Living Reviews in Relativity (2025)28:9
https://doi.org/10.1007/s41114-025-00056-1

WHITE PAPER

Waveform modelling for the Laser Interferometer Space Antenna

LISA Consortium Waveform Working Group · Niayesh Afshordi · Sarp Akçay · Pau Amaro Seoane · Andrea Antonelli · Josu C. Aurrekoetxea et al. ***[full author details at the end of the article]***

Received: 29 January 2024 / Accepted: 30 January 2025

Abstract

LISA, the Laser Interferometer Space Antenna, will usher in a new era in gravitational-wave astronomy. As the first anticipated space-based gravitational-wave detector, it will expand our view to the millihertz gravitational-wave sky, where a spectacular variety of interesting new sources abound: from millions of ultra-compact binaries in our Galaxy, to mergers of massive black holes at cosmological distances; from the early inspirals of stellar-mass black holes that will ultimately venture into the ground-based detectors' view to the death spiral of compact objects into massive black holes, and many sources in between. Central to realising LISA's discovery potential are waveform models, the theoretical and phenomenological predictions of the pattern of gravitational waves that these sources emit. This White Paper is presented on behalf of the Waveform Working Group for the LISA Consortium. It provides a review of the current state of waveform models for LISA sources, and describes the significant challenges that must yet be overcome.

Keywords LISA · Laser Interferometer Space Antenna · Gravitational waves · Gravitational wave detection · Gravitational wave sources · Astronomical black holes · Binary stars

The writing of this White Paper was coordinated by the co-chairs of the LISA Waveform Working Group: Maarten van de Meent, Deirdre Shoemaker, Niels Warburton, and Helvi Witek. Additional coordination was provided by the co-chairs of the LISA Waveform Work Package: Leor Barack, Anna Heffernan, and Harald Pfeiffer. The coordinators and contributors to individual sections of the White Paper are listed at the start of the each section.

Published online: 30 October 2025

Contents

1 Introduction

Waveforms, theoretical predictions for (GW) signals, play a vital role in GW astronomy. Many GW signal are buried deep in instrumental noise. By using waveforms as matched filters, such signals can be detected. Once a GW is found the properties of its source can be inferred by further comparing the system to theoretical waveforms. The Laser Interferometer Space Antenna (LISA), the recently adopted ESA-led space mission in collaboration with NASA (Colpi et al. 2024; Amaro-Seoane et al. 2017), will open a window on a new frequency band of GWs in the mHz regime. In this band we will encounter a slew of new sources of GWs ranging from local Galactic white-dwarf binaries to distant mergers of massive black holes (MBHs), and many sources in between. Realizing the science potential of LISA detection and measurement of GW signals will require new waveform models, which will need to cover a much wider range of sources while being significantly more accurate than the models used currently in ground based GW observations by LIGO, Virgo, and KAGRA (Pürrer and Haster 2020; Ferguson et al. 2021).

A large class of GW sources expected for LISA feature the inspiral of a binary of compact objects decaying under the emission of GWs, often leading to a merger at the end. Producing theoretical waveforms for such events requires solving the relativistic two body problem. This is a notoriously difficult problem with no known closed form solution for radiating binaries. There are four main approaches to obtain approximate solutions to the relativistic two-body problem from first principles. First, numerical relativity (NR) takes the non-linear partial differential equations (PDEs) of general relativity (GR), puts them on a grid, and evolves them on a supercomputer. Second, one can make a weak field approximation and obtain a perturbative analytical solution. This is known as the post-Minkowskian (PM) approximation, or – when an additional simultaneous slow motion approximation is introduced – the post-Newtonian (PN) approximation. Third, the gravitational self-force (GSF) formalism expands the two-body dynamics in powers of the (small) ratio of the masses of the two bodies. Finally, black hole perturbation theory (BHPT) uses homogeneous perturbations of isolated black holes (BHs) and associated quasi-normal mode (QNM) calculations to model the post-merger behaviour.

Each of these four approaches has its own natural domain of applicability. Due to its computational cost NR is limited to a relatively low number of orbits before merger and to systems with comparable masses. The PN and PM weak-field

approximations limit their application to the early inspiral, while GSF theory is at its best when dealing with binaries with relatively disparate mass-ratios. The post-merger phase of binaries containing a BH can be modelled with BHPT. As illustrated in Fig. 1, the natural domains of applicability of the four first-principle approaches to the relativistic two-body problem are largely complementary, and building waveforms for LISA will require input from all four — sometimes for modelling a single source. Effective waveform models like effective one-body (EOB) and the Phenom family combine inputs from the different approaches to provide waveforms that can straddle these domains.

The LISA Waveform Working Group (WavWG) serves as an interface between the LISA Science Group — tasked with realizing LISA's scientific mission — and the wider scientific community developing waveform models and studying the relativistic two-body problem. It serves to prioritize waveform development, inform the wider community of LISA's waveform modelling needs, and as a recruiting pool for waveform related tasks and projects in the LISA Science Group.

In this White Paper, the WavWG discusses the current status of waveform modelling and what further development is needed to realize LISA's science. It is organized in five main sections. In Sect. 2 we take a brief inventory of the sources LISA is expected to observe along with their expected parameters. This sets the primary goals for waveform model accuracy and parameter space coverage. Section 3 discusses what requirements LISA data analysis puts on waveform models in terms of accuracy, efficiency, and format. The main approaches to modelling waveforms from compact binaries are described in Sect. 4, discussing both their status to date, and challenges to be overcome to meet LISA's waveform requirements. Section 5 discusses methods for accelerating the production of waveform models. Finally, Sect. 6 covers the modeling for beyond GR, beyond Standard Model, and cosmic strings sources. We note that while stochastic signals are of considerable interest, this paper does not address them as the focus here is on individual detectable sources. For the reader's convenience, we have provided a table of notation used throughout the paper in Table 1 and a list of commonly used acronyms on the page proceeding this introduction.

2 LISA sources

LISA will be sensitive to a wide range of GW sources in the mHz regime. In this section, we take an inventory of anticipated sources that need to be modelled to extract useful scientific results *and* are well-enough understood at this stage to be modelled in some detail. A more extensive survey of LISA's expected sources and the science that can be done with them can be found in the White Paper produced by the LISA Astrophysics Working Group (Amaro-Seoane et al. 2023). The short summaries here mainly focus on the expected parameter ranges to provide a context for the modelling approaches discussed in the rest of the White Paper. Conventional long-lived astronomical sources include massive black hole binaries (MBHBs),

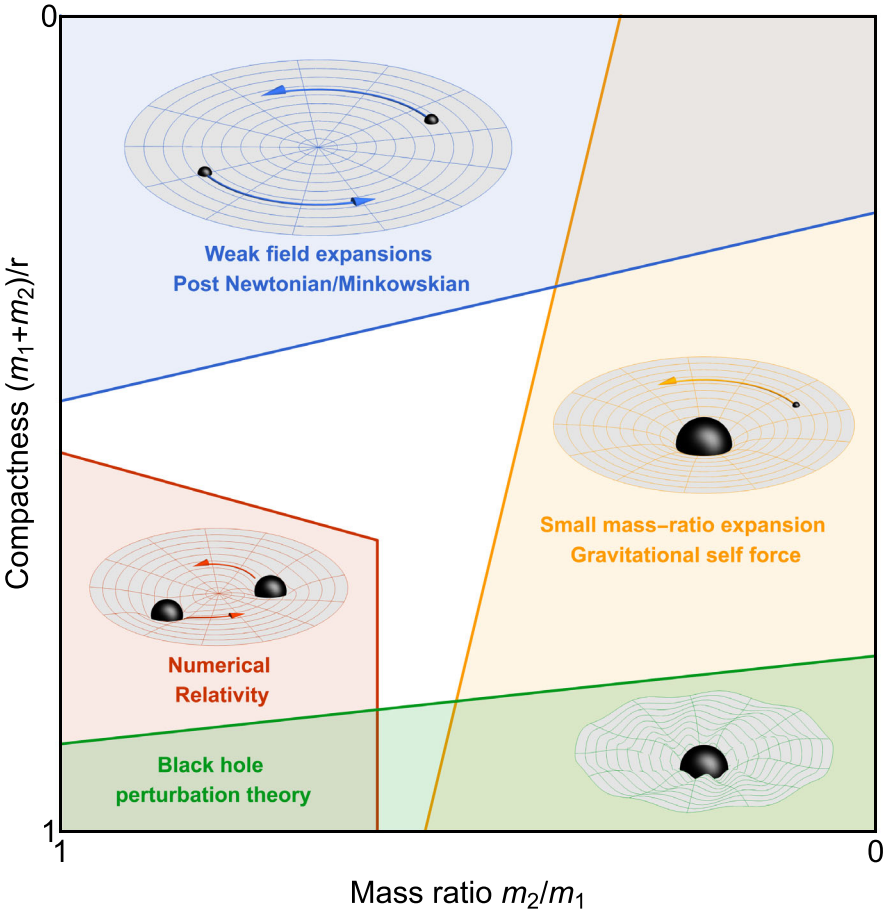

Fig. 1 A sketch of the natural domains of applicability of the four main approaches to solving the relativistic two-body problem. The approaches are largely complementary and building waveforms for LISA will require input from all four. The solid lines shown are illustrative of the reach of each approach. The precise reach of each region depends on the source type and the accuracy requirements of the model. In addition, the Effective-One-Body and Phenomenological models absorb information from the four main approaches to produce more global models that can compute waveforms sourced by binaries across large portions of the parameter space

extreme mass-ratio inspirals (EMRIs), intermediate mass-ratio inspirals (IMRIs), Galactic binaries (GBs) and stellar-origin black hole binaries (SOBHBs). These Sects. 2.1, 2.2, 2.3, 2.4, 2.5 present LISA sources in GR and the Standard Model. Theoretically interesting but empirically speculative sources include cosmic strings (CSs) and sources based on physics beyond GR and beyond the Standard Model are discussed in Sects. 2.6 and 2.7. These sources, and resulting science, will also be applicable to other mHz gravitational wave detectors (Luo et al. 2016; Hu and Wu 2017).

Table 1 Frequently used symbols throughout this White Paper; G and c are set to 1 throughout

G	Gravitational constant	
c	Speed of light	
m_1	Mass of the primary	$m_1 > m_2$
m_2	Mass of secondary	$m_2 < m_1$
M	Total mass	$m_1 + m_2$
μ	Reduced mass	$m_1 m_2 / M$
q	Large mass ratio	m_1 / m_2
ϵ	Small mass ratio	m_2 / m_1
ν	Symmetric mass ratio	$m_1 m_2 / M^2$
S_i	Spin angular momentum of body i	
a_i	Kerr spin parameter of body i	$S_i/(m_i c)$
χ_i	Dimensionless spin of body i	$a_i c^2/(G m_i) \equiv S_i c/(G m_i^2)$
e	Orbital eccentricity	
Ω	Orbital frequency	
μ_S	String tension	

A key metric for the detectability of sources is their signal-to-noise ratio (SNR). This is defined via the standard formula

$$\mathrm{SNR} = \sqrt{\langle h|h\rangle}, \tag{1}$$

where h is the GW strain and $\langle\cdot|\cdot\rangle$ is the noise weighted inner product,

$$\langle h_1|h_2\rangle = 4\Re \int \frac{\tilde{h}_1^*(f)\tilde{h}_2(f)}{S_n(f)} \mathrm{d}f, \tag{2}$$

with $\tilde{h}_i(f)$ denoting the Fourier transform of the strain, the star superscript (*) denoting complex conjugation, and $S_n(f)$ the noise power spectral density of the detector (Amaro-Seoane et al. 2017; Robson et al. 2019).

Unless otherwise stated this is computed for an observation period of up to 4 years.

2.1 Massive black hole binaries (MBHBs)

Coordinator: Enrico Barausse
Contributors: M. Bonetti, J. Garcia-Bellido

2.1.1 Description

In the local Universe, MBHs are observed in the centers of virtually all massive galaxies (Gehren et al. 1984; Kormendy and Richstone 1995; Heckman and Best 2014), as well as in many low mass dwarf galaxies (Reines et al. 2011, 2013; Baldassare et al. 2020). Their cosmic evolution is inextricably intertwined with that of their host galaxies. The latter provide MBHs with gas out of which they grow by accretion (thereby shining as quasars or active galactic nuclei (AGN)), and MBHs

influence the evolution of their hosts by injecting energy into their surroundings (AGN feedback) (Croton et al. 2006; Dickey et al. 2019; Sharma et al. 2020). This co-evolution of MBHs and galaxies is reflected in the scaling relations between MBH mass and galactic properties (Ferrarese and Merritt 2000; Gebhardt et al. 2000; Barger 2004; Kormendy and Ho 2013; McConnell and Ma 2013; Schramm and Silverman 2013), although the detailed physical processes leading to their emergence are still not fully understood.

Present day galaxies/dark matter haloes are believed to have formed hierarchically from the merger of smaller systems. Likewise, "seed" MBHs are expected to inhabit at least a fraction of the high redshift progenitors of today's galaxies (see Latif and Ferrara 2016 for a review). These seed BHs are expected to grow by a combination of gas accretion and mergers (Volonteri et al. 2008; Volonteri 2012; Lupi et al. 2014; Mayer et al. 2015; Valiante et al. 2016; Regan et al. 2017; Wise et al. 2019). Their coalescences, as well as those of the later generations of MBHs that they give rise to, are indeed a prime target for LISA (Sesana et al. 2004, 2005; Klein et al. 2016; Barausse et al. 2020a, 2023).

By detecting MBH mergers, LISA could confirm or disprove this hierarchical scenario for the evolution of MBHs. Indeed, considerable uncertainties exist about the timescale on which MBHs form a bound binary and eventually coalesce, after two galaxies have merged. The main uncertainty is whether MBH pairs can efficiently make their way from separations of hundreds of pc down to the sub-pc scales on which gravitational waves dominate the dynamics (Begelman et al. 1980; Yu 2002; Milosavljevic and Merritt 2003; Merritt and Milosavljevic 2005; Sesana et al. 2007; Lodato et al. 2009; Khan et al. 2011; Preto et al. 2011; Colpi 2014; Vasiliev et al. 2015; Sesana and Khan 2015; Dosopoulou and Antonini 2017; Tremmel et al. 2018; Bortolas et al. 2020; Barausse et al. 2020a). First dynamical friction and then stellar and/or gaseous hardening are the main drivers of the evolution of MBHs on their path to coalescence. Triple or quadruple MBH interactions, which naturally arise in models where the evolution of MBH pairs/binaries is slow or even stalls (Bonetti et al. 2019; Ryu et al. 2018; Mannerkoski et al. 2021), should in any case ensure LISA detection rates of at least a few per year (Bonetti et al. 2019; Barausse et al. 2020a).

Conversely, the observed detection rate will inform us about the efficiency with which MBH binaries come together and merge in nature (Barausse et al. 2020a), even though that information may be partly degenerate with the number of MBH seeds formed at high redshift. In that respect, it is worth pointing out the possibility that there may be massive primordial black holes (PBH) formed during the radiation era that may act as seeds for the MBH population (Clesse and García-Bellido 2015; García-Bellido 2019), resulting in high redshift MBHB mergers. PBHs of mass $\sim 10^6 M_\odot$ are believed to form at the electron-positron annihilation epoch (~ 1 second after the Big Bang) (Carr et al. 2024). They could start accreting gas very soon after recombination ($\sim 400,000$ years after the Big Bang) and grow to become supermassive ($10^9 M_\odot$) around $z \sim 10$ (470 Myr after the Big Bang). Close binaries of million-solar-mass PBHs could form very early and merge in a few million years. If

LISA detects MBHBs at $z = 25$ (130 Myr after the Big Bang) we should be confident they are PBH at $> 99.97\%$ confidence interval.

2.1.2 Expected source parameters

Further information on the underlying astrophysics can be gained by measuring the parameters of MBH binaries. Measurements of the component masses will allow for constraining the initial mass function of the seed black holes at high redshift (Sesana et al. 2004, 2005, 2011; Klein et al. 2016; Barausse et al. 2020a). Indeed, the latter may form as relatively low-mass black holes ($\sim 100 - 1000 M_\odot$), e.g. from the collapse of the first generation of stars (Madau and Rees 2001), or they may be born already as higher mass seeds of $\sim 10^4 - 10^5 M_\odot$ (e.g. from the collapse of massive quasi-stars (Begelman 2010), runaway instabilities in stellar clusters (Portegies Zwart and McMillan 2000; Stone et al. 2017), instabilities of protogalactic disks (Volonteri et al. 2008), etc.). Spin measurements, together with mass measurements, will clarify the properties of the accretion process and its importance in the evolution of MBHs relative to mergers (Berti and Volonteri 2008; Barausse 2012; Sesana et al. 2014). Measurements of distance will allow for placing the detected system at the right epoch in the history of the universe. Further help in this respect will naturally be provided by sufficiently accurate/precise sky localization, which might allow for the identification of an electromagnetic counterpart; and, therefore, a direct measurement of photometric or spectroscopic redshift (Tamanini et al. 2016; Mangiagli et al. 2020). In the presence of independent redshift and distance measurements, one may even attempt to construct a GW-based cosmography, potentially measuring the Hubble constant or the density of matter/dark energy in our universe (Tamanini et al. 2016). Finally, measurements of the eccentricity and mass ratio will provide insight on the mechanism driving MBH pairs to separations at which GW emission is enough to lead to a merger within a Hubble time (Bonetti et al. 2019; Barausse et al. 2020a).

In more detail, current expectations on the parameters of MBHBs and their seeds from astrophysical models are generally as follows:

- Source frame total masses range from a few 10^2 to a few $10^8 M_\odot$, with possible peaks around 10^3 and $10^5 M_\odot$ for respectively light and heavy seed formation in some models. See, e.g., Fig. 2 of Barausse et al. (2020a).
- Comparable mass binaries with mass ratio $\epsilon \equiv m_2/m_1$ between 0.1 and 1 are expected to make up the bulk of LISA detections, although tails extending down to $\epsilon \sim$ a few $\times 10^{-3}$ may be present (cf. Fig. 3 of Barausse et al. 2020a).
- Large uncertainties generally affect the prediction for spin magnitudes and orientations. Moderate to large spins $\gtrsim 0.7$ are expected in models calibrated to electromagnetic measurements (i.e. iron Kα) of MBH spins in local AGNs (Sesana et al. 2014), but the spins of the first generations of MBH mergers are relatively unknown. Similarly, spins may be approximately parallel at the peak of the star formation $z \sim 2 - 3$, where gas torques may align them with the orbital angular

momentum to within $10-30$ degrees (Dotti et al. 2010), but the situation may be different at higher and lower redshift.

- Eccentricity may be very significant and evolving in the LISA window ($e > 0.9$ upon entrance into the LISA band and up to 0.1 at plunge) if triple/quadruple MBH interactions are more efficient than gas and stellar interactions to drive the binary's evolution at $\sim$pc scales (Bonetti et al. 2019).
- Event rates and SNRs can vary significantly according to the underpinning astrophysical model (Sesana et al. 2011; Klein et al. 2016; Barausse et al. 2020a): in light seed scenarios rates may be as low as a few per year, especially if feedback from supernova explosions is included (Barausse et al. 2020a), which results in most events having small total masses and thus low SNRs (below 100). More generally, the number of light seed detections may be threshold limited (Bonetti et al. 2019; Barausse et al. 2020a). This is again especially true if supernova feedback is included, as most events have SNRs of a few tens in that case. In heavy seed scenarios, instead, irrespective of whether supernova feedback is included or not, rates and SNRs tend to be larger, i.e. roughly a few tens of detections in 4 years and SNRs up to several thousands.
- Environmental effects from gas and stars generally have negligible impact in the LISA observation window (Barausse et al. 2014), except under certain circumstances (Garg et al. 2022; Caputo et al. 2020). In addition, they might leave a recognizable imprint in the eccentricity distribution of detected events (Roedig and Sesana 2012). The same applies to MBH triple/quadruple interactions, which are expected to cause the aforementioned very high "relic" eccentricity when the binaries enter the LISA band (Bonetti et al. 2019).
- When delays between galaxy and MBH mergers are accounted for, the highest number of detections is expected around $z \sim 2-4$ (Barausse et al. 2020a).

In addition to the large parameter space described above, waveform templates for MBHBs will also need to accurately represent the waveform for many hundreds or thousands of cycles before merger — see, e.g., Fig. 16 of Mangiagli et al. (2020).

2.2 Extreme mass-ratio inspirals (EMRIs)

Coordinator: Huan Yang
Contributors: S. Akcay, P. Amaro Seoane, S. Bernuzzi, J. Gair, A. Heffernan, T. Hinderer, S. A. Hughes, S. Isoyama, G. Lukes-Gerakopoulos, A. Nagar, Z. Pan, Z. Sam, C. F. Sopuerta, V. Witzany

2.2.1 Description

EMRIs are binaries in which one member is substantially more massive than the other. The canonical EMRI is expected to be a stellar mass compact body (typically a black hole of 10–100 $M_\odot$) captured by a BH of 10^5–10^7 $M_\odot$ by multibody scattering processes in the core of a galaxy (Amaro-Seoane 2018b). EMRIs can also form via

the capture of other compact objects such as neutron stars or white dwarfs, though the small mass of these objects reduces their detectability with LISA (Hopman and Alexander 2006). A consequence of the large mass-ratio of EMRIs is the quite slow inspiral of the smaller body, executing 10^4–10^5 of orbits as it moves through the black hole's strong field (Finn and Thorne 2000; Berry et al. 2016). Binaries involving a MBH orbited by a substellar object, such as a brown dwarf, are called extremely-large mass-ratio inspirals (XMRIs) and these are potential LISA sources if they form around the MBH in the centre of the Milky Way (Amaro-Seoane 2019; Gourgoulhon et al. 2019). Measuring the gravitational waves generated by the strong-field orbits of E/XMRIs will make it possible to map the properties of massive black holes with great precision (Babak et al. 2017a; Vazquez-Aceves et al. 2023). See Table 2 for Summary of the anticipated parameters for LISA MBHB sources.

2.2.2 Expected source parameters

The expected LISA detection rate of EMRIs depends on several astrophysical ingredients (Babak et al. 2017a), including the mass/spin function of MBHs at different redshifts, the fraction of MBHs living in stellar cusps, stellar-mass compact objects (COs) capture rate per MBH, the characteristic mass of stellar-mass COs and their orbit eccentricities. The mass function of MBHs is usually modelled as a power law $dn/d\log M = n_0(M/3\times10^6 M_\odot)^{(-0.3,0.3)}$ (Gair et al. 2010), with n being the MBH number density and $n_0 \in (0.002, 0.005)$ Mpc^{-3}. MBHs can be extremely spinning with $a \approx 0.998$, slowly spinning with $\chi_1 \approx 0$ or of an extending spin distribution in the range $0 \leq \chi_1 \leq 1$, depending on their growth channels (accretion and/or mergers) (Dotti et al. 2013; Sesana et al. 2014; Pan and Yang 2020b). The fraction of MBHs living in stellar cusps is determined by how frequently MBHs

Table 2 Summary of the anticipated parameters for LISA MBHB sources

Parameter	Notation	Astrophysically relevant range
Total mass in the detector frame	M	10^5–$10^7 M_\odot$
Mass ratio (>1)	q	1–10
Dimensionless spin	$\lvert\chi_i\rvert$	0–0.998
Eccentricity entering LISA band	$e_{\rm init}$	0–0.99
Eccentricity at last stable orbit	$e_{\rm merge}$	<0.1
Signal to noise ratio	SNR	10–10^4

The total mass of a massive binary in the source frame ranges from 10^2–$10^8 M_\odot$ while moving to the detector frame picks up a factor of ~ 10 giving the range 10^3–$10^9 M_\odot$. This is squeezed on both ends by another factor of 10 (SNR and LISA band constrain the low and high limits respectively) giving a possible range of 10^4–$10^8 M_\odot$ with the majority of sources expected between 10^5–$10^7 M_\odot$ (Barausse et al. 2020a). The mass ratio, q is expected to range from 1–1000, again with the majority of sources expected to be in the 1–10 range (Barausse et al. 2020a). The maximum spin of 0.998 comes about because if a MBH accretes gas, the radiation emitted by the disk and falling into the hole has negative angular momentum, preventing a spin up past $\chi = 0.998$ (Thorne 1974)

merge, when the stellar cusps are destroyed, and their regrowth time after mergers. COs in stellar cusps captured by MBHs generically reside in low angular momentum orbits with large eccentricities, which subsequently decay to the range of $0 < e < 0.2$ at the final plunge (Babak et al. 2017a). The capture rate depends on the cusp relaxation time and the density profile of the cusp (Amaro-Seoane and Preto 2011). Taking into account of all these uncertainties with semi-analytic models, Babak et al. (2017a) forecasted that there will be several to thousands of EMRIs detected by LISA per year, assuming the contributing COs are BHs with mass 10 or 30 $M_{\odot}$, and a detection threshold of SNR $= 20$. On the other hand, recent rate studies predicted that accretion disk-assisted EMRI formation may be more common for LISA detection (Pan and Yang 2021a; Pan et al. 2021; Derdzinski and Mayer 2023), thanks to the high efficiency of disks in transporting stellar-mass black holes towards galaxy centers. These disk-assisted EMRIs tend to have negligible eccentricity comparing to the EMRIs formed by gravitational capture.

For XMRIs their extremely slow evolution means they will spend millions of years in the LISA band. Although the event rate of an XMRI forming is quite low, their long duration in band means in the Galactic centre there could be a few dozen sources, some of which may be highly eccentric. Due to the short distance between the centre of the Galaxy and the solar system, the SNRs can range from 10 to 10^4 (Amaro-Seoane 2019; Gourgoulhon et al. 2019). See Table 3 for Summary of the anticipated parameters for LISA EMRI sources.

2.2.3 Science with EMRIs

Constraining model parameters of EMRIs from their GW signals benefits from the large number of cycles completed in the LISA band (Babak et al. 2017a; Huerta and Gair 2009; Pan and Yang 2020b): all intrinsic parameters of an EMRI (the redshifted masses, the MBH spin magnitude, and the CO orbit eccentricity at plunge) can be measured with fractional uncertainty $\sim 10^{-6}$–10^{-4}; external parameters are mainly determined by the GW amplitude and its modulation with time, where the luminosity distance $D_{\rm L}$, the source sky location $\Omega_{\rm s}$ and the MBH spin direction Ω_a can be measured with fractional uncertainty $\sigma(\ln D_{\rm L}) \approx {\rm SNR}^{-1}$, median solid angle uncertainties $\sigma(\Omega_{\rm s}) \approx 0.05({\rm SNR}/100)^{-5/2}{\rm deg}^2$ and $\sigma(\Omega_{\rm a}) \approx 30\sigma(\Omega_{\rm s})$, respectively. In light of the source location constraints in both radial and transverse directions, a fraction of low-redshift EMRIs are expected to be traced back to their host galaxies without the aid of any electromagnetic counterparts (Pan and Yang 2020b).

To identify the nature of the secondary in an EMRI, in the case of a light black hole or a neutron star, the only potentially detectable parameter beyond its mass will be the component of its spin parallel to its orbital angular momentum (Witzany 2019; Skoupy et al. 2023). The detectability in the aligned-spin case has been discussed in Piovano et al. (2021) while more generic waveform model is being developed to address it in the general precessing-spin scenario (Drummond et al. 2024). For less compact objects, such as white dwarfs or brown dwarfs, there is a possibility of gaining some information about their quadrupoles (Rahman and Bhattacharyya 2023). However, all of the parameters of the secondary beyond its mass may be

Table 3 Summary of the anticipated parameters for LISA EMRI sources

Parameter	Notation	Astrophysically relevant range
Total mass in the detector frame	M	10^5–$10^7 M_\odot$
Mass ratio (> 1)	q	10^3–10^6
Dimensionless spin	$\max\lvert\chi_i\rvert$	0–0.998
Eccentricity entering LISA band	$e_{\rm init}$	0–0.8
Eccentricity at last stable orbit	$e_{\rm merge}$	0–0.2
Signal to noise ratio	SNR	20–100

Total masses of 10^4–$10^7 M_\odot$ can be seen by LISA (Gair et al. 2010) with those greater than $10^7 M_\odot$ ending outside the LISA band, although a rapidly spinning MBH may be detectable with a few $10^7 M_\odot$ as the ISCO is closer to the MBH (Amaro-Seoane 2018b). Regardless of formation channel, the smaller compact body as a typical $\mathcal{O}(10) M_\odot$ stellar mass black hole has an expected mass ratio of 10^3–10^6, or even 10^4–10^7 if neutron star EMRIs are included. Using MBH of $3 \times 10^6 M_\odot$ as a basis, the "loss-cone" EMRIs are expected to have high eccentricities, capped at ~ 0.8 entering the LISA band (Hopman and Alexander 2005), while the accretion channel tends to have smaller eccentricities (Pan et al. 2021). Evolving a large sample of compact bodies from capture results in a flat eccentricity distribution for the last stable orbit in the range $0 < e < 0.2$ (Babak et al. 2017a). A small tail of outlying higher eccentricities is possible. There is also the possibility of GW bursts from unbound / hyperbolic systems (Berry and Gair 2013a, b). Babak et al. (2017a) predicts the loudest EMRIs to have SNR ~ 100 for an observation time of a year

poorly constrained and partially or wholly degenerate with parameters controlling other sub-leading effects.

Detection of EMRIs will provide critical information with which to understand the growth history of MBHs and their environment. Different growth mechanisms, i.e., via mergers and/or via gas accretion, predict significantly different mass and spin distribution for MBHs (King et al. 2008; Berti and Volonteri 2008; Barausse 2012; Sesana et al. 2014). With a population of EMRI events, the co-evolution of MBH masses and spins over cosmic time can be measured to further reveal how they are formed and how they grew (Berti and Volonteri 2008; Barausse 2012; Sesana et al. 2014; Pan and Yang 2020b). N-body calculations have shown that EMRI rates sensitively depend on stellar distribution at galactic centers, so that the rate inferred from observation will also be able to constrain various distribution models (Babak et al. 2017a). Environmental effects, including the interaction with possible accretion disk around the MBH and close stellar objects near the EMRI system, may induce sizeable phase shifts to the EMRI waveform (Barausse et al. 2014; Bonga et al. 2019; Derdzinski et al. 2019, 2021). The accretion channel has illustrated that MBHs with AGNs will account for a significant number of EMRIs (Pan et al. 2021). Estimates of the resulting GW phase correction vary over many orders of magnitude (0.1–10^4 rad / year), depending on the assumed disk model (Yunes et al. 2011b; Barausse et al. 2015). Tidal resonances induced by the tidal field of nearby stars and stellar-mass black holes can generate a phase correction of $\mathcal{O}(1)$ in a significant fraction of the phase space (Gupta et al. 2022b). The main uncertainty comes from the population of nearby stellar-mass objects, which may come from the (disk)-migrating stellar-mass

objects in the AGN or leftovers from the previous AGN life cycle (Fig. 6 of Pan and Yang 2021b), or simply from the mass segregation effect (Emami and Loeb 2020, 2021).

By precisely mapping the background spacetime geometry of a MBH (Ryan 1995; Barack and Cutler 2007; Barausse et al. 2020b), EMRIs can be used to check whether the Kerr metric description is accurate and GR holds in the strong-field regime (Barausse et al. 2020b). At the innermost stable circular orbit (ISCO) of a typical MBH, the curvature scale is higher than Solar-system curvatures but lower than curvatures of some well-observed compact-binaries (Yunes et al. 2016). Consequently, modified gravities satisfying existing observational constraints generically predict very small deviations from GR in the standard EMRI scenario. However, since EMRIs are expected to be highly sensitive to small departures from the standard Kerr black hole background paradigm (Bambi 2011; Cardoso and Pani 2019), EMRIs will allow us to further tightly constrain any deviations caused by an additional scalar or vector channel for radiation in the long-term dissipation of energy and angular momentum (Chamberlain and Yunes 2017). In fact, even in the case where the field of the primary is just a generic stationary axisymmetric GR vacuum field, we should be able to determine the matter multipoles of the primary (Ryan 1995) and check possible violations of the no-hair theorem (Carter 1971), e.g., a deviation from the Kerr solution in the quadrupole moment (Glampedakis and Babak 2006; Barack and Cutler 2007).

In addition, as is true for all extragalactic LISA sources, various cosmological dispersion and propagation effects can be tightly constrained from EMRI signals (Chamberlain and Yunes 2017).

2.3 Intermediate mass-ratio inspirals (IMRIs)

Coordinator: Carlos F. Sopuerta
Contributors: M. Dhesi, M. Hannam, T. Hinderer, D. Neilsen, H. Pfeiffer, H. Sundar, N. Warburton

2.3.1 Description

An IMRI is a binary system with mass ratio in the range $10 \lesssim q \lesssim 10^4$ placing it between comparable mass binaries and EMRIs. IMRIs can come in two flavors, both of which contain an intermediate mass black hole (IMBH) with mass in the range 10^2–$10^4 M_\odot$. There is little observational evidence for BHs in the IMBH mass range, mainly because their main formation channel is inside globular clusters, the interiors of which are very difficult to observe (Greene et al. 2020). However, recent GW observations with ground-based detectors have found a population of BHs formed from binary black hole (BBH) mergers with a total mass greater than $10^2\, M_\odot$ (Abbott et al. 2023a, 2024). The largest confidently observed remnant (of GW190521) has a mass of $\sim 150 M_\odot$ (Abbott et al. 2020b, d). At the other end of the mass range, we have evidence of BHs with masses in the range 10^4–$10^5 M_\odot$ from observations of dwarf galaxies out to redshift ~ 2.4 (Mezcua et al. 2018; Greene et al. 2020). These

may correspond to an interpolation of the mass function observed for low MBH mass (Reines et al. 2013).

The two flavors in which IMRIs are expected to appear are: (i) Light IMRIs. A stellar-origin black hole (SOBH), or another sufficiently massive and compact object, inspiraling into an IMBH. For instance, dwarf galaxies or globular clusters may contain an IMBH which could capture an SOBH (Arca-Sedda et al. 2021). In this case, it is quite likely that the merger occurs outside the LISA frequency band, at higher frequencies. It is thus possible that an IMRI can be observed during its inspiral with LISA and have its merger seen by ground-based GW observatories (only for light IMBHs, with mass $\lesssim 10^3\, M_\odot$ (Gair et al. 2011)). (ii) Heavy IMRIs. Dynamical friction can produce the orbital decay of globular clusters into a galactic nucleus allowing the formation of an IMBH-MBH binary system, with the MBH in the LISA mass range (10^5–$10^7 M_\odot$) (Matsubayashi et al. 2007; Arca-Sedda and Gualandris 2018). Another possible channel to form heavy IMRIs is the merger of a dwarf galaxy satellite with its main galaxy (Bellovary et al. 2019). A third possibility is the formation of an IMBH in a galactic nuclei via hierarchical mergers (Gerosa and Fishbach 2021) via migration traps in AGN (Bellovary et al. 2016). Interestingly, GW190521 may have occurred in such an environment (Graham et al. 2020).

For more information on possible formation channels, and the uncertain event rates for these binaries, see the LISA Astrophysics Working Group White Paper (Amaro-Seoane et al. 2023) and Fragione and Leigh (2018), Jani et al. (2019), or the IMRI reviews (Amaro-Seoane 2018a, b). The nature of the different formation channels for IMRIs (both light and heavy) may lead to distinct IMRI dynamics so that LISA detections may shed some light on what are the most viable formation scenarios. See Table 4 for Summary of the anticipated parameters for LISA IMBH sources.

2.3.2 Science with IMRIs

As we only have evidence for IMBHs at the two ends of the mass range that defines these objects, the search for IMRIs with LISA is especially relevant with huge discovery potential. Event rates and parameter estimates for IMRIs can provide valuable information about the formation and growth of IMBHs in globular clusters, as well as details of stellar dynamics in those systems. This information is often difficult to glean from electromagnetic observations (Greene et al. 2020).

For heavy IMRIs the masses and spin of the MBH can be measured to within an relative error of a fraction of a percent (Huerta et al. 2012). Unlike EMRIs, where the spin on the secondary can be difficult to constrain (Piovano et al. 2021; Burke et al. 2024), the spin of the IMBH can be constrained to within $\sim 10\%$ (Huerta et al. 2012). IMRIs spend a long time orbiting in the strong field and due to their high SNR (relative to EMRIs) this makes then uniquely precise probes of GR and the Kerr hypothesis (Miller 2004). They can also be sensitive to modifications to Einstein's equations of GR or the presence of dark matter (Sopuerta and Yunes 2009; Dai et al. 2022).

Table 4 Summary of the anticipated parameters for LISA IMRI sources

Parameter	Notation	Heavy IMRIs	Light IMRIs
Binary mass	M	10^4–$10^7 M_\odot$	10^2–$10^4 M_\odot$
Mass ratio (> 1)	q	10–10^4	10–10^4
Dimensionless spin	$\max\|\chi_i\|$	0–0.998	0–0.998
Eccentricity entering LISA band	$e_{\rm init}$	0–1	0–0.9995
Eccentricity at last stable orbit or leaving LISA band	$e_{\rm merge}$	0–0.9	0–0.9
Signal to noise ratio	SNR	10–10^2	10–10^3

By defintion, light IMRIs' primary BH is from $10^2 M_\odot$ to $10^4 M_\odot$, i.e., an IMBH, while heavy IMRIs' primary BH is a MBH (Amaro-Seoane et al. 2023). Again the definition of an IMRI has a mass ratio from comparable (10) up to 10^5, above which the binary is defined as an EMRI. Eccentricity can be quite high for light IMRIs entering the LISA band (Amaro-Seoane 2018a). The initial eccentricity for heavy IMRIs is largely unknown. SNRs are taken from Table 11 of the Astrophysics Working Group White Paper (Amaro-Seoane et al. 2023)

Finally, *multiband* GW astronomy observations of light IMRIs consisting of observing the inspiral in the LISA detector and the merger in ground-based detectors (Aasi et al. 2015; Acernese et al. 2015; Sathyaprakash et al. 2012; Reitze et al. 2019) offers a range of increased science potential (Jani et al. 2019; Amaro-Seoane and Santamaría 2010; Sesana 2016). In particular, observing the inspiral with LISA can place tight constraints on the sky location and the merger time which can allow for targeted alerts for electromagnetic counterparts to the merger. Conversely, knowledge of the source parameters from ground-based observations of the merger can allow researchers to perform targeted searches for IMRIs in the archived LISA data (Wong et al. 2018). Multiband observations can also enhance the potential for performing tests of GR by breaking degeneracies between some parameters in the waveform models (Datta et al. 2021).

2.4 Galactic binaries (GBs)

Coordinator: Milton Ruiz
Contributors: V. Korol, H. Lim, V. Paschalidis, S. L. Shapiro, A. Tsokaros

2.4.1 Description

Our Galaxy is home to a variety of stellar binaries formed by white dwarfs, neutron stars, and black holes. Approximately a million years before their anticipated merger, these compact binaries transition into the millihertz GW frequency band accessible with LISA. Given such long evolution timescales, these systems will manifest as nearly-monochromatic sources of gravitational waves. Furthermore, these compact binaries will be detectable in large numbers by LISA, potentially emerging as the most numerous GW source within the millihertz band (Postnov and Yungelson 2014; Wagg et al. 2022; Lamberts et al. 2019; Marsh 2011).

Galactic compact binaries represent a key source class for the LISA mission. Firstly, their existence as GW sources is confirmed, as several have already been identified and characterised with electromagnetic telescopes (see e.g. Kupfer et al. 2024; Digman et al. 2023; Carvalho et al. 2022; Johnson et al. 2023; Yu et al. 2020; Biscoveanu et al. 2023; Wolz et al. 2020). Gravitational radiation from some of these known sources has already been measured indirectly by monitoring binary orbital contraction over extended periods (Hermes et al. 2012; Burdge et al. 2019; Munday et al. 2022). Secondly, as we can anticipate their GW signatures before the mission, these binaries have been suggested as "verification sources" for LISA (e.g. Stroeer and Vecchio 2006; Finch et al. 2023; Littenberg and Lali 2024; Shah et al. 2012b; Kilic et al. 2021). Most notably, Galactic compact object binaries accessible to LISA promise a wealth of insights into stellar and binary evolution. This encompasses understanding the nature of compact objects, unravelling the physical processes that govern binary interactions, and exploring their role in the formation and evolution of the Milky Way – see the LISA Astrophysics White Paper (Amaro-Seoane et al. 2023) for a review. Finally, it is noteworthy that a substantial portion of these binaries will not be individually resolvable by LISA, contributing to an unresolved stochastic foreground that will act as an additional source of noise for the instrument. Therefore, accurate characterization of this foreground is crucial to ensuring the precise characterization of other LISA sources.

Here we consider Galactic double compact objects, which we refer to as GBs, specifically those where at least one component is a compact object other than a black hole (binaries with two stellar origin black holes are treated in the next section). These can be categorised into various subtypes: binary white dwarfs (BWDs), with the subset of accreting BWDs, known as AM Canum Venaticorum or AM CVns in literature; binary neutron stars (BNSs); and mixed systems. The mixed systems encompass white dwarfneutron stars (WDNSs), which can emerge as ultra-compact X-ray binarys (UCXBs) in electromagnetic radiation, white dwarf-black holes (WDBHs), and binary black holeneutron stars (BHNSs).

2.4.2 Masses, mass-ratios, eccentricities, and known LISA verification sources

Observing GB using electromagnetic observatories poses a significant challenge due to their inherently small size and dimness (in some cases the entire absence of electromagnetic emissions). These features, when combined with selection effects and incompleteness of dedicated electromagnetic surveys, has limited our ability to know the true distributions of their parameters such as orbital separations, component masses, mass ratios, and eccentricities. Thus, much of our understanding of these binaries primarily hinges upon population synthesis studies. However, electromagnetic observations using Sloan Digital Sky Survey (SDSS) and Gaia have recently improved our understanding (Postnov and Yungelson 2014; Maoz et al. 2018; Brown et al. 2020; Kilic et al. 2021).

Binary population synthesis studies (e.g., Table 6 in Amaro-Seoane et al. 2023) show that for frequencies less than approximately 2 mHz, the BWDs form an unresolved foreground for LISA (see also Evans et al. 1987; Lipunov et al. 1987; Hils et al. 1990; Ruiter et al. 2010). Binaries with frequencies greater than

approximately 2 mHz and/or closer than a few kpc do not overlap with this background (Evans et al. 1987; Nelemans et al. 2001; Amaro-Seoane et al. 2023; Ruiter et al. 2010; Korsakova et al. 2024) and are called "resolvable". However, not all resolvable GBs are detectable, and unresolved GBs can also be detectable. Only binary systems with a significant SNR may be detected by LISA within a 4-year mission. Theoretical estimates suggest that among the hundreds of millions of binaries in the Galaxy, the number of resolvable binaries are about 6000–10000 BWDs, 100–300 WDNSs, 2–100 BNSs, 0–3 WDBHs and 0–20 BHNSs (Amaro-Seoane et al. 2023; Ruiter et al. 2010; Korsakova et al. 2024). However, the number of detectable binaries above the noise are about 6000 BWDs, 100 WDNSs, 30 BNSs, 3 WDBHs, 3 BHNSs and 2 hot subdwarf binaries (Nelemans et al. 2001; Kupfer et al. 2024).

The chirp mass, a key distinctive parameter among compact binary classes, varies significantly across different binary systems. For instance, BWDs typically peak at a chirp mass of around $0.25M_{\odot}$ (e.g. Korol et al. 2022; Li et al. 2020; Edlund et al. 2005), while BNS tend to have a chirp mass around $1.2M_{\odot}$ (Lau et al. 2020; Korol and Safarzadeh 2021). Systems comprising BHs and neutron stars (NSs) exhibit even higher chirp masses. However, it is important to note that LISA's limited ability to measure frequency derivatives for $f < 2$ mHz, and thus the chirp mass may introduce potential classification ambiguities (Lau et al. 2020; Korol and Safarzadeh 2021). For example, a nearby BWD system may be misidentified as a more distant BNS. Another discriminative feature could be the eccentricity measurements (Lau et al. 2020; Andrews and Mandel 2019). BWDs, typically formed via isolated binary evolution, are expected to be circularised due to recurrent mass transfer episodes. Contrastingly, BNS systems detectable in the LISA band might present measurable eccentricities due to natal kicks imparted by the supernova explosions that birth the NSs. Nevertheless, some rare eccentric BWD can form in globular clusters or via triple interactions (e.g. Kremer et al. 2018; Willems et al. 2007).

There are approximately 30 GBs, identified through electromagnetic detection, that have been confirmed as resolvable verification targets for the LISA mission. Notably, 18 of these are expected to be detectable within merely 3 months of scientific operations (Kupfer et al. 2024), proving invaluable in the early stages of the mission by assisting in the validation of LISA's performance relative to pre-launch expectations. These GBs are characterised by orbital periods ranging from ~ 300 to ~ 6000 seconds, equivalent to GW frequencies approximately between 0.5 and 6 mHz. Their total mass typically lies between 0.5 to $1.0M_{\odot}$, with mass ratios roughly between 0.1 and 0.7. Their estimated SNRs can exceed 100 after four years of integration (Finch et al. 2023; Liang et al. 2024; Kupfer et al. 2018).

Certain types of binaries can be sources of low and high frequencies, and hence can straddle both the LISA and ground-based detector bands. This is true for mixed binaries when unstable mass transfer leads to merger. Gravitational waves from the inspiral and merger of WDNSs may go from LISA to ground-based from potential oscillations of the NS after merger and/or its eventual collapse to a BH (Paschalidis et al. 2009, 2011a, b; Sun et al. 2018; Kang et al. 2024). The same straddling of LISA/ground-based frequency bands holds for stellar-mass black hole

binaries (Sesana 2016; Toubiana et al. 2020; Moore et al. 2019). See Table 5 for Summary of the anticipated parameters for LISA GB sources.

2.4.3 Modeling requirements & methods to improve/remove the Galactic background

GBs can be classified as detached or interacting (mass-transferring), depending on whether significant mass transfer occurs between the components. This classification is crucial for modelling their GW signals accurately. Although these systems are practically monochromatic to first order, the frequency does evolve with time. In particular, there is a difference in how the frequency evolves for detached binaries and interacting binaries. The orbital evolution of detached binaries is driven by the emission of gravitational waves, causing a gradual inward spiral of the binary (manifested as a negative frequency derivative in the GW signal). On the other hand, in accreting binaries, the redistribution of mass between the components results in an increase in their separation (leading to a positive frequency derivative in the GW signal) (Postnov and Yungelson 2014; Paschalidis et al. 2009). This leads to different requirements for waveform modelling. Note also that the shortest period binaries can be tidally-locked and corotating (Bildsten and Cutler 1992). For binaries near the Roche separation, tidal effects may have a non-negligible contribution to the phase evolution of the wave (Broek et al. 2012; Yu et al. 2021). Understanding the frequency evolution will help determine if mass transfer is taking place (Breivik et al. 2018; Littenberg et al. 2020) and/or tidal interactions are at play. A large number of mass-transferring systems may constrain the physics of mass transfer and the efficiency of angular momentum removal from the disk/companion system and its reinjection back into the orbit (Paschalidis et al. 2009).

Some of the GW sources that LISA will observe may be part of triple or higher-order multiple systems (e.g. Toonen et al. 2016; Rajamuthukumar et al. 2023). This includes sources in the Galactic disc that form through isolated triple evolution, as well as those in dense environments. When a BWD system — as the most common Galactic LISA source — is part of a larger system with an additional stellar or even a substellar object, the gravitational interaction with the substellar object introduces a modulation in the observed GW frequency due to the Doppler and related effects. This is a consequence of the motion of the BWD around the centre of mass of the three-body system. As the orbit of the tertiary must be larger than that of the inner binary for the system to remain stable, the modulation timescale will be longer than the GW frequency produced by the inner BWD. However, to detect this modulation with LISA, it should also be shorter than the mission's lifetime (Seto 2008; Tamanini and Danielski 2019; Katz et al. 2022).

Signals from many GBs will be below the BWD confusion background, which is generated both by detached and interaction/mass-transferring BWDs. Efforts have been made to remove this background in order to resolve more binaries (see e.g. Crowder and Cornish 2007; Littenberg 2011; Bouffanais and Porter 2016; Littenberg et al. 2020). Notice that the modeling of this confusion background may provide insight about the BWD population in the Milky Way (and nearby satellite galaxies).

Table 5 Summary of the anticipated parameters for LISA GB sources

Parameter	Notation	BWD	WDNS	BNS
Total chirp mass	M	$0.1–1M_\odot$	$0.4–1.2M_\odot$	$1–2.2M_\odot$
Mass ratio (> 1)	q	1–10	1–5	1–1.6
Eccentricity in LISA band	$e_{\rm init}$	0	0–1	0–1
Signal to noise ratio	SNR	<1000	<1000	<1000

BWDs can have a chirp mass between $0.1–1M_\odot$ Korol et al. (2017), mass ratios of 1–10 (which can reach 100 for AM CVns systems) and spins ranging from seconds to hours (Pelisoli et al. 2022; Kilic et al. 2021). WDNSs and BNSs will have chirp masses in the range $0.4–1.2M_\odot$ (Korol et al. 2024) and $1.0–2.2M_\odot$ (Vigna-Gómez et al. 2018; Wagg et al. 2022; Kruckow 2020) respectively. These binaries should exhibit spin periods ranging from seconds down to milliseconds, consistent with those observed in current systems, and near any eccentricity (Vigna-Gómez et al. 2018; Lau et al. 2020). As these sources are considered nearly monochomatic in the LISA band, their eccentricity is expected to evolve only a negligible amount inband

2.5 Stellar origin black hole binaries (SOBHBs)

Coordinators: Antoine Klein and Ilya Mandel
Contributor: D. Gerosa

2.5.1 Description

Stellar origin BH binaries are BBHs with component masses ranging from a few solar masses up to about $\sim 50–100M_\odot$, where models of pair-instability supernovae predict a mass gap to appear (Woosley 2017; Farmer et al. 2019; Woosley and Heger 2021). Those systems are in a mass range such that they can be observed by both LISA and by ground-based detectors, as they sweep through a few decades in frequency during the last stage of their inspiral. This broad coverage of the GW frequency spectrum makes it possible to probe the evolutionary history of such binaries (Sesana 2016; Mandel et al. 2018).

A circular BBH with two $45M_\odot$ components will merge in about 10 years from a GW frequency of ~ 10 mHz (Peters 1964; Sesana 2016). It is thus possible to track its evolution from the LISA band to the ground-based detector band, taking advantage of LISA's ability to better measure some of the system properties at low frequency and the improved measurements of parameters such as the remnant spin from high-frequency data. Of particular interest for LISA is the sky localisation capability, which is typically limited to tens of square degrees for BBHs in current ground-based detector data (Abbott et al. 2023a, 2024). The long duration of observations in the LISA band means that the detector will complete multiple orbits around the Sun, and thus effectively act as an instrument with a baseline of order the size of the orbit. The accuracy of sky localisation can be estimated as Mandel et al. (2018)

$$\sigma_\theta \sim 0.025 \frac{0.01\text{Hz}}{f} \frac{8}{\text{SNR}} \frac{\text{AU}}{\text{baseline}}, \tag{3}$$

where the GW frequency f should be replaced by the detector bandwidth for a source that evolves out of the band during the observation, and SNR is the signal-to-noise ratio. For a 2 AU baseline, this would yield sub-degree localization, though the exact localization accuracy would depend on the source location in the orbital plane. Another example could involve the measurements of BH spins and spin-orbit misalignments, which store information about formation scenarios (Vitale et al. 2017; Stevenson et al. 2017; Zevin et al. 2017; Farr et al. 2017; Gerosa and Fishbach 2021). While we may expect that high-frequency ground-based observations are best suited to measure mass ratios and spin-orbit couplings, which enter the waveform at higher orders in the orbital frequency, LIGO-Virgo-KAGRA Collaboration (LVK) observations to date have demonstrated the challenge of making such measurements precisely (Abbott et al. 2023a). LISA could observe $\gtrsim 10^5$ orbital cycles and therefore assist in making precise constraints for the handful of systems that will be observed by both LISA and ground-based detectors (Klein et al. 2022).

Beyond individual sources, LISA could track changes in the source population as binaries evolve in frequency. For example, LVK observations indicate that the majority of black holes in merging BBHs have masses $\lesssim 40 M_\odot$ (Abbott et al. 2023b), low to moderate spins (Roulet et al. 2020; Galaudage et al. 2021; Callister et al. 2021), and most have circularized by the time of merger (Romero-Shaw et al. 2019). On the other hand, LISA could observe BBHs while they are still eccentric, which would likely indicate dynamical formation (Abbott et al. 2016a; Romero-Shaw et al. 2021). The appearance of sources at higher frequencies would on its own indicate high birth eccentricity (McNeill and Seto 2022).

Another possibility worth mentioning is the detectability of a third body, particularly a massive black hole (MBH), through its impact on the binary's GW signature. Nuclear clusters around an MBH have been proposed as a possible BBH merger site, with possible assistance from gas in an active galactic nucleus (O'Leary et al. 2009; Bellovary et al. 2016; Tagawa et al. 2020). Mandel et al. (2018) argued that even when the orbital period of a binary of mass M_{bin} around an MBH of mass $M_{\text{MBH}} \gg M_{\text{bin}}$ is much longer than the observation duration T_{obs}, the orbital acceleration of the binary due to the MBH could still be detectable provided the GW frequency f_{GW} exceeds

$$f_{\text{GW}} \gtrsim 0.02\,\text{Hz} \left(\frac{M_{\text{MBH}}}{10^6\ M_\odot}\right)^{-1} \left(\frac{a}{\text{pc}}\right)^{2} \left(\frac{T_{\text{obs}}}{5\text{yr}}\right)^{-2} \left(\frac{\text{SNR}}{8}\right)^{-1}, \tag{4}$$

where a is the distance from the binary to the MBH. A BBH merger in a massive globular cluster of a similar mass could carry a comparable signature.

2.5.2 Expected source parameters

Judging by evidence from ground-based observations, the majority of BBHs observed so far have chirp masses between 5 and $\sim 40 M_\odot$ (Abbott et al. 2023b),

though BH masses could extend down to the maximum neutron star mass and up to the IMBH mass range, especially if hierarchical mergers in dense dynamical environments fill the mass gap from pair-instability supernovae (Yang et al. 2019b; Mapelli et al. 2021; Gerosa and Fishbach 2021). LISA will be particularly sensitive to more massive BBHs.

Most observed BBHs have mass ratios $q \lesssim 4$ (Abbott et al. 2023b), which is consistent with the bulk of model predictions, but systems with more extreme mass ratios are possible, such as GW190814, which involved a $\sim 23 M_\odot$ BH and a $\sim 2.6 M_\odot$ companion (Abbott et al. 2020c). As mentioned above, most observed BBHs have low to moderate companion spins, though it remains unclear whether this is a generic feature of stellar-mass BHs (Mandel and Fragos 2020; Fishbach and Kalogera 2022). Lastly, high eccentricities and generic spin-orbit misalignments could be a telltale sign of dynamical formation in dense stellar environments or in hierarchical triples (see Mandel and Farmer 2022; Mapelli 2020 for reviews of formation channels).

BBHs emit the bulk of their orbital energy above the LISA frequency band; therefore, moderate SNRs are expected except for fortuitously nearby sources (Sesana 2016). The minimal SNR for detection of BBHs will be influenced by the technical challenges associated with searching for signals with a complicated morphology and many in-band cycles (Moore et al. 2019). Furthermore, beyond an SNR threshold for detection, signals must also show evidence of frequency evolution in order for masses to be measurable, so that BBHs can be identified among the much larger population of signals from double white dwarfs (Lau et al. 2020). See Table 6 for Summary of the anticipated parameters for LISA SOBHB sources.

2.6 Cosmic strings

Coordinators: Barry Wardell
Contributors: D. Chernoff, J. Wachter

2.6.1 Description

Strings are effectively one-dimensional stress energy sources. If a network of strings is generated at early times then it can have many cosmological consequences including the production of gravitational waves (see Vilenkin and Shellard 2000 for a general review) that are potentially observable by LISA. String sources at energy scales comparable to those postulated in Grand Unified Theories (GUTs) have been ruled out by observations of the CMB (see Ade et al. 2014 for Planck-derived limits; the energy scale of the string-forming phase transition is $< 4.7 \times 10^{15}$ GeV, somewhat less than the characteristic GUT energy scale $\sim 10^{16}$ GeV). However, String Theory suggests new sources —fundamental strings and D-branes wrapped on

Table 6 Summary of the anticipated parameters for LISA SOBHB sources

Parameter	Notation	Range for majority of sources
Chirp mass	M	5–40
Mass ratio (> 1)	q	1–4
Effective spin	$\max\lvert\chi_{\rm eff}\rvert$	0–0.3
Eccentricity entering LISA band	$e_{\rm init}$	0–1
Eccentricity at last stable orbit	$e_{\rm merge}$	Out of band
Signal to noise ratio	SNR	<50

The most recent data release from LVK indicates a mass distribution of BBHs centred around $5–40M_\odot$ (Abbott et al. 2023b), however their masses could theoretically extend down to neutron star mass ($2M_\odot$) and up towards IMBH ($100M_\odot$) (Yang et al. 2019b; Mapelli et al. 2021; Gerosa and Fishbach 2021; Woosley and Heger 2021). LVK observations also show a mass ratio and effective spin magnitude distribution between 1–4 and 0–0.3 respectively (Abbott et al. 2023b), with more extreme mass ratio binaries observed (Abbott et al. 2020c) and the possibility of higher spins theoretically possible (Mandel and Fragos 2020; Fishbach and Kalogera 2022). Binary eccentricity decays with increasing gravitational-wave frequency roughly as $e \propto f^{-18/19}$ (Peters 1964), so sources that appear in the LISA band would circularise by the time they reach the LVK detector band; therefore, existing LVK observations do not constrain LISA band eccentricies. If we consider a SNR threshold for detection of 12, then $1-(12/50)^3 \approx 98.6\%$ of sources in an isotropic homogeneous Universe would have SNR <50

small dimensions— in the context of certain inflationary string theory scenarios (Witten 1998; Sen 1998b; Horava 1999; Dvali and Tye 1999; Sen 1998a; Giddings et al. 2002; Jones et al. 2002; Sarangi and Tye 2002; Kachru et al. 2003b; Copeland et al. 2004; Jones et al. 2003; Kachru et al. 2003a; Dvali and Vilenkin 2004; Henry Tye 2008). Macroscopic cosmic strings (CSs) are created and stretched to superhorizon scales by inflation (see Chernoff and Tye 2015; Baumann and McAllister 2015 for a review). Extensions to the Standard Model that introduce new symmetry breakings in-between the GUT and electro-weak scale can also produce viable strings Dror et al. (2020); Dunsky et al. (2022).

Irrespective of the detailed microscopic origin, these CSs may evolve to generate a network with some common features: after the Universe enters its radiation dominated phase the long, horizon-crossing strings begin to collide, break, reconnect and form small, sub-horizon scale loops. All string elements are dynamical, radiating gravitational waves and possibly other quanta (Brandenberger 1987; Srednicki and Theisen 1987; Bhattacharjee et al. 1992; Damour and Vilenkin 1997; Wichoski et al. 2002; Peloso and Sorbo 2003; Vachaspati 2010; Sabancilar 2010; Long et al. 2014). Isolated loops, for example, radiate their entire rest mass energy and eventually disappear. Together the string elements generate a stochastic GW background (Vilenkin 1981b; Vachaspati and Vilenkin 1985; Hogan and Rees 1984; Accetta and Krauss 1989; Bennett and Bouchet 1991; Caldwell and Allen 1992; Siemens et al. 2007; DePies and Hogan 2007; Olmez et al. 2010; Sanidas et al. 2012, 2013; Binetruy et al. 2012; Kuroyanagi et al. 2012, 2013; Sousa and Avelino 2013; Blanco-

Pillado et al. 2014; Sousa and Avelino 2014; Blanco-Pillado and Olum 2017; Chernoff and Tye 2018; Ringeval and Suyama 2017; Blanco-Pillado et al. 2018a; Cui et al. 2019; Jenkins and Sakellariadou 2018) and GW bursts (Damour and Vilenkin 2000, 2001; Siemens et al. 2007; Binetruy et al. 2009; Olmez et al. 2010; Regimbau et al. 2012; Kuroyanagi et al. 2012, 2013; Aasi et al. 2014a; Ringeval and Suyama 2017; Chernoff and Tye 2018; Abbott et al. 2018; Jenkins and Sakellariadou 2018). Detection and measurement of the string-generated gravitational waves by LISA will be informative for cosmology and high energy physics (see the White Paper from the LISA Cosmology Working Group for a summary (Auclair et al. 2023)).

The physics of CSs is sensitive to (1) the set of fields to which the string couples, (2) whether the strings are global or local, (3) the ratio of the characteristic string width to curvature scale. Here, we assume that the strings are minimally coupled (they interact with each other but only radiate gravitational waves), local and well-described in the classical limit by the Nambu–Goto action (see Aoyama et al. 2004 for a brief description and Zwiebach 2006 for string-theory applications). We refer to this as the "minimally coupled-string network". There are additional possibilities but this defines a wide, interesting arena for this White Paper.

Average properties of the minimally coupled string network are encapsulated in the Velocity One Scale (VOS) model (Martins and Shellard 1996, 2002; Martins et al. 2004; Sousa and Avelino 2013). It turns out that all quantitative features depend primarily on the string tension μ_S, or $G\mu_S/c^2$ in dimensionless terms. In particular, the total density in string components is parametrically small when the tension is small.

The VOS model is a valuable guide for forecasting the observations LISA may make. For specific numerical estimates below we assume minimally coupled local strings and adopt the following secondary parameters: intercommutation probability ~ 1 (intersecting field theory strings break and reconnect with probability of order unity (Shellard 1987) whereas string theory strings do so with smaller probability (Jackson et al. 2005)), number of string species 1 (multiple species exist in realistic string constructions, for a review see Chernoff and Tye (2015)), fraction ~ 0.2 of long length strings chopped into loops of size ~ 0.1 of the horizon (for review of the small and large components inferred from simulation see Chernoff 2009; Auclair et al. 2023) and rate of gravitational energy loss $dE/dt = \Gamma G\mu_S^2 c$ implied by dimensionless parameter $\Gamma = 50$ (Vachaspati and Vilenkin 1985; Burden 1985; Garfinkle and Vachaspati 1987; Blanco-Pillado and Olum 2017). Broadly speaking, changes to these adopted secondary values do not qualitatively change the network properties predicted by the VOS model. Many network properties are *not* included in VOS and have not yet been addressed in simulations. For example, isolated loops should evolve under the force of radiative backreaction (see Wachter and Olum 2017; Blanco-Pillado et al. 2018b; Chernoff et al. 2019; Blanco-Pillado et al. 2019) but that process is not included in current numerical simulations and so it is difficult to accurately incorporate into statistical descriptions. These model-dependent, as opposed to parameter-dependent, uncertainties are important systematic deficiencies in our understanding and hard to quantify.

2.6.2 Tension limits

The most well-studied modern scenario involves Type IIB string theory and low tension strings produced at the end of brane inflation. Strings — not monopoles nor domain walls — are produced when a brane and anti-brane pair annihilate and initiate the Big Bang cosmology (Jones et al. 2002; Sarangi and Tye 2002). The primary parameter, string tension, cannot currently be calculated a priori from theory. Instead we must turn to observations.

Empirical upper bounds on $G\mu_S/c^2$ have been derived from null results for experiments involving lensing (Vilenkin 1981a; Hogan and Narayan 1984; Vilenkin 1984; de Laix 1997; Bernardeau and Uzan 2001; Sazhin et al. 2003, 2006; Christiansen et al. 2008), GW background and bursts (Vachaspati and Vilenkin 1985; Economou et al. 1992; Battye et al. 1997; Damour and Vilenkin 2000, 2001, 2005; Siemens et al. 2006; Hogan 2006; Siemens et al. 2007; Abbott et al. 2009a, b; Aasi et al. 2014a; Abbott et al. 2018, 2019a, 2021e), pulsar timing (Bouchet and Bennett 1990; Caldwell and Allen 1992; Kaspi et al. 1994; Jenet et al. 2006; DePies and Hogan 2007; Blanco-Pillado and Olum 2017; Blanco-Pillado et al. 2018a), cosmic microwave background radiation (Smoot et al. 1992; Bennett et al. 1996; Pogosian et al. 2003, 2004; Tye et al. 2005; Wyman et al. 2005; Pogosian et al. 2006; Seljak et al. 2006; Spergel et al. 2007; Bevis et al. 2007; Fraisse 2007; Pogosian et al. 2009; Ade et al. 2014). It has long been recognized (Chernoff and Tye 2015) that all such bounds are model-dependent and typically involve observational and astrophysical uncertainties. Constraints from the CMB power spectrum rely on well-established gross properties of large-scale string networks and are relatively secure. Limits from optical lensing in fields of background galaxies rely on the theoretically well-understood deficit angle geometry of a string in spacetime but require a precise understanding of optical selection effects. Bounds from big bang nucleosynthesis rely on changes to the expansion rate from extra gravitational energy density but only constrain the strings formed prior to that epoch. Roughly speaking, these limits imply $G\mu_S/c^2 \lesssim 3 \times 10^{-8} - 3 \times 10^{-7}$ (see Siemens et al. (2007) for comparisons of limits). More stringent bounds on tension generally invoke additional assumptions (Battye and Moss 2010). Gravitational wave experiments (Siemens et al. 2007; Abbott et al. 2009a, 2018, 2019c) can monitor the occurrence of bursts. In particular, the LVK set a bound $G\mu_S/c^2 \lesssim 4 \times 10^{-15}$ based on non-detection of assumed cusp-like bursts (Abbott et al. 2021a). Long-term pulsar timing searches for a stochastic background have set the bound of $G\mu_S/c^2 \lesssim 1.5 \times 10^{-11}$ (Jenet et al. 2006; Ringeval and Suyama 2017; Blanco-Pillado and Olum 2017; Blanco-Pillado et al. 2018a). In the future LISA may achieve limits as low as $G\mu_S \sim 10^{-17}$ for Nambu-Goto strings (Auclair et al. 2023; Arun et al. 2022).

2.6.3 Loop sources for LISA

The VOS model for the minimally coupled string network generates a loop size distribution weighted towards small sizes (Chernoff and Tye 2018). For string tensions $G\mu_S/c^2 \ll 10^{-7}$ the string loops are the most important elements of the

network for GW science (Auclair et al. 2023). Small tensions imply weak GW damping. The undamped string is a non-linear oscillator with a fundamental period $T = \ell/(2c)$ and frequency $f = 1/T$. The Fourier transform of its motion yields power in all harmonics nf for $n \geq 1$. A survey of the loop dynamics reveals large scale motions and distinctive small scale feature: cusps (infinitesimal bits of the string that move at the speed of light twice per fundamental period) and kinks (discontinuous changes of slope that perpetually circumnavigate the loop). Gravitational wave emission is sourced not only by the large scale oscillations but also by cusps and kinks. All long-lived loops are expected to possess cusps or kinks else they intercommute and produce kinks. Cusp-generated power decays with harmonic n asymptotically $\propto n^{-4/3}$, kink-generated power $\propto n^{-5/3}$ and kink-kink collisions $\propto n^{-2}$ (Vachaspati and Vilenkin 1985; Damour and Vilenkin 2000, 2001; Binetruy et al. 2009). At high frequencies, cusps dominate if they are present. Conversely, the period-averaged area of the sky illuminated by gravitational radiation increases from cusps to kinks to large scale modes.

There are three scenarios for LISA detections. (1) Loop decay creates a stochastic GW background from a large number of unresolved sources (Auclair et al. 2023). (2) Specific cusp or kink containing sources produce bursts of emission that stand above the general background (Bartolo et al. 2022). (3) A few nearby loops, possibly associated with the Galaxy, produce emission that is strong, smooth and always on DePies and Hogan (2009); Chernoff (2009); Khakhaleva-Li and Hogan (2020); Jain and Vilenkin (2020).

2.6.4 Science with cosmic strings

(1) Interesting fundamental results are destined to emerge whether or not LISA detects evidence of gravitational radiation from strings. A positive result for the stochastic background will allow the inference of the string tension; a negative result will provide upper limits on the tension of any string component that might be present (Auclair et al. 2023). If the network has a String Theory origin then either determination helps guide progress towards a realistic model scenario for String Theory that incorporates the Standard Model.

(2) A positive detection (either background, burst or nearby loop) is also fundamentally significant for cosmology because loops of macroscopic size are created during an epoch of inflation, supporting the inflationary paradigm (Guth 1981; Linde 1982; Albrecht and Steinhardt 1982). The universe's precise inflationary scenario remains a profound problem for cosmology and for fundamental physics. The almost scale-invariant density perturbation spectrum predicted by inflation is strongly supported by cosmological observations, in particular the cosmic microwave background radiation (Ade et al. 2014).

A negative detection is also very informative. The production of string-like structures is a rather generic theoretical prediction whenever inflation does occur (Jeannerot et al. 2003; Dunsky et al. 2022). A negative result might be explained if the strings are unstable and/or couple to additional fields that promote their decay. This sort of result will guide the search for models that allow such interactions.

2.7 Beyond GR and beyond standard model sources

Coordinator: Paolo Pani, Helvi Witek
Contributors: N. Afshordi, R. Benkel, G. Bozzola, R. Brito, A. Cárdenas-Avendaño, E. Maggio, M. Okounkova, V. Paschalidis, C. Sopuerta

2.7.1 Introduction

BHs and compact binaries, and their GW emission have tremendous potential to probe for new physics beyond the Standard Model in the strong-field, nonlinear regime of gravity. LISA is likely to detect loud sources, such as MBHBs and EMRIs, which will allow us to test the nature of BHs, the validity of GR in the strong-field, highly-dynamical regime of gravity, or the presence of additional fundamental fields with unprecedented precision. These observations can help us address fundamental questions such as Arvanitaki and Dubovsky (2011); Yunes and Siemens (2013); Berti et al. (2015); Barack et al. (2019b); Cardoso and Pani (2019); Barausse et al. (2020b): (i) What is the nature of dark matter, and how can BH detections with LISA aid the search for new particles? (ii) What is the nature of gravity? Are there new fundamental fields and GW polarizations, as predicted by some extensions of GR and of the Standard Model? (iii) How do gravitational waves propagate over cosmological distances? (iv) Are the massive objects observed at galactic centers consistent with the rotating BHs predicted by GR? (v) Do exotic compact objects other than BHs and neutron stars exist in the universe? This complex topic in the context of LISA science is discussed in depth in the White paper of LISA's Fundamental Physics Working Group (Arun et al. 2022). Here we briefly summarize the most relevant sources for probing fundamental physics with LISA as a guide for the modelling of gravitational waveforms in GR and beyond.

2.7.2 Black holes and ultralight fields

2.7.2.1 Description Ultralight bosonic fields such as axions, axion-like particles or dark photons are predicted in several particle and theoretical physics models. A remarkable example is the string axiverse scenario, which predicts a multitude of axion-like particles emerging naturally from string theory compactifications (Arvanitaki et al. 2010). These ultralight particles play a crucial role in diverse areas of physics and have been proposed (i) as a solution to the strong CP problem in quantum chromodynamics (QCD) (Peccei and Quinn 1977), (ii) as compelling dark matter candidates (Hui et al. 2017; Ferreira 2021) and (iii) in cosmology (Marsh 2016). Excitingly, we can employ BHs to search for (or constrain) ultralight bosons in a mass range that is complementary to traditional particle colliders or direct detection experiments (Arvanitaki and Dubovsky 2011; Brito et al. 2015c; Bertone et al. 2020; Arvanitaki et al. 2015; Brito et al. 2017a, b). This surprising connection between BHs and particle physics is provided by the superradiant instability of BHs (Press and Teukolsky 1972; Starobinsky 1973; Bekenstein 1973; Teukolsky and Press 1974; Detweiler 1980b; Shlapentokh-Rothman 2014; Brito et al. 2015c): low-

frequency bosonic fields scatter off a rotating BH superradiantly, thereby extracting mass and angular momentum from the BH. Fields of mass-energy $\mu_{\rm B}$ are efficiently confined in the vicinity of a BH with mass M if the gravitational coupling $M\mu_{\rm B}\lesssim 0.4$ (Dolan 2007; Witek et al. 2013; Pani et al. 2012; East 2017; Wang et al. 2022), corresponding to $\mu_{\rm B}\lesssim 10^{-16}(M/10^6 M_\odot)$ eV. In this case they efficiently form a bosonic condensate ("cloud") around the BH. An alternative formation scenario involves accretion of such ultra-light fields onto BHs (Clough et al. 2019; Bamber et al. 2021) in the same mass range. If the bosonic field is complex, this process gives rise to hairy BHs (Herdeiro and Radu 2014, 2015; Herdeiro et al. 2016; Santos et al. 2020).

The details of the cloud's formation depends on the initial parameters such as the BH spin and the gravitational coupling between BH and bosonic field (Brito et al. 2015b; Ficarra et al. 2019; East and Pretorius 2017). Once formed, the condensate dissipates by emitting a quasi-monochromatic GW signal (Yoshino and Kodama 2014; Arvanitaki et al. 2015; Brito et al. 2015b; Okawa et al. 2014; Zilhão et al. 2015b; Brito et al. 2017a, b; East and Pretorius 2017; East 2018; Siemonsen and East 2020; Zhu et al. 2020; Brito et al. 2020). The presence of boson clouds can also significantly affect the dynamics of binaries, e.g., through "dragging" of the cloud (Zhang and Yang 2020), dynamical friction (Traykova et al. 2021) or tidal effects (Cardoso et al. 2020). Numerical simulations of comparable-mass BH binaries interacting with a high-density bosonic cloud have shown that scalar clouds may condense around the binary to form "gravitational molecules" (Ikeda et al. 2021), that yield scalar radiation. This interaction may yield a GW phase shift (Bamber et al. 2023) that is also present for low-eccentricity initial data (Cheng et al. 2024). The post-merger quasinormal ringdown frequency are changed in the presence of a scalar cloud (Choudhary et al. 2021). In EMRIs the GW signal is modified relative to the vacuum case (Macedo et al. 2013b; Wong 2020) and the presence of a secondary BH yields resonances (Baumann et al. 2019a, b, 2020; Berti et al. 2019). The detection of EMRIs can be used to infer the boson's mass (Hannuksela et al. 2019, 2020).

2.7.2.2 Expected source parameters All "traditional" GW sources in the LISA band, including compact, comparable-mass BH binaries, EMRIs, and isolated spinning massive BHs, are potentially affected by bosonic clouds. Therefore, they are also good sources to act as cosmic laboratories for ultralight fields. Because the underlying mechanism only relies on the gravitational coupling, but is independent from the coupling of the bosons to the Standard Model of particle physics, they probe all types of bosons, i.e., (pseudo-) scalars such as axion-like particles (Peccei and Quinn 1977; Arvanitaki et al. 2010), ultralight dark matter (Hui et al. 2017; Ferreira 2021), ultralight vector (Goodsell et al. 2009; Baryakhtar et al. 2017) and tensor (Brito et al. 2020; Dias et al. 2023) fields. LISA sources are particularly well suited for detecting or constraining ultra-light bosons in the mass range $\mu_{\rm B}\in[10^{-19},10^{-15}]$ eV (Brito et al. 2017a, b; Isi et al. 2019b; Stott 2020; Brito et al. 2020) (and even wider for massive spin-2 fields (Dias et al. 2023)), and they are suited for multi-wavelength searches in combination with ground-based instruments (Ng et al. 2020).

2.7.3 Binary black holes as probes of the nature of gravity

2.7.3.1 Description Does GR, our Standard Model of gravity, truly describe gravitational phenomena at all scales? It is expected to break down at high-energy scales as signaled by the presence of singularities inside BHs or at the Big Bang. At these scales a more complete theory of quantum gravity is needed that consistently combines gravity and quantum mechanics. However, GR cannot be quantized with standard approaches and it is not renormalizable. Therefore, GR (or a quantized version thereof) is not a viable candidate for quantum gravity. While a complete theory of quantum gravity remains elusive, most candidates predict similar extensions to GR such as higher curvature corrections or (non-minimial) coupling to new fields. BHs provide an ideal probe to search for such beyond-GR theories because, e.g., the presence of additional fields may endow BHs with scalar hair (or "charges"), thus violating the no-hair theorems of GR (Hawking 1972; Bekenstein 1996). More specifically, new fundamental fields arise in several low-energy effective field theories of gravity (Berti et al. 2015), e.g., in the low-energy limit of quantum gravity, in the Horndeski class of scalar-tensor theories (Horndeski 1974; Deffayet et al. 2009) tensor-vector-scalar theories (Moffat 2006), and in theories with quadratic curvature corrections (Kanti et al. 1996; Alexander and Yunes 2009; Kanti and Tamvakis 1995; Cano and Ruipérez 2022). Such fields also arise in extensions of the Standard Model of particle physics, e.g., hidden U(1) fields (including "dark photons") in mini-charged dark matter models (Cardoso et al. 2016c) , primordial magnetic monopoles (Preskill 1984), darkly charged dark-matter (Fan et al. 2013), and the aforementioned bosonic clouds formed around BHs due to the superradiant instability.

In comparable-mass compact binaries, the coalesence of such "hairy" BHs generates additional scalar radiation that accelerates the inspiral and yields a GW phase shift. Furthermore, new polarization channels can exist in modified gravity theories. The detection or absence of such extra polarizations will be an important probe for new physics. In addition to modifications to the background solutions and the GW emission, modified theories of gravity may also change the physical properties of the gravitational waves once they are emitted, e.g., by changing the dispersion relation, the polarization and the way they interact with matter and with the detector (Yunes and Siemens 2013). As modifications to the propagation of gravitational waves accumulate with the distance traveled, and the capability to put constraints on the mass of the graviton (Compton GW wavelength) scales with the chirp mass, comparable-mass binaries are the most effective systems for measuring these effects (Barausse et al. 2020b).

EMRIs will provide an excellent probe of the multipolar stucture of its primary object and, thus, test if the primary is consistent with the Kerr BH metric predicted by GR. GW measurements will reveal details of both the conservative (time-symmetric) and the dissipative (time-asymmetric) sectors of the gravitational theory. Additional degrees of freedom, such as dynamical scalar or vector fields, will introduce modifications to the motion of bodies, and additional sources of GW energy and angular momentum emission. Given that in most modified theories the gravitational field is described by a spin-2 metric tensor field and by additional fields (Berti et al.

2015), the interaction between matter and the new fields may give rise generally to an effective "fifth force", leading to deviations from the universality of free fall (Nordtvedt 1968), or in other words, to violations of the "strong" equivalence principle. How well a beyond-GR theory may be constrained depends on the relative PN order at which the correction enters and on the dimensions of the extra couplings (Cardenas-Avendano et al. 2020; Yunes et al. 2016; Chamberlain and Yunes 2017). For example, the best GW tests of theories with higher-order curvature invariants, such as the Gauss–Bonnet invariant (Metsaev and Tseytlin 1987; Campbell et al. 1992; Kanti et al. 1996) or the Pontryagin density (Alexander and Yunes 2009), involve small-mass BHs whose curvature is larger than that of supermassive BHs. Therefore, the best probes of higher curvature corrections are IMRIs and EMRIs in the LISA band (Sopuerta and Yunes 2009; Gair et al. 2013) or stellar-mass BBHs detected with ground-based GW instruments.

2.7.3.2 Expected source parameters Both MBHBs and EMRIs can be employed to test gravity and the nature of compact objects with LISA; see the LISA Fundamental Physics White Paper (Arun et al. 2022) for details. For example, with nearly equal-mass BHs, one can perform null tests with inspiral-merger-ringdown consistency and BH spectroscopy, as well as searching for specific deviations with parametrized inspiral and ringdown waveforms; see (Berti et al. 2015; Franchini and Völkel 2024; Colleoni et al. 2024). Given the different nature and mass range of the gravitational-wave sources that will be detected with LISA, tests of gravity with LISA will be complementary to the suite of tests that has been performed by the LVK collaboration (Abbott et al. 2019e, 2021c, d). The beyond-GR modifications in the modelling of these signals (including PN theory, BH perturbation theory, effective-one-body approaches, and numerical relativity) are discussed in Sect. 6.

With EMRIs one can constrain the multipolar structure of the primary object's spacetime with exquisite precision, thus testing whether the primary object is consistent with the Kerr BH metric predicted in GR , see, e.g., Cárdenas-Avendaño and Sopuerta (2024) and references therein. The parametrization of the waveforms will depend on the type of test carried out. For instance, when testing the geometry of the dark objects inhabiting galactic centers assuming GR, the parameters would describe the deviations from Kerr, e.g., multipole moments, tidal parameters or post-Kerr parameters. On the other hand, when testing GR, the parameters would describe the modifications of GR, e.g., additional coupling constants, length scale of extra dimensions or higher-order corrections.

With both types of sources one can search for novel radiation channels due to extra polarizations or additional charges present in beyond-GR theories.

2.7.4 Testing the Kerr-hypothesis: BH mimickers and echoes

2.7.4.1 Description Exotic compact objects (ECOs) are horizonless objects which are predicted in some quantum gravity extensions of GR (Nicolini et al. 2006; Bena and Warner 2008; Giddings 2014; Koshelev and Mazumdar 2017; Abedi et al. 2020) and in the presence of exotic matter fields in the context of GR (Liebling and

Palenzuela 2023; Giudice et al. 2016; Cardoso and Pani 2019). The theoretical motivations for ECOs are the regularity of their inner structure and the overcoming of semi-classical puzzles such as that of the information loss (Myers 1997; Das and Mathur 2000; Mathur 2009). These ideas have inspired a plethora of models including gravastars (Mazur and Mottola 2004, 2023), boson stars (Feinblum and McKinley 1968; Kaup 1968; Ruffini and Bonazzola 1969; Colpi et al. 1986; Seidel and Suen 1991), Proca stars (Brito et al. 2016a), wormholes (Einstein and Rosen 1935; Morris and Thorne 1988; Damour and Solodukhin 2007), fuzzballs (Mathur 2005, 2009) and others (Bowers and Liang 1974; Gimon and Horava 2009; Prescod-Weinstein et al. 2009; Brustein and Medved 2017; Holdom and Ren 2017; Buoninfante and Mazumdar 2019).

ECOs are classified in terms of their compactness, reflectivity and possible extra degrees of freedom related to additional fields (Cardoso and Pani 2019; Wang and Afshordi 2018). Two important categories are (Cardoso and Pani 2017): *ultracompact objects*, whose exterior spacetime has a photon sphere, and *clean-photon-sphere objects* (ClePhOs), so compact that the round-trip time of the light between the photon sphere and the object's surface is longer than the instability timescale of photon orbits. If the remnant of a merger is an ultracompact object, the ringdown signal differs from the BH ringdown at early stages and is dominated by the modified QNMs of the object (Urbano and Veermäe 2019; Maggio et al. 2020). Conversely if the remnant of the merger is a ClePhO, the prompt ringdown is nearly indistinguishable from that of a BH because it is excited at the light ring (Cardoso et al. 2016a). The details of the object's interior appear at late times in the form of a modulated train of GW echoes (Cardoso et al. 2016a, b; Price and Khanna 2017; Correia and Cardoso 2018; Burgess et al. 2018; Huang et al. 2020). The time delay between echoes depends on the compactness of the object and/or the energy scale of new physics (Oshita et al. 2020a), whereas the amplitude is related to the reflectivity of the object (Cardoso and Pani 2019).

Many of these ECOs could be ruled out based on theoretical grounds. Horizonless compact objects are affected by an ergoregion instability when spinning sufficiently fast (Friedman 1978; Comins and Schutz 1978; Yoshida and Eriguchi 1996; Kokkotas et al. 2004). The endpoint of the instability could be a slowly spinning ECO (Cardoso et al. 2014; Brito et al. 2015c) or dissipation within the object could lead to a stable remnant (Maggio et al. 2017, 2019a). Furthermore, ultracompact horizonless objects might be generically affected by a light-ring instability at the nonlinear level (Cardoso et al. 2014; Cunha et al. 2017, 2023). Current and future GW detectors will constrain models of ECOs in almost all the regions of their parameter space (Cardoso et al. 2008; Fan and Chen 2018; Barausse et al. 2018; Maggio et al. 2020). In particular, searching for echoes in the post-merger signal of MBHBs with LISA (Maggio et al. 2019b) will provide a clean smoking gun of deviations from the standard, "vacuum", BH prediction. Furthermore, EMRIs could constrain the reflectivity of the primary object to unprecedented levels (Maggio et al. 2021a).

2.7.5 Expected source parameters

The source parameters depend on the specific signal used to search for and constrain ECOs. The echo signal depends on the parameters of the remnant (in particular mass and spin), on its compactness, and especially on its effective reflectivity, which is zero for a classical BH (Cardoso and Pani 2019; Maggio et al. 2021b). The reflectivity can be generically a complex function of the frequency and of other remnant parameters. In an inspiral, besides the standard binary parameters, ECOs are characterized by anomalous multipole moments and nonvanishing tidal deformability, sharing in this case properties similar to those of BHs in modified gravity theories. In an EMRI, besides the different multipolar structure (Glampedakis and Pappas 2018; Raposo et al. 2019; Raposo and Pani 2020; Bianchi et al. 2020, 2021; Bena and Mayerson 2020, 2021; Herdeiro et al. 2021a; Bah et al. 2021; Fransen and Mayerson 2022; Loutrel et al. 2022; Vaglio et al. 2022) and tidal deformability (Pani and Maselli 2019; Piovano et al. 2023) of the central object, a key parameter is again the (frequency-dependent) reflectivity (Maggio et al. 2021a).

3 Modelling requirements from data analysis

Ideally, waveform models should be infinitely accurate, evaluate instantly and be available in any format desired. In practice, none of these are achievable. The practical accuracy, efficiency and format requirements are set by the way LISA data is analyzed. This section starts with a brief overview of how LISA data analysis is expected to work. (For a more detailed description, see the White Paper from the LISA Data Challenge Working Group (2022).) The remaining sections discuss how data analysis sets requirements on the accuracy, efficiency and formats of waveform models, providing the necessary framing for the discussion of waveform models in the rest of this White Paper.

3.1 Data analysis for LISA

Contributor: Tyson Littenberg

The foundation of gravitational wave data analysis is rooted in the conceptual simplicity of the measurement: observing relative changes in the separation between a collection of "proof masses" in free fall due to leading-order perturbations in the underlying spacetime metric, which propagate (effectively) uninhibited through the Universe. This is in stark contrast to, for example, electromagnetic observations, where the photons' propagation from source to detector is influenced by intervening material (e.g., dispersion, scattering, absorption, reprocessing), and then undergoes complicated interactions with the instruments themselves (e.g., focusing optics, filters, diffraction, absorption by the detector) before registering as a signal. This is not to take away from the heroic effort and ingenuity required to develop the measurement system that is sensitive to the unfathomably small space-time perturbations themselves. However, given a detector that can achieve the necessary

sensitivities, it is a tractable task to derive its response to incident gravitational waves from first principles.

As a result, GW data analysis methods have primarily developed around a *forward* problem, where the detector response is predicted from a hypothetical source and that predication is then tested against the data (Jaranowski and Krolak 2005). There are notable exceptions, particularly in some searches for unmodelled GW transients in ground-based interferometer data (Drago et al. 2021), which approach the analysis as an *inverse* problem, starting with the observed data and working backward to solve for the input signal.

Any analysis is only as good as the models that go into it. The phenomenal sensitivity, accuracy and precision of GW observations is not achievable without highly accurate, coherent models for the gravitational waveforms themselves (the focus of this whitepaper), as well as the detector response and noise characteristics.

Under the assumption that the noise is Gaussian, the likelihood that the hypothetical model, parameterized by θ, would produce the observed data $\mathbf{d}$ is

$$p(\mathbf{d}|\theta) = \frac{1}{\sqrt{\det(2\pi\mathbf{C})}} e^{-\frac{1}{2}\mathbf{r}^\dagger \mathbf{C}^{-1}\mathbf{r}}, \tag{5}$$

where $\mathbf{r} = \mathbf{d} - \sum_i \mathbf{h}_i$ is a vector of all residual data samples after the discrete GW signals $\mathbf{h}_i$ have been subtracted, $\mathbf{C}$ is the noise covariance matrix $C_{ij} \propto \langle n_i | n_j \rangle$, and $\mathbf{n}$ is noise such that, in the absence of any GW signals, $\mathbf{d} = \mathbf{n}$. The likelihood is testing whether the residual is consistent with the ansatz that, in the absence of discrete gravitational waves, the data is Gaussian characterized by $\mathbf{C}$. Note the emphasis on *discrete* gravitational waves – a stochastic background of GW signals appears in the data model as a "noise" term, which modifies $\mathbf{C}$ with particular covariances that set it apart from instrument noise. See Romano and Cornish (2017) for a detailed look at how the likelihood is derived, simplifications that produce slightly different forms of the equation in the literature, and a unified treatment of discrete and stochastic signals.

Also note that Eq. (5) does not prescribe a representation of the data. The game, as it were, is to represent the data in a way that minimizes the number of non-zero components of $\mathbf{C}^{-1}$ and thereby minimize the computational cost of evaluating the likelihood. It is the case under the assumption of stationary noise (i.e. $\mathbf{C}$ is constant over the observation time) that the discrete Fourier transform diagonalizes $\mathbf{C}$, which is why much of the GW analysis literature is based in the Fourier domain. For LISA, due to the long duration signals expected, the assumption of stationary noise will be dubious at best, and so analysis methods may trend towards other representations for the data (e.g., time-frequency methods with short Fourier transforms, discrete wavelet transforms, etc.), but the fundamental likelihood function remains the same.

The closest analog to the LISA analysis of individual sources is found in the analysis of ground-based interferometer data from the LVK collaboration, which are heavily reliant on waveform models. There are two major differences between LVK and LISA that limits the applicability of the analogy. First: At current detector sensitivities, the rate of detectable sources is such that they are still sparsely distributed through the data, with typical signals present in the most sensitive

frequency band of the detectors for $O(10\ \mathrm{s})$ at a rate of $O(\text{a few}/\text{week})$. LISA, on the other hand, will be signal-dominated, with tens of thousands of continuous Galactic sources overpowering the instrument noise below $O(3\ \mathrm{mHz})$ and, depending on the rate and mass distribution of massive black hole mergers, several extremely high SNR mergers in band for $O(\text{weeks})$ to $O(\text{months})$, overwhelming any other contributions to the data stream. Thus, whereas the LVK searches are primarily "data mining" endeavors, sifting through a large volume of noisy data for rare and comparatively weak signals, LISA's primary challenges are twofold: Source confusion due to the large number of sources simultaneously detectable; and model accuracy due to both the large number of waveform cycles over which models must stay phase coherent, and to contend with such high SNRs so as to not contaminate lower-amplitude sources with residual power.

The second key difference between the LVK collaboration and LISA experiences is the volume of the parameter space itself. Ground-based searches for compact mergers span a mass range for the components of O(1–100) $\mathrm{M}_\odot$. While challenging, this mass range is small enough that precomputed grids of template waveforms covering the parameter space can be used when searching for candidates (see, e.g., Abbott et al. 2016d, 2023a). The LISA parameter space for comparable-mass black hole mergers, for example, is several orders of magnitude larger, spanning $O(10^3 - 10^8\ \mathrm{M}_\odot)$, both eliminating the possibility of using grid-based methods and expanding the range of possible mass ratios encountered by the analysis. To date, the most successful prototype LISA analyses have used stochastic sampling algorithms (Katz 2022; Littenberg and Cornish 2023; Lackeos et al. 2023), still relying on template waveforms but using data-driven methods to concentrate waveform calculations in the high-probability regions of parameter space. While LVK analysis of compact mergers is hierarchical, with clear distinction between the "search" and "parameter estimation" steps, those two functions blur together for many prototype LISA pipelines. Stochastic sampling algorithms put more pressure on the computational efficiency of waveform calculations, since template generation is part of the analysis pipeline itself, as opposed to pre-computing and then reusing a (large) table of waveforms generated on a fixed grid.

Note that while 3rd generation ground-based GW detectors will trend towards higher event rates, signal durations and signal strengths, the LISA forecasted maximum signal strengths are uniquely in excess of signal-to-noise ratios $\sim 10^4$ (Kaiser and McWilliams 2021). As a result, while the continued improvement of ground-based detectors and analysis methods naturally leads to evolution of the waveform models that directly benefit analysis of LISA data, the waveform development for 3rd generation detectors is necessary but not sufficient to fully achieve LISA's potential. LISA puts unique pressure on the accuracy, breadth of parameter space and computational efficiency of waveform models.

It is also worth considering that the signal-processing part of the LISA science ground segment is divided between two paradigms: the so called "low latency" and "global" analyses. The global analysis is the joint fit to all GW signals in the data, and it is here where waveform accuracy is most important, in order to prevent mismatches with loud signals from contaminating weaker signals that are

simultaneously present in the data stream. The global analysis is computationally intensive, and having efficient waveform generation tools is necessary for it to be tractable. However, the global-fit processing speed is more forgiving than that of the low-latency analyses, since the goal is to produce thorough source catalogs with a relatively relaxed release schedule on a $O(\text{monthly})$ to $O(\text{yearly})$ cadence.

For the low-latency analysis the trade-off is inverted, as computational speed and localization information are prioritized over all else. The low-latency pipelines will run $\sim$daily, and will likely use a subset of the data (e.g. by bootstrapping based on the most recently completed analysis). The primary goal is to provide actionable information for joint multimessenger observations of transients. There are other functions of the low-latency pipelines, for example providing source-subtracted residuals to the instrument team for assessment of detector performance etc., but under the purview of waveform generation time is of the essence. One thing to therefore consider at the architectural level of the waveform generation software is the need for tools that can be responsive to different demands on the speed/accuracy spectrum for processing sources, depending on the primary goal of the analysis.

3.2 Accuracy requirements

Coordinators: Deborah Ferguson and Maarten van de Meent
Contributors: M. Haney, R. O'Shaughnessy

Inaccuracies in waveform models affect the analysis of LISA data in three main ways. First, if the modelled waveforms do not sufficiently resemble the signals produced by Nature, this can hamper our ability to detect and identify sources in the data. Second, errors in the model will introduce some level of bias in the estimation of the source parameters, and could potentially masquerade as beyond-GR effects. Finally, if particularly loud sources are not perfectly subtracted from the data stream, their residuals can contaminate the searches for other sources. Below, we discuss the impact of these effects and how they lead to accuracy requirements for LISA waveform models.

3.2.1 Detection and identification

The impact of modeling errors on detection rates are fairly well understood in the case of a matched filter search for a single source in the data (Flanagan and Hughes 1998; Lindblom et al. 2008; McWilliams et al. 2010). Suppose we have some waveform model, $h_{\text{model}}(\vec{\lambda})$, depending on some set of parameters $\vec{\lambda}$, and we are looking for some true waveform h_{true} in the data, then the *fitting factor* (Apostolatos 1995) is defined by

$$\mathcal{F} = \max_{\vec{\lambda}} \frac{\langle h_{\rm true} | h_{\rm model}(\vec{\lambda}) \rangle}{\sqrt{\langle h_{\rm true} | h_{\rm true} \rangle \langle h_{\rm model}(\vec{\lambda}) | h_{\rm model}(\vec{\lambda}) \rangle}}, \tag{6}$$

where $\langle \cdot | \cdot \rangle$ is the noise weighted inner product from (2). The fitting factor measures the effective loss in SNR due to using an imperfect model. Consequently, if the used models have a fitting factor $\mathcal{F}$ for a particular source, the maximum range at which such a source can be detected is reduced by a factor $\mathcal{F}$. Whether this has any impact on the detection rate depends on the type of source. Some LISA MBHB sources are so loud (in the higher mass seed scenario) that even the earliest (and therefore furthest) such events would be easily detectable (Barausse et al. 2020a), in which case the fitting factor of the used model has little to no effect on the detection rate. For other, quieter sources (such as EMRIs, SOBHBs, or GBs) the detection rate is more range limited, and a poor fitting factor $\mathcal{F}$ could lead to a reduction of the number of detections by a factor $\mathcal{F}^3$ (assuming a uniform distribution of the source through a spatially flat universe). An appropriate norm for what degree of loss of sources is deemed admissible for achieving LISA's science goals needs to be established. An additional consideration here is that increasing the number of unresolved sources could adversely affect the searches for others sources such as any cosmological GW backgrounds (Pan and Yang 2020a).

The above is valid for an idealized case, where the search is conducted using a continuous bank of templates. In practice, a search would use a discretized template bank, meaning that the effective fitting factor is increased due to the template spacing. Moreover, as noted in Sect. 3.1, a fully coherent search of the LISA data seems infeasible. Instead, LISA pipelines will most likely employ semi-coherent (Gair et al. 2004; Chua et al. 2017) or stochastic (Gair et al. 2008b; Cornish 2011) search strategies. In a semi-coherent search, template and data are both partitioned into short segments, and the template–data overlap for each segment is maximized over several extrinsic parameters. Waveforms used in such a search need only to stay phase-coherent over the shorter segments. For example, it was shown in Chua et al. (2017) that templates with $> 97\%$ overlap accuracy over $\gtrsim 10^6$ s will still be sufficient to detect $> 50\%$ of EMRIs detectable with fully coherent, precise templates.

3.2.2 Parameter estimation

LISA parameter inference nominally involves a joint multi-source fit for all available sources in the data (Vallisneri 2009; Babak et al. 2008a, b, 2010). For the purposes of the discussion below, we approximate this process as independent parameter inference for individual sources, resolving the source from detector noise and the confusion noise of all other signals in the data. Within that context, the impact of waveform sytematics on parameter inference has been historically estimated using well-understood analytic techniques; see, e.g., Vallisneri and Yunes (2013); Cutler and Vallisneri (2007). The most frequently used ingredients in analytic waveform standards are the match or *faithfulness* $\mathcal{M}$, which is the overlap between a signal $h_{\rm true}$ and template $h_{\rm template}$ maximized over the coalescence time and phase of the template;

the *Fisher matrix* $\langle \partial_a h(\lambda) | \partial_b h(\lambda) \rangle$; and the inner product $\langle \partial_a h | \delta h \rangle$ between derivatives of the waveform and residuals δh between two signal approximations. The simplest and most conservative waveform accuracy standards for parameter inference are expressed in terms of limits on the mismatch $1 - \mathcal{M}$, which nominally must be $\lesssim 1/SNR^2$ to avoid introducing systematic bias comparable to the statistical error *for a single source* (Flanagan and Hughes 1998; Lindblom et al. 2008; Chatziioannou et al. 2017). For a population of sources, in principle systematic biases could stack in hierarchical population inference, and the most conservative threshold would be $1/(N_s SNR^2)$ where N_s is the typical number of sources (Wysocki et al. 2019). However, these thresholds are likely to be much too conservative for many applications, see, e.g., Pürrer and Haster (2020).

Because the impact of systematic biases depends strongly on the nature and scale of the bias relative to astrophysical features, general conclusions about systematic bias cannot be drawn, and (barring negligible systematic error) must be assessed for each science goal individually by performing hierarchical population inference. For example, most SOBHBs in quasicircular orbits are in wide, relatively slowly-evolving orbits in the LISA band. For 90% of LISA-relevant SOBHBs (in population models consistent with current LVK observations), 2PN-accurate waveforms are sufficiently faithful for parameter estimation without biases (Mangiagli et al. 2019). At the other extreme, MBHBs will have extremely high amplitudes, with minute statistical error (Lang and Hughes 2008; Babak et al. 2008a, b, 2010). Nominally, the very conservative accuracy thresholds described above would suggest a mismatch error target of order $1/(N_s SNR^2) \simeq O(1/(10 * (1000)^2)) \simeq 10^{-7}$, for statistical errors to be small compared to statistical errors for the recovered population of MBHBs from $O(10)$ detections with $O(1000)$ SNR as could occur in certain MBHB formation scenarios (Barausse et al. 2020a). This threshold may be needed for applications that require joint inference on all massive MBHBs (e.g., tests of general relativity), but can be dramatically relaxed for any astrophysical interpretation of the MBHB population. Further studies will be necessary to establish specific requirements on waveform accuracy for each context in which parameter estimation is critical.

3.2.3 Contamination

Contamination effects occur when the residual from one source cannot be fully removed and impedes the interpretation of other, subdominant sources in the data. For such strong sources, systematic errors may be larger than statistical errors (Cutler and Vallisneri 2007). Though measurement error may have little impact on the astrophysical interpretation of the strong sources, the potentially substantial residuals produced by inaccurate models of their gravitational waves will introduce artifacts which contaminate downstream data analysis (Vallisneri 2009; Babak et al. 2008a, b, 2010; Porter 2015). For instance, for numerical relativity waveforms, insufficiently resolved grids can cause significant residuals even for simulations with precisely the same parameters as the observed signal (Ferguson et al. 2021). The impact of errors arising from such imperfect modeling of strong sources can only be

properly assessed with full joint hierarchical inference, using realistic models and contamination targets. Because of the diversity of sources that could be contaminated by residuals left by imperfect models for MBHB sources, much remains to be done to comprehensively assess key questions: How do modelling residuals from loud sources impact the detection and identification of other sources? Which sources are most affected? And what are the implications for the required modelling accuracy?

3.3 Efficiency considerations

Coordinators: Mark Hannam and Jonathan Thompson
Contributors: A. Chua and M. Katz

We shall discuss here the efficiency requirements imposed by search and inference for the two main classes of strong-field source that will be observable by LISA: MBHs and EMRIs. Relatively weaker-field sources such as GBs and SOBHs are a lesser concern; modeling of their signals (to the accuracy required for data analysis) is significantly easier, and computational cost is dominated by the need to attain a sampling resolution that is adequate for the typical duration, bandwidth and abundance of each source type. Thus the efficiency requirements for these sources may be addressed on the analysis end with suitable approximations, or at the modeling–analysis interface where techniques such as those in Sect. 5 may be applied.

3.3.1 Extreme-mass-ratio inspirals

EMRIs are the only LISA sources that combine the issue of strong-field complexity with that of long-lived signals (potentially staying in band for years), and thus they pose great challenges for both waveform modeling and data analysis. The main problem in EMRI search is *information volume*: the space of LISA-observable EMRIs is gargantuan, requiring 10^{30}–10^{40} templates to cover in a naive grid-based search (Gair et al. 2004).[1] This is unfeasible regardless of waveform efficiency. One possible solution relies on semi-coherent filtering, which essentially returns less informative templates that cover larger regions in parameter space, allowing extensive searches to be performed in a viable amount of time. Assuming that computing performance in the 2030 s lies around the 10^2-teraflop regime (achievable at present with $\sim 10^3$-node clusters), semi-coherent segments of $\lesssim 10^6$ s would enable the analysis to be completed over the mission lifetime (Gair et al. 2004).

In practice, EMRI search will probably use semi-coherent filtering within stochastic algorithms, rather than template banks. Thus the estimates in Gair et al. (2004) are very conservative, as stochastic searches are generally far more efficient than grid-based searches at the same number of template evaluations, even with a

[1] As a point of reference, banks of at most 10^5–10^8 templates are needed to detect LVK BBH mergers (Moore et al. 2019), and searches are often conducted with smaller banks of around 10^4 templates in practice (Sakon et al. 2024).

large multiplier (e.g., repeated runs) to ensure proper coverage of the parameter space. Note, however, that a potentially large number of additional templates will be required in the assessment of detection significance for each candidate source, although it remains unclear whether such an assessment will eventually be performed in the search or inference stage.

The efficiency requirements for inference are more straightforward, in that LISA analysis algorithms will be built on similar tools to those used in LVK parameter estimation, like Markov Chain Monte Carlo (MCMC) (Littenberg and Cornish 2023; Strub et al. 2024; Katz et al. 2025, e.g.). An estimated 10^6–10^9 templates will be required per source posterior distribution. If we want to produce a posterior in less than 10 days we need waveforms that can be produced in $\lesssim$1ms. LISA will detect $\sim 10^4$ sources, so parallelization resources are inherently considered in our scaling estimate considering each individual source posterior as a single parallelized process taking $\lesssim$10 days. The estimated number of template evaluations per posterior also assumes that the prior regions for posterior sampling can be sufficiently localized to begin with; this is certainly possible in principle, but may require multiple search stages beforehand in a hierarchical approach.

3.3.2 Massive black hole sources

Generally, MBH sources are expected to be detectable for $\sim$week to hours prior to the merger. Due to this detection time frame and large signal-to-noise ratio of MBH binaries, coherent analysis over the full waveform template will most likely be employed for both search and parameter estimation. Therefore, from a waveform production perspective, these two analyses are roughly the same even if search and parameter estimation employ different schemes for achieving their various goals (Cornish and Shuman 2020). One way a search algorithm may differ from a parameter estimation algorithm for MBHs, in terms of the waveform generation, is in the use of higher-order harmonics. Recent work (Katz et al. 2020; Marsat et al. 2021) has shown the importance of higher-order modes in parameter estimation for LISA. However, as detailed in Cornish and Shuman (2020), searching over the dominant harmonic may be acceptable for initially and roughly locating sources throughout the high-dimensional parameter space. With this said, this is a matter of adding or removing modes (that we assume are available in a model), not altering the fundamental waveform generation method.

Given this idea that the waveform generation is similar for both search and parameter estimation for MBHs, the following discusses how efficiency requirements relate to the stages of waveform creation. As discussed in Sect. 5.1, there are generally two main parts to waveform creation in the context of LISA: sparse, accurate waveform calculations and a scaling method to achieve a full waveform from the sparse information. MBH waveforms can be generated beginning with sparse calculations of the amplitude and phase for each harmonic mode with an accurate waveform model. Depending on the specific analysis type, these sparse calculations are then upsampled to the desired search or parameter estimation settings. Producing accurate and upsampled waveforms *directly* from the accurate

waveform generator is unnecessary and time-consuming: various methods allow for the upsampling of sparse, smooth functions in an accurate and much more efficient manner (e.g. see García-Quirós et al. 2021; Katz et al. 2021). This construction leads to two different waveform generation efficiency requirements. The first is the overall waveform (including upsampling). With similar requirements to EMRIs given in the section above, we expect to collect at least $\sim 10^6$ MCMC samples for a given source posterior distribution. To accomplish this in ~ 10 days, we need to generate waveforms at a rate of $\sim /1\text{s}$ on a single central processing unit (CPU) core.

The other efficiency requirement deals with the separation of the accurate waveform generation from the scaling operation. Generally, the scaling operation is the bottleneck for LISA where waveforms can have up to $\sim 10^6$–10^8 data points. Therefore, the requirement on the scaling part is that a waveform on a single CPU core be scaled in ~ 1 second or less. This condition, therefore, also sets the requirement for the accurate waveform portion assuming its sparsity prevents it from becoming the bottleneck. This requirement is that the sparsely sampled, accurate waveform must be of a similar or lower order of magnitude in timing when compared with the scaling operation.

3.4 Interface and data format requirements

Contributor: Tyson Littenberg

An additional key consideration for optimally supporting LISA analyses is the need for a flexible interface between waveform generation software and analysis pipelines. It is important for verification and validation of pipelines, and as a means for cross-checking results, to have independently developed algorithms targeting the same sources. (There is also the added benefit of a constructive competition between development teams.) As per the previous discussion around Eq. (5), different analysis pipelines will likely be built around different representations of the data. Template generation is generally the computational bottleneck, and so it needs to be optimized for the application. At the same time, the benefits of having independent pipelines become liabilities if the analyses are not interfacing to the same waveform generation tools. As a result, it is of paramount importance that the waveform and pipeline development teams are collaborating early and often to avoid unnecessary or redundant transformations of the waveforms by the analysis pipelines (consider, e.g., a waveform that is initially computed in the time domain but then output in the Fourier domain, being called by an analysis pipeline that uses a discrete wavelet domain representation of the data).

The demand for flexibility of the waveform-analysis interface affects more than just the choice of a basis set used to represent the template. There have been promising developments in low-cost likelihood evaluations that use the instantaneous amplitude and phase of the template waveform, sampled on an adaptive grid, to concentrate computations to regions where the signal is changing most rapidly (Cornish and Shuman 2020; Marsat et al. 2021). Such considerations are difficult to retroactively incorporate in established template generation algorithms, but present

opportunities for increased efficiency if they are part of the original waveform algorithm designs.

4 Modelling approaches for compact binaries

Detecting and inferring the parameters of compact binaries systems requires waveform template which, in turn, necessitates solving the relativistic two-body problem. Unlike in the Newtonian counterpart, it is not possible to only solve for the motion of the two bodies; one must solve for the dynamical evolution of the full spacetime. In general there are no known closed-form solutions to the nonlinear Einstein field equations for radiating binaries and so a variety of techniques have been developed to compute solutions either numerically or via perturbative expansions. The three main approaches that directly solve the Einstein field equations are numerical relativity (NR), post-Newtonian/Minkowskian (PN/PM) theory, and gravitational self-force (GSF).

Each of these approaches has strengths and weaknesses that leads them to being best employed in different regions of the binary configuration parameter space. Numerical Relativity directly solves the Einstein field equations to produce exact solutions up to numerical error. Post-Newtonian theory analytically computes relativistic corrections to the binary's motion and GW emission as a series expansion in powers of the orbital velocity as a fraction of the speed of light. The closely related post-Minkowskian approach expands field equations around flat Minkowski spacetime in powers of the gravitational constant without any restriction of the velocity of the binary. Gravitational self-force expands the Einstein field equations in powers of the (small) mass ratio. Figure 2 gives a quantitive description of the strengths and weakness of each approach in the orbital separation – mass-ratio parameter space for non-spinning quasi-circular binaries.

In addition to the above approaches there are also effective frameworks that attempt to cover large portions of the parameter space. The physically motivated Effective-One-Body model takes inspiration from the solution to the Newtonian problem and describes the binary as the motion of a test body in spacetime of a deformed single black hole. Much progress can be made analytically with this approach by absorbing post-Newtonian and post-Minkowskian corrections, and further calibration can be applied using numerical results from the NR and GSF methods. The Phenomenological (Phenom) waveform models do not attempt to solve the relativistic two-body problem. Instead they aim to directly model the waveforms by building upon fast post-Newtonian models with further calibration from NR and GSF. The EOB and Phenom models are heavily used in analysis of GW data from current ground-based detectors.

In this section we outline the status of the above approaches and discuss the required development needed to reach the accuracy requirements outlined in Sect. 3.2. Concerns about the speed of waveform generation are addressed in Sect. 5. The status and requires for LISA of these approaches can be found in Sect. 4.1 for numerical relativity, Sect. 4.2 for weak-field post-Newtonian and post-Minkowskian expansions, Sect. 4.3 GSF, Sect. 4.5 for EOB, and Sect. 4.6 for Phenomenological models. These sections focus on modelling within GR; see Sect. 6 for a discussion on modelling in alternate theories of gravity.

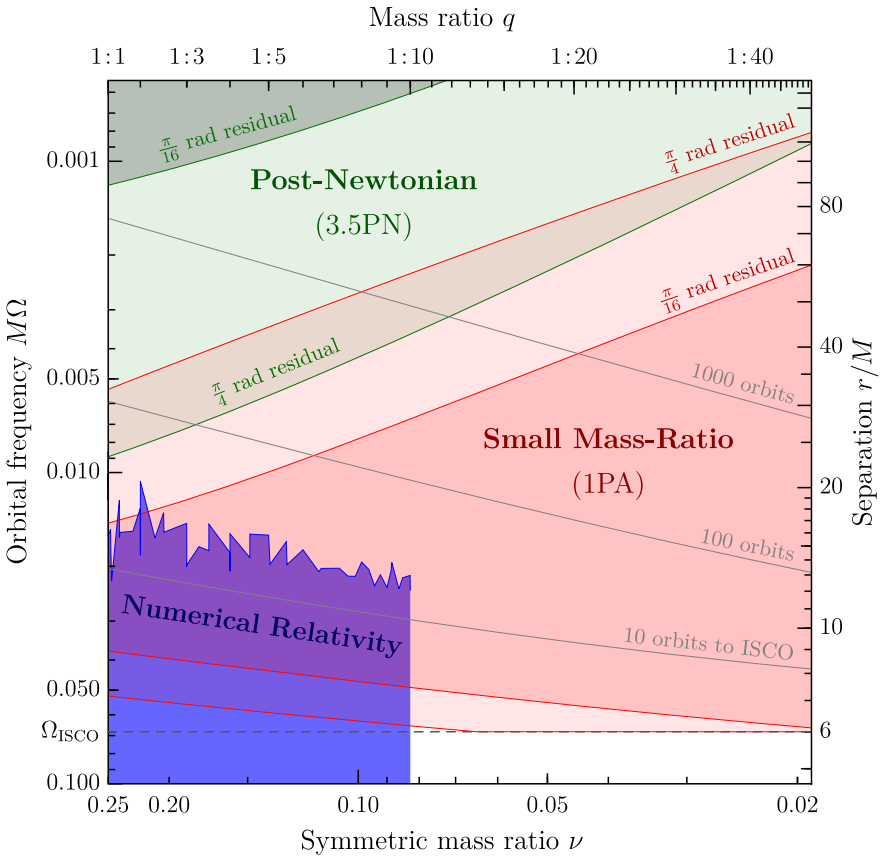

Fig. 2 Region of applicability of different approximation techniques for non-spinning quasi-circular binary BH inspiral. The 1PA region is a prediction derived from fitting NR data to an expansion of the form (14). The shaded regions indicate ranges within which the cumulative orbital phase-error is less than $\pi/4$ and $\pi/16$ radians, respectively. Recent direct calculations of post-adiabatic (1PA) waveforms suggest the 1PA region shown is over-optimistic for $\nu > 0.1$, but they have borne out the prediction for $\nu < 0.1$ (Albertini et al. 2022b). The gray lines show the location of binaries with 10 (resp. 100 and 1000) orbits left before they reach the ISCO. This figure is reproduced from van de Meent and Pfeiffer (2020)

4.1 Numerical relativity

Coordinators: Mekhi Dhesi, Deborah Ferguson and Deirdre Shoemaker
Contributors: Sebastiano Bernuzzi, Gabriele Bozzola, Katy Clough, Deborah Ferguson, William Gabella, Miguel Gracia, Roland Haas, Mark Hannam, Eliu Huerta, Sascha Husa, Larry Kidder, Pablo Laguna, Carlos Lousto, Geoffrey Lovelace, David Neilsen, Vasileios Paschalidis, Harald Pfeiffer, Geraint Pratten, Hannes Rüter, Milton Ruiz, Stuart Shapiro, Jonathan Thompson, Antonios Tsokaros, Miguel Zilhao

4.1.1 Description

Numerical relativity (NR) solves Einstein's field equations through direct numerical integration on supercomputers (see e.g. the books by Alcubierre 2008; Bona et al. 2009; Baumgarte and Shapiro 2010; Gourgoulhon 2012; Shibata 2016), providing the spacetime geometry and dynamics of the system in addition to the gravitational radiation emitted. Such solutions of the full nonlinear field equations without approximations are critical to our understanding of highly dynamic regimes without symmetries, such as the late inspiral and merger of compact binaries.

The first steps at numerical solutions of Einstein's equations date back several decades (Hahn and Lindquist 1964; Smarr et al. 1976) and tremendous progress since then enabled the first simulations of inspiraling and merging binary black holes (Pretorius 2005a; Campanelli et al. 2006a; Baker et al. 2006a). These breakthroughs initiated an explosive growth of the field, as illustrated, e.g. in the reviews by Lehner (2001); Centrella et al. (2010); Duez and Zlochower (2019); Foucart et al. (2022). By now, NR has become a critical part of the modeling the gravitational waves of the late inspiral and merger phase of coalescing binaries (e.g. Mroue et al. 2013; Husa et al. 2016; Boyle et al. 2019; Hamilton et al. 2024), which in turn underpins the analyses of all observed gravitational waves from coalescing binaries.

In order to solve Einstein's field equations, modern NR codes generally use the 3+1 approach (Arnowitt et al. 1962; York, Jr. 1979) in which the four-dimensional spacetime is sliced into three-dimensional hypersurfaces, and Einstein's equations are reformulated as a Cauchy problem with constraints. The first stage in numerically solving a compact binary inspiral is the construction of initial data, for which Einstein's constraint equations are reformulated as elliptic equations either in the context of the conformal-thin-sandwich formulation (York 1999; Pfeiffer and York 2003) or the puncture approach (Brandt and Brügmann 1997). The resulting coupled nonlinear partial differential equations are solved with custom-purpose elliptic solvers (Pfeiffer et al. 2003; Ansorg et al. 2004; Gourgoulhon et al. 2016). Numerous improvements over the years increased the generality of the physical conditions that can be achieved and the numerical quality of the solution, e.g. Lovelace et al. (2008); Foucart et al. (2008); Grandclement (2010); Ruchlin et al. (2017); Ossokine et al. (2015). Moreover, entirely new codes were developed (Dietrich et al. 2015b; Rashti et al. 2022; Assumpcao et al. 2022; Vu et al. 2022; Papenfort et al. 2021). The time evolution is encoded in a set of coupled, hyperbolic partial differential equations with suitable gauge conditions and boundary conditions, where three main approaches have emerged: the generalized-harmonic formulation (Pretorius 2005b; Lindblom et al. 2006; Szilagyi et al. 2009), the Baumgarte–Shapiro–Shibata–Nakamura formulation (Shibata and Nakamura 1995; Baumgarte and Shapiro 1998) and different versions of the Z4 formulation of Einstein's equations (Bona et al. 2003; Bernuzzi and Hilditch 2010; Ruiz et al. 2011; Weyhausen et al. 2012; Hilditch et al. 2013; Alic et al. 2012, 2013) (see Table 7). Gravitational radiation is typically

computed as gravitational strain (Reisswig and Pollney 2011) and must be propagated to future null infinity (see review by Bishop and Rezzolla 2016), which is often accomplished by extrapolation of GW modes extracted at finite radius (Boyle and Mroue 2009). Alternatively, Cauchy-Characteristic Extraction (Bishop et al. 1996; Handmer and Szilagyi 2015; Moxon et al. 2023) directly yields the waveforms at infinity, with improved recovery of non-oscillatory GW modes and GW memory effects (Mitman et al. 2020). Gauge conditions and transformations at future null infinity must be treated with care (Lehner and Moreschi 2007) to yield well-behaved numerical waveforms with well-defined waveform modes (Mitman et al. 2022). Cauchy codes have difficulty resolving the memory effect (Boyle et al. 2019; Mitman et al. 2020). Instead, most approaches to computing the memory effect use Cauchy NR waveforms (or NR calibrated waveform models) and the asymptotic Einstein equations to determine the unresolved memory effect in the Cauchy simulations that is required to satisfy Einstein's equations (Favata 2009; Talbot et al. 2018; Boersma et al. 2020; Khera et al. 2021; Mitman et al. 2021a; Liu et al. 2021a). This approximate approach agrees with the Cauchy-Characteristic extracted waveforms, though comparisons over a wider range of the BBH parameter space would be useful.

Once BBH simulations became possible, the NR community quickly achieved many firsts, including the first simulations of unequal-mass BBH coalescences (Baker et al. 2006b; Herrmann et al. 2006), the first with spinning binaries (Campanelli et al. 2006b), the first targeted eccentricity mergers (Hinder et al. 2010) and first comparisons with PN calculations (Baker et al. 2007b; Buonanno et al. 2007a; Hannam et al. 2008; Boyle et al. 2007). NR calculations of the merger revealed features of the non-linear regime, among them that BHs with spins positively aligned with the orbital angular momentum merge at higher frequency (Campanelli et al. 2006b), spin hang-up configurations (Lousto and Zlochower 2011a), as well as the calculation of the recoil velocity imparted on the remnant BH (Baker et al. 2006b; Gonzalez et al. 2007b; Herrmann et al. 2006); in particular it was found that BH spins oriented approximately parallel to the orbital plane can lead to recoil velocities of several 1000's km/s (Campanelli et al. 2007a; Gonzalez et al. 2007a; Campanelli et al. 2007b).

Analysis of GW observations requires waveforms that cover the entire frequency band of the relevant detector at high accuracy. This has motivated large efforts to improve the accuracy of NR simulations (Boyle et al. 2007; Husa et al. 2008; Szilagyi et al. 2009; Scheel et al. 2015; Rosato et al. 2021; Etienne 2024), length of the inspiral (Mroue et al. 2013; Szilágyi et al. 2015), and coverage of increasingly large portions of parameter space in increasing detail. Parameter space exploration was initially performed through community-wide Numerical INJection Analysis (NINJA) (Aylott et al. 2009; Ajith et al. 2012) and Numerical-Relativity-Analytical-Relativity (NRAR) (Hinder et al. 2014) collaborations, which also yielded important cross-checks between different codes (Hannam et al. 2009; Hinder et al. 2014). Newer and more extensive parameter space surveys are listed in Table 7. Waveform models developed with NR information are described in Sect. 4.5 and 4.6. NR surrogate models (Blackman et al. 2017b; Varma et al. 2019a) are directly built on NR simulations, and are particularly important for the analysis of high-mass BBH systems like GW190521 (Abbott et al. 2020b, d). NR simulations can also be directly

used for GW data-analysis, where they serve as synthetic signals (Schmidt et al. 2017) for quantifying the response of GW search and parameter-estimation pipelines (Aasi et al. 2014b; Abbott et al. 2017), and to conduct indirect analyses of observations (Abbott et al. 2016c; Lange et al. 2017; Gayathri et al. 2022).

NR also offers important information for the ringdown phase, characterized by an exponential decay as the remnant BH settles into a Kerr black hole. NR results determined the remnant parameters (mass, spin, recoil velocity) (Barausse and Rezzolla 2009; Healy et al. 2014; Hofmann et al. 2016; Healy and Lousto 2017, 2018; Varma et al. 2019a, c; Jiménez-Forteza et al. 2017). Detailed NR calculations of the emitted gravitational waves during merger and ringdown yield the initial amplitudes and phases of quasi-normal ringdown modes and underpin theoretical studies of what information about nonlinear processes are accessible through the emitted gravitational waves (Mitman et al. 2023; Cheung et al. 2023), and how the ringdown phase can be used to test GR and to probe the no-hair and area theorems (Abbott et al. 2021c, d; Ghosh et al. 2021; Islam 2021; Capano et al. 2023; Finch and Moore 2022; Isi et al. 2021; Cotesta et al. 2022).

Due to our focus on the role of NR in the LISA mission, this section primarily covers vacuum spacetimes with a short discussion on environmental effects that include matter; the important work of NR with neutron stars is not included.

4.1.2 Suitable for what sources?

The coalescence of BBHs is a primary source for LISA for a vast range of BH mass. Those BBH systems that merge in the LISA band require NR to produce the waveforms during the late inspiral and merger. In order to quantify the mass ranges that merge in the LISA band, we compute the masses for which the frequency of ringdown and inspiral are both in the LISA band. The dominant quasi-normal mode for a non-spinning black hole has a frequency of $f = 12.07\text{mHz}(M/10^6 M_\odot)^{-1}$ (Berti et al. 2006), which will be within the LISA band for BH masses of roughly $10^4 - 10^8 M_\odot$. Turning to the inspiral, NR simulations of massive BBHs typically cover a few tens of orbits before merger, starting at GW frequencies of $f \sim 1\text{mHz}(M/10^6 M_\odot)^{-1}$, placing this part of the inspiral into LISA band for $10^3 - 10^7 M_\odot$. This estimate implies that BBHs of mass $10^4 - 10^8 M_\odot$ will have at least part of its waveform within coverage of NR. NR is capable of modeling these binaries for comparable mass ratios of less than 1:20, with attempts to reach 1:1000 (Lousto and Healy 2023).

NR simulations become increasingly costly with increasing mass-ratio and with very large spins, whereas there is only minor dependence of computational cost on other BBH parameters like spin-direction and orbital eccentricity. Parameter space coverage is improving over time. The next section describes what parameters NR currently covers and in Sect. 4.1.5 we discuss where efforts are needed to achieve complete coverage of the potential range of source parameters.

4.1.3 Status of the field

Since the breakthrough in NR in 2005/2006 (Pretorius 2005a; Campanelli et al. 2006a; Baker et al. 2006a) and the subsequent "gold-rush" to explore nonlinear phenomena in black hole and neutron star mergers, NR has now matured into a reliable tool for accurately computing gravitational waveforms needed to characterize GW data. In this section we briefly describe the landscape of current and future numerical relativity codes, their cross-validation and the parameter space coverage of currently available numerical waveforms.

The community has developed a number of successful NR codes that target a variety of goals for BBH spacetimes including covering increasing fractions of the parameter space (so far mostly comparable mass ratios and moderate spins), increasing number of GW cycles, accuracy of waveforms and interactions with matter. Table 7 provides a comprehensive list of currently available NR codes, some of which are briefly described in Appendix A. Their capabilities have been sufficient for the detection and characterization of GW signals with current ground-based GW detectors. However, data collected with future space- or next generation ground-based instruments will have a higher SNR and its interpretation requires much improved NR waveforms.

In particular, LISA sources present a formidable challenge to NR (see Sect. 4.1.5), both with regard to the characteristic features of the target BBH systems (e.g., high spins, large mass ratios, eccentric orbits, etc.) and the quality of the GW data due to, e.g., high signal-to-noise ratios and sources remaining in band for very long times. Computational simulations that meet the accuracy requirements for these demanding BBH configurations, for sufficiently long times, will require exascale computational resources. It will also require continued research in NR to develop new algorithms, computational techniques and software to tackle these challenges faced by existing code bases. Some new codes are under development, and they are included in Table 7.

Given the complexity of NR codes, cross-validation is an important component of code verification and it is by no means trivial that results obtained with different code bases agree. They employ, for example, different theoretical formulations of Einstein's equations for the evolution and initial data and different methods for the GW extraction. They also employ different numerical techniques (e.g, pseudo-spectral or high-order finite differences discretization) and numerical implementations, e.g., for the grid structure. First systematic code comparisons and studies on the integration of NR with data analysis and analytical approximations have been conducted in Baker et al. (2007a); Aylott et al. (2009); Aasi et al. (2014b); Hannam et al. (2009); Hinder et al. (2014); Lovelace et al. (2016). For example, the NINJA project (Aylott et al. 2009; Aasi et al. 2014b) focused on building a NR data analysis framework and to develop first injection studies. The initial study presented a sample of 23 NR waveforms of BBHs with moderate mass ratios $q \lesssim 4$, considering only the dominant the $\ell = |m| = 2$ GW mode. The follow-up study increased to 60 NR waveforms. While no cross-validation between the NR waveforms were performed, NINJA was crucial to identify technical and conceptual issues, that a hybridization with PN or EOB may be needed and that more than only the dominant GW mode

may be necessary. The Samurai project (Hannam et al. 2009) conducted a detailed cross-validation of gravitational waveforms obtained with five different NR codes. It focused on one BBH system, namely an equal-mass, non-spinning, quasi-circular (eccentricity $\lesssim 0.0016$) binary completing about six orbits before their merger. Focusing on the dominant $\ell = |m| = 2$ multipole, it was found that the waveforms' amplitude and phase agree within numerical error. It was also found that these NR waveforms were indistinguishable for SNR ≤ 14 and would yield mismatches of $\lesssim 10^{-3}$ for binaries with $M \sim 60 M_{\odot}$ (using the anticipated detector noise curves at the time). The Numerical-Relativity–Analytical-Relativity (NRAR) collaboration (Hinder et al. 2014) made important strides towards constructing more accurate inspiral-merger-ringdown waveforms by combining analytical and NR computations, and by defining new accuracy standards that would be needed for GW parameter estimation. The collaboration pushed cross-validation of NR codes to new frontiers by considering quasi-circular BBHs (with initial eccentricity $\leq 2 \cdot 10^{-3}$) with both unequal mass (up to $q \leq 3$) and moderately spinning BHs (up to $\chi_i \sim \pm 0.6$) completing about 20 GW cycles before merger. The study also included a binary of non-spinning BHs with $q = 10$, the highest mass ratio for quasi-circular binaries at the time. For the first time, the seven involved NR codes performed 22 targeted simulations to meet the required accuracy standards. They employed the same analysis code to estimate the uncertainties due to the numerical resolution and waveform extractions. The simulations exhibited a relative amplitude error in the $\ell = |m| = 2$ multipole of $\lesssim 1\%$ and a cumulative phase error of $\lesssim 0.25$rad. Finally, Lovelace et al. (2016) presented a comparison of targeted simulations for the first GW event, GW150914, concluding that the waveforms were sufficiently accurate to effectively analyse LIGO data for comparable events. A comparison between different time evolution formulations of Einstein's equations, namely BSSN and Z4c, was performed in Zlochower et al. (2012); Hilditch et al. (2013).

The cross-validation studies between different NR codes have been crucial for building confidence in their results. As summarized above, they have been conducted in limited regions of parameter space (e.g., low mass ratios, some moderate spins, low eccentricity). As the demand on NR waveforms increases, such as covering a larger region of parameter space, including eccentric or spin-precessing BBHs, including higher multipoles (typically up to $\ell = 8$) that are excited by asymmetric systems and further improving their accuracy, extended validation studies become important. With the technical and computational developments, the numerical data becomes more and more sensitive to mismatches, e.g., in the initial data, evolution or wave extraction. Therefore, a careful study of the initial data and initial parameters, of wave extraction techniques (e.g., extrapolation of waveforms extracted at finite radii vs. Cauchy characteristic extraction vs. Cauchy characteristic matching) or the choice of asymptotic Bondi–van der Burg–Metzner–Sachs frame will be needed (Mitman et al. 2021b).

The starting point for any simulation is the construction of constraint satisfying initial data. After decades of work (see, e.g., Cook 1994; Brandt and Brügmann 1997; Cook 2000; Ansorg et al. 2004; Pfeiffer 2005; Gourgoulhon 2007; Lovelace 2009; Lovelace et al. 2008; Ruchlin et al. 2017; Tichy 2017 and references therein),

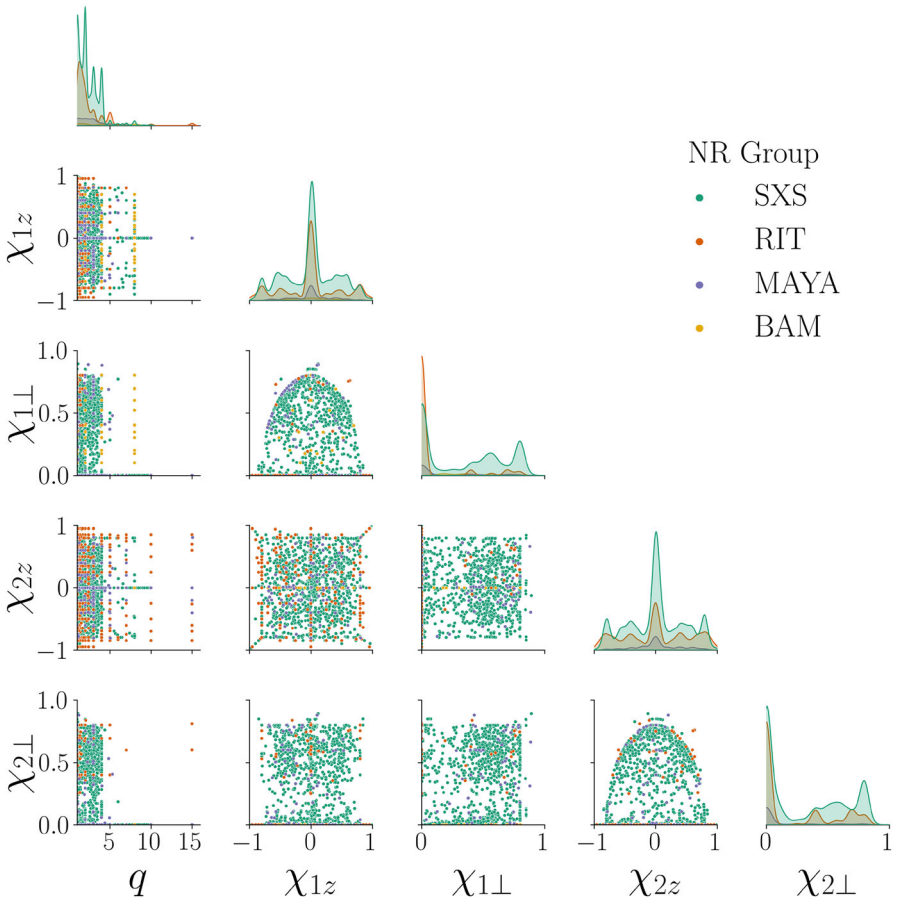

Fig. 3 Parameter space coverage of public waveform catalogs in the quasi-circular limit. Shown are mass-ratio q, projections of the BH spins onto the orbital angular momentum ($\chi_{1/2z}$), and magnitude of spin-components orthogonal to the orbital angular momentum ($\chi_{1/2\perp}$) for waveform catalogs of different NR groups. Data as of June 2023

multiple codes are now capable of generating BBH initial data where the BHs are on a quasi-circular orbit or where the orbit has non-zero eccentricity.

Several groups worldwide have created public catalogs of BBH merger simulations with approximately 5, 700 waveforms available at the time of this writing (Mroue et al. 2013; Jani et al. 2016; Healy et al. 2017; Boyle et al. 2019; Healy et al. 2019; Healy and Lousto 2020, 2022; Hamilton et al. 2024; Ferguson et al. 2023); see also Table 7. Nowadays, NR waveforms survey several configurations in the extensive BBH parameter space spanned by their mass ratios, spin magnitudes and directions, and eccentricity. Figure 3 illustrates the portion of the parameter space covered by the publicly available waveforms at the time of this paper's publication. Focussing on quasi-circular binaries, it shows that the parameter space is best sampled for moderate mass ratios and spins.

Consequently, there are three dimensions in the BBH parameter space — spin, mass ratio and eccentricity — that require further waveform development. For example, most runs with spinning BHs concentrate on spins $\chi \lesssim 0.9$, because simulating BHs with spin closer to the extremal Kerr limit is technically challenging. It requires a much higher numerical resolution and, more importantly, the initial data is more difficult to construct. There are some codes capable of constructing initial data for BHs with spins above $\chi = 0.95$; see, e.g., Lovelace et al. (2008); Healy et al. (2018); Zlochower et al. (2017). Another challenging regime in BBH simulations is that of unequal mass binaries. Most simulations in the public catalogs cover the regime $q \lesssim 8$ for spinning BHs, and up to $q \lesssim 18$ for nonspinning binaries, as can be seen in Fig. 3. However, simulations above $q = 20$ are scarce: the first high-mass ratio simulations up to $q = 100$ (Sperhake et al. 2011) (see also Fernando et al. 2019b) and, more recently, up to $q = 1024$ (Lousto and Healy 2023) were achieved for head-on collisions. The frontier for quasi-circular inspirals are mass ratios of $q = 128$ (Lousto and Healy 2020; Rosato et al. 2021). New techniques such as worldtube excision to model intermediate mass ratios of $q = 100\text{-}10^4$ are under development (Dhesi et al. 2021; Wittek et al. 2023).

In quasi-circular orbits, NR BBH simulations are well sampled in the regime of moderate mass ratios and spins, including precessing spins. As Fig. 3 illustrates, the parameter space is best sampled over spins when the mass ratio is less than 1:4. Increasing spins to the Kerr limit is challenging both as the resolution required for highly spinning black holes increases and, more importantly, the initial data are harder to construct. Some codes, however, are capable of pushing beyond $\chi = 0.95$ (Lovelace et al. 2008; Healy et al. 2018).

Most NR simulations to-date have focused on quasi-circular inspirals because it is expected that any eccentricity present during a binary's formation will have been emitted through GW radiation by the time of merger (Peters 1964); however, there are several astrophysics scenarios that predict eccentric MBHBs (Armitage and Natarajan 2005; Bonetti et al. 2019), produced eccentric numerical relativity waveforms (Hinder et al. 2008; Huerta et al. 2017, 2019; Ramos-Buades et al. 2020a; Hinder et al. 2018) and other beyond circular evolution such as head on (Zilhão et al. 2014b), hyperbolic (Healy et al. 2009a; Nelson et al. 2019) and zoom-whirl (Healy et al. 2009b; Gold and Brügmann 2010, 2013).

Arguably the most challenging regime to simulate is that of highly unequal mass BBHs. While codes have been pushed to simulate up to 1:128 mass ratio (Lousto and Healy 2020), there are few simulations above 1:20 and fewer with generic spins and/or eccentricity. The community has yet to achieve routine production of highly spinning ($\chi > 0.9$) and highly unequal ($q > 20$) configurations with or without eccentricity. Higher order modes are excited with greater amplitudes as the binary parameters move away from non-spinning and equal mass. Fortunately, NR codes routinely produce well resolved higher order modes up to and including about $\ell = 8$.

In summary, the BBH parameter space is currently covered as follows:

- Non-spinning BBH mergers with mass ratio $q \leq 18$ (Jani et al. 2016; Healy et al. 2017, 2019; Mroue et al. 2013; Boyle et al. 2019; Ajith et al. 2012; Gonzalez et al.

2009; Hinder et al. 2014; Husa et al. 2016) — see Lousto and Zlochower (2011b); Lousto and Healy (2020) for binaries with mass ratios $q = 64, 100$, and 128.

- BBHs with moderate random spins and $q \leq 8$ (Jani et al. 2016; Mroue et al. 2013; Healy et al. 2017, 2019; Hinder et al. 2014; Hamilton et al. 2024; Boyle et al. 2019), aligned-spin binaries of $\chi \leq 0.85$ with $q \leq 18$ (Husa et al. 2016; Healy and Lousto 2020), and a few with very high spins ($\chi \sim 0.99$) (Zlochower et al. 2017; Scheel et al. 2015; Liu et al. 2009).
- Eccentric BBHs with $q \leq 32$ (Hinder et al. 2008; Huerta et al. 2019; Ramos-Buades et al. 2020a; Gayathri et al. 2022; Healy and Lousto 2020) with limited cycles.

Note that BBH simulations in GR are scale-invariant with respect to the total mass of the system; therefore, a BBH waveform can be re-scaled for both ground-based and space-based gravitational wave detectors without having to repeat the NR computation. However, the mass scaling will determine the physical starting frequency of the signal, and therefore whether the NR waveform covers the entire sensitivity band of the detector.

4.1.4 Environmental effects

The NR community has made great strides in simulating binaries in a matter-rich environment. This Whitepaper focuses on ways the environment directly impacts the predicted gravitational waves; for EM signatures of BBH mergers, we refer to the Astrophysics Working Group White Paper (Amaro-Seoane et al. 2023) and references therein.

The gravitational waves emitted during the merger of a BBH in an accretion disk are likely unaffected by the accreting matter (Bode et al. 2010), although (Fedrow et al. 2017) indicates that accretion disk densities greater than $10^6 - 10^7$ g cm^{-3} would alter the coalescence dynamics enough to be relevant for ground-based GW detectors.

In addition to EM counterparts, there are other possible sources for LISA modeled by NR. One such class of signals arises from the magnetorotational collapse of a supermassive stars; see, e.g., Smith et al. (2017) for a recent review and Shibata et al. (2006) for early NR work. Recently the GW signatures from such collapsing supermassive stars were calculated in Shibata et al. (2016); Sun et al. (2017), where it was shown that LISA could observe such events out to redshift $z \simeq 3$. Sun et al. (2017) also computed possible EM counterparts and predicted that these systems could be sources of very long gamma-ray bursts.

Another potential source of gravitational waves detectable by LISA that is currently unmodeled comes from instabilities in accretion disks around BHs. The particular case of the Papaloizou–Pringle instability (Papaloizou and Pringle 1984) of self-gravitating disks has been studied in Kiuchi et al. (2011) without BH spin, and in Wessel et al. (2021) including spin. In Wessel et al. (2021) it was shown that BH spin could potentially increase the duration of the near monochromatic signal from the

instability, and that LISA could detect gravitational waves generated by the Papaloizou-Pringle instability around $10^5 M_\odot$ BHs out to redshift $z \simeq 1$.

Finally, for a detailed discussion of environmental effects and the challenges they could present for precision tests of GR, such as dark matter environments, we refer the interested reader to the Fundamental Physics White Paper (Arun et al. 2022) and references therein.

4.1.5 Challenges in NR

Improvements in hardware and numerical techniques continue to speed up simulations, yet some corners of the binary parameter space continue to demand challenging simulations that are costly in terms of runtime and computational resources. Three of the most pressing challenges facing NR are (i) producing waveforms that cover the anticipated parameter space of unequal mass, highly spinning, and eccentric binaries, (ii) producing long-lived waveforms with sufficient numbers of GW cycles, and (iii) producing these waveforms at standards of accuracy set by LISA's sensitivity.

Parameter coverage: The BBH parameter space for the LISA mission, as summarized in Table 2 has mass ratios that span from 1:1 to 1:1000, BH spins from 0 to 0.998, and a wide range of eccentricities. As discussed in § 4.1.3, almost all NR simulations to date are for $q \leq 8$, $\chi \leq 0.8$ and $e \approx 0$; and, therefore, there is significant work to be done to supply waveforms that cover the full potential parameter space for LISA. We also discuss LISA waveform catalogs.

Producing waveforms for systems with large mass ratios is a challenge for the broader waveform community with various approaches existing to bridge the gap between NR solutions and small mass ratio approximations. This is especially relevant for IMRIs. High-mass ratios are demanding due to the need to resolve the smaller mass black hole and provide appropriate gauge conditions (Rosato et al. 2021). As discussed in Sec. 4.1.3, several new codes are being developed by the NR community with the goal of having simulations with large mass ratios ($q > 50$) be routinely possible. In addition to pushing the NR capacity to larger mass ratios, new methods for modeling IMRIs are currently being explored (Schutz 2017; Dhesi et al. 2021), which combine black-hole perturbation theory and NR techniques to significantly increase the numerical efficiency of simulations. Coordination between the GSF and NR communities as well as the construction of open source platforms to share NR (Boyle et al. 2019; Healy et al. 2017; Jani et al. 2016) and GSF waveforms, such as the `Einstein Toolkit` (Löffler et al. 2012) and the `Black Hole Perturbation Toolkit` (BHPToolkit 2024), will streamline and accelerate such endeavors.

A second challenge is producing many generic simulations with BH spins that are very large in magnitude, i.e., approaching 1. The simplest approach to solving the initial data problem is to use the Bowen and York method (Bowen and York 1980; Brandt and Brügmann 1997); however, this method cannot construct BHs with high spins, $\chi \gtrsim 0.93$ (Cook and York 1990; Dain et al. 2002; Lovelace et al. 2011). In addition, resolving the region of spacetime near the horizons requires

computationally expensive, very high resolution. This is exacerbated in evolution methods using excision to handle the singularities (Scheel et al. 2015). As mentioned previously, NR codes have successfully achieved some high spins, including several aligned-spin binaries with spins ($\chi \sim 0.99$) (Zlochower et al. 2017; Scheel et al. 2015; Liu et al. 2009) by using new formulations that move beyond the conformally flat ansatz for puncture methods (Ruchlin et al. 2017) and new techniques for handling the excision region (Scheel et al. 2015).

Finally, several astrophysical scenarios produce non-zero eccentricity in the LISA frequency band (Armitage and Natarajan 2005). NR is capable of and has been producing eccentric runs (Hinder et al. 2008; Huerta et al. 2019; Ramos-Buades et al. 2020a; Gayathri et al. 2022; Ramos-Buades et al. 2022b; Joshi et al. 2023); the challenge is simulations must start with the BHs more widely separated than in quasi-circular configurations. This is again a computational cost.

The source modeling community has continued to improve the modeling of these sources, developing inspiral-merger-ringdown models that combine analytical approximations (Hinderer and Babak 2017) with eccentric NR waveforms (Hinder et al. 2008; Huerta et al. 2017; Ramos-Buades et al. 2020a; Hinder et al. 2018; Huerta et al. 2018; Cao and Han 2017; Chiaramello and Nagar 2020; Liu et al. 2020; Gayathri et al. 2022; Ferguson et al. 2023).

Gravitational wave cycles: The LISA frequency band may contain thousands of GW cycles, depending on the total mass of the massive binary, thus observing BBH signals for months or even years. Given the accuracy of approximate waveform models calibrated with NR (Hannam et al. 2014; Bohé et al. 2017; Khan et al. 2016; Blackman et al. 2017b; Husa et al. 2016), and the recent developments in the self-force community (Dhesi et al. 2021; Albertini et al. 2022b), it is likely unrealistic and unnecessary to use NR to describe the entire evolution of binary systems, from inspiral to ringdown. We point the reader to the rest of Sect. 4 for descriptions on the approaches for modeling the inspiral and inspiral-merger-ringdown waveforms.

Accuracy Massive BBH mergers in LISA could have high (up to 1×10^4) signal-to-noise (SNR) ratios and NR must model these loud signals accurately enough not only to infer the correct source properties, but also to subtract the signal from LISA data, revealing quieter, high-interest signals that may lay underneath. The full implications of these requirements for NR waveform accuracy have yet to be assessed, but an initial study (Ferguson et al. 2021) suggests that NR waveforms will require a substantial increase in accuracy, compared to today's most accurate waveforms, to be indistinguishable from a high-SNR observation with the same source properties. A similar assessment for next-generation ground-based detectors concluded that NR waveforms will need an order of magnitude more accuracy to avoid bias in the inferred source properties for the high signal-to-noise sources that these detectors will observe (Pürrer and Haster 2020). The impact of using insufficiently accurate templates is highlighted in Fig. 4.

These accuracy requirements are even more challenging for NR if the BHs are precessing, if one or both BHs are spinning nearly as rapidly as possible, or if one BH is much more massive than the other. Let us illustrate how quickly computational cost rises, by quantifying computational cost increases relative to a fiducial baseline

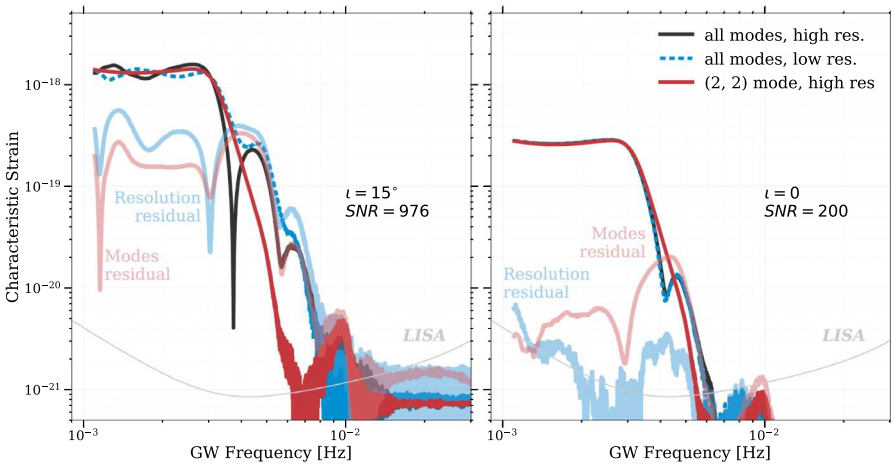

Fig. 4 Illustration of how numerical errors in a template may leave a residual in high-SNR signals. The left panel represents a BBH at high SNR (detector mass $M_{\rm det} = 5 \times 10^6 M_\odot$, aligned spin of $\chi = 0.2$ on the larger BH at distance $D_L = 30\,{\rm Gpc}$ and at inclination $\iota = 15°$). The black line is the characteristic strain ($2f\tilde{h}(f)$) obtained at high numerical resolution from all spherical harmonic modes. The blue dashed line is the corresponding quantity obtained from a low resolution simulation, with the light blue line denoting the difference to the high-resolution waveform. The solid red line is a high resolution template containing only the $(l, m) = (2, 2)$ mode, with the light red line showing the difference to the black line. If this system were searched for with the low-resolution (or (2,2)-mode only) waveforms, then the shaded lines would remain as residuals after subtraction. The SNR of the residual due to resolution in the left panel is 342, clearly indicating the need for higher accuracy NR simulations. The right panel represents a more frequently expected system, where the SNR is 200, $D_L = 158\,{\rm Gpc}$ and $\iota = 0°$. Here, the residual due to resolution has an SNR of 2.4. Figure adapted from Ferguson et al. (2021). The LISA noise curve can be found at Robson et al. (2019)

simulation with mass-ratio q_0 and initial frequency $M\Omega_0$. Cost increases arise for multiple reasons.

First, the explicit evolution schemes used in NR codes are subject to the Courant-Friedrichs-Levy (CFL) condition, which limits the possible time step to the dynamic time of the smaller BH, $\Delta t \propto m_2$. As the mass ratio increases, the number of time-steps per unit $M = m_1 + m_2$ of evolution time will therefore increase as

$$f_{\rm CFL} \sim \frac{q}{q_0}. \tag{7}$$

Second, the total inspiral time of a BBH can be estimated by PN expansions Blanchet (2024) as $T \propto 1/v(M\Omega)^{-8/3}$, where $M\Omega$ is the initial dimensionless frequency of a binary. A change in mass ratio and initial frequency will modify the computational cost in proportion to T, i.e. by a factor

$$f_{\Omega low} = \left(\frac{v}{v_0}\right)^{-1} \left(\frac{\Omega}{\Omega_0}\right)^{-8/3}. \tag{8}$$

Thirdly, LISA has higher accuracy requirements than current NR simulations. We

denote by $f_\tau(A)$ the increase in computational cost that is needed to reduce the truncation error τ by a factor $A > 1$, i.e. $\tau \to \tau/A$.

A fourth cause for increased computational cost arises from the desire of achieving a certain overall phase error, which is important for GW waveform modeling. For longer simulations, phase accuracy must be preserved over more cycles. From PN theory, the orbital phase to merger scales as $\Phi \propto v^{-1}(M\Omega_i)^{-5/3}$. To achieve a fixed overall phase-error (say, 1 radian), the relative phase error must decrease $\propto 1/\Phi$, yielding an increase in computational cost by a factor

$$f_\Phi \sim f_\tau\left(\left(\frac{v}{v_0}\right)^{-1}\left(\frac{\Omega}{\Omega_0}\right)^{-5/3}\right). \tag{9}$$

The challenge now is that in order to achieve higher mass ratio simulations starting at similar (or lower) initial frequency, and possibly also achieving higher accuracy, each of the factors just outlined increases very rapidly and that these factors multiply for an overall cost increase by a factor

$$C = f_{\rm CFL} f_{\Omega_{\rm low}} f_\tau f_\Phi. \tag{10}$$

To obtain concrete numerical estimates, we assume that f_τ is a power law, $f_\tau(A) = A^\alpha$. This assumption is satisfied for finite difference codes, where a convergence order of k in $(3+1)$ dimension yields $\alpha = 4/k$. In terms of α, the overall cost increase is given by

$$C \sim \left(\frac{q}{q_0}\right)^{2+\alpha}\left(\frac{\Omega_0}{\Omega}\right)^{8/3+5\alpha/3} A^\alpha, \tag{11}$$

where we have also used $v \approx 1/q$, which is valid at large q.

We can now make concrete estimates: Increasing the mass-ratio by a factor of 2, lowering the initial frequency by a factor of 1/2, and increasing accuracy by a factor of 2, and assuming the NR code under consideration maintains perfect 8-th order convergence into the regime of longer, more accurate simulations at higher mass-ratio (i.e. $\alpha = 1/2$), increases the computational cost two orders of magnitude. More ambitiously, increasing the mass-ratio by a factor of 10, reducing initial frequency by a factor 1/4 and increasing accuracy by a factor 10 increases the computational cost by five orders of magnitude. Codes based on spectral methods, e.g. SpEC, will likely result in a smaller f_τ; even so, increases in computational cost are very challenging as one goes to longer simulations at higher mass-ratio.

The NR codes that have been instrumental in providing public BBH waveforms use either a spectral method or box-in-box mesh refinement. These methods scale well to the order of 1000 cores, but they cannot scale to hundreds of thousands or millions of cores. For example, codes using high-order finite-difference stencils incur ever-increasing inter-core communication costs as the number of cores increases and this cost eventually becomes prohibitive. These codes are parallelization bound and do not parallelize beyond current usage. Since individual computer cores are no longer dramatically increasing in speed (Moore's law has 4) assessment of systematic bias in simulated LISA signals with currently available waveforms, and 5) the

development of NR waveform for all potential parameters at the necessary accuracy. For a more general discussion on waveform accuracy, see Sec. 3.2.

4.1.6 Future codes and catalogs

The LISA data analysis groups could have access to NR waveforms via a bespoke LISA catalog or as a public catalog. A bespoke catalog would have NR waveforms created specifically to meet those aforementioned requirements, potentially interfacing and merging existing catalogs and extending with its own dedicated entries (similar to the LVK catalog (P. Schmidt et al. 2017). If a bespoke LISA catalog is not created or deemed unnecessary due to a possible future abundance of NR public waveforms (current catalogs are indicated in Table 7) we will need a software interface with existing NR waveform catalogs that is curated and cultivated with time. A full catalog of NR waveforms achieving all requirements will take time, possibly until the launch of LISA. We put forth the following priorities for the NR waveforms: 1) an accuracy assessment of current and near-term achievable NR waveforms, 2) the assessment of current and near achievable parameter space, 3) the development of NR waveforms for the most likely LISA events at the required accuracy, 4) assessment of systematic bias in simulated LISA signals with currently available waveforms, and 5) the development of NR waveform for all potential parameters at the necessary accuracy.

4.2 Weak field approximations (post-Newtonian/post-Minkowskian)

Coordinators: Laura Bernard and Chris Kavanagh
Contributors: A. Antonelli, G. Faye, J. Garcia-Bellido, M. Haney, F. Larrouturou, A. Le Tiec, O. Long

4.2.1 Description

The PN formalism is an approximation method in GR that is well suited to describe the orbital motion of—and the GW emission from—binary systems of compact objects, in a regime where the typical orbital velocities are small compared to the vacuum speed of light c and the gravitational fields are weak. It has played and continues to play a central role in the construction of template banks for the detection and analysis of GW signals generated by binary systems of black holes and/or neutron stars, which are now routinely observed by the LVK collaboration's detectors (Abbott et al. 2019b, 2021b, 2023a). More precisely, PN results are at the core of

Table 7 List of numerical relativity evolution codes

Code	Open Source	Public catalog	Formulation	Hydro	Beyond GR
AMSS-NCKU	Y	–	BSSN/Z4c	–	Y
Cao et al. (2008, 2013); Cao and Hilditch (2012); Hilditch et al. (2013)					
BAM	–	–	BSSN/Z4c	Y	–
Brügmann et al. (2008b); Husa et al. (2008); Thierfelder et al. (2011); Dietrich et al. (2015a) Dietrich et al. (2018); Gonzalez et al. (2023b); Hamilton et al. (2024)					
BAMPS	–	–	GHG	Y	–
Bugner et al. (2016); Hilditch et al. (2016); Renkhoff et al. (2023)					
Dendro-GR	Y	–	BSSN/CCZ4	–	Y
Fernando et al. (2019b, 2023)					
Einstein Toolkit	Y	–	BSSN/Z4c	Y	Y
Löffler et al. (2012); Einstein Toolkit (2024)					
*Canuda	Y	–	BSSN	–	Y
Okawa et al. (2014); Zilhão et al. (2015b); Witek et al. (2019)					
*IllinoisGRMHD	Y	–	BSSN	Y	–
Etienne et al. (2015)					
*LazEv	–		BSSN/CCZ4	–	–
Campanelli et al. (2006a); Zlochower et al. (2005) Healy et al. (2017, 2019); Healy and Lousto (2020, 2022)					
*Lean	Partially	–	BSSN	–	Y
Sperhake (2007); Berti et al. (2013)					
*MAYA	–		BSSN	–	Y
Jani et al. (2016)					
*NRPy+	Y	–	BSSN	Y	–
Ruchlin et al. (2018)					
*SphericalNR	–	–	spherical BSSN	Y	–
Mewes et al. (2018, 2020)					
*Spritz	Y	–	BSSN	Y	–
Cipolletta et al. (2020); Spritz Code (2024)					
*THC	Y		BSSN/Z4c	Y	–
Radice and Rezzolla (2012); Radice et al. (2014a, b); Dietrich et al. (2018)					
*WhiskyMHD	–		BSSN	Y	–
Giacomazzo and Rezzolla (2007); WhiskyMHD (2024)					
ExaHyPE	Y	–	CCZ4	Y	–
Köppel (2018)					
FIL	–	–	BSSN/Z4c/CCZ4	Y	–
Most et al. (2019)					
GR-Athena++	Y	–	Z4c	Y	–
Daszuta et al. (2021)					
GRChombo	Y	–	BSSN/CCZ4	–	Y
Clough et al. (2015); GRChombo (2024); Andrade et al. (2021)					
HAD	–	–	CCZ4	Y	Y
HAD (2010); Liebling (2002); Lehner et al. (2006)					

Table 7 continued

Code	Open Source	Public catalog	Formulation	Hydro	Beyond GR
`Illinois GRMHD`	–	–	BSSN	Y	–
Etienne et al. (2010); Sun et al. (2022)					
`MANGA/NRPy+`	Partially	–	BSSN	Y	–
Chang and Etienne (2020)					
`BH@H/NRPy+`	–	–	BSSN	–	–
Ruchlin et al. (2018); BH@Home (2024)					
`MHDuet`	Y	–	CCZ4	Y	Y
Palenzuela et al. (2018); Liebling et al. (2020); MHDuet Code (2024)					
`Nmesh`	–	–	GHG	Y	–
Tichy et al. (2023)					
`SACRA`	–		BSSN/Z4c	Y	Y
Yamamoto et al. (2008); Kiuchi et al. (2017); Kuan et al. (2023)					
Shibata and Traykova (2023); Shibata and Yoshino (2010); SACRA (2024)					
`SACRA-SFS2D`	–	–	BSSN/Z4c	Y	–
Fujibayashi et al. (2018); Shibata et al. (2021)					
`SGRID`	Y	–	BSSN	–	–
Tichy (2006, 2009)					
`SpEC`	–		GHG	Y	Y
SpEC (2024); Boyle et al. (2019); Mroue et al. (2013); SXS catalog (2024)					
`SpECTRE`	Y	–	GHG	Y	–
Kidder et al. (2017); Deppe et al. (2023)					
`SPHINCS_BSSN`		–	BSSN	SPH	–
Rosswog and Diener (2021)					

We indicate if a code is open-source, if it has been used to produce public gravitational waveform catalogs, the formulation of Einstein's equation used (GHG: generalized harmonic, BSSN: Baumgarte–Shapiro–Shibata–Nakamura, CCZ4 / Z4c variants of the Z4 formulation, GCFE: generalised conformal field equations), if a code implements general relativistic hydrodynamics, and if it is capable of simulating compact objects beyond general relativity. SPH refers to smooth particle hydrodynamics. An asterisk indicates codes that are either (partially) based on the open-source Einstein Toolkit or are co-funded by its grant. Note this table was created jointly for this paper and Foucart et al. (2022)

several classes of waveform models, including phenomenological waveforms and effective one-body waveforms (see Sects. 4.5 and 4.6).

In PN theory, the general relativistic corrections to the Newtonian motion and to the leading GW emission (i.e. Einstein's quadrupole formulas) are computed in a systematic manner in powers of the small PN parameter $v^2/c^2 \sim GM/(c^2 r)$, where v and r are the typical binary relative velocity and separation, M is the sum of the component masses, and $v^2 \sim GM/r$ for bound orbits. Indeed, the most promising sources of gravitational waves for existing and planned interferometric detectors are bound systems of compact objects. By convention, a contribution of "nPN" order refers to equation-of-motion terms that are $O(1/c^{2n})$ smaller than the Newtonian

acceleration, or, in the radiation field, smaller by that factor relative to the standard quadrupolar field.

The PN approximation dates back to the pioneering works of Lorentz and Droste (1917), as well as Einstein et al. (1938) and Fock (1939), who computed the leading 1PN corrections to the Newtonian equations of motion in a system of N point masses. During the 1980s, those results were extended to 2.5PN to provide a rigorous basis for interpreting binary pulsar observations (Damour and Deruelle 1981a, b, 1985, 1986). For binary systems of compact objects, the state of the art corresponds to gravitational waveforms that include all of the relativistic corrections up to 4PN order (Damour et al. 2016; Marchand et al. 2018; Foffa and Sturani 2019; Foffa et al. 2019), in the simplest case of nonspinning bodies moving along a sequence of quasi-circular orbits.

Another complementary weak field approximation can be found by relaxing the small velocity assumption of the PN approximation and demanding only that $GM/(c^2 r) \ll 1$. This scheme, known as the PM approximation, has a long and venerable history, in the context of both unbound scattering where velocities can be arbitrarily large (Westpfahl and Goller 1979; Westpfahl and Hoyler 1980) and far-zone–near-zone matching for bound orbits within certain PN schemes (see e.g., Blanchet 2024).

As discussed below, much work has recently been dedicated to (i) push this accuracy to 4.5PN order, (ii) include the effects of the spins of the compact objects (see also Table 8), (iii) generalize the results from circular to eccentric orbits, and (iv) explore the overlap and synergies with other approximation methods (PM approximation, small-mass-ratio approximation, effective one-body model). The reader is referred to the review articles by Futamase and Itoh (2007); Blanchet (2011); Schäfer (2009); Blanchet (2024); Foffa and Sturani (2014); Rothstein (2014); Porto (2016); Schäfer and Jaranowski (2024); Levi (2020) and to the texbooks by Maggiore (2007); Poisson and Will (2014) for more information.

4.2.2 Suitable for what sources?

The PN approximation is well suited to describe the dynamics and gravitational emission of compact binary systems in the early inspiral stage. While it can in principle be applied to model BH binaries of any mass ratio, it is expected to be more accurate for comparable to intermediate mass BHBs, as the gravitational field should remain small until the final cycles. For mass ratio above $q \gtrsim 100$, when the small body remains for long timescales close to the supermassive BH, the gravitational field is strong and the weak-field approximation will lose accuracy (see Fig. 2).

The PM approximation is best suited to close hyperbolic encounters (CHE), which could be detected with LISA for a population of massive PBH in dense clusters forming part of the halos of galaxies, as studied in García-Bellido and Nesseris (2017); García-Bellido and Nesseris (2018) using a leading order PN approximation scheme. It also provides valuable resummations of terms in the PN approximation and is used to improve bound compact binary coalescence models when combined with PN results.

Table 8 State-of-the-art of known PN results for both the conservative and dissipative dynamics as well as for the gravitational flux

PN order	Dynamics				Dissipative flux			
	Non-spinning	Spinning			Non-spinning	Spinning		
		SO	SS	Higher spins		SO	SS	Higher spins
0	√	–	–	–	–	–	–	–
1	√	–	–	–	–	–	–	–
1.5	–	√	–	–	–	–	–	–
2	√	–	√	–	–	–	–	–
2.5	√	√	–	–	√	–	–	–
3	√	–	√	–	–	–	–	–
3.5	√	√	–	√ (S^3)	√	–	–	–
4	√	–	√	√ (S^4)	√	√	–	–
4.5	∗	√	–	√ (S^3)	√	–	√	–
5	∗	–	√	√ (S^4)	√	√	–	–
5.5	∗			√ (S^5)	√	√	√	–
6				√ (S^6)	√	√	√	√ (S^3)
6.5				★	√	√	√	
7				★	√			

Contrary to the text, everything is stated as absolute order. For example, the 6PN absolute order for the non-spinning flux in the table corresponds to the 3.5PN relative order results as stated in the text. Hereditary effects enter at 2.5PN order and subsequent odd PN orders in the non-spinning dynamics and usually contain non-local contributions. An instantaneous expression can be obtained by performing a low-eccentricity expansion. SO and SS refer to spin-orbit and spin-spin interactions respectively. ∗ means that only a partial result is known at those orders. At 5 and 5.5PN order, the results were obtained by the combination of PN traditional techniques with scattering amplitudes and self-force. ★ means that the dynamics is known at all leading order in the spin

PN waveforms are ideally suited to model binaries that are in an early stage of their inspiral while in the LISA band such as SOBHBs and GBs.

4.2.3 Status

4.2.3.1 Equations of motion and waveforms without spin For an isolated, non-spinning compact binary system, the phase evolution and GW modes during the inspiral stage are currently known up to 4.5PN and 4PN, respectively (Marchand et al. 2020; Henry et al. 2021; Larrouturou et al. 2022a, b; Blanchet et al. 2022; Trestini et al. 2023; Henry 2023; Blanchet et al. 2023b, c). As for the LISA requirements, it was established in Mangiagli et al. (2019) that the 2PN waveform will be enough for the parameter estimation of roughly 90% of the detectable SOBHBs, while the 3PN waveform phasing is needed for the systems that will merge within the mission lifetime. Nevertheless it will be quite valuable to push the current accuracy up to 4.5PN order for at least two main reasons. The first one is that it may be necessary for the parameter estimation of black hole binaries

with large masses. The second one is that this accuracy will be very beneficial for the calibration of numerical waveforms, and for testing the second-order self-force computations.

For quasi-circular orbits, the gravitational phase $\phi(t)$ is computed via the so-called energy *flux-balance equation*, $\frac{\mathrm{d}E}{\mathrm{d}t} = -\mathcal{F}_{\rm GW}$, where E is the conserved energy and $\mathcal{F}_{\rm GW}$ is the flux of radiation emitted. Both quantities are functions of the gravitational phase, which is thus obtained by a simple integration. The amplitude and polarizations are obtained by the same radiative multipole moments that are used when computing the flux, as explained later. For recent reviews, see Buonanno and Sathyaprakash (2014); Goldberger (2007); Foffa and Sturani (2014); Porto (2016); Blanchet (2024).

At 4PN precision, three different techniques are used to compute the binding energy: the canonical Hamiltonian formulation of General Relativity (Jaranowski and Schäfer 2013, 2015; Damour et al. 2014b, 2015, 2016), the Fokker Lagrangian approach (Bernard et al. 2016, 2017a, b; Marchand et al. 2018; Bernard et al. 2018) and effective field theory (EFT) (Foffa and Sturani 2013a, b; Galley et al. 2016; Porto 2016; Foffa and Sturani 2019; Foffa et al. 2019; Blümlein et al. 2020a). All of these methods derive the energy as a conserved quantity associated with the equations of motion for two point-like particles, and naturally give physically equivalent results. The Hamiltonian approach has been pushed up to 6PN, yielding incomplete results (Bini et al. 2020c), see Sect. 4.2.3.4. Exploiting synergies between traditional PN methods and EFT, the logarithmic contributions in the energy have also been computed up to 7PN (Blanchet et al. 2020).

The flux of gravitational radiation can be expressed as a generalisation of the famous Einstein quadrupole formula (Einstein 1918; Landau and Lifschits 1975), as Thorne (1980)

$$\begin{aligned}\mathcal{F}_{\rm GW} &= \sum_{\ell\geq 2}\frac{G}{c^{2\ell+1}}\left[\alpha_\ell\, U_L^{(1)}U_L^{(1)} + \frac{\beta_\ell}{c^2}\, V_L^{(1)}V_L^{(1)}\right]\\ &= \sum_{\ell\geq 2}\frac{G}{c^{2\ell+1}}\left[\alpha_\ell\, I_L^{(\ell+1)}I_L^{(\ell+1)} + \frac{\beta_\ell}{c^2}\, J_L^{(\ell+1)}J_L^{(\ell+1)}\right] + \mathcal{F}_{\rm tails}\,,\end{aligned} \tag{12}$$

where L is a multi-index, the U_L (resp. V_L) are the mass (current) radiative multipole moments and the I_L (resp. J_L) are the mass (current) source multipole moments, the $\{\alpha_\ell, \beta_\ell\}$ are collections of numbers and the superscript (n) denotes n time derivatives. To connect radiative moments to sources moments, their non-linear interactions (occurring during the propagation from the source to the detector) have been singled out in $\mathcal{F}_{\rm tails}$. The radiative moments are also directly involved in the computation of polarisations (Thorne 1980), and thus their determination is crucial.

The contribution $\mathcal{F}_{\rm tails}$ is known up to 4.5PN order, using traditional PN methods (Marchand et al. 2016), and was confirmed by an independent PN re-expansion of resummed waveforms (Messina and Nagar 2017). The computation of the required moments is currently done using the Multipolar-post-Minkowskian-post-Newtonian (MPM-PN) algorithm (Blanchet 2024). The major piece of this work is the derivation of the mass quadrupole ($\ell = 2$) up to 4PN order: the main result has

been obtained (Marchand et al. 2020; Larrouturou et al. 2022a, b; Blanchet et al. 2022; Trestini et al. 2023), including the tail-of-memory contribution (Trestini and Blanchet 2023). The other moments involved are the mass octupole and the current quadrupole, already known at the required order (3PN) (Faye et al. 2015; Henry et al. 2021), and higher moments that are either known or trivial (i.e. needed at the Newtonian order only), see notably Blanchet et al. (2008). Collecting all these results, the complete flux of gravitational radiation at infinity is fully known at 4PN (Blanchet et al. 2023b) and 4.5PN in the case of circular orbits (Marchand et al. 2016). In the case of horizonless objects such as neutron stars, the flux-balance equation is used to compute the gravitational phase for circular orbits at 4.5PN (Blanchet et al. 2023c). However, if at least one object is a black hole, one must include an extra contribution due to the absorption of gravitational waves by the black hole horizon(s) (Poisson and Sasaki 1995; Tagoshi et al. 1997; Alvi 2001; Porto 2008; Chatziioannou et al. 2013). Note that two other methods are able to deal with high PN multipole moments, both currently developed up to 2PN: the direct integration of the relaxed equations (DIRE) (Will and Wiseman 1996) and EFT (Leibovich et al. 2020). As half-PN orders are often easier to compute than integer ones, one can probably push the results up to 4.5PN order, including the amplitudes of the gravitational modes. A first step in this program is to control the dissipative, radiation reaction effects in the equations of motion. Table 8 summarizes the current knowledge regarding PN dynamics and flux without spin.

Finally, there have been some works trying to map the BMS (Bondi–Metzner–Sachs) flux-balance laws to equivalent PN results in the harmonic gauge (Compère et al. 2020c). By transforming the metric from harmonic coordinates to radiative Newman-Unti (NU) coordinates, they were able to obtain the mass and angular momentum aspects and the Bondi shear as a function of the quadrupole moment (Blanchet et al. 2021). In particular, they rederive the displacement memory effect (see also Favata 2009) and provide expressions for all Bondi aspects relevant to the study of leading and subleading memory effects (Blanchet et al. 2023a).

4.2.3.2 Equations of motion and waveforms with spin In the last decade, the effects of the proper rotation of the components of binary systems have been included in the orbital equations of motion to 4PN order, extending previous works dating back to the 1970s Barker and O'Connell (1975). In the post-Newtonian terminology, the spin variable S is rescaled as $S = cS_{\rm phys} = Gm^2\chi$, with χ the dimensionless spin parameter comprised between 0 and 1. The leading spin interactions, the so-called spin-orbit interaction (SO), couple the mass m_1 of a particle with the spin of the other, hence those contributions scale as $\frac{Gm_1}{c^2} \times \frac{S_2}{c} \sim \mathcal{O}(\frac{1}{c^3})$ and are regarded as being of 1.5PN order. Meanwhile the first effect due to spin-spin interaction, scaling as $\frac{G}{c^2} \times \frac{S_1}{c} \times \frac{S_2}{c} \sim \mathcal{O}(\frac{1}{c^4})$, is quadratic in spin (SS) and arises at 2PN order. We refer to the successive subleading PN contributions to a given spin interaction (e.g. SO or SS) as the next-to-leading (NL), next-to-next-to-leading (NNL) and so on. Moving beyond the 2PN two-body dynamics including SO interactions (Damour 1982), it becomes increasingly difficult to resort to an explicit model, where the bodies are described as small balls of fluid (Will 2005). The most

efficient strategy consists in adopting an effective point of view and considering that the two objects are point particles endowed with a classical spin.

The definition of spin in GR was first introduced by Mathisson (1937), and rephrased later by Tulczyjew (1959). The covariant equations of evolution obeyed by a spinning test particle were obtained in their usual form by Papapetrou (1951) and later generalized by Dixon (1974) to bodies endowed with higher-order multipole moments. The equations of motion and precession served as a starting point to investigate the dynamics of binary systems at next-to-leading (NL: 2.5PN) (Tagoshi et al. 2001; Faye et al. 2006) and NNL (3.5PN) order linear in spin (SO interactions) (Marsat et al. 2013b), assuming that all Dixon moments other than the masses and the spins vanish. The metric is obtained by solving iteratively Einstein's equations in harmonic coordinates (Bohe et al. 2013) for the pole-dipole stress-energy tensor. Later, to compute the SS corrections, first contributing at NL (3PN) order (Bohé et al. 2015), the Dixon quadrupoles were added, so as to account for the self deformation of the bodies produced by their own spins.

The direct computation of a generalized Lagrangian (i.e. depending on the accelerations) for two spinning particles, using EFT in harmonic coordinates, was performed in stages from the mid-2000's on by integrating out the gravitational field entering the full 'field plus matter' Lagrangian with the help of standard Feymann diagram expansions (Porto and Rothstein 2006; Porto 2006; Levi and Steinhoff 2015b). The NL S_1–S_2 (3PN) interactions (Porto and Rothstein 2008b; Levi 2010b) were computed first, before the NL S_1–S_1 (3PN) contributions (Porto and Rothstein 2008a) and NL SO (2.5PN) interactions (Levi 2010a; Porto 2010) were considered. Equivalent results were obtained in parallel by means of Hamiltonian methods based of the Arnowitt–Deser–Misner (ADM) formulation of GR (Steinhoff et al. 2008a, b, c).

After the canonical treatment of the spin was better understood (Steinhoff et al. 2008c; Steinhoff and Schäfer 2009), the computations of the Hamiltonian were pushed up to NNL (3.5PN) order for the SO (Hartung and Steinhoff 2011a; Hartung et al. 2013), to NNL (4PN) order for the S_1–S_2 interactions (Hartung and Steinhoff 2011b) and to NL (3PN) order for the S^2 interaction (Hergt et al. 2010). A fully equivalent Lagrangian for the latter effects was found using EFT (Levi 2012). Once the EFT degrees of freedom and the gauge choice corresponding to the spin-supplementary condition were clearly identified, the PN leading terms to all orders in spins were computed (Vines and Steinhoff 2018), then beyond leading order corrections were added (Levi and Steinhoff 2015a; Levi et al. 2021; Levi and Teng 2021) and the spin part of the harmonic Lagrangian was completed up to the NNNL (5PN) order (Kim et al. 2023c, b).

Note that reaction forces, dissipative in essence, are absent from the previous treatments, which exclusively describe the conservative dynamics. Nonetheless, they can be computed from balance equations (Zeng and Will 2007), or more directly from the Papapetrou evolution equations, or from the conservation of an appropriate stress-energy tensor (Wang and Will 2007). One may even construct a Schwinger–Keldysh Lagrangian where each degree of freedom is formally doubled. This was done for the NL SO and SS effects at 4PN and 4.5PN respectively in (Maia et al.

2017a, b), and to all orders in spin in (Siemonsen et al. 2018) (see also the approach developed for ADM Hamiltonians (Wang et al. 2011) at leading SO and SS orders).

Knowing the near-zone dynamics of two spinning particles, one can insert the corresponding PN metric into the right-hand side of Einstein's equations in harmonic coordinates, which yields the expression of the effective non-linear source entering the integrand of the multipole moments, as defined in the multipolar post-Minkowskian (MPM) formalism (Blanchet 1998), or, equivalently, in EFT (Ross 2012); hence one gets the relevant mass, current and gauge moments in the spinning case (Porto et al. 2012). The expression for the radiative moments in terms of the former quantities has been derived for general isolated systems (Faye et al. 2015), but the hereditary terms therein are more delicate to evaluate than for mere point-mass particles on circular orbits, since the orbital plane is now generically precessing. They have however been handled for the leading (Blanchet et al. 2011) and NL (Marsat et al. 2014) SO interactions, which required the full integration of the (approximately) conservative dynamics up to the considered order.

Finally concerning the gravitational radiation, the GW flux has been obtained to NNL (4PN) order both for the SO and SS contributions (Bohé et al. 2015; Cho et al. 2022b). The GW phase, built from the radiative moments and the Noetherian energy, has been obtained within the MPM formalism at the NNL (4PN) order for the SO contributions (Bohé et al. 2013; Marsat et al. 2014) (in continuation of previous works at leading order (2PN) (Kidder et al. 1993; Kidder 1995) and NL (3PN) orders (Blanchet et al. 2006)), at the NL (3PN) order for the SS terms (Bohé et al. 2015), and at leading order for the spin cube contributions (Marsat 2015). Similar results were obtained with the EFT formalism (Porto et al. 2011) for which state-of-the-art results are also the NNL (4PN) order (Cho et al. 2022b). The waveform modes have been obtained to NNL (3.5PN) order (Henry et al. 2022) in the quasi-circular orbit approximations. By contrast, the radiation amplitude has been computed up to the NL (2PN) order only (Buonanno et al. 2013), although it is currently provided in a ready-to-use form for precessing quasi-circular orbits to the even lower 1.5PN order (Arun et al. 2009b).

See Table 8 for a summary of on the current knowledge about the PN spinning dynamics and flux.

4.2.3.3 Eccentric-orbit waveforms The modeling of inspiral waveforms from compact binaries in eccentric orbits commonly relies on the quasi-Keplerian parametrization (QKP) as a semi-analytic representation of the perturbative, slowly precessing post-Newtonian motion. The conservative motion as well as instantaneous and hereditary contributions to the secular ("orbital averaged") evolution of the orbital elements are known to 3PN order, in both modified harmonic and ADM-type coordinates (Damour et al. 2004; Memmesheimer et al. 2004; Arun et al. 2008a, b, 2009a) and to 4PN order in the ADM-type coordinates only (Cho et al. 2022c).

The complete 3PN-accurate GW amplitudes from non-spinning eccentric binaries have been derived using the multipolar post-Minkowskian formalism, including all instantaneous, tail and non-linear contributions to the spherical harmonic modes

(Mishra et al. 2015; Boetzel et al. 2019; Ebersold et al. 2019). Going beyond the usual approximation of radiation reaction as an adiabatic process (and the associated "orbital averaging" in QKP), Damour et al. (2004); Königsdörffer and Gopakumar (2006); Moore et al. (2016); Boetzel et al. (2019) provide post-adiabatic, oscillatory corrections to the secular evolution of GW phase and amplitude.

For spinning eccentric binaries that have component spins aligned with the orbital angular momentum, the effects of spin-orbit and spin-spin couplings on the binary evolution and gravitational radiation have been worked out to leading order in QKP (i.e., up to 1.5PN and 2PN in the equations of motion) (Klein and Jetzer 2010). Subsequent work has aimed to extend the treatment of spins in QKP to higher PN orders (Tessmer et al. 2010, 2013). The waveforms modes to NL (3PN) order for aligned spins and eccentric orbits have been derived in Khalil et al. (2021); Henry and Khalil (2023), including tail and memory contributions. While the instantaneous contributions were derived for generic motion, the hereditary contributions were computed first in a small-eccentricity expansion, then extended to larger eccentricities using a resummation. Regarding precessing eccentric systems, gravitational waveforms have been obtained to leading order in the precessing equation (Klein 2021). A fully analytical treatment has also been proposed up to 2PN order in the spin, including higher harmonics (Paul and Mishra 2023).

In practice, the semi-analytic approach of QKP requires a numerical evolution of the orbit described by a coupled system of ordinary differential equations (ODEs) and a root-finding method to solve the Kepler problem, and therefore lacks the computational efficiency required for most data analysis applications. The post-circular (PC) formalism (Yunes et al. 2009) provides a method to recast the time-domain response function $h(t)$ into a form that permits an approximate fully analytic Fourier transform in stationary phase approximation (SPA), under the assumption that the eccentricity is small, leading to non-spinning, eccentric Fourier-domain inspiral waveforms as a simple extension to the quasi-circular PN approximant TaylorF2. More recent work has extended the PC formalism to 3PN, with a bivariate expansion in eccentricity and the PN parameter (Tanay et al. 2016; Moore et al. 2016), and has included previously unmodeled effects of periastron advance (Tiwari et al. 2019).

The parameter space coverage of Fourier-domain waveforms in the PC formalism is limited by the necessary expansion in small eccentricity. Newer models aim for validity in the range of moderate to high eccentricities, by utilizing numerical inversions in SPA and resummations of hypergeometric functions to solve orbital dynamics (Moore et al. 2018; Moore and Yunes 2019) or by applying Padé approximation on analytic PC schemes expanded into high orders in eccentricity. A semi-analytic frequency-domain model for eccentric inspiral waveforms in the presence of spin-induced precession has been developed with the help of a shifted uniform asymptotics (SUA) technique to approximate the Fourier transform, a numerical treatment of the secular evolution coupled to the orbital-averaged spin-precession, and relying on a small eccentricity expansion (Klein et al. 2018).

4.2.3.4 Insight from scattering One can gain surprising insight in the relativistic two-body problem by investigating *unbound* orbits. Studying such systems implies analyzing the scattering of compact objects and the approximation to the two-body problem most naturally applicable to it, the PM expansion. Recently, there has been renewed interest in the subject, as it has been realized that PM information from unbound systems can be transferred to bound ones, as done for instance via Hamiltonians (Damour 2016, 2018; Antonelli et al. 2019) or between gauge-invariant quantities (Kälin and Porto 2020a, b; Bjerrum-Bohr et al. 2020; Cho et al. 2022a; Saketh et al. 2022). Moreover, PM expansions can be independently obtained from scattering-amplitude calculations (Arkani-Hamed et al. 2021), as done at 3PM order (Bern et al. 2019a, b; Kälin et al. 2020a; Cheung and Solon 2020a; Kälin et al. 2023) for the nonspinning sector (see also earlier results at 2PM order (Cheung et al. 2018; Bjerrum-Bohr et al. 2018; Cristofoli et al. 2020; Kosower et al. 2019; Kälin and Porto 2020c) and preliminary results at 4PM (Bern et al. 2021b, 2022; Dlapa et al. 2022a, b, 2023)). Another method that has been successfully used is the worldline quantum field theory approach (Mogull et al. 2021; Jakobsen et al. 2021; Mougiakakos et al. 2021).

The 3PM radiative contribution, which cancels a divergence in the 3PM conservative part, has been obtained in Damour (2020b); Bjerrum-Bohr et al. (2021); Herrmann et al. (2021a, b); Di Vecchia et al. (2021a, b, 2020). The radiative effects in PM expansions have been further explored in Brandhuber et al. (2021); Damgaard et al. (2021); Riva and Vernizzi (2021); Manohar et al. (2022) and the radiative contributions to the scattering problem were obtained in a PN expansion (Bini et al. 2020e, 2021; Bini and Geralico 2021a, b, 2022a, b; Bini et al. 2023).

A Hamiltonian including spin-orbit coupling at the 2PM approximation has been obtained (Bini and Damour 2018) by extracting the dynamical information from a scattering situation with the help of "scattering holonomy" (Bini and Damour 2017; Kälin and Porto 2020b). Likewise effects at 'spin-squared' have been determined at the 2PM level using both amplitude (Kosmopoulos and Luna 2021) and the EFT formalism (Liu et al. 2021b; Chung et al. 2020; Bern et al. 2021a; Bautista et al. 2023; Jakobsen et al. 2022a, b). To 3PM order, SO and SS contributions have been determined (Jakobsen and Mogull 2023). Effects of arbitrary orders in spin in the scattering angle have also been studied by means of purely classical methods (Vines 2018; Siemonsen et al. 2018; Aoude et al. 2022). Those results have been recovered at 1PM order through the computation of quantum scattering amplitudes for minimally coupled massive spin-n particles and gravitons in the classical limit, as n goes to infinity (Maybee et al. 2019). Notably, the tree-level amplitude has been found to generate the full series of black-hole spin-induced multipole moments (Guevara et al. 2019). Tidal effects in PM expansions have also been investigated (Cheung and Solon 2020b; Bini et al. 2020b; Cheung et al. 2021; Bern et al. 2021c; Kälin et al. 2020b; Aoude et al. 2021; Haddad and Helset 2020; Mougiakakos et al. 2022).

The aforementioned results have naturally prompted discussions and comparisons between the GW astrophysics and scattering-amplitude communities, which is made possible by the use of pivotal gauge-invariant quantities for comparisons. The scattering angle of unbound compact-object interactions is one such pivotal quantity that, at least in a perturbative sense through the orders so-far considered, is thought to

encapsulate the complete conservative dynamics. Not only does it provide a common ground to exchange information between independent PM calculations (Cristofoli et al. 2019) or between PM and EOB schemes (Damour 2016, 2018; Vines 2018; Vines et al. 2019; Antonelli et al. 2020c; Damgaard and Vanhove 2021; Khalil et al. 2022; Damour and Rettegno 2023), but it has also proven extremely useful to PN theory.

The PM expansion of the scattering angle allows one to extract previously unknown PN information through a synergistic combination of constraints from its simple mass-ratio dependence and gravitational self-force (GSF) results, as first realized at 5PN (Bini et al. 2019, 2020a). Such construct has been exploited to partially calculate the 6PN dynamics (Bini et al. 2020c, d), allowing a nontrivial check at 3PM-6PN order of the 3PM result (Blümlein et al. 2020b; Cheung and Solon 2020a), as well as to the generic spin-orbit and aligned bilinear-in-spin sectors at NNNL (Antonelli et al. 2020a, b) (see also Siemonsen and Vines (2020) for more on the interface between PM and GSF theory). GSF scattering observables can also provide a powerful handle on PM dynamics across all mass ratios. Calculations of the scattering angle to first-order (second-order) in the mass ratio fully determine the complete two-body Hamiltonian through 4PM (6PM) order (Damour 2020a).

4.2.3.5 First laws and gauge invariant comparisons The orbital dynamics of a binary system of compact objects exhibits a fundamental property, known as the first law of binary mechanics, that takes the form of a simple variational relation. This formula relates local properties of the individual bodies (e.g. their masses, spins, redshifts, spin precession frequencies), to global properties of the binary system (e.g. gravitational binding energy, total angular momentum, radial action variable, fundamental frequencies). The first law was first established for binary systems of nonspinning compact objects moving along circular orbits (Le Tiec et al. 2012b), as a particular case of a more general variational relation, valid for systems of black holes and extended matter sources (Friedman et al. 2002). This first law was later extended to generic bound eccentric orbits (Le Tiec 2015), including the effect of the GW tails that appear at the leading 4PN order (Blanchet and Le Tiec 2017), as well as to spinning compact binaries, for spin aligned or anti-aligned with the orbital angular momentum (Blanchet et al. 2013). In the context of the small mass-ratio approximation (see Sect. 4.3), analogous relations were established for a test particle or a small self-gravitating body orbiting a Kerr black hole, by accounting for the conservative part of the first-order gravitational self-force (GSF) (Le Tiec 2014a; Fujita et al. 2017). These various first laws of binary mechanics have proven useful for a broad variety of applications, including to:

- Determine the numerical values of the "ambiguity parameters" that appeared in the derivations of the 4PN two-body equations of motion (Jaranowski and Schäfer 2012; Jaranowski and Schäfer 2013, 2015; Damour et al. 2014b, 2016; Bernard et al. 2016, 2017a, b);
- Compute the exact first-order conservative GSF contributions to the gravitational binding energy and angular momentum for circular-orbit nonspinning black hole

binaries, allowing for a coordinate-invariant comparison to NR results (Le Tiec et al. 2012a);

- Calculate the GSF-induced correction to the frequency of the ISCO for Schwarzschild (Le Tiec et al. 2012a; Akcay et al. 2012) and Kerr ISCO (Isoyama et al. 2014; van de Meent 2017);
- Calibrate the potentials that enter the EOB model for circular orbits (Barausse et al. 2012b; Akcay et al. 2012) and mildly eccentric orbits (Akcay and van de Meent 2016; Bini et al. 2016a, b), and spin-orbit couplings for spinning binaries (Bini et al. 2015);
- Test the cosmic censorship conjecture in a scenario where a massive particle subject to first-order GSF falls into a nonspinning black hole along unbound orbits (Colleoni et al. 2015);
- Define the analogue of the redshift variable of a particle for black holes in NR simulations, this allowing further comparisons to the predictions of the PN and GSF approximations (Zimmerman et al. 2016; Le Tiec and Grandclément 2018);
- Provide a benchmark for the calculations of the first-order GSF-induced frequency shift of the Schwarzschild innermost bound stable orbit (Barack et al. 2019a) and the second-order GSF contribution to the gravitational binding energy (Pound et al. 2020).

The first law of binary mechanics for circular orbits has been extended to account for finite-size effects such as the rotationally-induced and tidally-induced quadrupole moments of the compact objects (Ramond and Le Tiec 2021, 2022). Other interesting directions would be to extend the first law to generic precessing spinning compact binaries, and to establish it in the context of the PM approximation and for unbound orbits.

4.2.4 Environmental effects

The evolution of relativistic magneto-hydrodynamics, circumbinary disks around supermassive binary black holes has been studied in the weak-field approximation. This relies on the techniques of matched asymptotics to analytically describe a non-spinning binary system up to 2.5PN order (Johnson-McDaniel et al. 2009; Mundim et al. 2014), on which the magnetic field is then numerically evolved (Noble et al. 2012; Zilhão et al. 2015a). These results have later been extended to spinning, non-precessing binary black-holes (Gallouin et al. 2012; Ireland et al. 2016) and to spinning, precessing black-hole spacetimes (Nakano et al. 2016).

Another astrophysical environmental effect concerns the presence of a third body around a massive binary back hole. Hierarchical triples may undergo several type of resonances (Kuntz 2022), that can result for example in von Zeipel–Kozai–Lidov oscillations (von Zeipel 1910; Kozai 1962; Lidov 1962). This is an interchange between the eccentricity of the two-body inner orbit and its inclination relative to the plane of the third body studied. Such an effect is particularly interesting for LISA as it involves high eccentricity systems and can result in an enhancement of

gravitational radiation. A general-relativistic treatment of triple hierarchical systems has been performed in a weak-field approximation up to 2.5PN order in the dynamics (Bonetti et al. 2016). The quadrupolar and octupolar waveforms have also been obtained by numerically integrating the three-body system trajectories from the PN expansion (Bonetti et al. 2017; Will 2017; Chandramouli and Yunes 2022). Other studies on the von Zeipel–Kozai–Lidov oscillations in GR have employed an expansion in powers of the ratio between the two semi-major axes up the hexadecapole order (Bonetti et al. 2017) and later to second-order in the quadrupolar perturbation (Will 2021). Finally, an effective two-body approach to the hierarchical three-body problem has been proposed (Kuntz et al. 2021) and the mass quadrupole to 1PN order was derived under this formalism (Kuntz et al. 2023).

4.2.5 Challenges

Post-Newtonian information in data analysis enters primarily through the use of semi-analytical models (see Sects. 4.5, 4.6). To avoid parameter estimation biases due to waveform uncertainties, developments in PN theory will be needed to increase the accuracies of these models for the next generation of GW detectors (see Sect. 3 and Pürrer and Haster (2020) for a discussion in the context of third-generation ground-based detectors).

One of the most significant challenges in the PN formalism will be the completion of the 5PN order. First, due to the so-called "effacement principle" (Damour 1983), the point-particle approximation breaks at this order. Finite-size and tidal effects have to be taken into account, the latter being known up to 7.5PN (Flanagan and Hinderer 2008; Vines et al. 2011; Damour et al. 2012b; Bini et al. 2012; Henry et al. 2020). In addition, due to the complexity of the computations involved, it seems highly unlikely to achieve the derivation of the complete gravitational phase at 5PN during the next decade, even if partial results are already obtained. In this regard, the interplay with GSF and scattering amplitudes will be crucial to make significant progress in this direction.

Exploiting the links between asymptotic symmetries and hereditary effects in the PN formalism should improve the matching to NR as memory effects are starting to be included in NR waveforms (Mitman et al. 2021b) (see also Sect. 4.1).

Regarding spinning binary systems, although the orbital dynamics are known up to the 4PN order, it might not be sufficient for LISA data analysis. In the near future one should primarily focus, at lower orders, on the exterior gravitational field, outside the matter source, extending to infinity. Indeed, new multipole moments will have to be computed to reach the same level of accuracy for the GW amplitude as for the flux, notably the 3PN SS contributions to the current quadrupole. The next step will consist in moving on to 4PN order, to do as well as the current equations of evolution. For this purpose, the NNL SS piece of the 4PN mass quadrupole will be required.

Another important topic, in order to combine information coming from the PN framework and numerical relativity, will be to connect the magnitude of the spin used in PN expressions to the rigorous definitions employed in numerical simulations (Brown and York 1993; Ashtekar et al. 2001). The problem of comparing the

spin axis is even more intricate since, for now, its direction has not been given a satisfactory unambiguous meaning in any of these schemes (Owen et al. 2019).

Regarding eccentric waveforms, most current models have focused on a low eccentricity expansion and non-spinning or aligned spin systems. It is crucial to make progress in both directions. First one has to go beyond the small eccentricity approximation, as some have started investigating (Moore et al. 2018; Moore and Yunes 2019). Second, it will be important to have reliable fully precessing and eccentric waveforms in order to span all the parameter space expected for LISA sources.

Notwithstanding the amount of work and progress already made, studies of the scattering of compact objects still explore a relatively uncharted territory. Obvious extensions of the work reported above will involve pushing scattering calculations of both spinning and nonspinning systems to higher PM orders in the conservative sector, both from a fully classical and amplitude approach. Such new information would help in obtaining new nontrivial PN information via the continued exploitation of the scattering angle's mass-ratio dependence, as well as continuing the fruitful exchange between the communities. The interconnectedness of the PM, PN and GSF approximations should also be explored in the context of tidal effects (information from PM is available, e.g., Cheung and Solon 2020b). Scattering studies should also explore dissipative radiation-reaction effects. It is important to push these calculations, so that the accuracy gained in the dissipative dynamics goes on par with that of the conservative sector.

4.3 Small-mass-ratio approximation (gravitational self-force)

Coordinators: Marta Colleoni and Adam Pound
Contributors: S. Akcay, E. Barausse, B. Bonga, R. Brito, M. Casals, G. Compere, A. Druart, L. Durkan, A. Heffernan, T. Hinderer, S. A. Hughes, S. Isoyama, C. Kavanagh, L. Kuchler, A. Le Tiec, B. Leather, G. Lukes-Gerakopoulos, O. Long, P. Lynch, C. Markakis, A. Maselli, J. Mathews, C. O'Toole, Z. Sam, A. Spiers, S. D. Upton, M. van de Meent, N. Warburton, V. Witzany

4.3.1 Description

When the secondary object in a binary is significantly smaller than the primary, we can treat the mass ratio $\epsilon = m_2/m_1 = 1/q$ as a small parameter and seek a perturbative solution for the spacetime metric, $g_{\alpha\beta} = g^{(0)}_{\alpha\beta} + \epsilon h^{(1)}_{\alpha\beta} + \epsilon^2 h^{(2)}_{\alpha\beta} + \ldots$ The background metric $g^{(0)}_{\alpha\beta}$ then describes the spacetime of the primary in isolation, typically taken to be a Kerr BH. At zeroth order, the secondary behaves as a test mass in the background, moving on a geodesic of $g^{(0)}_{\alpha\beta}$. At subleading orders, it generates

the perturbations $h^{(n)}_{\alpha\beta}$, which then exert a *self-force* back on it, accelerating it away from geodesic motion and driving the inspiral. These perturbations $h^{(n)}_{\alpha\beta}$ also encode the emitted waveforms.

The perturbative field equations and trajectory of the secondary are determined using *GSF theory*, a collection of techniques for incorporating a small gravitating object into an external field (Poisson et al. 2011; Harte 2015; Pound 2015b; Barack and Pound 2019; Pound and Wardell 2021). Using matched asymptotic expansions (or EFT (Galley and Hu 2009)), the small object is reduced to a point particle, or more generally to a puncture in the spacetime geometry, equipped with the object's multipole moments. For a compact object, higher moments scale with higher powers of the small mass m_2, such that one additional multipole moment appears at each order in ϵ. This multipolar particle (or puncture) is found to obey a generalized equivalence principle, behaving as a test body in a certain effective, smooth, vacuum metric $g^{(0)}_{\alpha\beta} + \epsilon h^{\mathrm{R}(1)}_{\alpha\beta} + \epsilon^2 h^{\mathrm{R}(2)}_{\alpha\beta} + \ldots$ (Mino et al. 1997b; Quinn and Wald 1997; Detweiler 2001; Detweiler and Whiting 2003; Gralla and Wald 2008; Pound 2010a; Gralla 2011; Harte 2012; Detweiler 2012; Pound 2012b; Gralla 2012; Harte 2015; Pound 2017; Upton and Pound 2021).

The *regular fields* $h^{\mathrm{R(n)}}_{\alpha\beta}$ that influence the secondary's motion can be calculated directly, using a puncture scheme in which they are the numerical variables (Barack et al. 2007; Vega and Detweiler 2008). Alternatively, they can be extracted from the full fields $h^{(n)}_{\alpha\beta}$ using a mode-by-mode subtraction (Barack and Ori 2000, 2003a, b; Barack et al. 2002; Heffernan et al. 2012, 2014; Heffernan 2022) or other methods (Casals et al. 2009; Wardell et al. 2014), as reviewed in Barack (2009); Wardell and Warburton (2015); Pound and Wardell (2021). In either approach, the perturbative field equations can be solved using the methods of BHPT (Regge and Wheeler 1957; Zerilli 1970b; Teukolsky 1973; Wald 1973; Chrzanowski 1975; Wald

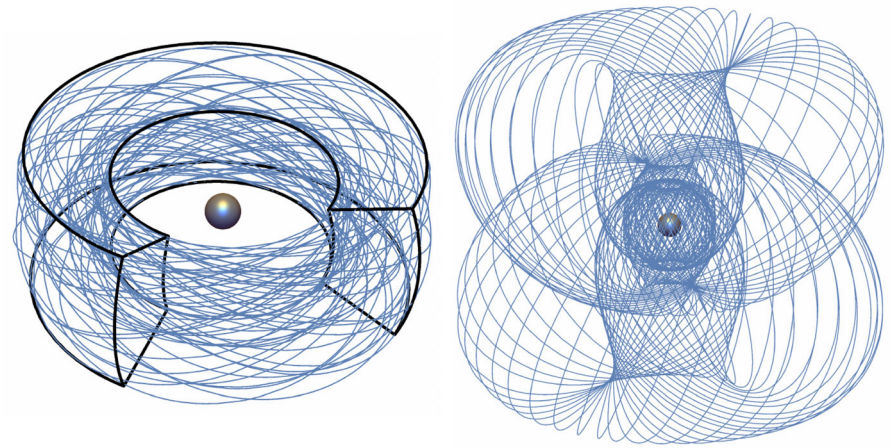

Fig. 5 Geodesics of Kerr spacetime. Left: a non-resonant geodesic, which fills a toroidal shape. Right: a resonant geodesic. Images taken from Barack and Pound (2019)

1978; Kegeles and Cohen 1979; Sasaki and Tagoshi 2003; Martel and Poisson 2005; Barack and Lousto 2005; BHPToolkit 2024; Pound and Wardell 2021).

A key feature of this model is its clean separation of time scales: because the self-force is small, inspirals occur slowly, over $\sim 1/\epsilon$ orbits. On the time scale of a few orbits, the secondary's trajectory is approximately a bound geodesic of $g^{(0)}_{\alpha\beta}$ (illustrated in Fig. 5), which in Kerr spacetime is generically triperiodic, undergoing radial, polar, and azimuthal motion with frequencies Ω_r, Ω_θ, and Ω_ϕ (Schmidt 2002; Mino 2003; Fujita and Hikida 2009; Grossman et al. 2012; Pound and Wardell 2021). Over the long inspiral, the frequencies slowly evolve due to dissipation. The field equations can therefore be solved using a two-timescale expansion (Mino and Price 2008; Hinderer and Flanagan 2008; Pound 2010b, 2015c; Miller and Pound 2021; Flanagan et al. 2024; Pound and Wardell 2021), $h^{(n)}_{\alpha\beta} = \sum_{k^A\in\mathbb{Z}} h^{(n,k^A)}_{\alpha\beta}(J^B, x^a)e^{ik^A\psi_A}$. Here x^a are spatial coordinates, and all time dependence is encoded in the set of system parameters J^A (the secondary's orbital energy, angular momentum, and Carter constant, the primary's mass and spin, etc.), and the set of orbital phases ψ_A. The parameters J^A evolve slowly, on the inspiral time scale $t \sim 2\pi/(\epsilon\Omega)$, while the phases ψ_A evolve on the orbital time scale $t \sim 2\pi/\Omega$, with evolution equations of the form Hinderer and Flanagan (2008); Van De Meent and Warburton (2018); Miller and Pound (2021); Flanagan et al. (2024); Pound and Wardell (2021)

$$\frac{dJ^A}{dt} = \epsilon G^A_{(1)}(J^B) + \epsilon^2 G^A_{(2)}(J^B) + O(\epsilon^3), \quad \frac{d\psi_A}{dt} = \Omega^{(0)}_A(J^B) + \epsilon\Omega^{(1)}_A(J^B) + O(\epsilon^2). \tag{13}$$

Formulating the problem in this way enables practical methods of solving the Einstein equations (Miller and Pound 2021; Pound and Wardell 2021) as well as facilitating rapid waveform generation (Van De Meent and Warburton 2018; Pound and Wardell 2021; Lynch et al. 2022).

The two-timescale description will frame much of the discussion below. However, there are some special cases of interest that it does not apply to, such as scattering orbits (Hopper 2018; Hopper and Cardoso 2018; Long and Barack 2021; Barack and Long 2022; Long 2022). Even in an inspiral, there are regions of parameter space in which the approximation breaks down: at the end of the inspiral, when the secondary transitions into a final plunge into the primary (Buonanno and Damour 2000; Ori and Thorne 2000; Apte and Hughes 2019; Burke et al. 2020; Compère et al. 2020b; Compère and Küchler 2022), and during resonances, which occur when at least two of the frequencies Ω_A have a rational ratio, causing a linear combination of phases, $k^A\psi_A$, to become approximately stationary (Tanaka 2006; Flanagan and Hinderer 2012; Lukes-Gerakopoulos and Witzany 2022). Such resonances can arise from a variety of physical causes, outlined below, with significant observational consequences.

Many of the core tools in GSF modelling, as well as advanced codes described in the sections below, have been consolidated in the open-source Black Hole Perturbation Toolkit (BHPToolkit 2024), which provides a hub for GSF code development, as well as in the Black Hole Perturbation Club (BHPClub 2024). In

particular, the Fast EMRI Waveforms (FEW) package (Katz et al. 2021), which exploits GSF models' multiscale structure, has provided a flexible framework for rapid waveform generation.

4.3.2 Suitable for what sources?

Historically, the GSF approximation has been motivated by EMRIs, with mass ratios in the interval $10^{-7} \lesssim \epsilon \lesssim 10^{-3}$ as far as LISA sources are concerned (see Table 3). The GSF model's accuracy for a typical EMRI can be estimated from the evolution Eq. (13). On the inspiral time scale, the solutions for the orbital phases, and therefore the GW phase, take the form

$$\psi_A = \frac{1}{\epsilon}\left[\psi_A^{(0)} + \epsilon\psi_A^{(1)} + O(\epsilon^2)\right]. \tag{14}$$

Following (Hinderer and Flanagan 2008), the leading term in this expansion is referred to as *adiabatic* order (0PA), and the nth subleading term as nth *post-adiabatic* order (nPA). An adiabatic approximation, which has large phase errors $\sim \epsilon^0$ over an inspiral, is expected to suffice for detection of EMRIs using the semi-coherent searches discussed in Sect. 3.3.1. A 1PA approximation, which will have phase errors $\sim \epsilon \ll 1$ rad over the final year of inspiral, should suffice for parameter extraction even for loud EMRIs with SNR > 50.

A large and growing body of evidence (Fitchett and Detweiler 1984; Anninos et al. 1995; Favata et al. 2004; Le Tiec et al. 2011, 2012a; Sperhake et al. 2011; Le Tiec et al. 2013; Nagar 2013; van de Meent 2017; Zimmerman et al. 2016; Le Tiec and Grandclément 2018; Rifat et al. 2020; van de Meent and Pfeiffer 2020; Warburton et al. 2021; Wardell et al. 2023; Albertini et al. 2022b; Ramos-Buades et al. 2022b) suggests that the GSF approximation can also accurately model IMRIs (see Table 4). It can even provide a useful model of CO binaries with *comparable* masses when it is re-expressed as an expansion in powers of the symmetric mass ratio $\nu \equiv m_1 m_2/(m_1+m_2)^2 = \epsilon + O(\epsilon^2)$. We refer to Le Tiec (2014b) for an early review and Albertini et al. (2022b); Ramos-Buades et al. (2022b) for recent analyses of the accuracy of 1PA models in the $1 \lesssim q \lesssim 100$ regime. Further study is required to assess whether 1PA models meet expected accuracy requirements for specific classes of astrophysical sources in this range of mass ratios.

Besides compact binary inspirals, the GSF approximation can be used for other classes of sources. A leading-order GSF model, comprising a point source on a geodesic trajectory, should be suitable for XMRIs (Amaro-Seoane 2019; Gourgoulhon et al. 2019) and fly-by burst signals (Hopper 2018; Hopper and Cardoso 2018; Long and Barack 2021; Barack and Long 2022; Long 2022). GSF theory may also be relevant for modelling gravitational waves from cosmic strings (Blanco-Pillado et al. 2018b; Chernoff et al. 2019; Blanco-Pillado et al. 2019). Inspirals of less compact bodies into MBHs (e.g., white or brown dwarfs or main-sequence stars prior to tidal disruption), and three-body "binary EMRIs", can be modelled by including sufficiently high multipole moments in the particle or puncture (Steinhoff and Puetzfeld 2012; Chen and Han 2018; Rahman and Bhattacharyya 2023).

4.3.3 Status

The current status of GSF models is summarized in Fig. 6, which also summarizes the necessary inputs for a waveform model at 0PA and 1PA order.

4.3.3.1 Adiabatic approximation At leading order in the two-timescale expansion, only the geodesic frequencies $\Omega_A^{(0)}$ and time-averaged dissipative piece $G^A_{(1)}$ of the first-order self-force are required to drive the evolution (Mino 2003, 2005). The secondary's motion in this approximation can be regarded as an adiabatic inspiral through a sequence of geodesic orbits (Hinderer and Flanagan 2008; Hughes et al. 2005). The waveform can then be built from a corresponding sequence of "snapshot" Fourier mode amplitudes together with the leading phases in Eq. (14). Alternatively, outside the two-timescale scheme, a time-domain field equation can be solved with an adiabatically inspiraling source particle (Sundararajan et al. 2008; Barausse et al. 2012a; Taracchini et al. 2014a; Harms et al. 2014; Rifat et al. 2020).

$G^A_{(1)}$ is most conveniently computed using "flux-balance" formulas (Gal'tsov 1982; Drasco et al. 2005; Sago et al. 2005; Isoyama et al. 2013, 2019), in which the "work" done by the dissipative self-force balances the fluxes of gravitational waves to infinity and down the horizon (or flux-like quantities in the case of the Carter constant). Methods of computing fluxes in GSF theory are well developed (Press and Teukolsky 1973; Teukolsky and Press 1974; Nakamura et al. 1987; Martel 2004; Poisson 2004; Sundararajan et al. 2007, 2008; Zenginoglu and Khanna 2011; Harms et al. 2014), and have been numerically implemented for generic (inclined and eccentric) geodesics about a Kerr BH (Hughes 2000; Glampedakis and Kennefick 2002; Drasco and Hughes 2006; Fujita et al. 2009). The fluxes have also been calculated analytically (by expanding $h^{(1)}_{\alpha\beta}$ in a PN series (Mano et al. 1996; Mino

Background Spacetime	Orbital Configuration	Adiabatic	Post-1-adiabatic			
		1SF (Dissipative)	1SF (Conservative)	2SF (Dissipative)	Spin Effects (Conservative)	Spin Effects (Dissipative)
Schwarzschild	Circular	✓✓✓	✓✓✓	✓✓✓	✓✓✓	✓✓✓
	Eccentric	✓✓✓	✓✓✓	✗	✓✓ , ✓✓✓*	✓, ✓✓*
Kerr	Circular	✓✓✓	✓✓	✗	✓,✓✓*	✓✓✓*
	Eccentric Equatorial	✓✓✓	✓✓	✗	✓,✓✓*	✓✓*
	Generic	✓✓✓	✓	✗	✓	✓*
	Resonances	✓✓✓	✓	✗	✗	✗

✓✓✓ Evolving Waveform ✓✓ Driven Inspiral ✓ Snapshot Calculation *(Anti-)Aligned Spin Only

Fig. 6 Progress in modelling EMRIs using GSF methods. '1SF' and '2SF' indicate calculations involving the first or second-order self-force, respectively, and 'spin effects' indicates calculations that take into account the secondary's spin (the spin of the primary is accounted for in all 'Kerr' calculations). 'Snapshot calculations' (single tick) are ones in which self-force effects are calculated on fixed geodesic orbits

et al. 1997a; Sasaki and Tagoshi 2003)) to high PN order for circular (Fujita 2012, 2015; Shah 2014), eccentric (Tagoshi 1995; Munna et al. 2020; Munna and Evans 2020), and generic orbital configurations (Sago et al. 2006; Ganz et al. 2007; Sago and Fujita 2015).

After decades of progress (Cutler et al. 1994; Finn and Thorne 2000; Hughes 2001; Fujita and Iyer 2010; Pan et al. 2011b; Gralla et al. 2016; Burke et al. 2020; Chua et al. 2021; Fujita and Shibata 2020), adiabatic inspirals and waveforms are now being computed for generic orbits in Kerr, both numerically (Hughes et al. 2021) and within the analytical BHPT-PN framework mentioned above (Isoyama et al. 2022).

Once fluxes and waveform mode amplitudes have been computed across the parameter space, adiabatic waveforms can be efficiently generated using a combination of neural network and reduced-order techniques (Chua et al. 2021; Katz et al. 2021), a method that lends itself to graphical processing unit (GPU) acceleration techniques; see Sect. 5.2. This approach should ultimately meet the efficiency requirements described in Sect. 3.3.1. However, due to the high-dimensional parameter space, significant work remains to populate the parameter space. As a consequence, data analysis development has so far relied on semirelativistic "kludge" models that seek to capture all the qualitative features of EMRI waveforms while sacrificing accuracy (Barack and Cutler 2004; Babak et al. 2007; Chua and Gair 2015; Chua et al. 2017; EMRI Kludge Suite 2024). These models typically combine (i) post-Newtonian information about the orbital dynamics, (ii) qualitative (and sometimes quantitative) features of the fully relativistic 0PA orbital evolution, and (iii) a post-Newtonian (e.g., Peters and Mathews 1963) multipolar formula for the emitted waveform. The most advanced of such models, the Augmented Analytical Kludge (Chua et al. 2017), is available in the the FEW package (Katz et al. 2021).

4.3.3.2 Post-1-adiabatic self-force effects: 1SF The 1PA terms in the two-timescale expansion ($\Omega_A^{(1)}$ and $G^A_{(2)}$) take as input the conservative piece of the first-order self-force (1SF, $\propto h^{(1)}_{\alpha\beta}$) and the dissipative piece of the second-order self-force (2SF, $\propto h^{(2)}_{\alpha\beta}$). Once these ingredients have been computed, a 1PA waveform-generation scheme takes the same form as a 0PA one (Miller and Pound 2021; Pound and Wardell 2021).

Numerical computations of the full first-order self-force have made tremendous progress, evolving from Lorenz-gauge calculations (Barack and Lousto 2005; Barack and Sago 2007, 2010; Dolan and Barack 2013; Akcay et al. 2013; Osburn et al. 2014; Isoyama et al. 2014; Wardell and Warburton 2015) to more efficient methods relying on radiation gauges (Keidl et al. 2010; Shah et al. 2011; Pound et al. 2014; Merlin and Shah 2015; van de Meent and Shah 2015; van de Meent 2016; Merlin et al. 2016; van De Meent 2017). These developments culminated in 1SF calculations along generic bound geodesics in Kerr spacetime (van de Meent 2018), and work is still ongoing to further improve 1SF methods (Toomani et al. 2022; Dolan et al. 2022; Panosso Macedo et al. 2022).

High-precision numerics and BHPT-PN methods have also made possible high-order PN expansions of numerous conservative invariants, such as the Detweiler redshift (Shah et al. 2012a, 2014; Bini and Damour 2014a; Hopper et al. 2016; van de Meent and Shah 2015; Johnson-McDaniel et al. 2015; Kavanagh et al. 2016; Bini et al. 2018a; Bini and Geralico 2019c), the periastron advance (van de Meent 2017; Bini and Geralico 2019a), and other invariants (Nolan et al. 2015; Shah and Pound 2015; Bini and Geralico 2015; Bini et al. 2018b; Bini and Geralico 2019b; Munna and Evans 2022), which have played a key role in the synergies with PN theory and EOB described in Sects. 4.2 and 4.5.

Modern 1SF calculations mostly rely on frequency-domain methods and mode-by-mode subtraction or puncture schemes to calculate $h^{\mathrm{R}(1)}_{\alpha\beta}$. However, there have also been advances in time domain (TD) calculations based on either finite-difference schemes (Barack and Giudice 2017; Hughes et al. 2005; Long and Barack 2021; Da Silva et al. 2023) or spectral methods (Canizares and Sopuerta 2009, 2010, 2011; Field et al. 2009; Diener et al. 2012; Markakis et al. 2021; Da Silva et al. 2023; Vishal et al. 2024), along with improved time-stepping methods (O'Boyle et al. 2022; Markakis et al. 2023; Da Silva et al. 2023; O'Boyle and Markakis 2023). There is also ongoing work to directly obtain the retarded Green function (Casals et al. 2013; Wardell et al. 2014; Casals et al. 2019; Yang et al. 2014; O'Toole et al. 2021), which would then allow direct evaluation of the self-force (Mino et al. 1997b; Quinn and Wald 1997).

As at 0PA, calculations of the self-force and of GW amplitudes across the parameter space have been used to simulate self-forced inspirals (Warburton et al. 2012; Osburn et al. 2016; Van De Meent and Warburton 2018; Lynch et al. 2022, 2024) and generate waveforms (Lackeos and Burko 2012; Osburn et al. 2016). To date, this has only been done for equatorial orbits and quasi-spherical orbits (Lynch et al. 2024), due to the computational expense of current 1SF calculations for generic orbits.

4.3.3.3 Post-1-adiabatic self-force effects: 2SF The dissipative piece of the second-order self-force ($G^{A}_{(2)}$) contributes to the GW phasing at the same 1PA order as the first-order conservative self-force, but calculations of it are less mature. After years of development of the governing formalism (Rosenthal 2006; Detweiler 2012; Pound 2012b; Gralla 2012; Pound 2012a, 2015a, 2017; Upton and Pound 2021) and of practical implementation methods (Pound and Miller 2014; Warburton and Wardell 2014; Wardell and Warburton 2015; Pound 2015c; Miller et al. 2016; Miller 2017; Pound and Wardell 2021; Durkan and Warburton 2022; Spiers et al. 2024b), (Pound et al. 2020; Warburton et al. 2021; Wardell et al. 2023) recently carried out the first concrete calculations of physical second-order quantitities in the restricted case of quasicircular orbits around a Schwarzschild BH. These calculations culminated in the first complete 1PA waveforms in Wardell et al. (2023). Figure 7 shows a comparison between one of these 1PA waveforms and an NR waveform for $q = 10$. As alluded to in Sect. 4.3.2, the 1PA approximation agrees well with NR even at this moderate mass ratio. These 1PA waveforms have also more recently been extended to include a slowly spinning primary (Mathews et al. 2024). Section 4.3.5 discusses the next

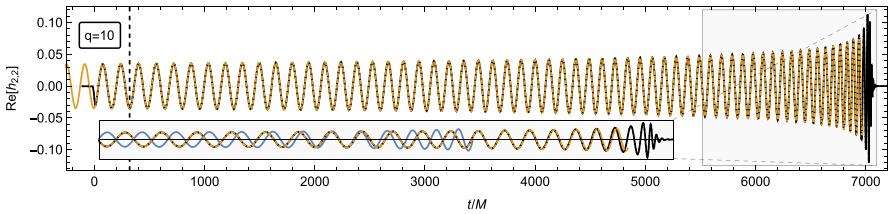

Fig. 7 1PA GSF waveform for a quasicircular, nonspinning binary with mass ratio $q = 10$ (orange). The inset shows a zoomed portion of the waveform near the merger. Also included for comparison are the 0PA GSF waveform (blue, inset only) and the waveform for the same binary produced using an NR simulation in the SXS catalog (Boyle et al. 2019) (SXS:BBH:1107, in black). The three waveforms are aligned in time and phase at $t = 320M$, when the orbital separation is $\approx 13.83M$. Image reproduced from Wardell et al. (2023)

major barrier in GSF calculations: 2SF calculations with a rapidly spinning primary, eccentricity, and inclination.

4.3.3.4 Transient resonances Resonances are a ubiquitous feature of the strong-field dynamics around BHs in GR (Brink et al. 2015a, b), and their observational imprints on waveforms can be significant. Transient self-force resonances, between the orbital frequencies Ω_r and Ω_θ, will have strong observational consequences for EMRIs (Mino 2005; Tanaka 2006; Levin and Perez-Giz 2008; Apostolatos et al. 2009; Flanagan and Hinderer 2012). Essentially *all* LISA-type EMRIs pass through at least one dynamically significant resonance, leading to a large, $O(1/\sqrt{\epsilon})$ (i.e., 0.5PA) contribution to the waveform phase (Ruangsri and Hughes 2014; Berry et al. 2016; Mihaylov and Gair 2017). The magnitude of this effect depends sensitively on the orbital phase at the resonance. As a result, modelling it requires 1PA accuracy prior to resonance. There are ongoing efforts to understand the impact of these resonances and include them in evolutions (Gair et al. 2012; Flanagan et al. 2014; van de Meent 2014a; Isoyama et al. 2013; Lewis et al. 2017; Isoyama et al. 2019, 2022; Lukes-Gerakopoulos and Witzany 2022; Nasipak and Evans 2021; Nasipak 2022; Gupta et al. 2022b).

There also occur resonances between the r and φ frequencies and between the θ and φ frequencies. These do not change the intrinsic inspiral dynamics, but they can lead to a strong net emission of linear momentum that results in a 'kick' to the system's center of mass (Hirata 2011; van de Meent 2014b). The maximum kick velocity can reach $\sim 30,000 \times \epsilon^{3/2}$ km/s (depending on the primary spin and on the orbital eccentricity): for IMRI systems, these values could be comparable to the escape velocities from globular clusters, which are typically of the order of a few tens of km/s (Merritt et al. 2004; Antonini and Rasio 2016).

4.3.3.5 Merger and ringdown The two-timescale expansion breaks down as the secondary object approaches the separatrix between bound and plunging orbits. There, the secondary enters a gradual transition across the separatrix (Buonanno and Damour 2000; Ori and Thorne 2000; Burke et al. 2020; Compère et al. 2020b) followed by an approximately geodesic plunge. The transition motion has been

mostly studied within the EOB framework using resummed PN expansions (Buonanno and Damour 2000; Buonanno et al. 2006; Nagar et al. 2007; Damour and Nagar 2007, 2009; Bernuzzi and Nagar 2010; Bernuzzi et al. 2011a, b; Pan et al. 2014) or within the GSF approach using simplifying approximations (Ori and Thorne 2000; Sundararajan 2008; Kesden 2011; Taracchini et al. 2014a; Apte and Hughes 2019; Compère et al. 2020b; Burke et al. 2020). Merger-ringdown waveforms have been generated from the final plunge at first order (Folacci and Ould El Hadj 2018; Rom and Sari 2022), and complete inspiral-merger-ringdown waveforms have been generated by solving time-domain equations for first-order perturbations sourced by the combined inspiral-transition-plunge motion (Barausse et al. 2012a; Taracchini et al. 2014a; Harms et al. 2014; Rifat et al. 2020; Islam et al. 2022). Only recently, (Compère and Küchler 2021, 2022; Küchler et al. 2024) took a first step toward 1PA/2SF inspiral-merger-ringdown waveforms by developing a systematic expansion of the transition motion and metric perturbation that matches to the two-timescale expansion for quasicircular, equatorial inspirals into a Kerr BH.

4.3.3.6 Spin and finite-size effects When its multipole structure is accounted for, the secondary obeys the Mathisson–Papapetrou–Dixon equations of a test body (Mathisson 1937; Papapetrou 1951; Dixon 1970a, b, 1974) in the effective metric; such a result is expected to hold to all perturbative orders for both BHs and material bodies (Thorne and Hartle 1984; Harte 2012, 2015).

The spin contributes first-order conservative and second-order dissipative forces in the equations of motion, leading to 1PA, $\mathcal{O}(\epsilon^0)$ contributions to the final inspiral phase (Mathews et al. 2022). Spin also generally breaks the integrability of Kerr geodesic motion (Suzuki and Maeda 1997); the resulting potential phenomena, like prolonged resonances, can leave a significant imprint on the gravitational waves (Rudiger 1983; Suzuki and Maeda 2000; Ruangsri et al. 2016; Witzany 2019; Zelenka et al. 2020) and may contribute $\mathcal{O}(1)$ to the GW phase. Away from these resonances, the spinning-particle motion is perturbatively separable to linear order in spin (Witzany 2019) and easily incorporated into a two-timescale approximation (Witzany et al. 2020; Mathews et al. 2022).

For dissipative effects, a spin-flux balance law has been established (Akcay et al. 2020), and GW fluxes were computed for a variety of binary configurations (Mino et al. 1996; Tanaka et al. 1996; Han 2010; Harms et al. 2016a, b; Lukes-Gerakopoulos et al. 2017; Nagar et al. 2019a; Akcay et al. 2020; Zelenka et al. 2020; Piovano et al. 2020; Skoupý and Lukes-Gerakopoulos 2021). Waveforms from generic inspirals into a Schwarzschild BH have also been computed including 1SF and first-order conservative spin effects (Warburton et al. 2017) but excluding dissipative spin effects. Waveforms including *all* 1PA spin effects from circular equatorial inspirals into Schwarzschild (Mathews et al. 2022) and Kerr BHs (Piovano et al. 2021) have been produced, and the spin's complete 1PA contribution to the GW phase has been calculated for eccentric equatorial inspirals into a Kerr BH (Skoupý and Lukes-Gerakopoulos 2022). A formulation of the first-order conservative spin-forced motion for generic orbits about a Kerr BH (Drummond and Hughes 2022a, b) paved the way for calculations of the spin's complete impact on fully generic 1PA

waveforms, beginning with recent snapshot computations of energy and angular momentum fluxes (Skoupy et al. 2023).

The secondary's higher moments are unlikely to contribute at 1PA order. The tidal quadrupole's contribution to the acceleration scales with ϵ^4 (Binnington and Poisson 2009) and can therefore only become relevant for non-compact objects. The spin also induces a quadrupole deformation of the secondary, which creates an acceleration $\sim\epsilon^2$ (Steinhoff and Puetzfeld 2012; Rahman and Bhattacharyya 2023) that is unlikely important for EMRIs (up to resonances) but might be relevant for IMRIs (Rahman and Bhattacharyya 2023).

4.3.4 Environmental effects

In the preceding sections, we have focused on the simplest GSF model: an isolated vacuum BH orbited by a single body. This will not fully describe astrophysical small-mass-ratio binaries. Accreting matter will be present at some level, and there are likely to be additional bodies nearby. Accounting for these effects will be necessary to achieve the stringent accuracy requirements that EMRIs, in particular, place on GSF models.

There are three ways we can modify GSF models to include such effects: (i) perturbatively, by adding "small" matter fields or metric perturbations to the spacetime, which then exert small forces on the secondary; (ii) non-perturbatively, by modifying the background spacetime and introducing "large" matter fields; (iii) by changing boundary conditions, imagining (for example) modifications very near the BH horizon or non-asymptotically flat perturbations due to external matter. Section 6 discusses how these classes of modifications can also be used to incorporate beyond-GR effects.

Although important aspects of the astrophysical environment of EMRIs are uncertain, it is expected that there will be other stellar-mass bodies nearby. These bodies create an additional metric perturbation, which should be sufficiently small to be treated as a linear perturbation. The influence of the perturbation is generally negligible, except at moments when two or more of the orbital frequencies characterising the perturbed EMRI system become commensurate. At those times, an EMRI experiences a tidal resonance (Yang and Casals 2017), an orbital resonance akin to the mean motion resonance known from planetary dynamics (Yang et al. 2019a). Calculations across the parameter space showed that a single resonance can dephase the waveform by several radians over the inspiral (Bonga et al. 2019; Gupta et al. 2021a, 2022a, b), and that most EMRIs will cross multiple tidal resonances before plunge. If LISA can reliably measure these resonances, they can be used to learn about the tidal environment of EMRI systems.

Accretion and gas interactions will also be present at some level in any astrophysical EMRI system. Order-of-magnitude estimates suggest they will be negligible unless the primary BH powers an AGN (in which case it would be surrounded by an accretion disk with which the secondary is likely to interact) (Barausse et al. 2014, 2015; Barausse and Rezzolla 2008; Suková et al. 2021). Since AGNs are believed to make up 1–10% of local galaxies, only a comparable

fraction of EMRIs are expected to be significantly affected by accretion and gas interactions. For those systems, accretion onto the primary and secondary, as well as dynamical friction from the disk and planetary-like migration within it, are expected to cause secular effects comparable to those of GW fluxes (Barausse et al. 2014, 2015; Barausse and Rezzolla 2008). Recently work has begun to incorporate the disk and other potential nonvacuum effects into GSF models by adding torques to 0PA Kerr models (Speri et al. 2023) or by working perturbatively on an exact nonvacuum background, assuming a spherically symmetric dark matter distribution (Cardoso et al. 2022b; Destounis et al. 2023b).

The direct gravitational pull from AGN disks is likely to be negligible (Barausse et al. 2014), but if more dense disks/rings exist in nature, the effect may be significant (Barausse et al. 2007). Exact spacetime solutions describing thin disks or rings around BHs (Lemos and Letelier 1994; Basovník and Semerák 2016; Semerák and Čížek 2020) show that orbits in such situations are non-integrable, exhibiting characteristic phenomena like chaos and prolonged resonances (Semerák and Suková 2015). If these effects are significant in realistic scenarios, GSF models should be able to account for them through perturbative corrections on top of a Kerr background (Yunes and Gonzalez 2006; Le Tiec et al. 2021; Gupta et al. 2022b; Polcar et al. 2022).

4.3.5 Challenges

The principal goal of GSF waveform modelling is to develop complete 1PA models for generic orbital configurations around a spinning, Kerr BH. To be complete, these models must include the spin of the companion, transitions across resonances, and the final plunge. They must also be sufficiently modular to incorporate beyond-GR and environmental effects, and there are strong motivations to explore other regions of the parameter space, such as scatter orbits and comparable masses. We summarize here the main challenges in developing and implementing such models.

4.3.5.1 Post-1-adiabatic calculations 1PA models are currently missing two ingredients: the effects of the companion's spin for generic binary configurations, and dissipative 2SF effects; see Fig. 6. Both must be incorporated into a unified two-timescale expansion of the field equations, the orbital motion, and the spin evolution.

While substantial work remains to calculate 1PA spin effects for generic binary configurations, these calculations can leverage existing methods for point-particle sources. Therefore, 2SF calculations represent the overriding obstacle to 1PA accuracy. Practical 2SF calculations have, thus far, been restricted to quasicircular orbits in a Schwarzschild background (Pound et al. 2020; Warburton et al. 2021; Wardell et al. 2023). As discussed in Sect. 2.2, the majority of EMRIs are expected to have significant eccentricity and may have highly precessing orbital planes when they enter the LISA band, meaning 2SF techniques need to be extended to cover generic orbital configurations. They must also be extended to the realistic case of a Kerr background.

Eccentricity and inclination bring multiple challenges. Most recent self-force calculations have utilized decompositions into Fourier modes (the natural setting of the two-timescale expansion) and angular harmonics. Eccentric, inclined orbits can require $\sim 10^5$ modes, all of which will couple to one another in the second-order source. The sum of Fourier modes can also suffer from poor convergence: in the existing 2SF puncture scheme, the source for $h^{\mathrm{R}(2)}_{\alpha\beta}$ has finite differentiability on the puncture's worldline, leading to slow power-law convergence (the Gibbs phenomenon). At first order, similar problems were overcome using methods of extended solutions (Barack et al. 2008; Warburton and Barack 2011; Hopper and Evans 2013; Akcay et al. 2013; Osburn et al. 2014; van de Meent and Shah 2015; van de Meent 2018) that restore exponential convergence. These have inspired a new scheme, applicable at second order, known as the method of extended effective sources (Leather and Warburton 2023), which has been demonstrated in the case of a scalar-field toy model for eccentric orbits about a Schwarzschild BH. Work now remains to apply it to gravitational perturbations, both at first and second order, and to orbits in Kerr spacetime.

The extension to Kerr spacetime brings more challenges. Second-order calculations in Schwarzschild have so far relied on directly solving the perturbative Einstein equations, which are not separable in Kerr spacetime. At first order, this problem was overcome using radiation-gauge methods, in which the metric perturbation is reconstructed from a solution to the (fully separable) Teukolsky equation (Teukolsky 1973; Chrzanowski 1975; Kegeles and Cohen 1979). One path to 2SF calculations is to extend that method to second order (Campanelli and Lousto 1999; Green et al. 2020; Toomani et al. 2022; Spiers et al. 2023). The standard method of metric reconstruction (Chrzanowski 1975; Kegeles and Cohen 1979) fails beyond linear order, but recent work found an extension to all orders (Green et al. 2020; Toomani et al. 2022). Recent work on second-order flux-balance laws (Grant 2023; Sam 2024) also suggests that 1PA rates of change of energy and angular momentum (though perhaps not the Carter constant) can be computed directly from a solution to the second-order Teukolsky equation, without the need for metric reconstruction.

An additional obstacle is that in radiation-gauge implementations, the first-order metric perturbation has gauge singularities that extend away from the particle. There is a rigorous procedure to extract physical 1SF quantities despite these singularities (Pound et al. 2014; Merlin et al. 2016; van De Meent 2017), but the singularities become ill defined in the second-order field equations (Toomani et al. 2022). Several avenues are being explored to resolve this problem (Toomani et al. 2022; Dolan et al. 2022; Osburn and Nishimura 2022; Dolan et al. 2024).

There are also challenges common to all these 2SF calculations: at second order, the field equations have a noncompact source that falls off slowly at large distances (Pound 2015c) and is burdensome to compute due to the strong nonlinear singularity at the particle (Miller et al. 2016). Recent work (Upton and Pound 2021; Spiers et al. 2023) has shown that both problems might be mitigated by using gauges adapted to the lightcone structure of the perturbed spacetime. However, additional work will be required to implement these gauge choices in a practical numerical scheme.

4.3.5.2 Covering the parameter space Even once numerical implementations of all necessary ingredients are available, spanning the full EMRI parameter space remains a considerable challenge at both 0PA and 1PA orders. This is due to the high dimensionality of the parameter space and the high computational burden of self-force calculations, particularly at second order. Covering the EMRI parameter space will likely involve a combination of (i) using analytic results to reduce the region of the parameter space where high-precision interpolation of numerical data is required, (ii) better interpolation methods, and (iii) improvements in computational efficiency of current numerical calculations. We address each of these three below in the context of 0PA inspirals, 1PA inspirals, and waveform calculations. Computing adiabatic inspirals requires interpolating the rates of change ($G^A_{(1)}$) of the orbital energy, angular momentum, and Carter constant across the four-dimensional parameter space of the primary spin and three orbital elements. For an adiabatic model sufficiently accurate to build 1PA corrections upon, we need to interpolate $G^A_{(1)}$ to better than a relative accuracy of ϵ^{-1}. The central challenge is then constructing such a high-accuracy interpolant over the 4D parameter space. Recent work has demonstrated advantages of Chebyshev interpolation for this purpose (Lynch et al. 2022). The region of the parameter space, and the accuracy of the interpolation of the numerical data, can also be reduced by constructing global fits informed by analytic results.

At 1PA order we must also compute the change in the mass of the primary during the inspiral (Miller and Pound 2021), and so the parameter space grows to five dimensions. There are also corrections due the spin of the secondary, but fortunately, these can be added on separately. At 1PA order the accuracy requirements of the contributions are much lower, at $\sim 10^{-2}$–10^{-3} relative (Osburn et al. 2016). This should allow analytic results to assist in reducing the parameter space that numerical results need to cover. Such analytical results could be obtained by extending BHPT-PN calculations. Alternatively, they could be obtained from EOB dynamics, following the programme in (Han and Cao 2011; Han 2014, 2016; Han et al. 2017; Zhang et al. 2021a, b; Shen et al. 2023). Regions of high eccentricity may also be more easily covered using advanced time-domain codes (Canizares et al. 2010; Field et al. 2009; Diener et al. 2012; Markakis et al. 2021; Barack and Giudice 2017; Long and Barack 2021; O'Boyle et al. 2022; Da Silva et al. 2023; Vishal et al. 2024).

4.3.5.3 Extending the parameter space The challenges above are centered on "vanilla" regions of the parameter space: the inspiral phase away from resonances, which is amenable to a two-timescale expansion. However, it is also critical to include accurate transitions across resonances, particularly in the EMRI regime. In addition to the dominant r-θ resonances that occur in a self-forced inspiral, prolonged resonances may occur due to spin, external matter, or a non-Kerr central object (Apostolatos et al. 2009; Destounis et al. 2021; Lukes-Gerakopoulos and Witzany 2022). Similarly, the transition from inspiral to plunge can also be important, particularly for more comparable masses (Rifat et al. 2020; van de Meent and Pfeiffer 2020; Albertini et al. 2022b). Both resonances and the plunge will require matching the two-timescale expansion to specialized approximations in those parameter regions (van de Meent 2014a; Berry et al. 2016; Pound and Wardell 2021;

Lukes-Gerakopoulos and Witzany 2022; Compère and Küchler 2021, 2022; Gupta et al. 2022b).

There are also reasons to compute self-force effects on scattering orbits, whether to model hyperbolic, burst sources or to inform PM and PN dynamics, as described in 4.2.3.4 (and possibly to infer properties of bound, self-forced orbits (Kälin and Porto 2020b; Gonzo and Shi 2023)). Explorations of scatter orbits have only recently begun (Barack and Long 2022; Long 2022; Barack et al. 2023; Whittall and Barack 2023). While bound-orbit self-force calculations can utilize the orbit's discrete Fourier spectrum, scatter orbits have a continuous spectrum (Hopper and Cardoso 2018; Hopper 2018), suggesting some clear advantages to simulations in the time domain (Barack et al. 2019a; Barack and Long 2022; Long 2022).

In addition to including more of the two-body GR parameter space, considerable work must be done to include possible beyond-GR and environmental effects in GSF models. Fortunately, the GSF model is relatively modular. This means most additional effects can be added separately, as described in Sect. 6.4, and are readily incorporated into frameworks such as FEW (Katz et al. 2021). However, modelling these additional effects will be particularly challenging if they are not amenable to a two-timescale treatment, or if they are too large to be treated perturbatively.

4.4 Perturbation theory for post-merger waveforms (quasi-normal modes)

Coordinators: Stephen R. Green and Laura Sberna
Contributors: E. Berti, R. P. Macedo, P. Mourier, N. Oshita, M. van de Meent

4.4.1 Description

Following a compact binary merger, the remnant object settles into a stationary state through a process known as the "ringdown". The ringdown signal is interesting because it involves a collection of discrete modes that encode information about the final object. For a BH merger, the no-hair theorems of general relativity predict that the final state is itself a Kerr BH (see, e.g., Chrusciel et al. 2012), yielding precise predictions for the ringdown frequencies. We consider this case here.

At late times, the ringdown is best described using BHPT. This involves expanding the spacetime metric $g_{\alpha\beta} = g^{(0)}_{\alpha\beta} + \epsilon g^{(1)}_{\alpha\beta} + \epsilon^2 g^{(2)}_{\alpha\beta} + \ldots$ (Regge and Wheeler 1957; Zerilli 1970a, b) and solving the Einstein equation order by order in ϵ. At zeroth order, the background metric $g^{(0)}_{\alpha\beta}$ describes the remnant Kerr BH. At first order, $g^{(1)}_{ab}$ satisfies the Einstein equation linearized about Kerr. Rather than work directly with the metric perturbation, it is convenient to use instead the Newman-

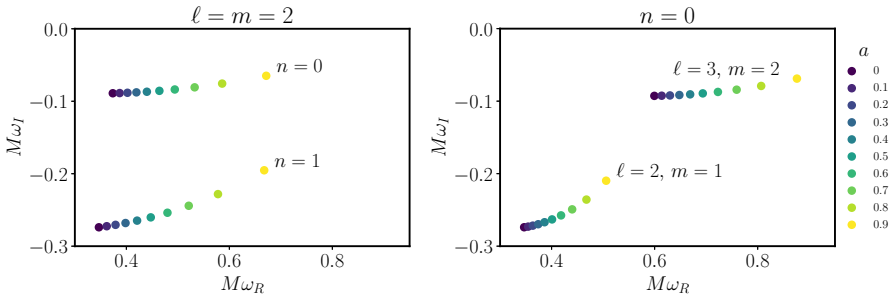

Fig. 8 Real and imaginary parts of the Kerr quasinormal mode frequencies, coloured by the BH spin (from $a = 0$ in dark blue to $a = 0.9$ in yellow). Left: $\ell = m = 2$ fundamental and first overtone modes. Right: modes with different angular numbers (ℓ, m)

Penrose formalism, expressing the perturbation in terms of the (complex) Weyl curvature scalars. Equations for the $s = \pm 2$ linearized Weyl scalars ψ_0 and ψ_4 famously decouple yielding a separable wave-like equation discovered by Teukolsky (Teukolsky 1972, 1973; Press and Teukolsky 1973; Teukolsky and Press 1974). Both ψ_0 and ψ_4 uniquely describe $g^{(1)}_{ab}$ up to gauge and perturbations to other Kerr spacetimes (Wald 1973), and in particular describe the GW degrees of freedom, with ψ_4 most relevant for gravitational radiation at infinity. Similarly, spin-weight $s = \pm 1$ and $s = 0$ Teukolsky equations describe electromagnetic and scalar-field perturbations, respectively.

Homogeneous solutions to the Teukolsky equation can be obtained by imposing boundary conditions corresponding to the physical requirement that radiation is outgoing at the BH horizon and outgoing at infinity. For each spin weight, this eigenvalue problem admits a countably infinite, discrete spectrum of complex-frequency *quasinormal modes (QNMs)* (Press 1971; Chandrasekhar and Detweiler 1975), see Fig. 8. Each QNM is labelled by three integers: two spin-weighted spheroidal-harmonic quantum numbers used to separate the angular dependence ($\ell \geq 2$, $-\ell \leq m \leq \ell$) and an "overtone number" $n \geq 0$, which sorts the frequencies in ascending order of the absolute value of their imaginary part. Negative (real) frequency modes are related to modes with negative m by the symmetry $-\omega^*_{n\ell m} = \omega_{n\ell -m}$. Kerr quasinormal frequencies (QNFs) have a strictly negative imaginary part, hence the modes decay with time, due to absorption by the BH horizon and radiation to infinity. These frequencies are moreover uniquely determined by the Kerr mass and spin in agreement with no-hair theorems. For detailed reviews on QNMs, see, e.g., Kokkotas and Schmidt (1999); Nollert (1999); Berti et al. (2009, 2018).

In contrast to normal modes, QNMs of Kerr do not form a complete basis, and therefore cannot fully describe the ringdown for all times, even at linear order. At *early* times, the linear response to a perturbation is dominated by a "direct" emission of radiation (also known as the prompt response) (Jensen and Candelas 1986; Leaver 1986; Nollert 1999). At *late* times, the perturbation is dominated by a power-law "tail" (associated with a branch cut in the frequency plane of the Green's function of the Teukolsky equation), which arises due to the asymptotic properties of the wave-

equation potential at large distances from the horizon (Leaver 1986; Price 1972). QNMs are most important at *intermediate* times, and for realistic inspirals they tend to dominate the majority of the post-merger signal. They have therefore proven extremely relevant for waveform modeling, either to analyze the ringdown in isolation or for combined inspiral-merger-ringdown waveforms. Indeed, a single QNM can be used to infer the mass and spin of the remnant, whereas additional modes or inspiral information enable consistency checks on GR (Detweiler 1980a; Dreyer et al. 2004; Berti et al. 2006; Isi et al. 2019a; Abbott et al. 2021d).

4.4.2 Suitable for what sources?

LISA is expected to detect the ringdown of MBHB and IMRI sources for which the merger occurs during the LISA observational time, and for which remnant QNFs fall within the LISA frequency band (Berti et al. 2006, 2007a, 2016). For EMRIs, the ringdown is likely to be too weak to resolve, a potential exception being those with near-extremal primaries (Compère et al. 2018; Oshita and Tsuna 2023).

One can easily estimate the mass range of remnants with ringdowns within the LISA band. Indeed, the longest lived (fundamental, $\ell = m = 2, n = 0$) QNM has frequency $f_0 \simeq 0.4/(2\pi M_{\rm final})$, with the exact value depending on the remnant's spin. For this to lie within the LISA band, $[10^{-4}, 10^{-1}]$ Hz, the mass of the remnant must therefore fall within the range $[10^8, 10^5]\ {\rm M}_\odot$. Ringdown modelling will be particularly important for MBHBs at the higher end of the mass spectrum, since their inspiral will take place outside the LISA band and contribute little to the SNR (Baibhav et al. 2020).

4.4.3 Status

At linear order in BHPT and for most of the duration of the signal, the ringdown is well described by a superposition of QNMs. For a given BH mass and spin, the Kerr QNFs were first computed numerically in Detweiler (1980a). The most accurate and reliable numerical method is Leaver's continued fraction approach (Leaver 1985; Nollert 1993; Onozawa 1997) (see Mathematica notebook and data at Berti 2024) and in particular its spectral refinement (Cook and Zalutskiy 2014; Hughes 2000) (implemented in the Python package `qnm` (Stein 2019)). Kerr QNFs can also be estimated analytically using WKB (Wentzel-Kramers-Brillouin) or WKB-inspired approximations (Blome and Mashhoon 1981; Schutz and Will 1985; Seidel and Iyer 1990; Kokkotas 1991; Dolan and Ottewill 2009; Dolan 2010). QNM modeling should be performed in a certain preferred BMS frame (Magaña Zertuche et al. 2022; Mitman et al. 2022). Afterwards it can be transformed to a different desired reference frame, e.g., a frame co-precessing with the binary (Hamilton et al. 2021, 2023), a frame set prior to a merger kick (Gerosa and Moore 2016), or the post-Newtonian preferred frame appropriate to modeling the early inspiral (Mitman et al. 2022).

In addition to the frequencies, the QNM component of the ringdown signal also comprises the amplitude and phase of each mode. Unlike the frequencies, these quantities are not uniquely determined by the remnant, but rather depend on the

particular initial conditions that led to its formation. In principle, the amplitudes and phases can be computed from the spacetime right after the formation of a common BH horizon (Leaver 1986; Berti and Cardoso 2006a), and hence from the binary parameters (Kamaretsos et al. 2012a, b). However, this data is hard to predict analytically, and moreover challenging to extract from NR simulations. Common practice is therefore to calibrate the desired mode amplitudes and phases by fitting against NR simulations (Berti et al. 2007b; Kamaretsos et al. 2012a; London et al. 2014; Baibhav et al. 2018; London 2020; Magaña Zertuche et al. 2022; Forteza et al. 2023; Baibhav et al. 2023). Alternatively, initial data can be estimated at the level of the Teukolsky equation using an Ori-Thorne procedure (Taracchini et al. 2014a; Lim et al. 2019; Hughes et al. 2019; Apte and Hughes 2019; Lim et al. 2022).

For binary BH mergers of comparable masses, the linear ringdown model—a superposition of a finite number of QNMs with arbitrary amplitudes and phases—has been extensively compared against NR simulations. At late times ($\gtrsim 10M$ after the peak of the waveform), the general consensus is that the linear model provides a good, stable, and consistent fit to the numerical waveform. At these times, the waveform is well described by a small number of overtones (dominated by the $\ell = m = 2$ multipole and overtones with $n \lesssim 2$), and fitting for the frequencies and decay rates allows for accurate inference of the remnant mass and spin (Buonanno et al. 2007a; Baibhav et al. 2018; Giesler et al. 2019; Cook 2020; Jiménez Forteza et al. 2020; Ota and Chirenti 2022; Li et al. 2022; Magaña Zertuche et al. 2022; Baibhav et al. 2023). More surprisingly, several studies indicate that the linear model applies even at much earlier times, provided higher (ℓ, m, n) modes are included in the model (Giesler et al. 2019; Cook 2020; Jiménez Forteza et al. 2020; Magaña Zertuche et al. 2022). However, the relevance of the linear model at these times ($\lesssim 10\,M$ after the peak of the waveform) and, in particular, the role of spherical-spheroidal mode mixing, nonlinear modes and higher overtones ($n > 2$), is still actively debated (Bhagwat et al. 2020; Magaña Zertuche et al. 2022; Forteza and Mourier 2021; Mitman et al. 2023; Ma et al. 2022a, 2023a, b; Baibhav et al. 2023; Nee et al. 2023; Zhu et al. 2024).

A complete linear-order model of the post-merger signal should also include back-scattering of radiation against the background potential. This is well approximated by a power-law tail $h \sim t^{-n_{\rm tail}}$ at late times, where $n_{\rm tail} = 7$ for generic gravitational perturbations of Kerr (Price 1972; Barack 2000; Tiglio et al. 2008). So far the tail contribution has not been confidently identified in NR simulations of binary BH mergers, so it is usually neglected in waveform modeling.

At very early times (around the peak amplitude) we expect higher order BHPT to become relevant. Beyond-linear-order perturbations satisfy the same equations as at linear order, but now with source terms made up of lower-order perturbations (Gleiser et al. 1996; Campanelli and Lousto 1999; Brizuela et al. 2009; Nakano and Ioka 2007; Pazos et al. 2010; Loutrel et al. 2021; Spiers et al. 2023). It is therefore natural to expect the signal to deviate from a simple superposition of linear QNMs. Such deviations could include new driven frequencies that are combinations of the first-order QNFs (Lagos and Hui 2023; Bucciotti et al. 2023), or corrections to the first order modes, in terms of the mode amplitudes, phases, and frequency spectrum (Sberna et al. 2022; Ripley et al. 2021). Indeed, a driven second-order mode

(which in quasicircular mergers appears in the $\ell = m = 4$ multipole, sourced by the square of the $\ell = m = 2$ fundamental mode) was recently identified in binary BH simulations (London et al. 2014; Ma et al. 2022a; Cheung et al. 2023; Mitman et al. 2023; Khera et al. 2023). Notably, the amplitude of the second-order mode is comparable to the amplitude from linear order, raising questions about perturbative convergence.

Detailed second-order calculations remain challenging, and are complicated by aspects of metric reconstruction and regularization of singularities. Nevertheless, second-order Kerr perturbations in the ringdown context were recently calculated numerically (Ripley et al. 2021). Additional analytic progress in the higher-order ringdown has included the development of a bilinear form under which Kerr QNMs are orthogonal (Green et al. 2023; Cannizzaro et al. 2024) (see also London 2023), new methods to reconstruct the metric in the presence of a first-order source (Green et al. 2020), and the use of analytic approximations (Bucciotti et al. 2023). These calculations have considerable overlap with the self-force problem, where significant progress has recently been made at second order, see Sect. 4.3.3.

4.4.4 Challenges

The main challenges in post-merger signal modeling using BHPT concern the inclusion of higher modes, the instability and quick damping of overtones, non-QNM ringdown components (e.g., from tails or the prompt response), and nonlinear effects.

Higher (ℓ, m, n) modes are predicted by BHPT to arise in generic binary mergers. However, there is no consensus on whether it is consistent to include more than a few overtones ($n \geq 1$) in a purely linear model (Giesler et al. 2019; Baibhav et al. 2023; Nee et al. 2023). The challenge lies in the fact that higher overtones decay rapidly, and therefore are relevant at early times, when nonlinearities are also expected to become more significant. Despite providing good fits to the signal, higher overtones might simply play the role of fitting noise, nonlinearities, or non-QNM components (such as tails or the prompt response) in the signal. For asymmetric binaries (with precession, eccentricity, or unequal mass ratios) angular modes beyond $\ell = m = 2$ may also have significant amplitudes (see e.g. Capano et al. 2023; Magaña Zertuche et al. 2022; Li et al. 2022; Oshita 2023), and their fundamental ($n = 0$) modes have lifetimes similar to the fundamental $\ell = m = 2$ mode.

Recent theoretical studies also indicate that the QNM spectrum itself could be unstable (Nollert 1996; Aguirregabiria and Vishveshwara 1996; Vishveshwara 1996; Jaramillo et al. 2021, 2022a; Cheung et al. 2022; Konoplya and Zhidenko 2023), with overtones particularly sensitive to nonlinear perturbations, small environmental effects, and deviations from vacuum general relativity. However the experimental implications of this instability are not fully understood.

The size of power-law tail contributions due to back-scattering has yet to be estimated for binary BHs in full GR. Baibhav et al. (2023) cautioned that, at the linear level, the tail contribution can be comparable to that of high-overtone QNMs with $n \simeq 5$. The tail might play an even larger role in eccentric binary mergers, as suggested by perturbative solutions (Albanesi et al. 2023) and some NR simulations

(Carullo and De Amicis 2023). This should motivate a more careful study of the contribution of back-scattering effects in the post-merger signal.

No study has yet quantified which (if any) LISA-band ringdown sources will require higher-order perturbation theory. Ideally, starting from a first-order perturbation, a nonlinear model would predict detailed corrections including the amplitude of driven modes, shifts in amplitudes and phases for first-order modes, and any frequency drifts. Some initial progress towards such a model includes agnostic fits of numerical relativity waveform catalogues (Baibhav et al. 2023), numerical studies (Ripley et al. 2021), and developments in BH perturbation theory (Green et al. 2023; Spiers et al. 2023).

Some studies have speculated that nonlinearities could be stronger for near-extreme remnants, whose spectrum contains long-lived modes with commensurate frequencies. In this limit, nonlinear effects could lead to gravitational turbulence (Yang et al. 2015) and connect with the Aretakis instability of extremal BHs (Aretakis 2012). To assess these possibilities, it will be necessary to extend calculations beyond scalar-field toy models (Yang et al. 2015) to full general relativity, see for example (Redondo-Yuste et al. 2024).

4.5 Effective-one-body waveform models

Coordinators: Tanja Hinderer, Geraint Pratten
Contributors: S. Akcay, A. Antonelli, S. Bernuzzi, A. Buonanno, J. Garcia-Bellido, A. Nagar, L. Pompili

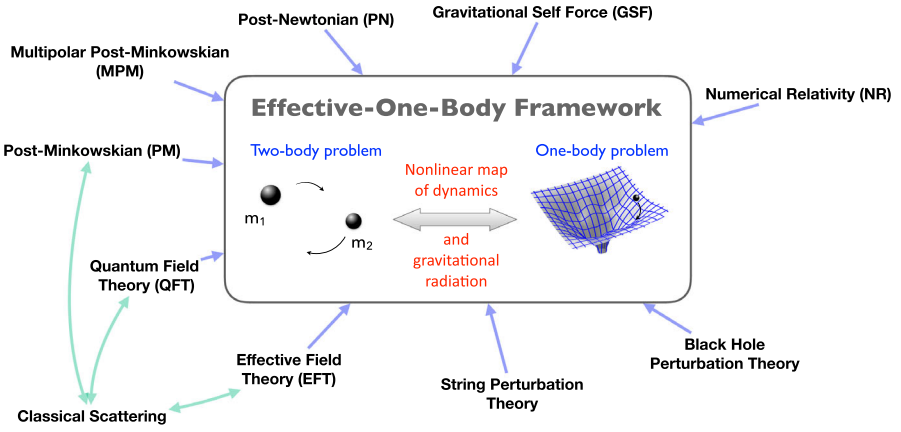

Fig. 9 Theoretical inputs to the EOB framework. The EOB theory draws on a variety of perturbative results from numerous approaches in different regimes, as well as from NR simulations, as illustrated here

4.5.1 General description

The effective-one-body (EOB) approach was originally introduced in Buonanno and Damour (1999, 2000); Damour et al. (2000); Damour (2001); Buonanno et al. (2006) with the aim of providing GW detectors with semianalytic waveform models for the entire coalescence of compact-object binaries (i.e., the inspiral, plunge, merger and ringdown), resumming PN information around the strong-field test-body limit. Since the breakthrough in NR in 2005 (Pretorius 2005a; Campanelli et al. 2006a; Baker et al. 2006a), the EOB framework has incorporated information from the NR simulations, thus producing highly-accurate waveform models for GW observations (e.g., see the review articles by Damour 2008; Buonanno and Sathyaprakash 2014; Damour and Nagar 2016 and discussion below). Over the years, the EOB framework has been extended to the scattering problem, and has incorporated analytical information from other methods, such as the PM approach and GSF theory, as illustrated in Fig. 9; see e.g. Berkovits et al. (2022); Buonanno et al. (2022) for overviews of the role of string perturbation theory, QFT, and worldline EFT.

The EOB waveform models consist of three main building blocks: (1) the Hamiltonian, which describes the conservative dynamics, (2) the radiation-reaction (RR) force, which accounts for the energy and angular momentum losses due to GW emission, and (3) the inspiral-merger-ringdown waveform modes, built upon improved PN resummations for the inspiral part, and functional forms calibrated to NR waveforms for the merger-ringdown signal. We now briefly review these three key ingredients.

A fundamental pillar of the EOB approach is the map of the real two-body dynamics into that of an effective test mass or test spin in a deformed Schwarzschild or Kerr background, with the deformation parameter being the symmetric mass ratio $\nu = \mu/M$, where $\mu = m_1 m_2/M$ is the reduced mass and $M = m_1 + m_2$ is the total mass. More specifically, the real or EOB Hamiltonian, $H_{\rm EOB}$, is related to the effective Hamiltonian, $H_{\rm eff}$, by Buonanno and Damour (1999)

$$H_{\rm EOB} = M\sqrt{1 + 2\nu\left(\frac{H_{\rm eff}}{\mu} - 1\right)}. \tag{15}$$

Interestingly, such a relation agrees with calculations in quantum electrodynamics (Brezin et al. 1970) aimed at deriving an approximate binding energy for charged particles with comparable masses in the eikonal approximation; it has been shown to hold exactly at 1PM order (Damour 2016), and it has been extensively used in scattering-theory computations (Damour 2016; Vines 2018; Vines et al. 2019; Damour 2018). The above energy-map (15) achieves a concise resummation of PN information into the Hamiltonian via a small number of terms. In the center-of-mass frame, the EOB equations of motion read:

$$\frac{d\boldsymbol{r}}{dt} = \frac{\partial H_{\rm EOB}}{\partial \boldsymbol{p}}\,, \qquad \frac{d\boldsymbol{p}}{dt} = -\frac{\partial H_{\rm EOB}}{\partial \boldsymbol{r}} + \boldsymbol{F}\,, \qquad \frac{d\boldsymbol{S}_{1,2}}{dt} = \frac{\partial H_{\rm EOB}}{\partial \boldsymbol{S}_{1,2}} \times \boldsymbol{S}_{1,2}, \tag{16}$$

where $\boldsymbol{r}$ and $\boldsymbol{p}$ are the canonical variables, notably the relative position and momentum, respectively, $\boldsymbol{F}$ is the RR force, and $\boldsymbol{S}_i$ with $i = 1, 2$ are the spins of the

compact objects. For example, in the nonspinning limit, where the dynamical variables reduce to (r, ϕ, p_r, p_ϕ), the effective Hamiltonian in the gauge of (Buonanno and Damour 1999; Damour et al. 2000) reads

$$H_{\rm eff} = \mu \sqrt{A_v(r)\left[\mu^2 + A_v(r)\bar{D}_v(r)\, p_r^2 + \frac{p_\phi^2}{r^2} + Q_v(r, p_r)\right]}\,, \tag{17}$$

where the potentials $A_v(r)$ and $\bar{D}_v(r)$ differ from the Schwarzschild ones due to PN corrections depending on v. The higher-order (yet) unknown PN corrections in $A_v(r)$ might be informed to NR simulations. The potential $Q_v(r)$ is a non-geodesic term that needs to be introduced at 3PN order (Damour et al. 2000) to preserve the mapping (15), and reduces to zero in the test-mass limit.

Precessing-spin EOB waveforms for the inspiral-merger-ringdown were first built in Buonanno et al. (2006) using the nonspinning EOB Hamiltonian (Buonanno and Damour 1999, 2000; Damour et al. 2000) augmented with a spinning PN Hamiltonian (Blanchet 2024). The EOB Hamiltonian for spinning objects was first developed in Damour (2001), and then in Damour et al. (2008a); Nagar (2011); Damour and Nagar (2014b); Balmelli and Damour (2015). These papers follow the structure of the Hamiltonian advocated in Damour (2001) that in the large mass-ratio limit reduces to the one of a (nonspinning) test mass on a Kerr background. Furthermore, another line of research, which started in Barausse et al. (2009); Barausse and Buonanno (2010), built EOB Hamiltonians for spinning objects such that, in the large mass-ratio limit, they reduce to the one of a test spin on a Kerr background (Barausse et al. 2009; Barausse and Buonanno 2011). The two different spinning Hamiltonians were comprehensively compared in Rettegno et al. (2020); Khalil et al. (2020).

In the original EOB model (Buonanno and Damour 2000), the radiation-reaction force of Eq. (16) was given by a suitable Padé resummation of the PN-expanded energy flux at 2.5PN order, following the seminal work of Damour et al. (1998). Subsequently, the (quasi-circular) radiation-reaction force, that is the flux of angular momentum, has been expressed as the sum of factorized and resummed multipoles according to the procedure introduced in Damour and Nagar (2007); Damour et al. (2009). This approach was then first extended to spinning bodies in Pan et al. (2011b) and then improved in Taracchini et al. (2012, 2014b); Nagar and Shah (2016); Messina et al. (2018); Nagar et al. (2019a); Cotesta et al. (2018) by means of additional factorizations and resummation of the orbital and spin parts, and the inclusion of higher-order PN terms.

The factorization of each waveform multipole proposed in Damour et al. (2009) reads

$$h_{\ell m}^{\rm insp-plunge}(t) = h_{\ell m}^{(N,\epsilon)}\, S_{\rm eff}^{(\epsilon)}\, T_{\ell m}\, e^{i\delta_{\ell m}}\, (\rho_{\ell m})^{\ell}\, h_{\ell m}^{\rm NQC}\,, \tag{18}$$

where $h_{\ell m}^{(N,\epsilon)}$ is the Newtonian contribution and ϵ denotes the parity of the mode. The factor $T_{\ell m}$ resums an infinite number of leading-order logarithms arising from tail effects (Damour and Nagar 2007) (see also Faye et al. 2015), the term $e^{i\delta_{\ell m}}$ is a

residual phase correction due to sub-leading order logarithms in hereditary contributions, and the functions $\rho_{\ell m}$ are the residual amplitude corrections. These functions were originally obtained as PN-expansions (Damour et al. 2009), but in some versions of the EOB models, it was found useful to further resum them using Padé approximants for improved strong-field robustness (Nagar and Shah 2016; Messina et al. 2018; Nagar et al. 2019a). Another approach consists of calibrating effective high-order PN parameters entering the $\rho_{\ell m}$'s to improve their accuracy, doing so either using NR data (Taracchini et al. 2012, 2014b; Cotesta et al. 2018; Pompili et al. 2023) or second-order GSF results (van de Meent et al. 2023).

The factor $h_{\ell m}^{\rm NQC}$ is the phenomenological next-to-quasi-circular (NQC) correction (Damour et al. 2003) to the waveform that is informed by NR simulations, and it is designed to correctly shape the waveform during the late plunge up to merger, where the motion is not quasi-circular and the resummed quasi-circular waveform lacks information. The complete EOB waveform is constructed by attaching the merger-ringdown mode, $h_{\ell m}^{\rm merger-RD}(t)$, to the inspiral-plunge one, $h_{\ell m}^{\rm insp-plunge}(t)$, at a suitable matching time $t = t_{\rm match}$, around the peak of the EOB orbital frequency (which approximately corresponds to merger time), that is Buonanno and Damour (2000):

$$h_{\ell m}(t) = h_{\ell m}^{\rm insp-plunge-merger}(t)\,\Theta\left(t_{\rm match}^{\ell m} - t\right) + h_{\ell m}^{\rm ringdown}(t)\,\Theta\left(t - t_{\rm match}^{\ell m}\right), \quad (19)$$

where $\Theta(t)$ is the Heaviside step function. Inspired by results for the infall of a test mass into a BH (Davis et al. 1972) and the close-limit approximation (Price and Pullin 1994), several EOB waveform models used a superposition of QNMs for the dominant mode (Buonanno and Damour 2000; Damour 2001; Buonanno et al. 2007a, b; Damour and Nagar 2009; Pan et al. 2011a; Barausse et al. 2012a; Taracchini et al. 2012; Damour et al. 2013; Pan et al. 2014; Taracchini et al. 2014b; Babak et al. 2017b). More recently, an NR-informed fit of the amplitude and phase has become standard (Damour and Nagar 2014a). This framework is similar in spirit to the rotating source approximation developed in Baker et al. (2008), but with significant technical differences. An important input into the merger-ringdown part of the EOB model is the mapping between progenitor binary parameters and the mass and spin of the final remnant. This is needed to determine the frequency of QNMs of the remnant, and it is obtained from NR results (Jiménez-Forteza et al. 2017; Hofmann et al. 2016).

There is considerable freedom in modeling and resumming the EOB Hamiltonian, radiation-reaction force and GW modes, and spin effects. Those different choices, together with variations in the gauge adopted and deformations of the potentials in the Kerr spacetime, have led to two main EOB families: `SEOBNR` (e.g., see Bohé et al. 2017; Cotesta et al. 2018; Ossokine et al. 2020; Ramos-Buades et al. 2023) and `TEOBResumS` (e.g., see Damour and Nagar (2014b); Nagar et al. (2018, 2020b); Gamba et al. (2022), which we discuss in detail in Sects. 4.5.3 and 4.5.4 below. The EOB waveform program advances along two interrelated directions. The first comprises theoretical advances on the underlying structure and mapping of analytical results from PN, PM and GSF approaches. The second involves testing and refining

the models using NR information and rendering them available for use in data analysis. The EOB waveform models are intrinsically in the time domain (TD), which provides a more direct relation between source physics and asymptotic radiation than frequency-domain models. Modeling both the dynamics and radiation is useful for gaining deeper insights into strong-field nonlinearities and it enables more thorough tests of the robustness of different aspects of the waveform based on examining the behavior of various characteristic quantities under changes in the binary's parameters, and on comparing different gauge-invariant quantities between EOB, NR, or perturbative results — for example the binding energy and fluxes (Boyle et al. 2008; Damour et al. 2012a; Le Tiec et al. 2012a; Bernuzzi et al. 2015b; Ossokine et al. 2018; Antonelli et al. 2019), periastron advance (Le Tiec et al. 2011, 2013; Hinderer et al. 2013), scattering angles (Damour et al. 2014a; Hopper et al. 2023; Khalil et al. 2022; Damour and Rettegno 2023) or spin-precession invariant (Hinderer et al. 2013) and redshift (Le Tiec et al. 2012a; Barausse et al. 2012b; Bini and Damour 2016; Akcay et al. 2012). At the same time, this also makes EOB models computationally more expensive than IMR waveform models, which describe only the asymptotic GW signals in the frequency domain (FD), as discussed in Sect. 4.6. However, the computational cost is not an insurmountable problem. Much recent work has significantly improved the computational efficiency of EOB models through the development of optimized codes (Devine et al. 2016; Knowles et al. 2018; Nagar and Rettegno 2019; Rettegno et al. 2020; Gamba et al. 2021), by building reduced-order models (ROMs) (Field et al. 2014; Pürrer 2014, 2016; Lackey et al. 2017, 2019; Cotesta et al. 2020; Gadre et al. 2024; Tissino et al. 2023; Khan and Green 2021; Thomas et al. 2022; Pompili et al. 2023), implementing the post-adiabatic approximation (Nagar and Rettegno 2019; Rettegno et al. 2020; Gamba et al. 2021; Mihaylov et al. 2021), and making use of machine-learning methods (Schmidt et al. 2021; Dax et al. 2023; Tissino et al. 2023; Thomas et al. 2022; Khan and Green 2021). Close Hyperbolic Encounters could also be searched for with both ground- and space-based interferometers using machine learning (Morrás et al. 2022).

EOB waveform models have been constructed for quasi-circular non-spinning (Buonanno and Damour 2000; Buonanno et al. 2007a, b; Damour and Nagar 2008; Damour et al. 2008c, d; Buonanno et al. 2009; Pan et al. 2011a; Damour et al. 2013; Nagar et al. 2020a) and spinning (Buonanno et al. 2006; Pan et al. 2010; Nagar 2011; Damour and Nagar 2014b; Taracchini et al. 2012, 2014b; Bohé et al. 2017; Cotesta et al. 2018; Pan et al. 2014; Babak et al. 2017b; Ossokine et al. 2020; Nagar et al. 2018, 2019b; Akcay et al. 2021; Gamba et al. 2022; Pompili et al. 2023; Ramos-Buades et al. 2023; Nagar et al. 2020b; Nagar and Rettegno 2021) binaries, building also on further developments of EOB Hamiltonians (Damour et al. 2000, 2015; Damour 2001; Damour et al. 2008a; Balmelli and Jetzer 2015; Balmelli and Damour 2015; Barausse and Buonanno 2010, 2011; Khalil et al. 2020) and resummations of the radiative sector (Damour et al. 2009). Furthermore, orbital eccentricity (Bini and Damour 2012; Hinderer and Babak 2017; Chiaramello and Nagar 2020; Nagar et al. 2021a; Khalil et al. 2021; Ramos-Buades et al. 2022a; Albanesi et al. 2022b) (see also Cao and Han 2017; Liu et al. 2022) and matter effects (Bernuzzi et al. 2015b; Hinderer et al. 2016; Steinhoff et al. 2016; Akcay et al.

2019; Steinhoff et al. 2021; Matas et al. 2020; Gonzalez et al. 2023a) (see Sect. 6.5), as well as information from PM (Damour 2016, 2018; Antonelli et al. 2019; Damgaard and Vanhove 2021; Khalil et al. 2022; Damour and Rettegno 2023) and conservative GSF information (Damour 2010; Yunes et al. 2010a, 2011a; Barausse et al. 2012b; Akcay et al. 2012; Antonelli et al. 2020c; Nagar and Albanesi 2022; Albertini et al. 2022a, b; van de Meent et al. 2023) have been also incorporated in EOB models. The required effort to advance the EOB modeling involves: (1) obtaining new analytical information and mapping it into the EOB framework; (2) resumming the results into full waveform models with additional flexibility for calibrations to NR; and (3) testing and comparing models to assess their performance and accuracy. We describe each of the two main EOB families in more detail in Sects. 4.5.3 and 4.5.4 below.

4.5.2 Suitable for what sources?

Inspiral-merger-ringdown signals from massive black-hole binaries (MBHBs) will be within the LISA band (see Sect. 2.1), making EOB models naturally applicable for these sources. The bulk of MBHB events observable by LISA are expected to have mass ratios $q \lesssim 10$, but some systems may have mass ratios of up to several hundreds. Most tests and calibrations of EOB models have been for $q \lesssim 20$, but the fact that EOB models interpolate between this regime and the test-body limit with information from BH perturbation theory makes them structurally well-suited for larger-q systems. Spin precession and eccentricity effects, both simultaneously relevant for MBHBs and IMRIs, have mainly been separately included in EOB models, and there has been recent progress on going beyond this, e.g. Gamba et al. (2024); Liu et al. (2024). These considerations apply not only for MBHBs but also for describing intermediate mass-ratio binaries (IMRIs) discussed in Sect. 2.3. Importantly, EOB models have been either validated (Albertini et al. 2022a, b) or improved using perturbation-theory and GSF information (Yunes et al. 2010a, 2011a; Barausse et al. 2012b; Antonelli et al. 2020c; Nagar and Albanesi 2022; van de Meent et al. 2023), which is relevant for IMRIs and also EMRIs. EOB models are also suitable to stellar-origin binaries Sect. 2.5, whose early-inspiral signals will be within the LISA band. For inspirals, EOB models provide a more accurate though less efficient description than pure PN-based models. Using EOB waveforms will further be important for connecting the LISA portion of SOBHB signals with the corresponding merger signals measurable in future ground-based detectors. The EOB approach also allows for the inclusion of additional physical effects, for instance, from gravity theories beyond GR and environmental effects as explained in Sect. 6.5.

As discussed in Sect. 4.5.6, while EOB models are naturally suited to the above sources, significant further advances in the modeling accuracy, complexity of physical effects, robustness over a wide range of parameter space, and efficiency will be required for their use in LISA data analysis.

4.5.3 The SEOBNR waveform models

The EOBNR family of waveform models [2] has been developed with two main goals: i) make use of the most accurate analytical information for the two-body dynamics and gravitational radiation (PN, PM, GSF) and results from NR and Teukolsky-code simulations to build physical, highly-accurate waveform models of compact-object binaries, and ii) make them available to GW detectors for searches and inference studies. The history, since 2007, and the current status of EOBNR models are illustrated in Table 9. These models have been implemented into the LIGO Algorithms Library (LALsuite) (LIGO Scientific Collaboration et al. 2024), and more recently in the open-source Python package pySEOBNR (Mihaylov et al. 2023). These codes were then reviewed by the LVK Collaboration. Here we summarize the main milestones, focusing on the binary BHs, while leaving details of the modeling improvements (two-body inspiraling dynamics, transition merger to ringdown, RR effects, GW modes, resummation of EOB potentials, etc.) to the corresponding publications.

Building on the original work on the EOB framework (Buonanno and Damour 1999, 2000; Damour et al. 2000; Buonanno et al. 2006), the first EOBNR model calibrated to nonspinning NR waveforms was developed in Buonanno et al. (2007b), following initial comparisons to NR equal-mass nonspinning binaries in Buonanno et al. (2007a), in which the importance of including overtones in the EOB description of the merger-ringdown signal was pointed out. EOBNRv1 was employed by Initial and Enhanced LIGO, and Virgo for the first searches of coalescing binary BHs (Ochsner 2010; Abadie et al. 2011, 2012; Aasi et al. 2013). The calibration to spinning binaries with equal masses was considered in Pan et al. (2010), employing an EOB Hamiltonian for a test mass in a deformed Kerr spacetime (Damour et al. 2008a). The nonspinning waveforms with higher modes were first modeled in (Pan et al. 2011a) with the improved factorized waveforms (Damour and Nagar 2007; Damour et al. 2009; Pan et al. 2011b), thus marking the second generation of EOBNR models.

The third-generation of EOBNR models encompassed significant advances in including spin effects in the two-body dynamics and radiation, resumming perturbative information, and calibration to NR simulations. An EOB Hamiltonian for a test spin in a deformed Kerr spacetime was derived in Barausse et al. (2009); Barausse and Buonanno (2010, 2011). It included all PN corrections in the test-body limit, at linear order in the test-body's spin. To enforce the presence of a photon orbit (and peak of the orbital frequency) for aligned-spin binary BHs, it used a logarithmic (instead of Padé) resummation of the EOB potentials. Those improvements led to the aligned-spin model SEOBNRv1 (Taracchini et al. 2012), and the first spin-precessing model, SEOBNRv2P (Pan et al. 2014), which adopted the co-precessing frame description of (Buonanno et al. 2003; Schmidt et al. 2011) to efficiently handle precessional effects. Those models also included information for the merger-ringdown waveforms from the test-body limit, notably from time-domain Teukolsky

[2] The generic name SEOBNRvnEPHM indicates that the version vn of the EOB model is calibrated to NR simulations (NR), includes spin (S) and precessional (P) effects, eccentricity (E) and higher modes (HM).

Table 9 Progress in the development of SEOBNR models

Family	Waveform model	Spins	Ecc./hyper	NR & Teukolsky calib. region	CP-frame modes $(\ell, \lvert m\rvert)$
1st	*EOBNRv1			$q \leq 4$	(2, 2)
	Buonanno et al. (2007b)				
2nd	EOBNRv2			$q \leq 3$	(2, 2)
	Buonanno et al. (2009)				
	SEOBNRv0			$q = 1, \chi_{1,2} = \pm 0.4$	(2, 2)
	Pan et al. (2010)				
	*EOBNRv2HM			$q \leq 6$	(2, 2), (2, 1), (3, 3),
	Pan et al. (2011a)				(4, 4), (5, 5)
	*EOBNRv2HM_ROM			$q \leq 6$	(2, 2), (2, 1), (3, 3),
	Marsat et al. (2021)				(4, 4), (5, 5)
3rd	*SEOBNRv1	✓		$q \leq 6, \chi_{1,2} = \pm 0.4$	(2, 2)
	Taracchini et al. (2012)				
	*SEOBNRv1_ROM	✓			
	Pürrer (2014)				
	*SEOBNRv2	✓		NR: $q \leq 8, \lvert\chi_{1,2}\rvert \leq 0.98$	
	Taracchini et al. (2014b)			Teuk.: $q = 1000, \lvert\chi_{1,2}\rvert \leq 0.99$	
	*SEOBNRv2_ROM	✓			
	Pürrer (2016)				
	SEOBNRv2P	✓✓			(2, 2), (2, 1)
	Pan et al. (2014)				
	*SEOBNRv3P	✓✓			
	Taracchini et al. (2014b); Babak et al. (2017b)				
4th	*SEOBNRv4	✓		NR: $q \leq 8, \lvert\chi_{1,2}\rvert \leq 0.995$	(2, 2)
	Bohé et al. (2017)			Teuk.: $q = 1000, \lvert\chi_{1,2}\rvert \leq 0.99$	
	*SEOBNRv4_ROM	✓			(2, 2)
	Bohé et al. (2017)				
	*SEOBNRv4P	✓✓			(2, 2), (2, 1)
	Ossokine et al. (2020)				

Table 9 continued

Family	Waveform model	Spins	Ecc./hyper	NR & Teukolsky calib. region	CP-frame modes $(\ell, \lvert m\rvert)$
	*SEOBNRv4HM	↗			(2, 2), (2, 1), (3, 3),
	Cotesta et al. (2018)				(4, 4), (5, 5)
	*SEOBNRv4HM_ROM	↗			
	Cotesta et al. (2020)				
	*SEOBNRv4PHM	↗↗			
	Ossokine et al. (2020)				
	*SEOBNRv4PHM_surr	↗↗			
	Gadre et al. (2024)				
	*SEOBNRv4EHM	↗	↗		
	Ramos-Buades et al. (2022a)				
	*SEOBNRv4PHM_4dq2	↗↗			(2, 2), (2, 1), (3, 3), (4, 4)
	Thomas et al. (2022)				
5th	*SEOBNRv5	↗		NR: $q \leq 20, \lvert\chi_{1,2}\rvert \leq 0.998$	(2, 2)
	Pompili et al. (2023)			Teuk.: $q = 1000, \lvert\chi_{1,2}\rvert \leq 0.99$	
	*SEOBNRv5_ROM	↗			
	Pompili et al. (2023)				
	*SEOBNRv5HM	↗			(2, 2), (2, 1), (3, 2), (3, 3),
	Pompili et al. (2023)				(4, 3), (4, 4), (5, 5)
	*SEOBNRv5PHM	↗↗			
	Ramos-Buades et al. (2023)				

The NR-calibration region refers only to calibration against aligned-spin NR waveforms. We indicate the coprecessing modes as CP modes. The surrogate models SEOBNRv4PHM_surr and SEOBNRv4PHM_4dq2, and the eccentric/hyperbolic model SEOBNRv4EHM are implemented in LALsuite, but they have not been reviewed, yet, and they are not publicly available at the moment. The surrogate models are limited in length and binary's parameter space (see Gadre et al. 2024; Thomas et al. 2022 for details)

↗ aligned spin, ↗↗ arbitrary spin orientations

* Implemented in LALsuite, and for the latest version (v5) in the open-source Python package pySEOBNR (Mihaylov et al. 2023)

waveforms obtained in Barausse et al. (2012a). With the availability of a larger set of accurate SXS NR waveforms, and further analytical results from PN theory, the model was upgraded to SEOBNRv2 (Taracchini et al. 2014b), with its precessing version known as SEOBNRv3P (Babak et al. 2017b), which is often also referred to simply as SEOBNRv3. The aligned-spin versions of these third-generation SEOBNR models were used in the template bank of the modeled searches in the gstLAL and pyCBC pipelines, and for parameter-estimation of GW signals detected during the first observing run (O1) of Advanced LIGO (Abbott et al. 2016b, e, 2019b).

The fourth generation of models included substantial and more efficient (via Markov-chain–Monte-Carlo methods) re-calibrations of the aligned-spin baseline models, such as SEOBNRv4 (Bohé et al. 2017), and phenomenological ansatzes for the merger-ringdown based on (Damour and Nagar 2014a). The SEOBNRv4 model was completed by including higher modes (Cotesta et al. 2018), arbitrary spin orientations (Ossokine et al. 2020), and extended to eccentric and hyperbolic orbits for aligned spins in Ramos-Buades et al. (2022a), using GW modes recast in factorized form in Khalil et al. (2021) (see also Cao and Han (2017); Liu et al. (2020, 2022); Hinderer and Babak (2017) for other eccentric EOBNR models). These updated models for quasi-circular orbits were used for the template banks of modeled searches, and extensively for inference studies during the second (O2) and third (O3) runs of Advanced LIGO and Virgo (Abbott et al. 2019b, 2020a, c, d, 2021b, 2023a).

Among the highlights of the fifth generation of models, they were calibrated to NR waveforms with larger mass-ratios and spins using a catalog of 442 SXS simulations (Pompili et al. 2023), and they incorporate for the first-time information from second-order GSF in the nonspinning modes and radiation-reaction force (van de Meent et al. 2023). The models include several higher modes, notably the $|m| = \ell$ modes for $\ell = 2$-- 5 and the $(2, \pm 1)$, $(3, \pm 2)$ and $(4, \pm 3)$ modes. Differently from the SEOBNRv3P and SEOBNRv4 Hamiltonians, the SEOBNRv5 reduces in the test-body limit to the one of a test mass in the Kerr spacetime. The accurate precessing-spin dynamics of SEOBNRv5PHM (Ramos-Buades et al. 2023) was obtained including partial precessing-spin information in the EOB Hamiltonian in the co-precessing frame by orbit averaging the in-plane spin components of the full precessing Hamiltonian at 4PN order (Khalil et al. 2023). Furthermore, the evolution equations for the spin and angular momentum vectors were computed in a PN-expanded, orbit-averaged form for quasi-circular orbits, similarly to what was done in Estellés et al. (2021); Ackley et al. (2020); Akcay et al. (2021), but with important differences due to the distinct gauge and spin supplementary conditions (Khalil et al. 2023), and the inclusion of orbit-average in-plane spin effects. Thanks to a simpler (but more approximated) precessing-spin inspiraling dynamics, which allows for the use of the post-adiabatic approximation (Rettegno et al. 2020; Mihaylov et al. 2021), and the new high-performance Python infrastructure pySEOBNR (Mihaylov et al. 2023), the computational efficiency of the SEOBNRv5PHM models has improved significantly, generally $\sim$8–20 times faster than the previous generation SEOBNRv4PHM. This is particularly important in view of the use of these waveform models with next-generation detectors on the ground and with LISA, which have a much broader bandwidth.

Furthermore, SEOBNR waveform models have also been used to extend the NR surrogate models (see Sect. 5.1) to lower frequencies, by hybridizing them (Varma et al. 2019b; Yoo et al. 2022, 2023), and to build IMR phenomenological waveform models (see Sect. 4.6). For the latter, SEOBNR models have been employed to construct time-domain hybrid NR waveforms, and also to calibrate the phenomenological models in regions of the parameter space where NR waveforms are not available (Khan et al. 2016; Pratten et al. 2020; Estellés et al. 2022b).

Quite importantly for LISA and next-generation detectors on the ground, the computational efficiency of the time-domain SEOBNR models can also be improved by building surrogate and ROM versions (Pürrer 2014, 2016; Bohé et al. 2017; Gadre et al. 2024; Pompili et al. 2023). Lastly, the efficient and flexible pySEOBNR infrastructure (Mihaylov et al. 2023), which uses Bayesian algorithms to calibrate waveforms against NR simulations, will allow to swiftly include and test new analytical information (PN,PM,GSF) (and their possible resummations) as soon as they become available. This is crucial to improve waveform models by at least two orders of magnitude to match the expected waveform accuracy requirements.

Extensions of the SEOBNR models to extreme mass-ratio inspirals were obtained in Yunes et al. (2010a, 2011a); Taracchini et al. (2014a, 2014b), and applications to non-vacuum binary systems and gravity theories beyond GR are discussed in Sect. 6.5.

4.5.4 The TEOBResumS waveform models

The TEOBResumS model builds upon early EOB developments at the Institut des Hautes Etudes Scientifiques (IHES) that define the basics structure of the model. The name suggests the key features: arbitrary compact binaries with tidal (T) and generic spins (S) interactions are modeled by making systematic use of analytical resummations. This name has first appeared in the tidal model of Bernuzzi et al. (2015b) and in the tidal and spinning model of Nagar et al. (2018). The latter include the factorized waveform described above (Damour et al. 2009; Damour and Nagar 2009), the systematic resummation of EOB potentials via Padé approximants (Damour et al. 2002, 2008a; Damour and Nagar 2009; Nagar 2011; Damour et al. 2013), NQC corrections (Nagar et al. 2007; Damour and Nagar 2007; Damour et al. 2008c, d, 2013), attachment of the ringdown around the peak of the orbital frequency (i.e., light-ring crossing) (Damour and Nagar 2007; Damour et al. 2013), the concept of centrifugal radius for incorporating spin-spin interactions (Damour and Nagar 2014b), resummed gyro-gravitomagnetic functions (Damour et al. 2008a; Nagar 2011; Damour and Nagar 2014b) and the factorized NR-informed ringdown waveform (Damour and Nagar 2014a). These developments made heavy use of results in the test-mass limit obtained by means of a new approach to black hole perturbation theory (Nagar et al. 2007; Damour and Nagar 2007; Bernuzzi et al. 2011a, b; Harms et al. 2014) to understand each physical element entering the structure of the waveform and striving for physical completeness, simplicity, accuracy and efficiency. Currently, TEOBResumS-GIOTTO is a unified framework to generate inspiral waveforms for any type of quasi-circular compact binary and

complete inspiral-merger-postmerger waveforms for BBH and BHNS binaries (Riemenschneider et al. 2021; Gonzalez et al. 2023a).

TEOBResumS-Dalí is the model's extension to generic orbits and describes bound orbits with arbitrary eccentricity (Chiaramello and Nagar 2020; Nagar et al. 2021a; Nagar and Rettegno 2021; Bonino et al. 2023), hyperbolic orbits and scattering (Nagar et al. 2021b; Gamba et al. 2023a; Hopper et al. 2023). The key features of the models are summarized in Table 10 and described in the following. An extension of the model that relies on GSF-informed potentials (Akcay and van de Meent 2016; Nagar and Albanesi 2022) so as to generate extreme-mass-ratio-inspirals (EMRIs) is available (Albertini et al. 2022a, b), and work on scalar-tensor gravity (building upon Julié and Deruelle 2017; Julié 2018c) is also currently in progress (Jain et al. 2023; Jain 2023a, b).

The structure of the spin-aligned effective TEOBResumS Hamiltonian is

$$H_{\rm eff} = H_{\rm eff}^{\rm orbital} + H_{\rm eff}^{\rm SO}, \tag{20}$$

where $H_{\rm eff}^{\rm orbital}$ incorporates even-in-spin contributions (spin-spin couplings), while $H_{\rm eff}^{\rm SO}$ incorporates odd-in-spin ones (spin-orbit couplings). The spin-orbit contribution reads

$$H_{\rm eff}^{\rm SO} = G_S S + G_{S_*} S_*, \tag{21}$$

where (G_S, G_{S_*}) are the gyro-gravitomagnetic functions and $S \equiv S_1 + S_2$, while $S_* = m_2/m_1 S_1 + m_1/m_2 S_2$ are useful combinations of the spins (Damour et al. 2008a, b; Nagar 2011). In the large-mass-ratio limit, S becomes the spin of the largest black hole, while S_* reduces to q times the spin of the small body. The orbital contribution $H_{\rm eff}^{\rm orbital}$ incorporates the three EOB potentials (A, D, Q). The A function employs the full 4PN information (Damour et al. 2015) augmented by an effective 5PN term, parametrized by the coefficient a_6^c, which is informed by NR simulations. In GIOTTO, both (D, Q) are kept at 3PN accuracy. In the latest versions of Dalí, the full 5PN information is being currently explored (Nagar et al. 2023). The spin-orbit sector includes next-to-next-to-leading-order (NNLO) analytical information (Nagar 2011) in the (resummed) gyro-gravitomagnetic functions (Damour and Nagar 2014b) augmented by an effective N^3LO coefficient c_3 that is informed by NR simulations. Spin-spin couplings are incorporated using the concept of centrifugal radius (Damour and Nagar 2014b), r_c, and starting from NLO accuracy. TEOBResumS can deal with generically oriented spins, thus incorporating the precession of the orbital plane and the related modulation of the waveform. Spin-precession in the quasicircular case is incorporated with an efficient yet accurate hybrid EOB-post-Newtonian scheme based on the common "twist approach" (Akcay et al. 2021; Gamba et al. 2022; Gonzalez et al. 2023a).

In GIOTTO, the radiation reaction and multipolar waveform (up to $\ell = m = 8$) are implemented as an upgraded version of the factorized and resummed procedure introduced in Damour et al. (2009); see Nagar et al. (2020b); Messina et al. (2018). In addition, NR information is used to determine NQC waveform corrections (multipole by multipole) so as to correctly shape the waveform around merger. The latter is then

Table 10 Current/default physics incorporated in `TEOBResumS`

Physical content		`GIOTTO`	`DALI`
Analytic information	$A(r)$	Pseudo 5PN, resummed	Pseudo 5PN, resummed
	$D(r)$	3PN, resummed	5PN, resummed
	$Q(r, p_{r_*})$	3PN	5PN (local)
	G_S, G_{S_*}	3.5PN	3.5PN
	r_c	NLO	NLO
NR information	a_c^6	Effective parameter in $A(r)$	
	$c_{\rm N3LO}$	Effective parameter in G_S, G_{S_*}	
	NQCs	Ensure correct transition between plunge and merger	
	Ringdown	Phenomenological model, quasi-circular	
	BBH NR Validation region	$q \leq 10$ and test-mass with $\lvert\chi_{1,2}\rvert \geq 0.99$; $10 < q < 128$ no-spins	
Spins	Aligned	✔	✔
	Precessing	✔	-
Orbital dynamics		Circular	Generic (bound & open)
CP modes	Inspiral to merger	$(\ell, \lvert m\rvert) \leq 8$	
	Merger/ringdown	$(\ell, \lvert m\rvert) = (2,2), (2,1), (3,2), (3,3), (4,2), (4,4), (5,5)$	

`TEOBResumS` is developed open source and publicly available at https://bitbucket.org/eob_ihes/teobresums/. Symbols are defined in the text. Historical milestones in the model developments and the associated references as well as robustness tests and the detailed parameter space coverage can be found on the Wiki page and are continuously updated. `TEOBResumS` can also be installed via `pip install teobresums`. The code is interfaced to state-of-art GW data-analysis pipelines, including Bilby and PyCBC. The code uses semantic versioning since the deployment of the `GIOTTO` version. Earlier versions of `TEOBResumS` are implemented in `LALsuite` (LIGO Scientific Collaboration et al. 2024) and reviewed by LVK

attached to a NR-informed, phenomenological description of the ringdown based on Nagar et al. (2020b). Importantly, NR information is included in such a way to maintain consistency between waveform and fluxes (Riemenschneider et al. 2021). The leading-order horizon absorption terms are implemented in the model since its early version (Damour and Nagar 2014b). In `Dalí`, the radiation reaction on generic orbits is obtained by incorporating generic Newtonian prefactors in the factorized quasicircular EOB waveform (Chiaramello and Nagar 2020; Nagar et al. 2021a). This approach, which is extended to include resummed 2PN terms, has been verified against exact Teukolsky fluxes for highly eccentric and hyperbolic geodesics and currently provides the best available representation of the radiation reaction (Placidi et al. 2022; Albanesi et al. 2021, 2022a). A new paradigm to incorporate PN results into EOB, which promises a further boost in performance, has been recently proposed in Albanesi et al. (2022b). The inclusion of matter effects and application to probing the nature of compact objects is discussed in Sect. 6.5.

On the algorithmic side, the development of `TEOBResumS` has introduced two key analytical acceleration techniques, namely the post-adiabatic (PA) approximation of the EOB dynamics (Nagar and Rettegno 2019) and the EOBSPA (Gamba et al.

2021). The PA approximation is an iterative procedure to solve the circularized EOB dynamics at given radii (or frequency) thus bypassing the need to numerically solve the system of ODEs. Performances are reported in e.g. Nagar and Rettegno (2019); Nagar et al. (2019b); Riemenschneider et al. (2021); Tissino et al. (2023) and show that `TEOBResumS`'s waveform generation times are competitive with some of the fastest waveforms and machine learning approximants for long signals (i.e. BNS inspirals), while retaining the original EOB accuracy. The EOBSPA is a technique to generate multipolar FD EOB waveforms using the stationary phase approximation. Gamba et al. (2021) illustrates that the EOBSPA is computationally competitive with current phenomenological and surrogate models, and can generate (virtually) arbitrarily long and faithful waveforms up to merger for any BNS. Currently, the EOBSPA is also the only alternative to PN methods for efficiently generating intermediate-mass binary black hole inspiral waveforms for LISA (Gamba et al. 2021).

4.5.5 Environmental effects

The EOB approach provides considerable freedom for incorporating yet unknown effects, such as beyond-GR gravity (see Sect. 6.6), exotic BH-like objects, or environmental effects. Analyzing the presence of such effects critically relies on accurate GR waveforms for comparison and benefits from the techniques developed for GR. While the modeling of astrophysical environments has not yet been explored directly within the EOB waveforms program, there is in principle no obstruction to incorporating them. For example, perturbative and numerical studies of environmental effects are already available (as discussed in Sects. 4.2, 4.3 and 4.1) and have identified key distinctive features, which could be mapped into EOB models similarly to what has already been accomplished for other physical effects. Likewise, existing capabilities of using EOB-baseline models for parameterized tests of GR could be extended to include environmental effects in a parameterized, phenomenological way at the level of waveforms. These two approaches could be useful for different purposes.

4.5.6 Challenges

Employing EOB waveforms for GW signals of LISA sources requires a significant continued effort to improve the accuracy and include all physical effects. Importantly, the waveform models must incorporate the simultaneous effects of high spins at generic orientations, eccentricity, and large mass ratios q, all of which also require many more higher modes. Furthermore, we require additional flexibility to discover new physics from beyond GR and the Standard Model of particle physics, as discussed in Sect. 6. In terms of accuracy, the models must describe high signal-to-noise-ratio events of MBHBs, at more than an order of magnitude higher than the calibration standards achieved to date, and they have to be tested for the expected LISA detector response.

The effort to meet these requirements involves substantial further model developments on the theoretical and computational fronts. On the theoretical side,

advances on the structure of the EOB models to incorporate more information from perturbative schemes are essential. This effort relies on inputs from higher-order calculations with more realistic physics from PN, PM, and GSF to develop robust EOB models for a wide range of the parameter space. While several proof-of-principle studies have been carried out on including PM and GSF information, more work is needed to incorporate them in full state-of-the-art models in a way that can readily be updated as more information becomes available. This also applies to the inclusion of memory effects. Methods for including precessing-spins and moderate eccentricity effects (where the systems circularize before merger) are in place but only separately. In principle, the EOB Hamiltonian is fully generic but other components of the model are not, and require further structural developments to incorporate larger eccentricities, as well as the simultaneous effect of precessing spins. Further considerations will also be required on the sets of dynamical variables used to evolve the inspirals, for example, action-angle variables versus the canonical Cartesian coordinates, or a mixture of them. The higher complexity when including both precession and eccentricity effects is challenging, and requires due care to ensure gauge-invariant comparisons. As for existing models, insights from the small-mass-ratio limit will likely prove useful to address this challenge.

On the practical side, significant further work on testing, calibrating, and optimizing the EOB models against NR results is crucial to attain the accuracy required for LISA sources discussed in Sect. 3.2. This in turn relies on the availability of accurate NR waveforms over a wider parameter space, as detailed in Sect. 4.1. Current EOB models are only calibrated in the aligned-spin sector. However, this would need to be changed, and the calibration be extended to precessing spins to achieve the much higher accuracy requirements of LISA sources.

Furthermore, accurate waveforms for LISA that include eccentricity, precessing spins, large mass ratio, higher modes, and means to test for new physics have a highly complex structure characterized by a large number of different frequencies. Accurately capturing these features significantly slows down the computations of waveforms and enlarges the dimensionality of the parameter space. While EOB waveforms are a priori less efficient than closed-form models, there exist a number of approaches to overcome these shortcomings, as discussed above in Sects. 4.5.1, 4.5.3 and 4.5.4.

4.6 Phenomenological waveform models

Coordinators: Sascha Husa, Maria Haney
Contributors: M. Colleoni, M. Hannam, A. Heffernan, J. Thompson

4.6.1 Description

After the binary black hole breakthrough of 2005, a pragmatic approach to developing waveform models for compact binary coalescence was required. Such models needed to describe the waveform from inspiral to ringdown, be tuned to NR, and suit a wide range of GW data analysis applications. Key requirements for broad

applicability were (and still are) computational efficiency and broad coverage of the parameter space. This has led to several generations of frequency-domain and more recently also time-domain models, which have been implemented in the open source `LALSuite` framework (LIGO Scientific Collaboration et al. 2024) under the name of IMRPhenom, and which are constructed in terms of piecewise closed form expressions for the amplitude and phase of spherical harmonic modes. A careful choice of the closed-form expressions allows the maximal compression of information about the waveform into a small number of coefficients that vary across the parameter space. More recently, fast ODE integration techniques have also been developed to model the evolution of the component spins in precessing binaries (Estellés et al. 2022a). The principal objective of the phenomenological waveform program has been to deliver waveform models that keep up with requirements of data analysis applications and are updated to become increasingly accurate as detectors become more sensitive.

To construct the models, one proceeds in three stages: First, an appropriate piecewise ansatz is developed for simple functions, e.g. the amplitude and phase of spherical or spheroidal harmonics. This ansatz is split into regions, for example corresponding to the inspiral, merger, and ringdown, where physical insight about the different regions can be exploited. Figure 10 shows the three regions used in current models, where in each such region closed-form expressions are developed to approximate a discrete data set of calibration waveforms. Future upgrades may increase the number of regions to increase accuracy. The analytical ansatz attempts to incorporate physical insight, e.g. regarding perturbative information concerning the inspiral and ringdown. For the inspiral, an ansatz is typically constructed as a deformation of a post-Newtonian description. In the ringdown, black hole perturbation theory can be used to link features in the waveform to the quasinormal frequencies determined by the final mass and spin of a black hole. The ansatz is then fitted to each waveform in a calibration data set, resulting in a set of generalized coefficients for each waveform. This stage is usually referred to as the "direct fit". The input data consist of NR data and perturbative descriptions at low frequency, such as post-Newtonian expansions or EOB models. Most typically, these types of input data are used in the form of hybrid waveforms, which are constructed by gluing inspiral approximants to shorter NR data. For the PhenomD, PhenomX and PhenomT models, waveforms from the `SEOBNR` family have been employed to construct such hybrids (Khan et al. 2016; Pratten et al. 2020; Estellés et al. 2022b). Finally, the coefficients are interpolated across the parameter space, which we will refer to as the "parameter space fit". In both stages of fits it is essential to avoid both overfitting and underfitting.

Waveform model development has been increasingly "data driven", adapting phenomenological descriptions to the available data sets, while also using physical insight and perturbative information. The inspiral descriptions, for example, extend post-Newtonian expansions, and the black hole ringdown is formulated in terms of exponentially damped oscillations with complex frequencies that depend on the dimensionless spin of the remnant. In addition, approximate maps have been used, e.g. to map the non-precessing waveforms to precessing ones. Such maps:

- Allow to increase the region of the parameter space where the models can be employed before sufficiently extensive catalogues of NR waveforms are available.
- Give guidance for future more sophisticated models that are calibrated to NR.

The "phenom" approach sketched above facilitates the development of simple and robust codes and very rapid evaluation of the waveforms, and is also well suited to benefit from parallelisation, e.g., through GPUs (Katz et al. 2020) or similar hardware. Phenom models have already been used in computationally efficient parameter estimation studies of MBHB sources for LISA (Katz et al. 2020). Initially, only frequency domain models were developed (Ajith et al. 2007, 2008, 2011; Santamaria et al. 2010; Hannam et al. 2014; Husa et al. 2016; Khan et al. 2016; Bohé et al. 2016; London et al. 2018; Khan et al. 2019, 2020; Dietrich et al. 2019b, c; Thompson et al. 2020; Pratten et al. 2020; García-Quirós et al. 2020, 2021; Pratten et al. 2021; Colleoni et al. 2023), since they are naturally adapted to matched filter techniques carried out in the frequency domain. More recently, time domain models have also been developed (Estellés et al. 2021, 2022a, b), which can simplify modelling complex phenomena such as precession or eccentricity.

Four generations of such models have been constructed to date in the frequency domain, progressing from the $\ell = |m| = 2$ mode for quasi-circular non-spinning binaries to multi-mode precessing waveforms, as will be described in Sect. 4.6.3. The flexibility of the phenomenological approach is also well suited to parameterize unknown information, e.g., beyond-GR effects (see Sect. 6.6).

4.6.2 Suitable for what sources?

Massive black hole binaries have already been modelled with the phenom approach, i.e., comparable-mass black-hole binaries, described in Sect. 2.1. The bulk of such binaries detected by LISA is expected to have mass ratios $q = m_1/m_2$ up to ~ 10 (see Sect. 2.1.2), where phenom models have already been calibrated to NR. The main challenge to model such binaries for LISA is to significantly increase the

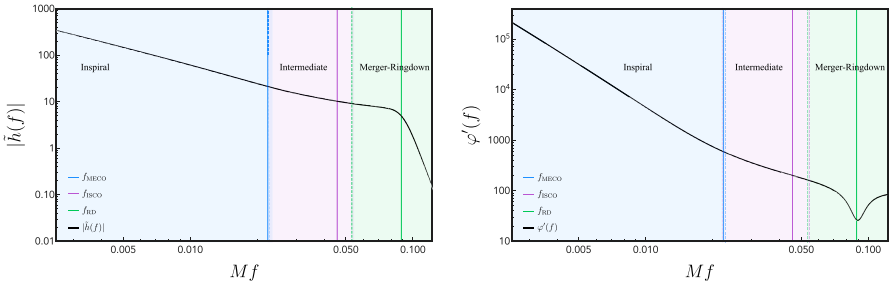

Fig. 10 Illustration of the regions used in Phenom models exemplified by the IMRPhenomX model. The plots show the Fourier domain amplitude (left) and phase derivative (right) of the $\ell = 2, m = -2$ spherical harmonic mode. Vertical lines mark the frequencies of the ISCO for the remnant black hole, the MECO (minimum energy circular orbit as defined in Cabero et al. (2017), see also Blanchet (2002)) and the ringdown frequency of the fundamental mode. Figure adapted from Pratten et al. (2020)

accuracy, corresponding to the much higher expected values for the signal-to-noise-ratio (SNR) with LISA. However, a tail up to mass ratios of a few times 10^3 also has to be expected (Sect. 2.1.2). The latest generation of phenom models has indeed already been calibrated to perturbative numerical waveforms that correspond to solutions of the Teukolsky equation (Pratten et al. 2020; García-Quirós et al. 2020) at mass ratios of $\approx 10^3$. Significant progress will still be required regarding both the input calibration waveforms and the models to increase the accuracy, in particular for larger spins and the inspiral. Developments and challenges toward computing large mass ratio NR waveforms are discussed in Sect. 4.1, including synergies between traditional numerical methods, analytical and self-force methods. In principle, the phenom approach may be well suited to some EMRI systems as well. Extension to EMRIs seems most feasible for non-precessing quasi-circular systems, but may not be practical for precessing or eccentric systems, where the signal can be extremely complex.

Stellar-origin binaries (Sect. 2.5) and Galactic binaries (Sect. 2.4) are types of sources for which the phenomenological approach is likely to provide a well suited framework. It can be adapted to produce computationally efficient models that can be tuned to data analysis requirements. However, to our knowledge, no work has yet been carried out in this direction. Finally, one of the strengths of the phenom approach is precisely that it allows for the easy inclusion of approximate phenomenological models of physical effects. In this sense, parameterised modifications to GR or models of environmental effects would in principle be straightforward to include.

4.6.3 Status

To date four generations of FD models have been developed, as well as a first generation of time domain models, which correspond to the most recent FD models in terms of parameter space coverage and accuracy. These models have been implemented in the LIGO Algorithms library (LALsuite) (LIGO Scientific Collaboration et al. 2024) and reviewed by the LIGO-Virgo-KAGRA collaboration. With the exception of (Hamilton et al. 2021; Thompson et al. 2024), these models have only been calibrated to non-precessing quasi-circular numerical waveforms, and precession has been implemented via the "twisting" approximation (Hannam et al. 2014; Bohé et al. 2016; London et al. 2018; Khan et al. 2019, 2020; Pratten et al. 2021; Estellés et al. 2021), which is based on the fact that in the inspiral the precession timescale is much smaller than the orbital timescale. Consequently, the precessing motion contributes little to the GW luminosity, and the inspiral rate is dominated by the non-precessing dynamics. One can thus approximately map non-precessing to precessing waveforms, and in a further step one can use fast PN approximants to describe the Euler angles that rotate the orbital plane and waveform. An effective analytical single-spin description for the Euler angles including next-to-next-to-leading order (NNLO) orbit-averaged PN effects has been developed in Marsat et al. (2013a), and a double spin approximation based on a multiple-scale analysis (MSA) has been developed in Chatziioannou et al. (2017). A key

shortcoming of implementations of the twisting-up approach in the frequency domain (Hannam et al. 2014; Bohé et al. 2016; London et al. 2018; Khan et al. 2019, 2020; Pratten et al. 2021) has been the use of the SPA, which is not appropriate for the late inspiral, merger and ringdown. Possible strategies for going beyond the SPA have been discussed in Marsat and Baker (2018), but will require further study and testing. Further shortcomings of the twisting-up approach have recently been discussed in Ramos-Buades et al. (2020b).

Before discussing the current generation of models we briefly summarize the historical development of the first three generations:

(i) The first generation consists of the PhenomA model for the $l = |m| = 2$ modes of non-spinning binaries (Ajith et al. 2007, 2008).

(ii) Second generation models PhenomB (Ajith et al. 2011) and PhenomC (Santamaria et al. 2010) included non-precessing spins, where the two spin degrees of freedom are described by a single effective spin. Also, the precessing PhenomP (Hannam et al. 2014) model was constructed from PhenomC using an approximate "twisting-up" map between precessing and non-precessing waveforms.

(iii) The PhenomD (Husa et al. 2016; Khan et al. 2016) model for the $l = |m| = 2$-mode significantly improved the fidelity of the phenomenological ansatz and the quality of the NR calibration. Several models have been derived from IMRPhenomD:

- PhenomPv2 (Bohé et al. 2016) updates the PhenomP model for precession.
- PhenomHM (London et al. 2018) adds subdominant harmonics based on an approximate map from the $l = |m| = 2$ mode to subdominant harmonics.
- PhenomPv3 (Khan et al. 2019) upgrades the NNLO effective single-spin description of precession that had been used for the first two versions of PhenomP to a double-spin description based on the MSA approximation (Chatziioannou et al. 2017).
- PhenomPv3HM (Khan et al. 2020) includes subdominant harmonics in the twisting-up construction.
- Matter effects have been included in terms of tidal phase corrections (Dietrich et al. 2019c, b) and amplitude corrections of NS-BH systems (Thompson et al. 2020).

The PhenomD model has been implemented for use in the LISA data challenge infrastructure (Babak and Petiteau 2024), and has been used in the "Radler" edition of the LISA data challenge. The PhenomD and PhenomPv2 models have been used for parameter estimation for observed GW events since the first detection of gravitational waves, the GW150914 event (Abbott et al. 2016f). Its derivatives including subdominant harmonics have also been used to analyse events during the third observing run. A detailed

study of waveform systematics (Abbott et al. 2017) found these models to be accurate enough for the GW150914 event, but also highlighted the need for further improvements. This is consistent with a more recent study concerning the need for further improvements for upcoming upgrades to ground-based GW detectors (Pürrer and Haster 2020).

The PhenomX (Pratten et al. 2020; García-Quirós et al. 2020, 2021; Pratten et al. 2021) family provides a thorough upgrade of third generation phenom models. PhenomXAS (Pratten et al. 2020) replaces PhenomD for the dominant mode, increasing the accuracy by roughly two orders of magnitude in terms of mismatch:

- The number of NR waveforms used for calibration is increased from 20 to ~ 400.
- Teukolsky waveforms are included in the data set in order to extend the model to EMRI waveforms.
- Final spin and mass include EMRI information derived from circular geodesics.
- Both spin degrees of freedom are calibrated to numerical data.
- Heuristic parameter space fits have been replaced by the systematic hierarchical fitting approach described in Jiménez-Forteza et al. (2017). An ansatz is selected among classes of polynomial and rational functions by minimizing not only the RMS errors, but also information criteria that approximate a full Bayesian approach, which avoids overfitting and underfitting. This method has, however, not yet been applied to dimensions larger than 3 (i.e. precession or spinning eccentric binaries).

PhenomXHM (García-Quirós et al. 2020) extends PhenomXAS to the sub-dominant modes, and PhenomXPHM (Pratten et al. 2021) adds precession via the twisting-up procedure, and allows to switch between the NNLO and MSA descriptions for the Euler angles. A first calibration of Phenom models to precessing NR simulations has recently been presented in the frequency domain (Hamilton et al. 2021, 2023), paving the way for further increasing the accuracy of precessing and eventually generic models in the future. Another important step in improving precessing models has been the incorporation of the mode asymmetry associated with large recoils (Brügmann et al. 2008a; Ramos-Buades et al. 2020b; Kalaghatgi and Hannam 2021) in the frequency domain (Ghosh et al. 2024; Thompson et al. 2024). Extensions to BNS and BHNS systems following the approaches of third generation models are in progress (Colleoni et al. 2023; Abac et al. 2024).

The fourth generation PhenomX family demonstrates that a significant increase in the accuracy of phenom models can be paired with a significant decrease in computational cost. Consequently, PhenomX provides the fastest Inspiral-Merger-Ringdown (IMR) waveforms currently available for data analysis without GPU acceleration (García-Quirós et al. 2021; Pratten et al. 2021). Parameter estimation application with GPU acceleration for PhenomHM has been presented in Katz et al. (2020). Part of the improvement in efficiency is due to the "multibanding method", which is based on Vinciguerra et al. (2017): analytical error estimates determine the

grid spacing for interpolation from a coarse grid, and a standard iterative scheme is used to rapidly evaluate the complex exponentials required to compute the waveform from the amplitude, phase, and the Euler angles used in "twisting up".

Most recently, the time-domain PhenomT model family (Estellés et al. 2021, 2022a, b) has been constructed to mirror the features of PhenomX in the time domain. A key motivation for the development of time domain models is that they do not require an analytical approximation to the Fourier transform in order to obtain explicit expressions for a "twisted-up" precessing waveform. This also simplifies the incorporation of analytical results, e.g., concerning the precessing ringdown frequencies; similar simplifications are hoped for when modelling eccentricity. The time domain model has also recently been extended to include the $\ell = 2, m = 0$ spherical harmonic, which contains the leading contribution to the gravitational wave memory effect (Rosselló-Sastre et al. 2024). For future developments, it is foreseen that both frequency and time domain models will be upgraded in parallel, and that each of the two "branches" will benefit from progress with the other.

The historical development and current status of phenom models is sketched in Table 11.

4.6.4 Environmental effects

The phenom approach provides significant freedom to incorporate additional features, such as poorly known subdominant GR effects, beyond-GR effects (see Sect. 6.6), and environmental effects. We note that analysing the presence of such effects also requires accurate GR waveforms for comparison and will benefit from the techniques developed for GR. Work toward tests of GR or the presence of environmental effects may call for improving the accuracy or other features of GR models. While the modelling of environmental effects has not yet been explored in the phenomenological waveform program, the phenomenological models are primed for their addition in two ways:

(i) The modular structure of phenomenological waveforms should facilitate the incorporation of known environmental effects, e.g. by augmenting PN information about the inspiral with information about environmental effects.
(ii) Environmental effects for which a quantitative model is not yet available could be incorporated into the phenom ansatz in a parameterised way, similar to existing GW tests for theory-agnostic deviations from GR.

In both cases it will be useful to have both frequency and time domain phenomenological waveform models available, allowing one to choose the natural domain for a given effect.

4.6.5 Challenges

Waveform modelling for comparable mass binaries in general faces four main challenges:

(i) The availability of a sufficient number of high-accuracy numerical relativity waveforms throughout the parameter space, including precession and eccentricity. (This is not specific for phenom models.)
(ii) The lack of accurate analytical descriptions, in particular for precession and eccentricity. Here, specific challenges arise for the phenom approach, which uses "deformed" PN expressions as the basis for constructing a computationally efficient inspiral ansatz. This will benefit in particular from further analytical developments in precession and eccentricity.
(iii) The development of modelling techniques that can produce efficient models from high-dimensional data sets. For the phenom approach, it may turn out to be difficult to develop closed form expressions that accurately represent the full morphology of precessing and eccentric binaries, and to accurately interpolate the full parameter space without compromising computational speed.
(iv) Development of an overall data analysis strategy and concrete code framework. The flexibility and modularity of the phenom approach could be exploited to develop variants of models with different tradeoffs between accuracy and speed, or accuracy and broad coverage of parameter space, which can then be utilised to optimise computational efficiency.

Significant coupling between these challenges is foreseen, e.g. the number and quality of NR waveforms required will also depend on the progress with analytical results. In addition, there will be more sophisticated data analysis approaches, which could exploit the advantages and disadvantages of different models, or tunable parameters, which could allow one to trade accuracy for speed. These could eventually give guidance for the development of waveform models that are designed as an integral part of the data analysis strategy. These challenges are not specific to LISA, but apply in general to further model improvements. LISA, however, poses particular challenges due to the extreme accuracies required for the loudest events, and also due to the more complicated nature of the detector response (see e.g. Marsat and Baker 2018). Strategies of how to best employ waveform models in data analysis applications, resolving tradeoffs of accuracy versus computational cost, can not be decoupled from considerations regarding the detector response, and new research will be required to exploit the simplicity and flexibility of phenomenological waveform models in order to accelerate the evaluation of the waveform together with the detector response.

The non-precessing quasi-circular sector will provide important initial guidance on how to connect with EMRI descriptions (or to which degree this is possible). This will provide an arena for toy-model explorations of highly accurate models in limited regions of parameter space, determining the limits of accuracy and computational efficiency that can be achieved, as well as studying issues of accuracy and efficiency related to the LISA detector response. It is therefore important to continue pushing to higher accuracies with these models.

The development of accurate phenomenological models of precessing systems is expected in both the time and frequency domains. Time-domain models will build on Estellés et al. (2021), which is foreseen to serve as a testing ground to further extend

Table 11 Progress in the development of phenomenological waveform models in frequency domain (FD) and time domain (TD)

Family	Domain	Waveform model	Spins	CP-Frame modes $(\ell, \lvert m \rvert)$	Eccentricity	Calibration region
1st gen	FD	`IMRPhenomA`	×	(2, 2)	No	$q \leq 4$
		Ajith et al. (2007, 2008)				
2nd gen.		`IMRPhenomB`	✓			$q \leq 4, \lvert\chi_{1,2}\rvert \leq 0.75$
		Ajith et al. (2011)				$\lvert\chi_{1,2}\rvert \leq 0.85$ (for $q = 1$)
		`IMRPhenomC`	✓			
		Santamaria et al. (2010)				
		`IMRPhenomP`	✓✓			
		Hannam et al. (2014)				
3rd gen.		`IMRPhenomD`	✓			$q \leq 18, \lvert\chi_{1,2}\rvert \leq 0.85$
		Husa et al. (2016); Khan et al. (2016)				$-0.95 \leq \lvert\chi_{1,2}\rvert \leq 0.98$
		`IMRPhenomPv2`	✓✓			(for $q = 1$)
		Bohé et al. (2016)				
		`IMRPhenomPv3`	✓✓			
		Khan et al. (2019)				
		`IMRPhenomHM`	✓	(2, 2), (2, 1), (3, 3),		
		London et al. (2018)		(4, 3), (4, 4)		
		`IMRPhenomPv3HM`	✓✓			
		Khan et al. (2020)				
4th gen.		`IMRPhenomXAS`	✓	(2, 2)	in dev.	NR:
		Pratten et al. (2020)				$q \leq 18, \lvert\chi_{1,2}\rvert \leq 0.99$
						Teukolsky:
						$q \leq 1000$

Table 11 continued

Family	Domain	Waveform model	Spins	CP-Frame modes $(\ell, \lvert m \rvert)$	Eccentricity	Calibration region
		`IMRPhenomP`	↗↗			
		Pratten et al. (2021)				
		`IMRPhenomXHM`	↗	(2, 2), (2, 1), (3, 2),		
		García-Quirós et al. (2020)		(3, 3), (4, 4)		
		`IMRPhenomPHM`	↗↗			
		Pratten et al. (2021)				
	TD	`IMRPhenomT`	↗	(2, 2)	in dev.	
		Estellés et al. (2021)				
		`IMRPhenomTP`	↗↗			
		Estellés et al. (2021)				
		`IMRPhenomTHM`	↗	(2, 2), (2, 1), (3, 3),		
		Estellés et al. (2022b)		(4, 4), (5, 5)		
		`IMRPhenomTPHM`	↗↗			
		Estellés et al. (2022a)				

`IMRPhenom` models are implemented in `LALSuite` (LIGO Scientific Collaboration et al. 2024) and reviewed by the LIGO-Virgo-KAGRA collaboration

× no spins ↗ spins aligned with orbital angular momentum ↗↗ precessing spins

CP: mode content in co-precessing frame

the calibration to NR, and will facilitate to use time domain implementations of the LISA response function. Further progress in the precessing inspiral will also crucially depend on progress with approximations that reduce the need for NR calibration for the inspiral across the large parameter space of precessing binaries, such as those based on the MSA (Chatziioannou et al. 2017) or dynamical renormalisation group (DRG) (Galley and Rothstein 2017; Yang and Leibovich 2019). In order to accurately describe the late inspiral, merger and ringdown of precessing systems in the frequency domain, further tests and implementations of the strategies discussed in Marsat and Baker (2018) will be required, such as analytical treatments that go beyond the SPA.

Eccentric waveform modes are again likely to require cross-pollination between frequency and time domain models (motivating in part the development of PhenomT in parallel to PhenomX), and significant advances in the development of analytical descriptions for the inspiral phase of spinning and eccentric binaries. This is particularly true where binary systems show both precession and eccentricity. It will be important to understand whether simple approaches twisting up eccentric waveforms will be sufficient for moderate SNR. Further investigations will determine if these prescriptions are adequate to determine binary parameters with sufficient accuracy, such that only a moderate number of NR waveforms is required to develop an accurate local model for high SNR events.

A key challenge is to develop models that are accurate across a large region of parameter space, describing well the changes of waveform morphology, e.g., as the mass ratio increases, or as spin alignment migrates between aligned and anti-aligned with the orbital angular momentum. For current ground-based detectors, parameter estimation posteriors are typically rather broad, so refined models in a smaller region of the parameter space would have very limited use. For LISA, however, it is foreseen that a hierarchy of models will be developed: those that are sufficiently accurate to identify signals across large portions of parameter space, and others that further increase the accuracy for smaller regions of parameter space, which would be used for the most accurate parameter estimation of the loudest signals. Models with parameters allowing one to trade accuracy for computational efficiency would be appropriate for hierarchical approaches to data analysis. This approach could also be extended further by mixing descriptions in terms of closed-form expressions with equation-solving, e.g. to improve the accuracy of describing eccentricity or precession. An important open question is how to incorporate results from the self-force program (see Sect. 4.3) into phenomenological models, and how to use ideas developed for the phenomenological waveforms program to accelerate self-force waveforms.

5 Waveform generation acceleration

Coordinators: Alvin Chua, Michael Katz
Contributor: S. Field

The stringent efficiency requirements described in Sect. 3.3 naturally necessitate the acceleration of waveform models, in order to enable the LISA science analysis. The two main strategies to achieve this are the development of improved computational techniques, and hardware acceleration.

5.1 Computational techniques

To maximize the science returns from highly relativistic LISA sources with exacting modeling requirements, we require waveform-acceleration techniques that do not compromise waveform accuracy. The general solution to this problem is to construct interpolants or fits for high-fidelity waveform data, where the data comes from an accurate underlying model that is too slow to use directly in data analysis studies (e.g., as it involves solving PDEs or coupled ODEs). This data can describe either the full time-/frequency-series representation of the waveform, or specific waveform components that are more computationally expensive. While many waveform acceleration techniques have appeared in the literature, most rely on the three steps summarized below and illustrated in Fig. 11.

5.1.1 Step 1: data representation

A gravitational waveform's parametric dependence is generally too complicated to model directly with an acceptable degree of accuracy. Instead, the waveform is typically decomposed into waveform data pieces that are simpler, more slowly varying functions of parameters and time. If we were to take a machine-learning viewpoint of the problem, data pieces are features of the data, and discovering what problem-specific features to extract is a feature engineering task. How should we define our features?

For non-precessing BBHs in quasi-circular orbits, an amplitude and phase decomposition for each (ℓ, m) angular-harmonic mode is an obvious choice for our data pieces. For precessing systems, the problem becomes significantly more complicated as the modes have a rich signal morphology. Here, the general approach has been to transform the modes to a co-rotating frame where the system has significantly reduced dynamical features (Blackman et al. 2017a, b; Varma et al. 2019a). It is often advantageous to further decompose the data into symmetric and asymmetric mode combinations (Blackman et al. 2017a, b; Varma et al. 2019a). The price of this simplification is that the frame dynamics must also be modeled, so that the co-rotating modes can be transformed back into the inertial frame of the detector. For eccentric BBH systems, which will be important for LISA science, the optimal data representation is currently unknown.

The highly disparate masses and large separation of timescales in EMRI systems allow their inspirals to be modeled within the two-timescale framework (Miller and Pound 2021). This allows the trajectory of the inspiral through the orbital configuration phase space to be computed in milliseconds (Katz et al. 2021; Wardell et al. 2023). The waveform is then computed by sampling the metric amplitudes along this inspiral typically by evaluating a precomputed interpolant of the amplitudes. Most often these amplitudes are computed in the frequency domain so

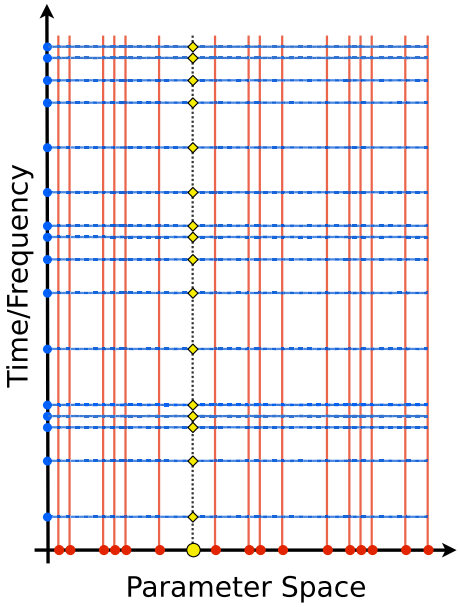

Fig. 11 Waveform acceleration can be achieved by building a surrogate model through a sequence of three steps. (Step 1) The red solid lines show the waveform training data evaluated at specific parameter values. (Step 2) Reduced-order modeling is used to compress the waveform data through a dimensional-reduction step, and the blue dots represent the data that needs to be modeled after compression. (Step 3) The blue lines indicate fits for the compressed waveform data across the parameter space. The yellow dot shows a generic parameter value, say λ_0, that is not in the training set. To compute the waveform for this value, each fit is evaluated at λ_0 (the yellow diamonds), and then the reduced-order representation is used to reconstruct the decompressed waveform (the dotted black line)

the waveform is decomposed into harmonics of not just angular dependence, but also the fundamental frequencies in the system (Hughes 2001; Drasco and Hughes 2006). Generically precessing and eccentric EMRI waveforms are extremely complex, but the above description effectively breaks the waveform down into slowly evolving sinusoids. The only drawback is that there are far more modes to compute and sum for a typical waveform ($\gtrsim 10^5$), though in practice many of these do not carry much power (Katz et al. 2021).

5.1.2 Step 2: reduced-order modeling

The waveform quantities of interest often reside in a representation space of extremely high dimensionality D, and must generally be interpolated or fitted over a parameter space of modest dimensionality d. For example, the full waveform itself for strong-field LISA sources typically has $D \gtrsim 10^4$ (signals of $\gtrsim 10^5$ s sampled at $\gtrsim 0.1$ Hz) and $d \sim 10$. These computational difficulties can often be mitigated through the use of dimensional-reduction tools (Prud'homme et al. 2001; Barrault et al. 2004; Binev et al. 2011; DeVore et al. 2013; Maday et al. 2002; Quarteroni et al.

2011; Cannon et al. 2010, 2011, 2012, 2013; Field et al. 2011; Herrmann et al. 2012), the collection of which is broadly referred to as ROMs.

ROMs aim to remove redundancies in large data sets, making them more amenable to analysis, and identifying relevant features for further approximation. Their construction typically begins with a greedy algorithm or singular value decomposition that identifies the set of n "most important" values in parameter space, whose associated waveform quantities span a *reduced-basis* space within which the model is well approximated (Field et al. 2011; Herrmann et al. 2012; Field et al. 2014; Pürrer 2014). This serves as both a dimensional-reduction step as well as a parametric-sampling step.

While invaluable for reducing computational cost on the representation end ($n \ll D$), the compression provided by ROMs does not actually lessen the intrinsic complexity of the model. Indeed, the successful application of ROMs relies on sufficient coverage of the parameter space with training data in the first place—or, more realistically, on truncation of the parameter domain to compensate. ROMs themselves also do not address the issue of interpolating or fitting the reduced representation at high accuracy, which can be challenging even in parameter-spaces with $d \gtrsim 3$.

5.1.3 Step 3: interpolation and fitting

The last step is to interpolate or fit each compressed data piece (viewed as scalar- or vector-field data) over the $d > 3$ dimensions of parameter space, and to do so both accurately ($\lesssim 10^{-6}$ error) and efficiently ($\lesssim 1$ seconds). In the context of sources and models for ground-based observing, a variety of choices have appeared, including polynomials (Field et al. 2014), splines (Pürrer 2014), Gaussian process regression (Doctor et al. 2017), deep neural networks (Chua et al. 2019; Khan and Green 2021; Thomas et al. 2022; Khan et al. 2022), and forward stepwise greedy regression using a custom basis (Blackman et al. 2017b). A recent review article provides informative comparisons between some methods (Setyawati et al. 2020). The accuracy and efficiency goals of models for ground-based observing are more modest, however, and it is unclear if these methods will continue to work for LISA MBHs (Pürrer and Haster 2020; Ferguson et al. 2021), or for EMRIs in full generality (Chua et al. 2021). As such, other interpolation and regression methods should continue to be explored.

5.1.4 Status of techniques

In the GW literature, the term surrogate modeling is sometimes used as a generalization of ROMs (for the full waveform) to include additional steps beyond dimensional reduction. ROM surrogates have been built for many different waveform families, regions of parameter space, and signal durations. Early models focused on closed-form waveform families largely as a proof-of-principle exercise (Herrmann et al. 2012; Field et al. 2011; Caudill et al. 2012; Cannon et al. 2010, 2011, 2012). Since then, ROM techniques have been further developed and

refined for various LVK (hence comparable-mass) applications: EOB (Field et al. 2014; Pürrer 2014, 2016; Cotesta et al. 2020; Gadre et al. 2024; Khan and Green 2021; Thomas et al. 2022), NR (Blackman et al. 2015, 2017a, b; Varma et al. 2019a, b), multiple subdominant modes (Field et al. 2014; Cotesta et al. 2020; Blackman et al. 2015, 2017a, b; Varma et al. 2019a, b), eccentric binaries (Islam et al. 2021), frequency-domain waveforms (Pürrer 2014, 2016; Cotesta et al. 2020), time-domain waveforms (Field et al. 2014; Blackman et al. 2015, 2017a, b; Varma et al. 2019a, b), generically precessing systems (Blackman et al. 2015, 2017a, b; Varma et al. 2019a), neutron star inspirals with tidal effects (Lackey et al. 2017, 2019; Barkett et al. 2020; Matas et al. 2020; Abac et al. 2024), and waveforms with $\sim 10^4$ cycles (Pürrer 2014, 2016; Cotesta et al. 2020; Varma et al. 2019b; Yoo et al. 2023).

When applied to computationally expensive models such as EOB or NR, ROM surrogates can accelerate the generation of a single waveform by factors of 10^2 (EOB models; described by ODEs) to 10^8 (NR models; described by partial differential equations), while being nearly indistinguishable to the underlying model. EOB surrogates are extensively used as part of LVK parameter-estimation efforts as well as template-bank detection (Abbott et al. 2016f, 2019b, 2021b, 2023a, 2024). NR surrogates have been used in numerous targeted follow-up studies on specific BBH events (Abbott et al. 2020a, b; Kumar et al. 2019; Islam et al. 2023). As such, ROM techniques have been essential to the widespread use of both EOB and NR waveforms for realistic data analysis efforts with LVK data.

The present surrogate framework is ill-suited to EMRI waveform modeling, where the increased duration and mode complexity combine to increase the information content of the model by at least 20 orders of magnitude (Gair et al. 2004; Chua et al. 2017; Moore et al. 2019). Surrogates might be useful in special cases of the IMRI regime, where these difficulties are lessened. There has been recent work on the first models (Rifat et al. 2020; Islam et al. 2022) for quasi-circular, non-spinning IMRI systems, based on solutions to the time-domain Teukolsky equation rescaled to fit NR results. The latest surrogate waveform model in this series covers the last 30,000M of the inspiral-merger-ringdown signal, with mass ratios ranging from 2.5 to 10^4. To put this in context, for a million-Solar-mass system, this is equivalent to approximately 2 days of signal, which is inadequate for the expected observable duration of months to years for an EMRI of that mass. However, it should suffice to describe an IMRI signal of similar total mass and a mass ratio of $\sim 10^3$.

In the angular- and frequency-based decomposition of an EMRI model, the problem separates naturally into two main parts: that of generating the inspiral trajectory (from which the waveform phasing is straightforwardly derived), and that of generating the waveform amplitude for each of the $\sim 10^5$ constituent modes. Fast frameworks for EMRI trajectory generation already exit (Van De Meent and Warburton 2018; Miller and Pound 2021). They present no computational difficulties at adiabatic order (for search); however, their extension to post-adiabatic order (for inference) will require interpolating the first-order fluxes to a relative precision of the mass ratio ($\sim \epsilon$) (Osburn et al. 2016). Trajectory-level interpolation with ROM is unlikely to be of practical use, due to issues of accuracy and parameter-space extensiveness. The accuracy requirements on the waveform amplitudes are far less

stringent, though, and it is here that ROM compression and neural-network interpolation has been applied to good effect (in the mode direction, rather than the time/frequency direction) (Chua et al. 2021).

5.1.5 Future challenges

LISA data analysis has three distinctive features that will require new ideas in waveform acceleration. First, the waveforms are significantly longer in duration, which will stress both computational resources and current ROM techniques. Second, as compared to LVK waveform modeling, LISA accuracy requirements are significantly more demanding. The fitting schemes will thus need to deliver higher accuracies while also contending with increased dimensionality. Finally, the orbital motion of LISA introduces a time-dependency in the response of the detector, which also needs to be modeled efficiently for data analysis applications; see, e.g., Marsat and Baker (2018).

In terms of source-specific challenges, eccentricity is expected to play a more important role in the modeling and interpretation of LISA MBHs. This will necessarily increase the problem from 7 to 9 parametric dimensions. While this should not pose significant difficulty for the dimensional-reduction step (Herrmann et al. 2012; Blackman et al. 2014), the parameter-fitting step will be vastly more difficult, and it is unlikely that any of the existing techniques will continue to perform well. For EMRIs, the main difficulty is ensuring that the waveform-amplitude fit retains its accuracy when extended from eccentric Schwarzschild orbits at present (Chua et al. 2021) to generic Kerr orbits with a much larger parameter and representation space.

5.2 Hardware accelerators/configurations

In addition to computational techniques, generating waveforms with a variety of hardware accelerators can vastly improve analysis time. Hardware acceleration, in a general sense, means hardware designed for a specific type of optimization when compared to general-purpose CPUs. Some examples of commonly used hardware accelerators include GPUs, Field-Programmable Gate Arrays (FPGAs) (Vanderbauwhede and Benkrid 2013), Tensor Processing Units (TPUs) (Paper 2021), and Artificial Intelligence (AI)-accelerators (Mishra et al. 2023).

GPUs are designed specifically for parallel computations. These devices leverage a large number of compute cores ($\sim 1000s$) and specialized memory structure to make a large number of independent calculations simultaneously. From an algorithmic standpoint, many of the methods discussed in Sect. 5.1 can be implemented on GPUs to achieve considerable gains in efficiency. These include, but are not limited to, artificial neural networks (matrix multiplication), interpolation, parallel sorting, and basis transformation. Additionally, some accurate waveform calculations can be implemented in parallel, allowing for all or parts of waveforms to be implemented entirely for GPUs. Programming for GPUs is generally performed in `C/C++` or, as of more recently, `Python`.

While GPUs take advantage of their parallel architecture, they are still programmed using specific software for a fixed hardware unit. FPGAs, on the other hand, represent "programmable hardware." These devices are programmed at the device level to implement customized hardware flow designed for specific tasks. Their most common usage is in neural networks and signal processing. Programming on FPGAs is done in `Verilog` or `VHDL` (Chu 2011), although some wrappers in `C/C++` are starting to become available.

5.2.1 Status

Recently FPGAs have started to be used by the GW community (Que et al. 2021; Martins et al. 2024) for data analysis but, to the best of our knowledge, they have not been used for waveform generation. In recent years, GPUs have seen increased interest from the community for use in waveform creation, as well as GW-related analysis in general. GPUs have been used for precessing waveforms, as well as population analysis related to ground-based observations from the LVK observing network (Talbot et al. 2019; Edwards et al. 2024). In this work, the waveform and the detector response were calculated directly on the GPU hardware. To limit the cost of Bayesian inference in ground-based observing, GPUs were recently used to greatly accelerate the creation of surrogate waveform models using techniques such as artificial neural networks (Khan and Green 2021). The creation of MBHB waveforms has also been implemented for LISA, including both the source-frame waveforms and the LISA response function for use in LISA parameter estimation studies (Katz et al. 2020) ($\sim$500x acceleration). The generation scheme for this work calculated, in parallel, accurate waveforms and LISA response information on sparse grids. Then, to scale to the full data stream, cubic spline interpolation was leveraged. This technique is generally well-suited for parallelization.

For EMRIs, GPUs have been used to improve the efficiency of black hole perturbation theory calculations within the GSF community (McKennon et al. 2012; Khanna and McKennon 2010; Field et al. 2023). In this work, the many harmonics of EMRI metric perturbation are computed in parallel as the orbit evolves. In terms of data-analysis related waveform creation for EMRIs, the Augmented Analytic Kludge (AAK) (Chua et al. 2017) waveform from the `EMRI Kludge Suite` was accelerated with GPUs (`gpuAAK`) for use in the LISA Data Challenges ($\sim$1000x). Additionally, the first fully relativistic fast and accurate EMRI waveform that goes beyond the kludge approximations was implemented on GPUs resulting in a considerable increase in efficiency ($\sim$2000x) (Chua et al. 2021; Katz et al. 2021). Both the `gpuAAK` and the fast and accurate EMRI waveforms generate sparse orbital and phase trajectories in serial on a CPU. These sparse trajectories are then scaled with spline interpolation to the full waveform sampling rate. This scaling is performed for each separate harmonic mode so that they can be properly and accurately combined into the final waveform. It is actually this summation over $\sim 10^6 - 10^7$ time points, each with a combination of $\sim$1000's of harmonic modes, that most requires the GPU architecture for optimal results.

5.2.2 Challenges

A central challenge when working with GPUs, FPGAs, or any other specialized hardware is the trade-off between efficiency and streamlined code creation and maintenance. For optimal efficiency, it is generally necessary to implement code specific to each type of hardware. This could mean implementation in an entirely different language with, for example, an FPGA, or an adjustment for different hardware or software requirements for each application. An example of this is the use of shared memory in GPUs. Shared memory is a small amount of memory available on the GPU chip, which is much faster to access in comparison to the larger global memory located off of the chip. Leveraging shared memory is essential to achieving optimal efficiency for many applications. There is no use of this form of shared memory on CPUs. Therefore, it may be desirable to implement a fast GPU version and a mirror CPU version that effectively uses the same exact code as the GPU version with slight adjustments. On the other hand, a CPU version optimized for a CPU may be needed, creating two separate codes. In general, it is helpful to minimize the amount of code duplication as much as possible, but that may be governed by efficiency requirements.

Many applications require some parallelization over CPUs in addition to specific hardware considerations. Understanding how to best leverage all resources is key to achieving maximal efficiency. With that said, maximal efficiency should be achieved while maintaining a constant user interface. This allows for the application of a waveform within a desired program while using a variety of hardware.

Another general concern about the use of specialized hardware is just that: it is specialized. Purchasing specialized hardware in place of CPUs will penalize the breadth at which the hardware can be used. This has generally hurt the availability of accelerators at large. Similarly, accelerators come at a variety of prices. Academic-grade GPUs (indicating they have strong performance in double precision) are generally expensive. However, the newest generations of accelerators combined with modern algorithms within the GW field have proven that efficiency is not only highly desirable, but cost efficient when compared to the equivalent number of CPUs (up to $\sim$ 1000's). Fortunately, researchers now often have access to clusters of CPUs, GPUs, TPUs, and AI-accelerators through local, national, and international scale computing centres. Ultimately, the combination of a variety of hardware will be necessary to accomplish the scientific goals of the LISA mission.

6 Modelling for beyond GR, beyond standard model, and cosmic string sources

Coordinators: Richard Brito and Daniele Vernieri
Contributors: J. Aurrekoetxea, L. Bernard, G. Bozzola, A. Cárdenas-Avendaño, D. Chernoff, K. Clough, T. Helfer, T. Hinderer, E. Lim, G. Lukes-Gerakopoulos, E. Maggio, A. Maselli, D. Nichols, J. Novák, M. Okounkova, P. Pani, G. Pappas, V. Paschalidis, M. Ruiz, A. Toubiana, A. Tsokaros, J. Wachter, B. Wardell, H. Witek

As explained in Sect. 2.7, the observation of gravitational waves with LISA has an enormous potential to probe physics beyond GR and the Standard Model of particle physics, in regimes that have so far not been explored (Barausse et al. 2020b; Arun et al. 2022). In order to fulfill this potential, we need to construct accurate waveforms that take into account signatures of new physics. As we will discuss in this section, this is in fact a very challenging task that for most cases is still at its early stages of development.

In this section we provide a brief summary of how beyond GR theories and the effect of beyond Standard Model physics can be modelled using the techniques presented in Sect. 4. The discussion will be mostly concerned with modelling the *generation* of gravitational waves by LISA sources in the presence of new physics. Beyond-GR effects can also affect the way gravitational waves *propagate* on cosmological scales, see e.g. Mirshekari et al. (2012); Saltas et al. (2014); Belgacem et al. (2018, 2019); Bonilla et al. (2020); D'Agostino and Nunes (2019); Allahyari et al. (2022); D'Agostino and Nunes (2022); Auclair et al. (2023). In general, separation of scales allows to add modifications to the GW propagation on top of any waveform model for which the generation problem is understood and therefore we do not discuss this possibility here. More details on this problem can be found in Belgacem et al. (2019); Auclair et al. (2023). We will also not discuss in detail the potential implications that LISA observations will have for fundamental physics, since a more detailed review on this issue can be found in LISA's Fundamental Physics Working Group White Paper (Arun et al. 2022).

This section follows a similar structure to Sect. 4 where various modelling approaches for compact binaries are discussed. However, the modelling of gravitational waves emitted by cosmic strings is discussed in a separate Sect. 6.7, mainly because these sources require modelling approaches that are specific to cosmic strings.

6.1 Numerical relativity

6.1.1 Beyond GR

NR simulations of BBH mergers in beyond-GR theories are only at their infancy and have only been performed in a handful of theories, e.g. Healy et al. (2012); Berti et al. (2013); Cao et al. (2013); Okounkova et al. (2017); Hirschmann et al. (2018); Witek et al. (2019); Okounkova et al. (2019, 2020); East and Ripley (2021b); Figueras and França (2022); East and Ripley (2021a); Aresté Saló et al. (2022); Ripley (2022); Cayuso et al. (2023). Even though most studies have so far focused on proof-of-principle simulations, in recent years there has been significant improvements in this topic.

The earliest NR simulations of BBH mergers in beyond GR theories focused on a particular class of scalar-tensor theories that are known to possess a well-posed initial value problem (Salgado et al. 2008; Healy et al. 2012; Berti et al. 2013; Cao et al. 2013). In these scalar-tensor theories, BHs satisfy no-hair theorems (Hawking 1972; Sotiriou and Faraoni 2012), and BBH mergers are indistinguishable from GR. However, in more complex extensions of GR, or for scalar matter with nontrivial

boundary conditions (e.g., cosmological boundary conditions or large scalar-field gradients), BHs can carry a scalar charge, and these solutions need not be unique.

One of the main difficulties when trying to do NR simulations in more complex theories is the fact that the well-posedness of the initial value problem (see e.g. Baumgarte and Shapiro 2010; Sarbach and Tiglio 2012; Hilditch 2013) in alternative theories is for most cases particularly challenging to establish (Delsate et al. 2015; Papallo and Reall 2017; Papallo 2017; Cayuso et al. 2017; Sarbach et al. 2019; Ripley and Pretorius 2019a, b; Kovács 2019; Kovács and Reall 2020a, b; Witek et al. 2020; Julié and Berti 2020; Bezares et al. 2021a; ter Haar et al. 2021; Silva et al. 2021; Aresté Saló et al. 2022; Ripley 2022; Barausse et al. 2022; de Rham et al. 2023).

To circumvent these problems, two treatments have been proposed in which alternative theories are considered as effective field theories of gravity. One approach uses an *order-by-order expansion* (Benkel et al. 2016, 2017; Okounkova et al. 2017; Witek et al. 2019; Okounkova et al. 2019, 2020; Doneva et al. 2022), in which the spacetime metric and extra fields are expanded around GR, order-by-order in the coupling constant,[3] to guarantee well-posedness. The second approach, the so-called *equation-fixing* method, proposes to use a scheme inspired by the Israel-Stewart treatment of viscous relativistic hydrodynamics, in which an effective damping controls higher frequency modes while preserving the physics of the low frequency modes (nearly) untouched (Cayuso et al. 2017; Allwright and Lehner 2019; Cayuso and Lehner 2020; Franchini et al. 2022; Cayuso et al. 2023). In this second approach the alternative theory equations of motion are viewed as a low-energy effective deviation from the Einstein equations, such that the theory can be captured by the low-energy degrees of freedom. Although these methods are quite generic, they have so far been mainly employed in theories with higher derivative terms in the metric (Benkel et al. 2016, 2017; Okounkova et al. 2017; Witek et al. 2019; Okounkova et al. 2019, 2020; Okounkova 2020; Cayuso and Lehner 2020; Silva et al. 2021; Doneva et al. 2022; Elley et al. 2022; Cayuso et al. 2023), such as quadratic theories of gravity with an extra scalar field (for which the order-by-order expansion was used), namely dynamical Chern-Simons gravity (dCS) (Alexander and Yunes 2009; Green and Schwarz 1984; Taveras and Yunes 2008; Mercuri and Taveras 2009), Einstein dilaton Gauss-Bonnet gravity (EdGB) (Kanti et al. 1996; Cayuso et al. 2023; Moura and Schiappa 2007; Berti et al. 2015) or more generic Einstein scalar Gauss-Bonnet theories (ESGB) (Doneva and Yazadjiev 2018; Silva et al. 2018; Antoniou et al. 2018). Unlike the simplest scalar-tensor theories, in dCS and EdGB BHs naturally possess scalar "hair", and therefore deviations from GR naturally occur. Some ESGB theories are prone to BH scalarization, i.e., a process in which GR BHs become unstable against the spontaneous development of scalar hair for large enough spacetime curvatures (Doneva and Yazadjiev 2018; Silva et al. 2018; Antoniou et al. 2018; Doneva et al. 2024) (see also Dima et al. (2020); Herdeiro et al. (2021b); Hod (2020); Berti et al. (2021); Doneva and Yazadjiev

[3] Sometimes this is also called "order-reduction scheme." This is not to be confused with order-reduction schemes in which the field equations themselves are used to replace higher-order curvature terms that are then kept only to a given (reduced) order in the coupling constant.

(2021a, b); Elley et al. (2022) for a similar process but where scalarization is controlled by the magnitude of the BH spin).

In particular, using the order-by-order expansion mentioned above, BBH simulations were done in dCS (Okounkova et al. 2019, 2020) and EdGB (Okounkova 2020; Witek et al. 2019). Importantly, this scheme also simplifies the problem of covering the parameter space needed to build IMR waveforms for parameter estimation purposes. Since NR is *scale-invariant* and the dCS and EdGB coupling parameters are scaled out of the order-by-order expansion scheme (Okounkova et al. 2019), a simulation for one set of BBH parameters (masses and spins) can be applied to any total mass, and any valid value of the coupling constants. With enough NR simulations, one can thus hope to cover the the full BBH parameter space, build a surrogate model for parameter estimation (Varma et al. 2019a), and perform model-dependent tests of GR with gravitational waves. Work towards model-dependent tests using full IMR signals obtained through this method has been done in Okounkova et al. (2023), where parameter estimation was performed on full BBH waveforms in dCS.

Despite their promises and advantages, the schemes mentioned above also suffer from some important problems. The main problem with the order-by-order expansion scheme is the fact that solutions may be plagued by secularly growing solutions signaling the breakdown of perturbation theory on long timescales. As proposed in Gálvez Ghersi and Stein (2021), such problem could potentially be solved using renormalization-group techniques that can be used to build solutions valid over the secular timescale. For the equation-fixing method on the other hand, there are first studies in spherical symmetry (Cayuso and Lehner 2020; Thaalba et al. 2024; Franchini et al. 2022; Bezares et al. 2021b) and for BBH mergers in some beyond-GR theories (Cayuso et al. 2023). A more detailed quantitative analysis is needed to identify how much a given "equation-fixing" choice affects low-energy modes in scenarios of interest, and to fully characterize the accuracy of these approximate schemes (Coates and Ramazanoğlu 2023).

These problems can be avoided for cases where a given theory in its full form can be shown to have a well posed initial value problem. Important work in this direction has recently been done. For example, nonlinear evolutions of BBHs in quadratic gravity were presented in Held and Lim (2023). Furthermore, BBHs simulations have been performed in cubic Horndeski theories (Figueras and França 2022) which are known to be well-posed in the standard gauges used in numerical GR (Kovács 2019). For more generic theories, it has been recently shown that, at sufficiently weak coupling, the equations of motion for Horndeski gravity theories possess a well posed initial value problem in a modified version of the generalized harmonic gauge formulation (Kovács and Reall 2020a, b). Quite remarkably, using this formulation it could in principle be possible to perform simulations in all Horndeski theories of gravity without having to resort to the two schemes mentioned above (Ripley 2022). In particular, (East and Ripley 2021b) used this modified generalized harmonic (MGH) formulation to perform the first numerical simulations of BBH mergers in shift-symmetric ESGB gravity, without approximations, which were also compared against PN results in Corman et al. (2023). Simulations of head-on BH collisions in ESGB theories that exhibit spontaneous BH scalarization (East and Ripley 2021a)

and simulations of binary neutron stars in shift-symmetric Einstein-scalar-Gauss-Bonnet (East and Pretorius 2022) have also been done. Based on the MGH formulation, a modified version of the CCZ4 formulation of Einstein's equations has also been proposed, which has been used to prove the well-posedness of the most general scalar-tensor theory of gravity with up to four derivatives, in singularity avoiding coordinates (Aresté Saló et al. 2022). This was then used to perform (circular and equal-mass) BBH merger simulations in such theories (Aresté Saló et al. 2022; Doneva et al. 2023). More recently, using shift-symmetric ESGB gravity as a benchmark theory, Corman et al. (2024) compared the results obtained with the MGH formulation against results obtained using the order-by-order expansion and equation-fixing methods. This work confirms that the order-by-order approach cannot faithfully track the solutions when the corrections to GR are non-negligible, whereas the equation-fixing method is able provide consistent solutions.

Finally, NR simulations have also been done in theories in which BHs possess an electric or magnetic charge (Zilhao et al. 2012; Zilhão et al. 2014a; Hirschmann et al. 2018; Bozzola and Paschalidis 2019, 2021; Luna et al. 2022), possibly coming from mini-charged dark matter (Cardoso et al. 2016c), primordial magnetic monopoles (Preskill 1984), or in specific classes of scalar-tensor-vector modified theories of gravity (Moffat 2006). In all these cases the field equations can be cast in a form that is mathematically equivalent to Einstein–Maxwell theory (or to Einstein–Maxwell with an extra scalar field for some theories (Hirschmann et al. 2018; Fernandes et al. 2019), which is known to possess a well-posed initial boundary value problem (Alcubierre et al. 2009).

6.1.2 Boson clouds

Simulations of BHs surrounded by massive bosonic fields have been widely studied, focusing mostly on the evolution of bosonic fields around isolated BHs (see e. g. Witek et al. 2013; Barranco et al. 2014; Okawa and Cardoso 2014; Okawa et al. 2014; Okawa 2015; Zilhão et al. 2015b; Sanchis-Gual et al. 2015, 2016; Clough et al. (2019; Bamber et al. 2021; Traykova et al. 2021; Wang et al. 2022; Clough et al. 2022; East 2022). This has led to the first successful nonlinear evolution of the superradiant instability of minimally-coupled Proca fields around a spinning BH in East and Pretorius (2017); East (2018). These works have laid down the possibility to study the impact of minimally-coupled bosonic fields in BBH systems within NR (Bernard et al. 2019; Cardoso et al. 2020; Ikeda et al. 2021; Choudhary et al. 2021; Zhang et al. 2023b; Bamber et al. 2023; Cheng et al. 2024) but such studies are still in their infancy.

6.1.3 Exotic compact objects

ECOs come in many different flavors, and the state of numerical simulations of ECO mergers vary widely, depending on the source. For example, simulations of string-theoretical models including fuzzballs, wormholes, firewalls or gravastars have not yet been performed because the theoretical foundations — the field content, equations of motion, equations of state (where applicable), solution space — are

under active investigation. Formulations suitable for numerical relativity are not yet available.

In contrast, binary boson stars that are compact objects composed of real or complex bosonic (scalar or vector) fields, with and without self interaction potentials, have received a lot of attention (Liebling and Palenzuela 2023; Palenzuela et al. 2007, 2008; Choptuik and Pretorius 2010; Brito et al. 2015a, 2016b; Cardoso et al. 2016b; Bezares et al. 2017; Palenzuela et al. 2017; Bezares and Palenzuela 2018; Helfer et al. 2019b; Widdicombe et al. 2020; Sanchis-Gual et al. 2019; Calderón Bustillo et al. 2021; Bezares et al. 2022b; Calderon Bustillo et al. 2023; Sanchis-Gual et al. 2022a, b; Jaramillo et al. 2022b; Freitas et al. 2024; Croft et al. 2023; Evstafyeva et al. 2023; Siemonsen and East 2023; Siemonsen 2024). These boson stars may be treated as potential dark matter components (see Sect. 2.7), or simply as toy model proxies for unknown exotic objects. Some works have also considered mixed collisions of BHs or neutron stars with these types of bosonic ECOs (Dietrich et al. 2019a; Clough et al. 2018) as well as collisions of fermion-boson stars (Bezares et al. 2019). Besides these, simulations of extremely compact perfect fluid stars have also been performed in Tsokaros et al. (2019, 2020). Most binary boson star simulations have explored new phenomena that arise during their merger or the qualitative structure of the gravitational radiation emitted. For model specific tests of gravity more accurate waveforms will be needed which, in turn, requires improved initial data and more accurate numerical evolutions.

In summary, despite the progress in the last few years, most of the studies mentioned above have only provided a proof of principle for the stable evolution of some families of ECOs and of fundamental fields around BHs in NR, and have primarily aimed at identifying significant qualitative differences between their signals and those of traditional binary candidates. Key areas for improvements include the numerical accuracy of such simulations and the quality of the initial data (Helfer et al. 2022; Aurrekoetxea et al. 2023; Bamber et al. 2023; Evstafyeva et al. 2023; Cheng et al. 2024). For example for boson stars, a formalism is currently lacking to ensure that the superimposed boosted objects are not in an excited state, the risk being that such artifacts in the initial data are wrongly attributed as features of the ECO signal. Less challenging, but equally important refinements are reducing the eccentricity of the initial orbits (most simulations thus far have been head-on mergers, or only achieve a few orbits before the plunge), and initial errors in the Hamiltonian and momentum constraints (many simulations rely on constraint damping which reduces control over the initial data parameters). Efforts to solve some of these problems are currently underway, in particular see Aurrekoetxea et al. (2023) where a novel method to solve the initial data constraints has been formulated and that could be particularly useful when the sources involve fundamental fields. See also Siemonsen and East (2023) where numerical simulations of binary boson stars were performed using constraint satisfying initial data.

Whilst feasible given these improvements, a significant effort would be required to create a template bank of waveforms of a similar quality to those used for BH and neutron star mergers. This is true even if the class of objects were restricted to a simple model, such as minimally coupled, non self-interacting, non spinning complex scalar boson stars. Refining the NR tools with which we study such objects

is work that is merited in the run up to the mission. In particular, key goals are (1) unambiguously identifying characteristic deviations in the merger signals of ECOs and of BHs surrounded by fundamental fields (e.g. to be used to motivate parameterised deviations from vacuum BBH waveforms) and (2) expanding the classes of objects for which simulations of mergers have been performed to qualitative examples in all sufficiently predictive ECO cases.

6.2 Weak-field approximations

6.2.1 Beyond GR

Applying weak field approximation techniques to theories beyond GR raises several difficulties which have prevented obtaining high-order PN results, with the exception of a small set of alternative theories of gravity. For most cases only the leading non-GR correction is known (see e.g. Yunes et al. 2016; Tahura and Yagi 2018). The most advanced results concern scalar-tensor theories, for which the equations of motion are known up to 3PN order (Mirshekari and Will 2013; Bernard 2018, 2019), including finite-size effects (Bernard et al. 2020; van Gemeren et al. 2023). The gravitational flux and waveform are known up to 2PN order (Lang 2014; Sennett et al. 2016) while the scalar energy flux is known to 1.5PN order beyond the quadrupolar formula (Lang 2015; Bernard et al. 2022). The scalar-tensor equations of motion have been used to obtain similar results in other theories such as Einstein-Maxwell-scalar (Julié 2018a, b) and ESGB theories (Julié and Berti 2019; Shiralilou et al. 2021, 2022; van Gemeren et al. 2023). The main difficulty encountered in more involved theories, such as the Horndeski family (Kobayashi 2019), is related to the need for a mechanism to screen the fifth force in the solar system. As an example, the Vainshtein mechanism requires to keep non-linearities in the description of the dynamics even in the weak field limit, rendering the definition of a perturbative method challenging (Chu and Trodden 2013; de Rham et al. 2013a, b; Barausse and Yagi 2015; McManus et al. 2017; Dar et al. 2019; Kuntz et al. 2019; Brax et al. 2020).

Given the many different alternative theories of gravity proposed over the years and the difficulty in constructing accurate waveforms in many of these theories, the most common approach to build beyond GR waveforms for data analysis purposes has been to use theory-agnostic phenomenological frameworks, such as the parametrised post-Einsteinian (ppE) formalism (Yunes and Pretorius 2009b), the TIGER pipeline (Agathos et al. 2014; Meidam et al. 2018) or the flexible theory-independent (FTI) approach (Mehta et al. 2023). In these frameworks, deviations from GR are assumed to be small and are treated as perturbative corrections to the signal predicted by GR. For example, in the ppE formalism the inspiral phase of the frequency domain waveform is given by:

$$\tilde{h}(f) = \tilde{h}_{GR}(f)[1 + \alpha_i(\pi\mathcal{M}f)^{a_i}]e^{i\beta_j(\pi\mathcal{M}f)^{b_j}}\,, \tag{22}$$

where $\tilde{h}_{GR}(f)$ is the frequency domain waveform of GR, $\mathcal{M}$ is the chirp mass of the binary, while the deviations from GR are described by the dimensionless parameters

α_i,β_j, a_i and b_j. The index i and j indicate the PN order at which the modification enters and are also introduced as a reminder that modifications could enter at different PN orders, in which case we should sum over all of them. Different values for the generic beyond GR parameters can be mapped to distinct physical effects and gravitational theories (see e.g. Barausse et al. 2016; Yagi et al. 2012, 2016; Yunes et al. 2010b; Yagi et al. 2011; Yunes and Stein 2011; Mirshekari et al. 2012; Carson and Yagi 2020; Perkins et al. 2021b), allowing to use this formalism to place constraints on such theories. Extensions of the ppE formalism to include higher-harmonic GW modes have also been recently formulated (Mezzasoma and Yunes 2022), as well as an extension for precessing binaries (Loutrel et al. 2023) (the TIGER framework already considers precessing BBH waveforms, however in this case the modifications to the GW phase are only applied in the coprecessing frame (Meidam et al. 2018)). The latter was based on the recent computation of time- and frequency-domain analytical waveforms emitted for quasicircular precessing BH binaries in dCS gravity (Loutrel and Yunes 2022) and in binaries composed of deformed compact objects with generic mass quadrupole moments (Loutrel et al. 2022).

As final remarks, we should note that while the ppE, TIGER and FTI approaches are very useful and powerful methods to perform null tests of GR, a qualitative and quantitative interpretation of a constraint on the beyond GR parameters (or measurements of a deviation from GR) only makes sense when accessed with respect to specific theories (Chua and Vallisneri 2020); see, e.g., (Nair et al. 2019; Perkins et al. 2021a). Theory-agnostic approaches should only be seen as complementary, and not as alternatives, to explicit computations of waveforms in specific alternative theories. Moreover, the mapping from the beyond GR parameters to specific theories also comes with important caveats. In particular, typically, only the leading-order modification to the PN coefficients is considered in the mapping (however see Perkins and Yunes (2022), where it was shown that, for a wide class of theories, the main effect of including higher-order terms is to mildly strengthen constraints when compared to constraints obtained using only the leading-order modification). Furthermore, these approaches break down in the high-frequency part of the signal, where the PN expansion is not applicable. In both the TIGER and the FTI framework, the beyond GR modifications to the phase are tapered off at some transition frequency, while also assuring that the waveform remains smooth at this transition point, to enforce that these modifications are only applied in the inspiral regime (in the TIGER approach the beyond GR coefficients are simply set to zero at the transition frequency between the inspiral and the "intermediate" regime, whereas the FTI method applies a tapering function over a given frequency window that ensures that the beyond GR coefficients smoothly transition to zero at high frequencies). There is no guarantee that these approaches provide a good description of specific beyond GR theories at high-frequencies. These issues motivate even further the need for computations of full waveforms in specific alternative theories.

6.2.2 Dark matter and boson clouds

Weak field approximations have been widely used to study the impact of dark matter environments on binary systems (Eda et al. 2013; Barausse et al. 2014; Cardoso and Maselli 2020). Such an environment can affect the binary dynamics through dynamical friction (Chandrasekhar 1943), accretion and the gravitational pull of the environment itself (Eda et al. 2013; Barausse et al. 2014; Cardoso and Maselli 2020). These effects typically modify the waveform at negative PN orders and can be captured within the ppE formalism presented above (Barausse et al. 2014; Cardoso and Maselli 2020).

In this context, Newtonian approximations have also been used to study binary systems moving inside bosonic structures, mainly motivated by the fact that ultralight bosons are promising candidates to describe dark matter (Hui et al. 2017). For example, Annulli et al. (2020a, b) studied how compact binaries travelling through these structures would be affected by dynamical friction and emission of scalar radiation. In particular, it was found that, for sources in the LISA band, scalar radiation affects the gravitational waveform at leading -6 PN order with respect to the dominant quadrupolar term (Annulli et al. 2020a, b). In addition, BHs surrounded by boson clouds have been studied within a weak-field approximation (Baumann et al. 2019a, b, 2020; Zhang and Yang 2019, 2020; Berti et al. 2019; Cardoso et al. 2020; Takahashi and Tanaka 2021; Takahashi et al. 2022; Tong et al. 2022) showing that a plethora of signatures, including tidally induced resonances (Baumann et al. 2019a, 2020), floating and kicking orbits (Cardoso et al. 2011; Zhang and Yang 2019; Baumann et al. 2020; Ferreira et al. 2017) and ionization of the cloud (Takahashi et al. 2022; Baumann et al. 2022a, b; Tomaselli et al. 2023) can occur. Finally, it was recently shown that sufficiently light bosonic fields can also be bound to and engulf a binary BH system as a whole, showing a rich phenomenology (Wong 2019, 2020; Ikeda et al. 2021), which could potentially lead to additional signatures besides the ones we discussed above. A main problem with those studies is that they have mostly been performed within a weak-field approximation, neglecting high PN corrections and nonlinear effects close to merger. It would be especially important to extend such studies beyond the weak-field regime and further explore the physics of ultralight fields around binary BHs with full NR simulations (see Sect. 6.1.2 for recent attempts).

6.2.3 Exotic compact objects

In the inspiral phase, the nature of the coalescing bodies can be studied through (i) their multipolar structure; (ii) (the absence of) tidal heating; and (iii) their tidal deformability. In particular, the multipole moments of an ECO will be different from those of their Kerr counterpart (Glampedakis and Pappas 2018; Raposo et al. 2019; Raposo and Pani 2020; Bianchi et al. 2020, 2021; Bena and Mayerson 2020, 2021; Herdeiro et al. 2021a; Bah et al. 2021; Fransen and Mayerson 2022; Loutrel et al. 2022; Vaglio et al. 2022), which at leading order enters as a 2PN correction to the GW phase due to the object's quadrupole moment (Poisson 1998; Loutrel et al. 2022). We note that in many cases the multipolar structure of the ECO is only

expected to be different from the Kerr metric if the ECO is spinning (as is the case for the simplest boson star models (Ryan 1997; Vaglio et al. 2022)), although examples of non-spinning (i.e. static) ECOs with a different multipolar structure from the Schwarzschild metric also exist (Raposo et al. 2019; Herdeiro et al. 2021a, 2024). In addition, tidal interactions during the coalescence also provide unique signatures able to disentangle BHs from ECOs in the form of tidal heating. For BH binaries a small fraction of the emitted radiation is lost through the horizon (Hughes 2001; Alvi 2001; Poisson 2009; Cardoso and Pani 2013; Poisson and Corrigan 2018). Absorption at the horizon introduces a 2.5PN (4PN) $\times \log v$ correction to the GW phase of spinning (nonspinning) binaries, relative to the leading term. On the other hand, exotic matter is expected to weakly interact with gravitational waves, leading to a smaller absorption during the inspiral, and therefore to a suppressed contribution to the accumulated GW phase from tidal heating (Maggio et al. 2017; Maselli et al. 2018; Oshita et al. 2020b; Datta et al. 2020; Datta 2020). Finally, tidal deformations can be strong enough, especially during the late stages of the inspiral, to modify the binary's orbital evolution leaving an imprint on the emitted waveform encoded in the ECO's tidal Love numbers (Pani 2015; Cardoso et al. 2017), which at leading order introduces a 5PN correction to the GW phase (Flanagan and Hinderer 2008). Overall more work is needed to construct fully consistent inspiral waveforms for ECOs that incorporate all these ingredients. For example, for the inspiral of boson stars with quartic interactions, such a waveform was only recently constructed in Pacilio et al. (2020); Vaglio et al. (2023). It would be important to extend this to other types of ECOs.

6.3 Perturbation theory for post-merger waveforms

6.3.1 Beyond GR

The ringdown phase of a GW signal emitted by a BBH merger event can be described using BH perturbation theory and is dominated by the QNMs of the remnant (Kokkotas and Schmidt 1999; Berti et al. 2009). Owing to the very large SNR with which LISA will be able to detect the ringdown phase of supermassive BHs (Berti et al. 2006; Kamaretsos et al. 2012a), we expect to be able to measure several QNMs for a single event up to very large distances (Dreyer et al. 2004; Berti et al. 2006, 2016; Baibhav and Berti 2019). This will allow to perform precise consistency tests of the QNMs and test the hypothesis that the remnant of a BBH merger is well described by the Kerr metric in GR (Dreyer et al. 2004; Berti et al. 2006; Kamaretsos et al. 2012a; Gossan et al. 2012; Meidam et al. 2014; Brito et al. 2018; Carullo et al. 2018, 2019; Giesler et al. 2019; Isi et al. 2019a; Maselli et al. 2020b; Bhagwat et al. 2020; Bao et al. 2019; Ota and Chirenti 2020; Hughes et al. 2019; Jiménez Forteza et al. 2020; Ghosh et al. 2021; Bhagwat et al. 2022; Forteza et al. 2023; Lim et al. 2022). Due to these prospects, significant work has been done in recent years in order to accurately model the ringdown phase of BBH mergers within GR (Damour and Nagar 2014a; London et al. 2014; London 2020; London and Fauchon-Jones 2019; Giesler et al. 2019; Cook 2020; Dhani 2021; Finch and

Moore 2021; Magaña Zertuche et al. 2022; Li et al. 2022; Lim et al. 2022; Mitman et al. 2023; Cheung et al. 2023).

For beyond GR theories, however, there has been significantly less progress, even though QNM measurements can, in principle, be powerful probes of beyond GR physics. In particular, for beyond GR theories, the ringdown of a BBH merger is typically expected to differ from the ringdown in GR (although not necessarily for all non-GR theories). Computations of QNMs in beyond GR theories are very challenging, especially for rotating BHs for which the separability of the perturbative equations present in GR (Teukolsky 1972) is in general absent. Then, one may employ numerical methods to compute QNMs for non-separable equations, (see, e.g., Dias et al. 2015, 2022a, b; Li et al. 2023; Chung et al. 2023, 2024; Chung and Yunes 2024a, b). In addition, most rotating BH solutions in alternative theories, for the cases where they differ from Kerr, are only known either perturbatively, through a small-spin expansion around non-spinning backgrounds (Pani et al. 2011b; Ayzenberg and Yunes 2014; Maselli et al. 2015; Cardoso et al. 2018b; Cano et al. 2024c), or they are given in the form of numerical solutions of the field equations (e.g., Kleihaus et al. 2011; Herdeiro and Radu 2014; Stein 2014; Herdeiro et al. 2016; Cunha et al. 2019; Sullivan et al. 2020, 2021), complicating the problem even further. Furthermore, BH spacetimes may change their character as compared to GR. For example, it was shown that BHs in ESGB and dCS gravity are of Petrov-type I (Owen et al. 2021) (instead of the more symmetric type-D spacetimes like the Kerr metric). Therefore, even though QNMs have been computed for a handful of theories and BH solutions (see e.g. Barausse and Sotiriou 2008; Molina et al. 2010; Barausse et al. 2014; Blázquez-Salcedo et al. 2016; Glampedakis and Pappas 2018; Tattersall et al. 2018; Franciolini et al. 2019; Cardoso et al. 2018b; McManus et al. 2019; Glampedakis and Silva 2019; Cardoso et al. 2019a; Silva and Glampedakis 2020; Pierini and Gualtieri 2021, 2022), up to very recently the vast majority of these results either assumed non-rotating or slowly-spinning BH backgrounds or relied on approximations such as the eikonal/geometric optics approximation. Methods to circumvent some of these problems were formulated in Cano et al. (2020); Li et al. (2023); Hussain and Zimmerman (2022); Ghosh et al. (2023); Wagle et al. (2024); Cano et al. (2023a, b, 2024a, b) where modified Teukolsky equations governing the perturbations of non-Kerr spinning BHs arising in theories beyond GR, were derived in the case where the deviations from the Kerr geometry are small. Another approach would be to rely on fits of time-domain waveforms computed from numerical simulations in selected classes of theories beyond GR. However, this is quite a challenging task, even in GR (London et al. 2014; Baibhav et al. 2018; London 2020; London and Fauchon-Jones 2019; Giesler et al. 2019; Cook 2020; Dhani 2021; Finch and Moore 2021; Forteza and Mourier 2021; Magaña Zertuche et al. 2022; Li et al. 2022; Mitman et al. 2023; Cheung et al. 2023), besides the fact that such simulations are still only possible for a handful of cases, has emphasized in Sect. 6.1.1.

6.3.2 Exotic compact objects

The vibration spectra of ECOs have been computed for a wide class of models, although mostly for spherically symmetric configurations, including: boson stars

(Berti and Cardoso 2006b; Macedo et al. 2013a), gravastars (Chirenti and Rezzolla 2007; Pani et al. 2009; Chirenti and Rezzolla 2016; Völkel and Kokkotas 2017), wormholes (Cardoso et al. 2016a; Konoplya and Zhidenko 2016; Bueno et al. 2018), quantum structures (Cardoso et al. 2006; Eperon et al. 2016; Cardoso et al. 2016b; Barceló et al. 2017; Brustein et al. 2017; Wang et al. 2020; Chakraborty et al. 2022), and in a model-indepedent fashion using the membrane paradigm (Maggio et al. 2020). Typically, the QNMs of ECOs differ from the BH QNMs due to the presence of a surface instead of an event horizon (Cardoso and Pani 2019) and the excitation of the internal oscillation modes of the objects (Ferrari and Kokkotas 2000; Pani and Ferrari 2018; Glampedakis and Pappas 2018). In addition, the isospectrality of axial and polar modes of spherically symmetric BHs in GR (Chandrasekhar and Detweiler 1975) is broken in ECOs, which are instead expected to emit a characteristic "mode doublet". The detection of such doublets would be a irrevocable signature of new physics (Berti et al. 2009; Brustein et al. 2017; Cardoso et al. 2019a; Maggio et al. 2020). The formation of an exotic ultracompact object may also lead to the emission of GW echoes in the post-merger signal (Cardoso et al. 2016a; Cardoso and Pani 2017) (see also Sect. 2.7). Several phenomenological GW templates for echoes have been developed based on standard GR ringdown templates with additional parameters (Abedi et al. 2017; Nakano et al. 2017; Wang and Afshordi 2018), the superposition of sine-Gaussians (Maselli et al. 2017), hybrid methods that put together information from perturbation theory and the pre-merger orbital dynamics (Longo Micchi et al. 2021; Ma et al. 2022b; Zhong et al. 2023), using the close-limit approximation (Annulli et al. 2022), and analytical models that explicitly depend on the physical parameters of the ECO (Mark et al. 2017; Testa and Pani 2018; Maggio et al. 2019b; Xin et al. 2021).

Finally, we note that although most of these works have so far relied on perturbative methods, fully nonlinear simulations of head-on collisions of boson stars in the large-mass-ratio regime, resulting in spinning horizonless remnants with stable light rings, have recently been performed (Siemonsen 2024). Those simulations confirm the picture that the prompt post-merger signal approaches that of Kerr black holes in the large-compactness limit with the subsequent emission containing periodically appearing bursts akin to GW echoes.

6.4 Small mass-ratio approximation

6.4.1 Beyond GR

Although there have been substantial advances in GSF models in GR (see Sect. 4.3), self-force calculations for theories beyond GR are in their infancy. The most detailed studies in this vein have so far investigated changes to the emitted GW flux for scalar-tensor and higher-order curvature theories of gravity (Sopuerta and Yunes 2009; Pani et al. 2011a; Cardoso et al. 2011; Yunes et al. 2012; Canizares et al. 2012; Blázquez-Salcedo et al. 2016; Fujita and Cardoso 2017), and for theories of massive gravity when assuming a Schwarzschild BH background (Cardoso et al. 2018a); there are only a few examples of formulations of a full self-force theory beyond GR (Zimmerman 2015; Spiers et al. 2024a). But recently it has been argued that for a

vast class of theories, no-hair theorems or separation of scales lead metric and scalar perturbations to decouple (Maselli et al. 2020a). In particular, in the large class of higher-derivative gravity models, the modification to GR scales with the curvature, i.e., with the inverse of the mass. Consider, for example, the Kretschmann curvature scalar $\mathcal{K} = R_{\mu\nu\rho\sigma}R^{\mu\nu\rho\sigma}$. On the horizon of a Schwarzschild BH of mass M it scales as $\mathcal{K} \sim M^{-4}$. Consequently, higher-curvature modifications to a supermassive BH are negligible. This allows the background spacetime to be treated as the Kerr solution, and changes in the binary's evolution to be fully controlled by the scalar field charge of the small BH (Maselli et al. 2020a, 2022; Barsanti et al. 2022; Zhang et al. 2023a; Guo et al. 2022). In this regard, the study of small-mass-ratio binaries in generalized scalar-tensor theories of gravity can benefit from efforts already devoted to investigating self-forces on scalar charges, and their orbital evolution around BHs (Barack and Burko 2000; Detweiler et al. 2003; Diaz-Rivera et al. 2004; Warburton and Barack 2010, 2011; Warburton 2015; Gralla et al. 2015; Castillo et al. 2018; Nasipak et al. 2019; Compère et al. 2020a; Nasipak and Evans 2021; Heffernan 2022; Barack and Long 2022; Nasipak 2022).

6.4.2 Dark matter and boson clouds

For EMRI and IMRI systems, the largest effect of dark matter is to produce a significant drag force through dynamical friction (Chandrasekhar 1943), which increases the rate of inspiral of the small compact object (Macedo et al. 2013b; Barausse et al. 2014; Eda et al. 2015; Cardoso and Maselli 2020; Vicente and Cardoso 2022) (accretion and the usual gravitational pull of the dark matter can be significant, but are in general subleading effects (Eda et al. 2013; Barausse et al. 2014; Yue and Han 2018; Cardoso and Maselli 2020)). This typically requires very high densities of dark matter surrounding the intermediate or supermassive BH (Barausse et al. 2014; Eda et al. 2015). The required densities can be achieved when the IMBH or SMBH adiabatically grows in a dark-matter halo, and the distribution of dark matter near the BH gets compressed into a "spike" with significantly higher densities than the surrounding halo (Quinlan et al. 1995; Gondolo and Silk 1999; Ullio et al. 2001; Kim et al. 2023a). Sufficiently large densities may also be achieved for clouds of ultralight bosons formed around MBHs, as discussed in Sect. 2.7. If they exist, these clouds would introduce additional metric perturbations that perturb the companion's orbit, and they would respond to the gravity of the companion. If the cloud contributes a sizable fraction of the BH's mass, its gravity would necessitate a change in the background geometry (see (Collodel et al. 2022; Delgado et al. 2023) for such an example), dramatically complicating the GSF model. Building accurate IMRI/EMRI waveforms evolving in a dark matter spike or boson cloud is also crucial to distinguish these environments from other astrophysical environments, such as accretion disks. In fact, recent studies strongly suggest that these different types of environments leave distinguishable signatures in IMRI or EMRI waveforms (Hannuksela et al. 2019, 2020; Coogan et al. 2022; Speri et al. 2023; Cole et al. 2023; Becker and Sagunski 2023; Kim et al. 2023a). Therefore

the detection of such systems could also be used to identify and learn about the environment surrounding supermassive BHs.

To date, studies of the gravitational effects of dark matter spikes and boson clouds on binary systems, such as EMRIs and IMRIs, have mostly relied on Newtonian or post-Newtonian approximations for the orbit and the matter distribution (Eda et al. 2013, 2015; Yue and Han 2018; Yue et al. 2019; Hannuksela et al. 2019, 2020; Ferreira et al. 2017; Berti et al. 2019; Baumann et al. 2019a; Zhang and Yang 2019, 2020; Kavanagh et al. 2020; Baumann et al. 2022a, b; Speeney et al. 2022; Kim et al. 2023a; Tomaselli et al. 2023). Generalizing some of these calculations to the fully relativistic case is in principle feasible. Indeed, first steps in this direction were recently done in Cardoso et al. (2022a); Destounis et al. (2023b); Cardoso et al. (2022b) where a generic and fully-relativistic formalism to study EMRI systems in spherically-symmetric, non-vacuum BH spacetimes was developed. For boson clouds, a fully relativistic framework that assumes that the impact of the cloud on the BH geometry can be treated perturbatively, was proposed in Brito and Shah (2023).

However, there are important open problems to be solved. First, generalizing the formulation of Cardoso et al. (2022a); Destounis et al. (2023b); Cardoso et al. (2022b); Brito and Shah (2023) to non-spherically-symmetric backgrounds is a non-trivial task, and secondly, for dynamic matter distributions (Kavanagh et al. 2020), evolving the matter environment coupled to the binary system at first post-adiabatic order will likely be a complex problem.

Finally, it is worth noting that boson clouds themselves can also be strong sources of nearly-monochromatic gravitational waves potentially detectable by LISA (Arvanitaki et al. 2010; Arvanitaki and Dubovsky 2011; Yoshino and Kodama 2014; Arvanitaki et al. 2015; Baryakhtar et al. 2017; Brito et al. 2017a; Isi et al. 2019b; Siemonsen and East 2020; Brito et al. 2020; Zhu et al. 2020; Siemonsen et al. 2023). The gravitational waves emitted by these sources can be computed using the same techniques typically used in the small mass-ratio approximation: one can consider the cloud as being a small perturber of a Kerr background geometry and use the Teukolsky formalism to compute GW emission from a boson cloud (Yoshino and Kodama 2014; Brito et al. 2017a; Siemonsen and East 2020; Brito et al. 2020; Siemonsen et al. 2023).

6.4.3 Beyond GR BHs and exotic compact objects

A key goal of the LISA mission, is to determine whether the dark central objects in galactic cores are genuine BHs, and if so, whether they are accurately described by GR BHs. With EMRIs we expect to be able to constrain fractional deviations from the quadrupole moment of the Kerr solution at a level smaller than 10^{-4} (Barack and Cutler 2007; Barausse et al. 2020b), which would allow to impose stringent constraints on ECOs and non-GR BHs. Work to include these modifications in GSF models has been done by considering the large central object as a "bumpy" BH. Bumpy BHs are spacetimes that include the Kerr limit, but that differ in a parameterized way, typically by modifying the spacetime's multipole moment structure (Manko and Novikov 1992; Ryan 1995; Collins and Hughes 2004;

Vigeland et al. 2011; Moore et al. 2017; Xin et al. 2019; Fransen and Mayerson 2022). The "bumps" can be introduced directly into the background metric, or (if they are sufficiently small) they can be treated as additional metric perturbations. A benefit of the bumpy BH framework is that it is agnostic about the mechanism which produces the BH's bumps. They could describe non-GR physics (to exactly recover BH solutions in specific alternative theories (Jackiw and Pi 2003; Yunes and Pretorius 2009a; Vigeland et al. 2011), for example), or if the central object is an ECO, they could be tidally induced by the companion, encoding the ECO's tidal Love numbers which are potentially detectable with EMRIs (Pani and Maselli 2019; Datta 2022; Piovano et al. 2023). Because bumpy BHs break the symmetries of Kerr that yield integrable motion (Carter 1968), orbits in these spacetimes are generically chaotic (Gair et al. 2008a; Lukes-Gerakopoulos and Kopáček 2017; Destounis et al. 2020; Destounis and Kokkotas 2021) and subject to prolonged resonances (Lukes-Gerakopoulos et al. 2010; Destounis et al. 2020, 2021; Destounis and Kokkotas 2021). Most of the work considering EMRIs around spacetimes with a multipolar structure different from Kerr, constructed approximate "kludge" waveforms (Xin et al. 2019; Chua et al. 2018; Fransen and Mayerson 2022) generated considering geodesics in a perturbed Kerr spacetime with parameters evolved using post-Newtonian equations (Glampedakis and Babak 2006; Barack and Cutler 2007; Gair et al. 2008a; Apostolatos et al. 2009; Moore et al. 2017). While these approaches are believed to reproduce the main features of the orbit, they will not be enough to get to the precision required to determine that the inspiral is indeed an inspiral into a Kerr BH or not (Sasaki and Tagoshi 2003; Gair et al. 2008a), and much more work is needed to build such waveforms. The additional parameters in such models will also typically increase the possibility of degeneracies, making it important to fully understand possible discernible features, such as characteristic variations of the amplitude and the energy emission rate (Suzuki and Maeda 2000) or the appearance of prolonged resonances (Apostolatos et al. 2009; Destounis et al. 2021; Destounis and Kokkotas 2021). If the central object is an ECO, in addition to nonintegrable motion and geodesic resonances (Destounis et al. 2023a), it will also lack a true event horizon. This causes a change in boundary conditions: in a BH spacetime, fields are purely ingoing on the horizon, while in an ECO spacetime, fields obey a boundary condition of (partial) reflection at the effective surface. The effect of this reflection has been taken into account for the dissipative first-order self-force in Li and Lovelace (2008); Cardoso et al. (2019b); Datta et al. (2020); Sago and Tanaka (2021); Maggio et al. (2021a); Sago and Tanaka (2022). In addition, the modes of the ECO could also be excited during the inspiral of the small compact object (Pani et al. 2010; Macedo et al. 2013a; Cardoso et al. 2019b; Asali et al. 2020; Fransen et al. 2021; Sago and Tanaka 2021; Maggio et al. 2021a; Cardoso and Duque 2022) (see (Cardoso and Duque 2022) where the conditions for such modes to be effectively excited during the inspiral were studied in more detail). Depending on the object's properties, this could cause the rate of the inspiral to change significantly in the vicinity of each resonance. For the dissipative first-order self-force, the effect on the emitted GW flux has been modelled for gravastars (Pani et al. 2010), boson stars (Macedo et al. 2013a) and an exotic ultracompact object with an exterior Schwarzschild or Kerr geometry but with a hard surface close to the would-be

horizon (Cardoso et al. 2019b; Sago and Tanaka 2021; Maggio et al. 2021a). An object plunging in the interior of an ECO would also be subject to additional forces that can dominate the dynamics, such as dynamical friction (Chandrasekhar 1943) and accretion. The impact of these effects on the orbit dynamics and GW waveforms has been modeled for small compact objects plunging onto boson stars using a Newtonian approximation (Macedo et al. 2013b) (see also Kesden et al. (2005) for earlier work on the same subject where dynamical friction and accretion had been neglected).

6.5 Effective-one-body waveform models

EOB waveforms with generic deviations from GR have been developed based on a parameterized form for performing theory-agnostic tests. These include deformations to the GW phase (see Eq. (22)) which are added as corrections to frequency-domain EOB waveforms in GR (Abbott et al. 2019d; Sennett et al. 2020; Mehta et al. 2023; Abbott et al. 2021c, d), or parameterized deformations of the QNMs in time-domain EOB waveforms, which have been used to perform tests of the no-hair theorem in GR and constrain higher-order curvature theories of gravity (Brito et al. 2018; Ghosh et al. 2021; Silva et al. 2023; Abbott et al. 2021c, d; Maggio et al. 2023).

Recent work has also computed the EOB dynamics for non-spinning binaries in various theories beyond GR as a foundational step towards enabling model-dependent tests. Results are available for scalar-tensor theories of gravity (Julié and Deruelle 2017; Julié 2018c; Jain et al. 2023; Julié et al. 2023; Jain 2023a, b), Einstein-Maxwell-dilaton theories (Khalil et al. 2018) and ESGB gravity (Julié et al. 2023). The EOB approach has also been used to compute the two-body potential energy of point-like particles in theories exhibiting a Vainshtein screening (Kuntz 2019). Developing these results into full EOB waveform models and including more realistic physics remains a challenging task, however important steps in this direction were recently done in Julié et al. (2025) where the first example of a full IMR waveform model for a beyond-GR theory, namely ESGB, was built. This waveform builds on top of SEOBNRv5PHM (Ramos-Buades et al. 2023), the state-of-the-art EOB multipolar waveform model for spin-precessing binary BHs, and includes corrections from ESGB gravity in both the inspiral and ringdown while also adding nuisance parameters to marginalize over the uncertainty in the merger morphology.

For non-vacuum binaries involving e.g. ECOs or boson clouds around BHs, a number of generic matter effects during the inspiral change the GW signals away from those of a BH binary (see discussion in previous subsections). Several of the dominant matter effects for neutron star binaries are included in EOB models that could also have broader applicability to ECOs or non-vacuum BHs. These effects are described in a parameterized form, where the nature of the object is encoded in characteristic coefficients such as the bodies' multipole moments, tidal and rotational Love numbers, and QNM frequencies. Specifically, the effects of rotational deformation and adiabatic tides are currently included in the TEOBResum family of models discussed in Sect. 4.5 in the way described in Damour and Nagar (2010); Bini et al. (2012); Bernuzzi et al. (2012); Bini and Damour (2014b); Bernuzzi et al. (2015b); Nagar et al. (2018); Nagar and Rettegno (2019); Akcay et al. (2019); Nagar

et al. (2019b); Gonzalez et al. (2023a), with the state-of-the-art models incorporating the known adiabatic gravitoelectric and -magnetic tidal terms up to $\ell = 8$ and $\ell = 3$ (Gamba et al. 2023b), respectively, in different resummation schemes (Bernuzzi et al. 2012; Bini and Damour 2014b; Bernuzzi et al. 2014; Akcay et al. 2019; Gamba et al. 2023b), dynamical tides from the fundamental modes (Gamba and Bernuzzi 2023; Steinhoff et al. 2016; Hinderer et al. 2016) as well as nonlinear-in-spin effects dependent on the nature and interior structure of the object (Nagar et al. 2018, 2019b). The SEOBNR models include tidal effects using the dynamical tidal models for the fundamental modes from (Steinhoff et al. 2016; Hinderer et al. 2016), which have recently been further developed (Steinhoff et al. 2021; Mandal et al. 2023; Gupta et al. 2021b). Matter effects have also been incorporated in the ROMs of SEOBNR waveforms in the frequency domain by augmenting the ROMs developed for BBHs with analytical closed-form expressions correcting the GW phase to include tidal and spin-induced multipole effects based on tidal models that are specific to calibrations to NR simulations of neutron star binaries, which could in principle be replaced by more general frequency-domain tidal models, and PN calculations for the spin-induced multipole effects (Dietrich et al. 2017, 2019c, b; Abac et al. 2024).

However, significant work remains. Besides the improvement of current EOB models already discussed in Sect. 4.5, other improvements that are specific to ECOs or non-vacuum BHs include, for example, incorporating more effects from spins and relativistic phenomena in the matter sector (which are likely to be more important for compact ECOs than for neutron stars); incorporating parameterized absorption coefficients; and the inclusion of effects specific to dark matter spikes and boson clouds already discussed in Secs. 6.2.2 and 6.4.2. In addition, a remaining challenge is to develop full IMR waveforms. Possible avenues for constructing full waveforms for binaries with matter have been explored, e.g., in the context of binary neutron stars (Breschi et al. 2019), by using NR-informed analytical models that build on quasiuniversal features found in these systems (Bernuzzi et al. 2015a; Breschi et al. 2019, 2022), and for the tidal disruption in BH-neutron-star binaries (Zappa et al. 2019; Matas et al. 2020; Gonzalez et al. 2023a). To achieve similar complete waveforms for ECOs, it is worth mentioning that a phenomenological model was proposed in Toubiana et al. (2021), which used EOB waveforms with tidal effects to describe the inspiral phase and a toy model inspired by Takami et al. (2015) to model the post-merger dynamics of the system. Whether this model is an accurate enough description for known ECOs, e.g. boson stars, remains to be fully studied.

6.6 Phenomenological waveform models

The phenomenological waveform models of Sect. 4.6 already provide standard tools for tests of GR with the current generation of ground-based detectors (Abbott et al. 2016g, 2019d, e, 2021c, d). In particular, parameterized tests (in the spirit of the ppE formalism, see Sect. 6.2.1) have been employed to probe theory-agnostic deviations from GR in the Phenom ansatz describing the phase evolution of an observed signal, namely using the TIGER pipeline (Agathos et al. 2014; Meidam et al. 2018) although, as shown in Mehta et al. (2023), the FTI framework can also be applied to

Phenom waveform models (note that in all LVK papers so far the FTI framework has only been applied on EOB waveforms, whereas parameterized tests with Phenom waveforms typically use the TIGER approach (Abbott et al. 2019d, e, 2021c, d)). Moreover, Phenom models have also been used to test the BH nature of compact binaries from waveform signatures of spin-induced quadrupole moments (Krishnendu et al. 2019). At a more fundamental level, such tests depend on the parameterization of the waveform model, and face a number of practical and conceptual problems, e. g., varying the phenomenological coefficients in such models by amounts that are too large, pathologies may arise in the waveform (see, e.g., Johnson-McDaniel et al. 2022). Some improvements can be expected from adding time domain models (Estellés et al. 2021, 2022a, b) to the existing frequency domain models, thus providing very different waveform parameterizations to be varied. Going beyond theory agnostic tests, the flexibility of phenomenological models also provides a natural ground to develop models for beyond GR theories or "exotic" physics, such as boson stars and boson clouds around BHs, possibly starting from recent work on BNS and BHNS models (Colleoni et al. 2023; Abac et al. 2024). A key problem is the very large parameter space for such theories, and significant technical and conceptual progress will be required to develop mature approaches. Natural first steps for the near future would be, for example, to calibrate accurate models to small "toy model" regions of some beyond GR theories, and to develop simple toy models that do not require any calibration to numerical waveforms.

6.7 Modeling cosmic strings

Waveform models for GW emission from cosmic strings are needed for LISA for three types of anticipated searches: for the stochastic background, for individual bursts and for individual, coherent, nonlinear oscillatory waveforms. There are significant uncertainties in the properties of the underlying string elements (the number of objects, the presence of cusps, kinks and small scale structure, the size distribution of the objects, the spatial and velocity distribution of the objects). Here, however, we concentrate on the modeling of the *waveforms* generated by one or more loops while also mentioning some of the incompletely known loop properties that will influence the waveforms.

6.7.1 Nambu–Goto, smooth loops with cusp/kink features

We begin with minimally coupled string networks with loops that are smooth on large scales and include cusps or kinks but no other small scale structure.

Early research on this topic focused on computing the individual loop waveforms to lowest order in the string tension μ_S, by considering relatively simple loops and using standard weak-field approximations for GW generation (Garfinkle and Vachaspati 1988; Vachaspati 1987; Burden 1985; Garfinkle and Vachaspati 1987; Allen and Shellard 1992; Allen et al. 1995; Allen and Casper 1994; Casper and Allen 1995; Allen and Ottewill 2001). Both the burst waveforms and the relevant statistical averages for the background implicitly follow. FFT techniques work well to estimate the power at low to moderate harmonics (Allen and Shellard 1992; Blanco-Pillado

and Olum 2017) and additional numerical techniques have been devised specifically to handle higher harmonics (Suresh and Chernoff 2024).

In the case of LVK, small scale features dominate emission at high frequencies. A similar situation pertains to LISA, which will be sensitive to the high frequencies of the astrophysically relevant low tension strings. The development of an asymptotic approach (Damour and Vilenkin 2000, 2001, 2005) was an important quantitative and qualitative advance. High frequency emission sourced by cusps and kinks is approximately independent of the large scale loop structure. The important features of cusp waveforms in this limit are that (1) the cusp power spectrum falls off at high frequencies as $f^{-4/3}$; and (2) the GWs from the cusp are strongly beamed in the direction of cusp motion and exponentially suppressed at frequencies $f \gtrsim 1/(\theta^3 T)$ for angle θ with respect to that direction (with T the periodicity of the string). The waveform's time dependence is $\propto |t - t_c|^{1/3}$, where t_c is the time at which the cusp formation event is noted by an observer situated in the beam of emission ($\theta = 0$), and so the cusp waveform is called *sharp* or *spiky*. This sharpness is softened for $0 < \theta \ll 1$. Similar analyses are applicable to kinks.

The genericity of the high frequency predictions for cusps and kinks, the independence with respect to the large scale loop structure and the simplicity of the templates are all important, and the results have been exploited in astrophysically-motivated searches (Siemens et al. 2006; Shapiro Key and Cornish 2009; Abbott et al. 2009b, 2019a).

The outlook and need for waveforms is as follows:

1. The existing asymptotic treatments of kink and cusp emission are likely to be sufficient for modeling an unresolved stochastic wave background. That is because the energy flux derived from averaging over time, space and angle, which is implicit in such a calculation, depends upon low-order moments of the loop's full beam pattern that can be derived from the asymptotic results.
2. More refined models of the burst waveform that do not, strictly speaking, lie in the asymptotic regime are needed. Such waveforms can account for geometric effects when the observer does not lie directly in the cusp direction and for anisotropies in the beam shape. These can be found by extending the asymptotic treatment.
3. Existing calculational methodologies for full loops are accurate and efficient at low to moderate modes. LISA and pulsar timing arrays will probe both low and high order modes. Hybridization methods giving models of the beam that span the full range of modes will be required for any loop sources that stand out above the stochastic background (Suresh and Chernoff 2024).

6.7.2 Nambu–Goto, small-scale structure

Each time a long horizon-crossing string intercommutes it gains two kinks. Small scale structure builds up on the string (Austin et al. 1993; Polchinski and Rocha 2007; Martins et al. 2014; Vieira et al. 2016; Martins et al. 2021). Gravitational backreaction probably smoothens the string at small scales (Bennett and Bouchet 1989; Quashnock and Spergel 1990; Siemens and Olum 2001; Siemens et al. 2002).

The wigglyness that remains has been evaluated (Austin et al. 1993; Polchinski and Rocha 2007) but never determined directly by simulation. Siemens and Olum (2003) found that small-scale structure near the cusp rounded off the sharpness of the cusp waveform but affected only observers very near to the direction of cusp motion. Alternatively, Polchinski and Rocha (2007) found that the small scale structure enhanced intercommutation on a newly formed loop and excised the cusp when it first begins to form. It will be important to investigate the effect of small structure on loop dynamics and the resultant waveforms. This can be done parametrically as the amount and character of the wigglyness increases on otherwise simple loops.

6.7.3 Nambu–Goto for Pseudocusps

As a last note, in addition to cusp waveforms, some authors (Stott et al. 2017) have studied the bursts due to "pseudocusps", i.e., string trajectories which very closely approach, but do not strictly reach, the cusp configuration. These pseudocusp burst waveforms are of lower amplitude than true cusps, and follow the same power spectrum decay of $f^{-4/3}$ at high frequencies. Accounting for them in a search can lead to an enhancement in the number of expected burst events.

6.7.4 Beyond Nambu–Goto for cusps

Gauge theory strings with energy scale $\mu_S^{1/2}$ have a characteristic core width $\sim \mu_S^{-1/2}$ whereas classical superstrings are always well-represented by the zero thickness Nambu–Goto limit. When a cusp forms the string instantaneously doubles back upon itself. Blanco-Pillado and Olum (1999) predicts that a region of string around the cusp, of the order of the string thickness, will annihilate into particles due to overlap. For strings with large tensions (near that of the GUT scale) this modification to the cusp shape is at a small enough scale that it does not meaningfully affect the cusp waveform. However, as tension decreases the physical scale increases. It may prove useful to compare the waveform of the gauge theory cusp to the superstring cusp. This can be done by parametrically varying the core width in Abelian-Higgs simulations.

A final assumption about the standard cusp waveform model is that it relies only on properties universal to all strings. However, superstrings possess additional features that could modify their cusp waveforms. Damour and Vilenkin (2005) suggested modifications to the amplitude based on the dimensionless loop-length parameter α. For example, cusps very near to Y-junctions will have their burst amplitude modified by a correction factor that depends on the nearby string geometry (Binetruy et al. 2009, 2010b, a), while the extra degrees of freedom on superstrings (extra dimensions) can lead to a strong suppression of both cusp rate and burst amplitude (O'Callaghan et al. 2010).

6.7.5 Cosmic strings and GW production in numerical relativity

While in most cases, perturbative methods (e.g., Nambu–Goto strings coupled to perturbative gravity (Quashnock and Spergel 1990)) are sufficient, situations may arise when perturbative methods are insufficient and gravitational backreaction becomes of $\mathcal{O}(1)$, even if the string tension $G\mu_S$ is small. For example, a string with a sharp kink can easily lead to a locally strong field situation (Jenkins and Sakellariadou 2020). In such strong field limits, the full machinery of NR must be employed. The construction of full NR solutions for cosmic strings was recently achieved by Helfer et al. (2019a); Aurrekoetxea et al. (2020), where stable dynamical solutions for an Abelian-Higgs string minimally coupled to gravity was found. This opens the door to not just the detailed exploration of the string dynamics, but also the characterization of the GW signals that can then be searched for.

The Abelian-Higgs model minimally coupled to gravity can be recast into the standard BSSN/CCZ4 formalism, and solved using finite differences (we refer the reader to Helfer et al. (2019a) for details). Presently, solutions for infinite static strings, planar loops (Helfer et al. 2019a) and single traveling wave solutions (Garfinkle and Vachaspati 1990) have been constructed. Once a string configuration is constructed and successfully evolved, the work required to extract useful GW signals from them follows very similarly to that of any standard NR simulations, see Sect. 4.1.

As an example, in Aurrekoetxea et al. (2020), the gravitational waveform emitted during the BH formation of a collapsing circular cosmic string was computed, and it was shown that the waveform is dominated by the BH formation and ringdown phase, with the primary contribution being the $\ell = 2$, $m = 0$ mode (as opposed to quasi-circular compact binary merger signals which are dominated by the $\ell = 2$, $m = 2$ mode). Intriguingly, due to the large asymmetric ejection of material in the formation process, a large GW memory was also seen.

The future prospects for using NR to compute GW signals from such strong gravity events is very promising. For example, a full general relativistic treatment of the GW emission from cosmic string cusps and kinks is long overdue, but is now within reach. Presently, the main obstacle to explore more complicated string configurations is the need for the construction of accurate initial conditions – a usual problem in any NR endeavor, here made more difficult by the presence of fundamental matter fields. Nevertheless, this area is ripe for further exploration.

7 Afterword

LISA will usher in an era of millihertz GW astronomy that will open a window to new classes of sources and offer unprecedented opportunities to probe our understanding of the universe. Integral to this scientific vision are predictions of the source waveforms, which are necessary for the detection and interpretation of GW events.

This White Paper has analyzed the question of waveform preparedness in the LISA era. It has reviewed the modelling requirements from astrophysical and data

analysis perspectives, and has analyzed the status of the main approaches to modelling waveforms from compact binaries both in vacuum GR and in the presence of environmental influences or effects from new physics beyond GR and the Standard Model. This white paper also provides guidance on new developments that are needed for the different approaches, both in terms of modelling accuracy and the covered parameter space, so that gravitational wave models will be ready for the LISA era.

The experience with ground-based GW detectors has to some extent prepared the community. For example, several approaches that predict the waveforms for comparable mass black hole binaries can be applied directly to massive black hole binaries due to the simple mass scaling of GR. However, these models are not currently sufficient to fully realize LISA's science goals. In particular they insufficiently cover the parameters of eccentricity, highly asymmetric mass-ratios, and high spin magnitudes. In addition, the possibility of very strong massive black hole binary signals places additional demands on the accuracy of these models, well beyond what can currently be achieved.

For extreme-mass-ratio inspirals, leading-order (adiabatic) models that are sufficient to enable some LISA science are becoming available, and these models can be evaluted fast enough for use in LISA data analysis. In order to enable the full spectrum of LISA science with EMRIs post-adiabatic models are needed. These have recently been developed for the simplest orbital configurations (non-spinning, quasi-circular). It also looks likely that these models can cover much of the intermediate mass ratio parameter space. Significant work remains to extend these post-adiabatic models to cover the full parameter space of precessing and eccentric parameter binaries where both components are spinning.

The modelling of sources in theories beyond GR is still in its infancy with significant effort needed. For example, the majority of computations have focused on higher derivative gravity, that are most interesting in the high curvature regime, or on Horndeski models. Moreover, simulations of compact binaries in extensions of GR are, at the time of writing this white paper, proof-of-concept. That is, they have been done for nearly equal-mass binaries, typically of non spinning black holes, and at relatively low resolution. This is comparable to the state of numerical relativity in GR about 15 years ago (i.e., few years after the breakthrough in 2005). Likewise, perturbative or PN calculations have only started to go beyond the leading order in the correction. To perform theory-specific tests of gravity, more work is needed, both in terms of modelling accuracy and in covering (parts of) the parameter space of black hole masses, spins and additional theory-specific parameters.

The good news is that in all approaches there are clear ideas of what needs to be done in order to reach the modelling requirements for LISA. Doing so will require a concerted effort over the next decade. Given sufficient resources, we are positive that all goals can be achieved.

We particularly recommend that the community conduct more investigations into the waveform standards and waveform interface. While lessons have been learned from ground-based detectors, LISA will offer unique challenges that will need to be addressed by the waveform and data analysis communities working together.

Appendix A: Descriptions of NR codes

Description of some numerical relativity codes that focus, in particular, on modelling LISA sources. A more extensive list is given in Table 7.

BAM BAM is a modular code framework initially developed at the University of Jena and is now maintained and further developed by the CoRe (Computational Relativity) Collaboration (Brügmann et al. 2008b; Husa et al. 2008; Thierfelder et al. 2011; Dietrich et al. 2015a). BAM employs finite differences for the discretization of spacetime fields, and high-resolution shock-capturing methods for the evolution of general relativistic hydrodynamics variables. It features automated code generation with Mathematica, adaptive mesh refinement (AMR) in space and time, and parallelization with MPI and OpenMP for large scale HPC, recently at 70% on up to 50k cores. BAM is employed for the simulation of compact binary mergers, e.g., Hamilton et al. (2024); Bernuzzi et al. (2012); Dietrich et al. (2015b); Kölsch et al. (2022). A major focus is on binary black hole, binary neutron star, and black hole - neutron star systems Chaurasia et al. (2021), plus more exotic compact objects or merger scenarios (Dietrich et al. 2019a). Recent updates allow the study of radiation hydrodynamics (Gieg et al. 2022), magnetohydrodynamics (Neuweiler et al. 2024), and the usage of an entropy-viscosity limiter for the flux computation (Doulis et al. 2022). BAM has contributed numerical data for the development and validation of e.g. Phenom-type and EOB waveform models. Several hundred binary neutron star merger simulations are available as part of the existing CoRe database (Dietrich et al. 2018; Gonzalez et al. 2023b).

BAMPS The Jena-Lisbon collaboration is developing the code bamps, a new and highly scalable NR code for exascale applications using pseudo-spectral and DG methods (Hilditch et al. 2016; Bugner et al. 2016). A key feature is hp-refinement for spectral element methods (Renkhoff et al. 2023), which allows highly scalable and accurate simulations, currently with a focus on smooth fields. To date, bamps has already been employed for the study of GW collapse (Hilditch et al. 2016; Fernández et al. 2022), simulations with scalar fields for collapse and for boson stars are in development. Further applications include simple neutron star spacetimes (Bugner et al. 2016), and studies of new techniques regarding the dual foliation framework (Bhattacharyya et al. 2021).

Dendro-GR Dendro-GR (Fernando et al. 2017, 2019a, b) uses an unstructured grid with a localized, wavelet-based refinement scheme to evolve the BSSN formulation of the Einstein equations using moving punctures. In test simulations of a BBH with a mass ratio of 10 : 1, Dendro-GR shows good scaling to over 10^5 cores.

Einstein Toolkit The Einstein Toolkit (Löffler et al. 2012; Einstein Toolkit 2024) is an open-source cyberinfrastructure for computational astrophysics, with more than 300 registered users worldwide. It implements Einstein's equations, or extensions thereof, in the BSSN or CCZ4 formulation together with the moving puncture gauge. It employs the method of lines, in which spatial derivatives are implemented as up to 8^{th} order finite differences together with a collection of direct time integration techniques (e.g., fourth order Runge–Kutta integrator). The Einstein Toolkit is based on the Cactus computational toolkit (Cactus Development Team 2024) and the Carpet boxes-in-boxes AMR package (Schnetter et al. 2004; Carpet developers 2024). It also provides a multipatch infrastructure consisting of Cartesian boxes-in-boxes meshes in the region where the binaries evolve (typical size $\sim 50\ldots100M$), and a spherical outer region in the wave zone (typical radius $\sim 1000\ldots2000M$) provided by the Llama code (LlamaWeb 2024).

Kreiss-Oliger dissipation is employed to reduce high frequency noise at refinement boundaries. The toolkit uses hybrid MPI/OpenMP parallelization.

The Einstein Toolkit has been a broad community project with a multitude of software that is based on its infrastructure or that has been developed within its framework. The additional software is indicated by asterisks in Table 7.

Einstein Toolkit – CarpetX The Einstein Toolkit consortium is developing a new AMR driver, CarpetX (Haas et al. 2022), for the Einstein Toolkit. CarpetX leverages the AMReX framework (Zhang et al. 2019) to provide scalable adaptive mesh refinement for physics modules. CarpetX will provide: efficient support for both CPUs and GPUs; parallelization via MPI and OpenMP; SIMD vectorization; scalable I/O based on the ADIOS2 file format (Godoy et al. 2020) and the openPMD metadata standard; and more. CarpetX offers block-structured AMR based on local error estimates, exact conservation across mesh interfaces, higher order prolongation operators, and scalable elliptic solvers based on PETSc (Balay et al. 2022). CarpetX is available as open source and was used in production in Shankar et al. (2023).

GR-Athena++ Another example is GR-Athena++(Daszuta et al. 2021) based on the astrophysical (radiation) magnetohydrodynamics code Athena++ (Stone et al. 2020). GR-Athena++ leverages on Athena++'s oct-tree AMR and exploits hybrid parallelism at different levels. The standard distributed approach is augmented by a dynamical tasklist for the procedures in each mesh block that overlaps calculation and communication (thus mitigating some of the overhead associated with high order finite differencing). In-core vectorization and other optimization techniques of the basic kernels (Alfieri et al. 2018) are also employed. This approach leads to a high parallel efficiency, with strong scaling efficiencies above 95% for up to 10^4 CPUs and excellent weak scaling is up to 10^5 CPUs measured in a production BBH setup with AMR.

GRChombo GRChombo (Clough et al. 2015; Andrade et al. 2021; GRChombo 2024) is an open-source NR code built using an optimized version of the publicly available library Chombo (Adams et al. 2024) developed at LBNL. It is based on established methods of solving the Einstein equations, but the highly flexible AMR capability and templating over physics classes makes it suited to strong gravity problems in beyond-GR scenarios (e.g. Horndeski gravity (Figueras and França 2020), cosmic strings (Aurrekoetxea et al. 2020)), which have been key targets of the code. GRChombo is written entirely in `C++14`, using hybrid MPI/OpenMP parallelism and vector intrinsics (in particular, the evolution calculations are explicitly vectorised) to achieve improved performance on the latest architectures. It has good strong scaling up to around 4,000 cores for typical binary BH problems, at which point it becomes limited by problem size as with most traditional codes.

The next release of Chombo is designed to be performance portable to different heterogeneous architectures (including GPUs), which GRChombo should be able to leverage to improve scaling further.

Illinois GRMHD The Illinois GRMHD evolution code (Duez et al. 2005; Etienne et al. 2010; Sun et al. 2022) solves the Einstein field equations via the BSSN scheme with puncture gauge conditions, utilizes a conservative high-resolution, shock-capturing (HRSC) scheme for the matter and adapts the Carpet infrastructure to implement AMR. The code solves the magnetic induction equation by introducing a magnetic vector potential, which guarantees that the B-field remains divergence-free for any interpolation scheme used on refinement level boundaries. This formulation reduces to a standard constrained transport (CT) scheme on uniform grids. An improved Lorenz gauge condition for evolving the vector potential in AMR without the appearance of spurious B-fields on refinement level boundaries is implemented. This gauge exhibits no zero-speed modes, enabling spurious magnetic effects to propagate off the grid quickly. The GRMHD code recently added a radiation module (Ruiz et al. 2023) built to handle transport (photons or neutrinos) via the M1 moment formalism. A version of the Illinois GRMHD code has been released as an open-source module that has been ported to the Einstein Toolkit (Etienne et al. 2015), where it has been documented and rewritten to make it more user-friendly, modular and efficient. The code has been used to simulate numerous scenarios related to LISA sources (e.g., BHBH mergers, BHBH mergers in gaseous clouds and magnetized disks, etc.) and their associated gravitational waveforms.

MHDuet The publicly available code MHDUET (MHDuet Code 2024; Palenzuela et al. 2018; Liebling et al. 2020; Viganò et al. 2020; Bezares et al. 2022a) is generated by the open-source platform SIMFLOWNY (Palenzuela et al. 2021) to run under the SAMRAI (SamraiWeb 2024) infrastructure, which provides the parallelization and the adaptive mesh refinement. There are different versions of the code, either to study alternative gravity theories or to include large-eddy-simulations and neutrino transport.

SACRA The SimulAtor for Compact objects in Relativistic Astrophysics (SACRA) code solves Einstein's equation with the BSSN-puncture formulation together with a Z4c constraint propagation prescription and the relativistic hydrodynamics equation with the HRSC scheme (Yamamoto et al. 2008; Kiuchi et al. 2017). It implements the box-in-box conservative AMR with parallelization by MPI and OpenMP. The code has been used to simulate compact binary mergers such as NSNS mergers, BHNS mergers, and BHBH mergers. The NSNS waveform catalog SACRA Gravitational Wave Data Bank is available at (SACRA 2024). The latest version of SACRA has a couple of branches, such as SACRA-TD, to simulate the tidal disruption of an ordinary star by the SMBH (Lam et al. 2023), or SACRA-MG to simulate a compact object in scalar-Gauss-Bonnet theory (Kuan et al. 2023) and scalar-tensor theory (Shibata and Traykova 2023). SACRA also has a version to solve high-dimensional Einstein's equation (Shibata and Yoshino 2010). In addition, it features modules for neutrino radiation transport (Sekiguchi et al. 2012), MHD (Shibata and Sekiguchi 2005; Kiuchi et al. 2022) and viscous hydrodynamics (Shibata et al. 2017).

SACRA-SFS2D is a viscous-radiation hydrodynamics (Fujibayashi et al. 2018) in axisymmetry and radiation magnetohydrodynamics code (Shibata et al. 2021) in full general relativity. These codes can be applied to the collapse of massive stars and supermassive stars to a stellar-mass and supermassive black hole (Uchida et al. 2017), to the post-merger evolution of the neutron-star binaries (Fujibayashi et al. 2023), and to collapsar modeling (Fujibayashi et al. 2024).

SpEC The Spectral Einstein Code (SpEC) (SpEC 2024) is a pseudo-spectral GR code developed by the Simulating eXtreme Spacetimes collaboration. SpEC is capable of evolving BBH and binaries with neutron stars. It incorporates an elliptic solver to construct initial data (Pfeiffer et al. 2003; Foucart et al. 2008; Ossokine et al. 2015), eccentricity reduction (Pfeiffer et al. 2007; Buonanno et al. 2011; Mroue and Pfeiffer 2012), constraint -preserving and non-reflective outer boundary conditions (Lindblom et al. 2006; Rinne 2006; Rinne et al. 2007), and implements hp-AMR (Lovelace et al. 2011; Szilágyi 2014). Extracted gravitational waves are extrapolated to future null infinity (Boyle and Mroue 2009; Taylor et al. 2013; Boyle et al. 2019) and corrected for center-of-mass drift (Woodford et al. 2019). SpEC is a highly accurate NR code for BBH, and has computed large waveform catalogs of BBH inspirals encompassing several tens of orbits (Mroue et al. 2013; Boyle et al. 2019). SpEC has evolved BBH with spins as large as 0.998 (Chatziioannou et al. 2018), inspirals as long as 170 orbits (Szilágyi et al. 2015) as well as eccentric binaries (Ramos-Buades et al. 2022b).

SpECTRE The Simulating eXtreme Spacetimes collaboration is developing the next-generation code SpECTRE (Deppe et al. 2023; Kidder et al. 2017), which uses a discontinuous-Galerkin-finite-difference hybrid method (Deppe et al. 2022a, b; Legred et al. 2023) for accurate and robust neutron star simulations combined with task-based parallelism, showing good scaling to over 600, 000 cores (Kidder et al. 2017). Using Cauchy-Characteristic extraction, SpECTRE is able to resolve gravitational wave memory (Moxon et al. 2023; Mitman et al. 2020) and improve hybridization with post-Newtonian waveforms by ensuring numerical relativity waveforms are in the same BMS frame as the post-Newtonian waveforms (Mitman et al. 2022). Improvements for efficiently simulating binary black holes with mass ratios $q > 10$ aim to reduce the computational cost of such simulations by a factor of q (Wittek et al. 2023). SpECTRE also incorporates a flexible elliptic solver (Fischer and Pfeiffer 2022; Vu et al. 2022, 2023).

Spritz `Spritz` is an open-source code that solves the equations of general relativistic magnetohydrodynamics and that can take into account finite temperature nuclear equations of state and neutrino emission (Cipolletta et al. 2020, 2021; Kalinani et al. 2022). The code is based on the Einstein Toolkit framework and implements also high-order methods for the hydrodynamic equations.

WhiskyMHD `WhiskyMHD` is a fully general relativistic magnetohydrodynamic code based on the Einstein Toolkit (Giacomazzo and Rezzolla 2007). The code has been used mainly to perform simulations of binary neutron star mergers, but it has also been used to perform the first simulations of magnetized plasma around merging supermassive black holes in the ideal magnetohydrodynamic approximation (Giacomazzo et al. 2012).

Acknowledgements We would like to thank our internal reviewers, Leor Barack, Christopher Berry, and Nelson Christensen for extremely helpful feedback. We are also grateful to two anonymous reviewers for their detailed comments which resulted in many improvements to this white paper. Sarp Akçay acknowledges University College Dublin's Ad Astra Fund. Pau Amaro Seoane acknowledges the funds from the "European Union NextGenerationEU/PRTR", Programa de Planes Complementarios I+D+I (ref. ASFAE/2022/014). Enrico Barausse acknowledges support from the European Union's H2020 ERC Consolidator Grant "GRavity from Astrophysical to Microscopic Scales" (Grant No. GRAMS-815673) and the EU Horizon 2020 Research and Innovation Programme under the Marie Sklodowska-Curie Grant Agreement No. 101007855. Emanuele Berti is supported by NSF Grants No. AST-2006538, PHY-2207502, PHY-090003 and PHY-20043; by NASA Grants No. 20-LPS20-0011 and 21-ATP21-0010; by the John Templeton Foundation Grant 62840; and by the ITA-USA Science and Technology Cooperation program, supported by the Ministry of Foreign Affairs of Italy (MAECI). Richard Brito acknowledges financial support provided by FCT/Portugal under the Scientific Employment Stimulus – Individual Call – 2020.00470.CEECIND and under project No. 2022.01324.PTDC. Marta Colleoni, Sascha Husa, Anna Heffernan and Pierre Mourier are supported by the Spanish Agencia Estatal de Investigaciòn grants PID2022-138626NB-I00, PID2019-106416GB-I00, IJC2019-041385, funded by MCIN/AEI/10.13039/501100011033; the MCIN with funding from the European Union NextGenerationEU/PRTR (PRTR-C17.I1); Comunitat Autonòma de les Illes Balears through the Direcció General de Recerca, Innovació I Transformació Digital with funds from the Tourist Stay Tax Law (PDR2020/11 - ITS2017-006), the Conselleria d'Economia, Hisenda i Innovació grant numbers SINCO2022/18146 and SINCO2022/6719, co-financed by the European Union and FEDER Operational Program 2021-2027 of the Balearic Islands; the "ERDF A way of making Europe"; Alvin J. K. Chua and Jonathan E. Thompson acknowledge support from the NASA LISA Preparatory Science grant 20-LPS20-0005. Katy Clough acknowledges funding from the UKRI Ernest Rutherford Fellowship (grant number ST/V003240/1). David A. Nichols acknowledges support from the NSF Grants No. PHY-2011784 and No. PHY-2309021. Vasileios Paschalidis is supported by NSF Grant No. PHY-2145421 and NASA Grant No. 80NSSC22K1605. Stuart Shapiro is supported by NSF Grants No. PHY-2006066 and PHY-2308242. Scott Field acknowledges support from US National Science Foundation Grants Nos. PHY-2110496, DMS-2309609, and by UMass Dartmouth's Marine and Undersea Technology (MUST) Research Program funded by the Office of Naval Research (ONR) under Grant No. N00014-23-1-2141. Davide Gerosa is supported by ERC Starting Grant No. 945155–GWmining, Cariplo Foundation Grant No. 2021-0555, MUR PRIN Grant No. 2022-Z9X4XS, Leverhulme Trust Grant No. RPG-2019-350, MSCA Fellowship No. 101064542–StochRewind, and the ICSC National Research Centre funded by NextGenerationEU. Eliu Huerta acknowledges support from the U.S. Department of Energy under Contract No. DE-AC02-06CH11357, and from the U.S. National Science Foundation (NSF) through award OAC-2209892. Scott A. Hughes has been supported by NASA ATP Grant 80NSSC18K1091, NSF Grants PHY-1707549 and PHY-2110384, by MIT's Margaret MacVicar Faculty Fellowship Program, and by the MIT Kavli Institute for Astrophysics and Space Research. Chris Kavanagh acknowledges support from Science Foundation Ireland under Grant number

21/PATH-S/9610. Gaurav Khanna acknowledges support from US National Science Foundation Grants No. PHY-2307236 and DMS-2309609. Larry Kidder acknowledges support from NSF OAC-2209655, PHY-2308615 and Sherman Fairchild Foundation. Pablo Laguna acknowledges support from US National Science Foundation Grants No. PHY-2114582 and 2207780. Georgios Lukes-Gerakopoulos has been supported by the fellowship Lumina Quaeruntur No. LQ100032102 of the Czech Academy of Sciences. Hyun Lim is supported by the LANL Laboratory Directed Research and Development program under project number 20220087DR. LANL is operated by Triad National Security, LLC, for the National Nuclear Security Administration of the U.S.DOE (Contract No. 89233218CNA000001). This work is authorized for unlimited release under LA-UR-23-31548. Tyson B. Littenberg is supported by the NASA LISA Study Office. Carlos O. Lousto gratefully acknowledge the National Science Foundation (NSF) for financial support from Grant No. PHY- 1912632 and PHY-2207920. Elisa Maggio acknowledges funding from the Deutsche Forschungsgemeinschaft (DFG) - project number: 386119226. Richard O'Shaughnessy acknowledges support from NSF PHY-2012057, PHY-2309172, and AST-2206321. Naritaka Oshita is supported by the Japan Society for the Promotion of Science (JSPS) KAKENHI Grant Number JP23K13111. Rodrigo P. Macedo and Maarten van de Meent acknowledge the financial support by the VILLUM Foundation (grant No. VIL37766), the DNRF Chair program (grant No. DNRF162) by the Danish National Research Foundation, and the European Union's H2020 ERC Advanced Grant "Black holes: gravitational engines of discovery" grant agreement No. Gravitas-101052587. Adam Pound acknowledges the support of a Royal Society University Research Fellowship and a UKRI Frontier Research Grant under the Horizon Europe Guarantee scheme [grant number EP/Y008251/1]. Milton Ruiz acknowledges support from the Generalitat Valenciana Grant CIDEGENT/2021/046 and the Spanish Agencia Estatal de Investigación Grant PID2021-125485NB-C21. Carlos F. Sopuerta CFS is supported by contracts PID2019-106515GB-I00 and PID2022-137674NB-I00 (MCIN/AEI/10.13039/501100011033) and partially supported by the program Unidad de Excelencia María de Maeztu CEX2020-001058-M (MCIN/AEI/10.13039/501100011033). Stuart L. Shapiro acknowledges support from NSF Grants No. PHY-2006066 and No. PHY-2308242. Deirdre Shoemaker acknowledges support from NASA 22-LPS22-0023, 80NSSC21K0900 and NSF 2207780. Antonios Tsokaros is supported by NSF Grants No. PHY-2308242 and OAC-2310548. Niels Warburton acknowledges support from a Royal Society - Science Foundation Ireland University Research Fellowship. This publication has emanated from research conducted with the financial support of Science Foundation Ireland under Grant numbers 16/RS-URF/3428, 17/RS-URF-RG/3490 and 22/RS-URF-R/3825. Helvi Witek acknowledges support provided by the National Science Foundation under NSF Awards No. OAC-2004879 and No. PHY-2110416. Huan Yang is supported by the Natural Sciences and Engineering Research Council of Canada and in part by Perimeter Institute for Theoretical Physics. Research at Perimeter Institute is supported in part by the Government of Canada through the Department of Innovation, Science and Economic Development Canada and by the Province of Ontario through the Ministry of Colleges and Universities. Miguel Zilhão acknowledges financial support by the Center for Research and Development in Mathematics and Applications (CIDMA) through the Portuguese Foundation for Science and Technology (FCT – Fundação para a Ciência e a Tecnologia) – references UIDB/04106/2020 and UIDP/04106/2020 – as well as FCT projects 2022.00721.CEECIND and 2022.04560.PTDC.

References

Aasi J et al (2013) Search for gravitational waves from binary black hole inspiral, merger, and ringdown in LIGO-Virgo data from 2009–2010. Phys Rev D 87(2):022002. https://doi.org/10.1103/PhysRevD.87.022002. arXiv:1209.6533 [gr-qc]

Aasi J et al (2014) Constraints on cosmic strings from the LIGO-Virgo gravitational-wave detectors. Phys Rev Lett 112:131101. https://doi.org/10.1103/PhysRevLett.112.131101. arXiv:1310.2384 [gr-qc]

Aasi J et al (2014) The NINJA-2 project: detecting and characterizing gravitational waveforms modelled using numerical binary black hole simulations. Class Quantum Grav 31:115004. https://doi.org/10.1088/0264-9381/31/11/115004. arXiv:1401.0939 [gr-qc]

Aasi J et al (2015) Advanced LIGO. Class Quantum Grav 32:074001. https://doi.org/10.1088/0264-9381/32/7/074001. arXiv:1411.4547 [gr-qc]

Abac A, Dietrich T, Buonanno A, Steinhoff J, Ujevic M (2024) New and robust gravitational-waveform model for high-mass-ratio binary neutron star systems with dynamical tidal effects. Phys Rev D 109 (2):024062. https://doi.org/10.1103/PhysRevD.109.024062. arXiv:2311.07456 [gr-qc]

Abadie J et al (2011) Search for gravitational waves from binary black hole inspiral, merger and ringdown. Phys Rev D 83:122005. [Erratum: Phys. Rev. D 86, 069903 (2012)]. https://doi.org/10.1103/PhysRevD.83.122005. arXiv:1102.3781 [gr-qc]

Abadie J et al (2012) Search for gravitational waves from low mass compact binary coalescence in LIGO's sixth science run and Virgo's science runs 2 and 3. Phys Rev D 85:082002. https://doi.org/10.1103/PhysRevD.85.082002. arXiv:1111.7314 [gr-qc]

Abbott BP et al (2009) An upper limit on the stochastic gravitational-wave background of cosmological origin. Nature 460:990. https://doi.org/10.1038/nature08278. arXiv:0910.5772 [astro-ph.CO]

Abbott BP et al (2009) First LIGO search for gravitational wave bursts from cosmic (super)strings. Phys Rev D 80:062002. https://doi.org/10.1103/PhysRevD.80.062002. arXiv:0904.4718 [astro-ph.CO]

Abbott BP et al (2016) Astrophysical implications of the binary black-hole merger GW150914. Astrophys J Lett 818(2):L22. https://doi.org/10.3847/2041-8205/818/2/L22. arXiv:1602.03846 [astro-ph.HE]

Abbott BP et al (2016) Binary Black Hole Mergers in the first Advanced LIGO Observing Run. Phys Rev X 6(4):041015. [Erratum: Phys Rev X 8, 039903 (2018)]. https://doi.org/10.1103/PhysRevX.6.041015. arXiv:1606.04856 [gr-qc]

Abbott BP et al (2016) Directly comparing GW150914 with numerical solutions of Einstein's equations for binary black hole coalescence. Phys Rev D 94(6):064035. https://doi.org/10.1103/PhysRevD.94.064035. arXiv:1606.01262 [gr-qc]

Abbott BP et al (2016) GW150914: first results from the search for binary black hole coalescence with Advanced LIGO. Phys Rev D 93(12):122003. https://doi.org/10.1103/PhysRevD.93.122003. arXiv:1602.03839 [gr-qc]

Abbott BP et al (2016) Observation of gravitational waves from a binary black hole merger. Phys Rev Lett 116(6):061102. https://doi.org/10.1103/PhysRevLett.116.061102. arXiv:1602.03837 [gr-qc]

Abbott BP et al (2016) Properties of the binary black hole merger GW150914. Phys Rev Lett 116 (24):241102. https://doi.org/10.1103/PhysRevLett.116.241102. arXiv:1602.03840 [gr-qc]

Abbott BP et al (2016) Tests of general relativity with GW150914. Phys Rev Lett 116(22):221101. [Erratum: Phys. Rev. Lett. 121, 129902 (2018)]. https://doi.org/10.1103/PhysRevLett.116.221101. arXiv:1602.03841 [gr-qc]

Abbott BP et al (2017) Effects of waveform model systematics on the interpretation of GW150914. Class Quantum Grav 34(10):104002. https://doi.org/10.1088/1361-6382/aa6854. arXiv:1611.07531 [gr-qc]

Abbott BP et al (2018) Constraints on cosmic strings using data from the first Advanced LIGO observing run. Phys Rev D 97(10):102002. https://doi.org/10.1103/PhysRevD.97.102002. arXiv:1712.01168 [gr-qc]

Abbott BP et al (2019) All-sky search for short gravitational-wave bursts in the second Advanced LIGO and Advanced Virgo run. Phys Rev D 100(2):024017. https://doi.org/10.1103/PhysRevD.100.024017. arXiv:1905.03457 [gr-qc]

Abbott BP et al (2019) GWTC-1: a gravitational-wave transient catalog of compact binary mergers observed by LIGO and Virgo during the first and second observing runs. Phys Rev X 9(3):031040. https://doi.org/10.1103/PhysRevX.9.031040. arXiv:1811.12907 [astro-ph.HE]

Abbott BP et al (2019) Search for the isotropic stochastic background using data from Advanced LIGO's second observing run. Phys Rev D 100(6):061101. https://doi.org/10.1103/PhysRevD.100.061101. arXiv:1903.02886 [gr-qc]

Abbott BP et al (2019) Tests of general relativity with GW170817. Phys Rev Lett 123(1):011102. https://doi.org/10.1103/PhysRevLett.123.011102. arXiv:1811.00364 [gr-qc]
Abbott BP et al (2019) Tests of general relativity with the binary black hole signals from the LIGO-Virgo catalog GWTC-1. Phys Rev D 100(10):104036. https://doi.org/10.1103/PhysRevD.100.104036. arXiv:1903.04467 [gr-qc]
Abbott R et al (2020) GW190412: observation of a binary-black-hole coalescence with asymmetric masses. Phys Rev D 102(4):043015. https://doi.org/10.1103/PhysRevD.102.043015. arXiv:2004.08342 [astro-ph.HE]
Abbott R et al (2020) GW190521: a binary black hole merger with a total mass of $150M_{\odot}$. Phys Rev Lett 125(10):101102. https://doi.org/10.1103/PhysRevLett.125.101102. arXiv:2009.01075 [gr-qc]
Abbott R et al (2020) GW190814: gravitational waves from the coalescence of a 23 solar mass black hole with a 2.6 solar mass compact object. Astrophys J Lett 896(2):L44. https://doi.org/10.3847/2041-8213/ab960f. arXiv:2006.12611 [astro-ph.HE]
Abbott R et al (2020) Properties and astrophysical implications of the 150 $M_{\odot}$ binary black hole merger GW190521. Astrophys J Lett 900(1):L13. https://doi.org/10.3847/2041-8213/aba493. arXiv:2009.01190 [astro-ph.HE]
Abbott R et al (2021) Constraints on cosmic strings using data from the third advanced LIGO-Virgo observing run. Phys Rev Lett 126(24):241102. https://doi.org/10.1103/PhysRevLett.126.241102. arXiv:2101.12248 [gr-qc]
Abbott R et al (2021) GWTC-2: compact binary coalescences observed by LIGO and Virgo during the first half of the third observing run. Phys Rev X 11:021053. https://doi.org/10.1103/PhysRevX.11.021053. arXiv:2010.14527 [gr-qc]
Abbott R et al (2021) Tests of general relativity with binary black holes from the second LIGO-Virgo gravitational-wave transient catalog. Phys Rev D 103(12):122002. https://doi.org/10.1103/PhysRevD.103.122002. arXiv:2010.14529 [gr-qc]
Abbott R, et al. (2021d) Tests of General Relativity with GWTC-3. arXiv e-prints arXiv:2112.06861 [gr-qc]
Abbott R et al (2021) Upper limits on the isotropic gravitational-wave background from Advanced LIGO and Advanced Virgo's third observing run. Phys Rev D 104(2):022004. https://doi.org/10.1103/PhysRevD.104.022004. arXiv:2101.12130 [gr-qc]
Abbott R et al (2023) GWTC-3: compact binary coalescences observed by LIGO and Virgo during the second part of the third observing run. Phys Rev X 13(4):041039. https://doi.org/10.1103/PhysRevX.13.041039. arXiv:2111.03606 [gr-qc]
Abbott R et al (2023) Population of merging compact binaries inferred using gravitational waves through GWTC-3. Phys Rev X 13(1):011048. https://doi.org/10.1103/PhysRevX.13.011048. arXiv:2111.03634 [astro-ph.HE]
Abbott R et al (2024) GWTC-2.1: Deep extended catalog of compact binary coalescences observed by LIGO and Virgo during the first half of the third observing run. Phys Rev D 109(2):022001. https://doi.org/10.1103/PhysRevD.109.022001. arXiv:2108.01045 [gr-qc]
Abedi J, Dykaar H, Afshordi N (2017) Echoes from the Abyss: tentative evidence for Planck-scale structure at black hole horizons. Phys Rev D 96(8):082004. https://doi.org/10.1103/PhysRevD.96.082004. arXiv:1612.00266 [gr-qc]
Abedi J, Afshordi N, Oshita N, Wang Q (2020) Quantum black holes in the sky. Universe 6(3):43. https://doi.org/10.3390/universe6030043. arXiv:2001.09553 [gr-qc]
Accetta FS, Krauss LM (1989) The stochastic gravitational wave spectrum resulting from cosmic string evolution. Nucl Phys B 319:747–764. https://doi.org/10.1016/0550-3213(89)90628-7
Acernese F et al (2015) Advanced virgo: a second-generation interferometric gravitational wave detector. Class Quantum Grav 32(2):024001. https://doi.org/10.1088/0264-9381/32/2/024001. arXiv:1408.3978 [gr-qc]
Ackley K et al (2020) Neutron star extreme matter observatory: a kilohertz-band gravitational-wave detector in the global network. Publ Astron Soc Austral 37:e047. https://doi.org/10.1017/pasa.2020.39. arXiv:2007.03128 [astro-ph.HE]
Adams M, Colella P, Graves DT, Johnson J, Keen N, Ligocki TJ, Martin DF, McCorquodale P, Modiano D, Schwartz P, Sternberg T, Straalen BV (2024) Chombo software package for amr applications - design document. https://commons.lbl.gov/display/chombo/Chombo+-+Software+for+Adaptive+Solutions+of+Partial+Differential+Equations

Ade PAR et al (2014) Planck 2013 results. XXV. Searches for cosmic strings and other topological defects. Astron Astrophys 571:A25. https://doi.org/10.1051/0004-6361/201321621. arXiv:1303.5085 [astro-ph.CO]

Agathos M, Del Pozzo W, Li T, Van Den Broeck C, Veitch J, Vitale S (2014) TIGER: a data analysis pipeline for testing the strong-field dynamics of general relativity with gravitational wave signals from coalescing compact binaries. Phys Rev D 89(8):082001. https://doi.org/10.1103/PhysRevD.89.082001. arXiv:1311.0420 [gr-qc]

Aguirregabiria JM, Vishveshwara CV (1996) Scattering by black holes: a simulated potential approach. Phys Lett A 210:251–254. https://doi.org/10.1016/0375-9601(95)00937-X

Ajith P et al (2007) Phenomenological template family for black-hole coalescence waveforms. Class Quantum Grav 24:S689–S700. https://doi.org/10.1088/0264-9381/24/19/S31. arXiv:0704.3764 [gr-qc]

Ajith P et al (2008) A Template bank for gravitational waveforms from coalescing binary black holes. I. Non-spinning binaries. Phys Rev D 77:104017. [Erratum: Phys. Rev. D 79, 129901 (2009)]. https://doi.org/10.1103/PhysRevD.77.104017. arXiv:0710.2335 [gr-qc]

Ajith P et al (2011) Inspiral-merger-ringdown waveforms for black-hole binaries with non-precessing spins. Phys Rev Lett 106:241101. https://doi.org/10.1103/PhysRevLett.106.241101. arXiv:0909.2867 [gr-qc]

Ajith P et al (2012) The NINJA-2 catalog of hybrid post-Newtonian/numerical-relativity waveforms for non-precessing black-hole binaries. Class Quantum Grav 29:124001. [Erratum: Class. Quant. Grav. 30, 199401 (2013)]. https://doi.org/10.1088/0264-9381/29/12/124001. arXiv:1201.5319 [gr-qc]

Akcay S, van de Meent M (2016) Numerical computation of the effective-one-body potential q using self-force results. Phys Rev D 93(6):064063. https://doi.org/10.1103/PhysRevD.93.064063. arXiv:1512.03392 [gr-qc]

Akcay S, Barack L, Damour T, Sago N (2012) Gravitational self-force and the effective-one-body formalism between the innermost stable circular orbit and the light ring. Phys Rev D 86:104041. https://doi.org/10.1103/PhysRevD.86.104041. arXiv:1209.0964 [gr-qc]

Akcay S, Warburton N, Barack L (2013) Frequency-domain algorithm for the Lorenz-gauge gravitational self-force. Phys Rev D 88(10):104009. https://doi.org/10.1103/PhysRevD.88.104009. arXiv:1308.5223 [gr-qc]

Akcay S, Bernuzzi S, Messina F, Nagar A, Ortiz N, Rettegno P (2019) Effective-one-body multipolar waveform for tidally interacting binary neutron stars up to merger. Phys Rev D 99(4):044051. https://doi.org/10.1103/PhysRevD.99.044051. arXiv:1812.02744 [gr-qc]

Akcay S, Dolan SR, Kavanagh C, Moxon J, Warburton N, Wardell B (2020) Dissipation in extreme-mass ratio binaries with a spinning secondary. Phys Rev D 102(6):064013. https://doi.org/10.1103/PhysRevD.102.064013. arXiv:1912.09461 [gr-qc]

Akcay S, Gamba R, Bernuzzi S (2021) Hybrid post-Newtonian effective-one-body scheme for spin-precessing compact-binary waveforms up to merger. Phys Rev D 103(2):024014. https://doi.org/10.1103/PhysRevD.103.024014. arXiv:2005.05338 [gr-qc]

Albanesi S, Nagar A, Bernuzzi S (2021) Effective one-body model for extreme-mass-ratio spinning binaries on eccentric equatorial orbits: testing radiation reaction and waveform. Phys Rev D 104(2):024067. https://doi.org/10.1103/PhysRevD.104.024067. arXiv:2104.10559 [gr-qc]

Albanesi S, Nagar A, Bernuzzi S, Placidi A, Orselli M (2022) Assessment of effective-one-body radiation reactions for generic planar orbits. Phys Rev D 105(10):104031. https://doi.org/10.1103/PhysRevD.105.104031. arXiv:2202.10063 [gr-qc]

Albanesi S, Placidi A, Nagar A, Orselli M, Bernuzzi S (2022) New avenue for accurate analytical waveforms and fluxes for eccentric compact binaries. Phys Rev D 105(12):L121503. https://doi.org/10.1103/PhysRevD.105.L121503. arXiv:2203.16286 [gr-qc]

Albanesi S, Bernuzzi S, Damour T, Nagar A, Placidi A (2023) Faithful effective-one-body waveform of small-mass-ratio coalescing black hole binaries: the eccentric, nonspinning case. Phys Rev D 108(8):084037. https://doi.org/10.1103/PhysRevD.108.084037. arXiv:2305.19336 [gr-qc]

Albertini A, Nagar A, Pound A, Warburton N, Wardell B, Durkan L, Miller J (2022) Comparing second-order gravitational self-force and effective one body waveforms from inspiralling, quasicircular and nonspinning black hole binaries. II. The large-mass-ratio case. Phys Rev D 106(8):084062. https://doi.org/10.1103/PhysRevD.106.084062. arXiv:2208.02055 [gr-qc]

Albertini A, Nagar A, Pound A, Warburton N, Wardell B, Durkan L, Miller J (2022) Comparing second-order gravitational self-force, numerical relativity, and effective one body waveforms from

inspiralling, quasicircular, and nonspinning black hole binaries. Phys Rev D 106(8):084061. https://doi.org/10.1103/PhysRevD.106.084061. arXiv:2208.01049 [gr-qc]
Albrecht A, Steinhardt PJ (1982) Cosmology for grand unified theories with radiatively induced symmetry breaking. Phys Rev Lett 48:1220–1223. https://doi.org/10.1103/PhysRevLett.48.1220
Alcubierre M (2008) Introduction to 3+1 Numerical Relativity. Oxford University Press, Oxford. https://doi.org/10.1093/acprof:oso/9780199205677.001.0001
Alcubierre M, Degollado JC, Salgado M (2009) The Einstein-Maxwell system in 3+1 form and initial data for multiple charged black holes. Phys Rev D 80:104022. https://doi.org/10.1103/PhysRevD.80.104022. arXiv:0907.1151 [gr-qc]
Alexander S, Yunes N (2009) Chern-simons modified general relativity. Phys Rept 480:1–55. https://doi.org/10.1016/j.physrep.2009.07.002. arXiv:0907.2562 [hep-th]
Alfieri R, Bernuzzi S, Perego A, Radice D (2018) Optimization of finite-differencing kernels for numerical relativity applications. J Low Power Electron Appl 8(2):15. https://doi.org/10.3390/jlpea8020015
Alic D, Bona-Casas C, Bona C, Rezzolla L, Palenzuela C (2012) Conformal and covariant formulation of the Z4 system with constraint-violation damping. Phys Rev D 85:064040. https://doi.org/10.1103/PhysRevD.85.064040. arXiv:1106.2254 [gr-qc]
Alic D, Kastaun W, Rezzolla L (2013) Constraint damping of the conformal and covariant formulation of the Z4 system in simulations of binary neutron stars. Phys Rev D 88(6):064049. https://doi.org/10.1103/PhysRevD.88.064049. arXiv:1307.7391 [gr-qc]
Allahyari A, Nunes RC, Mota DF (2022) No slip gravity in light of LISA standard sirens. Mon Not R Astron Soc 514(1):1274–1281. https://doi.org/10.1093/mnras/stac1445. arXiv:2110.07634 [astro-ph.CO]
Allen B, Casper P (1994) A Closed form expression for the gravitational radiation rate from cosmic strings. Phys Rev D 50:2496–2518. https://doi.org/10.1103/PhysRevD.50.2496. arXiv:gr-qc/9405005
Allen B, Ottewill AC (2001) Wave forms for gravitational radiation from cosmic string loops. Phys Rev D 63:063507. https://doi.org/10.1103/PhysRevD.63.063507. arXiv:gr-qc/0009091
Allen B, Shellard E (1992) Gravitational radiation from cosmic strings. Phys Rev D 45:1898–1912. https://doi.org/10.1103/PhysRevD.45.1898
Allen B, Casper P, Ottewill A (1995) Closed form expression for the momentum radiated from cosmic string loops. Phys Rev D 51:1546–1552. https://doi.org/10.1103/PhysRevD.51.1546. arXiv:gr-qc/9407023
Allwright G, Lehner L (2019) Towards the nonlinear regime in extensions to GR: assessing possible options. Class Quantum Grav 36(8):084001. https://doi.org/10.1088/1361-6382/ab0ee1. arXiv:1808.07897 [gr-qc]
Alvi K (2001) Energy and angular momentum flow into a black hole in a binary. Phys Rev D 64:104020. https://doi.org/10.1103/PhysRevD.64.104020. arXiv:gr-qc/0107080
Amaro-Seoane P (2018) Detecting intermediate-mass ratio inspirals from the ground and space. Phys Rev D 98(6):063018. https://doi.org/10.1103/PhysRevD.98.063018. arXiv:1807.03824 [astro-ph.HE]
Amaro-Seoane P (2018) Relativistic dynamics and extreme mass ratio inspirals. Living Rev Relativ 21:4. https://doi.org/10.1007/s41114-018-0013-8. arXiv:1205.5240 [astro-ph.CO]
Amaro-Seoane P (2019) Extremely large mass-ratio inspirals. Phys Rev D 99(12):123025. https://doi.org/10.1103/PhysRevD.99.123025. arXiv:1903.10871 [astro-ph.GA]
Amaro-Seoane P, Preto M (2011) The impact of realistic models of mass segregation on the event rate of extreme-mass ratio inspirals and cusp re-growth. Class Quantum Grav 28:094017. https://doi.org/10.1088/0264-9381/28/9/094017. arXiv:1010.5781 [astro-ph.CO]
Amaro-Seoane P, Santamaría L (2010) Detection of IMBHs with ground-based gravitational wave observatories: a biography of a binary of black holes, from birth to death. Astrophys J 722:1197–1206. https://doi.org/10.1088/0004-637X/722/2/1197. arXiv:0910.0254 [astro-ph.CO]
Amaro-Seoane P, et al. (2017) Laser Interferometer Space Antenna. arXiv arXiv:1702.00786 [astro-ph.IM]
Amaro-Seoane P et al (2023) Astrophysics with the Laser Interferometer Space Antenna. Living Rev Relativ 26:2. https://doi.org/10.1007/s41114-022-00041-y. arXiv:2203.06016 [gr-qc]
Andrade T et al (2021) GRChombo: an adaptable numerical relativity code for fundamental physics. J Open Source Softw 6(68):3703. https://doi.org/10.21105/joss.03703. arXiv:2201.03458 [gr-qc]
Andrews JJ, Mandel I (2019) Double neutron star populations and formation channels. Astrophys J Lett 880(1):L8. https://doi.org/10.3847/2041-8213/ab2ed1. arXiv:1904.12745 [astro-ph.HE]
Anninos P, Price RH, Pullin J, Seidel E, Suen WM (1995) Headon collision of two black holes: comparison of different approaches. Phys Rev D 52:4462–4480. https://doi.org/10.1103/PhysRevD.52.4462. arXiv:gr-qc/9505042

Annulli L, Cardoso V, Vicente R (2020) Response of ultralight dark matter to supermassive black holes and binaries. Phys Rev D 102(6):063022. https://doi.org/10.1103/PhysRevD.102.063022. arXiv:2009.00012 [gr-qc]

Annulli L, Cardoso V, Vicente R (2020) Stirred and shaken: dynamical behavior of boson stars and dark matter cores. Phys Lett B 811:135944. https://doi.org/10.1016/j.physletb.2020.135944. arXiv:2007.03700 [astro-ph.HE]

Annulli L, Cardoso V, Gualtieri L (2022) Applications of the close-limit approximation: horizonless compact objects and scalar fields. Class Quantum Grav 39(10):105005. https://doi.org/10.1088/1361-6382/ac6410. arXiv:2104.11236 [gr-qc]

Ansorg M, Brügmann B, Tichy W (2004) A Single-domain spectral method for black hole puncture data. Phys Rev D 70:064011. https://doi.org/10.1103/PhysRevD.70.064011. arXiv:gr-qc/0404056

Antonelli A, Buonanno A, Steinhoff J, van de Meent M, Vines J (2019) Energetics of two-body Hamiltonians in post-Minkowskian gravity. Phys Rev D 99(10):104004. https://doi.org/10.1103/PhysRevD.99.104004. arXiv:1901.07102 [gr-qc]

Antonelli A, Kavanagh C, Khalil M, Steinhoff J, Vines J (2020) Gravitational spin-orbit and aligned $spin_1$-$spin_2$ couplings through third-subleading post-Newtonian orders. Phys Rev D 102:124024. https://doi.org/10.1103/PhysRevD.102.124024. arXiv:2010.02018 [gr-qc]

Antonelli A, Kavanagh C, Khalil M, Steinhoff J, Vines J (2020) Gravitational spin-orbit coupling through third-subleading post-Newtonian order: from first-order self-force to arbitrary mass ratios. Phys Rev Lett 125(1):011103. https://doi.org/10.1103/PhysRevLett.125.011103. arXiv:2003.11391 [gr-qc]

Antonelli A, van de Meent M, Buonanno A, Steinhoff J, Vines J (2020) Quasicircular inspirals and plunges from nonspinning effective-one-body Hamiltonians with gravitational self-force information. Phys Rev D 101(2):024024. https://doi.org/10.1103/PhysRevD.101.024024. arXiv:1907.11597 [gr-qc]

Antonini F, Rasio FA (2016) Merging black hole binaries in galactic nuclei: implications for advanced-LIGO detections. Astrophys J 831(2):187. https://doi.org/10.3847/0004-637X/831/2/187. arXiv:1606.04889 [astro-ph.HE]

Antoniou G, Bakopoulos A, Kanti P (2018) Evasion of no-hair theorems and novel black-hole solutions in gauss-bonnet theories. Phys Rev Lett 120(13):131102. https://doi.org/10.1103/PhysRevLett.120.131102. arXiv:1711.03390 [hep-th]

Aoude R, Haddad K, Helset A (2021) Tidal effects for spinning particles. JHEP 03:097. https://doi.org/10.1007/JHEP03(2021)097. arXiv:2012.05256 [hep-th]

Aoude R, Haddad K, Helset A (2022) Classical gravitational spinning-spinless scattering at $O(G2S\infty)$. Phys Rev Lett 129(14):141102. https://doi.org/10.1103/PhysRevLett.129.141102. arXiv:2205.02809 [hep-th]

Aoyama H, Konechny A, Lemes V, Maggiore N, Sarandy M, Sorella S, Duplij S (2004) Nambu-goto action. In: Duplij S, Siegel W, Bagger J (eds) Concise Encyclopedia of Supersymmetry: And noncommutative structures in mathematics and physics. Springer, Dordrecht, pp 257. https://doi.org/10.1007/1-4020-4522-0_339

Apostolatos TA (1995) Search templates for gravitational waves from precessing, inspiraling binaries. Phys Rev D 52:605–620. https://doi.org/10.1103/PhysRevD.52.605

Apostolatos TA, Lukes-Gerakopoulos G, Contopoulos G (2009) How to observe a non-kerr spacetime using gravitational waves. Phys Rev Lett 103:111101. https://doi.org/10.1103/PhysRevLett.103.111101. arXiv:0906.0093 [gr-qc]

Apte A, Hughes SA (2019) Exciting black hole modes via misaligned coalescences: I. Inspiral, transition, and plunge trajectories using a generalized Ori-Thorne procedure. Phys Rev D 100(8):084031. https://doi.org/10.1103/PhysRevD.100.084031. arXiv:1901.05901 [gr-qc]

Arca-Sedda M, Gualandris A (2018) Gravitational wave sources from inspiralling globular clusters in the Galactic Centre and similar environments. Mon Not R Astron Soc 477(4):4423–4442. https://doi.org/10.1093/mnras/sty922. arXiv:1804.06116 [astro-ph.GA]

Arca-Sedda M, Amaro-Seoane P, Chen X (2021) Merging stellar and intermediate-mass black holes in dense clusters: implications for LIGO, LISA, and the next generation of gravitational wave detectors. Astron Astrophys 652:A54. https://doi.org/10.1051/0004-6361/202037785. arXiv:2007.13746 [astro-ph.GA]

Aresté Saló L, Clough K, Figueras P (2022) Well-posedness of the four-derivative scalar-tensor theory of gravity in singularity avoiding coordinates. Phys Rev Lett 129(26):261104. https://doi.org/10.1103/PhysRevLett.129.261104. arXiv:2208.14470 [gr-qc]

Aretakis S (2012) Decay of axisymmetric solutions of the wave equation on extreme Kerr backgrounds. J Funct Anal 263:2770–2831. https://doi.org/10.1016/j.jfa.2012.08.015. arXiv:1110.2006 [gr-qc]

Arkani-Hamed N, Huang TC, Huang Y (2021) Scattering amplitudes for all masses and spins. JHEP 11:070. https://doi.org/10.1007/JHEP11(2021)070. arXiv:1709.04891 [hep-th]
Armitage PJ, Natarajan P (2005) Eccentricity of supermassive black hole binaries coalescing from gas rich mergers. Astrophys J 634:921–928. https://doi.org/10.1086/497108. arXiv:astro-ph/0508493
Arnowitt R, Deser S, Misner CW (1962) The dynamics of general relativity. In: Witten L (ed) Gravitation: an introduction to current research. Wiley, New York
Arun KG, Blanchet L, Iyer BR, Qusailah M (2008) Inspiralling compact binaries in quasi-elliptical orbits: the complete 3PN energy flux. Phys Rev D 77:064035. https://doi.org/10.1103/PhysRevD.77.064035. arXiv:0711.0302 [gr-qc]
Arun KG, Blanchet L, Iyer BR, Qusailah M (2008) Tail effects in the 3PN gravitational wave energy flux of compact binaries in quasi-elliptical orbits. Phys Rev D 77:064034. https://doi.org/10.1103/PhysRevD.77.064034. arXiv:0711.0250 [gr-qc]
Arun KG, Blanchet L, Iyer BR, Sinha S (2009) Third post-Newtonian angular momentum flux and the secular evolution of orbital elements for inspiralling compact binaries in quasi-elliptical orbits. Phys Rev D 80:124018. https://doi.org/10.1103/PhysRevD.80.124018. arXiv:0908.3854 [gr-qc]
Arun KG, Buonanno A, Faye G, Ochsner E (2009) Higher-order spin effects in the amplitude and phase of gravitational waveforms emitted by inspiraling compact binaries: Ready-to-use gravitational waveforms. Phys Rev D 79:104023. [Erratum: Phys. Rev. D 84, 049901 (2011)]. https://doi.org/10.1103/PhysRevD.79.104023. arXiv:0810.5336 [gr-qc]
Arun KG et al (2022) New horizons for fundamental physics with LISA. Living Rev Relativ 25:4. https://doi.org/10.1007/s41114-022-00036-9. arXiv:2205.01597 [gr-qc]
Arvanitaki A, Dubovsky S (2011) Exploring the string axiverse with precision black hole physics. Phys Rev D 83:044026. https://doi.org/10.1103/PhysRevD.83.044026. arXiv:1004.3558 [hep-th]
Arvanitaki A, Dimopoulos S, Dubovsky S, Kaloper N, March-Russell J (2010) String Axiverse. Phys Rev D 81:123530. https://doi.org/10.1103/PhysRevD.81.123530. arXiv:0905.4720 [hep-th]
Arvanitaki A, Baryakhtar M, Huang X (2015) Discovering the QCD axion with black holes and gravitational waves. Phys Rev D 91(8):084011. https://doi.org/10.1103/PhysRevD.91.084011. arXiv:1411.2263 [hep-ph]
Asali Y, Pang P, Samajdar A, Van Den Broeck C (2020) Probing resonant excitations in exotic compact objects via gravitational waves. Phys Rev D 102(2):024016. https://doi.org/10.1103/PhysRevD.102.024016. arXiv:2004.05128 [gr-qc]
Ashtekar A, Beetle C, Lewandowski J (2001) Mechanics of rotating isolated horizons. Phys Rev D 64:044016. https://doi.org/10.1103/PhysRevD.64.044016. arXiv:gr-qc/0103026
Assumpcao T, Werneck LR, Jacques TP, Etienne ZB (2022) Fast hyperbolic relaxation elliptic solver for numerical relativity: conformally flat, binary puncture initial data. Phys Rev D 105(10):104037. https://doi.org/10.1103/PhysRevD.105.104037. arXiv:2111.02424 [gr-qc]
Auclair P et al (2023) Cosmology with the Laser Interferometer Space Antenna. Living Rev Relativ 26:5. https://doi.org/10.1007/s41114-023-00045-2. arXiv:2204.05434 [astro-ph.CO]
Aurrekoetxea JC, Helfer T, Lim EA (2020) Coherent gravitational waveforms and memory from cosmic string loops. Class Quantum Grav 37(20):204001. https://doi.org/10.1088/1361-6382/aba28b. arXiv:2002.05177 [gr-qc]
Aurrekoetxea JC, Clough K, Lim EA (2023) CTTK: a new method to solve the initial data constraints in numerical relativity. Class Quantum Grav 40(7):075003. https://doi.org/10.1088/1361-6382/acb883. arXiv:2207.03125 [gr-qc]
Austin D, Copeland EJ, Kibble T (1993) Evolution of cosmic string configurations. Phys Rev D 48:5594–5627. https://doi.org/10.1103/PhysRevD.48.5594. arXiv:hep-ph/9307325
Aylott B et al (2009) Status of NINJA: the numerical injection analysis project. Class Quantum Grav 26:114008. https://doi.org/10.1088/0264-9381/26/11/114008. arXiv:0905.4227 [gr-qc]
Ayzenberg D, Yunes N (2014) Slowly-Rotating Black Holes in Einstein-Dilaton-Gauss-Bonnet Gravity: Quadratic Order in Spin Solutions. Phys Rev D 90:044066. [Erratum: Phys. Rev. D 91, 069905 (2015)]. https://doi.org/10.1103/PhysRevD.90.044066. arXiv:1405.2133 [gr-qc]
Babak S, Petiteau A (2024) LISA Data Challenge Manual. https://lisa-ldc.lal.in2p3.fr/static/data/pdf/LDC-manual-002.pdf
Babak S, Fang H, Gair JR, Glampedakis K, Hughes SA (2007) Kludge gravitational waveforms for a test-body orbiting a Kerr black hole. Phys Rev D 75:024005. [Erratum: Phys. Rev. D 77, 04990 (2008)]. https://doi.org/10.1103/PhysRevD.75.024005. arXiv:gr-qc/0607007

Babak S, Gair J, Sesana A, Barausse E, Sopuerta CF, Berry CPL, Berti E, Amaro-Seoane P, Petiteau A, Klein A (2017) Science with the space-based interferometer LISA. V: Extreme mass-ratio inspirals. Phys Rev D 95(10):103012. https://doi.org/10.1103/PhysRevD.95.103012. arXiv:1703.09722 [gr-qc]

Babak S, Taracchini A, Buonanno A (2017) Validating the effective-one-body model of spinning, precessing binary black holes against numerical relativity. Phys Rev D 95(2):024010. https://doi.org/10.1103/PhysRevD.95.024010. arXiv:1607.05661 [gr-qc]

Babak S et al (2008) Report on the second Mock LISA Data Challenge. Class Quantum Grav 25:114037. https://doi.org/10.1088/0264-9381/25/11/114037. arXiv:0711.2667 [gr-qc]

Babak S et al (2008) The mock LISA data challenges: from challenge 1B to challenge 3. Class Quantum Grav 25:184026. https://doi.org/10.1088/0264-9381/25/18/184026. arXiv:0806.2110 [gr-qc]

Babak S et al (2010) The mock LISA data challenges: from challenge 3 to challenge 4. Class Quantum Grav 27:084009. https://doi.org/10.1088/0264-9381/27/8/084009. arXiv:0912.0548 [gr-qc]

Bah I, Bena I, Heidmann P, Li Y, Mayerson DR (2021) Gravitational footprints of black holes and their microstate geometries. JHEP 10:138. https://doi.org/10.1007/JHEP10(2021)138. arXiv:2104.10686 [hep-th]

Baibhav V, Berti E (2019) Multimode black hole spectroscopy. Phys Rev D 99(2):024005. https://doi.org/10.1103/PhysRevD.99.024005. arXiv:1809.03500 [gr-qc]

Baibhav V, Berti E, Cardoso V, Khanna G (2018) Black hole spectroscopy: systematic errors and ringdown energy estimates. Phys Rev D 97(4):044048. https://doi.org/10.1103/PhysRevD.97.044048. arXiv:1710.02156 [gr-qc]

Baibhav V, Berti E, Cardoso V (2020) LISA parameter estimation and source localization with higher harmonics of the ringdown. Phys Rev D 101(8):084053. https://doi.org/10.1103/PhysRevD.101.084053. arXiv:2001.10011 [gr-qc]

Baibhav V, Cheung M, Berti E, Cardoso V, Carullo G, Cotesta R, Del Pozzo W, Duque F (2023) Agnostic black hole spectroscopy: quasinormal mode content of numerical relativity waveforms and limits of validity of linear perturbation theory. Phys Rev D 108(10):104020. https://doi.org/10.1103/PhysRevD.108.104020. arXiv:2302.03050 [gr-qc]

Baker JG, Centrella J, Choi DI, Koppitz M, van Meter J (2006) Gravitational wave extraction from an inspiraling configuration of merging black holes. Phys Rev Lett 96:111102. https://doi.org/10.1103/PhysRevLett.96.111102. arXiv:gr-qc/0511103

Baker JG, Centrella J, Choi DI, Koppitz M, van Meter JR, Miller MC (2006) Getting a kick out of numerical relativity. Astrophys J Lett 653:L93–L96. https://doi.org/10.1086/510448. arXiv:astro-ph/0603204

Baker JG, Campanelli M, Pretorius F, Zlochower Y (2007) Comparisons of binary black hole merger waveforms. Class Quantum Grav 24:S25–S31. https://doi.org/10.1088/0264-9381/24/12/S03. arXiv:gr-qc/0701016

Baker JG, van Meter JR, McWilliams ST, Centrella J, Kelly BJ (2007) Consistency of post-Newtonian waveforms with numerical relativity. Phys Rev Lett 99:181101. https://doi.org/10.1103/PhysRevLett.99.181101. arXiv:gr-qc/0612024

Baker JG, Boggs WD, Centrella J, Kelly BJ, McWilliams ST, van Meter JR (2008) Mergers of non-spinning black-hole binaries: gravitational radiation characteristics. Phys Rev D 78:044046. https://doi.org/10.1103/PhysRevD.78.044046. arXiv:0805.1428 [gr-qc]

Balay S, Abhyankar S, Adams MF, Benson S, Brown J, Brune P, Buschelman K, Constantinescu EM, Dalcin L, Dener A, Eijkhout V, Faibussowitsch J, Gropp WD, Hapla V, Isaac T, Jolivet P, Karpeev D, Kaushik D, Knepley MG, Kong F, Kruger S, May DA, McInnes LC, Mills RT, Mitchell L, Munson T, Roman JE, Rupp K, Sanan P, Sarich J, Smith BF, Zampini S, Zhang H, Zhang H, Zhang J (2022) PETSc Web page. https://petsc.org/

Baldassare VF, Geha M, Greene J (2020) A search for optical AGN variability in 35,000 low-mass galaxies with the Palomar Transient Factory. Astrophys J 896(1):10. https://doi.org/10.3847/1538-4357/ab8936. arXiv:1910.06342 [astro-ph.HE]

Balmelli S, Damour T (2015) New effective-one-body Hamiltonian with next-to-leading order spin-spin coupling. Phys Rev D 92(12):124022. https://doi.org/10.1103/PhysRevD.92.124022. arXiv:1509.08135 [gr-qc]

Balmelli S, Jetzer P (2015) Effective-one-body Hamiltonian with next-to-leading order spin-spin coupling. Phys Rev D 91:064011. https://doi.org/10.1103/PhysRevD.91.064011. arXiv:1502.01343 [gr-qc]

Bamber J, Clough K, Ferreira PG, Hui L, Lagos M (2021) Growth of accretion driven scalar hair around Kerr black holes. Phys Rev D 103(4):044059. https://doi.org/10.1103/PhysRevD.103.044059. arXiv:2011.07870 [gr-qc]

Bamber J, Aurrekoetxea JC, Clough K, Ferreira PG (2023) Black hole merger simulations in wave dark matter environments. Phys Rev D 107(2):024035. https://doi.org/10.1103/PhysRevD.107.024035. arXiv:2210.09254 [gr-qc]
Bambi C (2011) Testing the Kerr black hole hypothesis. Mod Phys Lett A 26:2453–2468. https://doi.org/10.1142/S0217732311036929. arXiv:1109.4256 [gr-qc]
Bao J, Shi C, Wang H, Zhang J, Hu Y, Mei J, Luo J (2019) Constraining modified gravity with ringdown signals: an explicit example. Phys Rev D 100(8):084024. https://doi.org/10.1103/PhysRevD.100.084024. arXiv:1905.11674 [gr-qc]
Barack L (2000) Late time decay of scalar, electromagnetic, and gravitational perturbations outside rotating black holes. Phys Rev D 61:024026. https://doi.org/10.1103/PhysRevD.61.024026. arXiv:gr-qc/9908005
Barack L (2009) Gravitational self force in extreme mass-ratio inspirals. Class Quantum Grav 26:213001. https://doi.org/10.1088/0264-9381/26/21/213001. arXiv:0908.1664 [gr-qc]
Barack L, Burko LM (2000) Radiation reaction force on a particle plunging into a black hole. Phys Rev D 62:084040. https://doi.org/10.1103/PhysRevD.62.084040. arXiv:gr-qc/0007033
Barack L, Cutler C (2004) LISA capture sources: approximate waveforms, signal-to-noise ratios, and parameter estimation accuracy. Phys Rev D 69:082005. https://doi.org/10.1103/PhysRevD.69.082005. arXiv:gr-qc/0310125
Barack L, Cutler C (2007) Using LISA EMRI sources to test off-Kerr deviations in the geometry of massive black holes. Phys Rev D 75:042003. https://doi.org/10.1103/PhysRevD.75.042003. arXiv:gr-qc/0612029
Barack L, Giudice P (2017) Time-domain metric reconstruction for self-force applications. Phys Rev D 95 (10):104033. https://doi.org/10.1103/PhysRevD.95.104033. arXiv:1702.04204 [gr-qc]
Barack L, Long O (2022) Self-force correction to the deflection angle in black-hole scattering: a scalar charge toy model. Phys Rev D 106(10):104031. https://doi.org/10.1103/PhysRevD.106.104031. arXiv:2209.03740 [gr-qc]
Barack L, Lousto CO (2005) Perturbations of Schwarzschild black holes in the Lorenz gauge: formulation and numerical implementation. Phys Rev D 72:104026. https://doi.org/10.1103/PhysRevD.72.104026. arXiv:gr-qc/0510019
Barack L, Ori A (2000) Mode sum regularization approach for the selfforce in black hole space-time. Phys Rev D 61:061502. https://doi.org/10.1103/PhysRevD.61.061502. arXiv:gr-qc/9912010
Barack L, Ori A (2003) Gravitational selfforce on a particle orbiting a Kerr black hole. Phys Rev Lett 90:111101. https://doi.org/10.1103/PhysRevLett.90.111101. arXiv:gr-qc/0212103
Barack L, Ori A (2003) Regularization parameters for the selfforce in Schwarzschild space-time. 2. Gravitational and electromagnetic cases. Phys Rev D 67:024029. https://doi.org/10.1103/PhysRevD.67.024029. arXiv:gr-qc/0209072
Barack L, Pound A (2019) Self-force and radiation reaction in general relativity. Rept Prog Phys 82 (1):016904. https://doi.org/10.1088/1361-6633/aae552. arXiv:1805.10385 [gr-qc]
Barack L, Sago N (2007) Gravitational self force on a particle in circular orbit around a Schwarzschild black hole. Phys Rev D 75:064021. https://doi.org/10.1103/PhysRevD.75.064021. arXiv:gr-qc/0701069
Barack L, Sago N (2010) Gravitational self-force on a particle in eccentric orbit around a Schwarzschild black hole. Phys Rev D 81:084021. https://doi.org/10.1103/PhysRevD.81.084021. arXiv:1002.2386 [gr-qc]
Barack L, Mino Y, Nakano H, Ori A, Sasaki M (2002) Calculating the gravitational selfforce in Schwarzschild space-time. Phys Rev Lett 88:091101. https://doi.org/10.1103/PhysRevLett.88.091101. arXiv:gr-qc/0111001
Barack L, Golbourn DA, Sago N (2007) m-Mode regularization scheme for the self force in Kerr spacetime. Phys Rev D 76:124036. https://doi.org/10.1103/PhysRevD.76.124036. arXiv:0709.4588 [gr-qc]
Barack L, Ori A, Sago N (2008) Frequency-domain calculation of the self force: the high-frequency problem and its resolution. Phys Rev D 78:084021. https://doi.org/10.1103/PhysRevD.78.084021. arXiv:0808.2315 [gr-qc]
Barack L, Colleoni M, Damour T, Isoyama S, Sago N (2019) Self-force effects on the marginally bound zoom-whirl orbit in Schwarzschild spacetime. Phys Rev D 100(12):124015. https://doi.org/10.1103/PhysRevD.100.124015. arXiv:1909.06103 [gr-qc]
Barack L et al (2019) Black holes, gravitational waves and fundamental physics: a roadmap. Class Quantum Grav 36(14):143001. https://doi.org/10.1088/1361-6382/ab0587. arXiv:1806.05195 [gr-qc]

Barack L et al (2023) Comparison of post-Minkowskian and self-force expansions: scattering in a scalar charge toy model. Phys Rev D 108(2):024025. https://doi.org/10.1103/PhysRevD.108.024025. arXiv:2304.09200 [hep-th]

Barausse E (2012) The evolution of massive black holes and their spins in their galactic hosts. Mon Not R Astron Soc 423:2533–2557. https://doi.org/10.1111/j.1365-2966.2012.21057.x. arXiv:1201.5888 [astro-ph.CO]

Barausse E, Buonanno A (2010) Improved effective-one-body Hamiltonian for spinning black-hole binaries. Phys Rev D 81:084024. https://doi.org/10.1103/PhysRevD.81.084024. arXiv:0912.3517 [gr-qc]

Barausse E, Buonanno A (2011) Extending the effective-one-body Hamiltonian of black-hole binaries to include next-to-next-to-leading spin-orbit couplings. Phys Rev D 84:104027. https://doi.org/10.1103/PhysRevD.84.104027. arXiv:1107.2904 [gr-qc]

Barausse E, Rezzolla L (2008) The influence of the hydrodynamic drag from an accretion torus on extreme mass-ratio inspirals. Phys Rev D 77:104027. https://doi.org/10.1103/PhysRevD.77.104027. arXiv:0711.4558 [gr-qc]

Barausse E, Rezzolla L (2009) Predicting the direction of the final spin from the coalescence of two black holes. Astrophys J Lett 704:L40–L44. https://doi.org/10.1088/0004-637X/704/1/L40. arXiv:0904.2577 [gr-qc]

Barausse E, Sotiriou TP (2008) Perturbed Kerr black holes can probe deviations from general relativity. Phys Rev Lett 101:099001. https://doi.org/10.1103/PhysRevLett.101.099001. arXiv:0803.3433 [gr-qc]

Barausse E, Yagi K (2015) Gravitation-wave emission in shift-symmetric Horndeski theories. Phys Rev Lett 115(21):211105. https://doi.org/10.1103/PhysRevLett.115.211105. arXiv:1509.04539 [gr-qc]

Barausse E, Rezzolla L, Petroff D, Ansorg M (2007) Gravitational waves from extreme mass ratio inspirals in non-pure Kerr spacetimes. Phys Rev D 75:064026. https://doi.org/10.1103/PhysRevD.75.064026. arXiv:gr-qc/0612123

Barausse E, Racine E, Buonanno A (2009) Hamiltonian of a spinning test-particle in curved spacetime. Phys Rev D 80:104025. [Erratum: Phys. Rev. D 85, 069904 (2012)]. https://doi.org/10.1103/PhysRevD.85.069904. arXiv:0907.4745 [gr-qc]

Barausse E, Buonanno A, Hughes SA, Khanna G, O'Sullivan S, Pan Y (2012) Modeling multipolar gravitational-wave emission from small mass-ratio mergers. Phys Rev D 85:024046. https://doi.org/10.1103/PhysRevD.85.024046. arXiv:1110.3081 [gr-qc]

Barausse E, Buonanno A, Le Tiec A (2012) The complete non-spinning effective-one-body metric at linear order in the mass ratio. Phys Rev D 85:064010. https://doi.org/10.1103/PhysRevD.85.064010. arXiv:1111.5610 [gr-qc]

Barausse E, Cardoso V, Pani P (2014) Can environmental effects spoil precision gravitational-wave astrophysics? Phys Rev D 89(10):104059. https://doi.org/10.1103/PhysRevD.89.104059. arXiv:1404.7149 [gr-qc]

Barausse E, Cardoso V, Pani P (2015) Environmental effects for gravitational-wave astrophysics. J Phys: Conf Ser 610(1):012044. https://doi.org/10.1088/1742-6596/610/1/012044. arXiv:1404.7140 [astro-ph.CO]

Barausse E, Yunes N, Chamberlain K (2016) Theory-agnostic constraints on black-hole dipole radiation with multiband gravitational-wave astrophysics. Phys Rev Lett 116(24):241104. https://doi.org/10.1103/PhysRevLett.116.241104. arXiv:1603.04075 [gr-qc]

Barausse E, Brito R, Cardoso V, Dvorkin I, Pani P (2018) The stochastic gravitational-wave background in the absence of horizons. Class Quantum Grav 35(20):20LT01. https://doi.org/10.1088/1361-6382/aae1de. arXiv:1805.08229 [gr-qc]

Barausse E, Dvorkin I, Tremmel M, Volonteri M, Bonetti M (2020) Massive black hole merger rates: the effect of kiloparsec separation wandering and supernova feedback. Astrophys J 904(1):16. https://doi.org/10.3847/1538-4357/abba7f. arXiv:2006.03065 [astro-ph.GA]

Barausse E, Bezares M, Crisostomi M, Lara G (2022) The well-posedness of the Cauchy problem for self-interacting vector fields. JCAP 11:050. https://doi.org/10.1088/1475-7516/2022/11/050. arXiv:2207.00443 [gr-qc]

Barausse E, Dey K, Crisostomi M, Panayada A, Marsat S, Basak S (2023) Implications of the pulsar timing array detections for massive black hole mergers in the LISA band. Phys Rev D 108(10):103034. https://doi.org/10.1103/PhysRevD.108.103034. arXiv:2307.12245 [astro-ph.GA]

Barausse E et al (2020) Prospects for fundamental physics with LISA. Gen Relativ Gravit 52(8):81. https://doi.org/10.1007/s10714-020-02691-1. arXiv:2001.09793 [gr-qc]

Barceló C, Carballo-Rubio R, Garay LJ (2017) Gravitational wave echoes from macroscopic quantum gravity effects. JHEP 05:054. https://doi.org/10.1007/JHEP05(2017)054. arXiv:1701.09156 [gr-qc]
Barger AJ (2004) Supermassive black holes in the distant universe. Kluwer Academic, Dordrecht. https://doi.org/10.1007/978-1-4020-2471-9
Barker BM, O'Connell RF (1975) Gravitational two-body problem with arbitrary masses, spins, and quadrupole moments. Phys Rev D 12:329–335. https://doi.org/10.1103/PhysRevD.12.329
Barkett K, Chen Y, Scheel MA, Varma V (2020) Gravitational waveforms of binary neutron star inspirals using post-Newtonian tidal splicing. Phys Rev D 102(2):024031. https://doi.org/10.1103/PhysRevD.102.024031. arXiv:1911.10440 [gr-qc]
Barranco J, Bernal A, Degollado JC, Diez-Tejedor A, Megevand M, Alcubierre M, Núñez D, Sarbach O (2014) Schwarzschild scalar wigs: spectral analysis and late time behavior. Phys Rev D 89 (8):083006. https://doi.org/10.1103/PhysRevD.89.083006. arXiv:1312.5808 [gr-qc]
Barrault M, Maday Y, Nguyen NC, Patera AT (2004) An 'empirical interpolation'method: application to efficient reduced-basis discretization of partial differential equations. Comptes Rendus Math 339 (9):667–672. https://doi.org/10.1016/j.crma.2004.08.006
Barsanti S, Franchini N, Gualtieri L, Maselli A, Sotiriou TP (2022) Extreme mass-ratio inspirals as probes of scalar fields: eccentric equatorial orbits around Kerr black holes. Phys Rev D 106(4):044029. https://doi.org/10.1103/PhysRevD.106.044029. arXiv:2203.05003 [gr-qc]
Bartolo N et al (2022) Probing anisotropies of the stochastic gravitational wave background with LISA. JCAP 11:009. https://doi.org/10.1088/1475-7516/2022/11/009. arXiv:2201.08782 [astro-ph.CO]
Baryakhtar M, Lasenby R, Teo M (2017) Black hole superradiance signatures of ultralight vectors. Phys Rev D 96(3):035019. https://doi.org/10.1103/PhysRevD.96.035019. arXiv:1704.05081 [hep-ph]
Basovník M, Semerák O (2016) Geometry of deformed black holes. II. Schwarzschild hole surrounded by a Bach-Weyl ring. Phys Rev D 94(4):044007. https://doi.org/10.1103/PhysRevD.94.044007. arXiv:1608.05961 [gr-qc]
Battye R, Moss A (2010) Updated constraints on the cosmic string tension. Phys Rev D 82:023521. https://doi.org/10.1103/PhysRevD.82.023521. arXiv:1005.0479 [astro-ph.CO]
Battye RA, Caldwell RR, Shellard EPS (1997) Gravitational waves from cosmic strings. In: Conference on Topological Defects and CMB. pp 11–31. arXiv:astro-ph/9706013
Baumann D, McAllister L (2015) Inflation and String Theory. Cambridge Monographs on Mathematical Physics. Cambridge University Press, Cambridge. https://doi.org/10.1017/CBO9781316105733arXiv:1404.2601 [hep-th]
Baumann D, Chia HS, Porto RA (2019) Probing ultralight bosons with binary black holes. Phys Rev D 99 (4):044001. https://doi.org/10.1103/PhysRevD.99.044001. arXiv:1804.03208 [gr-qc]
Baumann D, Chia HS, Stout J, ter Haar L (2019) The spectra of gravitational atoms. JCAP 12:006. https://doi.org/10.1088/1475-7516/2019/12/006. arXiv:1908.10370 [gr-qc]
Baumann D, Chia HS, Porto RA, Stout J (2020) Gravitational collider physics. Phys Rev D 101 (8):083019. https://doi.org/10.1103/PhysRevD.101.083019. arXiv:1912.04932 [gr-qc]
Baumann D, Bertone G, Stout J, Tomaselli GM (2022) Ionization of gravitational atoms. Phys Rev D 105 (11):115036. https://doi.org/10.1103/PhysRevD.105.115036. arXiv:2112.14777 [gr-qc]
Baumann D, Bertone G, Stout J, Tomaselli GM (2022) Sharp signals of boson clouds in black hole binary inspirals. Phys Rev Lett 128(22):221102. https://doi.org/10.1103/PhysRevLett.128.221102. arXiv:2206.01212 [gr-qc]
Baumgarte TW, Shapiro SL (1998) On the numerical integration of Einstein's field equations. Phys Rev D 59:024007. https://doi.org/10.1103/PhysRevD.59.024007. arXiv:gr-qc/9810065
Baumgarte TW, Shapiro SL (2010) Numerical Relativity: Solving Einstein's Equations on the Computer. Cambridge University Press, Cambridge. https://doi.org/10.1017/CBO9781139193344
Bautista YF, Guevara A, Kavanagh C, Vines J (2023) Scattering in black hole backgrounds and higher-spin amplitudes. Part I. JHEP 03:136. https://doi.org/10.1007/JHEP03(2023)136. arXiv:2107.10179 [hep-th]
Becker N, Sagunski L (2023) Comparing accretion disks and dark matter spikes in intermediate mass ratio inspirals. Phys Rev D 107(8):083003. https://doi.org/10.1103/PhysRevD.107.083003. arXiv:2211.05145 [gr-qc]
Begelman MC (2010) Evolution of supermassive stars as a pathway to black hole formation. Mon Not R Astron Soc 402:673. https://doi.org/10.1111/j.1365-2966.2009.15916.x. arXiv:0910.4398 [astro-ph.CO]
Begelman MC, Blandford RD, Rees MJ (1980) Massive black hole binaries in active galactic nuclei. Nature 287:307–309. https://doi.org/10.1038/287307a0

Bekenstein JD (1973) Extraction of energy and charge from a black hole. Phys Rev D 7:949–953. https://doi.org/10.1103/PhysRevD.7.949

Bekenstein JD (1996) Black hole hair: 25 - years after. In: 2nd International Sakharov Conference on Physics. pp 216–219. arXiv:gr-qc/9605059

Belgacem E, Dirian Y, Foffa S, Maggiore M (2018) Gravitational-wave luminosity distance in modified gravity theories. Phys Rev D 97(10):104066. https://doi.org/10.1103/PhysRevD.97.104066. arXiv:1712.08108 [astro-ph.CO]

Belgacem E et al (2019) Testing modified gravity at cosmological distances with LISA standard sirens. JCAP 07:024. https://doi.org/10.1088/1475-7516/2019/07/024. arXiv:1906.01593 [astro-ph.CO]

Bellovary J, Cleary C, Munshi F, Tremmel M, Christensen C, Brooks A, Quinn T (2019) Multimessenger signatures of massive black holes in dwarf galaxies. Mon Not R Astron Soc 482(3):2913–2923. https://doi.org/10.1093/mnras/sty2842. arXiv:1806.00471 [astro-ph.GA]

Bellovary JM, Mac Low MM, McKernan B, Ford K (2016) Migration traps in disks around supermassive black holes. Astrophys J Lett 819(2):L17. https://doi.org/10.3847/2041-8205/819/2/L17. arXiv:1511.00005 [astro-ph.GA]

Bena I, Mayerson DR (2020) Multipole ratios: a new window into black holes. Phys Rev Lett 125 (22):221602. https://doi.org/10.1103/PhysRevLett.125.221602. arXiv:2006.10750 [hep-th]

Bena I, Mayerson DR (2021) Black holes lessons from multipole ratios. JHEP 03:114. https://doi.org/10.1007/JHEP03(2021)114. arXiv:2007.09152 [hep-th]

Bena I, Warner NP (2008) Black holes, black rings and their microstates. Lect Notes Phys 755:1–92. https://doi.org/10.1007/978-3-540-79523-0_1. arXiv:hep-th/0701216

Benkel R, Sotiriou TP, Witek H (2016) Dynamical scalar hair formation around a Schwarzschild black hole. Phys Rev D 94(12):121503. https://doi.org/10.1103/PhysRevD.94.121503. arXiv:1612.08184 [gr-qc]

Benkel R, Sotiriou TP, Witek H (2017) Black hole hair formation in shift-symmetric generalised scalar-tensor gravity. Class Quantum Grav 34(6):064001. https://doi.org/10.1088/1361-6382/aa5ce7. arXiv:1610.09168 [gr-qc]

Bennett CL, Banday A, Gorski KM, Hinshaw G, Jackson P, Keegstra P, Kogut A, Smoot GF, Wilkinson DT, Wright EL (1996) Four year COBE DMR cosmic microwave background observations: maps and basic results. Astrophys J Lett 464:L1–L4. https://doi.org/10.1086/310075. arXiv:astro-ph/9601067

Bennett DP, Bouchet FR (1989) Cosmic string evolution. Phys Rev Lett 63:2776. https://doi.org/10.1103/PhysRevLett.63.2776

Bennett DP, Bouchet FR (1991) Constraints on the gravity wave background generated by cosmic strings. Phys Rev D 43:2733–2735. https://doi.org/10.1103/PhysRevD.43.2733

Berkovits N, D'Hoker E, Green MB, Johansson H, Schlotterer O (2022) Snowmass white paper: string perturbation theory. In: Snowmass 2021. arXiv:2203.09099 [hep-th]

Bern Z, Cheung C, Roiban R, Shen CH, Solon MP, Zeng M (2019) Black hole binary dynamics from the double copy and effective theory. JHEP 10:206. https://doi.org/10.1007/JHEP10(2019)206. arXiv:1908.01493 [hep-th]

Bern Z, Cheung C, Roiban R, Shen CH, Solon MP, Zeng M (2019) Scattering amplitudes and the conservative hamiltonian for binary systems at third post-Minkowskian order. Phys Rev Lett 122 (20):201603. https://doi.org/10.1103/PhysRevLett.122.201603. arXiv:1901.04424 [hep-th]

Bern Z, Luna A, Roiban R, Shen CH, Zeng M (2021) Spinning black hole binary dynamics, scattering amplitudes, and effective field theory. Phys Rev D 104(6):065014. https://doi.org/10.1103/PhysRevD.104.065014. arXiv:2005.03071 [hep-th]

Bern Z, Parra-Martinez J, Roiban R, Ruf MS, Shen CH, Solon MP, Zeng M (2021) Scattering amplitudes and conservative binary dynamics at $\mathcal{O}(G^4)$. Phys Rev Lett 126(17):171601. https://doi.org/10.1103/PhysRevLett.126.171601. arXiv:2101.07254 [hep-th]

Bern Z, Parra-Martinez J, Roiban R, Sawyer E, Shen CH (2021) Leading nonlinear tidal effects and scattering amplitudes. JHEP 05:188. https://doi.org/10.1007/JHEP05(2021)188. arXiv:2010.08559 [hep-th]

Bern Z, Parra-Martinez J, Roiban R, Ruf MS, Shen CH, Solon MP, Zeng M (2022) Scattering amplitudes, the tail effect, and conservative binary dynamics at O(G4). Phys Rev Lett 128(16):161103. https://doi.org/10.1103/PhysRevLett.128.161103. arXiv:2112.10750 [hep-th]

Bernard L (2018) Dynamics of compact binary systems in scalar-tensor theories: Equations of motion to the third post-Newtonian order. Phys Rev D 98(4):044004. https://doi.org/10.1103/PhysRevD.98.044004. arXiv:1802.10201 [gr-qc]

Bernard L (2019) Dynamics of compact binary systems in scalar-tensor theories: II. Center-of-mass and conserved quantities to 3PN order. Phys Rev D 99(4):044047. https://doi.org/10.1103/PhysRevD.99.044047. arXiv:1812.04169 [gr-qc]

Bernard L, Blanchet L, Bohé A, Faye G, Marsat S (2016) Fokker action of nonspinning compact binaries at the fourth post-Newtonian approximation. Phys Rev D 93(8):084037. https://doi.org/10.1103/PhysRevD.93.084037. arXiv:1512.02876 [gr-qc]

Bernard L, Blanchet L, Bohé A, Faye G, Marsat S (2017) Dimensional regularization of the IR divergences in the Fokker action of point-particle binaries at the fourth post-Newtonian order. Phys Rev D 96 (10):104043. https://doi.org/10.1103/PhysRevD.96.104043. arXiv:1706.08480 [gr-qc]

Bernard L, Blanchet L, Bohé A, Faye G, Marsat S (2017) Energy and periastron advance of compact binaries on circular orbits at the fourth post-Newtonian order. Phys Rev D 95(4):044026. https://doi.org/10.1103/PhysRevD.95.044026. arXiv:1610.07934 [gr-qc]

Bernard L, Blanchet L, Faye G, Marchand T (2018) Center-of-Mass equations of motion and conserved integrals of compact binary systems at the fourth Post-Newtonian order. Phys Rev D 97(4):044037. https://doi.org/10.1103/PhysRevD.97.044037. arXiv:1711.00283 [gr-qc]

Bernard L, Cardoso V, Ikeda T, Zilhão M (2019) Physics of black hole binaries: geodesics, relaxation modes, and energy extraction. Phys Rev D 100(4):044002. https://doi.org/10.1103/PhysRevD.100.044002. arXiv:1905.05204 [gr-qc]

Bernard L, Bernard L, Bernard L (2020) Dipolar tidal effects in scalar-tensor theories. Phys Rev D 101 (2):021501. [Erratum: Phys. Rev. D 107, 069901 (2023)]. https://doi.org/10.1103/PhysRevD.101.021501. arXiv:1906.10735 [gr-qc]

Bernard L, Blanchet L, Trestini D (2022) Gravitational waves in scalar-tensor theory to one-and-a-half post-Newtonian order. JCAP 08(08):008. https://doi.org/10.1088/1475-7516/2022/08/008. arXiv:2201.10924 [gr-qc]

Bernardeau F, Uzan JP (2001) Cosmic string lens phenomenology: model of Poisson energy distribution. Phys Rev D 63:023005. https://doi.org/10.1103/PhysRevD.63.023005. arXiv:astro-ph/0004102

Bernuzzi S, Hilditch D (2010) Constraint violation in free evolution schemes: comparing BSSNOK with a conformal decomposition of Z4. Phys Rev D 81:084003. https://doi.org/10.1103/PhysRevD.81.084003. arXiv:0912.2920 [gr-qc]

Bernuzzi S, Nagar A (2010) Binary black hole merger in the extreme-mass-ratio limit: a multipolar analysis. Phys Rev D 81:084056. https://doi.org/10.1103/PhysRevD.81.084056. arXiv:1003.0597 [gr-qc]

Bernuzzi S, Nagar A, Zenginoglu A (2011) Binary black hole coalescence in the extreme-mass-ratio limit: testing and improving the effective-one-body multipolar waveform. Phys Rev D 83:064010. https://doi.org/10.1103/PhysRevD.83.064010. arXiv:1012.2456 [gr-qc]

Bernuzzi S, Nagar A, Zenginoglu A (2011) Binary black hole coalescence in the large-mass-ratio limit: the hyperboloidal layer method and waveforms at null infinity. Phys Rev D 84:084026. https://doi.org/10.1103/PhysRevD.84.084026. arXiv:1107.5402 [gr-qc]

Bernuzzi S, Nagar A, Thierfelder M, Brugmann B (2012) Tidal effects in binary neutron star coalescence. Phys Rev D 86:044030. https://doi.org/10.1103/PhysRevD.86.044030. arXiv:1205.3403 [gr-qc]

Bernuzzi S, Nagar A, Balmelli S, Dietrich T, Ujevic M (2014) Quasiuniversal properties of neutron star mergers. Phys Rev Lett 112:201101. https://doi.org/10.1103/PhysRevLett.112.201101. arXiv:1402.6244 [gr-qc]

Bernuzzi S, Dietrich T, Nagar A (2015) Modeling the complete gravitational wave spectrum of neutron star mergers. Phys Rev Lett 115(9):091101. https://doi.org/10.1103/PhysRevLett.115.091101. arXiv:1504.01764 [gr-qc]

Bernuzzi S, Nagar A, Dietrich T, Damour T (2015) Modeling the dynamics of tidally interacting binary neutron stars up to the merger. Phys Rev Lett 114(16):161103. https://doi.org/10.1103/PhysRevLett.114.161103. arXiv:1412.4553 [gr-qc]

Berry C, Gair JR (2013) Expectations for extreme-mass-ratio bursts from the Galactic Centre. Mon Not R Astron Soc 435:3521–3540. https://doi.org/10.1093/mnras/stt1543. arXiv:1307.7276 [astro-ph.HE]

Berry C, Gair JR (2013) Extreme-mass-ratio-bursts from extragalactic sources. Mon Not R Astron Soc 433:3572–3583. https://doi.org/10.1093/mnras/stt990. arXiv:1306.0774 [astro-ph.HE]

Berry C, Cole RH, Cañizares P, Gair JR (2016) Importance of transient resonances in extreme-mass-ratio inspirals. Phys Rev D 94(12):124042. https://doi.org/10.1103/PhysRevD.94.124042. arXiv:1608.08951 [gr-qc]

Berti E (2024) Emanuele Berti's ri2024wn web page. https://pages.jh.edu/eberti2/ri2024wn/

Berti E, Cardoso V (2006) Quasinormal ringing of Kerr black holes. I. The Excitation factors. Phys Rev D 74:104020. https://doi.org/10.1103/PhysRevD.74.104020. arXiv:gr-qc/0605118

Berti E, Cardoso V (2006) Supermassive black holes or boson stars? Hair counting with gravitational wave detectors. Int J Mod Phys D 15:2209–2216. https://doi.org/10.1142/S0218271806009637. arXiv:gr-qc/0605101

Berti E, Volonteri M (2008) Cosmological black hole spin evolution by mergers and accretion. Astrophys J 684:822–828. https://doi.org/10.1086/590379. arXiv:0802.0025 [astro-ph]

Berti E, Cardoso V, Will CM (2006) On gravitational-wave spectroscopy of massive black holes with the space interferometer LISA. Phys Rev D 73:064030. https://doi.org/10.1103/PhysRevD.73.064030. arXiv:gr-qc/0512160

Berti E, Cardoso J, Cardoso V, Cavaglia M (2007) Matched-filtering and parameter estimation of ringdown waveforms. Phys Rev D 76:104044. https://doi.org/10.1103/PhysRevD.76.104044. arXiv:0707.1202 [gr-qc]

Berti E, Cardoso V, Gonzalez JA, Sperhake U, Hannam M, Husa S, Brügmann B (2007) Inspiral, merger and ringdown of unequal mass black hole binaries: a multipolar analysis. Phys Rev D 76:064034. https://doi.org/10.1103/PhysRevD.76.064034. arXiv:gr-qc/0703053

Berti E, Cardoso V, Starinets AO (2009) Quasinormal modes of black holes and black branes. Class Quantum Grav 26:163001. https://doi.org/10.1088/0264-9381/26/16/163001. arXiv:0905.2975 [gr-qc]

Berti E, Cardoso V, Gualtieri L, Horbatsch M, Sperhake U (2013) Numerical simulations of single and binary black holes in scalar-tensor theories: circumventing the no-hair theorem. Phys Rev D 87 (12):124020. https://doi.org/10.1103/PhysRevD.87.124020. arXiv:1304.2836 [gr-qc]

Berti E, Sesana A, Barausse E, Cardoso V, Belczynski K (2016) Spectroscopy of Kerr black holes with Earth- and space-based interferometers. Phys Rev Lett 117(10):101102. https://doi.org/10.1103/PhysRevLett.117.101102. arXiv:1605.09286 [gr-qc]

Berti E, Yagi K, Yang H, Yunes N (2018) Extreme gravity tests with gravitational waves from compact binary coalescences: (II) ringdown. Gen Relativ Gravit 50(5):49. https://doi.org/10.1007/s10714-018-2372-6. arXiv:1801.03587 [gr-qc]

Berti E, Brito R, Macedo C, Raposo G, Rosa JL (2019) Ultralight boson cloud depletion in binary systems. Phys Rev D 99(10):104039. https://doi.org/10.1103/PhysRevD.99.104039. arXiv:1904.03131 [gr-qc]

Berti E, Collodel LG, Kleihaus B, Kunz J (2021) Spin-induced black-hole scalarization in Einstein-scalar-Gauss-Bonnet theory. Phys Rev Lett 126(1):011104. https://doi.org/10.1103/PhysRevLett.126.011104. arXiv:2009.03905 [gr-qc]

Berti E et al (2015) Testing general relativity with present and future astrophysical observations. Class Quantum Grav 32:243001. https://doi.org/10.1088/0264-9381/32/24/243001. arXiv:1501.07274 [gr-qc]

Bertone G et al (2020) Gravitational wave probes of dark matter: challenges and opportunities. SciPost Phys Core 3:007. https://doi.org/10.21468/SciPostPhysCore.3.2.007. arXiv:1907.10610 [astro-ph.CO]

Bevis N, Hindmarsh M, Kunz M, Urrestilla J (2007) CMB polarization power spectra contributions from a network of cosmic strings. Phys Rev D 76:043005. https://doi.org/10.1103/PhysRevD.76.043005. arXiv:0704.3800 [astro-ph]

Bezares M, Palenzuela C (2018) Gravitational Waves from Dark Boson Star binary mergers. Class Quantum Grav 35(23):234002. https://doi.org/10.1088/1361-6382/aae87c. arXiv:1808.10732 [gr-qc]

Bezares M, Palenzuela C, Bona C (2017) Final fate of compact boson star mergers. Phys Rev D 95 (12):124005. https://doi.org/10.1103/PhysRevD.95.124005. arXiv:1705.01071 [gr-qc]

Bezares M, Viganò D, Palenzuela C (2019) Gravitational wave signatures of dark matter cores in binary neutron star mergers by using numerical simulations. Phys Rev D 100(4):044049. https://doi.org/10.1103/PhysRevD.100.044049. arXiv:1905.08551 [gr-qc]

Bezares M, Crisostomi M, Palenzuela C, Barausse E (2021) K-dynamics: well-posed 1+1 evolutions in K-essence. JCAP 03:072. https://doi.org/10.1088/1475-7516/2021/03/072. arXiv:2008.07546 [gr-qc]

Bezares M, ter Haar L, Crisostomi M, Barausse E, Palenzuela C (2021) Kinetic screening in nonlinear stellar oscillations and gravitational collapse. Phys Rev D 104(4):044022. https://doi.org/10.1103/PhysRevD.104.044022. arXiv:2105.13992 [gr-qc]

Bezares M, Aguilera-Miret R, ter Haar L, Crisostomi M, Palenzuela C, Barausse E (2022) No evidence of kinetic screening in simulations of merging binary neutron stars beyond general relativity. Phys Rev Lett 128(9):091103. https://doi.org/10.1103/PhysRevLett.128.091103. arXiv:2107.05648 [gr-qc]

Bezares M, Bošković M, Liebling S, Palenzuela C, Pani P, Barausse E (2022) Gravitational waves and kicks from the merger of unequal mass, highly compact boson stars. Phys Rev D 105(6):064067. https://doi.org/10.1103/PhysRevD.105.064067. arXiv:2201.06113 [gr-qc]

Bhagwat S, Forteza XJ, Pani P, Ferrari V (2020) Ringdown overtones, black hole spectroscopy, and no-hair theorem tests. Phys Rev D 101(4):044033. https://doi.org/10.1103/PhysRevD.101.044033. arXiv:1910.08708 [gr-qc]

Bhagwat S, Pacilio C, Barausse E, Pani P (2022) Landscape of massive black-hole spectroscopy with LISA and the Einstein Telescope. Phys Rev D 105(12):124063. https://doi.org/10.1103/PhysRevD.105.124063. arXiv:2201.00023 [gr-qc]

Bhattacharjee P, Hill CT, Schramm DN (1992) Grand unified theories, topological defects and ultrahigh-energy cosmic rays. Phys Rev Lett 69:567–570. https://doi.org/10.1103/PhysRevLett.69.567

Bhattacharyya MK, Hilditch D, Rajesh Nayak K, Renkhoff S, Rüter HR, Brügmann B (2021) Implementation of the dual foliation generalized harmonic gauge formulation with application to spherical black hole excision. Phys Rev D 103(6):064072. https://doi.org/10.1103/PhysRevD.103.064072. arXiv:2101.12094 [gr-qc]

BH@Home (2024) BH@Home. https://blackholesathome.net/

BHPClub (2024) Black Hole Perturbation Club. (https://sites.google.com/view/bhpc1996/home)

BHPToolkit (2024) Black Hole Perturbation Toolkit. http://bhptoolkit.org/

Bianchi M, Consoli D, Grillo A, Morales JF, Pani P, Raposo G (2020) Distinguishing fuzzballs from black holes through their multipolar structure. Phys Rev Lett 125(22):221601. https://doi.org/10.1103/PhysRevLett.125.221601. arXiv:2007.01743 [hep-th]

Bianchi M, Consoli D, Grillo A, Morales JF, Pani P, Raposo G (2021) The multipolar structure of fuzzballs. JHEP 01:003. https://doi.org/10.1007/JHEP01(2021)003. arXiv:2008.01445 [hep-th]

Bildsten L, Cutler C (1992) Tidal interactions of inspiraling compact binaries. Astrophys J 400:175–180. https://doi.org/10.1086/171983

Binetruy P, Bohe A, Hertog T, Steer DA (2009) Gravitational wave bursts from cosmic superstrings with Y-junctions. Phys Rev D 80:123510. https://doi.org/10.1103/PhysRevD.80.123510. arXiv:0907.4522 [hep-th]

Binetruy P, Bohe A, Hertog T, Steer DA (2010) Gravitational wave signatures from kink proliferation on cosmic (super-) strings. Phys Rev D 82:126007. https://doi.org/10.1103/PhysRevD.82.126007. arXiv:1009.2484 [hep-th]

Binetruy P, Bohe A, Hertog T, Steer DA (2010) Proliferation of sharp kinks on cosmic (super-)string loops with junctions. Phys Rev D 82:083524. https://doi.org/10.1103/PhysRevD.82.083524. arXiv:1005.2426 [hep-th]

Binetruy P, Bohe A, Caprini C, Dufaux JF (2012) Cosmological backgrounds of gravitational waves and eLISA/NGO: phase transitions, cosmic strings and other sources. JCAP 06:027. https://doi.org/10.1088/1475-7516/2012/06/027. arXiv:1201.0983 [gr-qc]

Binev P, Cohen A, Dahmen W, DeVore RA, Petrova G, Wojtaszczyk P (2011) Convergence rates for greedy algorithms in reduced basis methods. SIAM J Math Analysis 43(3):1457. https://doi.org/10.1137/100795772

Bini D, Damour T (2012) Gravitational radiation reaction along general orbits in the effective one-body formalism. Phys Rev D 86:124012. https://doi.org/10.1103/PhysRevD.86.124012. arXiv:1210.2834 [gr-qc]

Bini D, Damour T (2014) Analytic determination of the eight-and-a-half post-Newtonian self-force contributions to the two-body gravitational interaction potential. Phys Rev D 89(10):104047. https://doi.org/10.1103/PhysRevD.89.104047. arXiv:1403.2366 [gr-qc]

Bini D, Damour T (2014) Gravitational self-force corrections to two-body tidal interactions and the effective one-body formalism. Phys Rev D 90(12):124037. https://doi.org/10.1103/PhysRevD.90.124037. arXiv:1409.6933 [gr-qc]

Bini D, Damour T (2016) Conservative second-order gravitational self-force on circular orbits and the effective one-body formalism. Phys Rev D 93(10):104040. https://doi.org/10.1103/PhysRevD.93.104040. arXiv:1603.09175 [gr-qc]

Bini D, Damour T (2017) Gravitational spin-orbit coupling in binary systems, post-Minkowskian approximation and effective one-body theory. Phys Rev D 96(10):104038. https://doi.org/10.1103/PhysRevD.96.104038. arXiv:1709.00590 [gr-qc]

Bini D, Damour T (2018) Gravitational spin-orbit coupling in binary systems at the second post-Minkowskian approximation. Phys Rev D 98(4):044036. https://doi.org/10.1103/PhysRevD.98.044036. arXiv:1805.10809 [gr-qc]
Bini D, Geralico A (2015) Tidal invariants along the worldline of an extended body in Kerr spacetime. Phys Rev D 91(8):084012. https://doi.org/10.1103/PhysRevD.91.084012. arXiv:1806.07696 [gr-qc]
Bini D, Geralico A (2019) Analytical determination of the periastron advance in spinning binaries from self-force computations. Phys Rev D 100(12):121502. https://doi.org/10.1103/PhysRevD.100.121502. arXiv:1907.11083 [gr-qc]
Bini D, Geralico A (2019) New gravitational self-force analytical results for eccentric equatorial orbits around a Kerr black hole: gyroscope precession. Phys Rev D 100(10):104003. https://doi.org/10.1103/PhysRevD.100.104003. arXiv:1907.11082 [gr-qc]
Bini D, Geralico A (2019) New gravitational self-force analytical results for eccentric equatorial orbits around a Kerr black hole: redshift invariant. Phys Rev D 100(10):104002. https://doi.org/10.1103/PhysRevD.100.104002. arXiv:1907.11080 [gr-qc]
Bini D, Geralico A (2021) Frequency domain analysis of the gravitational wave energy loss in hyperbolic encounters. Phys Rev D 104(10):104019. https://doi.org/10.1103/PhysRevD.104.104019. arXiv:2108.02472 [gr-qc]
Bini D, Geralico A (2021) Higher-order tail contributions to the energy and angular momentum fluxes in a two-body scattering process. Phys Rev D 104(10):104020. https://doi.org/10.1103/PhysRevD.104.104020. arXiv:2108.05445 [gr-qc]
Bini D, Geralico A (2022) Momentum recoil in the relativistic two-body problem: higher-order tails. Phys Rev D 105(8):084028. https://doi.org/10.1103/PhysRevD.105.084028. arXiv:2202.03037 [gr-qc]
Bini D, Geralico A (2022) Multipolar invariants and the eccentricity enhancement function parametrization of gravitational radiation. Phys Rev D 105(12):124001. https://doi.org/10.1103/PhysRevD.105.124001. arXiv:2204.08077 [gr-qc]
Bini D, Damour T, Faye G (2012) Effective action approach to higher-order relativistic tidal interactions in binary systems and their effective one body description. Phys Rev D 85:124034. https://doi.org/10.1103/PhysRevD.85.124034. arXiv:1202.3565 [gr-qc]
Bini D, Damour T, Geralico A (2015) Spin-dependent two-body interactions from gravitational self-force computations. Phys Rev D 92(12):124058. [Erratum: Phys. Rev. D 93, 109902 (2016)]. https://doi.org/10.1103/PhysRevD.92.124058. arXiv:1510.06230 [gr-qc]
Bini D, Damour T, Geralico A (2016) Confirming and improving post-Newtonian and effective-one-body results from self-force computations along eccentric orbits around a Schwarzschild black hole. Phys Rev D 93(6):064023. https://doi.org/10.1103/PhysRevD.93.064023. arXiv:1511.04533 [gr-qc]
Bini D, Damour T, Geralico A (2016) New gravitational self-force analytical results for eccentric orbits around a Schwarzschild black hole. Phys Rev D 93(10):104017. https://doi.org/10.1103/PhysRevD.93.104017. arXiv:1601.02988 [gr-qc]
Bini D, Damour T, Geralico A, Kavanagh C (2018) Detweiler's redshift invariant for spinning particles along circular orbits on a Schwarzschild background. Phys Rev D 97(10):104022. https://doi.org/10.1103/PhysRevD.97.104022. arXiv:1801.09616 [gr-qc]
Bini D, Damour T, Geralico A, Kavanagh C, van de Meent M (2018) Gravitational self-force corrections to gyroscope precession along circular orbits in the Kerr spacetime. Phys Rev D 98(10):104062. https://doi.org/10.1103/PhysRevD.98.104062. arXiv:1809.02516 [gr-qc]
Bini D, Damour T, Geralico A (2019) Novel approach to binary dynamics: application to the fifth post-Newtonian level. Phys Rev Lett 123(23):231104. https://doi.org/10.1103/PhysRevLett.123.231104. arXiv:1909.02375 [gr-qc]
Bini D, Damour T, Geralico A (2020) Binary dynamics at the fifth and fifth-and-a-half post-Newtonian orders. Phys Rev D 102(2):024062. https://doi.org/10.1103/PhysRevD.102.024062. arXiv:2003.11891 [gr-qc]
Bini D, Damour T, Geralico A (2020) Scattering of tidally interacting bodies in post-Minkowskian gravity. Phys Rev D 101(4):044039. https://doi.org/10.1103/PhysRevD.101.044039. arXiv:2001.00352 [gr-qc]
Bini D, Damour T, Geralico A (2020) Sixth post-Newtonian local-in-time dynamics of binary systems. Phys Rev D 102(2):024061. https://doi.org/10.1103/PhysRevD.102.024061. arXiv:2004.05407 [gr-qc]
Bini D, Damour T, Geralico A (2020) Sixth post-Newtonian nonlocal-in-time dynamics of binary systems. Phys Rev D 102(8):084047. https://doi.org/10.1103/PhysRevD.102.084047. arXiv:2007.11239 [gr-qc]

Bini D, Damour T, Geralico A, Laporta S, Mastrolia P (2020e) Gravitational dynamics at $O(G^6)$: perturbative gravitational scattering meets experimental mathematics. arXiv e-prints arXiv:2008.09389 [gr-qc]
Bini D, Damour T, Geralico A (2021) Radiative contributions to gravitational scattering. Phys Rev D 104 (8):084031. https://doi.org/10.1103/PhysRevD.104.084031. arXiv:2107.08896 [gr-qc]
Bini D, Damour T, Geralico A (2023) Radiated momentum and radiation reaction in gravitational two-body scattering including time-asymmetric effects. Phys Rev D 107(2):024012. https://doi.org/10.1103/PhysRevD.107.024012. arXiv:2210.07165 [gr-qc]
Binnington T, Poisson E (2009) Relativistic theory of tidal Love numbers. Phys Rev D 80:084018. https://doi.org/10.1103/PhysRevD.80.084018. arXiv:0906.1366 [gr-qc]
Biscoveanu S, Kremer K, Thrane E (2023) Probing the efficiency of tidal synchronization in outspiralling double white dwarf binaries with LISA. Astrophys J 949(2):95. https://doi.org/10.3847/1538-4357/acc585. arXiv:2206.15390 [astro-ph.HE]
Bishop NT, Rezzolla L (2016) Extraction of gravitational waves in numerical relativity. Living Rev Relativ 19:2. https://doi.org/10.1007/s41114-016-0001-9. arXiv:1606.02532 [gr-qc]
Bishop NT, Gomez R, Lehner L, Winicour J (1996) Cauchy-characteristic extraction in numerical relativity. Phys Rev D 54:6153–6165. https://doi.org/10.1103/PhysRevD.54.6153. arXiv:gr-qc/9705033
Bjerrum-Bohr N, Damgaard PH, Festuccia G, Planté L, Vanhove P (2018) General relativity from scattering amplitudes. Phys Rev Lett 121(17):171601. https://doi.org/10.1103/PhysRevLett.121.171601. arXiv:1806.04920 [hep-th]
Bjerrum-Bohr N, Cristofoli A, Damgaard PH (2020) Post-Minkowskian scattering angle in Einstein gravity. JHEP 08:038. https://doi.org/10.1007/JHEP08(2020)038. arXiv:1910.09366 [hep-th]
Bjerrum-Bohr N, Damgaard PH, Planté L, Vanhove P (2021) The amplitude for classical gravitational scattering at third Post-Minkowskian order. JHEP 08:172. https://doi.org/10.1007/JHEP08(2021)172. arXiv:2105.05218 [hep-th]
Blackman J, Szilagyi B, Galley CR, Tiglio M (2014) Sparse representations of gravitational waves from precessing compact binaries. Phys Rev Lett 113(2):021101. https://doi.org/10.1103/PhysRevLett.113.021101. arXiv:1401.7038 [gr-qc]
Blackman J, Field SE, Galley CR, Szilágyi B, Scheel MA, Tiglio M, Hemberger DA (2015) Fast and accurate prediction of numerical relativity waveforms from binary black hole coalescences using surrogate models. Phys Rev Lett 115(12):121102. https://doi.org/10.1103/PhysRevLett.115.121102. arXiv:1502.07758 [gr-qc]
Blackman J, Field SE, Scheel MA, Galley CR, Hemberger DA, Schmidt P, Smith R (2017) A surrogate model of gravitational waveforms from numerical relativity simulations of precessing binary black hole mergers. Phys Rev D 95(10):104023. https://doi.org/10.1103/PhysRevD.95.104023. arXiv:1701.00550 [gr-qc]
Blackman J, Field SE, Scheel MA, Galley CR, Ott CD, Boyle M, Kidder LE, Pfeiffer HP, Szilágyi B (2017) Numerical relativity waveform surrogate model for generically precessing binary black hole mergers. Phys Rev D 96(2):024058. https://doi.org/10.1103/PhysRevD.96.024058. arXiv:1705.07089 [gr-qc]
Blanchet L (1998) On the multipole expansion of the gravitational field. Class Quantum Grav 15:1971–1999. https://doi.org/10.1088/0264-9381/15/7/013. arXiv:gr-qc/9801101
Blanchet L (2002) Innermost circular orbit of binary black holes at the third post-Newtonian approximation. Phys Rev D 65:124009. https://doi.org/10.1103/PhysRevD.65.124009. arXiv:gr-qc/0112056
Blanchet L (2011) Post-Newtonian theory and the two-body problem. Fundam Theor Phys 162:125–166. https://doi.org/10.1007/978-90-481-3015-3_5. arXiv:0907.3596 [gr-qc]
Blanchet L (2024) Post-Newtonian theory for gravitational waves. Living Rev Relativ 27:4. https://doi.org/10.1007/s41114-024-00050-z. arXiv:1310.1528 [gr-qc]
Blanchet L, Le Tiec A (2017) First law of compact binary mechanics with gravitational-wave tails. Class Quantum Grav 34(16):164001. https://doi.org/10.1088/1361-6382/aa79d7. arXiv:1702.06839 [gr-qc]
Blanchet L, Buonanno A, Faye G (2006) Higher-order spin effects in the dynamics of compact binaries. II. Radiation field. Phys Rev D 74:104034. [Erratum: Phys. Rev. D 75, 049903 (2007), Erratum: Phys. Rev. D 81, 089901 (2010)]. https://doi.org/10.1103/PhysRevD.81.089901. arXiv:gr-qc/0605140
Blanchet L, Faye G, Iyer BR, Sinha S (2008) The Third post-Newtonian gravitational wave polarisations and associated spherical harmonic modes for inspiralling compact binaries in quasi-circular orbits.

Class Quantum Grav 25:165003. [Erratum: Class. Quant. Grav. 29, 239501 (2012)]. https://doi.org/10.1088/0264-9381/25/16/165003. arXiv:0802.1249 [gr-qc]
Blanchet L, Buonanno A, Faye G (2011) Tail-induced spin-orbit effect in the gravitational radiation of compact binaries. Phys Rev D 84:064041. https://doi.org/10.1103/PhysRevD.84.064041. arXiv:1104.5659 [gr-qc]
Blanchet L, Buonanno A, Le Tiec A (2013) First law of mechanics for black hole binaries with spins. Phys Rev D 87(2):024030. https://doi.org/10.1103/PhysRevD.87.024030. arXiv:1211.1060 [gr-qc]
Blanchet L, Foffa S, Larrouturou F, Sturani R (2020) Logarithmic tail contributions to the energy function of circular compact binaries. Phys Rev D 101(8):084045. https://doi.org/10.1103/PhysRevD.101.084045. arXiv:1912.12359 [gr-qc]
Blanchet L, Compère G, Faye G, Oliveri R, Seraj A (2021) Multipole expansion of gravitational waves: from harmonic to Bondi coordinates. JHEP 02:029. https://doi.org/10.1007/JHEP02(2021)029. arXiv:2011.10000 [gr-qc]
Blanchet L, Faye G, Larrouturou F (2022) The quadrupole moment of compact binaries to the fourth post-Newtonian order: from source to canonical moment. Class Quantum Grav 39(19):195003. https://doi.org/10.1088/1361-6382/ac840c. arXiv:2204.11293 [gr-qc]
Blanchet L, Compère G, Faye G, Oliveri R, Seraj A (2023) Multipole expansion of gravitational waves: memory effects and Bondi aspects. JHEP 07:123. https://doi.org/10.1007/JHEP07(2023)123. arXiv:2303.07732 [gr-qc]
Blanchet L, Faye G, Henry Q, Larrouturou F, Trestini D (2023) Gravitational-wave flux and quadrupole modes from quasicircular nonspinning compact binaries to the fourth post-Newtonian order. Phys Rev D 108(6):064041. https://doi.org/10.1103/PhysRevD.108.064041. arXiv:2304.11186 [gr-qc]
Blanchet L, Faye G, Henry Q, Larrouturou F, Trestini D (2023) Gravitational-wave phasing of quasicircular compact binary systems to the fourth-and-a-half post-newtonian order. Phys Rev Lett 131(12):121402. https://doi.org/10.1103/PhysRevLett.131.121402. arXiv:2304.11185 [gr-qc]
Blanco-Pillado JJ, Olum KD (1999) Form of cosmic string cusps. Phys Rev D 59:063508. [Erratum: Phys. Rev. D 103, 029902 (2021)]. https://doi.org/10.1103/PhysRevD.59.063508. arXiv:gr-qc/9810005
Blanco-Pillado JJ, Olum KD (2017) Stochastic gravitational wave background from smoothed cosmic string loops. Phys Rev D 96(10):104046. https://doi.org/10.1103/PhysRevD.96.104046. arXiv:1709.02693 [astro-ph.CO]
Blanco-Pillado JJ, Olum KD, Shlaer B (2014) The number of cosmic string loops. Phys Rev D 89(2):023512. https://doi.org/10.1103/PhysRevD.89.023512. arXiv:1309.6637 [astro-ph.CO]
Blanco-Pillado JJ, Olum KD, Siemens X (2018) New limits on cosmic strings from gravitational wave observation. Phys Lett B 778:392–396. https://doi.org/10.1016/j.physletb.2018.01.050. arXiv:1709.02434 [astro-ph.CO]
Blanco-Pillado JJ, Olum KD, Wachter JM (2018) Gravitational backreaction near cosmic string kinks and cusps. Phys Rev D 98(12):123507. https://doi.org/10.1103/PhysRevD.98.123507. arXiv:1808.08254 [gr-qc]
Blanco-Pillado JJ, Olum KD, Wachter JM (2019) Gravitational backreaction simulations of simple cosmic string loops. Phys Rev D 100(2):023535. https://doi.org/10.1103/PhysRevD.100.023535. arXiv:1903.06079 [gr-qc]
Blázquez-Salcedo JL, Macedo C, Cardoso V, Ferrari V, Gualtieri L, Khoo FS, Kunz J, Pani P (2016) Perturbed black holes in Einstein-dilaton-Gauss-Bonnet gravity: Stability, ringdown, and gravitational-wave emission. Phys Rev D 94(10):104024. https://doi.org/10.1103/PhysRevD.94.104024. arXiv:1609.01286 [gr-qc]
Blome HJ, Mashhoon B (1981) Quasi-normal oscillations of a schwarzschild black hole. Phys Lett A 100(5):231–234. https://doi.org/10.1016/0375-9601(84)90769-2
Blümlein J, Maier A, Marquard P, Schäfer G (2020) Fourth post-Newtonian Hamiltonian dynamics of two-body systems from an effective field theory approach. Nucl Phys B 955:115041. https://doi.org/10.1016/j.nuclphysb.2020.115041. arXiv:2003.01692 [gr-qc]
Blümlein J, Maier A, Marquard P, Schäfer G (2020) Testing binary dynamics in gravity at the sixth post-Newtonian level. Phys Lett B 807:135496. https://doi.org/10.1016/j.physletb.2020.135496. arXiv:2003.07145 [gr-qc]
Bode T, Haas R, Bogdanovic T, Laguna P, Shoemaker D (2010) Relativistic mergers of supermassive black holes and their electromagnetic signatures. Astrophys J 715:1117–1131. https://doi.org/10.1088/0004-637X/715/2/1117. arXiv:0912.0087 [gr-qc]

Boersma OM, Nichols DA, Schmidt P (2020) Forecasts for detecting the gravitational-wave memory effect with Advanced LIGO and Virgo. Phys Rev D 101(8):083026. https://doi.org/10.1103/PhysRevD.101.083026. arXiv:2002.01821 [astro-ph.HE]

Boetzel Y, Mishra CK, Faye G, Gopakumar A, Iyer BR (2019) Gravitational-wave amplitudes for compact binaries in eccentric orbits at the third post-Newtonian order: tail contributions and postadiabatic corrections. Phys Rev D 100(4):044018. https://doi.org/10.1103/PhysRevD.100.044018. arXiv:1904.11814 [gr-qc]

Bohé A, Marsat S, Blanchet L (2013) Next-to-next-to-leading order spin-orbit effects in the gravitational wave flux and orbital phasing of compact binaries. Class Quantum Grav 30:135009. https://doi.org/10.1088/0264-9381/30/13/135009. arXiv:1303.7412 [gr-qc]

Bohe A, Marsat S, Faye G, Blanchet L (2013) Next-to-next-to-leading order spin-orbit effects in the near-zone metric and precession equations of compact binaries. Class Quantum Grav 30:075017. https://doi.org/10.1088/0264-9381/30/7/075017. arXiv:1212.5520 [gr-qc]

Bohé A, Faye G, Marsat S, Porter EK (2015) Quadratic-in-spin effects in the orbital dynamics and gravitational-wave energy flux of compact binaries at the 3PN order. Class Quantum Grav 32 (19):195010. https://doi.org/10.1088/0264-9381/32/19/195010. arXiv:1501.01529 [gr-qc]

Bohé A, Hannam M, Husa S, Ohme F, Puerrer M, Schmidt P (2016) Phenompv2 - technical notes for lal implementation. Tech. Rep. LIGO-T1500602, LIGO Project. https://dcc.ligo.org/T1500602/public

Bohé A et al (2017) Improved effective-one-body model of spinning, nonprecessing binary black holes for the era of gravitational-wave astrophysics with advanced detectors. Phys Rev D 95(4):044028. https://doi.org/10.1103/PhysRevD.95.044028. arXiv:1611.03703 [gr-qc]

Bona C, Ledvinka T, Palenzuela C, Zacek M (2003) General covariant evolution formalism for numerical relativity. Phys Rev D 67:104005. https://doi.org/10.1103/PhysRevD.67.104005. arXiv:gr-qc/0302083

Bona C, Palenzuela-Luque C, Bona-Casas C (2009) Elements of Numerical Relativity and Relativistic Hydrodynamics, Lecture Notes in Physics, vol 783. Springer, Berlin, Heidelberg. https://doi.org/10.1007/978-3-642-01164-1

Bonetti M, Haardt F, Sesana A, Barausse E (2016) Post-Newtonian evolution of massive black hole triplets in galactic nuclei - I. Numerical implementation and tests. Mon Not R Astron Soc 461(4):4419–4434. https://doi.org/10.1093/mnras/stw1590. arXiv:1604.08770 [astro-ph.GA]

Bonetti M, Barausse E, Faye G, Haardt F, Sesana A (2017) About gravitational-wave generation by a three-body system. Class Quantum Grav 34(21):215004. https://doi.org/10.1088/1361-6382/aa8da5. arXiv:1707.04902 [gr-qc]

Bonetti M, Sesana A, Haardt F, Barausse E, Colpi M (2019) Post-Newtonian evolution of massive black hole triplets in galactic nuclei - IV. Implications for LISA. Mon Not R Astron Soc 486(3):4044–4060. https://doi.org/10.1093/mnras/stz903. arXiv:1812.01011 [astro-ph.GA]

Bonga B, Yang H, Hughes SA (2019) Tidal resonance in extreme mass-ratio inspirals. Phys Rev Lett 123 (10):101103. https://doi.org/10.1103/PhysRevLett.123.101103. arXiv:1905.00030 [gr-qc]

Bonilla A, D'Agostino R, Nunes RC, de Araujo J (2020) Forecasts on the speed of gravitational waves at high z. JCAP 03:015. https://doi.org/10.1088/1475-7516/2020/03/015. arXiv:1910.05631 [gr-qc]

Bonino A, Gamba R, Schmidt P, Nagar A, Pratten G, Breschi M, Rettegno P, Bernuzzi S (2023) Inferring eccentricity evolution from observations of coalescing binary black holes. Phys Rev D 107 (6):064024. https://doi.org/10.1103/PhysRevD.107.064024. arXiv:2207.10474 [gr-qc]

Bortolas E, Capelo PR, Zana T, Mayer L, Bonetti M, Dotti M, Davies MB, Madau P (2020) Global torques and stochasticity as the drivers of massive black hole pairing in the young Universe. Mon Not R Astron Soc 498(3):3601–3615. https://doi.org/10.1093/mnras/staa2628. arXiv:2005.02409 [astro-ph.GA]

Bouchet FR, Bennett DP (1990) Does the millisecond pulsar constrain cosmic strings? Phys Rev D 41:720–723. https://doi.org/10.1103/PhysRevD.41.720

Bouffanais Y, Porter EK (2016) Detecting compact galactic binaries using a hybrid swarm-based algorithm. Phys Rev D 93(6):064020. https://doi.org/10.1103/PhysRevD.93.064020. arXiv:1509.08867 [gr-qc]

Bowen JM, York JW Jr (1980) Time asymmetric initial data for black holes and black hole collisions. Phys Rev D 21:2047–2056. https://doi.org/10.1103/PhysRevD.21.2047

Bowers RL, Liang E (1974) Anisotropic spheres in general relativity. Astrophys J 188:657–665. https://doi.org/10.1086/152760

Boyle M, Mroue AH (2009) Extrapolating gravitational-wave data from numerical simulations. Phys Rev D 80:124045. https://doi.org/10.1103/PhysRevD.80.124045. arXiv:0905.3177 [gr-qc]

Boyle M, Brown DA, Kidder LE, Mroue AH, Pfeiffer HP, Scheel MA, Cook GB, Teukolsky SA (2007) High-accuracy comparison of numerical relativity simulations with post-Newtonian expansions. Phys Rev D 76:124038. https://doi.org/10.1103/PhysRevD.76.124038. arXiv:0710.0158 [gr-qc]

Boyle M, Buonanno A, Kidder LE, Mroue AH, Pan Y, Pfeiffer HP, Scheel MA (2008) High-accuracy numerical simulation of black-hole binaries: computation of the gravitational-wave energy flux and comparisons with post-Newtonian approximants. Phys Rev D 78:104020. https://doi.org/10.1103/PhysRevD.78.104020. arXiv:0804.4184 [gr-qc]

Boyle M et al (2019) The SXS Collaboration catalog of binary black hole simulations. Class Quantum Grav 36(19):195006. https://doi.org/10.1088/1361-6382/ab34e2. arXiv:1904.04831 [gr-qc]

Bozzola G, Paschalidis V (2019) Initial data for general relativistic simulations of multiple electrically charged black holes with linear and angular momenta. Phys Rev D 99(10):104044. https://doi.org/10.1103/PhysRevD.99.104044. arXiv:1903.01036 [gr-qc]

Bozzola G, Paschalidis V (2021) General relativistic simulations of the quasicircular inspiral and merger of charged black holes: GW150914 and fundamental physics implications. Phys Rev Lett 126 (4):041103. https://doi.org/10.1103/PhysRevLett.126.041103. arXiv:2006.15764 [gr-qc]

Brandenberger RH (1987) On the decay of cosmic string loops. Nucl Phys B 293:812–828. https://doi.org/10.1016/0550-3213(87)90092-7

Brandhuber A, Chen G, Travaglini G, Wen C (2021) Classical gravitational scattering from a gauge-invariant double copy. JHEP 10:118. https://doi.org/10.1007/JHEP10(2021)118. arXiv:2108.04216 [hep-th]

Brandt S, Brügmann B (1997) A simple construction of initial data for multiple black holes. Phys Rev Lett 78:3606–3609. https://doi.org/10.1103/PhysRevLett.78.3606. arXiv:gr-qc/9703066

Brax P, Heisenberg L, Kuntz A (2020) Unveiling the Galileon in a three-body system: scalar and gravitational wave production. JCAP 05:012. https://doi.org/10.1088/1475-7516/2020/05/012. arXiv:2002.12590 [gr-qc]

Breivik K, Kremer K, Bueno M, Larson SL, Coughlin S, Kalogera V (2018) Characterizing accreting double white dwarf binaries with the Laser Interferometer Space Antenna and Gaia. Astrophys J Lett 854(1):L1. https://doi.org/10.3847/2041-8213/aaaa23. arXiv:1710.08370 [astro-ph.SR]

Breschi M, Bernuzzi S, Zappa F, Agathos M, Perego A, Radice D, Nagar A (2019) Kilohertz gravitational waves from binary neutron star remnants: time-domain model and constraints on extreme matter. Phys Rev D 100(10):104029. https://doi.org/10.1103/PhysRevD.100.104029. arXiv:1908.11418 [gr-qc]

Breschi M, Gamba R, Borhanian S, Carullo G, Bernuzzi S (2022) Kilohertz gravitational waves from binary neutron star mergers: inference of postmerger signals with the Einstein Telescope. arXiv e-prints arXiv:2205.09979 [gr-qc]

Brezin E, Itzykson C, Zinn-Justin J (1970) Relativistic balmer formula including recoil effects. Phys Rev D 1:2349–2355. https://doi.org/10.1103/PhysRevD.1.2349

Brink J, Geyer M, Hinderer T (2015) Astrophysics of resonant orbits in the Kerr metric. Phys Rev D 91 (8):083001. https://doi.org/10.1103/PhysRevD.91.083001. arXiv:1501.07728 [gr-qc]

Brink J, Geyer M, Hinderer T (2015) Orbital resonances around Black holes. Phys Rev Lett 114 (8):081102. https://doi.org/10.1103/PhysRevLett.114.081102. arXiv:1304.0330 [gr-qc]

Brito R, Shah S (2023) Extreme mass-ratio inspirals into black holes surrounded by scalar clouds. Phys Rev D 108(8):084019. https://doi.org/10.1103/PhysRevD.108.084019. arXiv:2307.16093 [gr-qc]

Brito R, Cardoso V, Okawa H (2015) Accretion of dark matter by stars. Phys Rev Lett 115(11):111301. https://doi.org/10.1103/PhysRevLett.115.111301. arXiv:1508.04773 [gr-qc]

Brito R, Cardoso V, Pani P (2015) Black holes as particle detectors: evolution of superradiant instabilities. Class Quantum Grav 32(13):134001. https://doi.org/10.1088/0264-9381/32/13/134001. arXiv:1411.0686 [gr-qc]

Brito R, Cardoso V, Pani P (2015) Superradiance: New Frontiers in Black Hole Physics. Lect Notes Phys 906:1–237. https://doi.org/10.1007/978-3-319-19000-6. arXiv:1501.06570 [gr-qc]

Brito R, Cardoso V, Herdeiro C, Radu E (2016) Proca stars: Gravitating Bose-Einstein condensates of massive spin 1 particles. Phys Lett B 752:291–295. https://doi.org/10.1016/j.physletb.2015.11.051. arXiv:1508.05395 [gr-qc]

Brito R, Cardoso V, Macedo C, Okawa H, Palenzuela C (2016) Interaction between bosonic dark matter and stars. Phys Rev D 93(4):044045. https://doi.org/10.1103/PhysRevD.93.044045. arXiv:1512.00466 [astro-ph.SR]

Brito R, Ghosh S, Barausse E, Berti E, Cardoso V, Dvorkin I, Klein A, Pani P (2017) Gravitational wave searches for ultralight bosons with LIGO and LISA. Phys Rev D 96(6):064050. https://doi.org/10.1103/PhysRevD.96.064050. arXiv:1706.06311 [gr-qc]

Brito R, Ghosh S, Barausse E, Berti E, Cardoso V, Dvorkin I, Klein A, Pani P (2017) Stochastic and resolvable gravitational waves from ultralight bosons. Phys Rev Lett 119(13):131101. https://doi.org/10.1103/PhysRevLett.119.131101. arXiv:1706.05097 [gr-qc]

Brito R, Buonanno A, Raymond V (2018) Black-hole spectroscopy by making full use of gravitational-wave modeling. Phys Rev D 98(8):084038. https://doi.org/10.1103/PhysRevD.98.084038. arXiv:1805.00293 [gr-qc]

Brito R, Grillo S, Pani P (2020) Black hole superradiant instability from ultralight spin-2 fields. Phys Rev Lett 124(21):211101. https://doi.org/10.1103/PhysRevLett.124.211101. arXiv:2002.04055 [gr-qc]

Brizuela D, Martin-Garcia JM, Tiglio M (2009) A complete gauge-invariant formalism for arbitrary second-order perturbations of a Schwarzschild black hole. Phys Rev D 80:024021. https://doi.org/10.1103/PhysRevD.80.024021. arXiv:0903.1134 [gr-qc]

Broek D, Nelemans G, Dan M, Rosswog S (2012) On the point mass approximation to calculate the gravitational wave signal from white dwarf binaries. Mon Not R Astron Soc 425:24. https://doi.org/10.1111/j.1745-3933.2012.01294.x. arXiv:1206.0744 [astro-ph.HE]

Brown JD, York JW Jr (1993) Quasilocal energy and conserved charges derived from the gravitational action. Phys Rev D 47:1407–1419. https://doi.org/10.1103/PhysRevD.47.1407. arXiv:gr-qc/9209012

Brown WR, Kilic M, Kosakowski A, Andrews JJ, Heinke CO, Agüeros MA, Camilo F, Gianninas A, Hermes JJ, Kenyon SJ (2020) The ELM survey. VIII. Ninety-eight double white dwarf binaries. Astrophysical Journal 889(1):49. https://doi.org/10.3847/1538-4357/ab63cd. arXiv:2002.00064 [astro-ph.SR]

Brügmann B, Gonzalez JA, Hannam M, Husa S, Sperhake U (2008) Exploring black hole superkicks. Phys Rev D 77:124047. https://doi.org/10.1103/PhysRevD.77.124047. arXiv:0707.0135 [gr-qc]

Brügmann B, Gonzalez JA, Hannam M, Husa S, Sperhake U, Tichy W (2008) Calibration of moving puncture simulations. Phys Rev D 77:024027. https://doi.org/10.1103/PhysRevD.77.024027. arXiv:gr-qc/0610128

Brustein R, Medved A (2017) Black holes as collapsed polymers. Fortsch Phys 65(1):1600114. https://doi.org/10.1002/prop.201600114. arXiv:1602.07706 [hep-th]

Brustein R, Medved A, Yagi K (2017) When black holes collide: probing the interior composition by the spectrum of ringdown modes and emitted gravitational waves. Phys Rev D 96(6):064033. https://doi.org/10.1103/PhysRevD.96.064033. arXiv:1704.05789 [gr-qc]

Bucciotti B, Kuntz A, Serra F, Trincherini E (2023) Nonlinear quasi-normal modes: uniform approximation. JHEP 12:048. https://doi.org/10.1007/JHEP12(2023)048. arXiv:2309.08501 [hep-th]

Bueno P, Cano PA, Goelen F, Hertog T, Vercnocke B (2018) Echoes of Kerr-like wormholes. Phys Rev D 97(2):024040. https://doi.org/10.1103/PhysRevD.97.024040. arXiv:1711.00391 [gr-qc]

Bugner M, Dietrich T, Bernuzzi S, Weyhausen A, Brügmann B (2016) Solving 3D relativistic hydrodynamical problems with weighted essentially nonoscillatory discontinuous Galerkin methods. Phys Rev D 94(8):084004. https://doi.org/10.1103/PhysRevD.94.084004. arXiv:1508.07147 [gr-qc]

Buonanno A, Damour T (1999) Effective one-body approach to general relativistic two-body dynamics. Phys Rev D 59:084006. https://doi.org/10.1103/PhysRevD.59.084006. arXiv:gr-qc/9811091

Buonanno A, Damour T (2000) Transition from inspiral to plunge in binary black hole coalescences. Phys Rev D 62:064015. https://doi.org/10.1103/PhysRevD.62.064015. arXiv:gr-qc/0001013

Buonanno A, Sathyaprakash BS (2014) Sources of gravitational waves: theory and observations. In: Ashtekar A, Berger BK, Isenberg J, Maccallum M (eds) General relativity and gravitation: centennial perspective. Cambridge University Press, pp 287–346. arXiv:1410.7832 [gr-qc]

Buonanno A, Yb Chen, Vallisneri M (2003) Detecting gravitational waves from precessing binaries of spinning compact objects: Adiabatic limit. Phys Rev D 67:104025. [Erratum: Phys. Rev. D 74, 029904 (2006)]. https://doi.org/10.1103/PhysRevD.67.104025. arXiv:gr-qc/0211087

Buonanno A, Chen Y, Damour T (2006) Transition from inspiral to plunge in precessing binaries of spinning black holes. Phys Rev D 74:104005. https://doi.org/10.1103/PhysRevD.74.104005. arXiv:gr-qc/0508067

Buonanno A, Cook GB, Pretorius F (2007) Inspiral, merger and ring-down of equal-mass black-hole binaries. Phys Rev D 75:124018. https://doi.org/10.1103/PhysRevD.75.124018. arXiv:gr-qc/0610122

Buonanno A, Pan Y, Baker JG, Centrella J, Kelly BJ, McWilliams ST, van Meter JR (2007) Toward faithful templates for non-spinning binary black holes using the effective-one-body approach. Phys Rev D 76:104049. https://doi.org/10.1103/PhysRevD.76.104049. arXiv:0706.3732 [gr-qc]

Buonanno A, Pan Y, Pfeiffer HP, Scheel MA, Buchman LT, Kidder LE (2009) Effective-one-body waveforms calibrated to numerical relativity simulations: coalescence of non-spinning, equal-mass black holes. Phys Rev D 79:124028. https://doi.org/10.1103/PhysRevD.79.124028. arXiv:0902.0790 [gr-qc]

Buonanno A, Kidder LE, Mroue AH, Pfeiffer HP, Taracchini A (2011) Reducing orbital eccentricity of precessing black-hole binaries. Phys Rev D 83:104034. https://doi.org/10.1103/PhysRevD.83.104034. arXiv:1012.1549 [gr-qc]

Buonanno A, Faye G, Hinderer T (2013) Spin effects on gravitational waves from inspiraling compact binaries at second post-Newtonian order. Phys Rev D 87(4):044009. https://doi.org/10.1103/PhysRevD.87.044009. arXiv:1209.6349 [gr-qc]

Buonanno A, Khalil M, O'Connell D, Roiban R, Solon MP, Zeng M (2022) Snowmass white paper: gravitational waves and scattering amplitudes. In: Snowmass 2021. arXiv:2204.05194 [hep-th]

Buoninfante L, Mazumdar A (2019) Nonlocal star as a blackhole mimicker. Phys Rev D 100(2):024031. https://doi.org/10.1103/PhysRevD.100.024031. arXiv:1903.01542 [gr-qc]

Burden CJ (1985) Gravitational radiation from a particular class of cosmic strings. Phys Lett B 164:277–281. https://doi.org/10.1016/0370-2693(85)90326-0

Burdge KB et al (2019) General relativistic orbital decay in a seven-minute-orbital-period eclipsing binary system. Nature 571(7766):528–531. https://doi.org/10.1038/s41586-019-1403-0. arXiv:1907.11291 [astro-ph.SR]

Burgess CP, Plestid R, Rummel M (2018) Effective field theory of black hole echoes. JHEP 09:113. https://doi.org/10.1007/JHEP09(2018)113. arXiv:1808.00847 [gr-qc]

Burke O, Gair JR, Simón J (2020) Transition from inspiral to plunge: a complete near-extremal trajectory and associated waveform. Phys Rev D 101(6):064026. https://doi.org/10.1103/PhysRevD.101.064026. arXiv:1909.12846 [gr-qc]

Burke O, Piovano GA, Warburton N, Lynch P, Speri L, Kavanagh C, Wardell B, Pound A, Durkan L, Miller J (2024) Assessing the importance of first postadiabatic terms for small-mass-ratio binaries. Phys Rev D 109(12):124048. https://doi.org/10.1103/PhysRevD.109.124048. arXiv:2310.08927 [gr-qc]

Cabero M, Nielsen AB, Lundgren AP, Capano CD (2017) Minimum energy and the end of the inspiral in the post-Newtonian approximation. Phys Rev D 95(6):064016. https://doi.org/10.1103/PhysRevD.95.064016. arXiv:1602.03134 [gr-qc]

Cactus Development Team (2024) Cactus Code. http://www.cactuscode.org/

Calderón Bustillo J, Sanchis-Gual N, Torres-Forné A, Font JA, Vajpeyi A, Smith R, Herdeiro C, Radu E, Leong SHW (2021) GW190521 as a merger of proca stars: a potential new vector boson of 8.7×10^{-13} eV. Phys Rev Lett 126(8):081101. https://doi.org/10.1103/PhysRevLett.126.081101. arXiv:2009.05376 [gr-qc]

Calderon Bustillo J, Sanchis-Gual N, Leong S, Chandra K, Torres-Forne A, Font JA, Herdeiro C, Radu E, Wong I, Li T (2023) Searching for vector boson-star mergers within LIGO-Virgo intermediate-mass black-hole merger candidates. Phys Rev D 108(12):123020. https://doi.org/10.1103/PhysRevD.108.123020. arXiv:2206.02551 [gr-qc]

Caldwell RR, Allen B (1992) Cosmological constraints on cosmic string gravitational radiation. Phys Rev D 45:3447–3468. https://doi.org/10.1103/PhysRevD.45.3447

Callister TA, Haster CJ, Ng K, Vitale S, Farr WM (2021) Who Ordered That? Unequal-mass binary black hole mergers have larger effective spins. Astrophys J Lett 922(1):L5. https://doi.org/10.3847/2041-8213/ac2ccc. arXiv:2106.00521 [astro-ph.HE]

Campanelli M, Lousto CO (1999) Second order gauge invariant gravitational perturbations of a Kerr black hole. Phys Rev D 59:124022. https://doi.org/10.1103/PhysRevD.59.124022. arXiv:gr-qc/9811019

Campanelli M, Lousto CO, Marronetti P, Zlochower Y (2006) Accurate evolutions of orbiting black-hole binaries without excision. Phys Rev Lett 96:111101. https://doi.org/10.1103/PhysRevLett.96.111101. arXiv:gr-qc/0511048

Campanelli M, Lousto CO, Zlochower Y (2006) Spinning-black-hole binaries: the orbital hang up. Phys Rev D 74:041501. https://doi.org/10.1103/PhysRevD.74.041501. arXiv:gr-qc/0604012

Campanelli M, Lousto CO, Zlochower Y, Merritt D (2007) Large merger recoils and spin flips from generic black-hole binaries. Astrophys J Lett 659:L5–L8. https://doi.org/10.1086/516712. arXiv:gr-qc/0701164

Campanelli M, Lousto CO, Zlochower Y, Merritt D (2007) Maximum gravitational recoil. Phys Rev Lett 98:231102. https://doi.org/10.1103/PhysRevLett.98.231102. arXiv:gr-qc/0702133

Campbell BA, Kaloper N, Olive KA (1992) Classical hair for Kerr-Newman black holes in string gravity. Phys Lett B 285:199–205. https://doi.org/10.1016/0370-2693(92)91452-F
Canizares P, Sopuerta CF (2009) Simulations of extreme-mass-ratio inspirals using pseudospectral methods. J Phys: Conf Ser 154:012053. https://doi.org/10.1088/1742-6596/154/1/012053. arXiv:0811.0294 [gr-qc]
Canizares P, Sopuerta CF (2010) Modelling Extreme-Mass-Ratio Inspirals using Pseudospectral Methods. In: 12th Marcel Grossmann Meeting on General Relativity. pp 841–843. https://doi.org/10.1142/9789814374552_0072. arXiv:1001.4697 [gr-qc]
Canizares P, Sopuerta CF (2011) Time-domain modelling of extreme-mass-ratio inspirals for the Laser Interferometer Space Antenna. J Phys: Conf Ser 314:012075. https://doi.org/10.1088/1742-6596/314/1/012075. arXiv:1103.2149 [gr-qc]
Canizares P, Sopuerta CF, Jaramillo JL (2010) Pseudospectral collocation methods for the computation of the self-force on a charged particle: generic orbits around a Schwarzschild black hole. Phys Rev D 82:044023. https://doi.org/10.1103/PhysRevD.82.044023. arXiv:1006.3201 [gr-qc]
Canizares P, Gair JR, Sopuerta CF (2012) Testing Chern-Simons modified gravity with gravitational-wave detections of extreme-mass-ratio binaries. Phys Rev D 86:044010. https://doi.org/10.1103/PhysRevD.86.044010. arXiv:1205.1253 [gr-qc]
Cannizzaro E, Sberna L, Green SR, Hollands S (2024) Relativistic perturbation theory for black-hole boson clouds. Phys Rev Lett 132(5):051401. https://doi.org/10.1103/PhysRevLett.132.051401. arXiv:2309.10021 [gr-qc]
Cannon K, Chapman A, Hanna C, Keppel D, Searle AC, Weinstein AJ (2010) Singular value decomposition applied to compact binary coalescence gravitational-wave signals. Phys Rev D 82:044025. https://doi.org/10.1103/PhysRevD.82.044025. arXiv:1005.0012 [gr-qc]
Cannon K, Hanna C, Keppel D (2011) Efficiently enclosing the compact binary parameter space by singular-value decomposition. Phys Rev D 84:084003. https://doi.org/10.1103/PhysRevD.84.084003. arXiv:1101.4939 [gr-qc]
Cannon K, Hanna C, Keppel D (2012) Interpolating compact binary waveforms using the singular value decomposition. Phys Rev D 85:081504. https://doi.org/10.1103/PhysRevD.85.081504. arXiv:1108.5618 [gr-qc]
Cannon K, Emberson JD, Hanna C, Keppel D, Pfeiffer H (2013) Interpolation in waveform space: enhancing the accuracy of gravitational waveform families using numerical relativity. Phys Rev D 87(4):044008. https://doi.org/10.1103/PhysRevD.87.044008. arXiv:1211.7095 [gr-qc]
Cano PA, Ruipérez A (2022) String gravity in D=4. Phys Rev D 105(4):044022. https://doi.org/10.1103/PhysRevD.105.044022. arXiv:2111.04750 [hep-th]
Cano PA, Fransen K, Hertog T (2020) Ringing of rotating black holes in higher-derivative gravity. Phys Rev D 102(4):044047. https://doi.org/10.1103/PhysRevD.102.044047. arXiv:2005.03671 [gr-qc]
Cano PA, Fransen K, Hertog T, Maenaut S (2023) Quasinormal modes of rotating black holes in higher-derivative gravity. Phys Rev D 108(12):124032. https://doi.org/10.1103/PhysRevD.108.124032. arXiv:2307.07431 [gr-qc]
Cano PA, Fransen K, Hertog T, Maenaut S (2023) Universal Teukolsky equations and black hole perturbations in higher-derivative gravity. Phys Rev D 108(2):024040. https://doi.org/10.1103/PhysRevD.108.024040. arXiv:2304.02663 [gr-qc]
Cano PA, Capuano L, Franchini N, Maenaut S, Völkel SH (2024) Higher-derivative corrections to the Kerr quasinormal mode spectrum. Phys Rev D 110(12):124057. https://doi.org/10.1103/PhysRevD.110.124057. arXiv:2409.04517 [gr-qc]
Cano PA, Capuano L, Franchini N, Maenaut S, Völkel SH (2024) Parametrized quasinormal mode framework for modified Teukolsky equations. Phys Rev D 110(10):104007. https://doi.org/10.1103/PhysRevD.110.104007. arXiv:2407.15947 [gr-qc]
Cano PA, Deich A, Yunes N (2024) Accuracy of the slow-rotation approximation for black holes in modified gravity in light of astrophysical observables. Phys Rev D 109(2):024048. https://doi.org/10.1103/PhysRevD.109.024048. arXiv:2305.15341 [gr-qc]
Cao Z, Han WB (2017) Waveform model for an eccentric binary black hole based on the effective-one-body-numerical-relativity formalism. Phys Rev D 96(4):044028. https://doi.org/10.1103/PhysRevD.96.044028. arXiv:1708.00166 [gr-qc]
Cao Z, Hilditch D (2012) Numerical stability of the Z4c formulation of general relativity. Phys Rev D 85:124032. https://doi.org/10.1103/PhysRevD.85.124032. arXiv:1111.2177 [gr-qc]
Cao Z, Galaviz P, Li LF (2013) Binary black hole mergers in $f(R)$ theory. Phys Rev D 87(10):104029. https://doi.org/10.1103/PhysRevD.87.104029. arXiv:1608.07816 [gr-qc]

Cao Z, Yo HJ, Yu JP (2008) A reinvestigation of moving punctured black holes with a new code. Phys Rev D 78:124011. https://doi.org/10.1103/PhysRevD.78.124011. arXiv:0812.0641 [gr-qc]
Capano CD, Cabero M, Westerweck J, Abedi J, Kastha S, Nitz AH, Wang YF, Nielsen AB, Krishnan B (2023) Multimode quasinormal spectrum from a perturbed black hole. Phys Rev Lett 131 (22):221402. https://doi.org/10.1103/PhysRevLett.131.221402. arXiv:2105.05238 [gr-qc]
Caputo A, Sberna L, Toubiana A, Babak S, Barausse E, Marsat S, Pani P (2020) Gravitational-wave detection and parameter estimation for accreting black-hole binaries and their electromagnetic counterpart. Astrophys J 892(2):90. https://doi.org/10.3847/1538-4357/ab7b66. arXiv:2001.03620 [astro-ph.HE]
Cárdenas-Avendaño A, Sopuerta CF (2024) Testing gravity with Extreme-Mass-Ratio Inspirals. In: Bambi C, Cárdenas-Avendaño A (eds) Recent Progress on Gravity Tests: Challenges and Future Perspectives. Springer, Singapore, pp 275–359. https://doi.org/10.1007/978-981-97-2871-8_8. arXiv:2401.08085 [gr-qc]
Cardenas-Avendano A, Nampalliwar S, Yunes N (2020) Gravitational-wave versus X-ray tests of strong-field gravity. Class Quantum Grav 37(13):135008. https://doi.org/10.1088/1361-6382/ab8f64. arXiv:1912.08062 [gr-qc]
Cardoso V, Duque F (2022) Resonances, black hole mimickers, and the greenhouse effect: consequences for gravitational-wave physics. Phys Rev D 105(10):104023. https://doi.org/10.1103/PhysRevD.105.104023. arXiv:2204.05315 [gr-qc]
Cardoso V, Maselli A (2020) Constraints on the astrophysical environment of binaries with gravitational-wave observations. Astron Astrophys 644:A147. https://doi.org/10.1051/0004-6361/202037654. arXiv:1909.05870 [astro-ph.HE]
Cardoso V, Pani P (2013) Tidal acceleration of black holes and superradiance. Class Quantum Grav 30:045011. https://doi.org/10.1088/0264-9381/30/4/045011. arXiv:1205.3184 [gr-qc]
Cardoso V, Pani P (2017) Tests for the existence of black holes through gravitational wave echoes. Nature Astron 1(9):586–591. https://doi.org/10.1038/s41550-017-0225-y. arXiv:1709.01525 [gr-qc]
Cardoso V, Pani P (2019) Testing the nature of dark compact objects: a status report. Living Rev Relativ 22:4. https://doi.org/10.1007/s41114-019-0020-4. arXiv:1904.05363 [gr-qc]
Cardoso V, Dias O, Hovdebo JL, Myers RC (2006) Instability of non-supersymmetric smooth geometries. Phys Rev D 73:064031. https://doi.org/10.1103/PhysRevD.73.064031. arXiv:hep-th/0512277
Cardoso V, Pani P, Cadoni M, Cavaglia M (2008) Ergoregion instability of ultracompact astrophysical objects. Phys Rev D 77:124044. https://doi.org/10.1103/PhysRevD.77.124044. arXiv:0709.0532 [gr-qc]
Cardoso V, Chakrabarti S, Pani P, Berti E, Gualtieri L (2011) Floating and sinking: the imprint of massive scalars around rotating black holes. Phys Rev Lett 107:241101. https://doi.org/10.1103/PhysRevLett.107.241101. arXiv:1109.6021 [gr-qc]
Cardoso V, Crispino L, Macedo C, Okawa H, Pani P (2014) Light rings as observational evidence for event horizons: long-lived modes, ergoregions and nonlinear instabilities of ultracompact objects. Phys Rev D 90(4):044069. https://doi.org/10.1103/PhysRevD.90.044069. arXiv:1406.5510 [gr-qc]
Cardoso V, Franzin E, Pani P (2016) Is the gravitational-wave ringdown a probe of the event horizon? Phys Rev Lett 116(17):171101. [Erratum: Phys. Rev. Lett. 117, 089902 (2016)]. https://doi.org/10.1103/PhysRevLett.116.171101. arXiv:1602.07309 [gr-qc]
Cardoso V, Hopper S, Macedo C, Palenzuela C, Pani P (2016) Gravitational-wave signatures of exotic compact objects and of quantum corrections at the horizon scale. Phys Rev D 94(8):084031. https://doi.org/10.1103/PhysRevD.94.084031. arXiv:1608.08637 [gr-qc]
Cardoso V, Macedo CFB, Pani P, Ferrari V (2016) Black holes and gravitational waves in models of minicharged dark matter. JCAP 05:054. [Erratum: JCAP 04, E01 (2020)]. https://doi.org/10.1088/1475-7516/2016/05/054. arXiv:1604.07845 [hep-ph]
Cardoso V, Franzin E, Maselli A, Pani P, Raposo G (2017) Testing strong-field gravity with tidal Love numbers. Phys Rev D 95(8):084014. [Addendum: Phys. Rev. D 95, 089901 (2017)]. https://doi.org/10.1103/PhysRevD.95.084014. arXiv:1701.01116 [gr-qc]
Cardoso V, Castro G, Maselli A (2018) Gravitational waves in massive gravity theories: waveforms, fluxes and constraints from extreme-mass-ratio mergers. Phys Rev Lett 121(25):251103. https://doi.org/10.1103/PhysRevLett.121.251103. arXiv:1809.00673 [gr-qc]
Cardoso V, Kimura M, Maselli A, Senatore L (2018) Black Holes in an Effective Field Theory Extension of General Relativity. Phys Rev Lett 121(25):251105. [Erratum: Phys. Rev. Lett. 131, 109903 (2023)]. https://doi.org/10.1103/PhysRevLett.121.251105. arXiv:1808.08962 [gr-qc]

Cardoso V, Kimura M, Maselli A, Berti E, Macedo C, McManus R (2019) Parametrized black hole quasinormal ringdown: decoupled equations for nonrotating black holes. Phys Rev D 99(10):104077. https://doi.org/10.1103/PhysRevD.99.104077. arXiv:1901.01265 [gr-qc]

Cardoso V, del Rio A, Kimura M (2019) Distinguishing black holes from horizonless objects through the excitation of resonances during inspiral. Phys Rev D 100:084046. [Erratum: Phys. Rev. D 101, 069902 (2020)]. https://doi.org/10.1103/PhysRevD.100.084046. arXiv:1907.01561 [gr-qc]

Cardoso V, Duque F, Ikeda T (2020) Tidal effects and disruption in superradiant clouds: a numerical investigation. Phys Rev D 101(6):064054. https://doi.org/10.1103/PhysRevD.101.064054. arXiv:2001.01729 [gr-qc]

Cardoso V, Destounis K, Duque F, Macedo RP, Maselli A (2022) Black holes in galaxies: environmental impact on gravitational-wave generation and propagation. Phys Rev D 105(6):L061501. https://doi.org/10.1103/PhysRevD.105.L061501. arXiv:2109.00005 [gr-qc]

Cardoso V, Destounis K, Duque F, Panosso Macedo R, Maselli A (2022) Gravitational waves from extreme-mass-ratio systems in astrophysical environments. Phys Rev Lett 129(24):241103. https://doi.org/10.1103/PhysRevLett.129.241103. arXiv:2210.01133 [gr-qc]

Carpet developers (2024) Carpet: Adaptive mesh refinement for the Cactus framework. https://bitbucket.org/eschnett/carpet/src/master/

Carr B, Clesse S, Garcia-Bellido J, Hawkins M, Kuhnel F (2024) Observational evidence for primordial black holes: a positivist perspective. Phys Rept 1054:1–68. https://doi.org/10.1016/j.physrep.2023.11.005. arXiv:2306.03903 [astro-ph.CO]

Carson Z, Yagi K (2020) Parametrized and inspiral-merger-ringdown consistency tests of gravity with multiband gravitational wave observations. Phys Rev D 101(4):044047. https://doi.org/10.1103/PhysRevD.101.044047. arXiv:1911.05258 [gr-qc]

Carter B (1968) Global structure of the Kerr family of gravitational fields. Phys Rev 174:1559–1571. https://doi.org/10.1103/PhysRev.174.1559

Carter B (1971) Axisymmetric black hole has only two degrees of freedom. Phys Rev Lett 26:331–333. https://doi.org/10.1103/PhysRevLett.26.331

Carullo G, De Amicis M (2023) Late-time tails in nonlinear evolutions of merging black hole binaries. arXiv e-prints arXiv:2310.12968 [gr-qc]

Carullo G, Del Pozzo W, Veitch J (2019) Observational Black Hole Spectroscopy: A time-domain multimode analysis of GW150914. Phys Rev D 99(12):123029. [Erratum: Phys. Rev. D 100, 089903 (2019)]. https://doi.org/10.1103/PhysRevD.99.123029. arXiv:1902.07527 [gr-qc]

Carullo G et al (2018) Empirical tests of the black hole no-hair conjecture using gravitational-wave observations. Phys Rev D 98(10):104020. https://doi.org/10.1103/PhysRevD.98.104020. arXiv:1805.04760 [gr-qc]

Carvalho GA, Anjos RC, Coelho JG, Lobato RV, Malheiro M, Marinho RM, Rodriguez JF, Rueda JA, Ruffini R (2022) Orbital decay of double white dwarfs: beyond gravitational-wave radiation effects. Astrophys J 940(1):90. https://doi.org/10.3847/1538-4357/ac9841. arXiv:2208.00863 [gr-qc]

Casals M, Dolan SR, Ottewill AC, Wardell B (2009) Self-force calculations with matched expansions and quasinormal mode sums. Phys Rev D 79:124043. https://doi.org/10.1103/PhysRevD.79.124043. arXiv:0903.0395 [gr-qc]

Casals M, Dolan S, Ottewill AC, Wardell B (2013) Self-force and green function in Schwarzschild spacetime via Quasinormal modes and branch cut. Phys Rev D 88:044022. https://doi.org/10.1103/PhysRevD.88.044022. arXiv:1306.0884 [gr-qc]

Casals M, Nolan BC, Ottewill AC, Wardell B (2019) Regularized calculation of the retarded Green function in a Schwarzschild spacetime. Phys Rev D 100(10):104037. https://doi.org/10.1103/PhysRevD.100.104037. arXiv:1910.02567 [gr-qc]

Casper P, Allen B (1995) Gravitational radiation from realistic cosmic string loops. Phys Rev D 52:4337–4348. https://doi.org/10.1103/PhysRevD.52.4337. arXiv:gr-qc/9505018

Castillo J, Vega I, Wardell B (2018) Self-force on a scalar charge in a circular orbit about a Reissner-Nordström black hole. Phys Rev D 98(2):024024. https://doi.org/10.1103/PhysRevD.98.024024. arXiv:1804.09224 [gr-qc]

Caudill S, Field SE, Galley CR, Herrmann F, Tiglio M (2012) Reduced Basis representations of multi-mode black hole ringdown gravitational waves. Class Quantum Grav 29:095016. https://doi.org/10.1088/0264-9381/29/9/095016. arXiv:1109.5642 [gr-qc]

Cayuso J, Ortiz N, Lehner L (2017) Fixing extensions to general relativity in the nonlinear regime. Phys Rev D 96(8):084043. https://doi.org/10.1103/PhysRevD.96.084043. arXiv:1706.07421 [gr-qc]

Cayuso R, Lehner L (2020) Nonlinear, noniterative treatment of EFT-motivated gravity. Phys Rev D 102 (8):084008. https://doi.org/10.1103/PhysRevD.102.084008. arXiv:2005.13720 [gr-qc]
Cayuso R, Figueras P, França T, Lehner L (2023) Modelling self-consistently beyond general relativity. Phys Rev Lett 131:111403. https://doi.org/10.1103/PhysRevLett.131.111403. arXiv:2303.07246 [gr-qc]
Centrella J, Baker JG, Kelly BJ, van Meter JR (2010) Black-hole binaries, gravitational waves, and numerical relativity. Rev Mod Phys 82:3069. https://doi.org/10.1103/RevModPhys.82.3069. arXiv:1010.5260 [gr-qc]
Chakraborty S, Maggio E, Mazumdar A, Pani P (2022) Implications of the quantum nature of the black hole horizon on the gravitational-wave ringdown. Phys Rev D 106(2):024041. https://doi.org/10.1103/PhysRevD.106.024041. arXiv:2202.09111 [gr-qc]
Chamberlain K, Yunes N (2017) Theoretical physics implications of gravitational wave observation with future detectors. Phys Rev D 96(8):084039. https://doi.org/10.1103/PhysRevD.96.084039. arXiv:1704.08268 [gr-qc]
Chandramouli RS, Yunes N (2022) Ready-to-use analytic model for gravitational waves from a hierarchical triple with Kozai-Lidov oscillations. Phys Rev D 105(6):064009. https://doi.org/10.1103/PhysRevD.105.064009. arXiv:2107.00741 [gr-qc]
Chandrasekhar S (1943) Dynamical friction. I. General considerations: the coefficient of dynamical friction. Astrophys J 97:255. https://doi.org/10.1086/144517
Chandrasekhar S, Detweiler SL (1975) The quasi-normal modes of the Schwarzschild black hole. Proc R Soc Lond A 344:441–452. https://doi.org/10.1098/rspa.1975.0112
Chang P, Etienne Z (2020) General relativistic hydrodynamics on a moving-mesh I: static space-times. Mon Not R Astron Soc 496(1):206–214. https://doi.org/10.1093/mnras/staa1532. arXiv:2002.09613 [gr-qc]
Chatziioannou K, Poisson E, Yunes N (2013) Tidal heating and torquing of a Kerr black hole to next-to-leading order in the tidal coupling. Phys Rev D 87(4):044022. https://doi.org/10.1103/PhysRevD.87.044022. arXiv:1211.1686 [gr-qc]
Chatziioannou K, Klein A, Yunes N, Cornish N (2017) Constructing gravitational waves from generic spin-precessing compact binary inspirals. Phys Rev D 95(10):104004. https://doi.org/10.1103/PhysRevD.95.104004. arXiv:1703.03967 [gr-qc]
Chatziioannou K, Lovelace G, Boyle M, Giesler M, Hemberger DA, Katebi R, Kidder LE, Pfeiffer HP, Scheel MA, Szilágyi B (2018) Measuring the properties of nearly extremal black holes with gravitational waves. Phys Rev D 98(4):044028. https://doi.org/10.1103/PhysRevD.98.044028. arXiv:1804.03704 [gr-qc]
Chaurasia SV, Dietrich T, Rosswog S (2021) Black hole-neutron star simulations with the BAM code: first tests and simulations. Phys Rev D 104(8):084010. https://doi.org/10.1103/PhysRevD.104.084010. arXiv:2107.08752 [gr-qc]
Chen X, Han WB (2018) A new type of extreme-mass-ratio inspirals produced by tidal capture of binary black holes. Commun Phys 1:53. https://doi.org/10.1038/s42005-018-0053-0. arXiv:1801.05780 [astro-ph.HE]
Cheng-Hsin Cheng and Giuseppe Ficarra and Helvi Witek (2024) Binary black holes i2024rk matter environments. In prep
Chernoff DF (2009) Clustering of Superstring Loops. arXiv e-prints arXiv:0908.4077 [astro-ph.CO]
Chernoff DF, Tye S (2015) Inflation, string theory and cosmic strings. Int J Mod Phys D 24(03):1530010. https://doi.org/10.1142/S0218271815300104. arXiv:1412.0579 [astro-ph.CO]
Chernoff DF, Tye S (2018) Detection of low tension cosmic superstrings. JCAP 05:002. https://doi.org/10.1088/1475-7516/2018/05/002. arXiv:1712.05060 [astro-ph.CO]
Chernoff DF, Flanagan EE, Wardell B (2019) Gravitational backreaction on a cosmic string: formalism. Phys Rev D 99(8):084036. https://doi.org/10.1103/PhysRevD.99.084036. arXiv:1808.08631 [gr-qc]
Cheung C, Solon MP (2020) Classical gravitational scattering at $\mathcal{O}(G^3)$ from Feynman diagrams. JHEP 06:144. https://doi.org/10.1007/JHEP06(2020)144. arXiv:2003.08351 [hep-th]
Cheung C, Solon MP (2020) Tidal effects in the post-minkowskian expansion. Phys Rev Lett 125 (19):191601. https://doi.org/10.1103/PhysRevLett.125.191601. arXiv:2006.06665 [hep-th]
Cheung C, Rothstein IZ, Solon MP (2018) From scattering amplitudes to classical potentials in the post-minkowskian expansion. Phys Rev Lett 121(25):251101. https://doi.org/10.1103/PhysRevLett.121.251101. arXiv:1808.02489 [hep-th]

Cheung C, Shah N, Solon MP (2021) Mining the geodesic equation for scattering data. Phys Rev D 103 (2):024030. https://doi.org/10.1103/PhysRevD.103.024030. arXiv:2010.08568 [hep-th]
Cheung M, Destounis K, Macedo RP, Berti E, Cardoso V (2022) Destabilizing the fundamental mode of black holes: the elephant and the flea. Phys Rev Lett 128(11):111103. https://doi.org/10.1103/PhysRevLett.128.111103. arXiv:2111.05415 [gr-qc]
Cheung M et al (2023) Nonlinear effects in black hole ringdown. Phys Rev Lett 130(8):081401. https://doi.org/10.1103/PhysRevLett.130.081401. arXiv:2208.07374 [gr-qc]
Chiaramello D, Nagar A (2020) Faithful analytical effective-one-body waveform model for spin-aligned, moderately eccentric, coalescing black hole binaries. Phys Rev D 101(10):101501. https://doi.org/10.1103/PhysRevD.101.101501. arXiv:2001.11736 [gr-qc]
Chirenti C, Rezzolla L (2016) Did GW150914 produce a rotating gravastar? Phys Rev D 94(8):084016. https://doi.org/10.1103/PhysRevD.94.084016. arXiv:1602.08759 [gr-qc]
Chirenti C, Rezzolla L (2007) How to tell a gravastar from a black hole. Class Quantum Grav 24:4191–4206. https://doi.org/10.1088/0264-9381/24/16/013. arXiv:0706.1513 [gr-qc]
Cho G, Kälin G, Porto RA (2022) From boundary data to bound states. Part III. Radiative effects. JHEP 04:154. [Erratum: JHEP 07, 002 (2022)]. https://doi.org/10.1007/JHEP04(2022)154. arXiv:2112.03976 [hep-th]
Cho G, Porto RA, Yang Z (2022) Gravitational radiation from inspiralling compact objects: spin effects to the fourth post-Newtonian order. Phys Rev D 106(10):L101501. https://doi.org/10.1103/PhysRevD.106.L101501. arXiv:2201.05138 [gr-qc]
Cho G, Tanay S, Gopakumar A, Lee HM (2022) Generalized quasi-Keplerian solution for eccentric, nonspinning compact binaries at 4PN order and the associated inspiral-merger-ringdown waveform. Phys Rev D 105(6):064010. https://doi.org/10.1103/PhysRevD.105.064010. arXiv:2110.09608 [gr-qc]
Choptuik MW, Pretorius F (2010) Ultra relativistic particle collisions. Phys Rev Lett 104:111101. https://doi.org/10.1103/PhysRevLett.104.111101. arXiv:0908.1780 [gr-qc]
Choudhary S, Sanchis-Gual N, Gupta A, Degollado JC, Bose S, Font JA (2021) Gravitational waves from binary black hole mergers surrounded by scalar field clouds: numerical simulations and observational implications. Phys Rev D 103(4):044032. https://doi.org/10.1103/PhysRevD.103.044032. arXiv:2010.00935 [gr-qc]
Christiansen JL, Albin E, James KA, Goldman J, Maruyama D, Smoot GF (2008) Search for cosmic strings in the GOODS survey. Phys Rev D 77:123509. https://doi.org/10.1103/PhysRevD.77.123509. arXiv:0803.0027 [astro-ph]
Chrusciel PT, Lopes Costa J, Heusler M (2012) Stationary black holes: uniqueness and beyond. Living Rev Relativ 15:7. https://doi.org/10.12942/lrr-2012-7. arXiv:1205.6112 [gr-qc]
Chrzanowski PL (1975) Vector potential and metric perturbations of a rotating black hole. Phys Rev D 11:2042–2062. https://doi.org/10.1103/PhysRevD.11.2042
Chu P (2011) FPGA Prototyping by VHDL Examples: Xilinx Spartan-3 Version. Wiley, Hoboken
Chu YZ, Trodden M (2013) Retarded Green's function of a Vainshtein system and Galileon waves. Phys Rev D 87(2):024011. https://doi.org/10.1103/PhysRevD.87.024011. arXiv:1210.6651 [astro-ph.CO]
Chua A, Gair JR (2015) Improved analytic extreme-mass-ratio inspiral model for scoping out eLISA data analysis. Class Quantum Grav 32:232002. https://doi.org/10.1088/0264-9381/32/23/232002. arXiv:1510.06245 [gr-qc]
Chua AJK, Vallisneri M (2020) On parametric tests of relativity with false degrees of freedom. arXiv e-prints arXiv:2006.08918 [gr-qc]
Chua A, Moore CJ, Gair JR (2017) Augmented kludge waveforms for detecting extreme-mass-ratio inspirals. Phys Rev D 96(4):044005. https://doi.org/10.1103/PhysRevD.96.044005. arXiv:1705.04259 [gr-qc]
Chua A, Hee S, Handley WJ, Higson E, Moore CJ, Gair JR, Hobson MP, Lasenby AN (2018) Towards a framework for testing general relativity with extreme-mass-ratio-inspiral observations. Mon Not R Astron Soc 478(1):28–40. https://doi.org/10.1093/mnras/sty1079. arXiv:1803.10210 [gr-qc]
Chua A, Galley CR, Vallisneri M (2019) Reduced-order modeling with artificial neurons for gravitational-wave inference. Phys Rev Lett 122(21):211101. https://doi.org/10.1103/PhysRevLett.122.211101. arXiv:1811.05491 [astro-ph.IM]
Chua A, Katz ML, Warburton N, Hughes SA (2021) Rapid generation of fully relativistic extreme-mass-ratio-inspiral waveform templates for LISA data analysis. Phys Rev Lett 126(5):051102. https://doi.org/10.1103/PhysRevLett.126.051102. arXiv:2008.06071 [gr-qc]

Chung A, Yunes N (2024) Quasinormal mode frequencies and gravitational perturbations of black holes with any subextremal spin in modified gravity through METRICS: The scalar-Gauss-Bonnet gravity case. Phys Rev D 110(6):064019. https://doi.org/10.1103/PhysRevD.110.064019. arXiv:2406.11986 [gr-qc]

Chung A, Yunes N (2024) Ringing out general relativity: quasinormal mode frequencies for black holes of any spin in modified gravity. Phys Rev Lett 133(18):181401. https://doi.org/10.1103/PhysRevLett.133.181401. arXiv:2405.12280 [gr-qc]

Chung A, Wagle P, Yunes N (2023) Spectral method for the gravitational perturbations of black holes: Schwarzschild background case. Phys Rev D 107(12):124032. https://doi.org/10.1103/PhysRevD.107.124032. arXiv:2302.11624 [gr-qc]

Chung A, Wagle P, Yunes N (2024) Spectral method for metric perturbations of black holes: Kerr background case in general relativity. Phys Rev D 109(4):044072. https://doi.org/10.1103/PhysRevD.109.044072. arXiv:2312.08435 [gr-qc]

Chung MZ, Huang Y, Kim JW, Lee S (2020) Complete Hamiltonian for spinning binary systems at first post-Minkowskian order. JHEP 05:105. https://doi.org/10.1007/JHEP05(2020)105. arXiv:2003.06600 [hep-th]

Cipolletta F, Kalinani JV, Giacomazzo B, Ciolfi R (2020) Spritz: a new fully general-relativistic magnetohydrodynamic code. Class Quantum Grav 37(13):135010. https://doi.org/10.1088/1361-6382/ab8be8. arXiv:1912.04794 [astro-ph.HE]

Cipolletta F, Kalinani JV, Giangrandi E, Giacomazzo B, Ciolfi R, Sala L, Giudici B (2021) Spritz: general relativistic magnetohydrodynamics with neutrinos. Class Quantum Grav 38(8):085021. https://doi.org/10.1088/1361-6382/abebb7. arXiv:2012.10174 [astro-ph.HE]

Clesse S, García-Bellido J (2015) Massive primordial black holes from hybrid inflation as dark matter and the seeds of galaxies. Phys Rev D 92(2):023524. https://doi.org/10.1103/PhysRevD.92.023524. arXiv:1501.07565 [astro-ph.CO]

Clough K, Figueras P, Finkel H, Kunesch M, Lim EA, Tunyasuvunakool S (2015) GRChombo: numerical relativity with adaptive mesh refinement. Class Quantum Grav 32(24):245011. https://doi.org/10.1088/0264-9381/32/24/245011. arXiv:1503.03436 [gr-qc]

Clough K, Dietrich T, Niemeyer JC (2018) Axion star collisions with black holes and neutron stars in full 3D numerical relativity. Phys Rev D 98(8):083020. https://doi.org/10.1103/PhysRevD.98.083020. arXiv:1808.04668 [gr-qc]

Clough K, Ferreira PG, Lagos M (2019) Growth of massive scalar hair around a Schwarzschild black hole. Phys Rev D 100(6):063014. https://doi.org/10.1103/PhysRevD.100.063014. arXiv:1904.12783 [gr-qc]

Clough K, Helfer T, Witek H, Berti E (2022) Ghost instabilities in self-interacting vector fields: the problem with Proca fields. Phys Rev Lett 129(15):151102. https://doi.org/10.1103/PhysRevLett.129.151102. arXiv:2204.10868 [gr-qc]

Coates A, Ramazanoğlu FM (2023) Treatments and placebos for the pathologies of effective field theories. Phys Rev D 108(10):L101501. https://doi.org/10.1103/PhysRevD.108.L101501. arXiv:2307.07743 [gr-qc]

Cole PS, Bertone G, Coogan A, Gaggero D, Karydas T, Kavanagh BJ, Spieksma T, Tomaselli GM (2023) Distinguishing environmental effects on binary black hole gravitational waveforms. Nature Astron 7(8):943–950. https://doi.org/10.1038/s41550-023-01990-2. arXiv:2211.01362 [gr-qc]

Colleoni M, Barack L, Shah AG, van de Meent M (2015) Self-force as a cosmic censor in the Kerr overspinning problem. Phys Rev D 92(8):084044. https://doi.org/10.1103/PhysRevD.92.084044. arXiv:1508.04031 [gr-qc]

Colleoni M, Vidal FAR, Johnson-McDaniel NK, Dietrich T, Haney M, Pratten G (2023) IMRPhenomXP_NRTidalv2: An improved frequency-domain precessing binary neutron star waveform model. arXiv e-prints arXiv:2311.15978 [gr-qc]

Colleoni M, Krishnendu NV, Mourier P, Bera S, Jiménez-Forteza X (2024) Testing Gravity with Binary Black Hole Gravitational Waves. In: Bambi C, Cárdenas-Avendaño A (eds) Recent Progress on Gravity Tests: Challenges and Future Perspectives. Springer, Singapore, pp 239–274. https://doi.org/10.1007/978-981-97-2871-8_7. arXiv:2403.07682 [gr-qc]

Collins NA, Hughes SA (2004) Towards a formalism for mapping the space-times of massive compact objects: bumpy black holes and their orbits. Phys Rev D 69:124022. https://doi.org/10.1103/PhysRevD.69.124022. arXiv:gr-qc/0402063

Collodel LG, Doneva DD, Yazadjiev SS (2022) Equatorial extreme-mass-ratio inspirals in Kerr black holes with scalar hair spacetimes. Phys Rev D 105(4):044036. https://doi.org/10.1103/PhysRevD.105.044036. arXiv:2108.11658 [gr-qc]
Colpi M (2014) Massive binary black holes in galactic nuclei and their path to coalescence. Space Sci Rev 183(1–4):189–221. https://doi.org/10.1007/s11214-014-0067-1. arXiv:1407.3102 [astro-ph.GA]
Colpi M, Shapiro SL, Wasserman I (1986) Boson stars: gravitational equilibria of selfinteracting scalar fields. Phys Rev Lett 57:2485–2488. https://doi.org/10.1103/PhysRevLett.57.2485
Colpi M, et al. (2024) LISA Definition Study Report. arXiv e-prints arXiv:2402.07571 [astro-ph.CO]
Comins N, Schutz BF (1978) On the ergoregion instability. Proc R Soc London Ser A 364(1717):211–226. https://doi.org/10.1098/rspa.1978.0196
Compère G, Küchler L (2021) Self-consistent adiabatic inspiral and transition motion. Phys Rev Lett 126 (24):241106. https://doi.org/10.1103/PhysRevLett.126.241106. arXiv:2102.12747 [gr-qc]
Compère G, Küchler L (2022) Asymptotically matched quasi-circular inspiral and transition-to-plunge in the small mass ratio expansion. SciPost Phys 13(2):043. https://doi.org/10.21468/SciPostPhys.13.2.043. arXiv:2112.02114 [gr-qc]
Compère G, Fransen K, Hertog T, Long J (2018) Gravitational waves from plunges into Gargantua. Class Quantum Grav 35(10):104002. https://doi.org/10.1088/1361-6382/aab99e. arXiv:1712.07130 [gr-qc]
Compère G, Fransen K, Hertog T, Liu Y (2020) Scalar self-force for high spin black holes. Phys Rev D 101(6):064006. https://doi.org/10.1103/PhysRevD.101.064006. arXiv:1910.02081 [gr-qc]
Compère G, Fransen K, Jonas C (2020) Transition from inspiral to plunge into a highly spinning black hole. Class Quantum Grav 37(9):095013. https://doi.org/10.1088/1361-6382/ab79d3. arXiv:1909.12848 [gr-qc]
Compère G, Oliveri R, Seraj A (2020) The Poincaré and BMS flux-balance laws with application to binary systems. JHEP 10:116. [Erratum: JHEP 06, 045 (2024)]. https://doi.org/10.1007/JHEP10(2020)116. arXiv:1912.03164 [gr-qc]
Coogan A, Bertone G, Gaggero D, Kavanagh BJ, Nichols DA (2022) Measuring the dark matter environments of black hole binaries with gravitational waves. Phys Rev D 105(4):043009. https://doi.org/10.1103/PhysRevD.105.043009. arXiv:2108.04154 [gr-qc]
Cook GB (1994) Three-dimensional initial data for the collision of two black holes. 2: Quasicircular orbits for equal mass black holes. Phys Rev D 50:5025–5032. https://doi.org/10.1103/PhysRevD.50.5025. arXiv:gr-qc/9404043
Cook GB (2000) Initial data for numerical relativity. Living Rev Relativ 3:5. https://doi.org/10.12942/lrr-2000-5. arXiv:gr-qc/0007085
Cook GB (2020) Aspects of multimode Kerr ringdown fitting. Phys Rev D 102(2):024027. https://doi.org/10.1103/PhysRevD.102.024027. arXiv:2004.08347 [gr-qc]
Cook GB, York JW Jr (1990) Apparent horizons for boosted or spinning black holes. Phys Rev D 41:1077. https://doi.org/10.1103/PhysRevD.41.1077
Cook GB, Zalutskiy M (2014) Gravitational perturbations of the Kerr geometry: High-accuracy study. Phys Rev D 90(12):124021. https://doi.org/10.1103/PhysRevD.90.124021. arXiv:1410.7698 [gr-qc]
Copeland EJ, Myers RC, Polchinski J (2004) Cosmic F and D strings. JHEP 06:013. https://doi.org/10.1088/1126-6708/2004/06/013. arXiv:hep-th/0312067
Corman M, Ripley JL, East WE (2023) Nonlinear studies of binary black hole mergers in Einstein-scalar-Gauss-Bonnet gravity. Phys Rev D 107(2):024014. https://doi.org/10.1103/PhysRevD.107.024014. arXiv:2210.09235 [gr-qc]
Corman M, Lehner L, East WE, Dideron G (2024) Nonlinear studies of modifications to general relativity: comparing different approaches. Phys Rev D 110(8):084048. https://doi.org/10.1103/PhysRevD.110.084048. arXiv:2405.15581 [gr-qc]
Cornish NJ (2011) Detection strategies for extreme mass ratio inspirals. Class Quantum Grav 28:094016. https://doi.org/10.1088/0264-9381/28/9/094016. arXiv:0804.3323 [gr-qc]
Cornish NJ, Shuman K (2020) Black hole hunting with LISA. Phys Rev D 101(12):124008. https://doi.org/10.1103/PhysRevD.101.124008. arXiv:2005.03610 [gr-qc]
Correia MR, Cardoso V (2018) Characterization of echoes: a Dyson-series representation of individual pulses. Phys Rev D 97(8):084030. https://doi.org/10.1103/PhysRevD.97.084030. arXiv:1802.07735 [gr-qc]
Cotesta R, Buonanno A, Bohé A, Taracchini A, Hinder I, Ossokine S (2018) Enriching the symphony of gravitational waves from binary black holes by tuning higher harmonics. Phys Rev D 98(8):084028. https://doi.org/10.1103/PhysRevD.98.084028. arXiv:1803.10701 [gr-qc]

Cotesta R, Marsat S, Pürrer M (2020) Frequency domain reduced order model of aligned-spin effective-one-body waveforms with higher-order modes. Phys Rev D 101(12):124040. https://doi.org/10.1103/PhysRevD.101.124040. arXiv:2003.12079 [gr-qc]

Cotesta R, Carullo G, Berti E, Cardoso V (2022) Analysis of ringdown overtones in GW150914. Phys Rev Lett 129(11):111102. https://doi.org/10.1103/PhysRevLett.129.111102. arXiv:2201.00822 [gr-qc]

Cristofoli A, Bjerrum-Bohr N, Damgaard PH, Vanhove P (2019) Post-Minkowskian Hamiltonians in general relativity. Phys Rev D 100(8):084040. https://doi.org/10.1103/PhysRevD.100.084040. arXiv:1906.01579 [hep-th]

Cristofoli A, Damgaard PH, Di Vecchia P, Heissenberg C (2020) Second-order Post-Minkowskian scattering in arbitrary dimensions. JHEP 07:122. https://doi.org/10.1007/JHEP07(2020)122. arXiv:2003.10274 [hep-th]

Croft R, Helfer T, Ge BX, Radia M, Evstafyeva T, Lim EA, Sperhake U, Clough K (2023) The gravitational afterglow of boson stars. Class Quantum Grav 40(6):065001. https://doi.org/10.1088/1361-6382/acace4. arXiv:2207.05690 [gr-qc]

Croton DJ, Springel V, White SDM, De Lucia G, Frenk CS, Gao L, Jenkins A, Kauffmann G, Navarro JF, Yoshida N (2006) The Many lives of AGN: Cooling flows, black holes and the luminosities and colours of galaxies. Mon Not R Astron Soc 365:11–28. [Erratum: Mon. Not. R. Astron. Soc. 367, 864 (2006)]. https://doi.org/10.1111/j.1365-2966.2006.09994.x. arXiv:astro-ph/0602065

Crowder J, Cornish N (2007) A solution to the galactic foreground problem for LISA. Phys Rev D 75:043008. https://doi.org/10.1103/PhysRevD.75.043008. arXiv:astro-ph/0611546

Cui Y, Lewicki M, Morrissey DE, Wells JD (2019) Probing the pre-BBN universe with gravitational waves from cosmic strings. JHEP 01:081. https://doi.org/10.1007/JHEP01(2019)081. arXiv:1808.08968 [hep-ph]

Cunha P, Berti E, Herdeiro C (2017) Light-ring stability for ultracompact objects. Phys Rev Lett 119 (25):251102. https://doi.org/10.1103/PhysRevLett.119.251102. arXiv:1708.04211 [gr-qc]

Cunha P, Herdeiro C, Radu E (2019) Spontaneously scalarized kerr black holes in extended scalar-tensor-gauss-bonnet gravity. Phys Rev Lett 123(1):011101. https://doi.org/10.1103/PhysRevLett.123.011101. arXiv:1904.09997 [gr-qc]

Cunha P, Herdeiro C, Radu E, Sanchis-Gual N (2023) Exotic compact objects and the fate of the light-ring instability. Phys Rev Lett 130(6):061401. https://doi.org/10.1103/PhysRevLett.130.061401. arXiv:2207.13713 [gr-qc]

Cutler C, Vallisneri M (2007) LISA detections of massive black hole inspirals: parameter extraction errors due to inaccurate template waveforms. Phys Rev D 76:104018. https://doi.org/10.1103/PhysRevD.76.104018. arXiv:0707.2982 [gr-qc]

Cutler C, Kennefick D, Poisson E (1994) Gravitational radiation reaction for bound motion around a Schwarzschild black hole. Phys Rev D 50:3816–3835. https://doi.org/10.1103/PhysRevD.50.3816

Da Silva LJG, Panosso Macedo R, Thompson JE, Kroon JAV, Durkan L, Long O (2023) Hyperboloidal discontinuous time-symmetric numerical algorithm with higher order jumps for gravitational self-force computations in the time domain. arXiv e-prints arXiv:2306.13153 [gr-qc]

D'Agostino R, Nunes RC (2019) Probing observational bounds on scalar-tensor theories from standard sirens. Phys Rev D 100(4):044041. https://doi.org/10.1103/PhysRevD.100.044041. arXiv:1907.05516 [gr-qc]

D'Agostino R, Nunes RC (2022) Forecasting constraints on deviations from general relativity in f(Q) gravity with standard sirens. Phys Rev D 106(12):124053. https://doi.org/10.1103/PhysRevD.106.124053. arXiv:2210.11935 [gr-qc]

Dai N, Gong Y, Jiang T, Liang D (2022) Intermediate mass-ratio inspirals with dark matter minispikes. Phys Rev D 106(6):064003. https://doi.org/10.1103/PhysRevD.106.064003. arXiv:2111.13514 [gr-qc]

Dain S, Lousto CO, Takahashi R (2002) New conformally flat initial data for spinning black holes. Phys Rev D 65:104038. https://doi.org/10.1103/PhysRevD.65.104038. arXiv:gr-qc/0201062

Damgaard PH, Vanhove P (2021) Remodeling the effective one-body formalism in post-Minkowskian gravity. Phys Rev D 104(10):104029. https://doi.org/10.1103/PhysRevD.104.104029. arXiv:2108.11248 [hep-th]

Damgaard PH, Plante L, Vanhove P (2021) On an exponential representation of the gravitational S-matrix. JHEP 11:213. https://doi.org/10.1007/JHEP11(2021)213. arXiv:2107.12891 [hep-th]

Damour T (1982) Probléme des deux corps et freinage de rayonnement en relativité générale. C R Acad Sci Paris Sér II 294:1355–1357

Damour T (1983) Gravitational radiation and the motion of compact bodies. In: Deruelle N, Piran T (eds) Gravitational radiation: Proceedings of the Advanced Study Institute, Les Houches, Haute-Savoie, France, June 2-21, 1982. North-Holland Publishing, Amsterdam

Damour T (2001) Coalescence of two spinning black holes: an effective one-body approach. Phys Rev D 64:124013. https://doi.org/10.1103/PhysRevD.64.124013. arXiv:gr-qc/0103018

Damour T (2008) Introductory lectures on the effective one body formalism. Int J Mod Phys A 23:1130–1148. https://doi.org/10.1142/S0217751X08039992. arXiv:0802.4047 [gr-qc]

Damour T (2010) Gravitational self force in a Schwarzschild background and the effective one body formalism. Phys Rev D 81:024017. https://doi.org/10.1103/PhysRevD.81.024017. arXiv:0910.5533 [gr-qc]

Damour T (2016) Gravitational scattering, post-Minkowskian approximation and effective one-body theory. Phys Rev D 94(10):104015. https://doi.org/10.1103/PhysRevD.94.104015. arXiv:1609.00354 [gr-qc]

Damour T (2018) High-energy gravitational scattering and the general relativistic two-body problem. Phys Rev D 97(4):044038. https://doi.org/10.1103/PhysRevD.97.044038. arXiv:1710.10599 [gr-qc]

Damour T (2020) Classical and quantum scattering in post-Minkowskian gravity. Phys Rev D 102 (2):024060. https://doi.org/10.1103/PhysRevD.102.024060. arXiv:1912.02139 [gr-qc]

Damour T (2020) Radiative contribution to classical gravitational scattering at the third order in *G*. Phys Rev D 102(12):124008. https://doi.org/10.1103/PhysRevD.102.124008. arXiv:2010.01641 [gr-qc]

Damour T, Deruelle N (1981) Generalized lagrangian of two point masses in the post-post newtonian approximation of general relativity. Comptes Rendus des Seances de l'Academie des Sciences Serie 2 293(8):537–540

Damour T, Deruelle N (1981) Radiation reaction and angular momentum loss in small angle gravitational scattering. Phys Lett A 87:81. https://doi.org/10.1016/0375-9601(81)90567-3

Damour T, Deruelle N (1985) General relativistic celestial mechanics of binary systems I. The post-Newtonian motion. Ann Inst Henri Poincaré 43:107

Damour T, Deruelle N (1986) General relativistic celestial mechanics of binary systems II. The post-Newtonian timing formula. Ann Inst Henri Poincaré 44:263

Damour T, Nagar A (2007) Faithful effective-one-body waveforms of small-mass-ratio coalescing black-hole binaries. Phys Rev D 76:064028. https://doi.org/10.1103/PhysRevD.76.064028. arXiv:0705.2519 [gr-qc]

Damour T, Nagar A (2008) Comparing Effective-One-Body gravitational waveforms to accurate numerical data. Phys Rev D 77:024043. https://doi.org/10.1103/PhysRevD.77.024043. arXiv:0711.2628 [gr-qc]

Damour T, Nagar A (2009) An Improved analytical description of inspiralling and coalescing black-hole binaries. Phys Rev D 79:081503. https://doi.org/10.1103/PhysRevD.79.081503. arXiv:0902.0136 [gr-qc]

Damour T, Nagar A (2010) Effective One Body description of tidal effects in inspiralling compact binaries. Phys Rev D 81:084016. https://doi.org/10.1103/PhysRevD.81.084016. arXiv:0911.5041 [gr-qc]

Damour T, Nagar A (2014) A new analytic representation of the ringdown waveform of coalescing spinning black hole binaries. Phys Rev D 90(2):024054. https://doi.org/10.1103/PhysRevD.90.024054. arXiv:1406.0401 [gr-qc]

Damour T, Nagar A (2014) New effective-one-body description of coalescing nonprecessing spinning black-hole binaries. Phys Rev D 90(4):044018. https://doi.org/10.1103/PhysRevD.90.044018. arXiv:1406.6913 [gr-qc]

Damour T, Nagar A (2016) The effective-one-body approach to the general relativistic two body problem. Lect Notes Phys 905:273–312. https://doi.org/10.1007/978-3-319-19416-5_7

Damour T, Rettegno P (2023) Strong-field scattering of two black holes: numerical relativity meets post-Minkowskian gravity. Phys Rev D 107(6):064051. https://doi.org/10.1103/PhysRevD.107.064051. arXiv:2211.01399 [gr-qc]

Damour T, Solodukhin SN (2007) Wormholes as black hole foils. Phys Rev D 76:024016. https://doi.org/10.1103/PhysRevD.76.024016. arXiv:0704.2667 [gr-qc]

Damour T, Vilenkin A (1997) Cosmic strings and the string dilaton. Phys Rev Lett 78:2288–2291. https://doi.org/10.1103/PhysRevLett.78.2288. arXiv:gr-qc/9610005

Damour T, Vilenkin A (2000) Gravitational wave bursts from cosmic strings. Phys Rev Lett 85:3761–3764. https://doi.org/10.1103/PhysRevLett.85.3761. arXiv:gr-qc/0004075

Damour T, Vilenkin A (2001) Gravitational wave bursts from cusps and kinks on cosmic strings. Phys Rev D 64:064008. https://doi.org/10.1103/PhysRevD.64.064008. arXiv:gr-qc/0104026

Damour T, Vilenkin A (2005) Gravitational radiation from cosmic (super)strings: bursts, stochastic background, and observational windows. Phys Rev D 71:063510. https://doi.org/10.1103/PhysRevD.71.063510. arXiv:hep-th/0410222

Damour T, Iyer BR, Sathyaprakash BS (1998) Improved filters for gravitational waves from inspiralling compact binaries. Phys Rev D 57:885–907. https://doi.org/10.1103/PhysRevD.57.885. arXiv:gr-qc/9708034

Damour T, Jaranowski P, Schäfer G (2000) On the determination of the last stable orbit for circular general relativistic binaries at the third postNewtonian approximation. Phys Rev D 62:084011. https://doi.org/10.1103/PhysRevD.62.084011. arXiv:gr-qc/0005034

Damour T, Gourgoulhon E, Grandclement P (2002) Circular orbits of corotating binary black holes: comparison between analytical and numerical results. Phys Rev D 66:024007. https://doi.org/10.1103/PhysRevD.66.024007. arXiv:gr-qc/0204011

Damour T, Iyer BR, Jaranowski P, Sathyaprakash BS (2003) Gravitational waves from black hole binary inspiral and merger: the Span of third postNewtonian effective one-body templates. Phys Rev D 67:064028. https://doi.org/10.1103/PhysRevD.67.064028. arXiv:gr-qc/0211041

Damour T, Gopakumar A, Iyer BR (2004) Phasing of gravitational waves from inspiralling eccentric binaries. Phys Rev D 70:064028. https://doi.org/10.1103/PhysRevD.70.064028. arXiv:gr-qc/0404128

Damour T, Jaranowski P, Schäfer G (2008) Effective one body approach to the dynamics of two spinning black holes with next-to-leading order spin-orbit coupling. Phys Rev D 78:024009. https://doi.org/10.1103/PhysRevD.78.024009. arXiv:0803.0915 [gr-qc]

Damour T, Jaranowski P, Schäfer G (2008) Hamiltonian of two spinning compact bodies with next-to-leading order gravitational spin-orbit coupling. Phys Rev D 77:064032. https://doi.org/10.1103/PhysRevD.77.064032. arXiv:0711.1048 [gr-qc]

Damour T, Nagar A, Dorband EN, Pollney D, Rezzolla L (2008) Faithful effective-one-body waveforms of equal-mass coalescing black-hole binaries. Phys Rev D 77:084017. https://doi.org/10.1103/PhysRevD.77.084017. arXiv:0712.3003 [gr-qc]

Damour T, Nagar A, Hannam M, Husa S, Brügmann B (2008) Accurate effective-one-body waveforms of inspiralling and coalescing black-hole binaries. Phys Rev D 78:044039. https://doi.org/10.1103/PhysRevD.78.044039. arXiv:0803.3162 [gr-qc]

Damour T, Iyer BR, Nagar A (2009) Improved resummation of post-Newtonian multipolar waveforms from circularized compact binaries. Phys Rev D 79:064004. https://doi.org/10.1103/PhysRevD.79.064004. arXiv:0811.2069 [gr-qc]

Damour T, Nagar A, Pollney D, Reisswig C (2012) Energy versus angular momentum in black hole binaries. Phys Rev Lett 108:131101. https://doi.org/10.1103/PhysRevLett.108.131101. arXiv:1110.2938 [gr-qc]

Damour T, Nagar A, Villain L (2012) Measurability of the tidal polarizability of neutron stars in late-inspiral gravitational-wave signals. Phys Rev D 85:123007. https://doi.org/10.1103/PhysRevD.85.123007. arXiv:1203.4352 [gr-qc]

Damour T, Nagar A, Bernuzzi S (2013) Improved effective-one-body description of coalescing nonspinning black-hole binaries and its numerical-relativity completion. Phys Rev D 87 (8):084035. https://doi.org/10.1103/PhysRevD.87.084035. arXiv:1212.4357 [gr-qc]

Damour T, Guercilena F, Hinder I, Hopper S, Nagar A, Rezzolla L (2014) Strong-field scattering of two black holes: numerics versus analytics. Phys Rev D 89(8):081503. https://doi.org/10.1103/PhysRevD.89.081503. arXiv:1402.7307 [gr-qc]

Damour T, Jaranowski P, Schäfer G (2014) Nonlocal-in-time action for the fourth post-Newtonian conservative dynamics of two-body systems. Phys Rev D 89(6):064058. https://doi.org/10.1103/PhysRevD.89.064058. arXiv:1401.4548 [gr-qc]

Damour T, Jaranowski P, Schäfer G (2015) Fourth post-Newtonian effective one-body dynamics. Phys Rev D 91(8):084024. https://doi.org/10.1103/PhysRevD.91.084024. arXiv:1502.07245 [gr-qc]

Damour T, Jaranowski P, Schäfer G (2016) Conservative dynamics of two-body systems at the fourth post-Newtonian approximation of general relativity. Phys Rev D 93(8):084014. https://doi.org/10.1103/PhysRevD.93.084014. arXiv:1601.01283 [gr-qc]

Dar F, De Rham C, Deskins JT, Giblin JT, Tolley AJ (2019) Scalar gravitational radiation from binaries: vainshtein mechanism in time-dependent systems. Class Quantum Grav 36(2):025008. https://doi.org/10.1088/1361-6382/aaf5e8. arXiv:1808.02165 [hep-th]

Das SR, Mathur SD (2000) The quantum physics of black holes: results from string theory. Ann Rev Nucl Part Sci 50:153–206. https://doi.org/10.1146/annurev.nucl.50.1.153. arXiv:gr-qc/0105063

Daszuta B, Zappa F, Cook W, Radice D, Bernuzzi S, Morozova V (2021) GR-Athena++: puncture evolutions on vertex-centered oct-tree adaptive mesh refinement. Astrophys J Supp 257(2):25. https://doi.org/10.3847/1538-4365/ac157b. arXiv:2101.08289 [gr-qc]
Datta S (2020) Tidal heating of quantum black holes and their imprints on gravitational waves. Phys Rev D 102(6):064040. https://doi.org/10.1103/PhysRevD.102.064040. arXiv:2002.04480 [gr-qc]
Datta S (2022) Probing horizon scale quantum effects with Love. Class Quantum Grav 39(22):225016. https://doi.org/10.1088/1361-6382/ac9ae4. arXiv:2107.07258 [gr-qc]
Datta S, Brito R, Bose S, Pani P, Hughes SA (2020) Tidal heating as a discriminator for horizons in extreme mass ratio inspirals. Phys Rev D 101(4):044004. https://doi.org/10.1103/PhysRevD.101.044004. arXiv:1910.07841 [gr-qc]
Datta S, Gupta A, Kastha S, Arun KG, Sathyaprakash BS (2021) Tests of general relativity using multiband observations of intermediate mass binary black hole mergers. Phys Rev D 103(2):024036. https://doi.org/10.1103/PhysRevD.103.024036. arXiv:2006.12137 [gr-qc]
Davis M, Ruffini R, Tiomno J, Zerilli F (1972) Can synchrotron gravitational radiation exist? Phys Rev Lett 28:1352–1355. https://doi.org/10.1103/PhysRevLett.28.1352
Dax M, Green SR, Gair J, Pürrer M, Wildberger J, Macke JH, Buonanno A, Schölkopf B (2023) Neural importance sampling for rapid and reliable gravitational-wave inference. Phys Rev Lett 130(17):171403. https://doi.org/10.1103/PhysRevLett.130.171403. arXiv:2210.05686 [gr-qc]
van De Meent M (2017) The mass and angular momentum of reconstructed metric perturbations. Class Quantum Grav 34(12):124003. https://doi.org/10.1088/1361-6382/aa71c3. arXiv:1702.00969 [gr-qc]
Deffayet C, Esposito-Farese G, Vikman A (2009) Covariant Galileon. Phys Rev D 79:084003. https://doi.org/10.1103/PhysRevD.79.084003. arXiv:0901.1314 [hep-th]
Delgado J, Herdeiro C, Radu E (2023) EMRIs around j = 1 black holes with synchronised hair. JCAP 10:029. https://doi.org/10.1088/1475-7516/2023/10/029. arXiv:2305.02333 [gr-qc]
Delsate T, Hilditch D, Witek H (2015) Initial value formulation of dynamical Chern-Simons gravity. Phys Rev D 91(2):024027. https://doi.org/10.1103/PhysRevD.91.024027. arXiv:1407.6727 [gr-qc]
DePies MR, Hogan CJ (2007) Stochastic gravitational wave background from light cosmic strings. Phys Rev D 75:125006. https://doi.org/10.1103/PhysRevD.75.125006. arXiv:astro-ph/0702335
DePies MR, Hogan CJ (2009) Harmonic Gravitational Wave Spectra of Cosmic String Loops in the Galaxy. arXiv e-prints arXiv:0904.1052 [astro-ph.CO]
Deppe N, Hébert F, Kidder LE, Teukolsky SA (2022) A high-order shock capturing discontinuous Galerkin-finite difference hybrid method for GRMHD. Class Quantum Grav 39(19):195001. https://doi.org/10.1088/1361-6382/ac8864. arXiv:2109.11645 [gr-qc]
Deppe N, Throwe W, Kidder LE, Vu NL, Hébert F, Moxon J, Armaza C, Bonilla MS, Kim Y, Kumar P, Lovelace G, Macedo A, Nelli KC, O'Shea E, Pfeiffer HP, Scheel MA, Teukolsky SA, Wittek NA, et al. (2023) SpECTRE v2023.04.07. https://doi.org/10.5281/ze2024.7809262, https://spectre-code.org
Deppe N et al (2022) Simulating magnetized neutron stars with discontinuous Galerkin methods. Phys Rev D 105(12):123031. https://doi.org/10.1103/PhysRevD.105.123031. arXiv:2109.12033 [gr-qc]
Derdzinski A, Mayer L (2023) In situ extreme mass ratio inspirals via subparsec formation and migration of stars in thin, gravitationally unstable AGN discs. Mon Not Roy Astron Soc 521(3):4522–4543. https://doi.org/10.1093/mnras/stad749. arXiv:2205.10382 [astro-ph.GA]
Derdzinski A, D'Orazio D, Duffell P, Haiman Z, MacFadyen A (2021) Evolution of gas disc-embedded intermediate mass ratio inspirals in the *LISA* band. Mon Not R Astron Soc 501(3):3540–3557. https://doi.org/10.1093/mnras/staa3976. arXiv:2005.11333 [astro-ph.HE]
Derdzinski AM, D'Orazio D, Duffell P, Haiman Z, MacFadyen A (2019) Probing gas disc physics with LISA: simulations of an intermediate mass ratio inspiral in an accretion disc. Mon Not R Astron Soc 486(2):2754–2765. [Erratum: Mon. Not. R. Astron. Soc. 489, 4860-4861 (2019)]. https://doi.org/10.1093/mnras/stz1026. arXiv:1810.03623 [astro-ph.HE]
Destounis K, Kokkotas KD (2021) Gravitational-wave glitches: resonant islands and frequency jumps in nonintegrable extreme-mass-ratio inspirals. Phys Rev D 104(6):064023. https://doi.org/10.1103/PhysRevD.104.064023. arXiv:2108.02782 [gr-qc]
Destounis K, Suvorov AG, Kokkotas KD (2020) Testing spacetime symmetry through gravitational waves from extreme-mass-ratio inspirals. Phys Rev D 102(6):064041. https://doi.org/10.1103/PhysRevD.102.064041. arXiv:2009.00028 [gr-qc]
Destounis K, Suvorov AG, Kokkotas KD (2021) Gravitational-wave glitches in chaotic extreme-mass-ratio inspirals. Phys Rev Lett 126(14):141102. https://doi.org/10.1103/PhysRevLett.126.141102. arXiv:2103.05643 [gr-qc]

Destounis K, Angeloni F, Vaglio M, Pani P (2023) Extreme-mass-ratio inspirals into rotating boson stars: nonintegrability, chaos, and transient resonances. Phys Rev D 108(8):084062. https://doi.org/10.1103/PhysRevD.108.084062. arXiv:2305.05691 [gr-qc]

Destounis K, Kulathingal A, Kokkotas KD, Papadopoulos GO (2023) Gravitational-wave imprints of compact and galactic-scale environments in extreme-mass-ratio binaries. Phys Rev D 107(8):084027. https://doi.org/10.1103/PhysRevD.107.084027. arXiv:2210.09357 [gr-qc]

Detweiler S (2012) Gravitational radiation reaction and second order perturbation theory. Phys Rev D 85:044048. https://doi.org/10.1103/PhysRevD.85.044048. arXiv:1107.2098 [gr-qc]

Detweiler SL (1980) Black holes and gravitational waves. III. The resonant frequencies of rotating holes. Astrophys J 239:292–295. https://doi.org/10.1086/158109

Detweiler SL (1980) Klein-Gordon equation and rotating black holes. Phys Rev D 22:2323–2326. https://doi.org/10.1103/PhysRevD.22.2323

Detweiler SL (2001) Radiation reaction and the selfforce for a point mass in general relativity. Phys Rev Lett 86:1931–1934. https://doi.org/10.1103/PhysRevLett.86.1931. arXiv:gr-qc/0011039

Detweiler SL, Whiting BF (2003) Selfforce via a Green's function decomposition. Phys Rev D 67:024025. https://doi.org/10.1103/PhysRevD.67.024025. arXiv:gr-qc/0202086

Detweiler SL, Messaritaki E, Whiting BF (2003) Selfforce of a scalar field for circular orbits about a Schwarzschild black hole. Phys Rev D 67:104016. https://doi.org/10.1103/PhysRevD.67.104016. arXiv:gr-qc/0205079

Devine C, Etienne ZB, McWilliams ST (2016) Optimizing spinning time-domain gravitational waveforms for Advanced LIGO data analysis. Class Quantum Grav 33(12):125025. https://doi.org/10.1088/0264-9381/33/12/125025. arXiv:1601.03393 [astro-ph.HE]

DeVore R, Petrova G, Wojtaszczyk P (2013) Greedy algorithms for reduced bases in Banach spaces. Constr Approx 37(3):455. https://doi.org/10.1007/s00365-013-9186-2

Dhani A (2021) Importance of mirror modes in binary black hole ringdown waveform. Phys Rev D 103 (10):104048. https://doi.org/10.1103/PhysRevD.103.104048. arXiv:2010.08602 [gr-qc]

Dhesi M, Rüter HR, Pound A, Barack L, Pfeiffer HP (2021) Worldtube excision method for intermediate-mass-ratio inspirals: scalar-field toy model. Phys Rev D 104(12):124002. https://doi.org/10.1103/PhysRevD.104.124002. arXiv:2109.03531 [gr-qc]

Di Vecchia P, Heissenberg C, Russo R, Veneziano G (2020) Universality of ultra-relativistic gravitational scattering. Phys Lett B 811:135924. https://doi.org/10.1016/j.physletb.2020.135924. arXiv:2008.12743 [hep-th]

Di Vecchia P, Heissenberg C, Russo R, Veneziano G (2021) Radiation reaction from soft theorems. Phys Lett B 818:136379. https://doi.org/10.1016/j.physletb.2021.136379. arXiv:2101.05772 [hep-th]

Di Vecchia P, Heissenberg C, Russo R, Veneziano G (2021) The eikonal approach to gravitational scattering and radiation at $\mathcal{O}(G^3)$. JHEP 07:169. https://doi.org/10.1007/JHEP07(2021)169. arXiv:2104.03256 [hep-th]

Dias O, Godazgar M, Santos JE (2015) Linear mode stability of the Kerr-Newman black hole and its quasinormal modes. Phys Rev Lett 114(15):151101. https://doi.org/10.1103/PhysRevLett.114.151101. arXiv:1501.04625 [gr-qc]

Dias O, Godazgar M, Santos JE (2022) Eigenvalue repulsions and quasinormal mode spectra of Kerr-Newman: an extended study. JHEP 07:076. https://doi.org/10.1007/JHEP07(2022)076. arXiv:2205.13072 [gr-qc]

Dias O, Godazgar M, Santos JE, Carullo G, Del Pozzo W, Laghi D (2022) Eigenvalue repulsions in the quasinormal spectra of the Kerr-Newman black hole. Phys Rev D 105(8):084044. https://doi.org/10.1103/PhysRevD.105.084044. arXiv:2109.13949 [gr-qc]

Dias O, Lingetti G, Pani P, Santos JE (2023) Black hole superradiant instability for massive spin-2 fields. Phys Rev D 108(4):L041502. https://doi.org/10.1103/PhysRevD.108.L041502. arXiv:2304.01265 [gr-qc]

Diaz-Rivera LM, Messaritaki E, Whiting BF, Detweiler SL (2004) Scalar field self-force effects on orbits about a Schwarzschild black hole. Phys Rev D 70:124018. https://doi.org/10.1103/PhysRevD.70.124018. arXiv:gr-qc/0410011

Dickey CM, Geha M, Wetzel A, El-Badry K (2019) AGN all the way down? AGN-like line ratios are common in the lowest-mass isolated quiescent galaxies. Astrophys J 884(2):180. https://doi.org/10.3847/1538-4357/ab3220. arXiv:1902.01401 [astro-ph.GA]

Diener P, Vega I, Wardell B, Detweiler S (2012) Self-consistent orbital evolution of a particle around a Schwarzschild black hole. Phys Rev Lett 108:191102. https://doi.org/10.1103/PhysRevLett.108.191102. arXiv:1112.4821 [gr-qc]

Dietrich T, Bernuzzi S, Ujevic M, Brügmann B (2015) Numerical relativity simulations of neutron star merger remnants using conservative mesh refinement. Phys Rev D 91(12):124041. https://doi.org/10.1103/PhysRevD.91.124041. arXiv:1504.01266 [gr-qc]

Dietrich T, Moldenhauer N, Johnson-McDaniel NK, Bernuzzi S, Markakis CM, Brügmann B, Tichy W (2015) Binary neutron stars with generic spin, eccentricity, mass ratio, and compactness - quasi-equilibrium sequences and first evolutions. Phys Rev D 92(12):124007. https://doi.org/10.1103/PhysRevD.92.124007. arXiv:1507.07100 [gr-qc]

Dietrich T, Bernuzzi S, Tichy W (2017) Closed-form tidal approximants for binary neutron star gravitational waveforms constructed from high-resolution numerical relativity simulations. Phys Rev D 96(12):121501. https://doi.org/10.1103/PhysRevD.96.121501. arXiv:1706.02969 [gr-qc]

Dietrich T, Radice D, Bernuzzi S, Zappa F, Perego A, Brügmann B, Chaurasia SV, Dudi R, Tichy W, Ujevic M (2018) CoRe database of binary neutron star merger waveforms. Class Quantum Grav 35 (24):24LT01. https://doi.org/10.1088/1361-6382/aaebc0. arXiv:1806.01625 [gr-qc]

Dietrich T, Ossokine S, Clough K (2019) Full 3D numerical relativity simulations of neutron star-boson star collisions with BAM. Class Quantum Grav 36(2):025002. https://doi.org/10.1088/1361-6382/aaf43e. arXiv:1807.06959 [gr-qc]

Dietrich T, Samajdar A, Khan S, Johnson-McDaniel NK, Dudi R, Tichy W (2019) Improving the NRTidal model for binary neutron star systems. Phys Rev D 100(4):044003. https://doi.org/10.1103/PhysRevD.100.044003. arXiv:1905.06011 [gr-qc]

Dietrich T et al (2019) Matter imprints in waveform models for neutron star binaries: Tidal and self-spin effects. Phys Rev D 99(2):024029. https://doi.org/10.1103/PhysRevD.99.024029. arXiv:1804.02235 [gr-qc]

Digman MC, Hirata CM, Hirata CM (2023) LISA Galactic binaries in the Roman Galactic Bulge Time-Domain Survey. Mon Not R Astron Soc 525(1):393–401. https://doi.org/10.1093/mnras/stad2290. arXiv:2212.14887 [astro-ph.GA]

Dima A, Barausse E, Franchini N, Sotiriou TP (2020) Spin-induced black hole spontaneous scalarization. Phys Rev Lett 125(23):231101. https://doi.org/10.1103/PhysRevLett.125.231101. arXiv:2006.03095 [gr-qc]

Dixon WG (1970) Dynamics of extended bodies in general relativity. I. Momentum and angular momentum. Proc R Soc Lond A 314:499–527. https://doi.org/10.1098/rspa.1970.0020

Dixon WG (1970) Dynamics of extended bodies in general relativity. II. Moments of the charge-current vector. Proc R Soc Lond A 319:509–547. https://doi.org/10.1098/rspa.1970.0191

Dixon WG (1974) Dynamics of extended bodies in general relativity III. Equations of motion. Phil Trans R Soc Lond A 277(1264):59–119. https://doi.org/10.1098/rsta.1974.0046

Dlapa C, Kälin G, Liu Z, Porto RA (2022) Conservative dynamics of binary systems at fourth Post-Minkowskian order in the large-eccentricity expansion. Phys Rev Lett 128(16):161104. https://doi.org/10.1103/PhysRevLett.128.161104. arXiv:2112.11296 [hep-th]

Dlapa C, Kälin G, Liu Z, Porto RA (2022) Dynamics of binary systems to fourth Post-Minkowskian order from the effective field theory approach. Phys Lett B 831:137203. https://doi.org/10.1016/j.physletb.2022.137203. arXiv:2106.08276 [hep-th]

Dlapa C, Kälin G, Liu Z, Neef J, Porto RA (2023) Radiation reaction and gravitational waves at fourth Post-Minkowskian order. Phys Rev Lett 130(10):101401. https://doi.org/10.1103/PhysRevLett.130.101401. arXiv:2210.05541 [hep-th]

Doctor Z, Farr B, Holz DE, Pürrer M (2017) Statistical gravitational waveform models: what to simulate next? Phys Rev D 96(12):123011. https://doi.org/10.1103/PhysRevD.96.123011. arXiv:1706.05408 [astro-ph.HE]

Dolan SR (2007) Instability of the massive Klein-Gordon field on the Kerr spacetime. Phys Rev D 76:084001. https://doi.org/10.1103/PhysRevD.76.084001. arXiv:0705.2880 [gr-qc]

Dolan SR (2010) The quasinormal mode spectrum of a kerr black hole in the eikonal limit. Phys Rev D 82:104003. https://doi.org/10.1103/PhysRevD.82.104003. arXiv:1007.5097 [gr-qc]

Dolan SR, Barack L (2013) Self-force via *m*-mode regularization and 2+1D evolution: III. Gravitational field on Schwarzschild spacetime. Phys Rev D 87:084066. https://doi.org/10.1103/PhysRevD.87.084066. arXiv:1211.4586 [gr-qc]

Dolan SR, Ottewill AC (2009) On an expansion method for black hole quasinormal modes and regge poles. Class Quantum Grav 26:225003. https://doi.org/10.1088/0264-9381/26/22/225003. arXiv:0908.0329 [gr-qc]

Dolan SR, Kavanagh C, Wardell B (2022) Gravitational perturbations of rotating black holes in lorenz gauge. Phys Rev Lett 128(15):151101. https://doi.org/10.1103/PhysRevLett.128.151101. arXiv:2108.06344 [gr-qc]

Dolan SR, Durkan L, Kavanagh C, Wardell B (2024) Metric perturbations of Kerr spacetime in Lorenz gauge: circular equatorial orbits. Class Quantum Grav 41(15):155011. https://doi.org/10.1088/1361-6382/ad52e3. arXiv:2306.16459 [gr-qc]

Doneva DD, Yazadjiev SS (2018) New gauss-bonnet black holes with curvature-induced scalarization in extended scalar-tensor theories. Phys Rev Lett 120(13):131103. https://doi.org/10.1103/PhysRevLett.120.131103. arXiv:1711.01187 [gr-qc]

Doneva DD, Yazadjiev SS (2021) Dynamics of the nonrotating and rotating black hole scalarization. Phys Rev D 103(6):064024. https://doi.org/10.1103/PhysRevD.103.064024. arXiv:2101.03514 [gr-qc]

Doneva DD, Yazadjiev SS (2021) Spontaneously scalarized black holes in dynamical Chern-Simons gravity: dynamics and equilibrium solutions. Phys Rev D 103(8):083007. https://doi.org/10.1103/PhysRevD.103.083007. arXiv:2102.03940 [gr-qc]

Doneva DD, Vañó Viñuales A, Yazadjiev SS (2022) Dynamical descalarization with a jump during a black hole merger. Phys Rev D 106(6):L061502. https://doi.org/10.1103/PhysRevD.106.L061502. arXiv:2204.05333 [gr-qc]

Doneva DD, Aresté Saló L, Clough K, Figueras P, Yazadjiev SS (2023) Testing the limits of scalar-Gauss-Bonnet gravity through nonlinear evolutions of spin-induced scalarization. Phys Rev D 108(8):084017. https://doi.org/10.1103/PhysRevD.108.084017. arXiv:2307.06474 [gr-qc]

Doneva DD, Ramazanoğlu FM, Silva HO, Sotiriou TP, Yazadjiev SS (2024) Spontaneous scalarization. Rev Mod Phys 96(1):015004. https://doi.org/10.1103/RevModPhys.96.015004. arXiv:2211.01766 [gr-qc]

Dosopoulou F, Antonini F (2017) Dynamical friction and the evolution of Supermassive Black hole Binaries: the final hundred-parsec problem. Astrophys J 840(1):31. https://doi.org/10.3847/1538-4357/aa6b58. arXiv:1611.06573 [astro-ph.GA]

Dotti M, Volonteri M, Perego A, Colpi M, Ruszkowski M, Haardt F (2010) Dual black holes in merger remnants. II: spin evolution and gravitational recoil. Mon Not R Astron Soc 402:682. https://doi.org/10.1111/j.1365-2966.2009.15922.x. arXiv:0910.5729 [astro-ph.HE]

Dotti M, Colpi M, Pallini S, Perego A, Volonteri M (2013) On the orientation and magnitude of the black hole spin in galactic nuclei. Astrophys J 762:68. https://doi.org/10.1088/0004-637X/762/2/68. arXiv:1211.4871 [astro-ph.CO]

Doulis G, Atteneder F, Bernuzzi S, Brügmann B (2022) Entropy-limited higher-order central scheme for neutron star merger simulations. Phys Rev D 106(2):024001. https://doi.org/10.1103/PhysRevD.106.024001. arXiv:2202.08839 [gr-qc]

Drago M et al (2021) Coherent WaveBurst, a pipeline for unmodeled gravitational-wave data analysis. SoftwareX 14:100678. https://doi.org/10.1016/j.softx.2021.100678. arXiv:2006.12604 [gr-qc]

Drasco S, Hughes SA (2006) Gravitational wave snapshots of generic extreme mass ratio inspirals. Phys Rev D 73(2):024027. [Erratum: Phys. Rev. D 88, 109905 (2013), Erratum: Phys. Rev. D 90, 109905 (2014)]. https://doi.org/10.1103/PhysRevD.73.024027. arXiv:gr-qc/0509101

Drasco S, Flanagan EE, Hughes SA (2005) Computing inspirals in Kerr in the adiabatic regime. I. The Scalar case. Class Quantum Grav 22:S801-846. https://doi.org/10.1088/0264-9381/22/15/011. arXiv:gr-qc/0505075

Dreyer O, Kelly BJ, Krishnan B, Finn LS, Garrison D, Lopez-Aleman R (2004) Black hole spectroscopy: testing general relativity through gravitational wave observations. Class Quantum Grav 21:787–804. https://doi.org/10.1088/0264-9381/21/4/003. arXiv:gr-qc/0309007

Dror JA, Hiramatsu T, Kohri K, Murayama H, White G (2020) Testing the Seesaw mechanism and Leptogenesis with gravitational waves. Phys Rev Lett 124(4):041804. https://doi.org/10.1103/PhysRevLett.124.041804. arXiv:1908.03227 [hep-ph]

Drummond LV, Hughes SA (2022) Precisely computing bound orbits of spinning bodies around black holes. I. General framework and results for nearly equatorial orbits. Phys Rev D 105(12):124040. https://doi.org/10.1103/PhysRevD.105.124040. arXiv:2201.13334 [gr-qc]

Drummond LV, Hughes SA (2022) Precisely computing bound orbits of spinning bodies around black holes. II. Generic orbits. Phys Rev D 105(12):124041. https://doi.org/10.1103/PhysRevD.105.124041. arXiv:2201.13335 [gr-qc]

Drummond LV, Lynch P, Hanselman AG, Becker DR, Hughes SA (2024) Extreme mass-ratio inspiral and waveforms for a spinning body into a Kerr black hole via osculating geodesics and near-identity transformations. Phys Rev D 109(6):064030. https://doi.org/10.1103/PhysRevD.109.064030. arXiv:2310.08438 [gr-qc]
Duez MD, Zlochower Y (2019) Numerical relativity of compact binaries in the 21st century. Rept Prog Phys 82(1):016902. https://doi.org/10.1088/1361-6633/aadb16. arXiv:1808.06011 [gr-qc]
Duez MD, Liu YT, Shapiro SL, Stephens BC (2005) Relativistic magnetohydrodynamics in dynamical spacetimes: numerical methods and tests. Phys Rev D 72:024028. https://doi.org/10.1103/PhysRevD.72.024028. arXiv:astro-ph/0503420
Dunsky DI, Ghoshal A, Murayama H, Sakakihara Y, White G (2022) GUTs, hybrid topological defects, and gravitational waves. Phys Rev D 106(7):075030. https://doi.org/10.1103/PhysRevD.106.075030. arXiv:2111.08750 [hep-ph]
Durkan L, Warburton N (2022) Slow evolution of the metric perturbation due to a quasicircular inspiral into a Schwarzschild black hole. Phys Rev D 106(8):084023. https://doi.org/10.1103/PhysRevD.106.084023. arXiv:2206.08179 [gr-qc]
Dvali G, Vilenkin A (2004) Formation and evolution of cosmic D strings. JCAP 03:010. https://doi.org/10.1088/1475-7516/2004/03/010. arXiv:hep-th/0312007
Dvali GR, Tye S (1999) Brane inflation. Phys Lett B 450:72–82. https://doi.org/10.1016/S0370-2693(99)00132-X. arXiv:hep-ph/9812483
East WE (2017) Superradiant instability of massive vector fields around spinning black holes in the relativistic regime. Phys Rev D 96(2):024004. https://doi.org/10.1103/PhysRevD.96.024004. arXiv:1705.01544 [gr-qc]
East WE (2018) Massive boson superradiant instability of black holes: nonlinear growth, saturation, and gravitational radiation. Phys Rev Lett 121(13):131104. https://doi.org/10.1103/PhysRevLett.121.131104. arXiv:1807.00043 [gr-qc]
East WE (2022) Vortex string formation in black hole superradiance of a dark photon with the higgs mechanism. Phys Rev Lett 129(14):141103. https://doi.org/10.1103/PhysRevLett.129.141103. arXiv:2205.03417 [hep-ph]
East WE, Pretorius F (2017) Superradiant instability and backreaction of massive vector fields around kerr black holes. Phys Rev Lett 119(4):041101. https://doi.org/10.1103/PhysRevLett.119.041101. arXiv:1704.04791 [gr-qc]
East WE, Pretorius F (2022) Binary neutron star mergers in Einstein-scalar-Gauss-Bonnet gravity. Phys Rev D 106(10):104055. https://doi.org/10.1103/PhysRevD.106.104055. arXiv:2208.09488 [gr-qc]
East WE, Ripley JL (2021) Dynamics of spontaneous black hole scalarization and mergers in Einstein-Scalar-Gauss-Bonnet gravity. Phys Rev Lett 127(10):101102. https://doi.org/10.1103/PhysRevLett.127.101102. arXiv:2105.08571 [gr-qc]
East WE, Ripley JL (2021) Evolution of Einstein-scalar-Gauss-Bonnet gravity using a modified harmonic formulation. Phys Rev D 103(4):044040. https://doi.org/10.1103/PhysRevD.103.044040. arXiv:2011.03547 [gr-qc]
Ebersold M, Boetzel Y, Faye G, Mishra CK, Iyer BR, Jetzer P (2019) Gravitational-wave amplitudes for compact binaries in eccentric orbits at the third post-Newtonian order: memory contributions. Phys Rev D 100(8):084043. https://doi.org/10.1103/PhysRevD.100.084043. arXiv:1906.06263 [gr-qc]
Economou A, Harari D, Sakellariadou M (1992) Gravitational effects of traveling waves along global cosmic strings. Phys Rev D 45:433–440. https://doi.org/10.1103/PhysRevD.45.433
Eda K, Itoh Y, Kuroyanagi S, Silk J (2013) New probe of dark-matter properties: gravitational waves from an intermediate-mass black hole embedded in a dark-matter minispike. Phys Rev Lett 110(22):221101. https://doi.org/10.1103/PhysRevLett.110.221101. arXiv:1301.5971 [gr-qc]
Eda K, Itoh Y, Kuroyanagi S, Silk J (2015) Gravitational waves as a probe of dark matter minispikes. Phys Rev D 91(4):044045. https://doi.org/10.1103/PhysRevD.91.044045. arXiv:1408.3534 [gr-qc]
Edlund JA, Tinto M, Krolak A, Nelemans G (2005) Simulation of the White Dwarf - White Dwarf galactic background in the LISA data. Class Quantum Grav 22:S913–S926. https://doi.org/10.1088/0264-9381/22/18/S05. arXiv:gr-qc/0504026
Edwards T, Wong K, Lam K, Coogan A, Foreman-Mackey D, Isi M, Zimmerman A (2024) Differentiable and hardware-accelerated waveforms for gravitational wave data analysis. Phys Rev D 110(6):064028. https://doi.org/10.1103/PhysRevD.110.064028. arXiv:2302.05329 [astro-ph.IM]
Einstein A (1918) Über Gravitationswellen. Sitzungsber Preuss Akad Wiss Berlin (Math Phys) 1918:154–167

Einstein A, Rosen N (1935) The particle problem in the general theory of relativity. Phys Rev 48:73–77. https://doi.org/10.1103/PhysRev.48.73
Einstein A, Infeld L, Hoffmann B (1938) The gravitational equations and the problem of motion. Annals Math 39:65–100. https://doi.org/10.2307/1968714
Einstein Toolkit (2024) http://einsteintoolkit.org
Elley M, Silva HO, Witek H, Yunes N (2022) Spin-induced dynamical scalarization, descalarization, and stealthness in scalar-Gauss-Bonnet gravity during a black hole coalescence. Phys Rev D 106 (4):044018. https://doi.org/10.1103/PhysRevD.106.044018. arXiv:2205.06240 [gr-qc]
Emami R, Loeb A (2020) Observational signatures of the black hole mass distribution in the galactic center. JCAP 02:021. https://doi.org/10.1088/1475-7516/2020/02/021. arXiv:1903.02578 [astro-ph.HE]
Emami R, Loeb A (2021) Detectability of gravitational waves from a population of inspiralling black holes in Milky Way-mass galaxies. Mon Not R Astron Soc 502(3):3932–3941. https://doi.org/10.1093/mnras/stab290. arXiv:1903.02579 [astro-ph.HE]
EMRI Kludge Suite (2024) EMRI Kludge Suite. http://github.com/alvincjk/EMRI_Kludge_Suite/
Eperon FC, Reall HS, Santos JE (2016) Instability of supersymmetric microstate geometries. JHEP 10:031. https://doi.org/10.1007/JHEP10(2016)031. arXiv:1607.06828 [hep-th]
Estellés H, Ramos-Buades A, Husa S, García-Quirós C, Colleoni M, Haegel L, Jaume R (2021) Phenomenological time domain model for dominant quadrupole gravitational wave signal of coalescing binary black holes. Phys Rev D 103(12):124060. https://doi.org/10.1103/PhysRevD.103.124060. arXiv:2004.08302 [gr-qc]
Estellés H, Colleoni M, García-Quirós C, Husa S, Keitel D, Mateu-Lucena M, Planas ML, Ramos-Buades A (2022) New twists in compact binary waveform modeling: a fast time-domain model for precession. Phys Rev D 105(8):084040. https://doi.org/10.1103/PhysRevD.105.084040. arXiv:2105.05872 [gr-qc]
Estellés H, Husa S, Colleoni M, Keitel D, Mateu-Lucena M, García-Quirós C, Ramos-Buades A, Borchers A (2022) Time-domain phenomenological model of gravitational-wave subdominant harmonics for quasicircular nonprecessing binary black hole coalescences. Phys Rev D 105(8):084039. https://doi.org/10.1103/PhysRevD.105.084039. arXiv:2012.11923 [gr-qc]
Etienne ZB (2024) Improved moving-puncture techniques for compact binary simulations. Phys Rev D 110(6):064045. https://doi.org/10.1103/PhysRevD.110.064045. arXiv:2404.01137 [gr-qc]
Etienne ZB, Liu YT, Shapiro SL (2010) Relativistic magnetohydrodynamics in dynamical spacetimes: a new AMR implementation. Phys Rev D 82:084031. https://doi.org/10.1103/PhysRevD.82.084031. arXiv:1007.2848 [astro-ph.HE]
Etienne ZB, Paschalidis V, Haas R, Mösta P, Shapiro SL (2015) IllinoisGRMHD: an open-source, user-friendly GRMHD code for dynamical spacetimes. Class Quantum Grav 32:175009. https://doi.org/10.1088/0264-9381/32/17/175009. arXiv:1501.07276 [astro-ph.HE]
Evans CR, Iben I, Smarr L (1987) Degenerate dwarf binaries as promising, detectable sources of gravitational radiation. Astrophys J 323:129–139. https://doi.org/10.1086/165812
Evstafyeva T, Sperhake U, Helfer T, Croft R, Radia M, Ge BX, Lim EA (2023) Unequal-mass boson-star binaries: initial data and merger dynamics. Class Quantum Grav 40(8):085009. https://doi.org/10.1088/1361-6382/acc2a8. arXiv:2212.08023 [gr-qc]
Fan J, Katz A, Randall L, Reece M (2013) Double-disk dark matter. Phys Dark Univ 2:139–156. https://doi.org/10.1016/j.dark.2013.07.001. arXiv:1303.1521 [astro-ph.CO]
Fan XL, Chen YB (2018) Stochastic gravitational-wave background from spin loss of black holes. Phys Rev D 98(4):044020. https://doi.org/10.1103/PhysRevD.98.044020. arXiv:1712.00784 [gr-qc]
Farmer R, Renzo M, de Mink SE, Marchant P, Justham S (2019) Mind the gap: the location of the lower edge of the pair instability supernovae black hole mass gap. Astrophys J 887(1):53. https://doi.org/10.3847/1538-4357/ab518b. arXiv:1910.12874 [astro-ph.SR]
Farr WM, Stevenson S, Coleman Miller M, Mandel I, Farr B, Vecchio A (2017) Distinguishing spin-aligned and isotropic black hole populations with gravitational waves. Nature 548:426. https://doi.org/10.1038/nature23453. arXiv:1706.01385 [astro-ph.HE]
Favata M (2009) Nonlinear gravitational-wave memory from binary black hole mergers. Astrophys J Lett 696:L159–L162. https://doi.org/10.1088/0004-637X/696/2/L159. arXiv:0902.3660 [astro-ph.SR]
Favata M, Hughes SA, Holz DE (2004) How black holes get their kicks: gravitational radiation recoil revisited. Astrophys J Lett 607:L5–L8. https://doi.org/10.1086/421552. arXiv:astro-ph/0402056

Faye G, Blanchet L, Buonanno A (2006) Higher-order spin effects in the dynamics of compact binaries. I. Equations of motion. Phys Rev D 74:104033. https://doi.org/10.1103/PhysRevD.74.104033. arXiv:gr-qc/0605139

Faye G, Blanchet L, Iyer BR (2015) Non-linear multipole interactions and gravitational-wave octupole modes for inspiralling compact binaries to third-and-a-half post-Newtonian order. Class Quantum Grav 32(4):045016. https://doi.org/10.1088/0264-9381/32/4/045016. arXiv:1409.3546 [gr-qc]

Fedrow JM, Ott CD, Sperhake U, Blackman J, Haas R, Reisswig C, De Felice A (2017) Gravitational waves from binary black hole mergers inside stars. Phys Rev Lett 119(17):171103. https://doi.org/10.1103/PhysRevLett.119.171103. arXiv:1704.07383 [astro-ph.HE]

Feinblum DA, McKinley WA (1968) Stable states of a scalar particle in its own gravational field. Phys Rev 168(5):1445. https://doi.org/10.1103/PhysRev.168.1445

Ferguson D, Jani K, Laguna P, Shoemaker D (2021) Assessing the readiness of numerical relativity for LISA and 3G detectors. Phys Rev D 104(4):044037. https://doi.org/10.1103/PhysRevD.104.044037. arXiv:2006.04272 [gr-qc]

Ferguson D, et al. (2023) Second MAYA Catalog of Binary Black Hole Numerical Relativity Waveforms. arXiv e-prints arXiv:2309.00262 [gr-qc]

Fernandes PGS, Herdeiro CAR, Pombo AM, Radu E, Sanchis-Gual N (2019) Spontaneous Scalarisation of Charged Black Holes: Coupling Dependence and Dynamical Features. Class Quantum Grav 36 (13):134002. [Erratum: Class. Quantum Grav. 37, 049501 (2020)]. https://doi.org/10.1088/1361-6382/ab23a1. arXiv:1902.05079 [gr-qc]

Fernández IS, Renkhoff S, Cors D, Brügmann B, Hilditch D (2022) Evolution of Brill waves with an adaptive pseudospectral method. Phys Rev D 106(2):024036. https://doi.org/10.1103/PhysRevD.106.024036. arXiv:2205.04379 [gr-qc]

Fernando M, Duplyakin D, Sundar H (2017) Machine and application aware partitioning for adaptive mesh refinement applications. In: Proceedings of the 26th International Symposium on High-Performance Parallel and Distributed Computing. HPDC '17. Association for Computing Machinery, New York, p 231-242. https://doi.org/10.1145/3078597.3078610

Fernando M, Neilsen D, Hirschmann EW, Sundar H (2019a) A scalable framework for adaptive computational general relativity on heterogeneous clusters. In: Proceedings of the ACM International Conference on Supercomputing. ICS '19. Association for Computing Machinery, New York, NY, p 1-12. https://doi.org/10.1145/3330345.3330346

Fernando M, Neilsen D, Lim H, Hirschmann E, Sundar H (2019) Massively parallel simulations of binary black hole intermediate-mass-ratio inspirals. SIAM J Sci Comput 41(2):C97–C138. https://doi.org/10.1137/18M1196972. arXiv:1807.06128 [gr-qc]

Fernando M, Neilsen D, Zlochower Y, Hirschmann EW, Sundar H (2023) Massively parallel simulations of binary black holes with adaptive wavelet multiresolution. Phys Rev D 107(6):064035. https://doi.org/10.1103/PhysRevD.107.064035. arXiv:2211.11575 [gr-qc]

Ferrarese L, Merritt D (2000) A Fundamental relation between supermassive black holes and their host galaxies. Astrophys J Lett 539:L9. https://doi.org/10.1086/312838. arXiv:astro-ph/0006053

Ferrari V, Kokkotas KD (2000) Scattering of particles by neutron stars: time evolutions for axial perturbations. Phys Rev D 62:107504. https://doi.org/10.1103/PhysRevD.62.107504. arXiv:gr-qc/0008057

Ferreira E (2021) Ultra-light dark matter. Astron Astrophys Rev 29(1):7. https://doi.org/10.1007/s00159-021-00135-6. arXiv:2005.03254 [astro-ph.CO]

Ferreira MC, Macedo C, Cardoso V (2017) Orbital fingerprints of ultralight scalar fields around black holes. Phys Rev D 96(8):083017. https://doi.org/10.1103/PhysRevD.96.083017. arXiv:1710.00830 [gr-qc]

Ficarra G, Pani P, Witek H (2019) Impact of multiple modes on the black-hole superradiant instability. Phys Rev D 99(10):104019. https://doi.org/10.1103/PhysRevD.99.104019. arXiv:1812.02758 [gr-qc]

Field SE, Hesthaven JS, Lau SR (2009) Discontinuous Galerkin method for computing gravitational waveforms from extreme mass ratio binaries. Class Quantum Grav 26:165010. https://doi.org/10.1088/0264-9381/26/16/165010. arXiv:0902.1287 [gr-qc]

Field SE, Galley CR, Herrmann F, Hesthaven JS, Ochsner E, Tiglio M (2011) Reduced basis catalogs for gravitational wave templates. Phys Rev Lett 106:221102. https://doi.org/10.1103/PhysRevLett.106.221102. arXiv:1101.3765 [gr-qc]

Field SE, Galley CR, Hesthaven JS, Kaye J, Tiglio M (2014) Fast prediction and evaluation of gravitational waveforms using surrogate models. Phys Rev X 4(3):031006. https://doi.org/10.1103/PhysRevX.4.031006. arXiv:1308.3565 [gr-qc]

Field SE, Gottlieb S, Grant ZJ, Isherwood LF, Khanna G (2023) A GPU-accelerated mixed-precision WENO method for extremal black hole and gravitational wave physics computations. Appl Math Comput 5:97–115. https://doi.org/10.1007/s42967-021-00129-2. arXiv:2010.04760 [math.NA]
Figueras P, França T (2020) Gravitational collapse in cubic horndeski theories. Class Quantum Grav 37 (22):225009. https://doi.org/10.1088/1361-6382/abb693. arXiv:2006.09414 [gr-qc]
Figueras P, França T (2022) Black hole binaries in cubic Horndeski theories. Phys Rev D 105(12):124004. https://doi.org/10.1103/PhysRevD.105.124004. arXiv:2112.15529 [gr-qc]
Finch E, Moore CJ (2021) Modeling the ringdown from precessing black hole binaries. Phys Rev D 103 (8):084048. https://doi.org/10.1103/PhysRevD.103.084048. arXiv:2102.07794 [gr-qc]
Finch E, Moore CJ (2022) Searching for a ringdown overtone in GW150914. Phys Rev D 106(4):043005. https://doi.org/10.1103/PhysRevD.106.043005. arXiv:2205.07809 [gr-qc]
Finch E, Bartolucci G, Chucherko D, Patterson BG, Korol V, Klein A, Bandopadhyay D, Middleton H, Moore CJ, Vecchio A (2023) Identifying LISA verification binaries among the Galactic population of double white dwarfs. Mon Not R Astron Soc 522(4):5358–5373. https://doi.org/10.1093/mnras/stad1288. arXiv:2210.10812 [astro-ph.SR]
Finn LS, Thorne KS (2000) Gravitational waves from a compact star in a circular, inspiral orbit, in the equatorial plane of a massive, spinning black hole, as observed by LISA. Phys Rev D 62:124021. https://doi.org/10.1103/PhysRevD.62.124021. arXiv:gr-qc/0007074
Fischer NL, Pfeiffer HP (2022) Unified discontinuous Galerkin scheme for a large class of elliptic equations. Phys Rev D 105(2):024034. https://doi.org/10.1103/PhysRevD.105.024034. arXiv:2108.05826 [math.NA]
Fishbach M, Kalogera V (2022) Apples and Oranges: Comparing Black Holes in X-Ray Binaries and Gravitational-wave Sources. Astrophys J Lett 929(2):L26. https://doi.org/10.3847/2041-8213/ac64a5. arXiv:2111.02935 [astro-ph.HE]
Fitchett MJ, Detweiler SL (1984) Linear momentum and gravitational-waves - circular orbits around a schwarzschild black-hole. Mon Not R Astron Soc 211:933–942
Flanagan E, Hinderer T, Moxon J, Pound A (2024) The two-body problem in general relativity in the extreme-mass-ratio limit via multiscale expansions: Foundations, in preparation
Flanagan EE, Hinderer T (2008) Constraining neutron star tidal Love numbers with gravitational wave detectors. Phys Rev D 77:021502. https://doi.org/10.1103/PhysRevD.77.021502. arXiv:0709.1915 [astro-ph]
Flanagan EE, Hinderer T (2012) Transient resonances in the inspirals of point particles into black holes. Phys Rev Lett 109:071102. https://doi.org/10.1103/PhysRevLett.109.071102. arXiv:1009.4923 [gr-qc]
Flanagan EE, Hughes SA (1998) Measuring gravitational waves from binary black hole coalescences: 2. The Waves' information and its extraction, with and without templates. Phys Rev D 57:4566–4587. https://doi.org/10.1103/PhysRevD.57.4566. arXiv:gr-qc/9710129
Flanagan EE, Hughes SA, Ruangsri U (2014) Resonantly enhanced and diminished strong-field gravitational-wave fluxes. Phys Rev D 89(8):084028. https://doi.org/10.1103/PhysRevD.89.084028. arXiv:1208.3906 [gr-qc]
Fock VA (1939) On the motion of finite masses in the General Relativity Theory. Zh Eksp Teor Fiz 9:375
Foffa S, Sturani R (2013) Dynamics of the gravitational two-body problem at fourth post-Newtonian order and at quadratic order in the Newton constant. Phys Rev D 87(6):064011. https://doi.org/10.1103/PhysRevD.87.064011. arXiv:1206.7087 [gr-qc]
Foffa S, Sturani R (2013) Tail terms in gravitational radiation reaction via effective field theory. Phys Rev D 87(4):044056. https://doi.org/10.1103/PhysRevD.87.044056. arXiv:1111.5488 [gr-qc]
Foffa S, Sturani R (2014) Effective field theory methods to model compact binaries. Class Quantum Grav 31(4):043001. https://doi.org/10.1088/0264-9381/31/4/043001. arXiv:1309.3474 [gr-qc]
Foffa S, Sturani R (2019) Conservative dynamics of binary systems to fourth Post-Newtonian order in the EFT approach I: regularized Lagrangian. Phys Rev D 100(2):024047. https://doi.org/10.1103/PhysRevD.100.024047. arXiv:1903.05113 [gr-qc]
Foffa S, Porto RA, Rothstein I, Sturani R (2019) Conservative dynamics of binary systems to fourth Post-Newtonian order in the EFT approach II: renormalized Lagrangian. Phys Rev D 100(2):024048. https://doi.org/10.1103/PhysRevD.100.024048. arXiv:1903.05118 [gr-qc]
Folacci A, Ould El Hadj M (2018) Multipolar gravitational waveforms and ringdowns generated during the plunge from the innermost stable circular orbit into a Schwarzschild black hole. Phys Rev D 98 (8):084008. https://doi.org/10.1103/PhysRevD.98.084008. arXiv:1806.01577 [gr-qc]

Forteza XJ, Mourier P (2021) High-overtone fits to numerical relativity ringdowns: beyond the dismissed n=8 special tone. Phys Rev D 104(12):124072. https://doi.org/10.1103/PhysRevD.104.124072. arXiv:2107.11829 [gr-qc]

Forteza XJ, Bhagwat S, Kumar S, Pani P (2023) Novel ringdown amplitude-phase consistency test. Phys Rev Lett 130(2):021001. https://doi.org/10.1103/PhysRevLett.130.021001. arXiv:2205.14910 [gr-qc]

Foucart F, Kidder LE, Pfeiffer HP, Teukolsky SA (2008) Initial data for black hole-neutron star binaries: a flexible, high-accuracy spectral method. Phys Rev D 77:124051. https://doi.org/10.1103/PhysRevD.77.124051. arXiv:0804.3787 [gr-qc]

Foucart F, Laguna P, Lovelace G, Radice D, Witek H (2022) Snowmass2021 cosmic frontier white paper: numerical relativity for next-generation gravitational-wave probes of fundamental physics. arXiv e-prints arXiv:2203.08139 [gr-qc]

Fragione G, Leigh N (2018) Intermediate-mass ratio inspirals in galactic nuclei. Mon Not R Astron Soc 480(4):5160–5166. https://doi.org/10.1093/mnras/sty2233. arXiv:1807.09281 [astro-ph.GA]

Fraisse AA (2007) Limits on defects formation and hybrid inflationary models with three-year WMAP observations. JCAP 03:008. https://doi.org/10.1088/1475-7516/2007/03/008. arXiv:astro-ph/0603589

Franchini N, Völkel SH (2024) Testing General Relativity with Black Hole Quasi-Normal Modes. In: Bambi C, Cárdenas-Avendaño A (eds) Recent Progress on Gravity Tests: Challenges and Future Perspectives. Springer, Singapore, pp 361–416. https://doi.org/10.1007/978-981-97-2871-8_9. arXiv:2305.01696 [gr-qc]

Franchini N, Bezares M, Barausse E, Lehner L (2022) Fixing the dynamical evolution in scalar-Gauss-Bonnet gravity. Phys Rev D 106(6):064061. https://doi.org/10.1103/PhysRevD.106.064061. arXiv:2206.00014 [gr-qc]

Franciolini G, Hui L, Penco R, Santoni L, Trincherini E (2019) Effective field theory of black hole quasinormal modes in scalar-tensor theories. JHEP 02:127. https://doi.org/10.1007/JHEP02(2019)127. arXiv:1810.07706 [hep-th]

Fransen K, Mayerson DR (2022) Detecting equatorial symmetry breaking with LISA. Phys Rev D 106(6):064035. https://doi.org/10.1103/PhysRevD.106.064035. arXiv:2201.03569 [gr-qc]

Fransen K, Koekoek G, Tielemans R, Vercnocke B (2021) Modeling and detecting resonant tides of exotic compact objects. Phys Rev D 104(4):044044. https://doi.org/10.1103/PhysRevD.104.044044. arXiv:2005.12286 [gr-qc]

Freitas FF, Herdeiro C, Morais AP, Onofre A, Pasechnik R, Radu E, Sanchis-Gual N, Santos R (2024) Generating gravitational waveform libraries of exotic compact binaries with deep learning. Phys Rev D 109(12):124059. https://doi.org/10.1103/PhysRevD.109.124059. arXiv:2203.01267 [gr-qc]

Friedman JL (1978) Ergosphere instability. Commun Math Phys 63(3):243–255. https://doi.org/10.1007/BF01196933

Friedman JL, Uryu K, Shibata M (2002) Thermodynamics of binary black holes and neutron stars. Phys Rev D 65:064035. [Erratum: Phys. Rev. D 70, 129904 (2004)]. https://doi.org/10.1103/PhysRevD.70.129904. arXiv:gr-qc/0108070

Fujibayashi S, Kiuchi K, Nishimura N, Sekiguchi Y, Shibata M (2018) Mass ejection from the remnant of a binary neutron star merger: viscous-radiation hydrodynamics study. Astrophys J 860(1):64. https://doi.org/10.3847/1538-4357/aabafd. arXiv:1711.02093 [astro-ph.HE]

Fujibayashi S, Kiuchi K, Wanajo S, Kyutoku K, Sekiguchi Y, Shibata M (2023) Comprehensive study of mass ejection and nucleosynthesis in binary neutron star mergers leaving short-lived massive neutron stars. Astrophys J 942(1):39. https://doi.org/10.3847/1538-4357/ac9ce0. arXiv:2205.05557 [astro-ph.HE]

Fujibayashi S, Lam A, Shibata M, Sekiguchi Y (2024) Supernovalike explosions of massive rotating stars from disks surrounding a black hole. Phys Rev D 109(2):023031. https://doi.org/10.1103/PhysRevD.109.023031. arXiv:2309.02161 [astro-ph.HE]

Fujita R (2012) Gravitational waves from a particle in circular orbits around a schwarzschild black hole to the 22nd post-newtonian order. Prog Theor Phys 128:971–992. https://doi.org/10.1143/PTP.128.971. arXiv:1211.5535 [gr-qc]

Fujita R (2015) Gravitational waves from a particle in circular orbits around a rotating black hole to the 11th post-newtonian order. PTEP 2015(3):033E01. https://doi.org/10.1093/ptep/ptv012. arXiv:1412.5689 [gr-qc]

Fujita R, Cardoso V (2017) Ultralight scalars and resonances in black-hole physics. Phys Rev D 95(4):044016. https://doi.org/10.1103/PhysRevD.95.044016. arXiv:1612.00978 [gr-qc]

Fujita R, Hikida W (2009) Analytical solutions of bound timelike geodesic orbits in Kerr spacetime. Class Quantum Grav 26:135002. https://doi.org/10.1088/0264-9381/26/13/135002. arXiv:0906.1420 [gr-qc]

Fujita R, Iyer BR (2010) Spherical harmonic modes of 5.5 post-Newtonian gravitational wave polarisations and associated factorised resummed waveforms for a particle in circular orbit around a Schwarzschild black hole. Phys Rev D 82:044051. https://doi.org/10.1103/PhysRevD.82.044051. arXiv:1005.2266 [gr-qc]

Fujita R, Shibata M (2020) Extreme mass ratio inspirals on the equatorial plane in the adiabatic order. Phys Rev D 102(6):064005. https://doi.org/10.1103/PhysRevD.102.064005. arXiv:2008.13554 [gr-qc]

Fujita R, Hikida W, Tagoshi H (2009) An efficient numerical method for computing gravitational waves induced by a particle moving on eccentric inclined orbits around a kerr black hole. Prog Theor Phys 121:843–874. https://doi.org/10.1143/PTP.121.843. arXiv:0904.3810 [gr-qc]

Fujita R, Isoyama S, Le Tiec A, Nakano H, Sago N, Tanaka T (2017) Hamiltonian formulation of the conservative self-force dynamics in the kerr geometry. Class Quantum Grav 34(13):134001. https://doi.org/10.1088/1361-6382/aa7342. arXiv:1612.02504 [gr-qc]

Futamase T, Itoh Y (2007) The post-Newtonian approximation for relativistic compact binaries. Living Rev Relativ 10:2. https://doi.org/10.12942/lrr-2007-2

Gadre B, Pürrer M, Field SE, Ossokine S, Varma V (2024) Fully precessing higher-mode surrogate model of effective-one-body waveforms. Phys Rev D 110(12):124038. https://doi.org/10.1103/PhysRevD.110.124038. arXiv:2203.00381 [gr-qc]

Gair J, Yunes N, Bender CM (2012) Resonances in extreme mass-ratio inspirals: asymptotic and hyperasymptotic analysis. J Math Phys 53:032503. https://doi.org/10.1063/1.3691226. arXiv:1111.3605 [gr-qc]

Gair JR, Barack L, Creighton T, Cutler C, Larson SL, Phinney ES, Vallisneri M (2004) Event rate estimates for LISA extreme mass ratio capture sources. Class Quantum Grav 21:S1595–S1606. https://doi.org/10.1088/0264-9381/21/20/003. arXiv:gr-qc/0405137

Gair JR, Li C, Mandel I (2008) Observable properties of orbits in exact bumpy spacetimes. Phys Rev D 77:024035. https://doi.org/10.1103/PhysRevD.77.024035. arXiv:0708.0628 [gr-qc]

Gair JR, Porter EK, Babak S, Barack L (2008) A constrained metropolis-hastings search for EMRIs in the mock LISA data challenge 1B. Class Quantum Grav 25:184030. https://doi.org/10.1088/0264-9381/25/18/184030. arXiv:0804.3322 [gr-qc]

Gair JR, Tang C, Volonteri M (2010) LISA extreme-mass-ratio inspiral events as probes of the black hole mass function. Phys Rev D 81:104014. https://doi.org/10.1103/PhysRevD.81.104014. arXiv:1004.1921 [astro-ph.GA]

Gair JR, Mandel I, Miller MC, Volonteri M (2011) Exploring intermediate and massive black-hole binaries with the Einstein Telescope. Gen Relativ Gravit 43:485–518. https://doi.org/10.1007/s10714-010-1104-3. arXiv:0907.5450 [astro-ph.CO]

Gair JR, Vallisneri M, Larson SL, Baker JG (2013) Testing general relativity with low-frequency, space-based gravitational-wave detectors. Living Rev Relativ 16:7. https://doi.org/10.12942/lrr-2013-7. arXiv:1212.5575 [gr-qc]

Galaudage S et al (2021) Building Better Spin Models for Merging Binary Black Holes: Evidence for Nonspinning and Rapidly Spinning Nearly Aligned Subpopulations. Astrophys J Lett 921(1):L15. [Erratum: Astrophys. J. Lett. 936, L18 (2022), Erratum: Astrophys. J. 936, L18 (2022)]. https://doi.org/10.3847/2041-8213/ac2f3c. arXiv:2109.02424 [gr-qc]

Galley CR, Hu BL (2009) Self-force on extreme mass ratio inspirals via curved spacetime effective field theory. Phys Rev D 79:064002. https://doi.org/10.1103/PhysRevD.79.064002. arXiv:0801.0900 [gr-qc]

Galley CR, Rothstein IZ (2017) Deriving analytic solutions for compact binary inspirals without recourse to adiabatic approximations. Phys Rev D 95(10):104054. https://doi.org/10.1103/PhysRevD.95.104054. arXiv:1609.08268 [gr-qc]

Galley CR, Leibovich AK, Porto RA, Ross A (2016) Tail effect in gravitational radiation reaction: time nonlocality and renormalization group evolution. Phys Rev D 93:124010. https://doi.org/10.1103/PhysRevD.93.124010. arXiv:1511.07379 [gr-qc]

Gallouin L, Nakano H, Yunes N, Campanelli M (2012) Asymptotically matched spacetime metric for non-precessing, spinning black hole binaries. Class Quantum Grav 29:235013. https://doi.org/10.1088/0264-9381/29/23/235013. arXiv:1208.6489 [gr-qc]

Gal'tsov DV (1982) Radiation reaction in the Kerr gravitational field. J Phys A 15:3737–3749. https://doi.org/10.1088/0305-4470/15/12/025

Gálvez Ghersi JT, Stein LC (2021) Numerical renormalization-group-based approach to secular perturbation theory. Phys Rev E 104(3):034219. https://doi.org/10.1103/PhysRevE.104.034219. arXiv:2106.08410 [hep-th]

Gamba R, Bernuzzi S (2023) Resonant tides in binary neutron star mergers: analytical-numerical relativity study. Phys Rev D 107(4):044014. https://doi.org/10.1103/PhysRevD.107.044014. arXiv:2207.13106 [gr-qc]

Gamba R, Bernuzzi S, Nagar A (2021) Fast, faithful, frequency-domain effective-one-body waveforms for compact binary coalescences. Phys Rev D 104(8):084058. https://doi.org/10.1103/PhysRevD.104.084058. arXiv:2012.00027 [gr-qc]

Gamba R, Akçay S, Bernuzzi S, Williams J (2022) Effective-one-body waveforms for precessing coalescing compact binaries with post-Newtonian twist. Phys Rev D 106(2):024020. https://doi.org/10.1103/PhysRevD.106.024020. arXiv:2111.03675 [gr-qc]

Gamba R, Breschi M, Carullo G, Albanesi S, Rettegno P, Bernuzzi S, Nagar A (2023) GW190521 as a dynamical capture of two nonspinning black holes. Nature Astron 7(1):11–17. https://doi.org/10.1038/s41550-022-01813-w. arXiv:2106.05575 [gr-qc]

Gamba R, Chiaramello D, Neogi S (2024) Toward efficient effective-one-body models for generic, nonplanar orbits. Phys Rev D 110(2):024031. https://doi.org/10.1103/PhysRevD.110.024031. arXiv:2404.15408 [gr-qc]

Gamba R, et al. (2023b) Analytically improved and numerical-relativity informed effective-one-body model for coalescing binary neutron stars. arXiv e-prints arXiv:2307.15125 [gr-qc]

Ganz K, Hikida W, Nakano H, Sago N, Tanaka T (2007) Adiabatic evolution of three 'Constants' of motion for greatly inclined orbits in kerr spacetime. Prog Theor Phys 117:1041–1066. https://doi.org/10.1143/PTP.117.1041. arXiv:gr-qc/0702054

García-Bellido J (2019) Primordial black holes and the origin of the matter-antimatter asymmetry. Phil Trans R Soc Lond A 377(2161):20190091. https://doi.org/10.1098/rsta.2019.0091

García-Bellido J, Nesseris S (2017) Gravitational wave bursts from Primordial Black Hole hyperbolic encounters. Phys Dark Univ 18:123–126. https://doi.org/10.1016/j.dark.2017.10.002. arXiv:1706.02111 [astro-ph.CO]

García-Bellido J, Nesseris S (2018) Gravitational wave energy emission and detection rates of Primordial Black Hole hyperbolic encounters. Phys Dark Univ 21:61–69. https://doi.org/10.1016/j.dark.2018.06.001. arXiv:1711.09702 [astro-ph.HE]

García-Quirós C, Colleoni M, Husa S, Estellés H, Pratten G, Ramos-Buades A, Mateu-Lucena M, Jaume R (2020) Multimode frequency-domain model for the gravitational wave signal from nonprecessing black-hole binaries. Phys Rev D 102(6):064002. https://doi.org/10.1103/PhysRevD.102.064002. arXiv:2001.10914 [gr-qc]

García-Quirós C, Husa S, Mateu-Lucena M, Borchers A (2021) Accelerating the evaluation of inspiral-merger-ringdown waveforms with adapted grids. Class Quantum Grav 38(1):015006. https://doi.org/10.1088/1361-6382/abc36e. arXiv:2001.10897 [gr-qc]

Garfinkle D, Vachaspati T (1987) Radiation from kinky, cuspless cosmic loops. Phys Rev D 36:2229. https://doi.org/10.1103/PhysRevD.36.2229

Garfinkle D, Vachaspati T (1988) Fields due to kinky, cuspless, cosmic loops. Phys Rev D 37:257–262. https://doi.org/10.1103/PhysRevD.37.257

Garfinkle D, Vachaspati T (1990) Cosmic string traveling waves. Phys Rev D 42:1960–1963. https://doi.org/10.1103/PhysRevD.42.1960

Garg M, Derdzinski A, Zwick L, Capelo PR, Mayer L (2022) The imprint of gas on gravitational waves from LISA intermediate-mass black hole binaries. Mon Not R Astron Soc 517:1339–1354. https://doi.org/10.1093/mnras/stac2711. arXiv:2206.05292 [astro-ph.GA]

Gayathri V, Healy J, Lange J, O'Brien B, Szczepanczyk M, Bartos I, Campanelli M, Klimenko S, Lousto CO, O'Shaughnessy R (2022) Eccentricity estimate for black hole mergers with numerical relativity simulations. Nature Astron 6(3):344–349. https://doi.org/10.1038/s41550-021-01568-w. arXiv:2009.05461 [astro-ph.HE]

Gebhardt K et al (2000) A Relationship between nuclear black hole mass and galaxy velocity dispersion. Astrophys J Lett 539:L13. https://doi.org/10.1086/312840. arXiv:astro-ph/0006289

Gehren T, Fried J, Wehinger PA, Wyckoff S (1984) Host galaxies of quasars and their association with galaxy clusters. Astrophys J 278:11–27. https://doi.org/10.1086/161763

van Gemeren I, Shiralilou B, Hinderer T (2023) Dipolar tidal effects in gravitational waves from scalarized black hole binary inspirals in quadratic gravity. Phys Rev D 108(2):024026. [Erratum: Phys. Rev. D 109, 089901 (2024)]. https://doi.org/10.1103/PhysRevD.108.024026. arXiv:2302.08480 [gr-qc]

Gerosa D, Fishbach M (2021) Hierarchical mergers of stellar-mass black holes and their gravitational-wave signatures. Nature Astron 5(8):749–760. https://doi.org/10.1038/s41550-021-01398-w. arXiv:2105.03439 [astro-ph.HE]

Gerosa D, Moore CJ (2016) Black hole kicks as new gravitational wave observables. Phys Rev Lett 117 (1):011101. https://doi.org/10.1103/PhysRevLett.117.011101. arXiv:1606.04226 [gr-qc]

Ghosh A, Brito R, Buonanno A (2021) Constraints on quasinormal-mode frequencies with LIGO-Virgo binary-black-hole observations. Phys Rev D 103(12):124041. https://doi.org/10.1103/PhysRevD.103.124041. arXiv:2104.01906 [gr-qc]

Ghosh R, Franchini N, Völkel SH, Barausse E (2023) Quasinormal modes of nonseparable perturbation equations: the scalar non-Kerr case. Phys Rev D 108(2):024038. https://doi.org/10.1103/PhysRevD.108.024038. arXiv:2303.00088 [gr-qc]

Ghosh S, Kolitsidou P, Hannam M (2024) First frequency-domain phenomenological model of the multipole asymmetry in gravitational-wave signals from binary-black-hole coalescence. Phys Rev D 109(2):024061. https://doi.org/10.1103/PhysRevD.109.024061. arXiv:2310.16980 [gr-qc]

Giacomazzo B, Rezzolla L (2007) WhiskyMHD: a new numerical code for general relativistic magnetohydrodynamics. Class Quantum Grav 24:S235–S258. https://doi.org/10.1088/0264-9381/24/12/S16. arXiv:gr-qc/0701109

Giacomazzo B, Baker JG, Miller MC, Reynolds CS, van Meter JR (2012) General relativistic simulations of magnetized plasmas around merging supermassive black holes. Astrophys J Lett 752:L15. https://doi.org/10.1088/2041-8205/752/1/L15. arXiv:1203.6108 [astro-ph.HE]

Giddings SB (2014) Possible observational windows for quantum effects from black holes. Phys Rev D 90 (12):124033. https://doi.org/10.1103/PhysRevD.90.124033. arXiv:1406.7001 [hep-th]

Giddings SB, Kachru S, Polchinski J (2002) Hierarchies from fluxes in string compactifications. Phys Rev D 66:106006. https://doi.org/10.1103/PhysRevD.66.106006. arXiv:hep-th/0105097

Gieg H, Schianchi F, Dietrich T, Ujevic M (2022) Incorporating a radiative hydrodynamics scheme in the numerical-relativity code BAM. Universe 8(7):370. https://doi.org/10.3390/universe8070370. arXiv:2206.01337 [gr-qc]

Giesler M, Isi M, Scheel MA, Teukolsky S (2019) Black hole ringdown: the importance of overtones. Phys Rev X 9(4):041060. https://doi.org/10.1103/PhysRevX.9.041060. arXiv:1903.08284 [gr-qc]

Gimon EG, Horava P (2009) Astrophysical violations of the Kerr bound as a possible signature of string theory. Phys Lett B 672:299–302. https://doi.org/10.1016/j.physletb.2009.01.026. arXiv:0706.2873 [hep-th]

Giudice GF, McCullough M, Urbano A (2016) Hunting for dark particles with gravitational waves. JCAP 10:001. https://doi.org/10.1088/1475-7516/2016/10/001. arXiv:1605.01209 [hep-ph]

Glampedakis K, Babak S (2006) Mapping spacetimes with LISA: inspiral of a test-body in a 'quasi-Kerr' field. Class Quantum Grav 23:4167–4188. https://doi.org/10.1088/0264-9381/23/12/013. arXiv:gr-qc/0510057

Glampedakis K, Kennefick D (2002) Zoom and whirl: eccentric equatorial orbits around spinning black holes and their evolution under gravitational radiation reaction. Phys Rev D 66:044002. https://doi.org/10.1103/PhysRevD.66.044002. arXiv:gr-qc/0203086

Glampedakis K, Pappas G (2018) How well can ultracompact bodies imitate black hole ringdowns? Phys Rev D 97(4):041502. https://doi.org/10.1103/PhysRevD.97.041502. arXiv:1710.02136 [gr-qc]

Glampedakis K, Silva HO (2019) Eikonal quasinormal modes of black holes beyond general relativity. Phys Rev D 100(4):044040. https://doi.org/10.1103/PhysRevD.100.044040. arXiv:1906.05455 [gr-qc]

Gleiser RJ, Nicasio CO, Price RH, Pullin J (1996) Second order perturbations of a Schwarzschild black hole. Class Quantum Grav 13:L117–L124. https://doi.org/10.1088/0264-9381/13/10/001. arXiv:gr-qc/9510049

Godoy WF, Podhorszki N, Wang R, Atkins C, Eisenhauer G, Gu J, Davis P, Choi J, Germaschewski K, Huck K, Huebl A, Kim M, Kress J, Kurc T, Liu Q, Logan J, Mehta K, Ostrouchov G, Parashar M, Poeschel F, Pugmire D, Suchyta E, Takahashi K, Thompson N, Tsutsumi S, Wan L, Wolf M, Wu K, Klasky S (2020) Adios 2: the adaptable input output system. A framework for high-performance data management. SoftwareX 12:100561. https://doi.org/10.1016/j.softx.2020.100561

Gold R, Brügmann B (2010) Radiation from low-momentum zoom-whirl orbits. Class Quantum Grav 27:084035. https://doi.org/10.1088/0264-9381/27/8/084035. arXiv:0911.3862 [gr-qc]

Gold R, Brügmann B (2013) Eccentric black hole mergers and zoom-whirl behavior from elliptic inspirals to hyperbolic encounters. Phys Rev D 88(6):064051. https://doi.org/10.1103/PhysRevD.88.064051. arXiv:1209.4085 [gr-qc]

Goldberger WD (2007) Les Houches lectures on effective field theories and gravitational radiation. In: Les Houches Summer School - Session 86: Particle Physics and Cosmology: The Fabric of Spacetime. arXiv:hep-ph/0701129

Gondolo P, Silk J (1999) Dark matter annihilation at the galactic center. Phys Rev Lett 83:1719–1722. https://doi.org/10.1103/PhysRevLett.83.1719. arXiv:astro-ph/9906391

Gonzalez A, Gamba R, Breschi M, Zappa F, Carullo G, Bernuzzi S, Nagar A (2023) Numerical-relativity-informed effective-one-body model for black-hole-neutron-star mergers with higher modes and spin precession. Phys Rev D 107(8):084026. https://doi.org/10.1103/PhysRevD.107.084026. arXiv:2212.03909 [gr-qc]

Gonzalez A et al (2023) Second release of the CoRe database of binary neutron star merger waveforms. Class Quantum Grav 40(8):085011. https://doi.org/10.1088/1361-6382/acc231. arXiv:2210.16366 [gr-qc]

Gonzalez JA, Hannam MD, Sperhake U, Brügmann B, Husa S (2007) Supermassive recoil velocities for binary black-hole mergers with antialigned spins. Phys Rev Lett 98:231101. https://doi.org/10.1103/PhysRevLett.98.231101. arXiv:gr-qc/0702052

Gonzalez JA, Sperhake U, Brügmann B, Hannam M, Husa S (2007) Total recoil: the maximum kick from nonspinning black-hole binary inspiral. Phys Rev Lett 98:091101. https://doi.org/10.1103/PhysRevLett.98.091101. arXiv:gr-qc/0610154

Gonzalez JA, Sperhake U, Brügmann B (2009) Black-hole binary simulations: the mass ratio 10:1. Phys Rev D 79:124006. https://doi.org/10.1103/PhysRevD.79.124006. arXiv:0811.3952 [gr-qc]

Gonzo R, Shi C (2023) Boundary to bound dictionary for generic Kerr orbits. Phys Rev D 108(8):084065. https://doi.org/10.1103/PhysRevD.108.084065. arXiv:2304.06066 [hep-th]

Goodsell M, Jaeckel J, Redondo J, Ringwald A (2009) Naturally light hidden photons in LARGE volume string compactifications. JHEP 11:027. https://doi.org/10.1088/1126-6708/2009/11/027. arXiv:0909.0515 [hep-ph]

Gossan S, Veitch J, Sathyaprakash BS (2012) Bayesian model selection for testing the no-hair theorem with black hole ringdowns. Phys Rev D 85:124056. https://doi.org/10.1103/PhysRevD.85.124056. arXiv:1111.5819 [gr-qc]

Gourgoulhon E (2007) Construction of initial data for 3+1 numerical relativity. J Phys: Conf Ser 91:012001. https://doi.org/10.1088/1742-6596/91/1/012001. arXiv:0704.0149 [gr-qc]

Gourgoulhon E (2012) 3+1 Formalism in General Relativity: Bases of Numerical Relativity, Lecture Notes in Physics, vol 846. Springer, Berlin, Heidelberg. https://doi.org/10.1007/978-3-642-24525-1

Gourgoulhon E, Grandclément P, Marck JA, Novak J, Taniguchi K (2016) LORENE: Spectral methods differential equations solver. Astrophysics Source Code Library, record ascl:1608.018. https://lorene.obspm.fr/

Gourgoulhon E, Le Tiec A, Vincent FH, Warburton N (2019) Gravitational waves from bodies orbiting the Galactic Center black hole and their detectability by LISA. Astron Astrophys 627:A92. https://doi.org/10.1051/0004-6361/201935406. arXiv:1903.02049 [gr-qc]

Graham MJ et al (2020) Candidate electromagnetic counterpart to the binary black hole merger gravitational wave event S190521g. Phys Rev Lett 124(25):251102. https://doi.org/10.1103/PhysRevLett.124.251102. arXiv:2006.14122 [astro-ph.HE]

Gralla SE (2011) Gauge and averaging in gravitational self-force. Phys Rev D 84:084050. https://doi.org/10.1103/PhysRevD.84.084050. arXiv:1104.5635 [gr-qc]

Gralla SE (2012) Second order gravitational self force. Phys Rev D 85:124011. https://doi.org/10.1103/PhysRevD.85.124011. arXiv:1203.3189 [gr-qc]

Gralla SE, Wald RM (2008) A Rigorous Derivation of Gravitational Self-force. Class Quantum Grav 25:205009. [Erratum: Class. Quant. Grav. 28, 159501 (2011)]. https://doi.org/10.1088/0264-9381/25/20/205009. arXiv:0806.3293 [gr-qc]

Gralla SE, Porfyriadis AP, Warburton N (2015) Particle on the innermost stable circular orbit of a rapidly spinning black hole. Phys Rev D 92(6):064029. https://doi.org/10.1103/PhysRevD.92.064029. arXiv:1506.08496 [gr-qc]

Gralla SE, Hughes SA, Warburton N (2016) Inspiral into Gargantua. Class Quantum Grav 33(15):155002. [Erratum: Class. Quant. Grav. 37, 109501 (2020)]. https://doi.org/10.1088/0264-9381/33/15/155002. arXiv:1603.01221 [gr-qc]

Grandclement P (2010) Kadath: a spectral solver for theoretical physics. J Comput Phys 229:3334–3357. https://doi.org/10.1016/j.jcp.2010.01.005. arXiv:0909.1228 [gr-qc]

Grant A (2023) Flux-balance laws from an effective stress-energy tensor, talk given at the 26th Capra Meeting, Jun 2024. Available at https://www.caprameeting.org/capra-meetings/capra-26/timetable

GRChombo (2024) GRChombo a new AMR based open-source code for numerical-relativity simulations. https://www.grchombo.org
Green MB, Schwarz JH (1984) Anomaly cancellation in supersymmetric D=10 gauge theory and superstring theory. Phys Lett B 149:117–122. https://doi.org/10.1016/0370-2693(84)91565-X
Green SR, Hollands S, Zimmerman P (2020) Teukolsky formalism for nonlinear Kerr perturbations. Class Quantum Grav 37(7):075001. https://doi.org/10.1088/1361-6382/ab7075. arXiv:1908.09095 [gr-qc]
Green SR, Hollands S, Sberna L, Toomani V, Zimmerman P (2023) Conserved currents for a Kerr black hole and orthogonality of quasinormal modes. Phys Rev D 107(6):064030. https://doi.org/10.1103/PhysRevD.107.064030. arXiv:2210.15935 [gr-qc]
Greene JE, Strader J, Ho LC (2020) Intermediate-mass black holes. Ann Rev Astron Astrophys 58:257–312. https://doi.org/10.1146/annurev-astro-032620-021835. arXiv:1911.09678 [astro-ph.GA]
Grossman R, Levin J, Perez-Giz G (2012) The harmonic structure of generic Kerr orbits. Phys Rev D 85:023012. https://doi.org/10.1103/PhysRevD.85.023012. arXiv:1105.5811 [gr-qc]
Guevara A, Ochirov A, Vines J (2019) Black-hole scattering with general spin directions from minimal-coupling amplitudes. Phys Rev D 100(10):104024. https://doi.org/10.1103/PhysRevD.100.104024. arXiv:1906.10071 [hep-th]
Guo H, Liu Y, Zhang C, Gong Y, Qian WL, Yue RH (2022) Detection of scalar fields by extreme mass ratio inspirals with a Kerr black hole. Phys Rev D 106(2):024047. https://doi.org/10.1103/PhysRevD.106.024047. arXiv:2201.10748 [gr-qc]
Gupta P, Bonga B, Chua A, Tanaka T (2021) Importance of tidal resonances in extreme-mass-ratio inspirals. Phys Rev D 104(4):044056. https://doi.org/10.1103/PhysRevD.104.044056. arXiv:2104.03422 [gr-qc]
Gupta P, Kakehi T, Tanaka T (2022) Resonant jumps induced by stationary tidal perturbation: a two-for-one deal. Class Quantum Grav 39(24):245005. https://doi.org/10.1088/1361-6382/aca1a3. arXiv:2207.13369 [gr-qc]
Gupta P, Speri L, Bonga B, Chua A, Tanaka T (2022) Modeling transient resonances in extreme-mass-ratio inspirals. Phys Rev D 106(10):104001. https://doi.org/10.1103/PhysRevD.106.104001. arXiv:2205.04808 [gr-qc]
Gupta PK, Steinhoff J, Hinderer T (2021) Relativistic effective action of dynamical gravitomagnetic tides for slowly rotating neutron stars. Phys Rev Res 3(1):013147. https://doi.org/10.1103/PhysRevResearch.3.013147. arXiv:2011.03508 [gr-qc]
Guth AH (1981) The inflationary universe: a possible solution to the horizon and flatness problems. Phys Rev D 23:347–356. https://doi.org/10.1103/PhysRevD.23.347
ter Haar L, Bezares M, Crisostomi M, Barausse E, Palenzuela C (2021) Dynamics of screening in modified gravity. Phys Rev Lett 126:091102. https://doi.org/10.1103/PhysRevLett.126.091102. arXiv:2009.03354 [gr-qc]
Haas R, Cheng CH, Diener P, Etienne Z, Ficarra G, Ikeda T, Kalyanaraman H, Kuo N, Leung L, Tian C, Tsao BJ, Wen A, Alcubierre M, Alic D, Allen G, Ansorg M, Babiuc-Hamilton M, Baiotti L, Benger W, Bentivegna E, Bernuzzi S, Bode T, Bozzola G, Brandt SR, Brendal B, Bruegmann B, Campanelli M, Cipolletta F, Corvino G, Cupp S, Pietri RD, Dima A, Dimmelmeier H, Dooley R, Dorband N, Elley M, Khamra YE, Faber J, Font T, Frieben J, Giacomazzo B, Goodale T, Gundlach C, Hawke I, Hawley S, Hinder I, Huerta EA, Husa S, Iyer S, Ji L, Johnson D, Joshi AV, Kankani A, Kastaun W, Kellermann T, Knapp A, Koppitz M, Laguna P, Lanferman G, Lasky P, Löffler F, Macpherson H, Masso J, Menger L, Merzky A, Miller JM, Miller M, Moesta P, Montero P, Mundim B, Nelson P, Nerozzi A, Noble SC, Ott C, Paruchuri R, Pollney D, Price D, Radice D, Radke T, Reisswig C, Rezzolla L, Richards CB, Rideout D, Ripeanu M, Sala L, Schewtschenko JA, Schnetter E, Schutz B, Seidel E, Seidel E, Shalf J, Sible K, Sperhake U, Stergioulas N, Suen WM, Szilagyi B, Takahashi R, Thomas M, Thornburg J, Tobias M, Tonita A, Walker P, Wan MB, Wardell B, Werneck L, Witek H, Zilhão M, Zink B, Zlochower Y (2022). The einstein toolkit. https://doi.org/10.5281/zenodo.7245853
HAD (2010) HAD: Distributed AMR infrastructure for PDEs. http://had.liu.edu/
Haddad K, Helset A (2020) Tidal effects in quantum field theory. JHEP 12:024. https://doi.org/10.1007/JHEP12(2020)024. arXiv:2008.04920 [hep-th]
Hahn SG, Lindquist RW (1964) The two-body problem in geometrodynamics. Ann Phys 29(2):304–331. https://doi.org/10.1016/0003-4916(64)90223-4
Hamilton E, London L, Thompson JE, Fauchon-Jones E, Hannam M, Kalaghatgi C, Khan S, Pannarale F, Vano-Vinuales A (2021) Model of gravitational waves from precessing black-hole binaries through merger and ringdown. Phys Rev D 104(12):124027. https://doi.org/10.1103/PhysRevD.104.124027. arXiv:2107.08876 [gr-qc]

Hamilton E, London L, Hannam M (2023) Ringdown frequencies in black holes formed from precessing black-hole binaries. Phys Rev D 107(10):104035. https://doi.org/10.1103/PhysRevD.107.104035. arXiv:2301.06558 [gr-qc]
Hamilton E et al (2024) Catalog of precessing black-hole-binary numerical-relativity simulations. Phys Rev D 109(4):044032. https://doi.org/10.1103/PhysRevD.109.044032. arXiv:2303.05419 [gr-qc]
Han WB (2010) Gravitational radiations from a spinning compact object around a supermassive kerr black hole in circular orbit. Phys Rev D 82:084013. https://doi.org/10.1103/PhysRevD.82.084013. arXiv:1008.3324 [gr-qc]
Han WB (2014) Gravitational waves from extreme-mass-ratio inspirals in equatorially eccentric orbits. Int J Mod Phys D 23(7):1450064. https://doi.org/10.1142/S0218271814500643
Han WB (2016) Fast evolution and waveform generator for extreme-mass-ratio inspirals in equatorial-circular orbits. Class Quantum Grav 33(6):065009. https://doi.org/10.1088/0264-9381/33/6/065009. arXiv:1609.06817 [gr-qc]
Han WB, Cao Z (2011) Constructing EOB dynamics with numerical energy flux for intermediate-mass-ratio inspirals. Phys Rev D 84:044014. https://doi.org/10.1103/PhysRevD.84.044014. arXiv:1108.0995 [gr-qc]
Han WB, Cao Z, Hu YM (2017) Excitation of high frequency voices from intermediate-mass-ratio inspirals with large eccentricity. Class Quantum Grav 34(22):225010. https://doi.org/10.1088/1361-6382/aa891b. arXiv:1710.00147 [gr-qc]
Handmer CJ, Szilagyi B (2015) Spectral Characteristic Evolution: A New Algorithm for Gravitational Wave Propagation. Class Quantum Grav 32(2):025008. https://doi.org/10.1088/0264-9381/32/2/025008. arXiv:1406.7029 [gr-qc]
Hannam M, Husa S, Sperhake U, Brügmann B, Gonzalez JA (2008) Where post-Newtonian and numerical-relativity waveforms meet. Phys Rev D 77:044020. https://doi.org/10.1103/PhysRevD.77.044020. arXiv:0706.1305 [gr-qc]
Hannam M, Schmidt P, Bohé A, Haegel L, Husa S, Ohme F, Pratten G, Pürrer M (2014) Simple model of complete precessing black-hole-binary gravitational waveforms. Phys Rev Lett 113(15):151101. https://doi.org/10.1103/PhysRevLett.113.151101. arXiv:1308.3271 [gr-qc]
Hannam M et al (2009) The Samurai project: verifying the consistency of black-hole-binary waveforms for gravitational-wave detection. Phys Rev D 79:084025. https://doi.org/10.1103/PhysRevD.79.084025. arXiv:0901.2437 [gr-qc]
Hannuksela OA, Wong K, Brito R, Berti E, Li T (2019) Probing the existence of ultralight bosons with a single gravitational-wave measurement. Nature Astron 3(5):447–451. https://doi.org/10.1038/s41550-019-0712-4. arXiv:1804.09659 [astro-ph.HE]
Hannuksela OA, Ng K, Li T (2020) Extreme dark matter tests with extreme mass ratio inspirals. Phys Rev D 102(10):103022. https://doi.org/10.1103/PhysRevD.102.103022. arXiv:1906.11845 [astro-ph.CO]
Harms E, Bernuzzi S, Nagar A, Zenginoglu A (2014) A new gravitational wave generation algorithm for particle perturbations of the Kerr spacetime. Class Quantum Grav 31(24):245004. https://doi.org/10.1088/0264-9381/31/24/245004. arXiv:1406.5983 [gr-qc]
Harms E, Lukes-Gerakopoulos G, Bernuzzi S, Nagar A (2016) Asymptotic gravitational wave fluxes from a spinning particle in circular equatorial orbits around a rotating black hole. Phys Rev D 93(4):044015. [Addendum: Phys. Rev. D 100, 129901 (2019)]. https://doi.org/10.1103/PhysRevD.93.044015. arXiv:1510.05548 [gr-qc]
Harms E, Lukes-Gerakopoulos G, Bernuzzi S, Nagar A (2016) Spinning test body orbiting around a Schwarzschild black hole: Circular dynamics and gravitational-wave fluxes. Phys Rev D 94(10):104010. https://doi.org/10.1103/PhysRevD.94.104010. arXiv:1609.00356 [gr-qc]
Harte AI (2012) Mechanics of extended masses in general relativity. Class Quantum Grav 29:055012. https://doi.org/10.1088/0264-9381/29/5/055012. arXiv:1103.0543 [gr-qc]
Harte AI (2015) Motion in classical field theories and the foundations of the self-force problem. Fund Theor Phys 179:327–398. https://doi.org/10.1007/978-3-319-18335-0_12. arXiv:1405.5077 [gr-qc]
Hartung J, Steinhoff J (2011) Next-to-next-to-leading order post-Newtonian spin-orbit Hamiltonian for self-gravitating binaries. Annalen Phys 523:783–790. https://doi.org/10.1002/andp.201100094. arXiv:1104.3079 [gr-qc]
Hartung J, Steinhoff J (2011) Next-to-next-to-leading order post-Newtonian spin(1)-spin(2) Hamiltonian for self-gravitating binaries. Annalen Phys 523:919–924. https://doi.org/10.1002/andp.201100163. arXiv:1107.4294 [gr-qc]

Hartung J, Steinhoff J, Schafer G (2013) Next-to-next-to-leading order post-Newtonian linear-in-spin binary Hamiltonians. Annalen Phys 525:359–394. https://doi.org/10.1002/andp.201200271. arXiv:1302.6723 [gr-qc]
Hawking SW (1972) Black holes in the Brans-Dicke theory of gravitation. Commun Math Phys 25:167–171. https://doi.org/10.1007/BF01877518
Healy J, Lousto CO (2017) Remnant of binary black-hole mergers: new simulations and peak luminosity studies. Phys Rev D 95(2):024037. https://doi.org/10.1103/PhysRevD.95.024037. arXiv:1610.09713 [gr-qc]
Healy J, Lousto CO (2018) Hangup effect in unequal mass binary black hole mergers and further studies of their gravitational radiation and remnant properties. Phys Rev D 97(8):084002. https://doi.org/10.1103/PhysRevD.97.084002. arXiv:1801.08162 [gr-qc]
Healy J, Lousto CO (2020) Third RIT binary black hole simulations catalog. Phys Rev D 102(10):104018. https://doi.org/10.1103/PhysRevD.102.104018. arXiv:2007.07910 [gr-qc]
Healy J, Lousto CO (2022) Fourth RIT binary black hole simulations catalog: extension to eccentric orbits. Phys Rev D 105(12):124010. https://doi.org/10.1103/PhysRevD.105.124010. arXiv:2202.00018 [gr-qc]
Healy J, Herrmann F, Hinder I, Shoemaker DM, Laguna P, Matzner RA (2009) Superkicks in hyperbolic encounters of binary black holes. Phys Rev Lett 102:041101. https://doi.org/10.1103/PhysRevLett.102.041101. arXiv:0807.3292 [gr-qc]
Healy J, Levin J, Shoemaker D (2009) Zoom-whirl orbits in black hole binaries. Phys Rev Lett 103:131101. https://doi.org/10.1103/PhysRevLett.103.131101. arXiv:0907.0671 [gr-qc]
Healy J, Bode T, Haas R, Pazos E, Laguna P, Shoemaker D, Yunes N (2012) Late inspiral and merger of binary black holes in scalar-tensor theories of gravity. Class Quantum Grav 29:232002. https://doi.org/10.1088/0264-9381/29/23/232002. arXiv:1112.3928 [gr-qc]
Healy J, Lousto CO, Zlochower Y (2014) Remnant mass, spin, and recoil from spin aligned black-hole binaries. Phys Rev D 90(10):104004. https://doi.org/10.1103/PhysRevD.90.104004. arXiv:1406.7295 [gr-qc]
Healy J, Lousto CO, Zlochower Y, Campanelli M (2017) The RIT binary black hole simulations catalog. Class Quantum Grav 34(22):224001. https://doi.org/10.1088/1361-6382/aa91b1. arXiv:1703.03423 [gr-qc]
Healy J, Lousto CO, Ruchlin I, Zlochower Y (2018) Evolutions of unequal mass, highly spinning black hole binaries. Phys Rev D 97(10):104026. https://doi.org/10.1103/PhysRevD.97.104026. arXiv:1711.09041 [gr-qc]
Healy J, Lousto CO, Lange J, O'Shaughnessy R, Zlochower Y, Campanelli M (2019) Second RIT binary black hole simulations catalog and its application to gravitational waves parameter estimation. Phys Rev D 100(2):024021. https://doi.org/10.1103/PhysRevD.100.024021. arXiv:1901.02553 [gr-qc]
Heckman TM, Best P (2014) The coevolution of galaxies and supermassive black holes: insights from surveys of the contemporary universe. Ann Rev Astron Astrophys 52:589–660. https://doi.org/10.1146/annurev-astro-081913-035722. arXiv:1403.4620 [astro-ph.GA]
Heffernan A (2022) Regularization of a scalar charged particle for generic orbits in Kerr spacetime. Phys Rev D 106(6):064031. https://doi.org/10.1103/PhysRevD.106.064031. arXiv:2107.14750 [gr-qc]
Heffernan A, Ottewill A, Wardell B (2012) High-order expansions of the Detweiler-Whiting singular field in Schwarzschild spacetime. Phys Rev D 86:104023. https://doi.org/10.1103/PhysRevD.86.104023. arXiv:1204.0794 [gr-qc]
Heffernan A, Ottewill A, Wardell B (2014) High-order expansions of the Detweiler-Whiting singular field in Kerr spacetime. Phys Rev D 89(2):024030. https://doi.org/10.1103/PhysRevD.89.024030. arXiv:1211.6446 [gr-qc]
Held A, Lim H (2023) Nonlinear evolution of quadratic gravity in 3+1 dimensions. Phys Rev D 108(10):104025. https://doi.org/10.1103/PhysRevD.108.104025. arXiv:2306.04725 [gr-qc]
Helfer T, Aurrekoetxea JC, Lim EA (2019) Cosmic string loop collapse in full general relativity. Phys Rev D 99(10):104028. https://doi.org/10.1103/PhysRevD.99.104028. arXiv:1808.06678 [gr-qc]
Helfer T, Lim EA, Garcia M, Amin MA (2019) Gravitational wave emission from collisions of compact scalar solitons. Phys Rev D 99(4):044046. https://doi.org/10.1103/PhysRevD.99.044046. arXiv:1802.06733 [gr-qc]
Helfer T, Sperhake U, Croft R, Radia M, Ge BX, Lim EA (2022) Malaise and remedy of binary boson-star initial data. Class Quantum Grav 39(7):074001. https://doi.org/10.1088/1361-6382/ac53b7. arXiv:2108.11995 [gr-qc]

Henry Q (2023) Complete gravitational-waveform amplitude modes for quasicircular compact binaries to the 3.5PN order. Phys Rev D 107(4):044057. https://doi.org/10.1103/PhysRevD.107.044057. arXiv:2210.15602 [gr-qc]
Henry Q, Khalil M (2023) Spin effects in gravitational waveforms and fluxes for binaries on eccentric orbits to the third post-Newtonian order. Phys Rev D 108(10):104016. https://doi.org/10.1103/PhysRevD.108.104016. arXiv:2308.13606 [gr-qc]
Henry Q, Faye G, Blanchet L (2020) Tidal effects in the gravitational-wave phase evolution of compact binary systems to next-to-next-to-leading post-Newtonian order. Phys Rev D 102(4):044033. [Erratum: Phys. Rev. D 108, 089901 (2023)]. https://doi.org/10.1103/PhysRevD.102.044033. arXiv:2005.13367 [gr-qc]
Henry Q, Faye G, Blanchet L (2021) The current-type quadrupole moment and gravitational-wave mode (ℓ, m) = (2, 1) of compact binary systems at the third post-Newtonian order. Class Quantum Grav 38 (18):185004. https://doi.org/10.1088/1361-6382/ac1850. arXiv:2105.10876 [gr-qc]
Henry Q, Marsat S, Khalil M (2022) Spin contributions to the gravitational-waveform modes for spin-aligned binaries at the 3.5PN order. Phys Rev D 106(12):124018. https://doi.org/10.1103/PhysRevD.106.124018. arXiv:2209.00374 [gr-qc]
Henry Tye SH (2008) Brane inflation: string theory viewed from the cosmos. Lect Notes Phys 737:949–974 arXiv:hep-th/0610221
Herdeiro C, Radu E, Rúnarsson H (2016) Kerr black holes with Proca hair. Class Quantum Grav 33 (15):154001. https://doi.org/10.1088/0264-9381/33/15/154001. arXiv:1603.02687 [gr-qc]
Herdeiro C, Radu E (2014) Kerr black holes with scalar hair. Phys Rev Lett 112:221101. https://doi.org/10.1103/PhysRevLett.112.221101. arXiv:1403.2757 [gr-qc]
Herdeiro C, Radu E (2015) Asymptotically flat black holes with scalar hair: a review. Int J Mod Phys D 24 (09):1542014. https://doi.org/10.1142/S0218271815420146. arXiv:1504.08209 [gr-qc]
Herdeiro C, Kunz J, Perapechka I, Radu E, Shnir Y (2021) Multipolar boson stars: macroscopic Bose-Einstein condensates akin to hydrogen orbitals. Phys Lett B 812:136027. https://doi.org/10.1016/j.physletb.2020.136027. arXiv:2008.10608 [gr-qc]
Herdeiro C, Radu E, Silva HO, Sotiriou TP, Yunes N (2021) Spin-induced scalarized black holes. Phys Rev Lett 126(1):011103. https://doi.org/10.1103/PhysRevLett.126.011103. arXiv:2009.03904 [gr-qc]
Herdeiro CAR, Radu E, Sanchis-Gual N, Santos NM, dos Santos Costa Filho E (2024) The non-spherical ground state of Proca stars. Phys Lett B 852:138595. https://doi.org/10.1016/j.physletb.2024.138595. arXiv:2311.14800 [gr-qc]
Hergt S, Steinhoff J, Schäfer G (2010) Reduced Hamiltonian for next-to-leading order spin-squared dynamics of general compact binaries. Class Quantum Grav 27:135007. https://doi.org/10.1088/0264-9381/27/13/135007. arXiv:1002.2093 [gr-qc]
Hermes JJ, Kilic M, Brown WR, Winget DE, Allende Prieto C, Gianninas A, Mukadam AS, Cabrera-Lavers A, Kenyon SJ (2012) Rapid orbital decay in the 12.75-minute WD+WD binary J0651+2844. Astrophys J Lett 757:L21. https://doi.org/10.1088/2041-8205/757/2/L21. arXiv:1208.5051 [astro-ph.SR]
Herrmann E, Parra-Martinez J, Ruf MS, Zeng M (2021) Gravitational bremsstrahlung from reverse unitarity. Phys Rev Lett 126(20):201602. https://doi.org/10.1103/PhysRevLett.126.201602. arXiv:2101.07255 [hep-th]
Herrmann E, Parra-Martinez J, Ruf MS, Zeng M (2021) Radiative classical gravitational observables at $\mathcal{O}(G^3)$ from scattering amplitudes. JHEP 10:148. https://doi.org/10.1007/JHEP10(2021)148. arXiv:2104.03957 [hep-th]
Herrmann F, Hinder I, Shoemaker D, Laguna P (2006) Unequal Mass Binary Black Hole Plunges and Gravitational Recoil. In: New Frontiers in Numerical Relativity (NFNR 2006). arXiv:gr-qc/0601026
Herrmann F, Field SE, Galley CR, Ochsner E, Tiglio M (2012) Towards beating the curse of dimensionality for gravitational waves using Reduced Basis. Phys Rev D 86:084046. https://doi.org/10.1103/PhysRevD.86.084046. arXiv:1205.6009 [gr-qc]
Hilditch D (2013) An introduction to well-posedness and free-evolution. Int J Mod Phys A 28:1340015. https://doi.org/10.1142/S0217751X13400150. arXiv:1309.2012 [gr-qc]
Hilditch D, Bernuzzi S, Thierfelder M, Cao Z, Tichy W, Brügmann B (2013) Compact binary evolutions with the Z4c formulation. Phys Rev D 88:084057. https://doi.org/10.1103/PhysRevD.88.084057. arXiv:1212.2901 [gr-qc]
Hilditch D, Weyhausen A, Brügmann B (2016) Pseudospectral method for gravitational wave collapse. Phys Rev D 93(6):063006. https://doi.org/10.1103/PhysRevD.93.063006. arXiv:1504.04732 [gr-qc]

Hils D, Bender PL, Webbink RF (1990) Gravitational radiation from the Galaxy. Astrophys J 360:75–94. https://doi.org/10.1086/169098
Hinder I, Vaishnav B, Herrmann F, Shoemaker D, Laguna P (2008) Universality and final spin in eccentric binary black hole inspirals. Phys Rev D 77:081502. https://doi.org/10.1103/PhysRevD.77.081502. arXiv:0710.5167 [gr-qc]
Hinder I, Herrmann F, Laguna P, Shoemaker D (2010) Comparisons of eccentric binary black hole simulations with post-Newtonian models. Phys Rev D 82:024033. https://doi.org/10.1103/PhysRevD.82.024033. arXiv:0806.1037 [gr-qc]
Hinder I, Kidder LE, Pfeiffer HP (2018) Eccentric binary black hole inspiral-merger-ringdown gravitational waveform model from numerical relativity and post-Newtonian theory. Phys Rev D 98(4):044015. https://doi.org/10.1103/PhysRevD.98.044015. arXiv:1709.02007 [gr-qc]
Hinder I et al (2014) Error-analysis and comparison to analytical models of numerical waveforms produced by the NRAR Collaboration. Class Quantum Grav 31:025012. https://doi.org/10.1088/0264-9381/31/2/025012. arXiv:1307.5307 [gr-qc]
Hinderer T, Babak S (2017) Foundations of an effective-one-body model for coalescing binaries on eccentric orbits. Phys Rev D 96(10):104048. https://doi.org/10.1103/PhysRevD.96.104048. arXiv:1707.08426 [gr-qc]
Hinderer T, Flanagan EE (2008) Two timescale analysis of extreme mass ratio inspirals in Kerr. I. Orbital Motion. Phys Rev D 78:064028. https://doi.org/10.1103/PhysRevD.78.064028. arXiv:0805.3337 [gr-qc]
Hinderer T et al (2013) Periastron advance in spinning black hole binaries: comparing effective-one-body and numerical relativity. Phys Rev D 88(8):084005. https://doi.org/10.1103/PhysRevD.88.084005. arXiv:1309.0544 [gr-qc]
Hinderer T et al (2016) Effects of neutron-star dynamic tides on gravitational waveforms within the effective-one-body approach. Phys Rev Lett 116(18):181101. https://doi.org/10.1103/PhysRevLett.116.181101. arXiv:1602.00599 [gr-qc]
Hirata CM (2011) Resonant recoil in extreme mass ratio binary black hole mergers. Phys Rev D 83:104024. https://doi.org/10.1103/PhysRevD.83.104024. arXiv:1011.4987 [gr-qc]
Hirschmann EW, Lehner L, Liebling SL, Palenzuela C (2018) Black hole dynamics in Einstein-Maxwell-Dilaton theory. Phys Rev D 97(6):064032. https://doi.org/10.1103/PhysRevD.97.064032. arXiv:1706.09875 [gr-qc]
Hod S (2020) Onset of spontaneous scalarization in spinning Gauss-Bonnet black holes. Phys Rev D 102(8):084060. https://doi.org/10.1103/PhysRevD.102.084060. arXiv:2006.09399 [gr-qc]
Hofmann F, Barausse E, Rezzolla L (2016) The final spin from binary black holes in quasi-circular orbits. Astrophys J Lett 825(2):L19. https://doi.org/10.3847/2041-8205/825/2/L19. arXiv:1605.01938 [gr-qc]
Hogan C, Narayan R (1984) Gravitational lensing by cosmic strings. MNRAS 211:575–591. https://doi.org/10.1093/mnras/211.3.575
Hogan CJ (2006) Gravitational waves from light cosmic strings: backgrounds and bursts with large loops. Phys Rev D 74:043526. https://doi.org/10.1103/PhysRevD.74.043526. arXiv:astro-ph/0605567
Hogan CJ, Rees MJ (1984) Gravitational interactions of cosmic strings. Nature 311:109–113. https://doi.org/10.1038/311109a0
Holdom B, Ren J (2017) Not quite a black hole. Phys Rev D 95(8):084034. https://doi.org/10.1103/PhysRevD.95.084034. arXiv:1612.04889 [gr-qc]
Hopman C, Alexander T (2005) The Orbital statistics of stellar inspiral and relaxation near a massive black hole: characterizing gravitational wave sources. Astrophys J 629:362–372. https://doi.org/10.1086/431475. arXiv:astro-ph/0503672
Hopman C, Alexander T (2006) The effect of mass-segregation on gravitational wave sources near massive black holes. Astrophys J Lett 645:L133–L136. https://doi.org/10.1086/506273. arXiv:astro-ph/0603324
Hopper S (2018) Unbound motion on a Schwarzschild background: practical approaches to frequency domain computations. Phys Rev D 97(6):064007. https://doi.org/10.1103/PhysRevD.97.064007. arXiv:1706.05455 [gr-qc]
Hopper S, Cardoso V (2018) Scattering of point particles by black holes: gravitational radiation. Phys Rev D 97(4):044031. https://doi.org/10.1103/PhysRevD.97.044031. arXiv:1706.02791 [gr-qc]
Hopper S, Evans CR (2013) Metric perturbations from eccentric orbits on a Schwarzschild black hole: I. Odd-parity Regge-Wheeler to Lorenz gauge transformation and two new methods to circumvent the

Gibbs phenomenon. Phys Rev D 87(6):064008. https://doi.org/10.1103/PhysRevD.87.064008. arXiv:1210.7969 [gr-qc]
Hopper S, Kavanagh C, Ottewill AC (2016) Analytic self-force calculations in the post-Newtonian regime: eccentric orbits on a Schwarzschild background. Phys Rev D 93(4):044010. https://doi.org/10.1103/PhysRevD.93.044010. arXiv:1512.01556 [gr-qc]
Hopper S, Nagar A, Rettegno P (2023) Strong-field scattering of two spinning black holes: numerics versus analytics. Phys Rev D 107(12):124034. https://doi.org/10.1103/PhysRevD.107.124034. arXiv:2204.10299 [gr-qc]
Horava P (1999) Type IIA D-branes, K theory, and matrix theory. Adv Theor Math Phys 2:1373–1404. https://doi.org/10.4310/ATMP.1998.v2.n6.a5. arXiv:hep-th/9812135
Horndeski GW (1974) Second-order scalar-tensor field equations in a four-dimensional space. Int J Theor Phys 10:363–384. https://doi.org/10.1007/BF01807638
Hu WR, Wu YL (2017) The Taiji program in space for gravitational wave physics and the nature of gravity. Natl Sci Rev 4(5):685–686. https://doi.org/10.1093/nsr/nwx116
Huang YX, Xu JC, Zhou SY (2020) Fredholm approach to characterize gravitational wave echoes. Phys Rev D 101(2):024045. https://doi.org/10.1103/PhysRevD.101.024045. arXiv:1908.00189 [gr-qc]
Huerta EA, Gair JR (2009) Influence of conservative corrections on parameter estimation for extreme-mass-ratio inspirals. Phys Rev D 79:084021. [Erratum: Phys. Rev. D 84, 049903 (2011)]. https://doi.org/10.1103/PhysRevD.79.084021. arXiv:0812.4208 [gr-qc]
Huerta EA, Gair JR, Brown DA (2012) Importance of including small body spin effects in the modelling of intermediate mass-ratio inspirals II. Accurate parameter extraction of strong sources using higher-order spin effects. Phys Rev D 85:064023. https://doi.org/10.1103/PhysRevD.85.064023. arXiv:1111.3243 [gr-qc]
Huerta EA et al (2017) Complete waveform model for compact binaries on eccentric orbits. Phys Rev D 95 (2):024038. https://doi.org/10.1103/PhysRevD.95.024038. arXiv:1609.05933 [gr-qc]
Huerta EA et al (2018) Eccentric, nonspinning, inspiral, Gaussian-process merger approximant for the detection and characterization of eccentric binary black hole mergers. Phys Rev D 97(2):024031. https://doi.org/10.1103/PhysRevD.97.024031. arXiv:1711.06276 [gr-qc]
Huerta EA et al (2019) Physics of eccentric binary black hole mergers: a numerical relativity perspective. Phys Rev D 100(6):064003. https://doi.org/10.1103/PhysRevD.100.064003. arXiv:1901.07038 [gr-qc]
Hughes SA (2000) The Evolution of circular, nonequatorial orbits of Kerr black holes due to gravitational wave emission. Phys Rev D 61(8):084004. [Erratum: Phys. Rev. D 63, 049902 (2001), Erratum: Phys. Rev. D 65, 069902 (2002), Erratum: Phys. Rev. D 67, 089901 (2003), Erratum: Phys. Rev. D 78, 109902 (2008), Erratum: Phys. Rev. D 90, 109904 (2014)]. https://doi.org/10.1103/PhysRevD.65.069902. arXiv:gr-qc/9910091
Hughes SA (2001) Evolution of circular, nonequatorial orbits of Kerr black holes due to gravitational wave emission. II. Inspiral trajectories and gravitational wave forms. Phys Rev D 64:064004. [Erratum: Phys.Rev.D 88, 109902 (2013)]. https://doi.org/10.1103/PhysRevD.64.064004. arXiv:gr-qc/0104041
Hughes SA, Drasco S, Flanagan EE, Franklin J (2005) Gravitational radiation reaction and inspiral waveforms in the adiabatic limit. Phys Rev Lett 94:221101. https://doi.org/10.1103/PhysRevLett.94.221101. arXiv:gr-qc/0504015
Hughes SA, Apte A, Khanna G, Lim H (2019) Learning about black hole binaries from their ringdown spectra. Phys Rev Lett 123(16):161101. https://doi.org/10.1103/PhysRevLett.123.161101. arXiv:1901.05900 [gr-qc]
Hughes SA, Warburton N, Khanna G, Chua AJK, Katz ML (2021) Adiabatic waveforms for extreme mass-ratio inspirals via multivoice decomposition in time and frequency. Phys Rev D 103(10):104014. [Erratum: Phys. Rev. D 107, 089901 (2023)]. https://doi.org/10.1103/PhysRevD.103.104014. arXiv:2102.02713 [gr-qc]
Hui L, Ostriker JP, Tremaine S, Witten E (2017) Ultralight scalars as cosmological dark matter. Phys Rev D 95(4):043541. https://doi.org/10.1103/PhysRevD.95.043541. arXiv:1610.08297 [astro-ph.CO]
Husa S, Gonzalez JA, Hannam M, Brügmann B, Sperhake U (2008) Reducing phase error in long numerical binary black hole evolutions with sixth order finite differencing. Class Quantum Grav 25:105006. https://doi.org/10.1088/0264-9381/25/10/105006. arXiv:0706.0740 [gr-qc]
Husa S, Khan S, Hannam M, Pürrer M, Ohme F, Jiménez Forteza X, Bohé A (2016) Frequency-domain gravitational waves from nonprecessing black-hole binaries. I. New numerical waveforms and anatomy of the signal. Phys Rev D 93(4):044006. https://doi.org/10.1103/PhysRevD.93.044006. arXiv:1508.07250 [gr-qc]

Hussain A, Zimmerman A (2022) Approach to computing spectral shifts for black holes beyond Kerr. Phys Rev D 106(10):104018. https://doi.org/10.1103/PhysRevD.106.104018. arXiv:2206.10653 [gr-qc]
Ikeda T, Bernard L, Cardoso V, Zilhão M (2021) Black hole binaries and light fields: gravitational molecules. Phys Rev D 103(2):024020. https://doi.org/10.1103/PhysRevD.103.024020. arXiv:2010.00008 [gr-qc]
Ireland B, Mundim BC, Nakano H, Campanelli M (2016) Inspiralling, nonprecessing, spinning black hole binary spacetime via asymptotic matching. Phys Rev D 93(10):104057. https://doi.org/10.1103/PhysRevD.93.104057. arXiv:1512.05650 [gr-qc]
Isi M, Giesler M, Farr WM, Scheel MA, Teukolsky SA (2019) Testing the no-hair theorem with GW150914. Phys Rev Lett 123(11):111102. https://doi.org/10.1103/PhysRevLett.123.111102. arXiv:1905.00869 [gr-qc]
Isi M, Sun L, Brito R, Melatos A (2019) Directed searches for gravitational waves from ultralight bosons. Phys Rev D 99(8):084042. [Erratum: Phys. Rev. D 102, 049901 (2020)]. https://doi.org/10.1103/PhysRevD.99.084042. arXiv:1810.03812 [gr-qc]
Isi M, Farr WM, Giesler M, Scheel MA, Teukolsky SA (2021) Testing the Black-Hole Area Law with GW150914. Phys Rev Lett 127(1):011103. https://doi.org/10.1103/PhysRevLett.127.011103. arXiv:2012.04486 [gr-qc]
Islam T (2021) Applying higher-modes consistency test on GW190814 : lessons on no-hair theorem, nature of the secondary compact object and waveform modeling. arXiv e-prints arXiv:2111.00111 [gr-qc]
Islam T, Varma V, Lodman J, Field SE, Khanna G, Scheel MA, Pfeiffer HP, Gerosa D, Kidder LE (2021) Eccentric binary black hole surrogate models for the gravitational waveform and remnant properties: comparable mass, nonspinning case. Phys Rev D 103(6):064022. https://doi.org/10.1103/PhysRevD.103.064022. arXiv:2101.11798 [gr-qc]
Islam T, Field SE, Hughes SA, Khanna G, Varma V, Giesler M, Scheel MA, Kidder LE, Pfeiffer HP (2022) Surrogate model for gravitational wave signals from nonspinning, comparable-to large-mass-ratio black hole binaries built on black hole perturbation theory waveforms calibrated to numerical relativity. Phys Rev D 106(10):104025. https://doi.org/10.1103/PhysRevD.106.104025. arXiv:2204.01972 [gr-qc]
Islam T, Vajpeyi A, Shaik FH, Haster CJ, Varma V, Field SE, Lange J, O'Shaughnessy R, Smith R (2023) Analysis of GWTC-3 with fully precessing numerical relativity surrogate models. arXiv e-prints arXiv:2309.14473 [gr-qc]
Isoyama S, Fujita R, Nakano H, Sago N, Tanaka T (2013) Evolution of the Carter constant for resonant inspirals into a Kerr black hole: I. The scalar case. PTEP 6:063E01. https://doi.org/10.1093/ptep/ptt034. arXiv:1302.4035 [gr-qc]
Isoyama S, Barack L, Dolan SR, Le Tiec A, Nakano H, Shah AG, Tanaka T, Warburton N (2014) Gravitational self-force correction to the innermost stable circular equatorial orbit of a Kerr black hole. Phys Rev Lett 113(16):161101. https://doi.org/10.1103/PhysRevLett.113.161101. arXiv:1404.6133 [gr-qc]
Isoyama S, Fujita R, Nakano H, Sago N, Tanaka T (2019) Flux-balance formulae for extreme mass-ratio inspirals. PTEP 1:013E01. https://doi.org/10.1093/ptep/pty136. arXiv:1809.11118 [gr-qc]
Isoyama S, Fujita R, Chua A, Nakano H, Pound A, Sago N (2022) Adiabatic waveforms from extreme-mass-ratio inspirals: an analytical approach. Phys Rev Lett 128(23):231101. https://doi.org/10.1103/PhysRevLett.128.231101. arXiv:2111.05288 [gr-qc]
Jackiw R, Pi SY (2003) Chern-Simons modification of general relativity. Phys Rev D 68:104012. https://doi.org/10.1103/PhysRevD.68.104012. arXiv:gr-qc/0308071
Jackson MG, Jones NT, Polchinski J (2005) Collisions of cosmic F and D-strings. JHEP 10:013. https://doi.org/10.1088/1126-6708/2005/10/013. arXiv:hep-th/0405229
Jain M, Vilenkin A (2020) Clustering of cosmic string loops. JCAP 09:043. https://doi.org/10.1088/1475-7516/2020/09/043. arXiv:2006.15358 [astro-ph.CO]
Jain T (2023) Gravitational scattering up to third post-Newtonian approximation for conservative dynamics: scalar-tensor theories. Phys Rev D 108(10):104071. https://doi.org/10.1103/PhysRevD.108.104071. arXiv:2304.09052 [gr-qc]
Jain T (2023) Nonlocal-in-time effective one body Hamiltonian in scalar-tensor gravity at third post-Newtonian order. Phys Rev D 107(8):084018. https://doi.org/10.1103/PhysRevD.107.084018. arXiv:2301.01070 [gr-qc]

Jain T, Rettegno P, Agathos M, Nagar A, Turco L (2023) Effective-one-body Hamiltonian in scalar-tensor gravity at third post-Newtonian order. Phys Rev D 107(8):084017. https://doi.org/10.1103/PhysRevD.107.084017. arXiv:2211.15580 [gr-qc]

Jakobsen GU, Mogull G (2023) Linear response, Hamiltonian, and radiative spinning two-body dynamics. Phys Rev D 107(4):044033. https://doi.org/10.1103/PhysRevD.107.044033. arXiv:2210.06451 [hep-th]

Jakobsen GU, Mogull G, Plefka J, Steinhoff J (2021) Classical gravitational bremsstrahlung from a worldline quantum field theory. Phys Rev Lett 126(20):201103. https://doi.org/10.1103/PhysRevLett.126.201103. arXiv:2101.12688 [gr-qc]

Jakobsen GU, Mogull G, Plefka J, Steinhoff J (2022) Gravitational bremsstrahlung and hidden supersymmetry of spinning bodies. Phys Rev Lett 128(1):011101. https://doi.org/10.1103/PhysRevLett.128.011101. arXiv:2106.10256 [hep-th]

Jakobsen GU, Mogull G, Plefka J, Steinhoff J (2022) SUSY in the sky with gravitons. JHEP 01:027. https://doi.org/10.1007/JHEP01(2022)027. arXiv:2109.04465 [hep-th]

Jani K, Healy J, Clark JA, London L, Laguna P, Shoemaker D (2016) Georgia tech catalog of gravitational waveforms. Class Quantum Grav 33(20):204001. https://doi.org/10.1088/0264-9381/33/20/204001. arXiv:1605.03204 [gr-qc]

Jani K, Shoemaker D, Cutler C (2019) Detectability of intermediate-mass black holes in multiband gravitational wave astronomy. Nature Astron 4(3):260–265. https://doi.org/10.1038/s41550-019-0932-7. arXiv:1908.04985 [gr-qc]

Jaramillo JL, Panosso Macedo R, Al Sheikh L (2021) Pseudospectrum and black hole quasinormal mode instability. Phys Rev X 11(3):031003. https://doi.org/10.1103/PhysRevX.11.031003. arXiv:2004.06434 [gr-qc]

Jaramillo JL, Panosso Macedo R, Sheikh LA (2022) Gravitational wave signatures of black hole quasinormal mode instability. Phys Rev Lett 128(21):211102. https://doi.org/10.1103/PhysRevLett.128.211102. arXiv:2105.03451 [gr-qc]

Jaramillo V, Sanchis-Gual N, Barranco J, Bernal A, Degollado JC, Herdeiro C, Megevand M, Núñez D (2022) Head-on collisions of ℓ-boson stars. Phys Rev D 105(10):104057. https://doi.org/10.1103/PhysRevD.105.104057. arXiv:2202.00696 [gr-qc]

Jaranowski P, Krolak A (2005) Gravitational-wave data analysis. Formalism and sample applications: the gaussian case. Living Rev Relativ 8:3. https://doi.org/10.12942/lrr-2012-4. arXiv:0711.1115 [gr-qc]

Jaranowski P, Schafer G (2012) Towards the 4th post-Newtonian Hamiltonian for two-point-mass systems. Phys Rev D 86:061503. https://doi.org/10.1103/PhysRevD.86.061503. arXiv:1207.5448 [gr-qc]

Jaranowski P, Schäfer G (2013) Dimensional regularization of local singularities in the 4th post-Newtonian two-point-mass Hamiltonian. Phys Rev D 87:081503. https://doi.org/10.1103/PhysRevD.87.081503. arXiv:1303.3225 [gr-qc]

Jaranowski P, Schäfer G (2015) Derivation of local-in-time fourth post-Newtonian ADM Hamiltonian for spinless compact binaries. Phys Rev D 92(12):124043. https://doi.org/10.1103/PhysRevD.92.124043. arXiv:1508.01016 [gr-qc]

Jeannerot R, Rocher J, Sakellariadou M (2003) How generic is cosmic string formation in SUSY GUTs. Phys Rev D 68:103514. https://doi.org/10.1103/PhysRevD.68.103514. arXiv:hep-ph/0308134

Jenet FA, Hobbs GB, van Straten W, Manchester RN, Bailes M, Verbiest J, Edwards RT, Hotan AW, Sarkissian JM, Ord SM (2006) Upper bounds on the low-frequency stochastic gravitational wave background from pulsar timing observations: current limits and future prospects. Astrophys J 653:1571–1576. https://doi.org/10.1086/508702. arXiv:astro-ph/0609013

Jenkins AC, Sakellariadou M (2018) Anisotropies in the stochastic gravitational-wave background: formalism and the cosmic string case. Phys Rev D 98(6):063509. https://doi.org/10.1103/PhysRevD.98.063509. arXiv:1802.06046 [astro-ph.CO]

Jenkins AC, Sakellariadou M (2020) Primordial black holes from cusp collapse on cosmic strings. arXiv e-prints arXiv:2006.16249 [astro-ph.CO]

Jensen BP, Candelas P (1986) The Schwarzschild Radial Functions. Phys Rev D 33:1590. [Erratum: Phys. Rev. D 35, 4041 (1987)]. https://doi.org/10.1103/PhysRevD.35.4041

Jiménez-Forteza X, Keitel D, Husa S, Hannam M, Khan S, Pürrer M (2017) Hierarchical data-driven approach to fitting numerical relativity data for nonprecessing binary black holes with an application to final spin and radiated energy. Phys Rev D 95(6):064024. https://doi.org/10.1103/PhysRevD.95.064024. arXiv:1611.00332 [gr-qc]

Jiménez Forteza X, Bhagwat S, Pani P, Ferrari V (2020) Spectroscopy of binary black hole ringdown using overtones and angular modes. Phys Rev D 102(4):044053. https://doi.org/10.1103/PhysRevD.102.044053. arXiv:2005.03260 [gr-qc]

Johnson PT, Coughlin MW, Hamilton A, Bustamante-Rosell MJ, Ashton G, Corey S, Kupfer T, Littenberg TB, Reed D, Zimmerman A (2023) Multimessenger parameter inference of gravitational-wave and electromagnetic observations of white dwarf binaries. Mon Not R Astron Soc 525(3):4121–4128. https://doi.org/10.1093/mnras/stad2579. arXiv:2112.00145 [astro-ph.IM]

Johnson-McDaniel NK, Yunes N, Tichy W, Owen BJ (2009) Conformally curved binary black hole initial data including tidal deformations and outgoing radiation. Phys Rev D 80:124039. https://doi.org/10.1103/PhysRevD.80.124039. arXiv:0907.0891 [gr-qc]

Johnson-McDaniel NK, Shah AG, Whiting BF (2015) Experimental mathematics meets gravitational self-force. Phys Rev D 92(4):044007. https://doi.org/10.1103/PhysRevD.92.044007. arXiv:1503.02638 [gr-qc]

Johnson-McDaniel NK, Ghosh A, Ghonge S, Saleem M, Krishnendu NV, Clark JA (2022) Investigating the relation between gravitational wave tests of general relativity. Phys Rev D 105(4):044020. https://doi.org/10.1103/PhysRevD.105.044020. arXiv:2109.06988 [gr-qc]

Jones NT, Stoica H, Tye S (2002) Brane interaction as the origin of inflation. JHEP 07:051. https://doi.org/10.1088/1126-6708/2002/07/051. arXiv:hep-th/0203163

Jones NT, Stoica H, Tye S (2003) The Production, spectrum and evolution of cosmic strings in brane inflation. Phys Lett B 563:6–14. https://doi.org/10.1016/S0370-2693(03)00592-6. arXiv:hep-th/0303269

Joshi AV, Rosofsky SG, Haas R, Huerta EA (2023) Numerical relativity higher order gravitational waveforms of eccentric, spinning, nonprecessing binary black hole mergers. Phys Rev D 107(6):064038. https://doi.org/10.1103/PhysRevD.107.064038. arXiv:2210.01852 [gr-qc]

Julié FL (2018) Gravitational radiation from compact binary systems in Einstein-Maxwell-dilaton theories. JCAP 10:033. https://doi.org/10.1088/1475-7516/2018/10/033. arXiv:1809.05041 [gr-qc]

Julié FL (2018) On the motion of hairy black holes in Einstein-Maxwell-dilaton theories. JCAP 01:026. https://doi.org/10.1088/1475-7516/2018/01/026. arXiv:1711.10769 [gr-qc]

Julié FL (2018) Reducing the two-body problem in scalar-tensor theories to the motion of a test particle: a scalar-tensor effective-one-body approach. Phys Rev D 97(2):024047. https://doi.org/10.1103/PhysRevD.97.024047. arXiv:1709.09742 [gr-qc]

Julié FL, Berti E (2019) Post-Newtonian dynamics and black hole thermodynamics in Einstein-scalar-Gauss-Bonnet gravity. Phys Rev D 100(10):104061. https://doi.org/10.1103/PhysRevD.100.104061. arXiv:1909.05258 [gr-qc]

Julié FL, Berti E (2020) $d+1$ formalism in Einstein-scalar-Gauss-Bonnet gravity. Phys Rev D 101(12):124045. https://doi.org/10.1103/PhysRevD.101.124045. arXiv:2004.00003 [gr-qc]

Julié FL, Deruelle N (2017) Two-body problem in Scalar-Tensor theories as a deformation of General Relativity: an Effective-One-Body approach. Phys Rev D 95(12):124054. https://doi.org/10.1103/PhysRevD.95.124054. arXiv:1703.05360 [gr-qc]

Julié FL, Baibhav V, Berti E, Buonanno A (2023) Third post-Newtonian effective-one-body Hamiltonian in scalar-tensor and Einstein-scalar-Gauss-Bonnet gravity. Phys Rev D 107(10):104044. https://doi.org/10.1103/PhysRevD.107.104044. arXiv:2212.13802 [gr-qc]

Julié FL, Pompili L, Buonanno A (2025) Inspiral-merger-ringdown waveforms in Einstein-scalar-Gauss-Bonnet gravity within the effective-one-body formalism. Phys Rev D 111(2):024016. https://doi.org/10.1103/PhysRevD.111.024016. arXiv:2406.13654 [gr-qc]

Kachru S, Kallosh R, Linde AD, Maldacena JM, McAllister LP, Trivedi SP (2003) Towards inflation in string theory. JCAP 10:013. https://doi.org/10.1088/1475-7516/2003/10/013. arXiv:hep-th/0308055

Kachru S, Kallosh R, Linde AD, Trivedi SP (2003) De Sitter vacua in string theory. Phys Rev D 68:046005. https://doi.org/10.1103/PhysRevD.68.046005. arXiv:hep-th/0301240

Kaiser AR, McWilliams ST (2021) Sensitivity of present and future detectors across the black-hole binary gravitational wave spectrum. Class Quantum Grav 38(5):055009. https://doi.org/10.1088/1361-6382/abd4f6. arXiv:2010.02135 [gr-qc]

Kalaghatgi C, Hannam M (2021) Investigating the effect of in-plane spin directions for precessing binary black hole systems. Phys Rev D 103(2):024024. https://doi.org/10.1103/PhysRevD.103.024024. arXiv:2008.09957 [gr-qc]

Kälin G, Porto RA (2020) From boundary data to bound states. JHEP 01:072. https://doi.org/10.1007/JHEP01(2020)072. arXiv:1910.03008 [hep-th]

Kälin G, Porto RA (2020) From boundary data to bound states. Part II. Scattering angle to dynamical invariants (with twist). JHEP 02:120. https://doi.org/10.1007/JHEP02(2020)120. arXiv:1911.09130 [hep-th]

Kälin G, Porto RA (2020) Post-Minkowskian effective field theory for conservative binary dynamics. JHEP 11:106. https://doi.org/10.1007/JHEP11(2020)106. arXiv:2006.01184 [hep-th]

Kälin G, Liu Z, Porto RA (2020) Conservative dynamics of binary systems to third post-minkowskian order from the effective field theory approach. Phys Rev Lett 125(26):261103. https://doi.org/10.1103/PhysRevLett.125.261103. arXiv:2007.04977 [hep-th]

Kälin G, Liu Z, Porto RA (2020) Conservative tidal effects in compact binary systems to next-to-leading post-minkowskian order. Phys Rev D 102:124025. https://doi.org/10.1103/PhysRevD.102.124025. arXiv:2008.06047 [hep-th]

Kälin G, Neef J, Porto RA (2023) Radiation-reaction in the effective field theory approach to post-minkowskian dynamics. JHEP 01:140. https://doi.org/10.1007/JHEP01(2023)140. arXiv:2207.00580 [hep-th]

Kalinani JV, Ciolfi R, Kastaun W, Giacomazzo B, Cipolletta F, Ennoggi L (2022) Implementing a new recovery scheme for primitive variables in the general relativistic magnetohydrodynamic code Spritz. Phys Rev D 105(10):103031. https://doi.org/10.1103/PhysRevD.105.103031. arXiv:2107.10620 [astro-ph.HE]

Kamaretsos I, Hannam M, Husa S, Sathyaprakash BS (2012) Black-hole hair loss: learning about binary progenitors from ringdown signals. Phys Rev D 85:024018. https://doi.org/10.1103/PhysRevD.85.024018. arXiv:1107.0854 [gr-qc]

Kamaretsos I, Hannam M, Sathyaprakash B (2012) Is black-hole ringdown a memory of its progenitor? Phys Rev Lett 109:141102. https://doi.org/10.1103/PhysRevLett.109.141102. arXiv:1207.0399 [gr-qc]

Kang Y, Liu C, Zhu JP, Gao Y, Shao L, Zhang B, Sun H, Yin Y, Zhang BB (2024) Prospects for detecting neutron star-white dwarf mergers with decihertz gravitational-wave observatories. Mon Not R Astron Soc 528(3):5309–5322. https://doi.org/10.1093/mnras/stae340. arXiv:2309.16991 [astro-ph.HE]

Kanti P, Tamvakis K (1995) Classical moduli O (alpha-prime) hair. Phys Rev D 52:3506–3511. https://doi.org/10.1103/PhysRevD.52.3506. arXiv:hep-th/9504031

Kanti P, Mavromatos NE, Rizos J, Tamvakis K, Winstanley E (1996) Dilatonic black holes in higher curvature string gravity. Phys Rev D 54:5049–5058. https://doi.org/10.1103/PhysRevD.54.5049. arXiv:hep-th/9511071

Kaspi VM, Taylor JH, Ryba MF (1994) High - precision timing of millisecond pulsars. 3: Long - term monitoring of PSRs B1855+09 and B1937+21. Astrophys J 428:713. https://doi.org/10.1086/174280

Katz ML (2022) Fully automated end-to-end pipeline for massive black hole binary signal extraction from LISA data. Phys Rev D 105(4):044055. https://doi.org/10.1103/PhysRevD.105.044055. arXiv:2111.01064 [gr-qc]

Katz ML, Marsat S, Chua A, Babak S, Larson SL (2020) GPU-accelerated massive black hole binary parameter estimation with LISA. Phys Rev D 102(2):023033. https://doi.org/10.1103/PhysRevD.102.023033. arXiv:2005.01827 [gr-qc]

Katz ML, Chua A, Speri L, Warburton N, Hughes SA (2021) Fast extreme-mass-ratio-inspiral waveforms: new tools for millihertz gravitational-wave data analysis. Phys Rev D 104(6):064047. https://doi.org/10.1103/PhysRevD.104.064047. arXiv:2104.04582 [gr-qc]

Katz ML, Danielski C, Karnesis N, Korol V, Tamanini N, Cornish NJ, Littenberg TB (2022) Bayesian characterization of circumbinary sub-stellar objects with LISA. Mon Not R Astron Soc 517(1):697–711. https://doi.org/10.1093/mnras/stac2555. arXiv:2205.03461 [astro-ph.EP]

Katz ML, Karnesis N, Korsakova N, Gair JR, Stergioulas N (2025) Efficient GPU-accelerated multisource global fit pipeline for LISA data analysis. Phys Rev D 111(2):024060. https://doi.org/10.1103/PhysRevD.111.024060. arXiv:2405.04690 [gr-qc]

Kaup DJ (1968) Klein-Gordon Geon. Phys Rev 172:1331–1342. https://doi.org/10.1103/PhysRev.172.1331

Kavanagh BJ, Nichols DA, Bertone G, Gaggero D (2020) Detecting dark matter around black holes with gravitational waves: effects of dark-matter dynamics on the gravitational waveform. Phys Rev D 102(8):083006. https://doi.org/10.1103/PhysRevD.102.083006. arXiv:2002.12811 [gr-qc]

Kavanagh C, Ottewill AC, Wardell B (2016) Analytical high-order post-Newtonian expansions for spinning extreme mass ratio binaries. Phys Rev D 93(12):124038. https://doi.org/10.1103/PhysRevD.93.124038. arXiv:1601.03394 [gr-qc]

Kegeles LS, Cohen JM (1979) Constructive procedure for perturbations of space-times. Phys Rev D 19:1641–1664. https://doi.org/10.1103/PhysRevD.19.1641
Keidl TS, Shah AG, Friedman JL, Kim DH, Price LR (2010) Gravitational Self-force in a Radiation Gauge. Phys Rev D 82(12):124012. [Erratum: Phys. Rev. D 90, 109902 (2014)]. https://doi.org/10.1103/PhysRevD.82.124012. arXiv:1004.2276 [gr-qc]
Kesden M (2011) Transition from adiabatic inspiral to plunge into a spinning black hole. Phys Rev D 83:104011. https://doi.org/10.1103/PhysRevD.83.104011. arXiv:1101.3749 [gr-qc]
Kesden M, Gair J, Kamionkowski M (2005) Gravitational-wave signature of an inspiral into a supermassive horizonless object. Phys Rev D 71:044015. https://doi.org/10.1103/PhysRevD.71.044015. arXiv:astro-ph/0411478
Khakhaleva-Li Z, Hogan CJ (2020) Will LISA Detect Harmonic Gravitational Waves from Galactic Cosmic String Loops? arXiv e-prints arXiv:2006.00438 [astro-ph.CO]
Khalil M, Sennett N, Steinhoff J, Vines J, Buonanno A (2018) Hairy binary black holes in Einstein-Maxwell-dilaton theory and their effective-one-body description. Phys Rev D 98(10):104010. https://doi.org/10.1103/PhysRevD.98.104010. arXiv:1809.03109 [gr-qc]
Khalil M, Steinhoff J, Vines J, Buonanno A (2020) Fourth post-Newtonian effective-one-body Hamiltonians with generic spins. Phys Rev D 101(10):104034. https://doi.org/10.1103/PhysRevD.101.104034. arXiv:2003.04469 [gr-qc]
Khalil M, Buonanno A, Steinhoff J, Vines J (2021) Radiation-reaction force and multipolar waveforms for eccentric, spin-aligned binaries in the effective-one-body formalism. Phys Rev D 104(2):024046. https://doi.org/10.1103/PhysRevD.104.024046. arXiv:2104.11705 [gr-qc]
Khalil M, Buonanno A, Steinhoff J, Vines J (2022) Energetics and scattering of gravitational two-body systems at fourth post-Minkowskian order. Phys Rev D 106(2):024042. https://doi.org/10.1103/PhysRevD.106.024042. arXiv:2204.05047 [gr-qc]
Khalil M, Buonanno A, Estelles H, Mihaylov DP, Ossokine S, Pompili L, Ramos-Buades A (2023) Theoretical groundwork supporting the precessing-spin two-body dynamics of the effective-one-body waveform models SEOBNRv5. Phys Rev D 108(12):124036. https://doi.org/10.1103/PhysRevD.108.124036. arXiv:2303.18143 [gr-qc]
Khan A, Huerta EA, Zheng H (2022) Interpretable AI forecasting for numerical relativity waveforms of quasicircular, spinning, nonprecessing binary black hole mergers. Phys Rev D 105(2):024024. https://doi.org/10.1103/PhysRevD.105.024024. arXiv:2110.06968 [gr-qc]
Khan FM, Just A, Merritt D (2011) Efficient merger of binary supermassive black holes in merging galaxies. Astrophys J 732:89. https://doi.org/10.1088/0004-637X/732/2/89. arXiv:1103.0272 [astro-ph.CO]
Khan S, Green R (2021) Gravitational-wave surrogate models powered by artificial neural networks. Phys Rev D 103(6):064015. https://doi.org/10.1103/PhysRevD.103.064015. arXiv:2008.12932 [gr-qc]
Khan S, Husa S, Hannam M, Ohme F, Pürrer M, Jiménez Forteza X, Bohé A (2016) Frequency-domain gravitational waves from nonprecessing black-hole binaries. II. A phenomenological model for the advanced detector era. Phys Rev D 93(4):044007. https://doi.org/10.1103/PhysRevD.93.044007. arXiv:1508.07253 [gr-qc]
Khan S, Chatziioannou K, Hannam M, Ohme F (2019) Phenomenological model for the gravitational-wave signal from precessing binary black holes with two-spin effects. Phys Rev D 100(2):024059. https://doi.org/10.1103/PhysRevD.100.024059. arXiv:1809.10113 [gr-qc]
Khan S, Ohme F, Chatziioannou K, Hannam M (2020) Including higher order multipoles in gravitational-wave models for precessing binary black holes. Phys Rev D 101(2):024056. https://doi.org/10.1103/PhysRevD.101.024056. arXiv:1911.06050 [gr-qc]
Khanna G, McKennon J (2010) Numerical modeling of gravitational wave sources accelerated by OpenCL. Comput Phys Commun 181:1605–1611. https://doi.org/10.1016/j.cpc.2010.05.014. arXiv:1001.3631 [gr-qc]
Khera N, Krishnan B, Ashtekar A, De Lorenzo T (2021) Inferring the gravitational wave memory for binary coalescence events. Phys Rev D 103(4):044012. https://doi.org/10.1103/PhysRevD.103.044012. arXiv:2009.06351 [gr-qc]
Khera N, Ribes Metidieri A, Bonga B, Jiménez Forteza X, Krishnan B, Poisson E, Pook-Kolb D, Schnetter E, Yang H (2023) Nonlinear ringdown at the black hole horizon. Phys Rev Lett 131(23):231401. https://doi.org/10.1103/PhysRevLett.131.231401. arXiv:2306.11142 [gr-qc]
Kidder LE (1995) Coalescing binary systems of compact objects to postNewtonian 5/2 order. 5. Spin effects. Phys Rev D 52:821–847. https://doi.org/10.1103/PhysRevD.52.821. arXiv:gr-qc/9506022

Kidder LE, Will CM, Wiseman AG (1993) Spin effects in the inspiral of coalescing compact binaries. Phys Rev D 47(10):R4183–R4187. https://doi.org/10.1103/PhysRevD.47.R4183. arXiv:gr-qc/9211025
Kidder LE et al (2017) SpECTRE: a task-based discontinuous galerkin code for relativistic astrophysics. J Comput Phys 335:84–114. https://doi.org/10.1016/j.jcp.2016.12.059. arXiv:1609.00098 [astro-ph.HE]
Kilic M, Brown WR, Bedard A, Kosakowski A (2021) The discovery of Two LISA sources within 0.5 kpc. Astrophys J Lett 918(1):L14. https://doi.org/10.3847/2041-8213/ac1e2b. arXiv:2108.08324 [astro-ph.SR]
Kilic M, Kosakowski A, Moss AG, Bergeron P, Conly AA (2021) An isolated white dwarf with a 70 s spin period. Astrophys J Lett 923(1):L6. https://doi.org/10.3847/2041-8213/ac3b60. arXiv:2111.14902 [astro-ph.SR]
Kim H, Lenoci A, Stomberg I, Xue X (2023) Adiabatically compressed wave dark matter halo and intermediate-mass-ratio inspirals. Phys Rev D 107(8):083005. https://doi.org/10.1103/PhysRevD.107.083005. arXiv:2212.07528 [astro-ph.GA]
Kim JW, Levi M, Yin Z (2023) N^3LO quadratic-in-spin interactions for generic compact binaries. JHEP 03:098. https://doi.org/10.1007/JHEP03(2023)098. arXiv:2209.09235 [hep-th]
Kim JW, Levi M, Yin Z (2023) N^3LO spin-orbit interaction via the EFT of spinning gravitating objects. JHEP 05:184. https://doi.org/10.1007/JHEP05(2023)184. arXiv:2208.14949 [hep-th]
King AR, Pringle JE, Hofmann JA (2008) The evolution of black hole mass and spin in active galactic nuclei. Mon Not R Astron Soc 385:1621. https://doi.org/10.1111/j.1365-2966.2008.12943.x. arXiv:0801.1564 [astro-ph]
Kiuchi K, Shibata M, Montero PJ, Font JA (2011) Gravitational waves from the Papaloizou-Pringle instability in black hole-torus systems. Phys Rev Lett 106:251102. https://doi.org/10.1103/PhysRevLett.106.251102. arXiv:1105.5035 [astro-ph.HE]
Kiuchi K, Kawaguchi K, Kyutoku K, Sekiguchi Y, Shibata M, Taniguchi K (2017) Sub-radian-accuracy gravitational waveforms of coalescing binary neutron stars in numerical relativity. Phys Rev D 96(8):084060. https://doi.org/10.1103/PhysRevD.96.084060. arXiv:1708.08926 [astro-ph.HE]
Kiuchi K, Held LE, Sekiguchi Y, Shibata M (2022) Implementation of advanced Riemann solvers in a neutrino-radiation magnetohydrodynamics code in numerical relativity and its application to a binary neutron star merger. Phys Rev D 106(12):124041. https://doi.org/10.1103/PhysRevD.106.124041. arXiv:2205.04487 [astro-ph.HE]
Kleihaus B, Kunz J, Radu E (2011) Rotating black holes in Dilatonic Einstein-gauss-bonnet theory. Phys Rev Lett 106:151104. https://doi.org/10.1103/PhysRevLett.106.151104. arXiv:1101.2868 [gr-qc]
Klein A (2021) EFPE: Efficient fully precessing eccentric gravitational waveforms for binaries with long inspirals. arXiv e-prints arXiv:2106.10291 [gr-qc]
Klein A, Jetzer P (2010) Spin effects in the phasing of gravitational waves from binaries on eccentric orbits. Phys Rev D 81:124001. https://doi.org/10.1103/PhysRevD.81.124001. arXiv:1005.2046 [gr-qc]
Klein A, Boetzel Y, Gopakumar A, Jetzer P, de Vittori L (2018) Fourier domain gravitational waveforms for precessing eccentric binaries. Phys Rev D 98(10):104043. https://doi.org/10.1103/PhysRevD.98.104043. arXiv:1801.08542 [gr-qc]
Klein A et al (2016) Science with the space-based interferometer eLISA: supermassive black hole binaries. Phys Rev D 93(2):024003. https://doi.org/10.1103/PhysRevD.93.024003. arXiv:1511.05581 [gr-qc]
Klein A, et al. (2022) The last three years: multiband gravitational-wave observations of stellar-mass binary black holes. arXiv e-prints arXiv:2204.03423 [astro-ph.HE]
Knowles TD, Devine C, Buch DA, Bilgili SA, Adams TR, Etienne ZB, Mcwilliams ST (2018) Improving performance of SEOBNRv3 by $\sim$300x. Class Quantum Grav 35(15):155003. https://doi.org/10.1088/1361-6382/aacb8c. arXiv:1803.06346 [gr-qc]
Kobayashi T (2019) Horndeski theory and beyond: a review. Rept Prog Phys 82(8):086901. https://doi.org/10.1088/1361-6633/ab2429. arXiv:1901.07183 [gr-qc]
Kokkotas KD (1991) Normal modes of the Kerr black hole. Class Quantum Grav 8:2217–2224. https://doi.org/10.1088/0264-9381/8/12/006
Kokkotas KD, Schmidt BG (1999) Quasinormal modes of stars and black holes. Living Rev Relativ 2:2. https://doi.org/10.12942/lrr-1999-2. arXiv:gr-qc/9909058
Kokkotas KD, Ruoff J, Andersson N (2004) The w-mode instability of ultracompact relativistic stars. Phys Rev D 70:043003. https://doi.org/10.1103/PhysRevD.70.043003. arXiv:astro-ph/0212429

Kölsch M, Dietrich T, Ujevic M, Brügmann B (2022) Investigating the mass-ratio dependence of the prompt-collapse threshold with numerical-relativity simulations. Phys Rev D 106(4):044026. https://doi.org/10.1103/PhysRevD.106.044026. arXiv:2112.11851 [gr-qc]

Königsdörffer C, Gopakumar A (2006) Phasing of gravitational waves from inspiralling eccentric binaries at the third-and-a-half post-Newtonian order. Phys Rev D 73:124012. https://doi.org/10.1103/PhysRevD.73.124012. arXiv:gr-qc/0603056

Konoplya RA, Zhidenko A (2016) Wormholes versus black holes: quasinormal ringing at early and late times. JCAP 12:043. https://doi.org/10.1088/1475-7516/2016/12/043. arXiv:1606.00517 [gr-qc]

Konoplya RA, Zhidenko A (2023) General black-hole metric mimicking Schwarzschild spacetime. JCAP 08:008. https://doi.org/10.1088/1475-7516/2023/08/008. arXiv:2303.03130 [gr-qc]

Köppel S (2018) Towards an exascale code for GRMHD on dynamical spacetimes. J Phys: Conf Ser 1031 (1):012017. https://doi.org/10.1088/1742-6596/1031/1/012017. arXiv:1711.08221 [gr-qc]

Kormendy J, Ho LC (2013) Coevolution (Or Not) of supermassive black holes and host galaxies. Ann Rev Astron Astrophys 51:511–653. https://doi.org/10.1146/annurev-astro-082708-101811. arXiv:1304.7762 [astro-ph.CO]

Kormendy J, Richstone D (1995) Inward bound: the search for supermassive black holes in galactic nuclei. Ann Rev Astron Astrophys 33:581. https://doi.org/10.1146/annurev.aa.33.090195.003053

Korol V, Safarzadeh M (2021) How can LISA probe a population of GW190425-like binary neutron stars in the Milky Way? Mon Not R Astron Soc 502(4):5576–5583. https://doi.org/10.1093/mnras/stab310. arXiv:2012.03070 [astro-ph.HE]

Korol V, Rossi EM, Groot PJ, Nelemans G, Toonen S, Brown A (2017) Prospects for detection of detached double white dwarf binaries with Gaia, LSST and LISA. Mon Not R Astron Soc 470(2):1894–1910. https://doi.org/10.1093/mnras/stx1285. arXiv:1703.02555 [astro-ph.HE]

Korol V, Hallakoun N, Toonen S, Karnesis N (2022) Observationally driven Galactic double white dwarf population for LISA. Mon Not R Astron Soc 511(4):5936–5947. https://doi.org/10.1093/mnras/stac415. arXiv:2109.10972 [astro-ph.HE]

Korol V, Igoshev AP, Toonen S, Karnesis N, Moore CJ, Finch E, Klein A (2024) Neutron star - white dwarf binaries: probing formation pathways and natal kicks with LISA. Mon Not R Astron Soc 530 (1):844–860. https://doi.org/10.1093/mnras/stae889. arXiv:2310.06559 [astro-ph.HE]

Korsakova N, Babak S, Katz ML, Karnesis N, Khukhlaev S, Gair JR (2024) Neural density estimation for Galactic binaries in the LISA data analysis. Phys Rev D 110(10):104069. https://doi.org/10.1103/PhysRevD.110.104069. arXiv:2402.13701 [gr-qc]

Koshelev AS, Mazumdar A (2017) Do massive compact objects without event horizon exist in infinite derivative gravity? Phys Rev D 96(8):084069. https://doi.org/10.1103/PhysRevD.96.084069. arXiv:1707.00273 [gr-qc]

Kosmopoulos D, Luna A (2021) Quadratic-in-spin Hamiltonian at $\mathcal{O}(G^2)$ from scattering amplitudes. JHEP 07:037. https://doi.org/10.1007/JHEP07(2021)037. arXiv:2102.10137 [hep-th]

Kosower DA, Maybee B, O'Connell D (2019) Amplitudes, observables, and classical scattering. JHEP 02:137. https://doi.org/10.1007/JHEP02(2019)137. arXiv:1811.10950 [hep-th]

Kovács AD (2019) Well-posedness of cubic Horndeski theories. Phys Rev D 100(2):024005. https://doi.org/10.1103/PhysRevD.100.024005. arXiv:1904.00963 [gr-qc]

Kovács AD, Reall HS (2020) Well-posed formulation of Lovelock and Horndeski theories. Phys Rev D 101(12):124003. https://doi.org/10.1103/PhysRevD.101.124003. arXiv:2003.08398 [gr-qc]

Kovács AD, Reall HS (2020) Well-posed formulation of scalar-tensor effective field theory. Phys Rev Lett 124(22):221101. https://doi.org/10.1103/PhysRevLett.124.221101. arXiv:2003.04327 [gr-qc]

Kozai Y (1962) Secular perturbations of asteroids with high inclination and eccentricity. Astron J 67:591–598. https://doi.org/10.1086/108790

Kremer K, Chatterjee S, Breivik K, Rodriguez CL, Larson SL, Rasio FA (2018) LISA sources in milky way globular clusters. Phys Rev Lett 120(19):191103. https://doi.org/10.1103/PhysRevLett.120.191103. arXiv:1802.05661 [astro-ph.HE]

Krishnendu NV, Saleem M, Samajdar A, Arun KG, Del Pozzo W, Mishra CK (2019) Constraints on the binary black hole nature of GW151226 and GW170608 from the measurement of spin-induced quadrupole moments. Phys Rev D 100(10):104019. https://doi.org/10.1103/PhysRevD.100.104019. arXiv:1908.02247 [gr-qc]

Kruckow MU (2020) Masses of double neutron star mergers. Astron Astrophys 639:A123. https://doi.org/10.1051/0004-6361/202037519. arXiv:2002.08011 [astro-ph.SR]

Kuan HJ, Lam A, Doneva DD, Yazadjiev SS, Shibata M, Kiuchi K (2023) Dynamical scalarization during neutron star mergers in scalar-Gauss-Bonnet theory. Phys Rev D 108(6):063033. https://doi.org/10.1103/PhysRevD.108.063033. arXiv:2302.11596 [gr-qc]

Küchler L, Compère G, Durkan L, Pound A (2024) Self-force framework for transition-to-plunge waveforms. SciPost Phys 17(2):056. https://doi.org/10.21468/SciPostPhys.17.2.056. arXiv:2405.00170 [gr-qc]

Kumar P, Blackman J, Field SE, Scheel M, Galley CR, Boyle M, Kidder LE, Pfeiffer HP, Szilagyi B, Teukolsky SA (2019) Constraining the parameters of GW150914 and GW170104 with numerical relativity surrogates. Phys Rev D 99(12):124005. https://doi.org/10.1103/PhysRevD.99.124005. arXiv:1808.08004 [gr-qc]

Kuntz A (2019) Two-body potential of Vainshtein screened theories. Phys Rev D 100(2):024024. https://doi.org/10.1103/PhysRevD.100.024024. arXiv:1905.07340 [gr-qc]

Kuntz A (2022) Precession resonances in hierarchical triple systems. Phys Rev D 105(2):024017. https://doi.org/10.1103/PhysRevD.105.024017. arXiv:2112.05167 [gr-qc]

Kuntz A, Piazza F, Vernizzi F (2019) Effective field theory for gravitational radiation in scalar-tensor gravity. JCAP 05:052. https://doi.org/10.1088/1475-7516/2019/05/052. arXiv:1902.04941 [gr-qc]

Kuntz A, Serra F, Trincherini E (2021) Effective two-body approach to the hierarchical three-body problem. Phys Rev D 104(2):024016. https://doi.org/10.1103/PhysRevD.104.024016. arXiv:2104.13387 [hep-th]

Kuntz A, Serra F, Trincherini E (2023) Effective two-body approach to the hierarchical three-body problem: quadrupole to 1PN. Phys Rev D 107(4):044011. https://doi.org/10.1103/PhysRevD.107.044011. arXiv:2210.13493 [gr-qc]

Kupfer T, Korol V, Shah S, Nelemans G, Marsh TR, Ramsay G, Groot PJ, Steeghs D, Rossi EM (2018) LISA verification binaries with updated distances from Gaia Data Release 2. Mon Not R Astron Soc 480(1):302–309. https://doi.org/10.1093/mnras/sty1545. arXiv:1805.00482 [astro-ph.SR]

Kupfer T et al (2024) LISA galactic binaries with astrometry from Gaia DR3. Astrophys J 963(2):100. https://doi.org/10.3847/1538-4357/ad2068. arXiv:2302.12719 [astro-ph.SR]

Kuroyanagi S, Miyamoto K, Sekiguchi T, Takahashi K, Silk J (2012) Forecast constraints on cosmic string parameters from gravitational wave direct detection experiments. Phys Rev D 86:023503. https://doi.org/10.1103/PhysRevD.86.023503. arXiv:1202.3032 [astro-ph.CO]

Kuroyanagi S, Miyamoto K, Sekiguchi T, Takahashi K, Silk J (2013) Forecast constraints on cosmic strings from future CMB, pulsar timing and gravitational wave direct detection experiments. Phys Rev D 87(2):023522. [Erratum: Phys. Rev. D 87, 069903 (2013)]. https://doi.org/10.1103/PhysRevD.87.023522. arXiv:1210.2829 [astro-ph.CO]

Lackeos K, Littenberg TB, Cornish NJ, Thorpe JI (2023) The LISA data challenge radler analysis and time-dependent ultra-compact binary catalogues. Astron Astrophys 678:A123. https://doi.org/10.1051/0004-6361/202347222. arXiv:2308.12827 [gr-qc]

Lackeos KA, Burko LM (2012) Self-forced gravitational waveforms for extreme and intermediate mass ratio inspirals. Phys Rev D 86:084055. https://doi.org/10.1103/PhysRevD.86.084055. arXiv:1206.1452 [gr-qc]

Lackey BD, Bernuzzi S, Galley CR, Meidam J, Van Den Broeck C (2017) Effective-one-body waveforms for binary neutron stars using surrogate models. Phys Rev D 95(10):104036. https://doi.org/10.1103/PhysRevD.95.104036. arXiv:1610.04742 [gr-qc]

Lackey BD, Pürrer M, Taracchini A, Marsat S (2019) Surrogate model for an aligned-spin effective one body waveform model of binary neutron star inspirals using Gaussian process regression. Phys Rev D 100(2):024002. https://doi.org/10.1103/PhysRevD.100.024002. arXiv:1812.08643 [gr-qc]

Lagos M, Hui L (2023) Generation and propagation of nonlinear quasinormal modes of a Schwarzschild black hole. Phys Rev D 107(4):044040. https://doi.org/10.1103/PhysRevD.107.044040. arXiv:2208.07379 [gr-qc]

de Laix AA (1997) Observing long cosmic strings through gravitational lensing. Phys Rev D 56:6193–6204. https://doi.org/10.1103/PhysRevD.56.6193. arXiv:astro-ph/9705223

Lam A, Shibata M, Kiuchi K (2023) Numerical-relativity simulation for tidal disruption of white dwarfs by a supermassive black hole. Phys Rev D 107(4):043033. https://doi.org/10.1103/PhysRevD.107.043033. arXiv:2212.10891 [astro-ph.HE]

Lamberts A, Blunt S, Littenberg TB, Garrison-Kimmel S, Kupfer T, Sanderson RE (2019) Predicting the LISA white dwarf binary population in the Milky Way with cosmological simulations. Mon Not R Astron Soc 490(4):5888–5903. https://doi.org/10.1093/mnras/stz2834. arXiv:1907.00014 [astro-ph.HE]

Landau LD, Lifschits EM (1975) The Classical Theory of Fields, Course of Theoretical Physics, vol 2. Pergamon Press, Oxford

Lang RN (2014) Compact binary systems in scalar-tensor gravity. II. Tensor gravitational waves to second post-Newtonian order. Phys Rev D 89(8):084014. https://doi.org/10.1103/PhysRevD.89.084014. arXiv:1310.3320 [gr-qc]

Lang RN (2015) Compact binary systems in scalar-tensor gravity. III. Scalar waves and energy flux. Phys Rev D 91(8):084027. https://doi.org/10.1103/PhysRevD.91.084027. arXiv:1411.3073 [gr-qc]

Lang RN, Hughes SA (2008) Localizing coalescing massive black hole binaries with gravitational waves. Astrophys J 677:1184. https://doi.org/10.1086/528953. arXiv:0710.3795 [astro-ph]

Lange J et al (2017) Parameter estimation method that directly compares gravitational wave observations to numerical relativity. Phys Rev D 96(10):104041. https://doi.org/10.1103/PhysRevD.96.104041. arXiv:1705.09833 [gr-qc]

Larrouturou F, Blanchet L, Henry Q, Faye G (2022) The quadrupole moment of compact binaries to the fourth post-Newtonian order: II. Dimensional regularization and renormalization. Class Quantum Grav 39(11):115008. https://doi.org/10.1088/1361-6382/ac5ba0. arXiv:2110.02243 [gr-qc]

Larrouturou F, Henry Q, Blanchet L, Faye G (2022) The quadrupole moment of compact binaries to the fourth post-Newtonian order: I. Non-locality in time and infra-red divergencies. Class Quantum Grav 39(11):115007. https://doi.org/10.1088/1361-6382/ac5762. arXiv:2110.02240 [gr-qc]

Latif MA, Ferrara A (2016) Formation of supermassive black hole seeds. Publ Astron Soc Austral 33:e051. https://doi.org/10.1017/pasa.2016.41. arXiv:1605.07391 [astro-ph.GA]

Lau M, Mandel I, Vigna-Gómez A, Neijssel CJ, Stevenson S, Sesana A (2020) Detecting double neutron stars with LISA. Mon Not R Astron Soc 492(3):3061–3072. https://doi.org/10.1093/mnras/staa002. arXiv:1910.12422 [astro-ph.HE]

Le Tiec A (2014) A note on celestial mechanics in kerr spacetime. Class Quantum Grav 31:097001. https://doi.org/10.1088/0264-9381/31/9/097001. arXiv:1311.3836 [gr-qc]

Le Tiec A (2014) The overlap of numerical relativity, perturbation theory and post-newtonian theory in the binary black hole problem. Int J Mod Phys D 23(10):1430022. https://doi.org/10.1142/S0218271814300225. arXiv:1408.5505 [gr-qc]

Le Tiec A (2015) First law of mechanics for compact binaries on eccentric orbits. Phys Rev D 92 (8):084021. https://doi.org/10.1103/PhysRevD.92.084021. arXiv:1506.05648 [gr-qc]

Le Tiec A, Grandclément P (2018) Horizon surface gravity in corotating black hole binaries. Class Quantum Grav 35(14):144002. https://doi.org/10.1088/1361-6382/aac58c. arXiv:1710.03673 [gr-qc]

Le Tiec A, Mroue AH, Barack L, Buonanno A, Pfeiffer HP, Sago N, Taracchini A (2011) Periastron advance in black hole binaries. Phys Rev Lett 107:141101. https://doi.org/10.1103/PhysRevLett.107.141101. arXiv:1106.3278 [gr-qc]

Le Tiec A, Barausse E, Buonanno A (2012) Gravitational self-force correction to the binding energy of compact binary systems. Phys Rev Lett 108:131103. https://doi.org/10.1103/PhysRevLett.108.131103. arXiv:1111.5609 [gr-qc]

Le Tiec A, Blanchet L, Whiting BF (2012) The first law of binary black hole mechanics in general relativity and post-newtonian theory. Phys Rev D 85:064039. https://doi.org/10.1103/PhysRevD.85.064039. arXiv:1111.5378 [gr-qc]

Le Tiec A, Casals M, Franzin E (2021) Tidal love numbers of kerr black holes. Phys Rev D 103(8):084021. https://doi.org/10.1103/PhysRevD.103.084021. arXiv:2010.15795 [gr-qc]

Le Tiec A et al (2013) Periastron advance in spinning black hole binaries: gravitational self-force from numerical relativity. Phys Rev D 88(12):124027. https://doi.org/10.1103/PhysRevD.88.124027. arXiv:1309.0541 [gr-qc]

Leather B, Warburton N (2023) Applying the effective-source approach to frequency-domain self-force calculations for eccentric orbits. Phys Rev D 108(8):084045. https://doi.org/10.1103/PhysRevD.108.084045. arXiv:2306.17221 [gr-qc]

Leaver EW (1985) An Analytic representation for the quasi normal modes of Kerr black holes. Proc R Soc Lond A 402:285–298. https://doi.org/10.1098/rspa.1985.0119

Leaver EW (1986) Spectral decomposition of the perturbation response of the Schwarzschild geometry. Phys Rev D 34:384–408. [Erratum: Phys. Rev. D 38, 725 (1988)]. https://doi.org/10.1103/PhysRevD.34.384

Legred I, Kim Y, Deppe N, Chatziioannou K, Foucart F, Hébert F, Kidder LE (2023) Simulating neutron stars with a flexible enthalpy-based equation of state parametrization in spectre. Phys Rev D 107 (12):123017. https://doi.org/10.1103/PhysRevD.107.123017. arXiv:2301.13818 [astro-ph.HE]

Lehner L (2001) Numerical relativity: a review. Class Quantum Grav 18:R25–R86. https://doi.org/10.1088/0264-9381/18/17/202. arXiv:gr-qc/0106072
Lehner L, Moreschi OM (2007) Dealing with delicate issues in waveforms calculations. Phys Rev D 76:124040. https://doi.org/10.1103/PhysRevD.76.124040. arXiv:0706.1319 [gr-qc]
Lehner L, Liebling SL, Reula O (2006) AMR, stability and higher accuracy. Class Quantum Grav 23: S421–S446. https://doi.org/10.1088/0264-9381/23/16/S08. arXiv:gr-qc/0510111
Leibovich AK, Maia NT, Rothstein IZ, Yang Z (2020) Second post-Newtonian order radiative dynamics of inspiralling compact binaries in the effective field theory approach. Phys Rev D 101(8):084058. https://doi.org/10.1103/PhysRevD.101.084058. arXiv:1912.12546 [gr-qc]
Lemos J, Letelier PS (1994) Exact general relativistic thin disks around black holes. Phys Rev D 49:5135–5143. https://doi.org/10.1103/PhysRevD.49.5135
Levi M (2010) Next to leading order gravitational spin-orbit coupling in an effective field theory approach. Phys Rev D 82:104004. https://doi.org/10.1103/PhysRevD.82.104004. arXiv:1006.4139 [gr-qc]
Levi M (2010) Next to leading order gravitational Spin1-Spin2 coupling with Kaluza-Klein reduction. Phys Rev D 82:064029. https://doi.org/10.1103/PhysRevD.82.064029. arXiv:0802.1508 [gr-qc]
Levi M (2012) Binary dynamics from spin1-spin2 coupling at fourth post-Newtonian order. Phys Rev D 85:064043. https://doi.org/10.1103/PhysRevD.85.064043. arXiv:1107.4322 [gr-qc]
Levi M (2020) Effective field theories of post-newtonian gravity: a comprehensive review. Rept Prog Phys 83(7):075901. https://doi.org/10.1088/1361-6633/ab12bc. arXiv:1807.01699 [hep-th]
Levi M, Steinhoff J (2015) Leading order finite size effects with spins for inspiralling compact binaries. JHEP 06:059. https://doi.org/10.1007/JHEP06(2015)059. arXiv:1410.2601 [gr-qc]
Levi M, Steinhoff J (2015) Spinning gravitating objects in the effective field theory in the post-Newtonian scheme. JHEP 09:219. https://doi.org/10.1007/JHEP09(2015)219. arXiv:1501.04956 [gr-qc]
Levi M, Teng F (2021) NLO gravitational quartic-in-spin interaction. JHEP 01:066. https://doi.org/10.1007/JHEP01(2021)066. arXiv:2008.12280 [hep-th]
Levi M, Mougiakakos S, Vieira M (2021) Gravitational cubic-in-spin interaction at the next-to-leading post-Newtonian order. JHEP 01:036. https://doi.org/10.1007/JHEP01(2021)036. arXiv:1912.06276 [hep-th]
Levin J, Perez-Giz G (2008) A periodic table for black hole orbits. Phys Rev D 77:103005. https://doi.org/10.1103/PhysRevD.77.103005. arXiv:0802.0459 [gr-qc]
Lewis A, Zimmerman A, Pfeiffer HP (2017) Fundamental frequencies and resonances from eccentric and precessing binary black hole inspirals. Class Quantum Grav 34(12):124001. https://doi.org/10.1088/1361-6382/aa66f4. arXiv:1611.03418 [gr-qc]
Li C, Lovelace G (2008) A generalization of Ryan's theorem: probing tidal coupling with gravitational waves from nearly circular, nearly equatorial, extreme-mass-ratio inspirals. Phys Rev D 77:064022. https://doi.org/10.1103/PhysRevD.77.064022. arXiv:gr-qc/0702146
Li D, Wagle P, Chen Y, Yunes N (2023) Perturbations of spinning black holes beyond general relativity: modified Teukolsky equation. Phys Rev X 13(2):021029. https://doi.org/10.1103/PhysRevX.13.021029. arXiv:2206.10652 [gr-qc]
Li X, Sun L, Lo R, Payne E, Chen Y (2022) Angular emission patterns of remnant black holes. Phys Rev D 105(2):024016. https://doi.org/10.1103/PhysRevD.105.024016. arXiv:2110.03116 [gr-qc]
Li Z, Chen X, Chen HL, Li J, Yu S, Han Z (2020) Gravitational wave radiation of double degenerates with extremely low-mass WD companions. Astrophys J 893(1):2. https://doi.org/10.3847/1538-4357/ab7dc2. arXiv:2003.02480 [astro-ph.SR]
Liang ZC, Li ZY, Li EK, Zhang J, Hu YM (2024) Revisiting stochastic gravitational wave background in the strong signal case. Results Phys 63:107876. https://doi.org/10.1016/j.rinp.2024.107876. arXiv:2403.18709 [gr-qc]
Lidov ML (1962) The evolution of orbits of artificial satellites of planets under the action of gravitational perturbations of external bodies. Planet Space Sci 9(10):719–759. https://doi.org/10.1016/0032-0633(62)90129-0
Liebling SL (2002) The Singularity threshold of the nonlinear sigma model using 3-D adaptive mesh refinement. Phys Rev D 66:041703. https://doi.org/10.1103/PhysRevD.66.041703. arXiv:gr-qc/0202093
Liebling SL, Palenzuela C (2023) Dynamical boson stars. Living Rev Relativ 26:1. https://doi.org/10.1007/s41114-023-00043-4. arXiv:1202.5809 [gr-qc]
Liebling SL, Palenzuela C, Lehner L (2020) Toward fidelity and scalability in non-vacuum mergers. Class Quantum Grav 37(13):135006. https://doi.org/10.1088/1361-6382/ab8fcd. arXiv:2002.07554 [gr-qc]

LIGO Scientific Collaboration, Virgo Collaboration KAGRA, Collaboration, (2024) LVK Algorithm Library - LALSuite. Free software (GPL). https://doi.org/10.7935/GT1W-FZ16
Lim H, Khanna G, Apte A, Hughes SA (2019) Exciting black hole modes via misaligned coalescences: II. The mode content of late-time coalescence waveforms. Phys Rev D 100(8):084032. https://doi.org/10.1103/PhysRevD.100.084032. arXiv:1901.05902 [gr-qc]
Lim H, Hughes SA, Khanna G (2022) Measuring quasinormal mode amplitudes with misaligned binary black hole ringdowns. Phys Rev D 105(12):124030. https://doi.org/10.1103/PhysRevD.105.124030. arXiv:2204.06007 [gr-qc]
Lindblom L, Scheel MA, Kidder LE, Owen R, Rinne O (2006) A New generalized harmonic evolution system. Class Quantum Grav 23:S447–S462. https://doi.org/10.1088/0264-9381/23/16/S09. arXiv:gr-qc/0512093
Lindblom L, Owen BJ, Brown DA (2008) Model waveform accuracy standards for gravitational wave data analysis. Phys Rev D 78:124020. https://doi.org/10.1103/PhysRevD.78.124020. arXiv:0809.3844 [gr-qc]
Linde AD (1982) A new inflationary universe scenario: a possible solution of the horizon, flatness, homogeneity, isotropy and primordial monopole problems. Phys Lett B 108:389–393. https://doi.org/10.1016/0370-2693(82)91219-9
Lipunov VM, Postnov KA, Prokhorov ME (1987) The sources of gravitational waves with continuous and discrete spectra. Astron Astrophys 176(1):L1–L4
LISA Data Challenge Working Group (2022) LISA Data Challenge White Paper. In preparation
Littenberg T, Cornish N, Lackeos K, Robson T (2020) Global analysis of the gravitational wave signal from galactic binaries. Phys Rev D 101(12):123021. https://doi.org/10.1103/PhysRevD.101.123021. arXiv:2004.08464 [gr-qc]
Littenberg TB (2011) A detection pipeline for galactic binaries in LISA data. Phys Rev D 84:063009. https://doi.org/10.1103/PhysRevD.84.063009. arXiv:1106.6355 [gr-qc]
Littenberg TB, Cornish NJ (2023) Prototype global analysis of LISA data with multiple source types. Phys Rev D 107(6):063004. https://doi.org/10.1103/PhysRevD.107.063004. arXiv:2301.03673 [gr-qc]
Littenberg TB, Lali AK (2024) Have any LISA verification binaries been found? arXiv e-prints arXiv:2404.03046 [astro-ph.HE]
Liu X, Cao Z, Shao L (2020) Validating the effective-one-body numerical-relativity waveform models for spin-aligned binary black holes along eccentric orbits. Phys Rev D 101(4):044049. https://doi.org/10.1103/PhysRevD.101.044049. arXiv:1910.00784 [gr-qc]
Liu X, He X, Cao Z (2021) Accurate calculation of gravitational wave memory. Phys Rev D 103 (4):043005. https://doi.org/10.1103/PhysRevD.103.043005. arXiv:2302.02642 [gr-qc]
Liu X, Cao Z, Zhu ZH (2022) A higher-multipole gravitational waveform model for an eccentric binary black holes based on the effective-one-body-numerical-relativity formalism. Class Quantum Grav 39 (3):035009. https://doi.org/10.1088/1361-6382/ac4119. arXiv:2102.08614 [gr-qc]
Liu X, Cao Z, Zhu ZH (2024) Effective-one-body numerical-relativity waveform model for eccentric spin-precessing binary black hole coalescence. Class Quantum Grav 41(19):195019. https://doi.org/10.1088/1361-6382/ad72ca. arXiv:2310.04552 [gr-qc]
Liu YT, Etienne ZB, Shapiro SL (2009) Evolution of near-extremal-spin black holes using the moving puncture technique. Phys Rev D 80:121503. https://doi.org/10.1103/PhysRevD.80.121503. arXiv:1001.4077 [gr-qc]
Liu Z, Porto RA, Yang Z (2021) Spin effects in the effective field theory approach to post-minkowskian conservative dynamics. JHEP 06:012. https://doi.org/10.1007/JHEP06(2021)012. arXiv:2102.10059 [hep-th]
LlamaWeb (2024) Llama. https://llamacode.bitbucket.io
Lodato G, Nayakshin S, King AR, Pringle JE (2009) Black hole mergers: can gas discs solve the 'final parsec' problem? Mon Not R Astron Soc 398:1392. https://doi.org/10.1111/j.1365-2966.2009.15179.x. arXiv:0906.0737 [astro-ph.CO]
Löffler F et al (2012) The Einstein Toolkit: a community computational infrastructure for relativistic astrophysics. Class Quantum Grav 29:115001. https://doi.org/10.1088/0264-9381/29/11/115001. arXiv:1111.3344 [gr-qc]
London L, Fauchon-Jones E (2019) On modeling for Kerr black holes: basis learning, QNM frequencies, and spherical-spheroidal mixing coefficients. Class Quantum Grav 36(23):235015. https://doi.org/10.1088/1361-6382/ab2f11. arXiv:1810.03550 [gr-qc]

London L, Shoemaker D, Healy J (2014) Modeling ringdown: Beyond the fundamental quasinormal modes. Phys Rev D 90(12):124032. [Erratum: Phys. Rev. D 94, 069902 (2016)]. https://doi.org/10.1103/PhysRevD.90.124032. arXiv:1404.3197 [gr-qc]

London L, Khan S, Fauchon-Jones E, García C, Hannam M, Husa S, Jiménez-Forteza X, Kalaghatgi C, Ohme F, Pannarale F (2018) First higher-multipole model of gravitational waves from spinning and coalescing black-hole binaries. Phys Rev Lett 120(16):161102. https://doi.org/10.1103/PhysRevLett.120.161102. arXiv:1708.00404 [gr-qc]

London LT (2020) Modeling ringdown. II. Aligned-spin binary black holes, implications for data analysis and fundamental theory. Phys Rev D 102(8):084052. https://doi.org/10.1103/PhysRevD.102.084052. arXiv:1801.08208 [gr-qc]

London LT (2023) Biorthogonal harmonics for the decomposition of gravitational radiation. I. Angular modes, completeness, and the introduction of adjoint-spheroidal harmonics. Phys Rev D 107 (4):044056. https://doi.org/10.1103/PhysRevD.107.044056. arXiv:2006.11449 [gr-qc]

Long AJ, Hyde JM, Vachaspati T (2014) Cosmic strings in hidden sectors: 1. Radiation of standard model particles. JCAP 09:030. https://doi.org/10.1088/1475-7516/2014/09/030. arXiv:1405.7679 [hep-ph]

Long O (2022) Self-force in hyperbolic black hole encounters. PhD thesis, Southampton U. arXiv:2209.03836 [gr-qc]

Long O, Barack L (2021) Time-domain metric reconstruction for hyperbolic scattering. Phys Rev D 104 (2):024014. https://doi.org/10.1103/PhysRevD.104.024014. arXiv:2105.05630 [gr-qc]

Longo Micchi LF, Afshordi N, Chirenti C (2021) How loud are echoes from exotic compact objects? Phys Rev D 103(4):044028. https://doi.org/10.1103/PhysRevD.103.044028. arXiv:2010.14578 [gr-qc]

Lorentz HA, Droste J (1917) De beweging van een stelsel lichamen onder den invloed van hunne onderlinge aantrekking, behandeld volgens de theorie van Einstein I,II. Versl K Akad Wet Amsterdam 26:392 & 649

Lousto CO, Healy J (2020) Exploring the small mass ratio binary black hole merger via Zeno's dichotomy approach. Phys Rev Lett 125(19):191102. https://doi.org/10.1103/PhysRevLett.125.191102. arXiv:2006.04818 [gr-qc]

Lousto CO, Healy J (2023) Study of the intermediate mass ratio black hole binary merger up to 1000:1 with numerical relativity. Class Quantum Grav 40(9):09LT01. https://doi.org/10.1088/1361-6382/acc7ef. arXiv:2203.08831 [gr-qc]

Lousto CO, Zlochower Y (2011) Hangup kicks: still larger recoils by partial spin/orbit alignment of black-hole binaries. Phys Rev Lett 107:231102. https://doi.org/10.1103/PhysRevLett.107.231102. arXiv:1108.2009 [gr-qc]

Lousto CO, Zlochower Y (2011) Orbital evolution of extreme-mass-ratio black-hole binaries with numerical relativity. Phys Rev Lett 106:041101. https://doi.org/10.1103/PhysRevLett.106.041101. arXiv:1009.0292 [gr-qc]

Loutrel N, Yunes N (2022) Parity violation in spin-precessing binaries: gravitational waves from the inspiral of black holes in dynamical Chern-Simons gravity. Phys Rev D 106(6):064009. https://doi.org/10.1103/PhysRevD.106.064009. arXiv:2205.02675 [gr-qc]

Loutrel N, Ripley JL, Giorgi E, Pretorius F (2021) Second order perturbations of kerr black holes: reconstruction of the metric. Phys Rev D 103(10):104017. https://doi.org/10.1103/PhysRevD.103.104017. arXiv:2008.11770 [gr-qc]

Loutrel N, Brito R, Maselli A, Pani P (2022) Inspiraling compact objects with generic deformations. Phys Rev D 105(12):124050. https://doi.org/10.1103/PhysRevD.105.124050. arXiv:2203.01725 [gr-qc]

Loutrel N, Pani P, Yunes N (2023) Parametrized post-Einsteinian framework for precessing binaries. Phys Rev D 107(4):044046. https://doi.org/10.1103/PhysRevD.107.044046. arXiv:2210.10571 [gr-qc]

Lovelace G (2009) Reducing spurious gravitational radiation in binary-black-hole simulations by using conformally curved initial data. Class Quantum Grav 26:114002. https://doi.org/10.1088/0264-9381/26/11/114002. arXiv:0812.3132 [gr-qc]

Lovelace G, Owen R, Pfeiffer HP, Chu T (2008) Binary-black-hole initial data with nearly-extremal spins. Phys Rev D 78:084017. https://doi.org/10.1103/PhysRevD.78.084017. arXiv:0805.4192 [gr-qc]

Lovelace G, Scheel MA, Szilagyi B (2011) Simulating merging binary black holes with nearly extremal spins. Phys Rev D 83:024010. https://doi.org/10.1103/PhysRevD.83.024010. arXiv:1010.2777 [gr-qc]

Lovelace G et al (2016) Modeling the source of GW150914 with targeted numerical-relativity simulations. Class Quantum Grav 33(24):244002. https://doi.org/10.1088/0264-9381/33/24/244002. arXiv:1607.05377 [gr-qc]

Lukes-Gerakopoulos G, Kopáček O (2017) Recurrence Analysis as a tool to study chaotic dynamics of extreme mass ratio inspiral in signal with noise. Int J Mod Phys D 27(02):1850010. https://doi.org/10.1142/S0218271818500104. arXiv:1709.08446 [gr-qc]

Lukes-Gerakopoulos G, Witzany V (2022) Non-linear effects in EMRI dynamics and their imprints on gravitational waves. In: Bambi C, Katsanevas S, Kokkotas KD (eds) Handbook of Gravitational Wave Astronomy. Springer, Singapore, pp 1625–1668. https://doi.org/10.1007/978-981-16-4306-4_42. arXiv:2103.06724 [gr-qc]

Lukes-Gerakopoulos G, Apostolatos TA, Contopoulos G (2010) Observable signature of a background deviating from the Kerr metric. Phys Rev D 81:124005. https://doi.org/10.1103/PhysRevD.81.124005. arXiv:1003.3120 [gr-qc]

Lukes-Gerakopoulos G, Harms E, Bernuzzi S, Nagar A (2017) Spinning test-body orbiting around a Kerr black hole: circular dynamics and gravitational-wave fluxes. Phys Rev D 96(6):064051. https://doi.org/10.1103/PhysRevD.96.064051. arXiv:1707.07537 [gr-qc]

Luna R, Bozzola G, Cardoso V, Paschalidis V, Zilhão M (2022) Kicks in charged black hole binaries. Phys Rev D 106(8):084017. https://doi.org/10.1103/PhysRevD.106.084017. arXiv:2207.06429 [gr-qc]

Luo J et al (2016) TianQin: a space-borne gravitational wave detector. Class Quantum Grav 33(3):035010. https://doi.org/10.1088/0264-9381/33/3/035010. arXiv:1512.02076 [astro-ph.IM]

Lupi A, Colpi M, Devecchi B, Galanti G, Volonteri M (2014) Constraining the high redshift formation of black hole seeds in nuclear star clusters with gas inflows. Mon Not R Astron Soc 442(4):3616–3626. https://doi.org/10.1093/mnras/stu1120. arXiv:1406.2325 [astro-ph.GA]

Lynch P, van de Meent M, Warburton N (2022) Eccentric self-forced inspirals into a rotating black hole. Class Quantum Grav 39(14):145004. https://doi.org/10.1088/1361-6382/ac7507. arXiv:2112.05651 [gr-qc]

Lynch P, van de Meent M, Warburton N (2024) Self-forced inspirals with spin-orbit precession. Phys Rev D 109(8):084072. https://doi.org/10.1103/PhysRevD.109.084072. arXiv:2305.10533 [gr-qc]

Ma S, Mitman K, Sun L, Deppe N, Hébert F, Kidder LE, Moxon J, Throwe W, Vu NL, Chen Y (2022) Quasinormal-mode filters: a new approach to analyze the gravitational-wave ringdown of binary black-hole mergers. Phys Rev D 106(8):084036. https://doi.org/10.1103/PhysRevD.106.084036. arXiv:2207.10870 [gr-qc]

Ma S, Wang Q, Deppe N, Hébert F, Kidder LE, Moxon J, Throwe W, Vu NL, Scheel MA, Chen Y (2022) Gravitational-wave echoes from numerical-relativity waveforms via spacetime construction near merging compact objects. Phys Rev D 105(10):104007. https://doi.org/10.1103/PhysRevD.105.104007. arXiv:2203.03174 [gr-qc]

Ma S, Sun L, Chen Y (2023) Black hole spectroscopy by mode cleaning. Phys Rev Lett 130(14):141401. https://doi.org/10.1103/PhysRevLett.130.141401. arXiv:2301.06705 [gr-qc]

Ma S, Sun L, Chen Y (2023) Using rational filters to uncover the first ringdown overtone in GW150914. Phys Rev D 107(8):084010. https://doi.org/10.1103/PhysRevD.107.084010. arXiv:2301.06639 [gr-qc]

Macedo C, Pani P, Cardoso V, Crispino L (2013) Astrophysical signatures of boson stars: quasinormal modes and inspiral resonances. Phys Rev D 88(6):064046. https://doi.org/10.1103/PhysRevD.88.064046. arXiv:1307.4812 [gr-qc]

Macedo C, Pani P, Cardoso V, Crispino L (2013) Into the lair: gravitational-wave signatures of dark matter. Astrophys J 774:48. https://doi.org/10.1088/0004-637X/774/1/48. arXiv:1302.2646 [gr-qc]

Madau P, Rees MJ (2001) Massive black holes as population III remnants. Astrophys J Lett 551:L27–L30. https://doi.org/10.1086/319848. arXiv:astro-ph/0101223

Maday Y, Patera AT, Turinici G (2002) A priori convergence theory for reduced-basis approximations of single-parameter elliptic partial differential equations. J Sci Comput 17(1–4):437. https://doi.org/10.1023/A:1015145924517

Maggio E, Pani P, Ferrari V (2017) Exotic compact objects and how to quench their ergoregion instability. Phys Rev D 96(10):104047. https://doi.org/10.1103/PhysRevD.96.104047. arXiv:1703.03696 [gr-qc]

Maggio E, Cardoso V, Dolan SR, Pani P (2019) Ergoregion instability of exotic compact objects: electromagnetic and gravitational perturbations and the role of absorption. Phys Rev D 99(6):064007. https://doi.org/10.1103/PhysRevD.99.064007. arXiv:1807.08840 [gr-qc]

Maggio E, Testa A, Bhagwat S, Pani P (2019) Analytical model for gravitational-wave echoes from spinning remnants. Phys Rev D 100(6):064056. https://doi.org/10.1103/PhysRevD.100.064056. arXiv:1907.03091 [gr-qc]

Maggio E, Buoninfante L, Mazumdar A, Pani P (2020) How does a dark compact object ringdown? Phys Rev D 102(6):064053. https://doi.org/10.1103/PhysRevD.102.064053. arXiv:2006.14628 [gr-qc]

Maggio E, van de Meent M, Pani P (2021) Extreme mass-ratio inspirals around a spinning horizonless compact object. Phys Rev D 104(10):104026. https://doi.org/10.1103/PhysRevD.104.104026. arXiv:2106.07195 [gr-qc]

Maggio E, Pani P, Raposo G (2021b) Testing the nature of dark compact objects with gravitational waves. In: Bambi C, Katsanevas S, Kokkotas KD (eds) Handbook of Gravitational Wave Astronomy. Springer, Singapore. https://doi.org/10.1007/978-981-15-4702-7_29-1. arXiv:2105.06410 [gr-qc]

Maggio E, Silva HO, Buonanno A, Ghosh A (2023) Tests of general relativity in the nonlinear regime: a parametrized plunge-merger-ringdown gravitational waveform model. Phys Rev D 108(2):024043. https://doi.org/10.1103/PhysRevD.108.024043. arXiv:2212.09655 [gr-qc]

Maggiore M (2007) Gravitational Waves. Vol. 1: Theory and Experiments. Oxford University Press. https://doi.org/10.1093/acprof:oso/9780198570745.001.0001

Maia NT, Galley CR, Leibovich AK, Porto RA (2017) Radiation reaction for spinning bodies in effective field theory I: Spin-orbit effects. Phys Rev D 96(8):084064. https://doi.org/10.1103/PhysRevD.96.084064. arXiv:1705.07934 [gr-qc]

Maia NT, Galley CR, Leibovich AK, Porto RA (2017) Radiation reaction for spinning bodies in effective field theory II: Spin-spin effects. Phys Rev D 96(8):084065. https://doi.org/10.1103/PhysRevD.96.084065. arXiv:1705.07938 [gr-qc]

Mandal MK, Mastrolia P, Silva HO, Patil R, Steinhoff J (2023) Gravitoelectric dynamical tides at second post-Newtonian order. JHEP 11:067. https://doi.org/10.1007/JHEP11(2023)067. arXiv:2304.02030 [hep-th]

Mandel I, Farmer A (2022) Merging stellar-mass binary black holes. Phys Rept 955:1–24. https://doi.org/10.1016/j.physrep.2022.01.003. arXiv:1806.05820 [astro-ph.HE]

Mandel I, Fragos T (2020) An alternative interpretation of GW190412 as a binary black hole merger with a rapidly spinning secondary. Astrophys J Lett 895(2):L28. https://doi.org/10.3847/2041-8213/ab8e41. arXiv:2004.09288 [astro-ph.HE]

Mandel I, Sesana A, Vecchio A (2018) The astrophysical science case for a decihertz gravitational-wave detector. Class Quantum Grav 35(5):054004. https://doi.org/10.1088/1361-6382/aaa7e0. arXiv:1710.11187 [astro-ph.HE]

Mangiagli A, Klein A, Sesana A, Barausse E, Colpi M (2019) Post-Newtonian phase accuracy requirements for stellar black hole binaries with LISA. Phys Rev D 99(6):064056. https://doi.org/10.1103/PhysRevD.99.064056. arXiv:1811.01805 [gr-qc]

Mangiagli A, Klein A, Bonetti M, Katz ML, Sesana A, Volonteri M, Colpi M, Marsat S, Babak S (2020) Observing the inspiral of coalescing massive black hole binaries with LISA in the era of Multi-Messenger Astrophysics. Phys Rev D 102:084056. https://doi.org/10.1103/PhysRevD.102.084056. arXiv:2006.12513 [astro-ph.HE]

Manko VS, Novikov ID (1992) Generalizations of the Kerr and Kerr-Newman metrics possessing an arbitrary set of mass-multipole moments. Class Quantum Gravity 9(11):2477–2487. https://doi.org/10.1088/0264-9381/9/11/013

Mannerkoski M, Johansson PH, Rantala A, Naab T, Liao S (2021) Resolving the complex evolution of a supermassive black hole triplet in a cosmological simulation. Astrophys J Lett 912(2):L20. https://doi.org/10.3847/2041-8213/abf9a5. arXiv:2103.16254 [astro-ph.GA]

Mano S, Suzuki H, Takasugi E (1996) Analytic solutions of the Teukolsky equation and their low frequency expansions. Prog Theor Phys 95:1079–1096. https://doi.org/10.1143/PTP.95.1079. arXiv:gr-qc/9603020

Manohar AV, Ridgway AK, Shen CH (2022) Radiated angular momentum and dissipative effects in classical scattering. Phys Rev Lett 129(12):121601. https://doi.org/10.1103/PhysRevLett.129.121601. arXiv:2203.04283 [hep-th]

Maoz D, Hallakoun N, Badenes C (2018) The separation distribution and merger rate of double white dwarfs: improved constraints. Mon Not R Astron Soc 476(2):2584–2590. https://doi.org/10.1093/mnras/sty339. arXiv:1801.04275 [astro-ph.SR]

Mapelli M (2020) Astrophysics of stellar black holes. Proc Int Sch Phys Fermi 200:87–121. https://doi.org/10.3254/ENFI200005. arXiv:1809.09130 [astro-ph.HE]

Mapelli M, Santoliquido F, Bouffanais Y, Sedda MA, Artale MC, Ballone A (2021) Mass and rate of hierarchical black hole mergers in young, globular and nuclear star clusters. Symmetry 13(9):1678. https://doi.org/10.3390/sym13091678. arXiv:2007.15022 [astro-ph.HE]

Marchand T, Blanchet L, Faye G (2016) Gravitational-wave tail effects to quartic non-linear order. Class Quantum Grav 33(24):244003. https://doi.org/10.1088/0264-9381/33/24/244003. arXiv:1607.07601 [gr-qc]

Marchand T, Bernard L, Blanchet L, Faye G (2018) Ambiguity-free completion of the equations of motion of compact binary systems at the fourth post-newtonian order. Phys Rev D 97(4):044023. https://doi.org/10.1103/PhysRevD.97.044023. arXiv:1707.09289 [gr-qc]

Marchand T, Henry Q, Larrouturou F, Marsat S, Faye G, Blanchet L (2020) The mass quadrupole moment of compact binary systems at the fourth post-Newtonian order. Class Quantum Grav 37(21):215006. https://doi.org/10.1088/1361-6382/ab9ce1. arXiv:2003.13672 [gr-qc]

Mark Z, Zimmerman A, Du SM, Chen Y (2017) A recipe for echoes from exotic compact objects. Phys Rev D 96(8):084002. https://doi.org/10.1103/PhysRevD.96.084002. arXiv:1706.06155 [gr-qc]

Markakis C, O'Boyle MF, Brubeck PD, Barack L (2021) Discontinuous collocation methods and gravitational self-force applications. Class Quantum Grav 38(7):075031. https://doi.org/10.1088/1361-6382/abdf27. arXiv:1406.4865 [math.NA]

Markakis C, Bray S, Zenginoğlu A (2023) Symmetric integration of the 1+1 Teukolsky equation on hyperboloidal foliations of Kerr spacetimes. arXiv e-prints arXiv:2303.08153 [gr-qc]

Marsat S (2015) Cubic order spin effects in the dynamics and gravitational wave energy flux of compact object binaries. Class Quantum Grav 32(8):085008. https://doi.org/10.1088/0264-9381/32/8/085008. arXiv:1411.4118 [gr-qc]

Marsat S, Baker JG (2018) Fourier-domain modulations and delays of gravitational-wave signals. arXiv e-prints arXiv:1806.10734 [gr-qc]

Marsat S, Blanchet L, Bohe A, Faye G (2013a) Gravitational waves from spinning compact object binaries: New post-Newtonian results. arXiv e-prints arXiv:1312.5375 [gr-qc]

Marsat S, Bohe A, Faye G, Blanchet L (2013) Next-to-next-to-leading order spin-orbit effects in the equations of motion of compact binary systems. Class Quantum Grav 30:055007. https://doi.org/10.1088/0264-9381/30/5/055007. arXiv:1210.4143 [gr-qc]

Marsat S, Bohé A, Blanchet L, Buonanno A (2014) Next-to-leading tail-induced spin-orbit effects in the gravitational radiation flux of compact binaries. Class Quantum Grav 31:025023. https://doi.org/10.1088/0264-9381/31/2/025023. arXiv:1307.6793 [gr-qc]

Marsat S, Baker JG, Dal Canton T (2021) Exploring the Bayesian parameter estimation of binary black holes with LISA. Phys Rev D 103(8):083011. https://doi.org/10.1103/PhysRevD.103.083011. arXiv:2003.00357 [gr-qc]

Marsh D (2016) Axion cosmology. Phys Rept 643:1–79. https://doi.org/10.1016/j.physrep.2016.06.005. arXiv:1510.07633 [astro-ph.CO]

Marsh TR (2011) Double white dwarfs and LISA. Class Quantum Grav 28:094019. https://doi.org/10.1088/0264-9381/28/9/094019. arXiv:1101.4970 [astro-ph.SR]

Martel K (2004) Gravitational wave forms from a point particle orbiting a Schwarzschild black hole. Phys Rev D 69:044025. https://doi.org/10.1103/PhysRevD.69.044025. arXiv:gr-qc/0311017

Martel K, Poisson E (2005) Gravitational perturbations of the Schwarzschild spacetime: a practical covariant and gauge-invariant formalism. Phys Rev D 71:104003. https://doi.org/10.1103/PhysRevD.71.104003. arXiv:gr-qc/0502028

Martins A, Lopez M, Meijer Q, Baltus G, van der Sluys M, Van Den Broeck C, Caudill S (2024) Improving Early Detection of Gravitational Waves from Binary Neutron Stars Using CNNs and FPGAs. arXiv e-prints arXiv:2409.05068 [astro-ph.IM]

Martins C, Shellard E (1996) Quantitative string evolution. Phys Rev D 54:2535–2556. https://doi.org/10.1103/PhysRevD.54.2535. arXiv:hep-ph/9602271

Martins C, Shellard E (2002) Extending the velocity dependent one scale string evolution model. Phys Rev D 65:043514. https://doi.org/10.1103/PhysRevD.65.043514. arXiv:hep-ph/0003298

Martins C, Moore JN, Shellard E (2004) A Unified model for vortex string network evolution. Phys Rev Lett 92:251601. https://doi.org/10.1103/PhysRevLett.92.251601. arXiv:hep-ph/0310255

Martins C, Shellard E, Vieira J (2014) Models for small-scale structure on cosmic strings: mathematical formalism. Phys Rev D 90(4):043518. https://doi.org/10.1103/PhysRevD.90.043518. arXiv:1405.7722 [hep-ph]

Martins C, Peter P, Rybak IY, Shellard E (2021) Generalized velocity-dependent one-scale model for current-carrying strings. Phys Rev D 103(4):043538. https://doi.org/10.1103/PhysRevD.103.043538. arXiv:2011.09700 [astro-ph.CO]

Maselli A, Pani P, Gualtieri L, Ferrari V (2015) Rotating black holes in Einstein-Dilaton-Gauss-Bonnet gravity with finite coupling. Phys Rev D 92(8):083014. https://doi.org/10.1103/PhysRevD.92.083014. arXiv:1507.00680 [gr-qc]

Maselli A, Völkel SH, Kokkotas KD (2017) Parameter estimation of gravitational wave echoes from exotic compact objects. Phys Rev D 96(6):064045. https://doi.org/10.1103/PhysRevD.96.064045. arXiv:1708.02217 [gr-qc]
Maselli A, Pani P, Cardoso V, Abdelsalhin T, Gualtieri L, Ferrari V (2018) Probing Planckian corrections at the horizon scale with LISA binaries. Phys Rev Lett 120(8):081101. https://doi.org/10.1103/PhysRevLett.120.081101. arXiv:1703.10612 [gr-qc]
Maselli A, Franchini N, Gualtieri L, Sotiriou TP (2020) Detecting scalar fields with extreme mass ratio inspirals. Phys Rev Lett 125(14):141101. https://doi.org/10.1103/PhysRevLett.125.141101. arXiv:2004.11895 [gr-qc]
Maselli A, Pani P, Gualtieri L, Berti E (2020) Parametrized ringdown spin expansion coefficients: a data-analysis framework for black-hole spectroscopy with multiple events. Phys Rev D 101(2):024043. https://doi.org/10.1103/PhysRevD.101.024043. arXiv:1910.12893 [gr-qc]
Maselli A, Franchini N, Gualtieri L, Sotiriou TP, Barsanti S, Pani P (2022) Detecting fundamental fields with LISA observations of gravitational waves from extreme mass-ratio inspirals. Nature Astron 6 (4):464–470. https://doi.org/10.1038/s41550-021-01589-5. arXiv:2106.11325 [gr-qc]
Matas A et al (2020) Aligned-spin neutron-star-black-hole waveform model based on the effective-one-body approach and numerical-relativity simulations. Phys Rev D 102(4):043023. https://doi.org/10.1103/PhysRevD.102.043023. arXiv:2004.10001 [gr-qc]
Mathews J, Pound A, Wardell B (2022) Self-force calculations with a spinning secondary. Phys Rev D 105 (8):084031. https://doi.org/10.1103/PhysRevD.105.084031. arXiv:2112.13069 [gr-qc]
Mathews J, Wardell B, Pound A, Warburton N (2024) Post-adiabatic self-force waveforms: slowly spinning primary and precessing secondary, (in preparation)
Mathisson M (1937) Neue Mechanik materieller Systeme. Acta Phys Polon 6:163–200. Transl. and republ. in Gen. Relativ. Gravit. 42, 1011–1048 (2010)
Mathur SD (2005) The Fuzzball proposal for black holes: an elementary review. Fortsch Phys 53:793–827. https://doi.org/10.1002/prop.200410203. arXiv:hep-th/0502050
Mathur SD (2009) Fuzzballs and the information paradox: a summary and conjectures. Adv Sci Lett 2 (2):133–150. https://doi.org/10.1166/asl.2009.1021. arXiv:0810.4525 [hep-th]
Matsubayashi T, Makino J, Ebisuzaki T (2007) Evolution of galactic nuclei. 1. Orbital evolution of IMBH. Astrophys J 656:879–896. https://doi.org/10.1086/510344. arXiv:astro-ph/0511782
Maybee B, O'Connell D, Vines J (2019) Observables and amplitudes for spinning particles and black holes. JHEP 12:156. https://doi.org/10.1007/JHEP12(2019)156. arXiv:1906.09260 [hep-th]
Mayer L, Fiacconi D, Bonoli S, Quinn T, Roskar R, Shen S, Wadsley J (2015) Direct formation of supermassive black holes in metal-enriched gas at the heart of high-redshift galaxy mergers. Astrophys J 810(1):51. https://doi.org/10.1088/0004-637X/810/1/51. arXiv:1411.5683 [astro-ph.GA]
Mazur PO, Mottola E (2004) Gravitational vacuum condensate stars. Proc Nat Acad Sci 101:9545–9550. https://doi.org/10.1073/pnas.0402717101. arXiv:gr-qc/0407075
Mazur PO, Mottola E (2023) Gravitational condensate stars: an alternative to black holes. Universe 9 (2):88. https://doi.org/10.3390/universe9020088. arXiv:gr-qc/0109035
McConnell NJ, Ma CP (2013) Revisiting the scaling relations of black hole masses and host galaxy properties. Astrophys J 764:184. https://doi.org/10.1088/0004-637X/764/2/184. arXiv:1211.2816 [astro-ph.CO]
McKennon J, Forrester G, Khanna G (2012) High Accuracy Gravitational Waveforms from Black Hole Binary Inspirals Using OpenCL. arXiv e-prints arXiv:1206.0270 [gr-qc]
McManus R, Lombriser L, Peñarrubia J (2017) Parameterised post-newtonian expansion in screened regions. JCAP 12:031. https://doi.org/10.1088/1475-7516/2017/12/031. arXiv:1705.05324 [gr-qc]
McManus R, Berti E, Macedo CFB, Kimura M, Maselli A, Cardoso V (2019) Parametrized black hole quasinormal ringdown. II. Coupled equations and quadratic corrections for nonrotating black holes. Phys Rev D 100(4):044061. https://doi.org/10.1103/PhysRevD.100.044061. arXiv:1906.05155 [gr-qc]
McNeill LO, Seto N (2022) Probing the formation of double neutron star binaries around 1 mHz with LISA. Phys Rev D 106(12):123031. https://doi.org/10.1103/PhysRevD.106.123031. arXiv:2210.04407 [astro-ph.HE]
McWilliams ST, Kelly BJ, Baker JG (2010) Observing mergers of non-spinning black-hole binaries. Phys Rev D 82:024014. https://doi.org/10.1103/PhysRevD.82.024014. arXiv:1004.0961 [gr-qc]
van de Meent M (2014) Conditions for sustained orbital resonances in extreme mass ratio inspirals. Phys Rev D 89(8):084033. https://doi.org/10.1103/PhysRevD.89.084033. arXiv:1311.4457 [gr-qc]

van de Meent M (2014) Resonantly enhanced kicks from equatorial small mass-ratio inspirals. Phys Rev D 90(4):044027. https://doi.org/10.1103/PhysRevD.90.044027. arXiv:1406.2594 [gr-qc]
van de Meent M (2016) Gravitational self-force on eccentric equatorial orbits around a Kerr black hole. Phys Rev D 94(4):044034. https://doi.org/10.1103/PhysRevD.94.044034. arXiv:1606.06297 [gr-qc]
van de Meent M (2017) Self-force corrections to the periapsis advance around a spinning black hole. Phys Rev Lett 118(1):011101. https://doi.org/10.1103/PhysRevLett.118.011101. arXiv:1610.03497 [gr-qc]
van de Meent M (2018) Gravitational self-force on generic bound geodesics in Kerr spacetime. Phys Rev D 97(10):104033. https://doi.org/10.1103/PhysRevD.97.104033. arXiv:1711.09607 [gr-qc]
van de Meent M, Pfeiffer HP (2020) Intermediate mass-ratio black hole binaries: applicability of small mass-ratio perturbation theory. Phys Rev Lett 125(18):181101. https://doi.org/10.1103/PhysRevLett.125.181101. arXiv:2006.12036 [gr-qc]
van de Meent M, Shah AG (2015) Metric perturbations produced by eccentric equatorial orbits around a Kerr black hole. Phys Rev D 92(6):064025. https://doi.org/10.1103/PhysRevD.92.064025. arXiv:1506.04755 [gr-qc]
van de Meent M, Buonanno A, Mihaylov DP, Ossokine S, Pompili L, Warburton N, Pound A, Wardell B, Durkan L, Miller J (2023) Enhancing the SEOBNRv5 effective-one-body waveform model with second-order gravitational self-force fluxes. Phys Rev D 108(12):124038. https://doi.org/10.1103/PhysRevD.108.124038. arXiv:2303.18026 [gr-qc]
Mehta AK, Buonanno A, Cotesta R, Ghosh A, Sennett N, Steinhoff J (2023) Tests of general relativity with gravitational-wave observations using a flexible theory-independent method. Phys Rev D 107(4):044020. https://doi.org/10.1103/PhysRevD.107.044020. arXiv:2203.13937 [gr-qc]
Meidam J, Agathos M, Van Den Broeck C, Veitch J, Sathyaprakash BS (2014) Testing the no-hair theorem with black hole ringdowns using TIGER. Phys Rev D 90(6):064009. https://doi.org/10.1103/PhysRevD.90.064009. arXiv:1406.3201 [gr-qc]
Meidam J et al (2018) Parametrized tests of the strong-field dynamics of general relativity using gravitational wave signals from coalescing binary black holes: Fast likelihood calculations and sensitivity of the method. Phys Rev D 97(4):044033. https://doi.org/10.1103/PhysRevD.97.044033. arXiv:1712.08772 [gr-qc]
Memmesheimer RM, Gopakumar A, Schäfer G (2004) Third post-Newtonian accurate generalized quasi-Keplerian parametrization for compact binaries in eccentric orbits. Phys Rev D 70:104011. https://doi.org/10.1103/PhysRevD.70.104011. arXiv:gr-qc/0407049
Mercuri S, Taveras V (2009) Interaction of the Barbero-Immirzi field with matter and pseudo-scalar perturbations. Phys Rev D 80:104007. https://doi.org/10.1103/PhysRevD.80.104007. arXiv:0903.4407 [gr-qc]
Merlin C, Shah AG (2015) Self-force from reconstructed metric perturbations: numerical implementation in Schwarzschild spacetime. Phys Rev D 91(2):024005. https://doi.org/10.1103/PhysRevD.91.024005. arXiv:1410.2998 [gr-qc]
Merlin C, Ori A, Barack L, Pound A, van de Meent M (2016) Completion of metric reconstruction for a particle orbiting a Kerr black hole. Phys Rev D 94(10):104066. https://doi.org/10.1103/PhysRevD.94.104066. arXiv:1609.01227 [gr-qc]
Merritt D, Milosavljevic M (2005) Massive black hole binary evolution. Living Rev Relativ 8:8. https://doi.org/10.12942/lrr-2005-8. arXiv:astro-ph/0410364
Merritt D, Milosavljevic M, Favata M, Hughes SA, Holz DE (2004) Consequences of gravitational radiation recoil. Astrophys J Lett 607:L9–L12. https://doi.org/10.1086/421551. arXiv:astro-ph/0402057
Messina F, Nagar A (2017) Parametrized-4.5PN TaylorF2 approximants and tail effects to quartic nonlinear order from the effective one body formalism. Phys Rev D 95(12):124001. [Erratum: Phys. Rev.D 96, 049907 (2017)]. https://doi.org/10.1103/PhysRevD.95.124001. arXiv:1703.08107 [gr-qc]
Messina F, Maldarella A, Nagar A (2018) Factorization and resummation: a new paradigm to improve gravitational wave amplitudes. II: the higher multipolar modes. Phys Rev D 97(8):084016. https://doi.org/10.1103/PhysRevD.97.084016. arXiv:1801.02366 [gr-qc]
Metsaev RR, Tseytlin AA (1987) Order alpha-prime (Two Loop) equivalence of the string equations of motion and the sigma model weyl invariance conditions: dependence on the dilaton and the antisymmetric tensor. Nucl Phys B 293:385–419. https://doi.org/10.1016/0550-3213(87)90077-0
Mewes V, Zlochower Y, Campanelli M, Ruchlin I, Etienne ZB, Baumgarte TW (2018) Numerical relativity in spherical coordinates with the Einstein Toolkit. Phys Rev D 97(8):084059. https://doi.org/10.1103/PhysRevD.97.084059. arXiv:1802.09625 [gr-qc]

Mewes V, Zlochower Y, Campanelli M, Baumgarte TW, Etienne ZB, Lopez Armengol FG, Cipolletta F (2020) Numerical relativity in spherical coordinates: a new dynamical spacetime and general relativistic MHD evolution framework for the Einstein Toolkit. Phys Rev D 101(10):104007. https://doi.org/10.1103/PhysRevD.101.104007. arXiv:2002.06225 [gr-qc]

Mezcua M, Civano F, Marchesi S, Suh H, Fabbiano G, Volonteri M (2018) Intermediate-mass black holes in dwarf galaxies out to redshift $\sim$2.4 in the Chandra COSMOS-Legacy Survey. MNRAS 478 (2):2576–2591. https://doi.org/10.1093/mnras/sty1163. arXiv:1802.01567 [astro-ph.GA]

Mezzasoma S, Yunes N (2022) Theory-agnostic framework for inspiral tests of general relativity with higher-harmonic gravitational waves. Phys Rev D 106(2):024026. https://doi.org/10.1103/PhysRevD.106.024026. arXiv:2203.15934 [gr-qc]

MHDuet Code (2024) MHDuet: A distributed AMR, GRMHD code with LES and neutrinos. http://mhduet.liu.edu/

Mihaylov DP, Gair JR (2017) Transition of EMRIs through resonance: corrections to higher order in the on-resonance flux modification. J Math Phys 58(11):112501. https://doi.org/10.1063/1.5006336. arXiv:1706.06639 [gr-qc]

Mihaylov DP, Ossokine S, Buonanno A, Ghosh A (2021) Fast post-adiabatic waveforms in the time domain: applications to compact binary coalescences in LIGO and Virgo. Phys Rev D 104 (12):124087. https://doi.org/10.1103/PhysRevD.104.124087. arXiv:2105.06983 [gr-qc]

Mihaylov DP, Ossokine S, Buonanno A, Estelles H, Pompili L, Pürrer M, Ramos-Buades A (2023) pySEOBNR: a software package for the next generation of effective-one-body multipolar waveform models. arXiv e-prints arXiv:2303.18203 [gr-qc]

Miller J (2017) The second-order gravitational self-force. PhD thesis, Southampton U

Miller J, Pound A (2021) Two-timescale evolution of extreme-mass-ratio inspirals: waveform generation scheme for quasicircular orbits in Schwarzschild spacetime. Phys Rev D 103(6):064048. https://doi.org/10.1103/PhysRevD.103.064048. arXiv:2006.11263 [gr-qc]

Miller J, Wardell B, Pound A (2016) Second-order perturbation theory: the problem of infinite mode coupling. Phys Rev D 94(10):104018. https://doi.org/10.1103/PhysRevD.94.104018. arXiv:1608.06783 [gr-qc]

Miller MC (2004) Probing general relativity with mergers of supermassive and intermediate-mass black holes. Astrophys J 618:426–431. https://doi.org/10.1086/425910. arXiv:astro-ph/0409331

Milosavljevic M, Merritt D (2003) Long term evolution of massive black hole binaries. Astrophys J 596:860. https://doi.org/10.1086/378086. arXiv:astro-ph/0212459

Mino Y (2003) Perturbative approach to an orbital evolution around a supermassive black hole. Phys Rev D 67:084027. https://doi.org/10.1103/PhysRevD.67.084027. arXiv:gr-qc/0302075

Mino Y (2005) Self-force in the radiation reaction formula. Prog Theor Phys 113:733–761. https://doi.org/10.1143/PTP.113.733. arXiv:gr-qc/0506003

Mino Y, Price R (2008) Two-timescale adiabatic expansion of a scalar field model. Phys Rev D 77:064001. https://doi.org/10.1103/PhysRevD.77.064001. arXiv:0801.0179 [gr-qc]

Mino Y, Shibata M, Tanaka T (1996) Gravitational waves induced by a spinning particle falling into a rotating black hole. Phys Rev D 53:622–634. [Erratum: Phys. Rev. D 59, 047502 (1999)]. https://doi.org/10.1103/PhysRevD.53.622

Mino Y, Sasaki M, Shibata M, Tagoshi H, Tanaka T (1997a) Black hole perturbation: Chapter 1. Prog Theor Phys Suppl 128:1–121. https://doi.org/10.1143/PTPS.128.1. arXiv:gr-qc/9712057

Mino Y, Sasaki M, Tanaka T (1997) Gravitational radiation reaction to a particle motion. Phys Rev D 55:3457–3476. https://doi.org/10.1103/PhysRevD.55.3457. arXiv:gr-qc/9606018

Mirshekari S, Will CM (2013) Compact binary systems in scalar-tensor gravity: equations of motion to 2.5 post-Newtonian order. Phys Rev D 87(8):084070. https://doi.org/10.1103/PhysRevD.87.084070. arXiv:1301.4680 [gr-qc]

Mirshekari S, Yunes N, Will CM (2012) Constraining generic lorentz violation and the speed of the graviton with gravitational waves. Phys Rev D 85:024041. https://doi.org/10.1103/PhysRevD.85.024041. arXiv:1110.2720 [gr-qc]

Mishra A, Cha J, Park H, Kim S (2023) Artificial intelligence and hardware accelerators. Springer, Cham. https://doi.org/10.1007/978-3-031-22170-5

Mishra CK, Arun KG, Iyer BR (2015) Third post-Newtonian gravitational waveforms for compact binary systems in general orbits: instantaneous terms. Phys Rev D 91(8):084040. https://doi.org/10.1103/PhysRevD.91.084040. arXiv:1501.07096 [gr-qc]

Mitman K, Moxon J, Scheel MA, Teukolsky SA, Boyle M, Deppe N, Kidder LE, Throwe W (2020) Computation of displacement and spin gravitational memory in numerical relativity. Phys Rev D 102 (10):104007. https://doi.org/10.1103/PhysRevD.102.104007. arXiv:2007.11562 [gr-qc]
Mitman K et al (2021) Adding gravitational memory to waveform catalogs using BMS balance laws. Phys Rev D 103(2):024031. https://doi.org/10.1103/PhysRevD.103.024031. arXiv:2011.01309 [gr-qc]
Mitman K et al (2021) Fixing the BMS frame of numerical relativity waveforms. Phys Rev D 104 (2):024051. https://doi.org/10.1103/PhysRevD.104.024051. arXiv:2105.02300 [gr-qc]
Mitman K et al (2022) Fixing the BMS frame of numerical relativity waveforms with BMS charges. Phys Rev D 106(8):084029. https://doi.org/10.1103/PhysRevD.106.084029. arXiv:2208.04356 [gr-qc]
Mitman K et al (2023) Nonlinearities in black hole ringdowns. Phys Rev Lett 130(8):081402. https://doi.org/10.1103/PhysRevLett.130.081402. arXiv:2208.07380 [gr-qc]
Moffat JW (2006) Scalar-tensor-vector gravity theory. JCAP 03:004. https://doi.org/10.1088/1475-7516/2006/03/004. arXiv:gr-qc/0506021
Mogull G, Plefka J, Steinhoff J (2021) Classical black hole scattering from a worldline quantum field theory. JHEP 02:048. https://doi.org/10.1007/JHEP02(2021)048. arXiv:2010.02865 [hep-th]
Molina C, Pani P, Cardoso V, Gualtieri L (2010) Gravitational signature of Schwarzschild black holes in dynamical Chern-Simons gravity. Phys Rev D 81:124021. https://doi.org/10.1103/PhysRevD.81.124021. arXiv:1004.4007 [gr-qc]
Moore B, Yunes N (2019) A 3PN fourier domain waveform for non-spinning binaries with moderate eccentricity. Class Quantum Grav 36(18):185003. https://doi.org/10.1088/1361-6382/ab3778. arXiv:1903.05203 [gr-qc]
Moore B, Favata M, Arun KG, Mishra CK (2016) Gravitational-wave phasing for low-eccentricity inspiralling compact binaries to 3PN order. Phys Rev D 93(12):124061. https://doi.org/10.1103/PhysRevD.93.124061. arXiv:1605.00304 [gr-qc]
Moore B, Robson T, Loutrel N, Yunes N (2018) Towards a Fourier domain waveform for non-spinning binaries with arbitrary eccentricity. Class Quantum Grav 35(23):235006. https://doi.org/10.1088/1361-6382/aaea00. arXiv:1807.07163 [gr-qc]
Moore CJ, Chua A, Gair JR (2017) Gravitational waves from extreme mass ratio inspirals around bumpy black holes. Class Quantum Grav 34(19):195009. https://doi.org/10.1088/1361-6382/aa85fa. arXiv:1707.00712 [gr-qc]
Moore CJ, Gerosa D, Klein A (2019) Are stellar-mass black-hole binaries too quiet for LISA? Mon Not R Astron Soc 488(1):L94–L98. https://doi.org/10.1093/mnrasl/slz104. arXiv:1905.11998 [astro-ph.HE]
Morrás G, García-Bellido J, Nesseris S (2022) Search for black hole hyperbolic encounters with gravitational wave detectors. Phys Dark Univ 35:100932. https://doi.org/10.1016/j.dark.2021.100932. arXiv:2110.08000 [astro-ph.HE]
Morris MS, Thorne KS (1988) Wormholes in space-time and their use for interstellar travel: a tool for teaching general relativity. Am J Phys 56:395–412. https://doi.org/10.1119/1.15620
Most ER, Papenfort LJ, Rezzolla L (2019) Beyond second-order convergence in simulations of magnetized binary neutron stars with realistic microphysics. Mon Not R Astron Soc 490(3):3588–3600. https://doi.org/10.1093/mnras/stz2809. arXiv:1907.10328 [astro-ph.HE]
Mougiakakos S, Riva MM, Vernizzi F (2021) Gravitational Bremsstrahlung in the post-Minkowskian effective field theory. Phys Rev D 104(2):024041. https://doi.org/10.1103/PhysRevD.104.024041. arXiv:2102.08339 [gr-qc]
Mougiakakos S, Riva MM, Vernizzi F (2022) Gravitational Bremsstrahlung with tidal effects in the post-minkowskian expansion. Phys Rev Lett 129(12):121101. https://doi.org/10.1103/PhysRevLett.129.121101. arXiv:2204.06556 [hep-th]
Moura F, Schiappa R (2007) Higher-derivative corrected black holes: perturbative stability and absorption cross-section in heterotic string theory. Class Quantum Grav 24:361–386. https://doi.org/10.1088/0264-9381/24/2/006. arXiv:hep-th/0605001
Moxon J, Scheel MA, Teukolsky SA, Deppe N, Fischer N, Hébert F, Kidder LE, Throwe W (2023) SpECTRE Cauchy-characteristic evolution system for rapid, precise waveform extraction. Phys Rev D 107(6):064013. https://doi.org/10.1103/PhysRevD.107.064013. arXiv:2110.08635 [gr-qc]
Mroue AH, Pfeiffer HP (2012) Precessing Binary Black Holes Simulations: Quasicircular Initial Data. arXiv e-prints arXiv:1210.2958 [gr-qc]
Mroue AH et al (2013) Catalog of 174 binary black hole simulations for gravitational wave astronomy. Phys Rev Lett 111(24):241104. https://doi.org/10.1103/PhysRevLett.111.241104. arXiv:1304.6077 [gr-qc]

Munday J et al (2022) Two decades of optical timing of the shortest-period binary star system HM Cancri. Mon Not R Astron Soc 518(4):5123–5139. https://doi.org/10.1093/mnras/stac3385. arXiv:2211.09834 [astro-ph.SR]

Mundim BC, Nakano H, Yunes N, Campanelli M, Noble SC, Zlochower Y (2014) Approximate black hole binary spacetime via asymptotic matching. Phys Rev D 89(8):084008. https://doi.org/10.1103/PhysRevD.89.084008. arXiv:1312.6731 [gr-qc]

Munna C, Evans CR (2020) Eccentric-orbit extreme-mass-ratio-inspiral radiation II: 1PN correction to leading-logarithm and subleading-logarithm flux sequences and the entire perturbative 4PN flux. Phys Rev D 102(10):104006. https://doi.org/10.1103/PhysRevD.102.104006. arXiv:2009.01254 [gr-qc]

Munna C, Evans CR (2022) Post-Newtonian expansion of the spin-precession invariant for eccentric-orbit nonspinning extreme-mass-ratio inspirals to 9PN and e16. Phys Rev D 106(4):044058. https://doi.org/10.1103/PhysRevD.106.044058. arXiv:2206.04085 [gr-qc]

Munna C, Evans CR, Hopper S, Forseth E (2020) Determination of new coefficients in the angular momentum and energy fluxes at infinity to 9PN order for eccentric Schwarzschild extreme-mass-ratio inspirals using mode-by-mode fitting. Phys Rev D 102(2):024047. https://doi.org/10.1103/PhysRevD.102.024047. arXiv:2005.03044 [gr-qc]

Myers RC (1997) Pure states don't wear black. Gen Relativ Gravit 29:1217–1222. https://doi.org/10.1023/A:1018855611972. arXiv:gr-qc/9705065

Nagar A (2011) Effective one body Hamiltonian of two spinning black-holes with next-to-next-to-leading order spin-orbit coupling. Phys Rev D 84:084028. [Erratum: Phys. Rev. D 88, 089901 (2013)]. https://doi.org/10.1103/PhysRevD.84.084028. arXiv:1106.4349 [gr-qc]

Nagar A (2013) Gravitational recoil in nonspinning black hole binaries: the span of test-mass results. Phys Rev D 88(12):121501. https://doi.org/10.1103/PhysRevD.88.121501. arXiv:1306.6299 [gr-qc]

Nagar A, Albanesi S (2022) Toward a gravitational self-force-informed effective-one-body waveform model for nonprecessing, eccentric, large-mass-ratio inspirals. Phys Rev D 106(6):064049. https://doi.org/10.1103/PhysRevD.106.064049. arXiv:2207.14002 [gr-qc]

Nagar A, Rettegno P (2019) Efficient effective one body time-domain gravitational waveforms. Phys Rev D 99(2):021501. https://doi.org/10.1103/PhysRevD.99.021501. arXiv:1805.03891 [gr-qc]

Nagar A, Rettegno P (2021) Next generation: impact of high-order analytical information on effective one body waveform models for noncircularized, spin-aligned black hole binaries. Phys Rev D 104(10):104004. https://doi.org/10.1103/PhysRevD.104.104004. arXiv:2108.02043 [gr-qc]

Nagar A, Shah A (2016) Factorization and resummation: a new paradigm to improve gravitational wave amplitudes. Phys Rev D 94(10):104017. https://doi.org/10.1103/PhysRevD.94.104017. arXiv:1606.00207 [gr-qc]

Nagar A, Damour T, Tartaglia A (2007) Binary black hole merger in the extreme mass ratio limit. Class Quantum Grav 24:S109–S124. https://doi.org/10.1088/0264-9381/24/12/S08. arXiv:gr-qc/0612096

Nagar A, Messina F, Kavanagh C, Lukes-Gerakopoulos G, Warburton N, Bernuzzi S, Harms E (2019) Factorization and resummation: a new paradigm to improve gravitational wave amplitudes. III: the spinning test-body terms. Phys Rev D 100(10):104056. https://doi.org/10.1103/PhysRevD.100.104056. arXiv:1907.12233 [gr-qc]

Nagar A, Messina F, Rettegno P, Bini D, Damour T, Geralico A, Akcay S, Bernuzzi S (2019) Nonlinear-in-spin effects in effective-one-body waveform models of spin-aligned, inspiralling, neutron star binaries. Phys Rev D 99(4):044007. https://doi.org/10.1103/PhysRevD.99.044007. arXiv:1812.07923 [gr-qc]

Nagar A, Pratten G, Riemenschneider G, Gamba R (2020) Multipolar effective one body model for nonspinning black hole binaries. Phys Rev D 101(2):024041. https://doi.org/10.1103/PhysRevD.101.024041. arXiv:1904.09550 [gr-qc]

Nagar A, Riemenschneider G, Pratten G, Rettegno P, Messina F (2020) Multipolar effective one body waveform model for spin-aligned black hole binaries. Phys Rev D 102(2):024077. https://doi.org/10.1103/PhysRevD.102.024077. arXiv:2001.09082 [gr-qc]

Nagar A, Bonino A, Rettegno P (2021) Effective one-body multipolar waveform model for spin-aligned, quasicircular, eccentric, hyperbolic black hole binaries. Phys Rev D 103(10):104021. https://doi.org/10.1103/PhysRevD.103.104021. arXiv:2101.08624 [gr-qc]

Nagar A, Rettegno P, Gamba R, Bernuzzi S (2021) Effective-one-body waveforms from dynamical captures in black hole binaries. Phys Rev D 103(6):064013. https://doi.org/10.1103/PhysRevD.103.064013. arXiv:2009.12857 [gr-qc]

Nagar A, Rettegno P, Gamba R, Albanesi S, Albertini A, Bernuzzi S (2023) Analytic systematics in next generation of effective-one-body gravitational waveform models for future observations. Phys Rev D 108(12):124018. https://doi.org/10.1103/PhysRevD.108.124018. arXiv:2304.09662 [gr-qc]

Nagar A et al (2018) Time-domain effective-one-body gravitational waveforms for coalescing compact binaries with nonprecessing spins, tides and self-spin effects. Phys Rev D 98(10):104052. https://doi.org/10.1103/PhysRevD.98.104052. arXiv:1806.01772 [gr-qc]

Nair R, Perkins S, Silva HO, Yunes N (2019) Fundamental physics implications for higher-curvature theories from binary black hole signals in the LIGO-Virgo catalog GWTC-1. Phys Rev Lett 123 (19):191101. https://doi.org/10.1103/PhysRevLett.123.191101. arXiv:1905.00870 [gr-qc]

Nakamura T, Oohara K, Kojima Y (1987) General relativistic collapse to black holes and gravitational waves from black holes. Prog Theor Phys Suppl 90:1–218. https://doi.org/10.1143/PTPS.90.1

Nakano H, Ioka K (2007) Second order quasi-normal mode of the schwarzschild black hole. Phys Rev D 76:084007. https://doi.org/10.1103/PhysRevD.76.084007. arXiv:0708.0450 [gr-qc]

Nakano H, Ireland B, Campanelli M, West EJ (2016) Spinning, precessing, black hole binary spacetime via asymptotic matching. Class Quantum Grav 33(24):247001. https://doi.org/10.1088/0264-9381/33/24/247001. arXiv:1608.01033 [gr-qc]

Nakano H, Sago N, Tagoshi H, Tanaka T (2017) Black hole ringdown echoes and howls. PTEP 7:071E01. https://doi.org/10.1093/ptep/ptx093. arXiv:1704.07175 [gr-qc]

Nasipak Z (2022) Adiabatic evolution due to the conservative scalar self-force during orbital resonances. Phys Rev D 106(6):064042. https://doi.org/10.1103/PhysRevD.106.064042. arXiv:2207.02224 [gr-qc]

Nasipak Z, Evans CR (2021) Resonant self-force effects in extreme-mass-ratio binaries: a scalar model. Phys Rev D 104(8):084011. https://doi.org/10.1103/PhysRevD.104.084011. arXiv:2105.15188 [gr-qc]

Nasipak Z, Osburn T, Evans CR (2019) Repeated faint quasinormal bursts in extreme-mass-ratio inspiral waveforms: evidence from frequency-domain scalar self-force calculations on generic Kerr orbits. Phys Rev D 100(6):064008. https://doi.org/10.1103/PhysRevD.100.064008. arXiv:1905.13237 [gr-qc]

Nee PJ, Völkel SH, Pfeiffer HP (2023) Role of black hole quasinormal mode overtones for ringdown analysis. Phys Rev D 108(4):044032. https://doi.org/10.1103/PhysRevD.108.044032. arXiv:2302.06634 [gr-qc]

Nelemans G, Yungelson LR, Portegies Zwart SF (2001) The gravitational wave signal from the galactic disk population of binaries containing two compact objects. Astron Astrophys 375:890–898. https://doi.org/10.1051/0004-6361:20010683. arXiv:astro-ph/0105221

Nelson PE, Etienne ZB, McWilliams ST, Nguyen V (2019) Induced spins from scattering experiments of initially nonspinning black holes. Phys Rev D 100(12):124045. https://doi.org/10.1103/PhysRevD.100.124045. arXiv:1909.08621 [gr-qc]

Neuweiler A, Dietrich T, Brügmann B, Giangrandi E, Kiuchi K, Schianchi F, Mösta P, Shankar S, Giacomazzo B, Shibata M (2024) General relativistic magnetohydrodynamic simulations with bam: Implementation and code comparison. Phys Rev D 110(8):084046. https://doi.org/10.1103/PhysRevD.110.084046. arXiv:2407.20946 [gr-qc]

Ng K, Isi M, Haster CJ, Vitale S (2020) Multiband gravitational-wave searches for ultralight bosons. Phys Rev D 102(8):083020. https://doi.org/10.1103/PhysRevD.102.083020. arXiv:2007.12793 [gr-qc]

Nicolini P, Smailagic A, Spallucci E (2006) Noncommutative geometry inspired Schwarzschild black hole. Phys Lett B 632:547–551. https://doi.org/10.1016/j.physletb.2005.11.004. arXiv:gr-qc/0510112

Noble SC, Mundim BC, Nakano H, Krolik JH, Campanelli M, Zlochower Y, Yunes N (2012) Circumbinary MHD accretion into inspiraling binary black holes. Astrophys J 755:51. https://doi.org/10.1088/0004-637X/755/1/51. arXiv:1204.1073 [astro-ph.HE]

Nolan P, Kavanagh C, Dolan SR, Ottewill AC, Warburton N, Wardell B (2015) Octupolar invariants for compact binaries on quasicircular orbits. Phys Rev D 92(12):123008. https://doi.org/10.1103/PhysRevD.92.123008. arXiv:1505.04447 [gr-qc]

Nollert HP (1993) Quasinormal modes of Schwarzschild black holes: the determination of quasinormal frequencies with very large imaginary parts. Phys Rev D 47:5253–5258. https://doi.org/10.1103/PhysRevD.47.5253

Nollert HP (1996) About the significance of quasinormal modes of black holes. Phys Rev D 53:4397–4402. https://doi.org/10.1103/PhysRevD.53.4397. arXiv:gr-qc/9602032

Nollert HP (1999) Topical review: quasinormal modes: the characteristic 'sound' of black holes and neutron stars. Class Quantum Grav 16:R159–R216. https://doi.org/10.1088/0264-9381/16/12/201

Nordtvedt K (1968) Equivalence principle for massive bodies. 1. Phenomenology. Phys Rev 169:1014–1016. https://doi.org/10.1103/PhysRev.169.1014
O'Boyle MF, Markakis C (2023) Discontinuous collocation and symmetric integration methods for distributionally-sourced hyperboloidal partial differential equations. arXiv e-prints arXiv:2308.02385 [math.NA]
O'Boyle MF, Markakis C, Da Silva LJG, Panosso Macedo R, Kroon JAV (2022) Conservative Evolution of Black Hole Perturbations with Time-Symmetric Numerical Methods. arXiv e-prints arXiv:2210.02550 [gr-qc]
O'Callaghan E, Chadburn S, Geshnizjani G, Gregory R, Zavala I (2010) The effect of extra dimensions on gravity wave bursts from cosmic string cusps. JCAP 09:013. https://doi.org/10.1088/1475-7516/2010/09/013. arXiv:1005.3220 [hep-th]
Ochsner E (2010) Improving analytical templates and searching for gravitational waves from coalescing black hole binaries. PhD thesis, Maryland U., College Park
Okawa H (2015) Nonlinear evolutions of bosonic clouds around black holes. Class Quantum Grav 32 (21):214003. https://doi.org/10.1088/0264-9381/32/21/214003
Okawa H, Cardoso V (2014) Black holes and fundamental fields: hair, kicks, and a gravitational Magnus effect. Phys Rev D 90(10):104040. https://doi.org/10.1103/PhysRevD.90.104040. arXiv:1405.4861 [gr-qc]
Okawa H, Witek H, Cardoso V (2014) Black holes and fundamental fields in numerical relativity: initial data construction and evolution of bound states. Phys Rev D 89(10):104032. https://doi.org/10.1103/PhysRevD.89.104032. arXiv:1401.1548 [gr-qc]
Okounkova M (2020) Numerical relativity simulation of GW150914 in Einstein dilaton Gauss-Bonnet gravity. Phys Rev D 102(8):084046. https://doi.org/10.1103/PhysRevD.102.084046. arXiv:2001.03571 [gr-qc]
Okounkova M, Stein LC, Scheel MA, Hemberger DA (2017) Numerical binary black hole mergers in dynamical Chern-Simons gravity: scalar field. Phys Rev D 96(4):044020. https://doi.org/10.1103/PhysRevD.96.044020. arXiv:1705.07924 [gr-qc]
Okounkova M, Stein LC, Scheel MA, Teukolsky SA (2019) Numerical binary black hole collisions in dynamical Chern-Simons gravity. Phys Rev D 100(10):104026. https://doi.org/10.1103/PhysRevD.100.104026. arXiv:1906.08789 [gr-qc]
Okounkova M, Stein LC, Moxon J, Scheel MA, Teukolsky SA (2020) Numerical relativity simulation of GW150914 beyond general relativity. Phys Rev D 101(10):104016. https://doi.org/10.1103/PhysRevD.101.104016. arXiv:1911.02588 [gr-qc]
Okounkova M, Isi M, Chatziioannou K, Farr WM (2023) Gravitational wave inference on a numerical-relativity simulation of a black hole merger beyond general relativity. Phys Rev D 107(2):024046. https://doi.org/10.1103/PhysRevD.107.024046. arXiv:2208.02805 [gr-qc]
O'Leary RM, Kocsis B, Loeb A (2009) Gravitational waves from scattering of stellar-mass black holes in galactic nuclei. Mon Not R Astron Soc 395(4):2127–2146. https://doi.org/10.1111/j.1365-2966.2009.14653.x. arXiv:0807.2638 [astro-ph]
Olmez S, Mandic V, Siemens X (2010) Gravitational-wave stochastic background from kinks and cusps on cosmic strings. Phys Rev D 81:104028. https://doi.org/10.1103/PhysRevD.81.104028. arXiv:1004.0890 [astro-ph.CO]
Onozawa H (1997) A Detailed study of quasinormal frequencies of the Kerr black hole. Phys Rev D 55:3593–3602. https://doi.org/10.1103/PhysRevD.55.3593. arXiv:gr-qc/9610048
Ori A, Thorne KS (2000) The transition from inspiral to plunge for a compact body in a circular equatorial orbit around a massive, spinning black hole. Phys Rev D 62:124022. https://doi.org/10.1103/PhysRevD.62.124022. arXiv:gr-qc/0003032
Osburn T, Nishimura N (2022) New self-force method via elliptic partial differential equations for Kerr inspiral models. Phys Rev D 106(4):044056. https://doi.org/10.1103/PhysRevD.106.044056. arXiv:2206.07031 [gr-qc]
Osburn T, Forseth E, Evans CR, Hopper S (2014) Lorenz gauge gravitational self-force calculations of eccentric binaries using a frequency domain procedure. Phys Rev D 90(10):104031. https://doi.org/10.1103/PhysRevD.90.104031. arXiv:1409.4419 [gr-qc]
Osburn T, Warburton N, Evans CR (2016) Highly eccentric inspirals into a black hole. Phys Rev D 93 (6):064024. https://doi.org/10.1103/PhysRevD.93.064024. arXiv:1511.01498 [gr-qc]
Oshita N (2023) Thermal ringdown of a Kerr black hole: overtone excitation, Fermi-Dirac statistics and greybody factor. JCAP 04:013. https://doi.org/10.1088/1475-7516/2023/04/013. arXiv:2208.02923 [gr-qc]

Oshita N, Tsuna D (2023) Slowly decaying ringdown of a rapidly spinning black hole: probing the no-hair theorem by small mass-ratio mergers with LISA. Phys Rev D 108(10):104031. https://doi.org/10.1103/PhysRevD.108.104031. arXiv:2210.14049 [gr-qc]

Oshita N, Tsuna D, Afshordi N (2020) Quantum black hole seismology I: echoes, ergospheres, and spectra. Phys Rev D 102(2):024045. https://doi.org/10.1103/PhysRevD.102.024045. arXiv:2001.11642 [gr-qc]

Oshita N, Wang Q, Afshordi N (2020) On reflectivity of quantum black hole horizons. JCAP 04:016. https://doi.org/10.1088/1475-7516/2020/04/016. arXiv:1905.00464 [hep-th]

Ossokine S, Foucart F, Pfeiffer HP, Boyle M, Szilágyi B (2015) Improvements to the construction of binary black hole initial data. Class Quantum Grav 32:245010. https://doi.org/10.1088/0264-9381/32/24/245010. arXiv:1506.01689 [gr-qc]

Ossokine S, Dietrich T, Foley E, Katebi R, Lovelace G (2018) Assessing the energetics of spinning binary black hole systems. Phys Rev D 98(10):104057. https://doi.org/10.1103/PhysRevD.98.104057. arXiv:1712.06533 [gr-qc]

Ossokine S et al (2020) Multipolar effective-one-body waveforms for precessing binary black holes: construction and validation. Phys Rev D 102(4):044055. https://doi.org/10.1103/PhysRevD.102.044055. arXiv:2004.09442 [gr-qc]

Ota I, Chirenti C (2020) Overtones or higher harmonics? Prospects for testing the no-hair theorem with gravitational wave detections. Phys Rev D 101(10):104005. https://doi.org/10.1103/PhysRevD.101.104005. arXiv:1911.00440 [gr-qc]

Ota I, Chirenti C (2022) Black hole spectroscopy horizons for current and future gravitational wave detectors. Phys Rev D 105(4):044015. https://doi.org/10.1103/PhysRevD.105.044015. arXiv:2108.01774 [gr-qc]

O'Toole C, Ottewill A, Wardell B (2021) Characteristic formulation of the Regge-Wheeler and Zerilli Green functions. Phys Rev D 103:124022. https://doi.org/10.1103/PhysRevD.103.124022. arXiv:2010.15818 [gr-qc]

Owen CB, Yunes N, Witek H (2021) Petrov type, principal null directions, and Killing tensors of slowly rotating black holes in quadratic gravity. Phys Rev D 103(12):124057. https://doi.org/10.1103/PhysRevD.103.124057. arXiv:2103.15891 [gr-qc]

Owen R, Fox AS, Freiberg JA, Jacques TP (2019) Black hole spin axis in numerical relativity. Phys Rev D 99(8):084031. https://doi.org/10.1103/PhysRevD.99.084031. arXiv:1708.07325 [gr-qc]

Pacilio C, Vaglio M, Maselli A, Pani P (2020) Gravitational-wave detectors as particle-physics laboratories: constraining scalar interactions with a coherent inspiral model of boson-star binaries. Phys Rev D 102(8):083002. https://doi.org/10.1103/PhysRevD.102.083002. arXiv:2007.05264 [gr-qc]

Palenzuela C, Olabarrieta I, Lehner L, Liebling SL (2007) Head-on collisions of boson stars. Phys Rev D 75:064005. https://doi.org/10.1103/PhysRevD.75.064005. arXiv:gr-qc/0612067

Palenzuela C, Lehner L, Liebling SL (2008) Orbital dynamics of binary boson star systems. Phys Rev D 77:044036. https://doi.org/10.1103/PhysRevD.77.044036. arXiv:0706.2435 [gr-qc]

Palenzuela C, Pani P, Bezares M, Cardoso V, Lehner L, Liebling S (2017) Gravitational wave signatures of highly compact boson star binaries. Phys Rev D 96(10):104058. https://doi.org/10.1103/PhysRevD.96.104058. arXiv:1710.09432 [gr-qc]

Palenzuela C, Miñano B, Viganò D, Arbona A, Bona-Casas C, Rigo A, Bezares M, Bona C, Massó J (2018) A Simflowny-based finite-difference code for high-performance computing in numerical relativity. Class Quantum Grav 35(18):185007. https://doi.org/10.1088/1361-6382/aad7f6. arXiv:1806.04182 [physics.comp-ph]

Palenzuela C, Miñano B, Arbona A, Bona-Casas C, Bona C, Massó J (2021) Simflowny 3: an upgraded platform for scientific modeling and simulation. Comput Phys Commun 259:107675. https://doi.org/10.1016/j.cpc.2020.107675. arXiv:2010.00902 [physics.comp-ph]

Pan Y, Buonanno A, Buchman LT, Chu T, Kidder LE, Pfeiffer HP, Scheel MA (2010) Effective-one-body waveforms calibrated to numerical relativity simulations: coalescence of non-precessing, spinning, equal-mass black holes. Phys Rev D 81:084041. https://doi.org/10.1103/PhysRevD.81.084041. arXiv:0912.3466 [gr-qc]

Pan Y, Buonanno A, Boyle M, Buchman LT, Kidder LE, Pfeiffer HP, Scheel MA (2011) Inspiral-merger-ringdown multipolar waveforms of nonspinning black-hole binaries using the effective-one-body formalism. Phys Rev D 84:124052. https://doi.org/10.1103/PhysRevD.84.124052. arXiv:1106.1021 [gr-qc]

Pan Y, Buonanno A, Fujita R, Racine E, Tagoshi H (2011) Post-Newtonian factorized multipolar waveforms for spinning, non-precessing black-hole binaries. Phys Rev D 83:064003. [Erratum: Phys. Rev. D 87, 109901 (2013)]. https://doi.org/10.1103/PhysRevD.83.064003. arXiv:1006.0431 [gr-qc]

Pan Y, Buonanno A, Taracchini A, Kidder LE, Mroué AH, Pfeiffer HP, Scheel MA, Szilágyi B (2014) Inspiral-merger-ringdown waveforms of spinning, precessing black-hole binaries in the effective-one-body formalism. Phys Rev D 89(8):084006. https://doi.org/10.1103/PhysRevD.89.084006. arXiv:1307.6232 [gr-qc]

Pan Z, Yang H (2020) Probing Primordial Stochastic Gravitational Wave Background with Multi-band Astrophysical Foreground Cleaning. Class Quantum Grav 37(19):195020. https://doi.org/10.1088/1361-6382/abb074. arXiv:1910.09637 [astro-ph.CO]

Pan Z, Yang H (2020) Probing the Growth of Massive Black Holes with Black Hole-Host Galaxy Spin Correlations. Astrophys J 901(2):163. https://doi.org/10.3847/1538-4357/abb1b1. arXiv:2007.03783 [astro-ph.CO]

Pan Z, Yang H (2021) Formation Rate of Extreme Mass Ratio Inspirals in Active Galactic Nuclei. Phys Rev D 103(10):103018. https://doi.org/10.1103/PhysRevD.103.103018. arXiv:2101.09146 [astro-ph.HE]

Pan Z, Yang H (2021) Supercritical Accretion of Stellar-mass Compact Objects in Active Galactic Nuclei. Astrophys J 923(2):173. https://doi.org/10.3847/1538-4357/ac249c. arXiv:2108.00267 [astro-ph.HE]

Pan Z, Lyu Z, Yang H (2021) Wet extreme mass ratio inspirals may be more common for spaceborne gravitational wave detection. Phys Rev D 104(6):063007. https://doi.org/10.1103/PhysRevD.104.063007. arXiv:2104.01208 [astro-ph.HE]

Pani P (2015) I-Love-Q relations for gravastars and the approach to the black-hole limit. Phys Rev D 92 (12):124030. [Erratum: Phys. Rev. D 95, 049902 (2017)]. https://doi.org/10.1103/PhysRevD.95.049902. arXiv:1506.06050 [gr-qc]

Pani P, Ferrari V (2018) On gravitational-wave echoes from neutron-star binary coalescences. Class Quantum Grav 35(15):15LT01. https://doi.org/10.1088/1361-6382/aacb8f. arXiv:1804.01444 [gr-qc]

Pani P, Maselli A (2019) Love in Extrema Ratio. Int J Mod Phys D 28(14):1944001. https://doi.org/10.1142/S0218271819440012. arXiv:1905.03947 [gr-qc]

Pani P, Berti E, Cardoso V, Chen Y, Norte R (2009) Gravitational wave signatures of the absence of an event horizon. I. Nonradial oscillations of a thin-shell gravastar. Phys Rev D 80:124047. https://doi.org/10.1103/PhysRevD.80.124047. arXiv:0909.0287 [gr-qc]

Pani P, Berti E, Cardoso V, Chen Y, Norte R (2010) Gravitational-wave signatures of the absence of an event horizon. II. Extreme mass ratio inspirals in the spacetime of a thin-shell gravastar. Phys Rev D 81:084011. https://doi.org/10.1103/PhysRevD.81.084011. arXiv:1001.3031 [gr-qc]

Pani P, Cardoso V, Gualtieri L (2011) Gravitational waves from extreme mass-ratio inspirals in dynamical Chern-Simons gravity. Phys Rev D 83:104048. https://doi.org/10.1103/PhysRevD.83.104048. arXiv:1104.1183 [gr-qc]

Pani P, Macedo C, Crispino L, Cardoso V (2011) Slowly rotating black holes in alternative theories of gravity. Phys Rev D 84:087501. https://doi.org/10.1103/PhysRevD.84.087501. arXiv:1109.3996 [gr-qc]

Pani P, Cardoso V, Gualtieri L, Berti E, Ishibashi A (2012) Black hole bombs and photon mass bounds. Phys Rev Lett 109:131102. https://doi.org/10.1103/PhysRevLett.109.131102. arXiv:1209.0465 [gr-qc]

Panosso Macedo R, Leather B, Warburton N, Wardell B, Zenginoğlu A (2022) Hyperboloidal method for frequency-domain self-force calculations. Phys Rev D 105(10):104033. https://doi.org/10.1103/PhysRevD.105.104033. arXiv:2202.01794 [gr-qc]

Papallo G (2017) On the hyperbolicity of the most general Horndeski theory. Phys Rev D 96(12):124036. https://doi.org/10.1103/PhysRevD.96.124036. arXiv:1710.10155 [gr-qc]

Papallo G, Reall HS (2017) On the local well-posedness of Lovelock and Horndeski theories. Phys Rev D 96(4):044019. https://doi.org/10.1103/PhysRevD.96.044019. arXiv:1705.04370 [gr-qc]

Papaloizou J, Pringle JE (1984) The dynamical stability of differentially rotating discs with constant specific angular momentum. MNRAS 208:721–750. https://doi.org/10.1093/mnras/208.4.721

Papapetrou A (1951) Spinning test particles in general relativity. 1. Proc R Soc Lond A 209:248–258. https://doi.org/10.1098/rspa.1951.0200

Papenfort LJ, Tootle SD, Grandclément P, Most ER, Rezzolla L (2021) New public code for initial data of unequal-mass, spinning compact-object binaries. Phys Rev D 104(2):024057. https://doi.org/10.1103/PhysRevD.104.024057. arXiv:2103.09911 [gr-qc]

Paper D (2021) State-of-the-Art Deep Learning Models in TensorFlow: Modern Machine Learning in the Google Colab Ecosystem. Apress
Paschalidis V, MacLeod M, Baumgarte TW, Shapiro SL (2009) Merger of white dwarf-neutron star binaries: prelude to hydrodynamic simulations in general relativity. Phys Rev D 80:024006. https://doi.org/10.1103/PhysRevD.80.024006. arXiv:0910.5719 [astro-ph.HE]
Paschalidis V, Etienne Z, Liu YT, Shapiro SL (2011) Head-on collisions of binary white dwarf-neutron stars: simulations in full general relativity. Phys Rev D 83:064002. https://doi.org/10.1103/PhysRevD.83.064002. arXiv:1009.4932 [astro-ph.HE]
Paschalidis V, Liu YT, Etienne Z, Shapiro SL (2011) The merger of binary white dwarf-neutron stars: simulations in full general relativity. Phys Rev D 84:104032. https://doi.org/10.1103/PhysRevD.84.104032. arXiv:1109.5177 [astro-ph.HE]
Paul K, Mishra CK (2023) Spin effects in spherical harmonic modes of gravitational waves from eccentric compact binary inspirals. Phys Rev D 108(2):024023. https://doi.org/10.1103/PhysRevD.108.024023. arXiv:2211.04155 [gr-qc]
Pazos E, Brizuela D, Martin-Garcia JM, Tiglio M (2010) Mode coupling of Schwarzschild perturbations: ringdown frequencies. Phys Rev D 82:104028. https://doi.org/10.1103/PhysRevD.82.104028. arXiv:1009.4665 [gr-qc]
Peccei RD, Quinn HR (1977) CP conservation in the presence of instantons. Phys Rev Lett 38:1440–1443. https://doi.org/10.1103/PhysRevLett.38.1440
Pelisoli I, Marsh TR, Dhillon VS, Breedt E, Brown AJ, Dyer MJ, Green MJ, Kerry P, Littlefair SP, Parsons SG, Sahman DI, Wild JF (2022) Found: a rapidly spinning white dwarf in LAMOST J024048.51+195226.9. MNRAS 509:L31–L36. https://doi.org/10.1093/mnrasl/slab116. arXiv:2108.11396 [astro-ph.SR]
Peloso M, Sorbo L (2003) Moduli from cosmic strings. Nucl Phys B 649:88–100. https://doi.org/10.1016/S0550-3213(02)01020-9. arXiv:hep-ph/0205063
Perkins S, Yunes N (2022) Are parametrized tests of general relativity with gravitational waves robust to unknown higher post-Newtonian order effects? Phys Rev D 105(12):124047. https://doi.org/10.1103/PhysRevD.105.124047. arXiv:2201.02542 [gr-qc]
Perkins SE, Nair R, Silva HO, Yunes N (2021) Improved gravitational-wave constraints on higher-order curvature theories of gravity. Phys Rev D 104(2):024060. https://doi.org/10.1103/PhysRevD.104.024060. arXiv:2104.11189 [gr-qc]
Perkins SE, Yunes N, Berti E (2021) Probing fundamental physics with gravitational waves: the next generation. Phys Rev D 103(4):044024. https://doi.org/10.1103/PhysRevD.103.044024. arXiv:2010.09010 [gr-qc]
Peters PC (1964) Gravitational radiation and the motion of two point masses. Phys Rev 136:B1224–B1232. https://doi.org/10.1103/PhysRev.136.B1224
Peters PC, Mathews J (1963) Gravitational radiation from point masses in a Keplerian orbit. Phys Rev 131:435–439. https://doi.org/10.1103/PhysRev.131.435
Pfeiffer HP (2005) Initial data for black hole evolutions. PhD thesis, Cornell U. arXiv:gr-qc/0510016
Pfeiffer HP, York JW Jr (2003) Extrinsic curvature and the Einstein constraints. Phys Rev D 67:044022. https://doi.org/10.1103/PhysRevD.67.044022. arXiv:gr-qc/0207095
Pfeiffer HP, Kidder LE, Scheel MA, Teukolsky SA (2003) A Multidomain spectral method for solving elliptic equations. Comput Phys Commun 152:253–273. https://doi.org/10.1016/S0010-4655(02)00847-0. arXiv:gr-qc/0202096
Pfeiffer HP, Brown DA, Kidder LE, Lindblom L, Lovelace G, Scheel MA (2007) Reducing orbital eccentricity in binary black hole simulations. Class Quantum Grav 24:S59–S82. https://doi.org/10.1088/0264-9381/24/12/S06. arXiv:gr-qc/0702106
Pierini L, Gualtieri L (2021) Quasi-normal modes of rotating black holes in Einstein-dilaton Gauss-Bonnet gravity: the first order in rotation. Phys Rev D 103:124017. https://doi.org/10.1103/PhysRevD.103.124017. arXiv:2103.09870 [gr-qc]
Pierini L, Gualtieri L (2022) Quasinormal modes of rotating black holes in Einstein-dilaton Gauss-Bonnet gravity: The second order in rotation. Phys Rev D 106(10):104009. https://doi.org/10.1103/PhysRevD.106.104009. arXiv:2207.11267 [gr-qc]
Piovano GA, Maselli A, Pani P (2020) Extreme mass ratio inspirals with spinning secondary: a detailed study of equatorial circular motion. Phys Rev D 102(2):024041. https://doi.org/10.1103/PhysRevD.102.024041. arXiv:2004.02654 [gr-qc]

Piovano GA, Brito R, Maselli A, Pani P (2021) Assessing the detectability of the secondary spin in extreme mass-ratio inspirals with fully relativistic numerical waveforms. Phys Rev D 104 (12):124019. https://doi.org/10.1103/PhysRevD.104.124019. arXiv:2105.07083 [gr-qc]

Piovano GA, Maselli A, Pani P (2023) Constraining the tidal deformability of supermassive objects with extreme mass ratio inspirals and semianalytical frequency-domain waveforms. Phys Rev D 107 (2):024021. https://doi.org/10.1103/PhysRevD.107.024021. arXiv:2207.07452 [gr-qc]

Placidi A, Albanesi S, Nagar A, Orselli M, Bernuzzi S, Grignani G (2022) Exploiting Newton-factorized, 2PN-accurate waveform multipoles in effective-one-body models for spin-aligned noncircularized binaries. Phys Rev D 105(10):104030. https://doi.org/10.1103/PhysRevD.105.104030. arXiv:2112.05448 [gr-qc]

Pogosian L, Tye SHH, Wasserman I, Wyman M (2003) Observational constraints on cosmic string production during brane inflation. Phys Rev D 68:023506. [Erratum: Phys. Rev. D 73, 089904 (2006)]. https://doi.org/10.1103/PhysRevD.68.023506. arXiv:hep-th/0304188

Pogosian L, Wyman MC, Wasserman I (2004) Observational constraints on cosmic strings: Bayesian analysis in a three dimensional parameter space. JCAP 09:008. https://doi.org/10.1088/1475-7516/2004/09/008. arXiv:astro-ph/0403268

Pogosian L, Wasserman I, Wyman M (2006) On vector mode contribution to CMB temperature and polarization from local strings. arXiv e-prints arXiv:astro-ph/0604141

Pogosian L, Tye S, Wasserman I, Wyman M (2009) Cosmic strings as the source of small-scale microwave background anisotropy. JCAP 02:013. https://doi.org/10.1088/1475-7516/2009/02/013. arXiv:0804.0810 [astro-ph]

Poisson E (1998) Gravitational waves from inspiraling compact binaries: The Quadrupole moment term. Phys Rev D 57:5287–5290. https://doi.org/10.1103/PhysRevD.57.5287. arXiv:gr-qc/9709032

Poisson E (2004) Absorption of mass and angular momentum by a black hole: Time-domain formalisms for gravitational perturbations, and the small-hole / slow-motion approximation. Phys Rev D 70:084044. https://doi.org/10.1103/PhysRevD.70.084044. arXiv:gr-qc/0407050

Poisson E (2009) Tidal interaction of black holes and Newtonian viscous bodies. Phys Rev D 80:064029. https://doi.org/10.1103/PhysRevD.80.064029. arXiv:0907.0874 [gr-qc]

Poisson E, Corrigan E (2018) Nonrotating black hole in a post-Newtonian tidal environment II. Phys Rev D 97(12):124048. https://doi.org/10.1103/PhysRevD.97.124048. arXiv:1804.01848 [gr-qc]

Poisson E, Sasaki M (1995) Gravitational radiation from a particle in circular orbit around a black hole. 5: Black hole absorption and tail corrections. Phys Rev D 51:5753–5767. https://doi.org/10.1103/PhysRevD.51.5753. arXiv:gr-qc/9412027

Poisson E, Will CM (2014) Gravity: Newtonian, post-Newtonian, relativistic. Cambridge University Press, Cambridge

Poisson E, Pound A, Vega I (2011) The Motion of point particles in curved spacetime. Living Rev Relativ 14:7. https://doi.org/10.12942/lrr-2011-7

Polcar L, Lukes-Gerakopoulos G, Witzany V (2022) Extreme mass ratio inspirals into black holes surrounded by matter. Phys Rev D 106(4):044069. https://doi.org/10.1103/PhysRevD.106.044069. arXiv:2205.08516 [gr-qc]

Polchinski J, Rocha JV (2007) Cosmic string structure at the gravitational radiation scale. Phys Rev D 75:123503. https://doi.org/10.1103/PhysRevD.75.123503. arXiv:gr-qc/0702055

Pompili L et al (2023) Laying the foundation of the effective-one-body waveform models SEOBNRv5: Improved accuracy and efficiency for spinning nonprecessing binary black holes. Phys Rev D 108 (12):124035. https://doi.org/10.1103/PhysRevD.108.124035. arXiv:2303.18039 [gr-qc]

Portegies Zwart SF, McMillan S (2000) Black hole mergers in the universe. Astrophys J Lett 528:L17. https://doi.org/10.1086/312422. arXiv:astro-ph/9910061

Porter EK (2015) The challenges in gravitational wave astronomy for space-based detectors. Astrophys Space Sci Proc 40:267–279. https://doi.org/10.1007/978-3-319-10488-1_23. arXiv:1406.6891 [gr-qc]

Porto RA (2006) Post-Newtonian corrections to the motion of spinning bodies in NRGR. Phys Rev D 73:104031. https://doi.org/10.1103/PhysRevD.73.104031. arXiv:gr-qc/0511061

Porto RA (2008) Absorption effects due to spin in the worldline approach to black hole dynamics. Phys Rev D 77:064026. https://doi.org/10.1103/PhysRevD.77.064026. arXiv:0710.5150 [hep-th]

Porto RA (2010) Next to leading order spin-orbit effects in the motion of inspiralling compact binaries. Class Quantum Grav 27:205001. https://doi.org/10.1088/0264-9381/27/20/205001. arXiv:1005.5730 [gr-qc]

Porto RA (2016) The effective field theorist's approach to gravitational dynamics. Phys Rept 633:1–104. https://doi.org/10.1016/j.physrep.2016.04.003. arXiv:1601.04914 [hep-th]

Porto RA, Rothstein IZ (2006) The hyperfine Einstein-Infeld-Hoffmann potential. Phys Rev Lett 97:021101. https://doi.org/10.1103/PhysRevLett.97.021101. arXiv:gr-qc/0604099
Porto RA, Rothstein IZ (2008) Next to Leading Order Spin(1)Spin(1) Effects in the Motion of Inspiralling Compact Binaries. Phys Rev D 78:044013. [Erratum: Phys. Rev. D 81, 029905 (2010)]. https://doi.org/10.1103/PhysRevD.78.044013. arXiv:0804.0260 [gr-qc]
Porto RA, Rothstein IZ (2008) Spin(1)Spin(2) Effects in the Motion of Inspiralling Compact Binaries at Third Order in the Post-Newtonian Expansion. Phys Rev D 78:044012. [Erratum: Phys. Rev. D 81, 029904 (2010)]. https://doi.org/10.1103/PhysRevD.78.044012. arXiv:0802.0720 [gr-qc]
Porto RA, Ross A, Rothstein IZ (2011) Spin induced multipole moments for the gravitational wave flux from binary inspirals to third Post-Newtonian order. JCAP 03:009. https://doi.org/10.1088/1475-7516/2011/03/009. arXiv:1007.1312 [gr-qc]
Porto RA, Ross A, Rothstein IZ (2012) Spin induced multipole moments for the gravitational wave amplitude from binary inspirals to 2.5 Post-Newtonian order. JCAP 09:028. https://doi.org/10.1088/1475-7516/2012/09/028. arXiv:1203.2962 [gr-qc]
Postnov KA, Yungelson LR (2014) The evolution of compact binary star systems. Living Rev Relativ 17:3. https://doi.org/10.12942/lrr-2014-3. arXiv:1403.4754 [astro-ph.HE]
Pound A (2010) Self-consistent gravitational self-force. Phys Rev D 81:024023. https://doi.org/10.1103/PhysRevD.81.024023. arXiv:0907.5197 [gr-qc]
Pound A (2010) Singular perturbation techniques in the gravitational self-force problem. Phys Rev D 81:124009. https://doi.org/10.1103/PhysRevD.81.124009. arXiv:1003.3954 [gr-qc]
Pound A (2012) Nonlinear gravitational self-force. I. Field outside a small body. Phys Rev D 86:084019. https://doi.org/10.1103/PhysRevD.86.084019. arXiv:1206.6538 [gr-qc]
Pound A (2012) Second-order gravitational self-force. Phys Rev Lett 109:051101. https://doi.org/10.1103/PhysRevLett.109.051101. arXiv:1201.5089 [gr-qc]
Pound A (2015) Gauge and motion in perturbation theory. Phys Rev D 92(4):044021. https://doi.org/10.1103/PhysRevD.92.044021. arXiv:1506.02894 [gr-qc]
Pound A (2015) Motion of small objects in curved spacetimes: an introduction to gravitational self-force. Fund Theor Phys 179:399–486. https://doi.org/10.1007/978-3-319-18335-0_13. arXiv:1506.06245 [gr-qc]
Pound A (2015) Second-order perturbation theory: problems on large scales. Phys Rev D 92(10):104047. https://doi.org/10.1103/PhysRevD.92.104047. arXiv:1510.05172 [gr-qc]
Pound A (2017) Nonlinear gravitational self-force: second-order equation of motion. Phys Rev D 95 (10):104056. https://doi.org/10.1103/PhysRevD.95.104056. arXiv:1703.02836 [gr-qc]
Pound A, Miller J (2014) Practical, covariant puncture for second-order self-force calculations. Phys Rev D 89(10):104020. https://doi.org/10.1103/PhysRevD.89.104020. arXiv:1403.1843 [gr-qc]
Pound A, Wardell B (2021) Black hole perturbation theory and gravitational self-force. In: Bambi C, Katsanevas S, Kokkotas KD (eds) Handbook of Gravitational Wave Astronomy. Springer, Singapore. https://doi.org/10.1007/978-981-15-4702-7_38-1. arXiv:2101.04592 [gr-qc]
Pound A, Merlin C, Barack L (2014) Gravitational self-force from radiation-gauge metric perturbations. Phys Rev D 89(2):024009. https://doi.org/10.1103/PhysRevD.89.024009. arXiv:1310.1513 [gr-qc]
Pound A, Wardell B, Warburton N, Miller J (2020) Second-order self-force calculation of gravitational binding energy in compact binaries. Phys Rev Lett 124(2):021101. https://doi.org/10.1103/PhysRevLett.124.021101. arXiv:1908.07419 [gr-qc]
Pratten G, Husa S, Garcia-Quiros C, Colleoni M, Ramos-Buades A, Estelles H, Jaume R (2020) Setting the cornerstone for a family of models for gravitational waves from compact binaries: the dominant harmonic for nonprecessing quasicircular black holes. Phys Rev D 102(6):064001. https://doi.org/10.1103/PhysRevD.102.064001. arXiv:2001.11412 [gr-qc]
Pratten G et al (2021) Computationally efficient models for the dominant and subdominant harmonic modes of precessing binary black holes. Phys Rev D 103(10):104056. https://doi.org/10.1103/PhysRevD.103.104056. arXiv:2004.06503 [gr-qc]
Prescod-Weinstein C, Afshordi N, Balogh ML, Afshordi N, Balogh ML (2009) Stellar black holes and the origin of cosmic acceleration. Phys Rev D 80:043513. https://doi.org/10.1103/PhysRevD.80.043513. arXiv:0905.3551 [astro-ph.CO]
Preskill J (1984) MAGNETIC MONOPOLES IN PARTICLE PHYSICS AND COSMOLOGY. In: Inner Space/ Outer Space: Conference on Physics at the Interface of Astrophysics / Cosmology and Particle Physics
Press WH (1971) Long wave trains of gravitational waves from a vibrating black hole. Astrophys J Lett 170:L105–L108. https://doi.org/10.1086/180849

Press WH, Teukolsky SA (1972) Floating orbits, superradiant scattering and the black-hole bomb. Nature 238:211–212. https://doi.org/10.1038/238211a0
Press WH, Teukolsky SA (1973) Perturbations of a rotating black hole. II. Dynamical stability of the kerr metric. Astrophys J 185:649–674. https://doi.org/10.1086/152445
Preto M, Berentzen I, Berczik P, Spurzem R (2011) Fast coalescence of massive black hole binaries from mergers of galactic nuclei: implications for low-frequency gravitational-wave astrophysics. Astrophys J Lett 732:L26. https://doi.org/10.1088/2041-8205/732/2/L26. arXiv:1102.4855 [astro-ph.GA]
Pretorius F (2005) Evolution of binary black hole spacetimes. Phys Rev Lett 95:121101. https://doi.org/10.1103/PhysRevLett.95.121101. arXiv:gr-qc/0507014
Pretorius F (2005) Numerical relativity using a generalized harmonic decomposition. Class Quantum Grav 22:425–452. https://doi.org/10.1088/0264-9381/22/2/014. arXiv:gr-qc/0407110
Price RH (1972) Nonspherical perturbations of relativistic gravitational collapse. 1. Scalar and gravitational perturbations. Phys Rev D 5:2419–2438. https://doi.org/10.1103/PhysRevD.5.2419
Price RH, Khanna G (2017) Gravitational wave sources: reflections and echoes. Class Quantum Grav 34 (22):225005. https://doi.org/10.1088/1361-6382/aa8f29. arXiv:1702.04833 [gr-qc]
Price RH, Pullin J (1994) Colliding black holes: The Close limit. Phys Rev Lett 72:3297–3300. https://doi.org/10.1103/PhysRevLett.72.3297. arXiv:gr-qc/9402039
Prud'homme C, Maday Y, Patera AT, Turinici G, Rovas DV, Veroy K, Machiels L (2001) Reliable real-time solution of parametrized partial differential equations: Reduced-basis output bound methods. J Fluids Eng 10(1115/1):1448332
Pürrer M (2014) Frequency domain reduced order models for gravitational waves from aligned-spin compact binaries. Class Quantum Grav 31(19):195010. https://doi.org/10.1088/0264-9381/31/19/195010. arXiv:1402.4146 [gr-qc]
Pürrer M (2016) Frequency domain reduced order model of aligned-spin effective-one-body waveforms with generic mass-ratios and spins. Phys Rev D 93(6):064041. https://doi.org/10.1103/PhysRevD.93.064041. arXiv:1512.02248 [gr-qc]
Pürrer M, Haster CJ (2020) Gravitational waveform accuracy requirements for future ground-based detectors. Phys Rev Res 2(2):023151. https://doi.org/10.1103/PhysRevResearch.2.023151. arXiv:1912.10055 [gr-qc]
Quarteroni A, Rozza G, Manzoni A (2011) Certified reduced basis approximation for parametrized partial differential equations and applications. J Math Industry 1(1):1–49. https://doi.org/10.1186/2190-5983-1-3
Quashnock JM, Spergel DN (1990) Gravitational Selfinteractions of Cosmic Strings. Phys Rev D 42:2505–2520. https://doi.org/10.1103/PhysRevD.42.2505
Que Z, et al. (2021) Accelerating Recurrent Neural Networks for Gravitational Wave Experiments. In: 32nd IEEE International Conference on Application-specific Systems, Architectures and Processors. https://doi.org/10.1109/ASAP52443.2021.00025. arXiv:2106.14089 [cs.LG]
Quinlan GD, Hernquist L, Sigurdsson S (1995) Models of galaxies with central black holes: adiabatic growth in spherical galaxies. Astrophys J 440:554–564. https://doi.org/10.1086/175295. arXiv:astro-ph/9407005
Quinn TC, Wald RM (1997) An Axiomatic approach to electromagnetic and gravitational radiation reaction of particles in curved space-time. Phys Rev D 56:3381–3394. https://doi.org/10.1103/PhysRevD.56.3381. arXiv:gr-qc/9610053
Radice D, Rezzolla L (2012) THC: a new high-order finite-difference high-resolution shock-capturing code for special-relativistic hydrodynamics. Astron Astrophys 547:A26. https://doi.org/10.1051/0004-6361/201219735. arXiv:1206.6502 [astro-ph.IM]
Radice D, Rezzolla L, Galeazzi F (2014) Beyond second-order convergence in simulations of binary neutron stars in full general-relativity. Mon Not R Astron Soc 437:L46–L50. https://doi.org/10.1093/mnrasl/slt137. arXiv:1306.6052 [gr-qc]
Radice D, Rezzolla L, Galeazzi F (2014) High-order fully general-relativistic hydrodynamics: new approaches and tests. Class Quantum Grav 31:075012. https://doi.org/10.1088/0264-9381/31/7/075012. arXiv:1312.5004 [gr-qc]
Rahman M, Bhattacharyya A (2023) Prospects for determining the nature of the secondaries of extreme mass-ratio inspirals using the spin-induced quadrupole deformation. Phys Rev D 107(2):024006. https://doi.org/10.1103/PhysRevD.107.024006. arXiv:2112.13869 [gr-qc]
Rajamuthukumar AS, Hamers AS, Neunteufel P, Pakmor R, de mink SE (2023) Triple evolution: an important channel in the formation of type Ia supernovae. Astrophys J 950(1):9. https://doi.org/10.3847/1538-4357/acc86c. arXiv:2211.04463 [astro-ph.SR]

Ramond P, Le Tiec A (2021) Multipolar particles in helically symmetric spacetimes. Class Quantum Grav 38(13):135022. https://doi.org/10.1088/1361-6382/abebef. arXiv:2005.00602 [gr-qc]
Ramond P, Le Tiec A (2022) First law of mechanics for spinning compact binaries: dipolar order. Phys Rev D 106(4):044057. https://doi.org/10.1103/PhysRevD.106.044057. arXiv:2202.09345 [gr-qc]
Ramos-Buades A, Husa S, Pratten G, Estellés H, García-Quirós C, Mateu-Lucena M, Colleoni M, Jaume R (2020) First survey of spinning eccentric black hole mergers: numerical relativity simulations, hybrid waveforms, and parameter estimation. Phys Rev D 101(8):083015. https://doi.org/10.1103/PhysRevD.101.083015. arXiv:1909.11011 [gr-qc]
Ramos-Buades A, Schmidt P, Pratten G, Husa S (2020) Validity of common modeling approximations for precessing binary black holes with higher-order modes. Phys Rev D 101(10):103014. https://doi.org/10.1103/PhysRevD.101.103014. arXiv:2001.10936 [gr-qc]
Ramos-Buades A, Buonanno A, Khalil M, Ossokine S (2022) Effective-one-body multipolar waveforms for eccentric binary black holes with nonprecessing spins. Phys Rev D 105(4):044035. https://doi.org/10.1103/PhysRevD.105.044035. arXiv:2112.06952 [gr-qc]
Ramos-Buades A, van de Meent M, Pfeiffer HP, Rüter HR, Scheel MA, Boyle M, Kidder LE (2022) Eccentric binary black holes: comparing numerical relativity and small mass-ratio perturbation theory. Phys Rev D 106(12):124040. https://doi.org/10.1103/PhysRevD.106.124040. arXiv:2209.03390 [gr-qc]
Ramos-Buades A, Buonanno A, Estellés H, Khalil M, Mihaylov DP, Ossokine S, Pompili L, Shiferaw M (2023) Next generation of accurate and efficient multipolar precessing-spin effective-one-body waveforms for binary black holes. Phys Rev D 108(12):124037. https://doi.org/10.1103/PhysRevD.108.124037. arXiv:2303.18046 [gr-qc]
Raposo G, Pani P (2020) Axisymmetric deformations of neutron stars and gravitational-wave astronomy. Phys Rev D 102(4):044045. https://doi.org/10.1103/PhysRevD.102.044045. arXiv:2002.02555 [gr-qc]
Raposo G, Pani P, Emparan R (2019) Exotic compact objects with soft hair. Phys Rev D 99(10):104050. https://doi.org/10.1103/PhysRevD.99.104050. arXiv:1812.07615 [gr-qc]
Rashti A, Fabbri FM, Brügmann B, Chaurasia SV, Dietrich T, Ujevic M, Tichy W (2022) New pseudospectral code for the construction of initial data. Phys Rev D 105(10):104027. https://doi.org/10.1103/PhysRevD.105.104027. arXiv:2109.14511 [gr-qc]
Redondo-Yuste J, Carullo G, Ripley JL, Berti E, Cardoso V (2024) Spin dependence of black hole ringdown nonlinearities. Phys Rev D 109(10):L101503. https://doi.org/10.1103/PhysRevD.109.L101503. arXiv:2308.14796 [gr-qc]
Regan J, Visbal E, Wise JH, Haiman Z, Johansson PH, Bryan GL (2017) Rapid Formation of Massive Black Holes in close proximity to Embryonic Proto-Galaxies. arXiv e-prints arXiv:1703.03805 [astro-ph.GA]
Regge T, Wheeler JA (1957) Stability of a Schwarzschild singularity. Phys Rev 108:1063–1069. https://doi.org/10.1103/PhysRev.108.1063
Regimbau T, Giampanis S, Siemens X, Mandic V (2012) The stochastic background from cosmic (super) strings: popcorn and (Gaussian) continuous regimes. Phys Rev D 85:066001. https://doi.org/10.1103/PhysRevD.85.066001. arXiv:1111.6638 [astro-ph.CO]
Reines AE, Sivakoff GR, Johnson KE, Brogan CL (2011) An actively accreting massive black hole in the dwarf starburst galaxy Henize 2–10. Nature 470:66–68. https://doi.org/10.1038/nature09724. arXiv:1101.1309 [astro-ph.CO]
Reines AE, Greene JE, Geha M (2013) Dwarf galaxies with optical signatures of active massive black holes. Astrophys J 775:116. https://doi.org/10.1088/0004-637X/775/2/116. arXiv:1308.0328 [astro-ph.CO]
Reisswig C, Pollney D (2011) Notes on the integration of numerical relativity waveforms. Class Quantum Grav 28:195015. https://doi.org/10.1088/0264-9381/28/19/195015. arXiv:1006.1632 [gr-qc]
Reitze D et al (2019) Cosmic explorer: The U.S. contribution to gravitational-wave astronomy beyond LIGO. Bull Am Astron Soc 51(7):035 arXiv:1907.04833 [astro-ph.IM]
Renkhoff S, Cors D, Hilditch D, Brügmann B (2023) Adaptive hp refinement for spectral elements in numerical relativity. Phys Rev D 107(10):104043. https://doi.org/10.1103/PhysRevD.107.104043. arXiv:2302.00575 [gr-qc]
Rettegno P, Martinetti F, Nagar A, Bini D, Riemenschneider G, Damour T (2020) Comparing effective one body hamiltonians for spin-aligned coalescing binaries. Phys Rev D 101(10):104027. https://doi.org/10.1103/PhysRevD.101.104027. arXiv:1911.10818 [gr-qc]

de Rham C, Matas A, Tolley AJ (2013) Galileon radiation from binary systems. Phys Rev D 87(6):064024. https://doi.org/10.1103/PhysRevD.87.064024. arXiv:1212.5212 [hep-th]
de Rham C, Tolley AJ, Wesley DH (2013) Vainshtein mechanism in binary pulsars. Phys Rev D 87 (4):044025. https://doi.org/10.1103/PhysRevD.87.044025. arXiv:1208.0580 [gr-qc]
de Rham C, Kozuszek J, Tolley AJ, Wiseman T (2023) Dynamical formulation of ghost-free massive gravity. Phys Rev D 108(8):084052. https://doi.org/10.1103/PhysRevD.108.084052. arXiv:2302.04876 [hep-th]
Riemenschneider G, Rettegno P, Breschi M, Albertini A, Gamba R, Bernuzzi S, Nagar A (2021) Assessment of consistent next-to-quasicircular corrections and postadiabatic approximation in effective-one-body multipolar waveforms for binary black hole coalescences. Phys Rev D 104 (10):104045. https://doi.org/10.1103/PhysRevD.104.104045. arXiv:2104.07533 [gr-qc]
Rifat N, Field SE, Khanna G, Varma V (2020) Surrogate model for gravitational wave signals from comparable and large-mass-ratio black hole binaries. Phys Rev D 101(8):081502. https://doi.org/10.1103/PhysRevD.101.081502. arXiv:1910.10473 [gr-qc]
Ringeval C, Suyama T (2017) Stochastic gravitational waves from cosmic string loops in scaling. JCAP 12:027. https://doi.org/10.1088/1475-7516/2017/12/027. arXiv:1709.03845 [astro-ph.CO]
Rinne O (2006) Stable radiation-controlling boundary conditions for the generalized harmonic Einstein equations. Class Quantum Grav 23:6275–6300. https://doi.org/10.1088/0264-9381/23/22/013. arXiv:gr-qc/0606053
Rinne O, Lindblom L, Scheel MA (2007) Testing outer boundary treatments for the Einstein equations. Class Quantum Grav 24:4053–4078. https://doi.org/10.1088/0264-9381/24/16/006. arXiv:0704.0782 [gr-qc]
Ripley JL (2022) Numerical relativity for Horndeski gravity. Int J Mod Phys D 31(13):2230017. https://doi.org/10.1142/S0218271822300178. arXiv:2207.13074 [gr-qc]
Ripley JL, Pretorius F (2019) Gravitational collapse in Einstein dilaton-Gauss-Bonnet gravity. Class Quantum Grav 36(13):134001. https://doi.org/10.1088/1361-6382/ab2416. arXiv:1903.07543 [gr-qc]
Ripley JL, Pretorius F (2019) Hyperbolicity in Spherical Gravitational Collapse in a Horndeski Theory. Phys Rev D 99(8):084014. https://doi.org/10.1103/PhysRevD.99.084014. arXiv:1902.01468 [gr-qc]
Ripley JL, Loutrel N, Giorgi E, Pretorius F (2021) Numerical computation of second order vacuum perturbations of Kerr black holes. Phys Rev D 103:104018. https://doi.org/10.1103/PhysRevD.103.104018. arXiv:2010.00162 [gr-qc]
Riva MM, Vernizzi F (2021) Radiated momentum in the post-Minkowskian worldline approach via reverse unitarity. JHEP 11:228. https://doi.org/10.1007/JHEP11(2021)228. arXiv:2110.10140 [hep-th]
Robson T, Cornish NJ, Liu C (2019) The construction and use of LISA sensitivity curves. Class Quantum Grav 36(10):105011. https://doi.org/10.1088/1361-6382/ab1101. arXiv:1803.01944 [astro-ph.HE]
Roedig C, Sesana A (2012) Origin and Implications of high eccentricities in massive black hole binaries at sub-pc scales. J Phys: Conf Ser 363:012035. https://doi.org/10.1088/1742-6596/363/1/012035. arXiv:1111.3742 [astro-ph.CO]
Rom B, Sari R (2022) Extreme mass-ratio binary black hole merger: Characteristics of the test-particle limit. Phys Rev D 106(10):104040. https://doi.org/10.1103/PhysRevD.106.104040. arXiv:2204.11738 [gr-qc]
Romano JD, Cornish NJ (2017) Detection methods for stochastic gravitational-wave backgrounds: a unified treatment. Living Rev Relativ 20:2. https://doi.org/10.1007/s41114-017-0004-1. arXiv:1608.06889 [gr-qc]
Romero-Shaw IM, Lasky PD, Thrane E (2019) Searching for Eccentricity: Signatures of Dynamical Formation in the First Gravitational-Wave Transient Catalogue of LIGO and Virgo. Mon Not R Astron Soc 490(4):5210–5216. https://doi.org/10.1093/mnras/stz2996. arXiv:1909.05466 [astro-ph.HE]
Romero-Shaw IM, Kremer K, Lasky PD, Thrane E, Samsing J (2021) Gravitational waves as a probe of globular cluster formation and evolution. Mon Not R Astron Soc 506(2):2362–2372. https://doi.org/10.1093/mnras/stab1815. arXiv:2011.14541 [astro-ph.HE]
Rosato N, Healy J, Lousto CO (2021) Adapted gauge to small mass ratio binary black hole evolutions. Phys Rev D 103(10):104068. https://doi.org/10.1103/PhysRevD.103.104068. arXiv:2103.09326 [gr-qc]
Rosenthal E (2006) Second-order gravitational self-force. Phys Rev D 74:084018. https://doi.org/10.1103/PhysRevD.74.084018. arXiv:gr-qc/0609069
Ross A (2012) Multipole expansion at the level of the action. Phys Rev D 85:125033. https://doi.org/10.1103/PhysRevD.85.125033. arXiv:1202.4750 [gr-qc]

Rosselló-Sastre M, Husa S, Bera S (2024) Waveform model for the missing quadrupole mode from black hole coalescence: Memory effect and ringdown of the (ℓ=2, m=0) spherical harmonic. Phys Rev D 110(8):084074. https://doi.org/10.1103/PhysRevD.110.084074. arXiv:2405.17302 [gr-qc]

Rosswog S, Diener P (2021) SPHINCS_BSSN: A general relativistic Smooth Particle Hydrodynamics code for dynamical spacetimes. Class Quantum Grav 38(11):115002. https://doi.org/10.1088/1361-6382/abee65. arXiv:2012.13954 [gr-qc]

Rothstein IZ (2014) Progress in effective field theory approach to the binary inspiral problem. Gen Relativ Gravit 46:1726. https://doi.org/10.1007/s10714-014-1726-y

Roulet J, Venumadhav T, Zackay B, Dai L, Zaldarriaga M (2020) Binary Black Hole Mergers from LIGO/Virgo O1 and O2: Population Inference Combining Confident and Marginal Events. Phys Rev D 102 (12):123022. https://doi.org/10.1103/PhysRevD.102.123022. arXiv:2008.07014 [astro-ph.HE]

Ruangsri U, Hughes SA (2014) Census of transient orbital resonances encountered during binary inspiral. Phys Rev D 89(8):084036. https://doi.org/10.1103/PhysRevD.89.084036. arXiv:1307.6483 [gr-qc]

Ruangsri U, Vigeland SJ, Hughes SA (2016) Gyroscopes orbiting black holes: A frequency-domain approach to precession and spin-curvature coupling for spinning bodies on generic Kerr orbits. Phys Rev D 94(4):044008. https://doi.org/10.1103/PhysRevD.94.044008. arXiv:1512.00376 [gr-qc]

Ruchlin I, Healy J, Lousto CO, Zlochower Y (2017) Puncture Initial Data for Black-Hole Binaries with High Spins and High Boosts. Phys Rev D 95(2):024033. https://doi.org/10.1103/PhysRevD.95.024033. arXiv:1410.8607 [gr-qc]

Ruchlin I, Etienne ZB, Baumgarte TW (2018) SENR/NRPy+: Numerical Relativity in Singular Curvilinear Coordinate Systems. Phys Rev D 97(6):064036. https://doi.org/10.1103/PhysRevD.97.064036. arXiv:1712.07658 [gr-qc]

Rudiger R (1983) Conserved Quantities of Spinning Test Particles in General Relativity. II. Proceedings of the Royal Society of London Series A 385(1788):229–239. https://doi.org/10.1098/rspa.1983.0012

Ruffini R, Bonazzola S (1969) Systems of selfgravitating particles in general relativity and the concept of an equation of state. Phys Rev 187:1767–1783. https://doi.org/10.1103/PhysRev.187.1767

Ruiter AJ, Belczynski K, Benacquista M, Larson SL, Williams G (2010) The LISA gravitational wave foreground: a study of double white dwarfs. Astrophys J 717:1006–1021. https://doi.org/10.1088/0004-637X/717/2/1006. arXiv:0705.3272 [astro-ph]

Ruiz M, Hilditch D, Bernuzzi S (2011) Constraint preserving boundary conditions for the Z4c formulation of general relativity. Phys Rev D 83:024025. https://doi.org/10.1103/PhysRevD.83.024025. arXiv:1010.0523 [gr-qc]

Ruiz M, Tsokaros A, Shapiro SL (2023) General relativistic magnetohydrodynamic simulations of accretion disks around tilted binary black holes of unequal mass. Phys Rev D 108(12):124043. https://doi.org/10.1103/PhysRevD.108.124043. arXiv:2302.09083 [astro-ph.HE]

Ryan FD (1995) Gravitational waves from the inspiral of a compact object into a massive, axisymmetric body with arbitrary multipole moments. Phys Rev D 52:5707–5718. https://doi.org/10.1103/PhysRevD.52.5707

Ryan FD (1997) Spinning boson stars with large selfinteraction. Phys Rev D 55:6081–6091. https://doi.org/10.1103/PhysRevD.55.6081

Ryu T, Perna R, Haiman Z, Ostriker JP, Stone NC (2018) Interactions between multiple supermassive black holes in galactic nuclei: a solution to the final parsec problem. Mon Not R Astron Soc 473(3):3410–3433. https://doi.org/10.1093/mnras/stx2524. arXiv:1709.06501

Sabancilar E (2010) Cosmological Constraints on Strongly Coupled Moduli from Cosmic Strings. Phys Rev D 81:123502. https://doi.org/10.1103/PhysRevD.81.123502. arXiv:0910.5544 [hep-ph]

SACRA (2024) http://www2.yukawa.kyoto-u.ac.jp/∼nr_kyoto/SACRA_PUB/catalog.html

Sago N (2015) Calculation of radiation reaction effect on orbital parameters in Kerr spacetime. PTEP 7:073E03. https://doi.org/10.1093/ptep/ptv092. arXiv:1505.01600 [gr-qc]

Sago N, Tanaka T (2021) Oscillations in the extreme mass-ratio inspiral gravitational wave phase correction as a probe of a reflective boundary of the central black hole. Phys Rev D 104(6):064009. https://doi.org/10.1103/PhysRevD.104.064009. arXiv:2106.07123 [gr-qc]

Sago N, Tanaka T (2022) Efficient search method of anomalous reflection by the central object in an extreme mass-ratio inspiral system by future space gravitational wave detectors. Phys Rev D 106 (2):024032. https://doi.org/10.1103/PhysRevD.106.024032. arXiv:2202.04249 [gr-qc]

Sago N, Tanaka T, Hikida W, Nakano H (2005) Adiabatic radiation reaction to the orbits in Kerr spacetime. Prog Theor Phys 114:509–514. https://doi.org/10.1143/PTP.114.509. arXiv:gr-qc/0506092

Sago N, Tanaka T, Hikida W, Ganz K, Nakano H (2006) The Adiabatic evolution of orbital parameters in the Kerr spacetime. Prog Theor Phys 115:873–907. https://doi.org/10.1143/PTP.115.873. arXiv:gr-qc/0511151

Saketh M, Vines J, Steinhoff J, Buonanno A (2022) Conservative and radiative dynamics in classical relativistic scattering and bound systems. Phys Rev Res 4(1):013127. https://doi.org/10.1103/PhysRevResearch.4.013127. arXiv:2109.05994 [gr-qc]

Sakon S et al (2024) Template bank for compact binary mergers in the fourth observing run of Advanced LIGO, Advanced Virgo, and KAGRA. Phys Rev D 109(4):044066. https://doi.org/10.1103/PhysRevD.109.044066. arXiv:2211.16674 [gr-qc]

Salgado M, Martinez-del Rio D, Alcubierre M, Nunez D (2008) Hyperbolicity of scalar-tensor theories of gravity. Phys Rev D 77:104010. https://doi.org/10.1103/PhysRevD.77.104010. arXiv:0801.2372 [gr-qc]

Saltas ID, Sawicki I, Amendola L, Kunz M (2014) Anisotropic stress as a signature of nonstandard propagation of gravitational waves. Phys Rev Lett 113(19):191101. https://doi.org/10.1103/PhysRevLett.113.191101. arXiv:1406.7139 [astro-ph.CO]

Sam Z (2024) Flux balance derivation using generic approach, talk given at the 27th Capra Meeting, Jun 2024. Available at https://www.caprameeting.org/capra-27/abstracts

SamraiWeb (2024) Samrai. https://wwwrel.ph.utexas.edu/openGR/samrai-dox/html/main.html

Sanchis-Gual N, Degollado JC, Montero PJ, Font JA, Mewes V (2015) Quasistationary solutions of self-gravitating scalar fields around collapsing stars. Phys Rev D 92(8):083001. https://doi.org/10.1103/PhysRevD.92.083001. arXiv:1507.08437 [gr-qc]

Sanchis-Gual N, Degollado JC, Izquierdo P, Font JA, Montero PJ (2016) Quasistationary solutions of scalar fields around accreting black holes. Phys Rev D 94(4):043004. https://doi.org/10.1103/PhysRevD.94.043004. arXiv:1606.05146 [gr-qc]

Sanchis-Gual N, Herdeiro C, Font JA, Radu E, Di Giovanni F (2019) Head-on collisions and orbital mergers of Proca stars. Phys Rev D 99(2):024017. https://doi.org/10.1103/PhysRevD.99.024017. arXiv:1806.07779 [gr-qc]

Sanchis-Gual N, Calderón Bustillo J, Herdeiro C, Radu E, Font JA, Leong S, Torres-Forné A (2022) Impact of the wavelike nature of Proca stars on their gravitational-wave emission. Phys Rev D 106 (12):124011. https://doi.org/10.1103/PhysRevD.106.124011. arXiv:2208.11717 [gr-qc]

Sanchis-Gual N, Zilhão M, Cardoso V (2022) Electromagnetic emission from axionic boson star collisions. Phys Rev D 106(6):064034. https://doi.org/10.1103/PhysRevD.106.064034. arXiv:2207.05494 [gr-qc]

Sanidas SA, Battye RA, Stappers BW (2012) Constraints on cosmic string tension imposed by the limit on the stochastic gravitational wave background from the European Pulsar Timing Array. Phys Rev D 85:122003. https://doi.org/10.1103/PhysRevD.85.122003. arXiv:1201.2419 [astro-ph.CO]

Sanidas SA, Battye RA, Stappers BW (2013) Projected constraints on the cosmic (super)string tension with future gravitational wave detection experiments. Astrophys J 764:108. https://doi.org/10.1088/0004-637X/764/1/108. arXiv:1211.5042 [astro-ph.CO]

Santamaria L et al (2010) Matching post-Newtonian and numerical relativity waveforms: systematic errors and a new phenomenological model for non-precessing black hole binaries. Phys Rev D 82:064016. https://doi.org/10.1103/PhysRevD.82.064016. arXiv:1005.3306 [gr-qc]

Santos NM, Benone CL, Crispino L, Herdeiro C, Radu E (2020) Black holes with synchronised Proca hair: linear clouds and fundamental non-linear solutions. JHEP 07:010. https://doi.org/10.1007/JHEP07(2020)010. arXiv:2004.09536 [gr-qc]

Sarangi S, Tye S (2002) Cosmic string production towards the end of brane inflation. Phys Lett B 536:185–192. https://doi.org/10.1016/S0370-2693(02)01824-5. arXiv:hep-th/0204074

Sarbach O, Tiglio M (2012) Continuum and discrete initial-boundary-value problems and Einstein's field equations. Living Rev Relativ 15:9. https://doi.org/10.12942/lrr-2012-9. arXiv:1203.6443 [gr-qc]

Sarbach O, Barausse E, Preciado-López JA (2019) Well-posed cauchy formulation for Einstein-æther theory. Class Quantum Grav 36(16):165007. https://doi.org/10.1088/1361-6382/ab2e13. arXiv:1902.05130 [gr-qc]

Sasaki M, Tagoshi H (2003) Analytic black hole perturbation approach to gravitational radiation. Living Rev Relativ 6:6. https://doi.org/10.12942/lrr-2003-6. arXiv:gr-qc/0306120

Sathyaprakash B et al (2012) Scientific Objectives of Einstein Telescope. Class Quantum Grav 29:124013. [Erratum: Class. Quant. Grav. 30, 079501 (2013)]. https://doi.org/10.1088/0264-9381/29/12/124013. arXiv:1206.0331 [gr-qc]

Sazhin M, Longo G, Alcalá JM, Silvotti R, Covone G, Khovanskaya O, Pavlov M, Pannella M, Radovich M, Testa V (2003) CSL-1: A chance projection effect or serendipitous discovery of a gravitational lens induced by a cosmic string? Mon Not R Astron Soc 343:353. https://doi.org/10.1046/j.1365-8711.2003.06568.x. arXiv:astro-ph/0302547

Sazhin MV, Capaccioli M, Longo G, Paolillo M, Khovanskaya OS (2006) The true nature of CSL-1. arXiv e-prints arXiv:astro-ph/0601494

Sberna L, Bosch P, East WE, Green SR, Lehner L (2022) Nonlinear effects in the black hole ringdown: Absorption-induced mode excitation. Phys Rev D 105(6):064046. https://doi.org/10.1103/PhysRevD.105.064046. arXiv:2112.11168 [gr-qc]

Schäfer G (2009) Post-Newtonian methods: Analytic results on the binary problem. In: Blanchet L, Spallicci A, Whiting B (eds) Mass and Motion in General Relativity. Fundamental Theories of Physics, vol 162. Springer, Dordrecht, pp 167–210. https://doi.org/10.1007/978-90-481-3015-3_6. arXiv:0910.2857 [gr-qc]

Schäfer G, Jaranowski P (2024) Hamiltonian formulation of general relativity and post-Newtonian dynamics of compact binaries. Living Rev Relativ 27:2. https://doi.org/10.1007/s41114-024-00048-7. arXiv:1805.07240 [gr-qc]

Scheel MA, Giesler M, Hemberger DA, Lovelace G, Kuper K, Boyle M, Szilágyi B, Kidder LE (2015) Improved methods for simulating nearly extremal binary black holes. Class Quantum Grav 32 (10):105009. https://doi.org/10.1088/0264-9381/32/10/105009. arXiv:1412.1803 [gr-qc]

Schmidt P, Hannam M, Husa S, Ajith P (2011) Tracking the precession of compact binaries from their gravitational-wave signal. Phys Rev D 84:024046. https://doi.org/10.1103/PhysRevD.84.024046. arXiv:1012.2879 [gr-qc]

Schmidt P, Harry IW, Pfeiffer HP (2017) Numerical Relativity Injection Infrastructure. arXiv e-prints arXiv:1703.01076 [gr-qc]

Schmidt S, Breschi M, Gamba R, Pagano G, Rettegno P, Riemenschneider G, Bernuzzi S, Nagar A, Del Pozzo W (2021) Machine learning gravitational waves from binary black hole mergers. Phys Rev D 103(4):043020. https://doi.org/10.1103/PhysRevD.103.043020. arXiv:2011.01958 [gr-qc]

Schmidt W (2002) Celestial mechanics in Kerr space-time. Class Quantum Grav 19:2743. https://doi.org/10.1088/0264-9381/19/10/314. arXiv:gr-qc/0202090

Schnetter E, Hawley SH, Hawke I (2004) Evolutions in 3-D numerical relativity using fixed mesh refinement. Class Quantum Grav 21:1465–1488. https://doi.org/10.1088/0264-9381/21/6/014. arXiv:gr-qc/0310042

Schramm M, Silverman JD (2013) The black hole - bulge mass relation of Active Galactic Nuclei in the extended chandra deep field - South Survey. Astrophys J 767:13. https://doi.org/10.1088/0004-637X/767/1/13. arXiv:1212.2999 [astro-ph.CO]

Schutz B (2017) Discussion on EMRI/IMRI using numerical relativity, https://wasabi.physics.unc.edu/event/6/contributions/47/attachments/19/19/Schutz.NR_IMRI.pdf, 20th Capra Meeting

Schutz BF, Will CM (1985) Black hole normal modes: a semianalytical approach. Astrophys J Lett 291: L33–L36. https://doi.org/10.1086/184453

Seidel E, Iyer S (1990) Black hole normal modes: a WKB approach. IV. Kerr black holes. Phys Rev D 41:374–382. https://doi.org/10.1103/PhysRevD.41.374

Seidel E, Suen WM (1991) Oscillating soliton stars. Phys Rev Lett 66:1659–1662. https://doi.org/10.1103/PhysRevLett.66.1659

Sekiguchi Y, Kiuchi K, Kyutoku K, Shibata M (2012) Current status of numerical-relativity simulations in Kyoto. PTEP 2012:01A304. https://doi.org/10.1093/ptep/pts011. arXiv:1206.5927 [astro-ph.HE]

Seljak U, Slosar A, McDonald P (2006) Cosmological parameters from combining the Lyman-alpha forest with CMB, galaxy clustering and SN constraints. JCAP 10:014. https://doi.org/10.1088/1475-7516/2006/10/014. arXiv:astro-ph/0604335

Semerák O, Suková P (2015) On geodesic dynamics in deformed black-hole fields. In: Puetzfeld D, Lämmerzahl C, Schutz B (eds) Equations of Motion in Relativistic Gravity. Fundamental Theories of Physics, vol 179. Springer, Cham, pp 561–586. https://doi.org/10.1007/978-3-319-18335-0_17. arXiv:1509.08536 [gr-qc]

Semerák O, Čížek P (2020) Rotating Disc around a Schwarzschild Black Hole. Universe 6(2):27. https://doi.org/10.3390/universe6020027

Sen A (1998) SO(32) spinors of type I and other solitons on brane-antibrane pair. JHEP 09:023. https://doi.org/10.1088/1126-6708/1998/09/023. arXiv:hep-th/9808141

Sen A (1998) Stable nonBPS bound states of BPS D-branes. JHEP 08:010. https://doi.org/10.1088/1126-6708/1998/08/010. arXiv:hep-th/9805019

Sennett N, Marsat S, Buonanno A (2016) Gravitational waveforms in scalar-tensor gravity at 2PN relative order. Phys Rev D 94(8):084003. https://doi.org/10.1103/PhysRevD.94.084003. arXiv:1607.01420 [gr-qc]

Sennett N, Brito R, Buonanno A, Gorbenko V, Senatore L (2020) Gravitational-wave constraints on an effective field-theory extension of general relativity. Phys Rev D 102(4):044056. https://doi.org/10.1103/PhysRevD.102.044056. arXiv:1912.09917 [gr-qc]

Sesana A (2016) Prospects for multiband gravitational-wave astronomy after GW150914. Phys Rev Lett 116(23):231102. https://doi.org/10.1103/PhysRevLett.116.231102. arXiv:1602.06951 [gr-qc]

Sesana A, Khan FM (2015) Scattering experiments meet N-body - I. A practical recipe for the evolution of massive black hole binaries in stellar environments. Mon Not R Astron Soc 454(1):L66–L70. https://doi.org/10.1093/mnrasl/slv131. arXiv:1505.02062 [astro-ph.GA]

Sesana A, Haardt F, Madau P, Volonteri M (2004) Low-frequency gravitational radiation from coalescing massive black hole binaries in hierarchical cosmologies. Astrophys J 611:623–632. https://doi.org/10.1086/422185. arXiv:astro-ph/0401543

Sesana A, Haardt F, Madau P, Volonteri M (2005) The gravitational wave signal from massive black hole binaries and its contribution to the LISA data stream. Astrophys J 623:23–30. https://doi.org/10.1086/428492. arXiv:astro-ph/0409255

Sesana A, Volonteri M, Haardt F (2007) The imprint of massive black hole formation models on the LISA data stream. Mon Not R Astron Soc 377:1711–1716. https://doi.org/10.1111/j.1365-2966.2007.11734.x. arXiv:astro-ph/0701556

Sesana A, Gair J, Berti E, Volonteri M (2011) Reconstructing the massive black hole cosmic history through gravitational waves. Phys Rev D 83:044036. https://doi.org/10.1103/PhysRevD.83.044036. arXiv:1011.5893 [astro-ph.CO]

Sesana A, Barausse E, Dotti M, Rossi EM (2014) Linking the spin evolution of massive black holes to galaxy kinematics. Astrophys J 794:104. https://doi.org/10.1088/0004-637X/794/2/104. arXiv:1402.7088 [astro-ph.CO]

Seto N (2008) Detecting planets around compact binaries with gravitational wave detectors in space. Astrophys J Lett 677:L55–L58. https://doi.org/10.1086/587785. arXiv:0802.3411 [astro-ph]

Setyawati Y, Pürrer M, Ohme F (2020) Regression methods in waveform modeling: a comparative study. Class Quantum Grav 37(7):075012. https://doi.org/10.1088/1361-6382/ab693b. arXiv:1909.10986 [astro-ph.IM]

Shah AG (2014) Gravitational-wave flux for a particle orbiting a Kerr black hole to 20th post-Newtonian order: a numerical approach. Phys Rev D 90(4):044025. https://doi.org/10.1103/PhysRevD.90.044025. arXiv:1403.2697 [gr-qc]

Shah AG, Pound A (2015) Linear-in-mass-ratio contribution to spin precession and tidal invariants in Schwarzschild spacetime at very high post-Newtonian order. Phys Rev D 91(12):124022. https://doi.org/10.1103/PhysRevD.91.124022. arXiv:1503.02414 [gr-qc]

Shah AG, Keidl TS, Friedman JL, Kim DH, Price LR (2011) Conservative, gravitational self-force for a particle in circular orbit around a Schwarzschild black hole in a Radiation Gauge. Phys Rev D 83:064018. https://doi.org/10.1103/PhysRevD.83.064018. arXiv:1009.4876 [gr-qc]

Shah AG, Friedman JL, Keidl TS (2012) EMRI corrections to the angular velocity and redshift factor of a mass in circular orbit about a Kerr black hole. Phys Rev D 86:084059. https://doi.org/10.1103/PhysRevD.86.084059. arXiv:1207.5595 [gr-qc]

Shah AG, Friedman JL, Whiting BF (2014) Finding high-order analytic post-Newtonian parameters from a high-precision numerical self-force calculation. Phys Rev D 89(6):064042. https://doi.org/10.1103/PhysRevD.89.064042. arXiv:1312.1952 [gr-qc]

Shah S, van der Sluys M, Nelemans G (2012) Using electromagnetic observations to aid gravitational-wave parameter estimation of compact binaries observed with LISA. Astron Astrophys 544:A153. https://doi.org/10.1051/0004-6361/201219309. arXiv:1207.6770 [astro-ph.IM]

Shankar S, Mösta P, Brandt SR, Haas R, Schnetter E, de Graaf Y (2023) GRaM-X: a new GPU-accelerated dynamical spacetime GRMHD code for Exascale computing with the Einstein Toolkit. Class Quantum Grav 40(20):205009. https://doi.org/10.1088/1361-6382/acf2d9. arXiv:2210.17509 [astro-ph.IM]

Shapiro Key J, Cornish NJ (2009) Characterizing the gravitational wave signature from cosmic string cusps. Phys Rev D 79:043014. https://doi.org/10.1103/PhysRevD.79.043014. arXiv:0812.1590 [gr-qc]

Sharma RS, Brooks AM, Somerville RS, Tremmel M, Bellovary J, Wright AC, Quinn TR (2020) Black hole growth and feedback in isolated ROMULUS25 dwarf galaxies. Astrophys J 897(1):103. https://doi.org/10.3847/1538-4357/ab960e. arXiv:1912.06646 [astro-ph.GA]

Shellard E (1987) Cosmic string interactions. Nucl Phys B 283:624–656. https://doi.org/10.1016/0550-3213(87)90290-2

Shen P, Han WB, Zhang C, Yang SC, Zhong XY, Jiang Y, Cui Q (2023) Influence of mass-ratio corrections in extreme-mass-ratio inspirals for testing general relativity. Phys Rev D 108(6):064015. https://doi.org/10.1103/PhysRevD.108.064015. arXiv:2303.13749 [gr-qc]

Shibata M (2016) Numerical Relativity, 100 Years of General Relativity, vol 1. World Scientific. https://doi.org/10.1142/9692

Shibata M, Nakamura T (1995) Evolution of three-dimensional gravitational waves: Harmonic slicing case. Phys Rev D 52:5428–5444. https://doi.org/10.1103/PhysRevD.52.5428

Shibata M, Sekiguchi Y (2005) Magnetohydrodynamics in full general relativity: formulation and tests. Phys Rev D 72:044014. https://doi.org/10.1103/PhysRevD.72.044014. arXiv:astro-ph/0507383

Shibata M, Traykova D (2023) Properties of scalar wave emission in a scalar-tensor theory with kinetic screening. Phys Rev D 107(4):044068. https://doi.org/10.1103/PhysRevD.107.044068. arXiv:2210.12139 [gr-qc]

Shibata M, Yoshino H (2010) Bar-mode instability of rapidly spinning black hole in higher dimensions: Numerical simulation in general relativity. Phys Rev D 81:104035. https://doi.org/10.1103/PhysRevD.81.104035. arXiv:1004.4970 [gr-qc]

Shibata M, Liu YT, Shapiro SL, Stephens BC (2006) Magnetorotational collapse of massive stellar cores to neutron stars: simulations in full general relativity. Phys Rev D 74:104026. https://doi.org/10.1103/PhysRevD.74.104026. arXiv:astro-ph/0610840

Shibata M, Sekiguchi Y, Uchida H, Umeda H (2016) Gravitational waves from supermassive stars collapsing to a supermassive black hole. Phys Rev D 94(2):021501. https://doi.org/10.1103/PhysRevD.94.021501. arXiv:1606.07147 [astro-ph.HE]

Shibata M, Kiuchi K, Sekiguchi Y (2017) General relativistic viscous hydrodynamics of differentially rotating neutron stars. Phys Rev D 95(8):083005. https://doi.org/10.1103/PhysRevD.95.083005. arXiv:1703.10303 [astro-ph.HE]

Shibata M, Fujibayashi S, Sekiguchi Y (2021) Long-term evolution of neutron-star merger remnants in general relativistic resistive magnetohydrodynamics with a mean-field dynamo term. Phys Rev D 104(6):063026. https://doi.org/10.1103/PhysRevD.104.063026. arXiv:2109.08732 [astro-ph.HE]

Shiralilou B, Hinderer T, Nissanke S, Ortiz N, Witek H (2021) Nonlinear curvature effects in gravitational waves from inspiralling black hole binaries. Phys Rev D 103(12):L121503. https://doi.org/10.1103/PhysRevD.103.L121503. arXiv:2012.09162 [gr-qc]

Shiralilou B, Hinderer T, Nissanke SM, Ortiz N, Witek H (2022) Post-Newtonian gravitational and scalar waves in scalar-Gauss-Bonnet gravity. Class Quantum Grav 39(3):035002. https://doi.org/10.1088/1361-6382/ac4196. arXiv:2105.13972 [gr-qc]

Shlapentokh-Rothman Y (2014) Exponentially growing finite energy solutions for the Klein-Gordon equation on sub-extremal Kerr spacetimes. Commun Math Phys 329:859–891. https://doi.org/10.1007/s00220-014-2033-x. arXiv:1302.3448 [gr-qc]

Siemens X, Olum KD (2001) Gravitational radiation and the small-scale structure of cosmic strings. Nucl Phys B 611:125–145. [Erratum: Nucl. Phys. B 645, 367-367 (2002)]. https://doi.org/10.1016/S0550-3213(01)00353-4. arXiv:gr-qc/0104085

Siemens X, Olum KD (2003) Cosmic string cusps with small scale structure: their forms and gravitational wave forms. Phys Rev D 68:085017. https://doi.org/10.1103/PhysRevD.68.085017. arXiv:gr-qc/0307113

Siemens X, Olum KD, Vilenkin A (2002) On the size of the smallest scales in cosmic string networks. Phys Rev D 66:043501. https://doi.org/10.1103/PhysRevD.66.043501. arXiv:gr-qc/0203006

Siemens X, Creighton J, Maor I, Ray Majumder S, Cannon K, Read J (2006) Gravitational wave bursts from cosmic (super)strings: quantitative analysis and constraints. Phys Rev D 73:105001. https://doi.org/10.1103/PhysRevD.73.105001. arXiv:gr-qc/0603115

Siemens X, Mandic V, Creighton J (2007) Gravitational wave stochastic background from cosmic (super) strings. Phys Rev Lett 98:111101. https://doi.org/10.1103/PhysRevLett.98.111101. arXiv:astro-ph/0610920

Siemonsen N (2024) Nonlinear treatment of a black hole mimicker ringdown. Phys Rev Lett 133(3):031401. https://doi.org/10.1103/PhysRevLett.133.031401. arXiv:2404.14536 [gr-qc]

Siemonsen N, East WE (2020) Gravitational wave signatures of ultralight vector bosons from black hole superradiance. Phys Rev D 101(2):024019. https://doi.org/10.1103/PhysRevD.101.024019. arXiv:1910.09476 [gr-qc]
Siemonsen N, East WE (2023) Binary boson stars: merger dynamics and formation of rotating remnant stars. Phys Rev D 107(12):124018. https://doi.org/10.1103/PhysRevD.107.124018. arXiv:2302.06627 [gr-qc]
Siemonsen N, Vines J (2020) Test black holes, scattering amplitudes and perturbations of Kerr spacetime. Phys Rev D 101(6):064066. https://doi.org/10.1103/PhysRevD.101.064066. arXiv:1909.07361 [gr-qc]
Siemonsen N, Steinhoff J, Vines J (2018) Gravitational waves from spinning binary black holes at the leading post-Newtonian orders at all orders in spin. Phys Rev D 97(12):124046. https://doi.org/10.1103/PhysRevD.97.124046. arXiv:1712.08603 [gr-qc]
Siemonsen N, May T, East WE (2023) Modeling the black hole superradiance gravitational waveform. Phys Rev D 107(10):104003. https://doi.org/10.1103/PhysRevD.107.104003. arXiv:2211.03845 [gr-qc]
Silva HO, Glampedakis K (2020) Eikonal quasinormal modes of black holes beyond general relativity. II. Generalized scalar-tensor perturbations. Phys Rev D 101(4):044051. https://doi.org/10.1103/PhysRevD.101.044051. arXiv:1912.09286 [gr-qc]
Silva HO, Sakstein J, Gualtieri L, Sotiriou TP, Berti E (2018) Spontaneous scalarization of black holes and compact stars from a Gauss-Bonnet coupling. Phys Rev Lett 120(13):131104. https://doi.org/10.1103/PhysRevLett.120.131104. arXiv:1711.02080 [gr-qc]
Silva HO, Witek H, Elley M, Yunes N (2021) Dynamical descalarization in binary black hole mergers. Phys Rev Lett 127(3):031101. https://doi.org/10.1103/PhysRevLett.127.031101. arXiv:2012.10436 [gr-qc]
Silva HO, Ghosh A, Buonanno A (2023) Black-hole ringdown as a probe of higher-curvature gravity theories. Phys Rev D 107(4):044030. https://doi.org/10.1103/PhysRevD.107.044030. arXiv:2205.05132 [gr-qc]
Skoupý V, Lukes-Gerakopoulos G (2021) Spinning test body orbiting around a Kerr black hole: eccentric equatorial orbits and their asymptotic gravitational-wave fluxes. Phys Rev D 103(10):104045. https://doi.org/10.1103/PhysRevD.103.104045. arXiv:2102.04819 [gr-qc]
Skoupý V, Lukes-Gerakopoulos G (2022) Adiabatic equatorial inspirals of a spinning body into a Kerr black hole. Phys Rev D 105(8):084033. https://doi.org/10.1103/PhysRevD.105.084033. arXiv:2201.07044 [gr-qc]
Skoupy V, Lukes-Gerakopoulos G, Drummond LV, Hughes SA (2023) Asymptotic gravitational-wave fluxes from a spinning test body on generic orbits around a Kerr black hole. Phys Rev D 108(4):044041. https://doi.org/10.1103/PhysRevD.108.044041. arXiv:2303.16798 [gr-qc]
Smarr L, Cadez A, DeWitt BS, Eppley K (1976) Collision of two black holes: theoretical framework. Phys Rev D 14:2443–2452. https://doi.org/10.1103/PhysRevD.14.2443
Smith A, Bromm V, Loeb A (2017) The first supermassive black holes. Astron Geophys 58(3):3.22-3.26. https://doi.org/10.1093/astrogeo/atx099. arXiv:1703.03083 [astro-ph.GA]
Smoot GF et al (1992) Structure in the COBE differential microwave radiometer first year maps. Astrophys J Lett 396:L1–L5. https://doi.org/10.1086/186504
Sopuerta CF, Yunes N (2009) Extreme and intermediate-mass ratio inspirals in dynamical chern-simons modified gravity. Phys Rev D 80:064006. https://doi.org/10.1103/PhysRevD.80.064006. arXiv:0904.4501 [gr-qc]
Sotiriou TP, Faraoni V (2012) Black holes in scalar-tensor gravity. Phys Rev Lett 108:081103. https://doi.org/10.1103/PhysRevLett.108.081103. arXiv:1109.6324 [gr-qc]
Sousa L, Avelino PP (2013) Stochastic gravitational wave background generated by cosmic string networks: velocity-dependent one-scale model versus scale-invariant evolution. Phys Rev D 88(2):023516. https://doi.org/10.1103/PhysRevD.88.023516. arXiv:1304.2445 [astro-ph.CO]
Sousa L, Avelino PP (2014) Stochastic gravitational wave background generated by cosmic string networks: the small-loop regime. Phys Rev D 89(8):083503. https://doi.org/10.1103/PhysRevD.89.083503. arXiv:1403.2621 [astro-ph.CO]
SpEC (2024) The Spectral Einstein Code. http://www.black-holes.org/SpEC.html
Speeney N, Antonelli A, Baibhav V, Berti E (2022) Impact of relativistic corrections on the detectability of dark-matter spikes with gravitational waves. Phys Rev D 106(4):044027. https://doi.org/10.1103/PhysRevD.106.044027. arXiv:2204.12508 [gr-qc]

Spergel DN et al (2007) Wilkinson Microwave Anisotropy Probe (WMAP) three year results: implications for cosmology. Astrophys J Suppl 170:377. https://doi.org/10.1086/513700. arXiv:astro-ph/0603449
Sperhake U (2007) Binary black-hole evolutions of excision and puncture data. Phys Rev D 76:104015. https://doi.org/10.1103/PhysRevD.76.104015. arXiv:gr-qc/0606079
Sperhake U, Cardoso V, Ott CD, Schnetter E, Witek H (2011) Extreme black hole simulations: collisions of unequal mass black holes and the point particle limit. Phys Rev D 84:084038. https://doi.org/10.1103/PhysRevD.84.084038. arXiv:1105.5391 [gr-qc]
Speri L, Antonelli A, Sberna L, Babak S, Barausse E, Gair JR, Katz ML (2023) Probing accretion physics with gravitational waves. Phys Rev X 13(2):021035. https://doi.org/10.1103/PhysRevX.13.021035. arXiv:2207.10086 [gr-qc]
Spiers A, Pound A, Moxon J (2023) Second-order Teukolsky formalism in Kerr spacetime: formulation and nonlinear source. Phys Rev D 108(6):064002. https://doi.org/10.1103/PhysRevD.108.064002. arXiv:2305.19332 [gr-qc]
Spiers A, Maselli A, Sotiriou TP (2024) Measuring scalar charge with compact binaries: high accuracy modeling with self-force. Phys Rev D 109(6):064022. https://doi.org/10.1103/PhysRevD.109.064022. arXiv:2310.02315 [gr-qc]
Spiers A, Pound A, Wardell B (2024) Second-order perturbations of the Schwarzschild spacetime: practical, covariant, and gauge-invariant formalisms. Phys Rev D 110(6):064030. https://doi.org/10.1103/PhysRevD.110.064030. arXiv:2306.17847 [gr-qc]
Spritz Code (2024) The Spritz Code. https://ze2024.org/record/4350072
Srednicki M, Theisen S (1987) Nongravitational decay of cosmic strings. Phys Lett B 189:397. https://doi.org/10.1016/0370-2693(87)90648-4
Starobinsky AA (1973) Amplification of waves reflected from a rotating black hole. Sov Phys JETP 37 (1):28–32
Stein LC (2014) Rapidly rotating black holes in dynamical Chern-Simons gravity: decoupling limit solutions and breakdown. Phys Rev D 90(4):044061. https://doi.org/10.1103/PhysRevD.90.044061. arXiv:1407.2350 [gr-qc]
Stein LC (2019) qnm: A Python package for calculating Kerr quasinormal modes, separation constants, and spherical-spheroidal mixing coefficients. J Open Source Softw 4(42):1683. https://doi.org/10.21105/joss.01683. arXiv:1908.10377 [gr-qc]
Steinhoff J, Puetzfeld D (2012) Influence of internal structure on the motion of test bodies in extreme mass ratio situations. Phys Rev D 86:044033. https://doi.org/10.1103/PhysRevD.86.044033. arXiv:1205.3926 [gr-qc]
Steinhoff J, Schäfer G (2009) Canonical formulation of self-gravitating spinning-object systems. EPL 87 (5):50004. https://doi.org/10.1209/0295-5075/87/50004. arXiv:0907.1967 [gr-qc]
Steinhoff J, Hergt S, Schäfer G (2008) On the next-to-leading order gravitational spin(1)-spin(2) dynamics. Phys Rev D 77:081501. https://doi.org/10.1103/PhysRevD.77.081501. arXiv:0712.1716 [gr-qc]
Steinhoff J, Hergt S, Schäfer G (2008) Spin-squared Hamiltonian of next-to-leading order gravitational interaction. Phys Rev D 78:101503. https://doi.org/10.1103/PhysRevD.78.101503. arXiv:0809.2200 [gr-qc]
Steinhoff J, Schäfer G, Hergt S (2008) ADM canonical formalism for gravitating spinning objects. Phys Rev D 77:104018. https://doi.org/10.1103/PhysRevD.77.104018. arXiv:0805.3136 [gr-qc]
Steinhoff J, Hinderer T, Buonanno A, Taracchini A (2016) Dynamical tides in general relativity: effective action and effective-one-body hamiltonian. Phys Rev D 94(10):104028. https://doi.org/10.1103/PhysRevD.94.104028. arXiv:1608.01907 [gr-qc]
Steinhoff J, Hinderer T, Dietrich T, Foucart F (2021) Spin effects on neutron star fundamental-mode dynamical tides: phenomenology and comparison to numerical simulations. Phys Rev Res 3 (3):033129. https://doi.org/10.1103/PhysRevResearch.3.033129. arXiv:2103.06100 [gr-qc]
Stevenson S, Berry C, Mandel I (2017) Hierarchical analysis of gravitational-wave measurements of binary black hole spin-orbit misalignments. Mon Not R Astron Soc 471(3):2801–2811. https://doi.org/10.1093/mnras/stx1764. arXiv:1703.06873 [astro-ph.HE]
Stone JM, Tomida K, White CJ, Felker KG (2020) The Athena++ adaptive mesh refinement framework: design and magnetohydrodynamic solvers. ApJS 249(1):4. https://doi.org/10.3847/1538-4365/ab929b. arXiv:2005.06651 [astro-ph.IM]
Stone NC, Küpper A, Ostriker JP (2017) Formation of massive black holes in galactic nuclei: runaway tidal encounters. Mon Not R Astron Soc 467(4):4180–4199. https://doi.org/10.1093/mnras/stx097. arXiv:1606.01909 [astro-ph.GA]

Stott MJ (2020) Ultralight Bosonic Field Mass Bounds from Astrophysical Black Hole Spin. arXiv e-prints arXiv:2009.07206 [hep-ph]
Stott MJ, Elghozi T, Sakellariadou M (2017) Gravitational wave bursts from cosmic string cusps and pseudocusps. Phys Rev D 96(2):023533. https://doi.org/10.1103/PhysRevD.96.023533. arXiv:1612.07599 [hep-th]
Stroeer A, Vecchio A (2006) The LISA verification binaries. Class Quantum Grav 23:S809–S818. https://doi.org/10.1088/0264-9381/23/19/S19. arXiv:astro-ph/0605227
Strub SH, Ferraioli L, Schmelzbach C, Stähler SC, Giardini D (2024) Global analysis of LISA data with Galactic binaries and massive black hole binaries. Phys Rev D 110(2):024005. https://doi.org/10.1103/PhysRevD.110.024005. arXiv:2403.15318 [gr-qc]
Suková P, Zajaček M, Witzany V, Karas V (2021) Stellar transits across a magnetized accretion torus as a mechanism for plasmoid ejection. Astrophys J 917(1):43. https://doi.org/10.3847/1538-4357/ac05c6. arXiv:2102.08135 [astro-ph.HE]
Sullivan A, Yunes N, Sotiriou TP (2020) Numerical black hole solutions in modified gravity theories: spherical symmetry case. Phys Rev D 101(4):044024. https://doi.org/10.1103/PhysRevD.101.044024. arXiv:1903.02624 [gr-qc]
Sullivan A, Yunes N, Sotiriou TP (2021) Numerical black hole solutions in modified gravity theories: axial symmetry case. Phys Rev D 103(12):124058. https://doi.org/10.1103/PhysRevD.103.124058. arXiv:2009.10614 [gr-qc]
Sun L, Paschalidis V, Ruiz M, Shapiro SL (2017) Magnetorotational collapse of supermassive stars: black hole formation, gravitational waves and jets. Phys Rev D 96(4):043006. https://doi.org/10.1103/PhysRevD.96.043006. arXiv:1704.04502 [astro-ph.HE]
Sun L, Ruiz M, Shapiro SL (2018) Simulating the magnetorotational collapse of supermassive stars: incorporating gas pressure perturbations and different rotation profiles. Phys Rev D 98(10):103008. https://doi.org/10.1103/PhysRevD.98.103008. arXiv:1807.07970 [astro-ph.HE]
Sun L, Ruiz M, Shapiro SL, Tsokaros A (2022) Jet launching from binary neutron star mergers: incorporating neutrino transport and magnetic fields. Phys Rev D 105(10):104028. https://doi.org/10.1103/PhysRevD.105.104028. arXiv:2202.12901 [astro-ph.HE]
Sundararajan PA (2008) The transition from adiabatic inspiral to geodesic plunge for a compact object around a massive Kerr black hole: generic orbits. Phys Rev D 77:124050. https://doi.org/10.1103/PhysRevD.77.124050. arXiv:0803.4482 [gr-qc]
Sundararajan PA, Khanna G, Hughes SA (2007) Towards adiabatic waveforms for inspiral into Kerr black holes. I. A new model of the source for the time domain perturbation equation. Phys Rev D 76:104005. https://doi.org/10.1103/PhysRevD.76.104005. arXiv:gr-qc/0703028
Sundararajan PA, Khanna G, Hughes SA, Drasco S (2008) Towards adiabatic waveforms for inspiral into Kerr black holes: II. Dynamical sources and generic orbits. Phys Rev D 78:024022. https://doi.org/10.1103/PhysRevD.78.024022. arXiv:0803.0317 [gr-qc]
Suresh N, Chernoff DF (2024) Modeling the beam of gravitational radiation from a cosmic string loop. Phys Rev D 109(12):123540. https://doi.org/10.1103/PhysRevD.109.123540. arXiv:2310.00825 [astro-ph.CO]
Suzuki S, Maeda K (1997) Chaos in Schwarzschild space-time: the motion of a spinning particle. Phys Rev D 55:4848–4859. https://doi.org/10.1103/PhysRevD.55.4848. arXiv:gr-qc/9604020
Suzuki S, Maeda K (2000) Signature of chaos in gravitational waves from a spinning particle. Phys Rev D 61:024005. https://doi.org/10.1103/PhysRevD.61.024005. arXiv:gr-qc/9910064
SXS catalog (2024) SXS catalog. http://www.black-holes.org/waveforms
Szilágyi B (2014) Key elements of robustness in binary black hole evolutions using spectral methods. Int J Mod Phys D 23(7):1430014. https://doi.org/10.1142/S0218271814300146. arXiv:1405.3693 [gr-qc]
Szilagyi B, Lindblom L, Scheel MA (2009) Simulations of binary black hole mergers using spectral methods. Phys Rev D 80:124010. https://doi.org/10.1103/PhysRevD.80.124010. arXiv:0909.3557 [gr-qc]
Szilágyi B, Blackman J, Buonanno A, Taracchini A, Pfeiffer HP, Scheel MA, Chu T, Kidder LE, Pan Y (2015) Approaching the post-newtonian regime with numerical relativity: a compact-object binary simulation spanning 350 gravitational-wave cycles. Phys Rev Lett 115(3):031102. https://doi.org/10.1103/PhysRevLett.115.031102. arXiv:1502.04953 [gr-qc]
Tagawa H, Haiman Z, Kocsis B (2020) Formation and evolution of compact object binaries in AGN disks. Astrophys J 898(1):25. https://doi.org/10.3847/1538-4357/ab9b8c. arXiv:1912.08218 [astro-ph.GA]

Tagoshi H (1995) PostNewtonian expansion of gravitational waves from a particle in slightly eccentric orbit around a rotating black hole. Prog Theor Phys 93:307–333. [Erratum: Prog. Theor. Phys. 118, 577-579 (2007)]. https://doi.org/10.1143/PTP.118.577

Tagoshi H, Mano S, Takasugi E (1997) PostNewtonian expansion of gravitational waves from a particle in circular orbits around a rotating black hole: effects of black hole absorption. Prog Theor Phys 98:829–850. https://doi.org/10.1143/PTP.98.829. arXiv:gr-qc/9711072

Tagoshi H, Ohashi A, Owen BJ (2001) Gravitational field and equations of motion of spinning compact binaries to 2.5 postNewtonian order. Phys Rev D 63:044006. https://doi.org/10.1103/PhysRevD.63.044006. arXiv:gr-qc/0010014

Tahura S, Yagi K (2018) Parameterized Post-Einsteinian Gravitational Waveforms in Various Modified Theories of Gravity. Phys Rev D 98(8):084042. [Erratum: Phys. Rev. D 101, 109902 (2020)]. https://doi.org/10.1103/PhysRevD.98.084042. arXiv:1809.00259 [gr-qc]

Takahashi T, Tanaka T (2021) Axion clouds may survive the perturbative tidal interaction over the early inspiral phase of black hole binaries. JCAP 10:031. https://doi.org/10.1088/1475-7516/2021/10/031. arXiv:2106.08836 [gr-qc]

Takahashi T, Omiya H, Tanaka T (2022) Axion cloud evaporation during inspiral of black hole binaries: the effects of backreaction and radiation. PTEP 4:043E01. https://doi.org/10.1093/ptep/ptac044. arXiv:2112.05774 [gr-qc]

Takami K, Rezzolla L, Baiotti L (2015) Spectral properties of the post-merger gravitational-wave signal from binary neutron stars. Phys Rev D 91(6):064001. https://doi.org/10.1103/PhysRevD.91.064001. arXiv:1412.3240 [gr-qc]

Talbot C, Thrane E, Lasky PD, Lin F (2018) Gravitational-wave memory: waveforms and phenomenology. Phys Rev D 98(6):064031. https://doi.org/10.1103/PhysRevD.98.064031. arXiv:1807.00990 [astro-ph.HE]

Talbot C, Smith R, Thrane E, Poole GB (2019) Parallelized inference for gravitational-wave astronomy. Phys Rev D 100(4):043030. https://doi.org/10.1103/PhysRevD.100.043030. arXiv:1904.02863 [astro-ph.IM]

Tamanini N, Danielski C (2019) The gravitational-wave detection of exoplanets orbiting white dwarf binaries using LISA. Nature Astron 3(9):858–866. https://doi.org/10.1038/s41550-019-0807-y. arXiv:1812.04330 [astro-ph.EP]

Tamanini N, Caprini C, Barausse E, Sesana A, Klein A, Petiteau A (2016) Science with the space-based interferometer eLISA. III: probing the expansion of the Universe using gravitational wave standard sirens. JCAP 04:002. https://doi.org/10.1088/1475-7516/2016/04/002. arXiv:1601.07112 [astro-ph.CO]

Tanaka T (2006) Gravitational radiation reaction. Prog Theor Phys Suppl 163:120–145. https://doi.org/10.1143/PTPS.163.120. arXiv:gr-qc/0508114

Tanaka T, Mino Y, Sasaki M, Shibata M (1996) Gravitational waves from a spinning particle in circular orbits around a rotating black hole. Phys Rev D 54:3762–3777. https://doi.org/10.1103/PhysRevD.54.3762. arXiv:gr-qc/9602038

Tanay S, Haney M, Gopakumar A (2016) Frequency and time domain inspiral templates for comparable mass compact binaries in eccentric orbits. Phys Rev D 93(6):064031. https://doi.org/10.1103/PhysRevD.93.064031. arXiv:1602.03081 [gr-qc]

Taracchini A, Pan Y, Buonanno A, Barausse E, Boyle M, Chu T, Lovelace G, Pfeiffer HP, Scheel MA (2012) Prototype effective-one-body model for nonprecessing spinning inspiral-merger-ringdown waveforms. Phys Rev D 86:024011. https://doi.org/10.1103/PhysRevD.86.024011. arXiv:1202.0790 [gr-qc]

Taracchini A, Buonanno A, Khanna G, Hughes SA (2014) Small mass plunging into a Kerr black hole: anatomy of the inspiral-merger-ringdown waveforms. Phys Rev D 90(8):084025. https://doi.org/10.1103/PhysRevD.90.084025. arXiv:1404.1819 [gr-qc]

Taracchini A et al (2014) Effective-one-body model for black-hole binaries with generic mass ratios and spins. Phys Rev D 89(6):061502. https://doi.org/10.1103/PhysRevD.89.061502. arXiv:1311.2544 [gr-qc]

Tattersall OJ, Ferreira PG, Lagos M (2018) General theories of linear gravitational perturbations to a Schwarzschild Black Hole. Phys Rev D 97(4):044021. https://doi.org/10.1103/PhysRevD.97.044021. arXiv:1711.01992 [gr-qc]

Taveras V, Yunes N (2008) The Barbero-Immirzi parameter as a scalar field: K-Inflation from loop quantum gravity? Phys Rev D 78:064070. https://doi.org/10.1103/PhysRevD.78.064070. arXiv:0807.2652 [gr-qc]

Taylor NW, Boyle M, Reisswig C, Scheel MA, Chu T, Kidder LE, Szilágyi B (2013) Comparing gravitational waveform extrapolation to cauchy-characteristic extraction in binary black hole simulations. Phys Rev D 88(12):124010. https://doi.org/10.1103/PhysRevD.88.124010. arXiv:1309.3605 [gr-qc]

Tessmer M, Hartung J, Schafer G (2010) Motion and gravitational wave forms of eccentric compact binaries with orbital-angular-momentum-aligned spins under next-to-leading order in spin-orbit and leading order in spin(1)-spin(2) and spin-squared couplings. Class Quantum Grav 27:165005. https://doi.org/10.1088/0264-9381/27/16/165005. arXiv:1003.2735 [gr-qc]

Tessmer M, Hartung J, Schafer G (2013) Aligned spins: orbital elements, decaying orbits, and last stable circular orbit to high post-newtonian orders. Class Quantum Grav 30:015007. https://doi.org/10.1088/0264-9381/30/1/015007. arXiv:1207.6961 [gr-qc]

Testa A, Pani P (2018) Analytical template for gravitational-wave echoes: signal characterization and prospects of detection with current and future interferometers. Phys Rev D 98(4):044018. https://doi.org/10.1103/PhysRevD.98.044018. arXiv:1806.04253 [gr-qc]

Teukolsky SA (1972) Rotating black holes - separable wave equations for gravitational and electromagnetic perturbations. Phys Rev Lett 29:1114–1118. https://doi.org/10.1103/PhysRevLett.29.1114

Teukolsky SA (1973) Perturbations of a rotating black hole. 1. Fundamental equations for gravitational electromagnetic and neutrino field perturbations. Astrophys J 185:635–647. https://doi.org/10.1086/152444

Teukolsky SA, Press WH (1974) Perturbations of a rotating black hole. III - Interaction of the hole with gravitational and electromagnet IC radiation. Astrophys J 193:443–461. https://doi.org/10.1086/153180

Thaalba F, Bezares M, Franchini N, Sotiriou TP (2024) Spherical collapse in scalar-Gauss-Bonnet gravity: taming ill-posedness with a Ricci coupling. Phys Rev D 109(4):L041503. https://doi.org/10.1103/PhysRevD.109.L041503. arXiv:2306.01695 [gr-qc]

Thierfelder M, Bernuzzi S, Brügmann B (2011) Numerical relativity simulations of binary neutron stars. Phys Rev D 84:044012. https://doi.org/10.1103/PhysRevD.84.044012. arXiv:1104.4751 [gr-qc]

Thomas LM, Pratten G, Schmidt P (2022) Accelerating multimodal gravitational waveforms from precessing compact binaries with artificial neural networks. Phys Rev D 106(10):104029. https://doi.org/10.1103/PhysRevD.106.104029. arXiv:2205.14066 [gr-qc]

Thompson JE, Fauchon-Jones E, Khan S, Nitoglia E, Pannarale F, Dietrich T, Hannam M (2020) Modeling the gravitational wave signature of neutron star black hole coalescences. Phys Rev D 101(12):124059. https://doi.org/10.1103/PhysRevD.101.124059. arXiv:2002.08383 [gr-qc]

Thompson JE, Hamilton E, London L, Ghosh S, Kolitsidou P, Hoy C, Hannam M (2024) PhenomXO4a: a phenomenological gravitational-wave model for precessing black-hole binaries with higher multipoles and asymmetries. Phys Rev D 109(6):063012. https://doi.org/10.1103/PhysRevD.109.063012. arXiv:2312.10025 [gr-qc]

Thorne KS (1974) Disk accretion onto a black hole. 2. Evolution of the hole. Astrophys J 191:507–520. https://doi.org/10.1086/152991

Thorne KS (1980) Multipole expansions of gravitational radiation. Rev Mod Phys 52:299–339. https://doi.org/10.1103/RevModPhys.52.299

Thorne KS, Hartle JB (1984) Laws of motion and precession for black holes and other bodies. Phys Rev D 31:1815–1837. https://doi.org/10.1103/PhysRevD.31.1815

Tichy W (2006) Black hole evolution with the BSSN system by pseudo-spectral methods. Phys Rev D 74:084005. https://doi.org/10.1103/PhysRevD.74.084005. arXiv:gr-qc/0609087

Tichy W (2009) Long term black hole evolution with the BSSN system by pseudo-spectral methods. Phys Rev D 80:104034. https://doi.org/10.1103/PhysRevD.80.104034. arXiv:0911.0973 [gr-qc]

Tichy W (2017) The initial value problem as it relates to numerical relativity. Rept Prog Phys 80(2):026901. https://doi.org/10.1088/1361-6633/80/2/026901. arXiv:1610.03805 [gr-qc]

Tichy W, Ji L, Adhikari A, Rashti A, Pirog M (2023) The new discontinuous Galerkin methods based numerical relativity program Nmesh. Class Quantum Grav 40(2):025004. https://doi.org/10.1088/1361-6382/acaae7. arXiv:2212.06340 [gr-qc]

Tiglio M, Kidder LE, Teukolsky SA (2008) High accuracy simulations of Kerr tails: Coordinate dependence and higher multipoles. Class Quantum Grav 25:105022. https://doi.org/10.1088/0264-9381/25/10/105022. arXiv:0712.2472 [gr-qc]

Tissino J, Carullo G, Breschi M, Gamba R, Schmidt S, Bernuzzi S (2023) Combining effective-one-body accuracy and reduced-order-quadrature speed for binary neutron star merger parameter estimation

with machine learning. Phys Rev D 107(8):084037. https://doi.org/10.1103/PhysRevD.107.084037. arXiv:2210.15684 [gr-qc]
Tiwari S, Achamveedu G, Haney M, Hemantakumar P (2019) Ready-to-use Fourier domain templates for compact binaries inspiraling along moderately eccentric orbits. Phys Rev D 99(12):124008. https://doi.org/10.1103/PhysRevD.99.124008. arXiv:1905.07956 [gr-qc]
Tomaselli GM, Spieksma T, Bertone G (2023) Dynamical friction in gravitational atoms. JCAP 07:070. https://doi.org/10.1088/1475-7516/2023/07/070. arXiv:2305.15460 [gr-qc]
Tong X, Wang Y, Zhu HY (2022) Termination of superradiance from a binary companion. Phys Rev D 106 (4):043002. https://doi.org/10.1103/PhysRevD.106.043002. arXiv:2205.10527 [gr-qc]
Toomani V, Zimmerman P, Spiers A, Hollands S, Pound A, Green SR (2022) New metric reconstruction scheme for gravitational self-force calculations. Class Quantum Grav 39(1):015019. https://doi.org/10.1088/1361-6382/ac37a5. arXiv:2108.04273 [gr-qc]
Toonen S, Hamers A, Portegies Zwart S (2016) The evolution of hierarchical triple star-systems. Comput Astrophys Cosmol 3(1):6. https://doi.org/10.1186/s40668-016-0019-0. arXiv:1612.06172 [astro-ph.SR]
Toubiana A, Marsat S, Babak S, Baker J, Dal Canton T (2020) Parameter estimation of stellar-mass black hole binaries with LISA. Phys Rev D 102:124037. https://doi.org/10.1103/PhysRevD.102.124037. arXiv:2007.08544 [gr-qc]
Toubiana A, Babak S, Barausse E, Lehner L (2021) Modeling gravitational waves from exotic compact objects. Phys Rev D 103(6):064042. https://doi.org/10.1103/PhysRevD.103.064042. arXiv:2011.12122 [gr-qc]
Traykova D, Clough K, Helfer T, Berti E, Ferreira PG, Hui L (2021) Dynamical friction from scalar dark matter in the relativistic regime. Phys Rev D 104(10):103014. https://doi.org/10.1103/PhysRevD.104.103014. arXiv:2106.08280 [gr-qc]
Tremmel M, Governato F, Volonteri M, Quinn TR, Pontzen A (2018) Dancing to CHANGA: a self-consistent prediction for close SMBH pair formation time-scales following galaxy mergers. MNRAS 475(4):4967–4977. https://doi.org/10.1093/mnras/sty139. arXiv:1708.07126 [astro-ph.GA]
Trestini D, Blanchet L (2023) Gravitational-wave tails of memory. Phys Rev D 107(10):104048. https://doi.org/10.1103/PhysRevD.107.104048. arXiv:2301.09395 [gr-qc]
Trestini D, Larrouturou F, Blanchet L (2023) The quadrupole moment of compact binaries to the fourth post-Newtonian order: relating the harmonic and radiative metrics. Class Quantum Grav 40 (5):055006. https://doi.org/10.1088/1361-6382/acb5de. arXiv:2209.02719 [gr-qc]
Tsokaros A, Ruiz M, Sun L, Shapiro SL, Uryū K (2019) Dynamically stable ergostars exist: general relativistic models and simulations. Phys Rev Lett 123(23):231103. https://doi.org/10.1103/PhysRevLett.123.231103. arXiv:1907.03765 [gr-qc]
Tsokaros A, Ruiz M, Shapiro SL, Sun L, Uryū K (2020) Great impostors: extremely compact, merging binary neutron stars in the mass gap posing as binary black holes. Phys Rev Lett 124(7):071101. https://doi.org/10.1103/PhysRevLett.124.071101. arXiv:1911.06865 [astro-ph.HE]
Tulczyjew W (1959) Equations of motion of rotating bodies in general relativity theory. Acta Phys Polon 18:37–55. [Erratum: Acta Phys. Polon. 18, 534 (1959)]
Tye SHH, Wasserman I, Wyman M (2005) Scaling of multi-tension cosmic superstring networks. Phys Rev D 71:103508. [Erratum: Phys. Rev. D 71, 129906 (2005)]. https://doi.org/10.1103/PhysRevD.71.103508. arXiv:astro-ph/0503506
Uchida H, Shibata M, Yoshida T, Sekiguchi Y, Umeda H (2017) Gravitational Collapse of Rotating Supermassive Stars including Nuclear Burning Effects. Phys Rev D 96(8):083016. [Erratum: Phys. Rev. D 98, 129901 (2018)]. https://doi.org/10.1103/PhysRevD.96.083016. arXiv:1704.00433 [astro-ph.HE]
Ullio P, Zhao H, Kamionkowski M (2001) A Dark matter spike at the galactic center? Phys Rev D 64:043504. https://doi.org/10.1103/PhysRevD.64.043504. arXiv:astro-ph/0101481
Upton SD, Pound A (2021) Second-order gravitational self-force in a highly regular gauge. Phys Rev D 103(12):124016. https://doi.org/10.1103/PhysRevD.103.124016. arXiv:2101.11409 [gr-qc]
Urbano A, Veermäe H (2019) On gravitational echoes from ultracompact exotic stars. JCAP 04:011. https://doi.org/10.1088/1475-7516/2019/04/011. arXiv:1810.07137 [gr-qc]
Vachaspati T (1987) Gravity of cosmic loops. Phys Rev D 35:1767–1775. https://doi.org/10.1103/PhysRevD.35.1767
Vachaspati T (2010) Cosmic rays from cosmic strings with condensates. Phys Rev D 81:043531. https://doi.org/10.1103/PhysRevD.81.043531. arXiv:0911.2655 [astro-ph.CO]

Vachaspati T, Vilenkin A (1985) Gravitational radiation from cosmic strings. Phys Rev D 31:3052. https://doi.org/10.1103/PhysRevD.31.3052
Vaglio M, Pacilio C, Maselli A, Pani P (2022) Multipolar structure of rotating boson stars. Phys Rev D 105 (12):124020. https://doi.org/10.1103/PhysRevD.105.124020. arXiv:2203.07442 [gr-qc]
Vaglio M, Pacilio C, Maselli A, Pani P (2023) Bayesian parameter estimation on boson-star binary signals with a coherent inspiral template and spin-dependent quadrupolar corrections. Phys Rev D 108 (2):023021. https://doi.org/10.1103/PhysRevD.108.023021. arXiv:2302.13954 [gr-qc]
Valiante R, Schneider R, Volonteri M, Omukai K (2016) From the first stars to the first black holes. MNRAS 457(3):3356–3371. https://doi.org/10.1093/mnras/stw225. arXiv:1601.07915 [astro-ph.GA]
Vallisneri M (2009) A LISA data-analysis primer. Class Quantum Grav 26:094024. https://doi.org/10.1088/0264-9381/26/9/094024. arXiv:0812.0751 [gr-qc]
Vallisneri M, Yunes N (2013) Stealth bias in gravitational-wave parameter estimation. Phys Rev D 87 (10):102002. https://doi.org/10.1103/PhysRevD.87.102002. arXiv:1301.2627 [gr-qc]
Van De Meent M, Warburton N (2018) Fast self-forced inspirals. Class Quantum Grav 35(14):144003. https://doi.org/10.1088/1361-6382/aac8ce. arXiv:1802.05281 [gr-qc]
Vanderbauwhede W, Benkrid K (2013) High-performance computing using FPGAs. Springer, New York. https://doi.org/10.1007/978-1-4614-1791-0
Varma V, Field SE, Scheel MA, Blackman J, Gerosa D, Stein LC, Kidder LE, Pfeiffer HP (2019) Surrogate models for precessing binary black hole simulations with unequal masses. Phys Rev Research 1:033015. https://doi.org/10.1103/PhysRevResearch.1.033015. arXiv:1905.09300 [gr-qc]
Varma V, Field SE, Scheel MA, Blackman J, Kidder LE, Pfeiffer HP (2019) Surrogate model of hybridized numerical relativity binary black hole waveforms. Phys Rev D 99(6):064045. https://doi.org/10.1103/PhysRevD.99.064045. arXiv:1812.07865 [gr-qc]
Varma V, Gerosa D, Stein LC, Hébert F, Zhang H (2019) High-accuracy mass, spin, and recoil predictions of generic black-hole merger remnants. Phys Rev Lett 122(1):011101. https://doi.org/10.1103/PhysRevLett.122.011101. arXiv:1809.09125 [gr-qc]
Vasiliev E, Antonini F, Merritt D (2015) The final-parsec problem in the collisionless limit. Astrophys J 810(1):49. https://doi.org/10.1088/0004-637X/810/1/49. arXiv:1505.05480 [astro-ph.GA]
Vazquez-Aceves V, Lin Y, Torres-Orjuela A (2023) Sgr A* spin and mass estimates through the detection of an extremely large mass-ratio inspiral. Astrophys J 952(2):139. https://doi.org/10.3847/1538-4357/acde51. arXiv:2206.14399 [astro-ph.HE]
Vega I, Detweiler SL (2008) Regularization of fields for self-force problems in curved spacetime: foundations and a time-domain application. Phys Rev D 77:084008. https://doi.org/10.1103/PhysRevD.77.084008. arXiv:0712.4405 [gr-qc]
Vicente R, Cardoso V (2022) Dynamical friction of black holes in ultralight dark matter. Phys Rev D 105 (8):083008. https://doi.org/10.1103/PhysRevD.105.083008. arXiv:2201.08854 [gr-qc]
Vieira JPP, Martins CJAP, Shellard EPS (2016) Models for small-scale structure on cosmic strings. II. Scaling and its stability. Phys Rev D 94(9):096005. [Erratum: Phys.Rev.D 94, 099907 (2016)]. https://doi.org/10.1103/PhysRevD.94.096005. arXiv:1611.06103 [astro-ph.CO]
Viganò D, Aguilera-Miret R, Carrasco F, Miñano B, Palenzuela C (2020) General relativistic MHD large eddy simulations with gradient subgrid-scale model. Phys Rev D 101(12):123019. https://doi.org/10.1103/PhysRevD.101.123019. arXiv:2004.00870 [gr-qc]
Vigeland S, Yunes N, Stein L (2011) Bumpy black holes in alternate theories of gravity. Phys Rev D 83:104027. https://doi.org/10.1103/PhysRevD.83.104027. arXiv:1102.3706 [gr-qc]
Vigna-Gómez A et al (2018) On the formation history of Galactic double neutron stars. Mon Not R Astron Soc 481(3):4009–4029. https://doi.org/10.1093/mnras/sty2463. arXiv:1805.07974 [astro-ph.SR]
Vilenkin A (1981) Gravitational field of vacuum domain walls and strings. Phys Rev D 23:852–857. https://doi.org/10.1103/PhysRevD.23.852
Vilenkin A (1981) Gravitational radiation from cosmic strings. Phys Lett B 107:47–50. https://doi.org/10.1016/0370-2693(81)91144-8
Vilenkin A (1984) Cosmic strings as gravitational lenses. Astrophys J Lett 282:L51–L53. https://doi.org/10.1086/184303
Vilenkin A, Shellard E (2000) Cosmic strings and other topological defects. Cambridge University Press
Vinciguerra S, Veitch J, Mandel I (2017) Accelerating gravitational wave parameter estimation with multi-band template interpolation. Class Quantum Grav 34(11):115006. https://doi.org/10.1088/1361-6382/aa6d44. arXiv:1703.02062 [gr-qc]

Vines J (2018) Scattering of two spinning black holes in post-Minkowskian gravity, to all orders in spin, and effective-one-body mappings. Class Quantum Grav 35(8):084002. https://doi.org/10.1088/1361-6382/aaa3a8. arXiv:1709.06016 [gr-qc]
Vines J, Steinhoff J (2018) Spin-multipole effects in binary black holes and the test-body limit. Phys Rev D 97(6):064010. https://doi.org/10.1103/PhysRevD.97.064010. arXiv:1606.08832 [gr-qc]
Vines J, Flanagan EE, Hinderer T (2011) Post-1-Newtonian tidal effects in the gravitational waveform from binary inspirals. Phys Rev D 83:084051. https://doi.org/10.1103/PhysRevD.83.084051. arXiv:1101.1673 [gr-qc]
Vines J, Steinhoff J, Buonanno A (2019) Spinning-black-hole scattering and the test-black-hole limit at second post-Minkowskian order. Phys Rev D 99(6):064054. https://doi.org/10.1103/PhysRevD.99.064054. arXiv:1812.00956 [gr-qc]
Vishal M, Field SE, Rink K, Gottlieb S, Khanna G (2024) Toward exponentially-convergent simulations of extreme-mass-ratio inspirals: a time-domain solver for the scalar Teukolsky equation with singular source terms. Phys Rev D 110(10):104009. https://doi.org/10.1103/PhysRevD.110.104009. arXiv:2307.01349 [gr-qc]
Vishveshwara CV (1996) On the black hole trail: a personal journey. Curr Sci 71(11):824–830
Vitale S, Lynch R, Sturani R, Graff P (2017) Use of gravitational waves to probe the formation channels of compact binaries. Class Quantum Grav 34(3):03LT01. https://doi.org/10.1088/1361-6382/aa552e. arXiv:1503.04307 [gr-qc]
Völkel SH, Kokkotas KD (2017) A semi-analytic study of axial perturbations of ultra compact stars. Class Quantum Grav 34(12):125006. https://doi.org/10.1088/1361-6382/aa68cc. arXiv:1703.08156 [gr-qc]
Volonteri M (2012) The formation and evolution of massive black holes. Science 337:544. https://doi.org/10.1126/science.1220843. arXiv:1208.1106 [astro-ph.CO]
Volonteri M, Lodato G, Natarajan P (2008) The evolution of massive black hole seeds. Mon Not R Astron Soc 383:1079. https://doi.org/10.1111/j.1365-2966.2007.12589.x. arXiv:0709.0529 [astro-ph]
von Zeipel H (1910) Sur l'application des séries de M. Lindstedt à l'étude du mouvement des comètes périodiques. Astronomische Nachrichten 183(22):345. https://doi.org/10.1002/asna.19091832202
Vu NL et al (2022) A scalable elliptic solver with task-based parallelism for the SpECTRE numerical relativity code. Phys Rev D 105(8):084027. https://doi.org/10.1103/PhysRevD.105.084027. arXiv:2111.06767 [gr-qc]
Vu NL et al (2023) High-accuracy numerical models of Brownian thermal noise in thin mirror coatings. Class Quantum Grav 40:025015. https://doi.org/10.1088/1361-6382/acad62. arXiv:2111.06893 [astro-ph.IM]
Wachter JM, Olum KD (2017) Gravitational backreaction on piecewise linear cosmic string loops. Phys Rev D 95(2):023519. https://doi.org/10.1103/PhysRevD.95.023519. arXiv:1609.01685 [gr-qc]
Wagg T, Broekgaarden FS, de Mink SE, van Son L, Frankel N, Justham S (2022) Gravitational wave sources in our galactic backyard: predictions for BHBH, BHNS, and NSNS binaries detectable with LISA. Astrophys J 937(2):118. https://doi.org/10.3847/1538-4357/ac8675. arXiv:2111.13704 [astro-ph.HE]
Wagle P, Li D, Chen Y, Yunes N (2024) Perturbations of spinning black holes in dynamical Chern-Simons gravity: slow rotation equations. Phys Rev D 109(10):104029. https://doi.org/10.1103/PhysRevD.109.104029. arXiv:2311.07706 [gr-qc]
Wald RM (1973) On perturbations of a Kerr black hole. J Math Phys 14(10):1453–1461
Wald RM (1978) Construction of solutions of gravitational, electromagnetic, or other perturbation equations from solutions of decoupled equations. Phys Rev Lett 41:203–206. https://doi.org/10.1103/PhysRevLett.41.203
Wang H, Will CM (2007) Post-Newtonian gravitational radiation and equations of motion via direct integration of the relaxed Einstein equations. IV. Radiation reaction for binary systems with spin-spin coupling. Phys Rev D 75:064017. https://doi.org/10.1103/PhysRevD.75.064017. arXiv:gr-qc/0701047
Wang H, Steinhoff J, Zeng J, Schafer G (2011) Leading-order spin-orbit and spin(1)-spin(2) radiation-reaction Hamiltonians. Phys Rev D 84:124005. https://doi.org/10.1103/PhysRevD.84.124005. arXiv:1109.1182 [gr-qc]
Wang Q, Afshordi N (2018) Black hole echology: the observer's manual. Phys Rev D 97(12):124044. https://doi.org/10.1103/PhysRevD.97.124044. arXiv:1803.02845 [gr-qc]
Wang Q, Oshita N, Afshordi N (2020) Echoes from quantum black holes. Phys Rev D 101(2):024031. https://doi.org/10.1103/PhysRevD.101.024031. arXiv:1905.00446 [gr-qc]

Wang Z, Helfer T, Clough K, Berti E (2022) Superradiance in massive vector fields with spatially varying mass. Phys Rev D 105(10):104055. https://doi.org/10.1103/PhysRevD.105.104055. arXiv:2201.08305 [gr-qc]
Warburton N (2015) Self force on a scalar charge in Kerr spacetime: inclined circular orbits. Phys Rev D 91(2):024045. https://doi.org/10.1103/PhysRevD.91.024045. arXiv:1408.2885 [gr-qc]
Warburton N, Barack L (2010) Self force on a scalar charge in Kerr spacetime: circular equatorial orbits. Phys Rev D 81:084039. https://doi.org/10.1103/PhysRevD.81.084039. arXiv:1003.1860 [gr-qc]
Warburton N, Barack L (2011) Self force on a scalar charge in Kerr spacetime: eccentric equatorial orbits. Phys Rev D 83:124038. https://doi.org/10.1103/PhysRevD.83.124038. arXiv:1103.0287 [gr-qc]
Warburton N, Wardell B (2014) Applying the effective-source approach to frequency-domain self-force calculations. Phys Rev D 89(4):044046. https://doi.org/10.1103/PhysRevD.89.044046. arXiv:1311.3104 [gr-qc]
Warburton N, Akcay S, Barack L, Gair JR, Sago N (2012) Evolution of inspiral orbits around a Schwarzschild black hole. Phys Rev D 85:061501. https://doi.org/10.1103/PhysRevD.85.061501. arXiv:1111.6908 [gr-qc]
Warburton N, Osburn T, Evans CR (2017) Evolution of small-mass-ratio binaries with a spinning secondary. Phys Rev D 96(8):084057. https://doi.org/10.1103/PhysRevD.96.084057. arXiv:1708.03720 [gr-qc]
Warburton N, Pound A, Wardell B, Miller J, Durkan L (2021) Gravitational-wave energy flux for compact binaries through second order in the mass ratio. Phys Rev Lett 127(15):151102. https://doi.org/10.1103/PhysRevLett.127.151102. arXiv:2107.01298 [gr-qc]
Wardell B, Warburton N (2015) Applying the effective-source approach to frequency-domain self-force calculations: Lorenz-gauge gravitational perturbations. Phys Rev D 92(8):084019. https://doi.org/10.1103/PhysRevD.92.084019. arXiv:1505.07841 [gr-qc]
Wardell B, Galley CR, Zenginoğlu A, Casals M, Dolan SR, Ottewill AC (2014) Self-force via Green functions and worldline integration. Phys Rev D 89(8):084021. https://doi.org/10.1103/PhysRevD.89.084021. arXiv:1401.1506 [gr-qc]
Wardell B, Pound A, Warburton N, Miller J, Durkan L, Le Tiec A (2023) Gravitational waveforms for compact binaries from second-order self-force theory. Phys Rev Lett 130(24):241402. https://doi.org/10.1103/PhysRevLett.130.241402. arXiv:2112.12265 [gr-qc]
Wessel E, Paschalidis V, Tsokaros A, Ruiz M, Shapiro SL (2021) Gravitational waves from disks around spinning black holes: simulations in full general relativity. Phys Rev D 103(4):043013. https://doi.org/10.1103/PhysRevD.103.043013. arXiv:2011.04077 [astro-ph.HE]
Westpfahl K, Goller M (1979) Gravitational scattering of two relativistic particles in post-linear approximation. Lett Nuovo Cim 26:573–576. https://doi.org/10.1007/BF02817047
Westpfahl K, Hoyler H (1980) Gravitational bremsstrahlung in post-linear fast-motion approximation. Lett Nuovo Cim 27:581–585. https://doi.org/10.1007/BF02750304
Weyhausen A, Bernuzzi S, Hilditch D (2012) Constraint damping for the Z4c formulation of general relativity. Phys Rev D 85:024038. https://doi.org/10.1103/PhysRevD.85.024038. arXiv:1107.5539 [gr-qc]
WhiskyMHD (2024) WhiskyMHD waveforms. https://bitbucket.org/ciolfir/bns-waveforms/src/master/
Whittall C, Barack L (2023) Frequency-domain approach to self-force in hyperbolic scattering. Phys Rev D 108(6):064017. https://doi.org/10.1103/PhysRevD.108.064017. arXiv:2305.09724 [gr-qc]
Wichoski UF, MacGibbon JH, Brandenberger RH (2002) High-energy neutrinos, photons and cosmic ray fluxes from VHS cosmic strings. Phys Rev D 65:063005. https://doi.org/10.1103/PhysRevD.65.063005. arXiv:hep-ph/9805419
Widdicombe JY, Helfer T, Lim EA (2020) Black hole formation in relativistic Oscillaton collisions. JCAP 01:027. https://doi.org/10.1088/1475-7516/2020/01/027. arXiv:1910.01950 [astro-ph.CO]
Will CM (2005) Post-Newtonian gravitational radiation and equations of motion via direct integration of the relaxed Einstein equations. III. Radiation reaction for binary systems with spinning bodies. Phys Rev D 71:084027. https://doi.org/10.1103/PhysRevD.71.084027. arXiv:gr-qc/0502039
Will CM (2017) Orbital flips in hierarchical triple systems: relativistic effects and third-body effects to hexadecapole order. Phys Rev D 96(2):023017. https://doi.org/10.1103/PhysRevD.96.023017. arXiv:1705.03962 [astro-ph.EP]
Will CM (2021) Higher-order effects in the dynamics of hierarchical triple systems. Quadrupole-squared terms. Phys Rev D 103(6):063003. https://doi.org/10.1103/PhysRevD.103.063003. arXiv:2011.13286 [astro-ph.EP]

Will CM, Wiseman AG (1996) Gravitational radiation from compact binary systems: gravitational wave forms and energy loss to second postNewtonian order. Phys Rev D 54:4813–4848. https://doi.org/10.1103/PhysRevD.54.4813. arXiv:gr-qc/9608012

Willems B, Kalogera V, Vecchio A, Ivanova N, Rasio FA, Fregeau JM, Belczynski K (2007) Eccentric double white dwarfs as LISA sources in globular clusters. Astrophys J Lett 665:L59. https://doi.org/10.1086/521049. arXiv:0705.4287 [astro-ph]

Wise JH, Regan JA, O'Shea BW, Norman ML, Downes TP, Xu H (2019) Formation of massive black holes in rapidly growing pre-galactic gas clouds. Nature 566(7742):85–88. https://doi.org/10.1038/s41586-019-0873-4. arXiv:1901.07563 [astro-ph.GA]

Witek H, Cardoso V, Ishibashi A, Sperhake U (2013) Superradiant instabilities in astrophysical systems. Phys Rev D 87(4):043513. https://doi.org/10.1103/PhysRevD.87.043513. arXiv:1212.0551 [gr-qc]

Witek H, Gualtieri L, Pani P, Sotiriou TP (2019) Black holes and binary mergers in scalar Gauss-Bonnet gravity: scalar field dynamics. Phys Rev D 99(6):064035. https://doi.org/10.1103/PhysRevD.99.064035. arXiv:1810.05177 [gr-qc]

Witek H, Gualtieri L, Pani P (2020) Towards numerical relativity in scalar Gauss-Bonnet gravity: 3 + 1 decomposition beyond the small-coupling limit. Phys Rev D 101(12):124055. https://doi.org/10.1103/PhysRevD.101.124055. arXiv:2004.00009 [gr-qc]

Wittek NA et al (2023) Worldtube excision method for intermediate-mass-ratio inspirals: Scalar-field model in 3+1 dimensions. Phys Rev D 108(2):024041. https://doi.org/10.1103/PhysRevD.108.024041. arXiv:2304.05329 [gr-qc]

Witten E (1998) D-branes and K-theory. JHEP 12:019. https://doi.org/10.1088/1126-6708/1998/12/019. arXiv:hep-th/9810188

Witzany V (2019) Hamilton-Jacobi equation for spinning particles near black holes. Phys Rev D 100 (10):104030. https://doi.org/10.1103/PhysRevD.100.104030. arXiv:1903.03651 [gr-qc]

Witzany V, Pound A, Barack L (2020) Finite-size effects in large mass ratio inspirals. Unpublished manuscript

Wolz A, Yagi K, Anderson N, Taylor AJ (2020) Measuring individual masses of binary white dwarfs with space-based gravitational-wave interferometers. Mon Not R Astron Soc 500(1):L52–L56. https://doi.org/10.1093/mnrasl/slaa183. arXiv:2011.04722 [astro-ph.HE]

Wong K, Kovetz ED, Cutler C, Berti E (2018) Expanding the LISA horizon from the ground. Phys Rev Lett 121(25):251102. https://doi.org/10.1103/PhysRevLett.121.251102. arXiv:1808.08247 [astro-ph.HE]

Wong LK (2019) Superradiant scattering by a black hole binary. Phys Rev D 100(4):044051. https://doi.org/10.1103/PhysRevD.100.044051. arXiv:1905.08543 [hep-th]

Wong LK (2020) Evolution of diffuse scalar clouds around binary black holes. Phys Rev D 101 (12):124049. https://doi.org/10.1103/PhysRevD.101.124049. arXiv:2004.03570 [hep-th]

Woodford CJ, Boyle M, Pfeiffer HP (2019) Compact binary waveform center-of-mass corrections. Phys Rev D 100(12):124010. https://doi.org/10.1103/PhysRevD.100.124010. arXiv:1904.04842 [gr-qc]

Woosley SE (2017) Pulsational pair-instability supernovae. Astrophys J 836(2):244. https://doi.org/10.3847/1538-4357/836/2/244. arXiv:1608.08939 [astro-ph.HE]

Woosley SE, Heger A (2021) The pair-instability mass gap for black holes. Astrophys J Lett 912(2):L31. https://doi.org/10.3847/2041-8213/abf2c4. arXiv:2103.07933 [astro-ph.SR]

Wyman M, Pogosian L, Wasserman I (2005) Bounds on cosmic strings from WMAP and SDSS. Phys Rev D 72:023513. [Erratum: Phys. Rev. D 73, 089905 (2006)], https://doi.org/10.1103/PhysRevD.72.023513. arXiv:astro-ph/0503364

Wysocki D, Lange J, O'Shaughnessy R (2019) Reconstructing phenomenological distributions of compact binaries via gravitational wave observations. Phys Rev D 100(4):043012. https://doi.org/10.1103/PhysRevD.100.043012. arXiv:1805.06442 [gr-qc]

Xin S, Han WB, Yang SC (2019) Gravitational waves from extreme-mass-ratio inspirals using general parametrized metrics. Phys Rev D 100(8):084055. https://doi.org/10.1103/PhysRevD.100.084055. arXiv:1812.04185 [gr-qc]

Xin S, Chen B, Lo R, Sun L, Han WB, Zhong X, Srivastava M, Ma S, Wang Q, Chen Y (2021) Gravitational-wave echoes from spinning exotic compact objects: numerical waveforms from the Teukolsky equation. Phys Rev D 104(10):104005. https://doi.org/10.1103/PhysRevD.104.104005. arXiv:2105.12313 [gr-qc]

Yagi K, Tanahashi N, Tanaka T (2011) Probing the size of extra dimension with gravitational wave astronomy. Phys Rev D 83:084036. https://doi.org/10.1103/PhysRevD.83.084036. arXiv:1101.4997 [gr-qc]

Yagi K, Stein LC, Yunes N, Tanaka T (2012) Post-Newtonian, Quasi-Circular Binary Inspirals in Quadratic Modified Gravity. Phys Rev D 85:064022. [Erratum: Phys. Rev. D 93, 029902 (2016)]. https://doi.org/10.1103/PhysRevD.85.064022. arXiv:1110.5950 [gr-qc]

Yagi K, Stein LC, Yunes N (2016) Challenging the presence of scalar charge and dipolar radiation in binary pulsars. Phys Rev D 93(2):024010. https://doi.org/10.1103/PhysRevD.93.024010. arXiv:1510.02152 [gr-qc]

Yamamoto T, Shibata M, Taniguchi K (2008) Simulating coalescing compact binaries by a new code SACRA. Phys Rev D 78:064054. https://doi.org/10.1103/PhysRevD.78.064054. arXiv:0806.4007 [gr-qc]

Yang H, Casals M (2017) General relativistic dynamics of an extreme mass-ratio binary interacting with an external body. Phys Rev D 96(8):083015. https://doi.org/10.1103/PhysRevD.96.083015. arXiv:1704.02022 [gr-qc]

Yang H, Zhang F, Zimmerman A, Chen Y (2014) Scalar green function of the kerr spacetime. Phys Rev D 89(6):064014. https://doi.org/10.1103/PhysRevD.89.064014. arXiv:1311.3380 [gr-qc]

Yang H, Zimmerman A, Lehner L (2015) Turbulent black holes. Phys Rev Lett 114:081101. https://doi.org/10.1103/PhysRevLett.114.081101. arXiv:1402.4859 [gr-qc]

Yang H, Bonga B, Peng Z, Li G (2019) Relativistic mean motion resonance. Phys Rev D 100(12):124056. https://doi.org/10.1103/PhysRevD.100.124056. arXiv:1910.07337 [gr-qc]

Yang Y et al (2019) Hierarchical black hole mergers in active galactic nuclei. Phys Rev Lett 123 (18):181101. https://doi.org/10.1103/PhysRevLett.123.181101. arXiv:1906.09281 [astro-ph.HE]

Yang Z, Leibovich AK (2019) Analytic solutions to compact binary inspirals with leading order spin-orbit contribution using the dynamical renormalization group. Phys Rev D 100(8):084021. https://doi.org/10.1103/PhysRevD.100.084021. arXiv:1908.05688 [gr-qc]

Yoo J, Varma V, Giesler M, Scheel MA, Haster CJ, Pfeiffer HP, Kidder LE, Boyle M (2022) Targeted large mass ratio numerical relativity surrogate waveform model for GW190814. Phys Rev D 106 (4):044001. https://doi.org/10.1103/PhysRevD.106.044001. arXiv:2203.10109 [gr-qc]

Yoo J et al (2023) Numerical relativity surrogate model with memory effects and post-Newtonian hybridization. Phys Rev D 108(6):064027. https://doi.org/10.1103/PhysRevD.108.064027. arXiv:2306.03148 [gr-qc]

York JW Jr (1999) Conformal 'thin sandwich' data for the initial-value problem. Phys Rev Lett 82:1350–1353. https://doi.org/10.1103/PhysRevLett.82.1350. arXiv:gr-qc/9810051

York JW Jr (1979) Kinematics and dynamics of general relativity. In: Smarr LL (ed) Sources of Gravitational Radiation. Cambridge University Press, Cambridge, England, p 83

Yoshida S, Eriguchi Y (1996) Ergoregion instability revisited - a new and general method for numerical analysis of stability. MNRAS 282(2):580–586. https://doi.org/10.1093/mnras/282.2.580

Yoshino H, Kodama H (2014) Gravitational radiation from an axion cloud around a black hole: superradiant phase. PTEP 2014:043E02. https://doi.org/10.1093/ptep/ptu029. arXiv:1312.2326 [gr-qc]

Yu H, Weinberg NN, Fuller J (2020) Non-linear dynamical tides in white dwarf binaries. Mon Not R Astron Soc 496(4):5482–5502. https://doi.org/10.1093/mnras/staa1858. arXiv:2005.03058 [astro-ph.SR]

Yu Q (2002) Evolution of massive binary black holes. Mon Not R Astron Soc 331:935. https://doi.org/10.1046/j.1365-8711.2002.05242.x. arXiv:astro-ph/0109530

Yu S, Lu Y, Jeffery CS (2021) Orbital evolution of neutron-star-white-dwarf binaries by Roche lobe overflow and gravitational wave radiation. Mon Not R Astron Soc 503(2):2776–2790. https://doi.org/10.1093/mnras/stab626. arXiv:2103.01884 [astro-ph.HE]

Yue XJ, Han WB (2018) Gravitational waves with dark matter minispikes: the combined effect. Phys Rev D 97(6):064003. https://doi.org/10.1103/PhysRevD.97.064003. arXiv:1711.09706 [gr-qc]

Yue XJ, Han WB, Chen X (2019) Dark matter: an efficient catalyst for intermediate-mass-ratio-inspiral events. Astrophys J 874(1):34. https://doi.org/10.3847/1538-4357/ab06f6. arXiv:1802.03739 [gr-qc]

Yunes N, Gonzalez J (2006) Metric of a tidally perturbed spinning black hole. Phys Rev D 73(2):024010. [Erratum: Phys. Rev. D 89, 089902 (2014)]. https://doi.org/10.1103/PhysRevD.89.089902. arXiv:gr-qc/0510076

Yunes N, Pretorius F (2009) Dynamical chern-simons modified gravity. I. Spinning black holes in the slow-rotation approximation. Phys Rev D 79:084043. https://doi.org/10.1103/PhysRevD.79.084043. arXiv:0902.4669 [gr-qc]

Yunes N, Pretorius F (2009) Fundamental theoretical bias in gravitational wave astrophysics and the parameterized post-einsteinian framework. Phys Rev D 80:122003. https://doi.org/10.1103/PhysRevD.80.122003. arXiv:0909.3328 [gr-qc]

Yunes N, Siemens X (2013) Gravitational-wave tests of general relativity with ground-based detectors and pulsar timing-arrays. Living Rev Relativ 16:9. https://doi.org/10.12942/lrr-2013-9. arXiv:1304.3473 [gr-qc]

Yunes N, Stein LC (2011) Non-spinning black holes in alternative theories of gravity. Phys Rev D 83:104002. https://doi.org/10.1103/PhysRevD.83.104002. arXiv:1101.2921 [gr-qc]
Yunes N, Arun KG, Berti E, Will CM (2009) Post-Circular Expansion of Eccentric Binary Inspirals: Fourier-Domain Waveforms in the Stationary Phase Approximation. Phys Rev D 80(8):084001. [Erratum: Phys. Rev. D 89, 109901 (2014)]. https://doi.org/10.1103/PhysRevD.80.084001. arXiv:0906.0313 [gr-qc]
Yunes N, Buonanno A, Hughes SA, Coleman Miller M, Pan Y (2010) Modeling extreme mass ratio inspirals within the effective-one-body approach. Phys Rev Lett 104:091102. https://doi.org/10.1103/PhysRevLett.104.091102. arXiv:0909.4263 [gr-qc]
Yunes N, Pretorius F, Spergel D (2010) Constraining the evolutionary history of Newton's constant with gravitational wave observations. Phys Rev D 81:064018. https://doi.org/10.1103/PhysRevD.81.064018. arXiv:0912.2724 [gr-qc]
Yunes N, Buonanno A, Hughes SA, Pan Y, Barausse E, Miller MC, Throwe W (2011) Extreme Mass-Ratio Inspirals in the Effective-One-Body Approach: Quasi-Circular, Equatorial Orbits around a Spinning Black Hole. Phys Rev D 83:044044. [Erratum: Phys. Rev. D 88, 109904 (2013)]. https://doi.org/10.1103/PhysRevD.83.044044. arXiv:1009.6013 [gr-qc]
Yunes N, Kocsis B, Loeb A, Haiman Z (2011) Imprint of accretion disk-induced migration on gravitational waves from extreme mass ratio inspirals. Phys Rev Lett 107:171103. https://doi.org/10.1103/PhysRevLett.107.171103. arXiv:1103.4609 [astro-ph.CO]
Yunes N, Pani P, Cardoso V (2012) Gravitational waves from quasicircular extreme mass-ratio inspirals as probes of scalar-tensor theories. Phys Rev D 85:102003. https://doi.org/10.1103/PhysRevD.85.102003. arXiv:1112.3351 [gr-qc]
Yunes N, Yagi K, Pretorius F (2016) Theoretical physics implications of the binary black-hole mergers GW150914 and GW151226. Phys Rev D 94(8):084002. https://doi.org/10.1103/PhysRevD.94.084002. arXiv:1603.08955 [gr-qc]
Zappa F, Bernuzzi S, Pannarale F, Mapelli M, Giacobbo N (2019) Black-hole remnants from black-hole-neutron-star mergers. Phys Rev Lett 123(4):041102. https://doi.org/10.1103/PhysRevLett.123.041102. arXiv:1903.11622 [gr-qc]
Zelenka O, Lukes-Gerakopoulos G, Witzany V, Kopáček O (2020) Growth of resonances and chaos for a spinning test particle in the Schwarzschild background. Phys Rev D 101(2):024037. https://doi.org/10.1103/PhysRevD.101.024037. arXiv:1911.00414 [gr-qc]
Zeng J, Will CM (2007) Application of energy and angular momentum balance to gravitational radiation reaction for binary systems with spin-orbit coupling. Gen Relativ Gravit 39:1661–1673. https://doi.org/10.1007/s10714-007-0475-6. arXiv:0704.2720 [gr-qc]
Zenginoglu A, Khanna G (2011) Null infinity waveforms from extreme-mass-ratio inspirals in Kerr spacetime. Phys Rev X 1:021017. https://doi.org/10.1103/PhysRevX.1.021017. arXiv:1108.1816 [gr-qc]
Zerilli FJ (1970) Effective potential for even parity Regge-Wheeler gravitational perturbation equations. Phys Rev Lett 24:737–738. https://doi.org/10.1103/PhysRevLett.24.737
Zerilli FJ (1970) Gravitational field of a particle falling in a schwarzschild geometry analyzed in tensor harmonics. Phys Rev D 2:2141–2160. https://doi.org/10.1103/PhysRevD.2.2141
Magaña Zertuche L et al (2022) High precision ringdown modeling: multimode fits and BMS frames. Phys Rev D 105(10):104015. https://doi.org/10.1103/PhysRevD.105.104015. arXiv:2110.15922 [gr-qc]
Zevin M, Pankow C, Rodriguez CL, Sampson L, Chase E, Kalogera V, Rasio FA (2017) Constraining formation models of binary black holes with gravitational-wave observations. Astrophys J 846(1):82. https://doi.org/10.3847/1538-4357/aa8408. arXiv:1704.07379 [astro-ph.HE]
Zhang C, Han WB, Yang SC (2021) Analytical effective one-body formalism for extreme-mass-ratio inspirals with eccentric orbits. Commun Theor Phys 73(8):085401. https://doi.org/10.1088/1572-9494/abfbe4. arXiv:2001.06763 [gr-qc]
Zhang C, Han WB, Zhong XY, Wang G (2021) Geometrized effective-one-body formalism for extreme-mass-ratio limits: generic orbits. Phys Rev D 104(2):024050. https://doi.org/10.1103/PhysRevD.104.024050. arXiv:2102.05391 [gr-qc]
Zhang C, Gong Y, Liang D, Wang B (2023) Gravitational waves from eccentric extreme mass-ratio inspirals as probes of scalar fields. JCAP 06:054. https://doi.org/10.1088/1475-7516/2023/06/054. arXiv:2210.11121 [gr-qc]
Zhang J, Yang H (2019) Gravitational floating orbits around hairy black holes. Phys Rev D 99(6):064018. https://doi.org/10.1103/PhysRevD.99.064018. arXiv:1808.02905 [gr-qc]
Zhang J, Yang H (2020) Dynamic signatures of black hole binaries with superradiant clouds. Phys Rev D 101(4):043020. https://doi.org/10.1103/PhysRevD.101.043020. arXiv:1907.13582 [gr-qc]

Zhang W, Almgren A, Beckner V, Bell J, Blaschke J, Chan C, Day M, Friesen B, Gott K, Graves D, Katz M, Myers A, Nguyen T, Nonaka A, Rosso M, Williams S, Zingale M (2019) AMReX: a framework for block-structured adaptive mesh refinement. J Open Source Softw 4(37):1370. https://doi.org/10.21105/joss.01370

Zhang YP, Gracia-Linares M, Laguna P, Shoemaker D, Liu YX (2023) Gravitational recoil from binary black hole mergers in scalar field clouds. Phys Rev D 107(4):044039. https://doi.org/10.1103/PhysRevD.107.044039. arXiv:2209.11814 [gr-qc]

Zhong XY, Han WB, Jiang Y, Shen P, Yang SC, Zhang C (2023) Detecting properties of echoes from the inspiraling stage with ground-based detectors. Eur Phys J Plus 138(8):761. https://doi.org/10.1140/epjp/s13360-023-04398-z. arXiv:2212.11175 [gr-qc]

Zhu H, Ripley JL, Cárdenas-Avendaño A, Pretorius F (2024) Challenges in quasinormal mode extraction: perspectives from numerical solutions to the Teukolsky equation. Phys Rev D 109(4):044010. https://doi.org/10.1103/PhysRevD.109.044010. arXiv:2309.13204 [gr-qc]

Zhu SJ, Baryakhtar M, Papa MA, Tsuna D, Kawanaka N, Eggenstein HB (2020) Characterizing the continuous gravitational-wave signal from boson clouds around Galactic isolated black holes. Phys Rev D 102(6):063020. https://doi.org/10.1103/PhysRevD.102.063020. arXiv:2003.03359 [gr-qc]

Zilhão M, Cardoso V, Herdeiro C, Lehner L, Sperhake U (2014) Collisions of oppositely charged black holes. Phys Rev D 89(4):044008. https://doi.org/10.1103/PhysRevD.89.044008. arXiv:1311.6483 [gr-qc]

Zilhão M, Cardoso V, Herdeiro C, Lehner L, Sperhake U (2014b) Head-on collisions of charged black holes from rest. In: García-Parrado A, Mena FC, Moura F, Vaz E (eds) Progress in Mathematical Relativity, Gravitation and Cosmology. vol 60. Springer, Berlin, Heidelberg, pp 451–455. https://doi.org/10.1007/978-3-642-40157-2_69

Zilhão M, Noble SC, Campanelli M, Zlochower Y (2015) Resolving the relative influence of strong field spacetime dynamics and MHD on circumbinary disk physics. Phys Rev D 91(2):024034. https://doi.org/10.1103/PhysRevD.91.024034. arXiv:1409.4787 [gr-qc]

Zilhão M, Witek H, Cardoso V (2015) Nonlinear interactions between black holes and Proca fields. Class Quantum Grav 32:234003. https://doi.org/10.1088/0264-9381/32/23/234003. arXiv:1505.00797 [gr-qc]

Zilhao M, Cardoso V, Herdeiro C, Lehner L, Sperhake U (2012) Collisions of charged black holes. Phys Rev D 85:124062. https://doi.org/10.1103/PhysRevD.85.124062. arXiv:1205.1063 [gr-qc]

Zimmerman A, Lewis A, Pfeiffer HP (2016) Redshift factor and the first law of binary black hole mechanics in numerical simulations. Phys Rev Lett 117(19):191101. https://doi.org/10.1103/PhysRevLett.117.191101. arXiv:1606.08056 [gr-qc]

Zimmerman P (2015) Gravitational self-force in scalar-tensor gravity. Phys Rev D 92(6):064051. https://doi.org/10.1103/PhysRevD.92.064051. arXiv:1507.04076 [gr-qc]

Zlochower Y, Baker JG, Campanelli M, Lousto CO (2005) Accurate black hole evolutions by fourth-order numerical relativity. Phys Rev D 72:024021. https://doi.org/10.1103/PhysRevD.72.024021. arXiv:gr-qc/0505055

Zlochower Y, Ponce M, Lousto CO (2012) Accuracy issues for numerical waveforms. Phys Rev D 86:104056. https://doi.org/10.1103/PhysRevD.86.104056. arXiv:1208.5494 [gr-qc]

Zlochower Y, Healy J, Lousto CO, Ruchlin I (2017) Evolutions of nearly maximally spinning black hole binaries using the moving puncture approach. Phys Rev D 96(4):044002. https://doi.org/10.1103/PhysRevD.96.044002. arXiv:1706.01980 [gr-qc]

Zwiebach B (2006) A first course in string theory. Cambridge University Press, Cambridge. https://doi.org/10.1017/CBO9780511841682

Authors and Affiliations

LISA Consortium Waveform Working Group[106] · Niayesh Afshordi[1] · Sarp Akçay[2] · Pau Amaro Seoane[3,4,5,6] · Andrea Antonelli[7] · Josu C. Aurrekoetxea[8] · Leor Barack[9] · Enrico Barausse[10,11] · Robert Benkel[12] · Laura Bernard[13] · Sebastiano Bernuzzi[14] ·

Emanuele Berti[7] · Matteo Bonetti[15,16] · Béatrice Bonga[17] · Gabriele Bozzola[18] · Richard Brito[19] · Alessandra Buonanno[12] · Alejandro Cárdenas-Avendaño[20] · Marc Casals[2,21,22] · David F. Chernoff[23] · Alvin J. K. Chua[24,25] · Katy Clough[26] · Marta Colleoni[27] · Geoffrey Compère[28] · Mekhi Dhesi[9] · Adrien Druart[29] · Leanne Durkan[30] · Guillaume Faye[31] · Deborah Ferguson[30,32] · Scott E. Field[33] · William E. Gabella[34] · Juan García-Bellido[35] · Miguel Gracia-Linares[30] · Davide Gerosa[15,16,36] · Stephen R. Green[37] · Maria Haney[38] · Mark Hannam[39] · Anna Heffernan[1,26,40] · Tanja Hinderer[41] · Thomas Helfer[42] · Scott A. Hughes[43] · Sascha Husa[39,44] · Soichiro Isoyama[23] · Michael L. Katz[12,45] · Chris Kavanagh[2] · Gaurav Khanna[46] · Larry E. Kidder[47] · Valeriya Korol[48] · Lorenzo Küchler[9,29,49] · Pablo Laguna[30] · François Larrouturou[50] · Alexandre Le Tiec[13] · Benjamin Leather[2,12] · Eugene A. Lim[51] · Hyun Lim[52] · Tyson B. Littenberg[45] · Oliver Long[9,12] · Carlos O. Lousto[53] · Geoffrey Lovelace[54] · Georgios Lukes-Gerakopoulos[55] · Philip Lynch[2,12] · Rodrigo P. Macedo[56] · Charalampos Markakis[26] · Elisa Maggio[12] · Ilya Mandel[57,58] · Andrea Maselli[59,60] · Josh Mathews[24] · Pierre Mourier[26] · David Neilsen[61] · Alessandro Nagar[62,63] · David A. Nichols[64] · Jan Novák[65] · Maria Okounkova[66] · Richard O'Shaughnessy[53] · Naritaka Oshita[67,68,69] · Conor O'Toole[2] · Zhen Pan[1] · Paolo Pani[70] · George Pappas[71] · Vasileios Paschalidis[72] · Harald P. Pfeiffer[12] · Lorenzo Pompili[12] · Adam Pound[9] · Geraint Pratten[36] · Hannes R. Rüter[12] · Milton Ruiz[32,73] · Zeyd Sam[9] · Laura Sberna[12] · Stuart L. Shapiro[32] · Deirdre M. Shoemaker[30] · Carlos F. Sopuerta[44,74] · Andrew Spiers[9] · Hari Sundar[75] · Nicola Tamanini[76] · Jonathan E. Thompson[39,77] · Alexandre Toubiana[12] · Antonios Tsokaros[32,78] · Samuel D. Upton[9,55] · Maarten van de Meent[12,56] · Daniele Vernieri[79] · Jeremy M. Wachter[80] · Niels Warburton[2] · Barry Wardell[2] · Helvi Witek[32] · Vojtěch Witzany[81] · Huan Yang[1,40] · Miguel Zilhão[82] · Angelica Albertini[55,81] · K. G. Arun[83] · Miguel Bezares[84,85] · Alexander Bonilla[36] · Christian Chapman-Bird[86] · Bradley Cownden[2] · Kevin Cunningham[2] · Chris Devitt[2] · Sam Dolan[87] · Francisco Duque[12] · Conor Dyson[56] · Chris L. Fryer[52] · Jonathan R. Gair[12] · Bruno Giacomazzo[15,16,88] · Priti Gupta[89] · Wen-Biao Han[90] · Roland Haas[91] · Eric W. Hirschmann[61] · E. A. Huerta[92,93,94] · Philippe Jetzer[95] · Bernard Kelly[96,97,98] · Mohammed Khalil[1] · Jack Lewis[9] · Nicole Lloyd-Ronning[99] · Sylvain Marsat[76] · Germano Nardini[100] · Jakob Neef[2] · Adrian Ottewill[2] · Christiana Pantelidou[2] · Gabriel Andres Piovano[2] · Jaime Redondo-Yuste[56] · Laura Sagunski[101] · Leo C. Stein[102] · Viktor Skoupý[55,81] · Ulrich Sperhake[103] · Lorenzo Speri[12] · Thomas F. M. Spieksma[56] · Chris Stevens[104] · David Trestini[105] · Alex Vañó-Viñuales[19]

✉ LISA Consortium Waveform Working Group
wav-wg-chairs@lisamission.org

[1] Perimeter Institute for Theoretical Physics, Waterloo, Ontario N2L 2Y5, Canada

[2] School of Mathematics and Statistics, University College Dublin, Belfield, Dublin 4, Ireland

[3] Universitat Politècnica de València, València, Spain

[4] Max Planck Institute for Extraterrestrial Physics, Garching, Germany

[5] Higgs Centre for Theoretical Physics, Edinburgh, UK

[6] Kavli Institute for Astronomy and Astrophysics, Beijing 100871, China

[7] William H. Miller III Department of Physics and Astronomy, Johns Hopkins University, Baltimore, Maryland 21218, USA

[8] Astrophysics, University of Oxford, Denys Wilkinson Building, Keble Road, Oxford OX1 3RH, UK

[9] School of Mathematical Sciences and STAG Research Centre, University of Southampton, Southampton SO17 1BJ, UK

[10] SISSA, Via Bonomea 265, 34136 Trieste, Italy

[11] INFN Sezione di Trieste IFPU - Institute for Fundamental Physics of the Universe, Via Beirut 2, 34014 Trieste, Italy

[12] Max Planck Institute for Gravitational Physics (Albert Einstein Institute), D-14476 Potsdam, Germany

[13] Laboratoire Univers et Théories, CNRS, Observatoire de Paris, Université PSL, Université Paris Cité, 92190 Meudon, France

[14] Theoretisch-Physikalisches Institut, Friedrich-Schiller-Universität Jena, 07743 Jena, Germany

[15] Dipartimento di Fisica “G. Occhialini”, Universitá degli Studi di Milano-Bicocca, Piazza della Scienza 3, 20126 Milano, Italy

[16] INFN, Sezione di Milano-Bicocca, Piazza della Scienza 3, 20126 Milano, Italy

[17] Institute for Mathematics, Astrophysics and Particle Physics, Radboud University, 6525 Nijmegen, AJ, The Netherlands

[18] Department of Astronomy, The University of Arizona, Tucson, AZ 85721, USA

[19] CENTRA, Departamento de Física, Instituto Superior Técnico – IST, Universidade de Lisboa – UL, Avenida Rovisco Pais 1, 1049-001 Lisboa, Portugal

[20] Princeton Gravity Initiative, Princeton University, Princeton, New Jersey 08544, USA

[21] Institut für Theoretische Physik, Universität Leipzig, Brüderstraße 16, 04103 Leipzig, Germany

[22] Centro Brasileiro de Pesquisas Físicas (CBPF), Rio de Janeiro CEP 22290-180, Brazil

[23] Department of Astronomy, Cornell University, Ithaca, New York 14853, USA

[24] Department of Physics, National University of Singapore, Singapore 117551, Singapore

[25] Department of Mathematics, National University of Singapore, Singapore 119076, Singapore

[26] School of Mathematical Sciences, Queen Mary University of London, Mile End Rd, London E1 4NS, UK

[27] Departament de Física, Universitat de les Illes Balears, IAC3 – IEEC, Crta. Valldemossa km 7.5, E-07122 Palma, Spain

[28] Université Libre de Bruxelles, International Solvay Institutes, CP 231, 1050 Brussels, Belgium

[29] Université Libre de Bruxelles, Gravitational Wave Centre, International Solvay Institutes, CP 231, 1050 Brussels, Belgium

[30] Center of Gravitational Physics, Weinberg Institute, University of Texas at Austin, Austin, TX 78712, USA

[31] GReCO, Institut d'Astrophysique de Paris, UMR 7095, CNRS, Sorbonne Université, 98bis boulevard Arago, 75014 Paris, France

[32] Department of Physics and Illinois Center for Advanced Studies of the Universe, University of Illinois at Urbana-Champaign, Urbana, Illinois 61801, USA

[33] Department of Mathematics and Center for Scientific Computing & Data Science Research, University of Massachusetts, Dartmouth, MA 02747, USA

[34] Department of Physics and Astronomy, Vanderbilt University, Nashville, TN 37235, USA

[35] Instituto de Física Teórica IFT-UAM/CSIC, Universidad Autónoma de Madrid, 28049 Madrid, Spain

[36] School of Physics and Astronomy & Institute for Gravitational Wave Astronomy, University of Birmingham, Birmingham B15 2TT, UK

[37] School of Mathematical Sciences, University of Nottingham, University Park, Nottingham NG7 2RD, UK

[38] Nikhef, Science Park 105, 1098 Amsterdam, XG, The Netherlands

[39] School of Physics and Astronomy, Cardiff University, Queens Buildings, Cardiff CF24 3AA, UK

[40] University of Guelph, Guelph, Ontario N1G 2W1, Canada

[41] Institute for Theoretical Physics, Utrecht University, Princetonplein 5, 3584CC Utrecht, The Netherlands

[42] Institute for Advanced Computational Science, Stony Brook University, Stony Brook, NY 11794, USA

[43] Department of Physics and MIT Kavli Institute, Massachusetts Institute of Technology, Cambridge, MA 02139, USA

[44] Institut de Ciències de l'Espai (ICE, CSIC), Campus UAB, Carrer de Can Magrans s/n, 08193 Cerdanyola del Vallès, Spain

[45] NASA Marshall Space Flight Center, Huntsville, Alabama 35811, USA

[46] Department of Physics and Center for Computational Research, University of Rhode Island, Kingston, RI 02881, USA

[47] Cornell Center for Astrophysics and Planetary Science, Cornell University, Ithaca, NY 14853, USA

[48] Max-Planck-Institut für Astrophysik, Karl-Schwarzschild-Straße 1, 85741 Garching, Germany

[49] Institute for Theoretical Physics, KU Leuven, Celestijnenlaan 200D, 3001 Leuven, Belgium

[50] Deutsches Elektronen-Synchrotron DESY, Notkestr. 85, 22607 Hamburg, Germany

[51] Theoretical Particle Physics and Cosmology Group, Physics Department, Kings College London, Strand, London WC2R 2LS, UK

[52] Center for Theoretical Astrophysics, Los Alamos National Laboratory, Los Alamos, NM 87545, USA

[53] Center for Computational Relativity and Gravitation, School of Mathematical Sciences, Rochester Institute of Technology, 85 Lomb Memorial Drive, Rochester, New York 14623, USA

[54] Nicholas and Lee Begovich Center for Gravitational-Wave Physics and Astronomy, California State University, Fullerton, Fullerton, California 92831, USA

[55] Astronomical Institute of the Czech Academy of Sciences, Boční II 1401/1a, 141 00 Prague, Czech Republic

[56] Niels Bohr International Academy, Niels Bohr Institute, Blegdamsvej 17, 2100 Copenhagen, Denmark

[57] School of Physics and Astronomy, Monash University, Clayton, VIC 3800, Australia

[58] OzGrav: The ARC Centre of Excellence for Gravitational Wave Discovery, Hawthorn, Australia

[59] Gran Sasso Science Institute (GSSI), 67100 L'Aquila, Italy

[60] INFN, Laboratori Nazionali del Gran Sasso, 67100 Assergi, Italy

[61] Department of Physics and Astronomy, Brigham Young University, Provo, UT 84602, USA

[62] INFN Sezione di Torino, Via P. Giuria 1, 10125 Torino, Italy

[63] Institut des Hautes Etudes Scientifiques, 91440 Bures-sur-Yvette, France

[64] Department of Physics, University of Virginia, P.O. Box 400714, Charlottesville, VA 22904-4714, USA

[65] Department of Physics, Faculty of Mechanical Engineering, Czech Technical University in Prague, Technická 1902/4, 16607 Prague 6, Czech Republic

[66] Department of Physics, Pasadena City College, Pasadena, California 91106, USA

[67] Center for Gravitational Physics and Quantum Information (CGPQI), Yukawa Institute for Theoretical Physics (YITP), Kyoto University, Kyoto 606-8502, Japan

[68] The Hakubi Center for Advanced Research, Kyoto University, Yoshida Ushinomiyacho, Sakyo-ku, Kyoto 606-8501, Japan

[69] RIKEN iTHEMS, Wako, Saitama 351-0198, Japan

[70] Dipartimento di Fisica, Sapienza Università di Roma & INFN Sezione di Roma, Piazzale Aldo Moro 5, 00185 Roma, Italy

[71] Department of Physics, Aristotle University of Thessaloniki, 54124 Thessaloniki, Greece

[72] Departments of Astronomy and Physics, The University of Arizona, Tucson, AZ 85721, USA

[73] Departamento de Astronomía y Astrofísica, Universitat de Valéncia, Dr. Moliner 50, 46100 Burjassot (València), Spain

[74] Institut d'Estudis Espacials de Catalunya (IEEC), Edifici Nexus, Carrer del Gran Capità 2-4, despatx 201, 08034 Barcelona, Spain

[75] University of Utah, Salt Lake City, UT 84112, USA

[76] Laboratoire des 2 Infinis - Toulouse (L2IT-IN2P3), Université de Toulouse, CNRS, UPS, F-31062 Toulouse Cedex 9, France

[77] Theoretical Astrophysics Group, California Institute of Technology, Pasadena, CA 91125, USA

[78] Research Center for Astronomy and Applied Mathematics, Academy of Athens, 11527 Athens, Greece

[79] Dipartimento di Fisica "E. Pancini", Università di Napoli "Federico II" and INFN, Sezione di Napoli, Compl. Univ. di Monte S. Angelo, Edificio G, Via Cinthia, 80126 Napoli, Italy

[80] School of Sciences & Humanities, Wentworth Institute of Technology, Boston, MA 02155, USA

[81] Institute of Theoretical Physics, Faculty of Mathematics and Physics, Charles University, 180 00 Prague, Czech Republic

[82] Centre for Research and Development in Mathematics and Applications, Department of Mathematics, University of Aveiro, 3810-193 Aveiro, Portugal

[83] Chennai Mathematical Institute, Siruseri 603103, India

[84] Nottingham Centre of Gravity, University of Nottingham, University Park, Nottingham NG7 2RD, UK

[85] Observatório Nacional, Rua General José Cristino 77, São Cristóvço, Rio de Janeiro, RJ 20921-400 , Brazil

[86] SUPA, University of Glasgow, Glasgow G128QQ, UK

[87] Consortium for Fundamental Physics, School of Mathematics and Statistics, University of Sheffield, Hicks Building, Hounsfield Road, Sheffield S3 7RH, UK

[88] INAF, Osservatorio Astronomico di Brera, Via E. Bianchi 46, 23807 Merate, Italy

[89] Department of Physics, Indian Institute of Science, Bangalore 560012, India

[90] Shanghai Astronomical Observatory, CAS, Shanghai 200030, China

[91] University of Illinois, Champaign, USA

[92] Data Science and Learning Division, Argonne National Laboratory, Lemont, Illinois 60439, USA

[93] Department of Computer Science, The University of Chicago, Chicago, Illinois 60637, USA

[94] Department of Physics, University of Illinois at Urbana-Champaign, Urbana, Illinois 61801, USA

[95] Department of Physics, University of Zürich, Winterthurerstrasse 190, 8057 Zürich, Switzerland

[96] Center for Space Sciences and Technology, University of Maryland Baltimore County, 1000 Hilltop Circle, Baltimore, MD 21250, USA

[97] Gravitational Astrophysics Lab, NASA Goddard Space Flight Center, Greenbelt, MD 20771, USA

[98] Center for Research and Exploration in Space Science and Technology, NASA Goddard Space Flight Center, Greenbelt, MD 20771, USA

[99] Computational Physics and Methods Group, Los Alamos National Lab, Los Alamos, NM 87544, USA

[100] Faculty of Science and Technology, University of Stavanger, 4036 Stavanger, Norway

[101] Institute for Theoretical Physics, Goethe University, 60438 Frankfurt am Main, Germany

[102] Department of Physics and Astronomy, University of Mississippi, University, MS 38677, USA

[103] Department of Applied Mathematics and Theoretical Physics, University of Cambridge, Wilberforce Road, Cambridge CB3 0WA, UK

[104] School of Mathematics and Statistics, University of Canterbury, Christchurch 8041, New Zealand

[105] CEICO, Institute of Physics of the Czech Academy of Sciences, Na Slovance 2, 182 21 Praha 8, Czechia

[106] Paris, France